STUDY OF WATER RESOURCES BY USING 3D GROUNDWATER MODELLING IN AL-NAJAF REGION, IRAQ

A thesis submitted to Cardiff University

In candidature for the degree of

Doctor of Philosophy

By

Hayder Hatif Kareem

Hydro-environmental Research Centre

School of Engineering

Cardiff University

May, 2018

ACKNOWLEDGEMENTS

Dedication

To Ashab Al-Kasa "Mohammed, Ali, Fatima, Hassan, and Hussein" I dedicate my humble work ... with my great hope in accepting it with the best of acceptance ... and to be my intercessors in my eternal life

DECLARATION AND STATEMENTS

DECLARATION

This work has not been submitted in substance for any other degree or award at this or any other university or place of learning, nor is being submitted concurrently in candidature for any degree or other award.

Signed …………………….…… (Hayder H. Kareem)   Date……….……….

STATEMENT 1

This thesis is being submitted in partial fulfilment of the requirements for the degree of Doctor of Philosophy (PhD).

Signed …………………….…… (Hayder H. Kareem)   Date……….……….

STATEMENT 2

This thesis is the result of my own independent work/investigation, except where otherwise stated, and the thesis has not been edited by a third party beyond what is permitted by Cardiff University's Policy on the Use of Third Party Editors by Research Degree Students. Other sources are acknowledged by explicit references. The views expressed are my own.

Signed …………………….…… (Hayder H. Kareem)   Date……….……….

STATEMENT 3

I hereby give consent for my thesis, if accepted, to be available online in the University's Open Access repository and for inter-library loan, and for the title and summary to be made available to outside organisations.

Signed …………………….…… (Hayder H. Kareem)   Date……….……….

ABSTRACT

Groundwater is a vital water resource in many areas in the world, particularly in the Middle-East region where the water resources become scarce and depleting. Sustainable management and planning of the groundwater resources become essential and urgent given the impact of the global climate change. This research will use a new hydraulic conductivity estimation "Distributed Value Property Zones" approach, which is integrated into a state-of-the-art computer model—the Visual MODFLOW (version 4.6)—to assess the current state of groundwater resources and the risk of future water resource security in the region centred at Al-Najaf province, which is located in the mid-west of Iraq and adjacent to the Euphrates River. It will also explore and assess the groundwater aquifer-Euphrates River interaction. The impact of the interface soil layer located between the two soils of Al-Najaf region aquifer is studied, which is considered to be the second novelty in this research.

The model is calibrated both statically and dynamically. The new hydraulic conductivity approach is highly improved the calibration process, particularly the dynamic process. Where, the application of the dynamic calibration with a 16.5 mm/year recharge rate shows the best correspondence with the field observations. After considering the new approach, sensitivity analysis and validation process are also carried out to evaluate the behaviour of the model, which reveals acceptable convergence. Ignoring the interface soil layer from the conceptualisation process and considering the aquifer as one layer only has affected the model's results. Specifically, only 0.24 km^2 dry area appears in the aquifer as compared with the current state's results of the groundwater aquifer when the interface soil layer is modelled. In addition, the Euphrates River leakage results are different due to the impact of the interface soil layer when compared with those results when ignoring it from the modelling process. Calibration is also affected. The calculated heads were high and dispersed when compared with those heads when the interface soil layer is modelled. This affects the accuracy and acceptability of the model's calibration results.

The results of the current state of Al-Najaf region show a general flow pattern from the west to east of the study area, which agrees well with the observations and the gradient of the ground surface. With the current discharges taken from 69 wells in the study area, a dry area is found in the top and bottom layers, which equals 39 km^2 and 1.32 km^2, respectively. This indicated a degree of insufficiency of water resources in the study area because the groundwater aquifer supplies only 84% of the current water demand from the pumping schedules. The computed groundwater balance shows that the Euphrates River supplies water of 5354 m^3/day into the groundwater aquifer, instead of gaining water from the recharge of 23527 m^3/day if no water is

pumped from the wells. The predicted impact of climate change cases concludes that the largest effect on the groundwater-Euphrates River connection is when reducing the recharge rate and the western constant head. In particular, the groundwater aquifer's dry area will increase dramatically and will reach 150 km^2 and 120 km^2 in the top and bottom layers, respectively. The Euphrates River will also suffer hugely through the loss of 14100 m^3/day due to the reduction of either the recharge rate or the western constant head. Increasing the pumping schedule for future use will also impact on both the groundwater aquifer and the Euphrates River. Reducing the Euphrates River level by 0.5m or 1m will slightly affect the leakage from the river and the study area's dryness. To control the impact on the groundwater aquifer and its connection with the Euphrates River, it is highly recommended to remove some wells from the pumping schedule and reduce the pumping rate of the other wells, and constantly monitoring the behaviour of both over time. It is expected that the results obtained from the study can provide important information for the sustainable and effective planning and management of the groundwater resources for Al-Najaf City and the surrounding area.

TABLE OF CONTENTS

Chapter One: Introduction

Chapter Two: Literature Review

Chapter Three: Methodology

Chapter Four: Study Area

Chapter Five: Model Setup and Validation

Chapter Six: Results and Discussions

TABLE OF FIGURES

XIII

LIST OF TABLES

Chapter One

Introduction

1.1 Introduction

Water plays a key role in social and economic development around the world. Water resources are commonly referred to the surface water from rivers, lakes and streams, and subsurface water from groundwater, springs and others. The surface water gathered through the constructions of reservoirs, dams and barrages is seen as the main supplier to the needs of the world (Aesh 2009). As stated by Quevauviller (2008), of 37 million km^3 of drinking water which is available on the planet, about 8 million km^3 is found in groundwater resources. With the rapid economic development and the population growth at the global scale in recent years, the use of surface water has been seen significantly increased. The change of climate from the greenhouse gas emission, which is the main cause of the global warming, may also lead to the shortage of the surface water resources, especially in the Middle East region (Quevauviller 2008). In recent decades, in many countries of the world, evidently groundwater has become one of the most crucial natural resources. As this source has the ability to supply water, it provides a number of essential advantages as compared with surface water source, such as higher quality to use it for various life's aspects; better protection from contaminants which may infect this source; less prone to seasonal and long-term fluctuations, and uniformly spread over large areas as compared with surface water where it is very often available in regions which devoid of surface water (Igor and Lorne 2004). Therefore, for domestic uses, industry, and especially agriculture, the freshwater supplied by groundwater source will ultimately become very important, particularly when surface water sources have exposed for depletion problem (Siebert et al. 2010). As a result, the use of groundwater is inevitably increased at the present and in the future. To control the sustainable and effective management of the surface and subsurface water resources, water security becomes an extremely urgent issue at the global level.

Middle-East countries are located in the more arid lands in the world, which includes North Africa and the Arabian Peninsula. In these regions, there are only three major rivers (surface water sources), the Nile (in Egypt), the Tigris (originated from Turkey and terminated in southern of Iraq in the Shatt al-Arab), and the Euphrates (originated from Turkey and passes through Syria and terminated in southern of Iraq in the Shatt al-Arab) which provide water for narrow sections (areas) throughout the year. The rest of the regions are being forced to rely mainly on the desalination process of seawater for drinking purposes, especially in the Gulf

region. However, the other countries have to rely heavily on groundwater for human consumption and agricultural activities. Therefore, the groundwater is a major component of life particularly in the Middle-East region (El-Baz 2013).

The total Tigris River Basin area is around 375,000 km^2. The average annual runoff is estimated at 21.33x10^9 m^3 when entering Iraq. The Tigris River contains many tributaries, the most important ones are the Great Zab, the Small Zab, Al-Edheim River, Diyala River, and others. Regarding the Euphrates River, its basin area is around 500,000 km^2. The average annual flow of the Euphrates River when entering the Iraqi borders is estimated at 30x10^9 m^3, with a fluctuating annual value from 10x10^9 to 40x10^9 m^3. This quantity is allowed to enter Iraq under the agreement between Iraq and Syria as it often changes under political changes that negatively affect these agreements. Unlike the Tigris River, the Euphrates River is not connected to any tributaries when it runs through the Iraqi lands where it only discharges of around 10x10^9 m^3/year to Hor al-Hamar (one of the marshes in south of Iraq). The annual runoff in both rivers which has been entered from Turkey and Syria, has changed over the successive decades where in the period from 1938 to 1980, the total annual runoff rate of both was reaching up to 68x10^9 m^3, while the records showed that in certain years in the mid-sixties and mid-seventies, the annual runoff rate has exceeded 84x10^9 m^3. On the other hand, in the early 1960s, records illustrated a severe drought where the discharge rate of both rivers was 30 x10^9 m^3. Therefore, this large variation in the annual discharge rates makes it difficult to develop an appropriate water allocation plan to address the competitive demand for water from all sectors, as well as to ensure fair water sharing among neighbouring countries (MOWR 2015). Iraq had not experienced any shortage of water from the Tigris and the Euphrates Rivers previously, but the changes that have emerged in recent years (such as wars, population increase, excessive increase in water demand for various purposes) have been increasing the effect on the water security in Iraq. The Iraqi government has also called for Turkey and Syria to change their water policy with the riparian countries, which has led to the building-up of the tension in Iraqi-Turkish and Iraqi-Syrian relations.

In Iraq, the lack of application of modern technological methods in the management of water resources has led to the country lagging behind global development for several decades. Where twelve years of blockade and economic sanctions, which have imposed on Iraq, have deprived the engineers and scientists of the opportunities for the cooperation with the modern world and transfer of modern technologies to the Iraqi Ministry of Water Resources (MOWR); therefore, the negligence in the field of water resources was very large and need for strenuous efforts to promote this vital sector. Iraq has gone scarce of water through successive years since 1933, the

worst of which were 1999, 2000 and 2001, and now the situation is repeated since 2008 and so far. This indicates the impact of global warming on the scarcity of rainfall and climate change as well as the several factors which have contributed to the current water crisis and led to a major impact on water resources in Iraq. Climate change or global warming represents one of the factors that led to the drought phenomenon, which included the entire Middle East, not just Iraq, resulting in a significant decrease in the amount of rain and snow and a clear decline in the water revenues of the Tigris and Euphrates Rivers and their tributaries. The behaviour of neighbouring countries such as Turkey and Syria is changed where the fresh water flowed from the mountains in Turkey to Iraq and through Syria to Iraqi territory, flows from the immemorial time without any barriers like dams. In the early 1970s, neighbouring countries have started to build storage dams and irrigation projects and continue to establish more of these dams without taking into account the consequent shortage of water imported to Iraq and deterioration of its quality, where these dams located on the Euphrates River in Turkey and Syria have the ability to control the quantities of water received in Iraq. The management of water inside Iraq represents another problem, where there is poor planning of this source in general due to the previous policies of successive governments, which led to the disruption of the development process in irrigation projects and the deterioration of services in the water resources sector. All of these issues have produced the failure to develop clear plans to manage this vital source, which in turns led to some agricultural lands becoming dead and unsuitable for agriculture. Currently, the agricultural sector in Iraq contributes only to 8% of the Iraqi economic output although it is the second largest sector in the country. This is due to years of negligence for this sector, international sanctions, and the lack of investment and deterioration in recent years due to the decrease of the Tigris and the Euphrates Rivers' levels, which consider the main sources of water for agricultural and life purposes (MOWR 2015).

Al-Najaf province feeds mainly from the surface water supplied by the Euphrates river, which passes on the eastern side of it. Four provinces south of Al-Najaf are feeding mainly on surface waters provided by the Euphrates River, where vast areas of arable land are left without being sown due to the drought, which further exacerbated its decline level, leading to severe water shortages in the region. The low water level in the Euphrates River (Figure 1.1) forced farmers to cultivate a quarter of the land which normally cultivates previously. In addition, the decrease in the Euphrates River's level resulted in a shortage of those waters quantities required to meet the needs of the population for drinking and irrigation (MOWR 2015).

Figure 1.1: Declining of the river level and appearing the riverbed (Adopted from MOWR 2015)

The problem has become worsen and led to the drying up of some of the subsidiary irrigation canals which are branching from those tributaries of the Tigris and Euphrates Rivers, but far from the main flowing water of the Tigris and/or the Euphrates River. The dryness of these canals has resulted in the inability to cultivate agricultural land in the areas around of these canals despite the presence of the source of groundwater in some of these areas, but the poor management by the decision-makers has prevented the use of this vital resource due to the absence of extracted wells available in those areas (MOWR 2015).

With the sharp decline in the Tigris and Euphrates Rivers' levels in Iraq as reported by the Iraqi Ministry of Water Resources (MOWR 2015), the Tigris and Euphrates Rivers' running water are reduced by 30% and 35% respectively, which has caused the destruction of large tracts of agricultural land, significant livestock, and fisheries losses in the country, government efforts with neighbouring Turkey and Syria to increase water supply flowing in these rivers are increased. Where the agriculture in Iraq suffers from a significant decline compared to the actual production which was available before 2003. The most important reasons that contributed to this decline are the lack of successive governments to support farmers in funding and crop requirements, and the absence of a general agricultural plan for irrigation. In addition, the shortage of precipitation aggravates the problem in the last ten years on those lands away from the river or those that do not have groundwater, to increase non-planted areas, although those areas are cultivable (Figure 1.2). More than that, the rise in temperature significantly led to highlighting the phenomenon of desertification and drought, which led to a clear impact on the areas of arable land and thus on the agricultural sector in general (MOWR 2015).

Figure 1.2: Drought of arable lands due to the unavailability of water (Adopted from MOWR 2015)

A good groundwater quantity was discovered at the slopes of the mountains in the north-east toward south-east in the area on the right bank of the Euphrates River. The safe yield of the water that is stored in the groundwater reservoir in northeastern-southeastern of Iraq is estimated to be between 10 m^3/s and 40 m^3/s at a depth of between 5 m and 50 m. The aquifers located on the right bank of the Euphrates River (such as Dibdibba formation, Injana formation, and others) are between a layer of gypsum and dolomite at levels that are increasing in its deep to the west, with water at a depth of 200 m (after Abu Jir fault, such as Dammam formation, Umm Er Radhuma formation, and others), with an estimated safe yield of 13 m^3/s from the western formations. The salinity of groundwater in these formations is estimated to be suitable for agriculture, industry aspects and often for drinking. In other parts of the country, good groundwater quality is to some extent limited due to high levels of salinity (MOWR 2015). Some of groundwater reservoirs in Iraq are receiving groundwater from Saudi Arabia such as Umm Er Radhuma formation in the south-west of Iraq, which is received of about $8x10^7$ m^3/year. The renewable groundwater resources in Iraq are estimated to be $35.2x10^9$ m^3/year. According to the MOWR (2015), the total amount of water withdrawn from the groundwater resources in 2012 was estimated at 66 $x10^9$ m^3, 79% for agricultural purposes, 6.5% for domestic supply and 14.5% for industrial use.

In Iraq, there are many urban; agricultural, and desert areas that own a large stock of water and can take advantage of it for multiple purposes. In the current research, it will address the City of Al-Najaf and its surrounding area, in particular, to the importance of this province and the large number of arrivals from all over the world as a sacred area. Geographically, Al-Diwaniyah, Al-Muthanna, Al-Nasiriyah and Al-Basrah represent the provinces which are neighbouring to the province of Al-Najaf and depend upon the water of the Euphrates River. These provinces are all feeding on this river through the daily life for all purposes and nowadays these provinces are suffering from a lack of water supplied for drinking, economic, and agriculture. Therefore, it

requires the provision of appropriate additional amounts of water without relying only on Euphrates River.

Al-Najaf province is located in southwestern part of Iraq and borders with Saudi Arabia. It shares its internal boundaries with the provinces of Al-Anbar, Babil, Karbala, Al-Muthanna and Al-Qadissiya as shown in Figure 1.3. It is located on the south-west of the Iraqi capital centre Baghdad with a distance about 161 km. On the western border of this province, there is the Western desert, which extends to the borders of Saudi Arabia. The total area of Al-Najaf is about 28824×10^6 m^2. There is a sea also in this province, which is called Al-Najaf Sea, it is dry at this time, but sometimes owns oscillating level during the rainy seasons of the year and it is located adjacent to the Western Sahara. The desert plains dominate the landscape in this city. A strip of irrigated agricultural land (farmland) runs along the most right and left sides of the Euphrates River, which is passed through the eastern border. Typical dry desert weather represents the climate of this province through the most seasons. Summer season is hot and dry, and the rainfall is very low and limited to the winter months. On the yearly average, Al-Najaf province receives only about 100 mm of rainfall. On the eastern side of this province and close to the Euphrates River, there is Al-Kufa City, which represents the second capital populated area in this province. Water users in this region are dependent mainly on the water running in the Euphrates River and the groundwater quantities which are pumped from the wells field to support their livelihoods. There are a lot of groundwater formations in this province, some are near from the ground surface (such as Dibdibba aquifer) and some are located deeper (such as Dammam and Umm Er Radhuma aquifers). Some of these formations have huge quantities of water, especially those aquifers located on the western part of this province (Western Sahara) and some have limited water quantity. Due to the availability of this renewable source, it is intended by policy makers and water planners to maximize the long-term economic development of this source to be ready for future oscillating hydrologic constraints. Recharge and total holding water capacity represent the most important annual constraints that facing the aquifers of groundwater. Due to the aridity, and various climate changes, an extra attention is needed for these regions to prepare some scenarios that can deal with difficult situations. Most of the aquifers in Al-Najaf province are composed of limestone, dolomite, dolomitic limestone, coarse sand, fine pebbles, gypcrete, claystone, sandstone, chalky limestone with marl beds, and others (Jassim and Goff 2006).
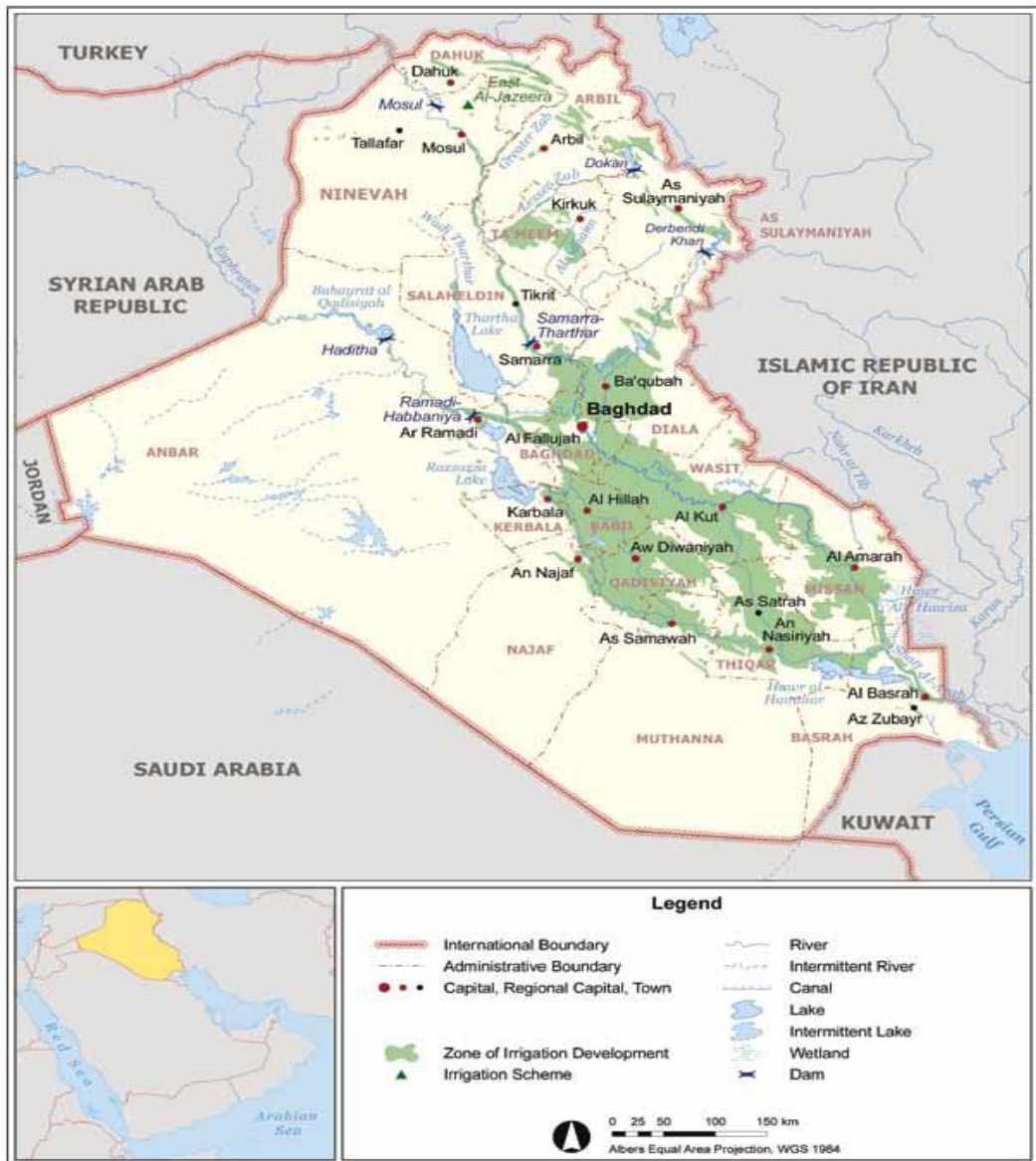
Figure 1.3: Iraqi governorates map with the Iraqi geographical neighbours (Adopted from MOWR 2015)

In recent years, Al-Najaf province suffers from increasing the level of groundwater in some areas. The main reasons for the rise of the groundwater in this province are, the weakness of the infrastructure system in some regions to collect water from residential houses, rainfall that falls on the region, and the seepage from the Euphrates River. Moreover, seeping a part of river water into the groundwater, and the little use of the groundwater source in multiple aspects of life in some areas which do not have wells-field, all of these factors together led to a rise in the groundwater levels in this city and its surrounding area. The effect of rising groundwater level has caused some issues. For example, the groundwater in this region contains chemicals that effect through the time on these foundations as shown in Figure 1.4, or its flow could cause soil erosion from under or around of these foundations. Some populated areas may be affected by

the rising of humidity due to the presence of groundwater, especially in the event of heavy rains, which lead to the rise of water level in the groundwater reservoir. In the region of Al-Najaf, there are some buildings that suffer from the problem of the rise of groundwater due to the proximity of these structures from the agricultural lands, which rely mainly on the water from the river in its irrigation despite the presence of groundwater in these lands (no wells available), which causes the increase of soil moisture which will affect the foundations of those structures (MOWR 2015).

Figure 1.4: Effect of groundwater on the foundations of buildings

The regions surrounding Al-Najaf province have large areas of agricultural lands in both east and west areas of this province where it is one of the Iraqi provinces that produce a section of crops that feed the country's economy, such as wheat and rice crops. Surface water represents the main factor in feeding agricultural crops in the province of Al-Najaf, represented by the Euphrates River and there are some areas feeds on groundwater. As the result of the high levels of groundwater in this province and the non-use of this source in some areas, led to the rise of groundwater to immerse the land and flooded many agricultural areas as illustrated in Figure 1.5. Where, due to the lack of drains to drain these waters on the long-term, it has led to damage of those areas to become unsuitable for agriculture because of the salinity, resulting in a significant loss in the local product crops of this province (MOWR 2015).

Figure 1.5: Immersing agricultural areas by groundwater

The rise of the groundwater level was not limited to the agricultural areas only, but also in the desert areas which have small agricultural areas as shown in Figure 1.6. Where these areas contain a good stock of groundwater and lack of population for the purpose of investment of this source as well as the lack of the management plans that should be prepared by the government to reclaim of these areas. Therefore, in the event of a high rate of precipitation, this will lead to increasing the groundwater levels and thus dumping large areas of agricultural lands and others (MOWR 2015).

Figure 1.6: Groundwater seen in the desert areas of Al-Najaf province

1.2 Motivations

The most important reasons for doing this work can be summarized by the followings:

1. Exploring the groundwater resources in Al-Najaf region and its connection with the surface water source represented by the Euphrates River to assess both of these sources, whether there is an impact applied on them from the current pumping schedule or not and whether the interaction between them will affect each other or not.

2. Due to some issues affecting the source of surface water represented by the Euphrates River, such as 1) the excessive use for the surface water source for all life purposes agriculturally, industrially, household, and drinking, 2) high temperatures which increase the evaporations from the surface water source, 3) shortage that may happen in the surface

water source after GAP project (22 dams on Tigris and Euphrates rivers) completes and becomes under operation, 4) population increase, and many more, it needs to use another source of water such as the groundwater source to reduce the impact of these issues and participate by providing water for some daily life's activities.

3. Sustaining the groundwater source to ensure its durability for future demand without any impact that may lead to damaging it.

4. Reducing the dependence or excessive use of the waters supplied by the Euphrates River where it will keep large amounts of water for future use in addition to maintaining the level of the river, which will help the arrival of the Euphrates River water to those provinces southern of Al-Najaf province.

5. Using the groundwater resource for the purposes of agricultural development through the reclamation of some agricultural land and the provision of water for this land from this source, which will help reduce the use of the surface water source represented by the Euphrates River and expand the scope of use of this vital source (groundwater source).

6. Helping the decision-makers in Al-Najaf region by providing an integrated view of the groundwater and surface water resources available in the governorate and the damage to these sources and how to manage them in the best manner, which in turn will reduce the future damage and provide the quantities of water in these sources for the potential future water scarcity.

7. Providing a specialised study on the source of groundwater, the effects applied on this source, and how to manage it in the best manner so that this study can be applied in other places of Al-Najaf province or Iraq, especially as Iraq contains many groundwater aquifers containing large amounts of water and most of them are not invested and/or studied so far.

1.3 Aims and objectives

This study is to use the modern state-of-the-art-Visual MODFLOW (version 4.6), which is classified as an accurate code in groundwater modelling (Kumar 2015), to assess the water resources (groundwater and surface water) in Al-Najaf region, Iraq as well as the interaction between these two resources. The scientific objectives of this thesis are to:

1. Build a 3D groundwater flow model for Al-Najaf region by using a novel approach of hydraulic conductivity estimation/interpolation that is provided by Visual MODFLOW to simulate the resources of water through establishing a conceptual model.

2. Explore the impact of the existing interface soil layer that separating the single unconfined aquifer (Dibdibba aquifer) into two soil layers to assess its impact on model entire domain conceptualisation and model results.

3. Assess and estimate the available groundwater quantities as a basic aspect of the current groundwater management.

4. Study the impact of the river level, which passes through Al-Najaf province on the groundwater level in the area close to the river and in Western Sahara region. In addition, explore the impact of groundwater exploitation on the aquifer by building a model that can simulate the river and the aquifer at the same time.

5. Estimate the vulnerability of groundwater resource (Dibdibba aquifer) and the Euphrates River by the impact of dry climate changes which are highly expected to happen in the future.

6. Identify the ideal locations for the pumping wells which will be used for the appropriate purposes in Al-Najaf region as well as maintaining the sustainability of this water source through the development of appropriate decisions to manage well locations. This will provide the ability to supply an extra water for population usage.

7. Create a management plan for the groundwater in Al-Najaf province so as to ensure the provision of scheduling of wells extraction amounts, locations, and effects on the groundwater aquifer system for the present and future advantages.

1.4 Thesis layout

The scientific and logical sequence that should be followed for the purpose of preparing a rigorous scientific research is as described in the chapters below with the required sequence, as follows:

An introduction explains some important information about the groundwater issue overall the world nowadays and the motivation leads to studying the groundwater problem in Iraq and specifically in Al-Najaf region, are illustrated in Chapter 1. Gaps which are leading to address Al-Najaf region to be under study are also explained in this chapter.

Chapter 2 presents a comprehensive review on the previous studies conducted by other researchers which are relevant to the current study/study site. The chapter focuses on the studies which were developed or modelled by MODFLOW program, but at the same time presents the other studies which were carried out using different codes or programs deal with groundwater analysis such as GMS program (Groundwater Modelling System), PMWIN (Processing MODFLOW for Windows), FEFLOW (Finite Element Subsurface Flow System), and others. A general view on the novelties intended to apply in this study is explained.

Chapter 3 describes the basic equations of groundwater flow which are governing the movement of groundwater flow for an area through the confined and unconfined aquifers, groundwater-surface water interaction (groundwater-river interaction), and some other equations related with methods to estimate some of the boundary conditions needed to build the groundwater model. The boundary conditions and those criteria needed to calibrate and validate of any groundwater model are also explored.

In Chapter 4 will describe the geology and hydrogeology parameters of the study area in terms of the nature of the topography and stratigraphy of the region and nutrition, which are mainly affected the movement of groundwater. This chapter will analyze the geological and hydrogeological collected data to extract the boundary conditions. In addition, the methodology used to calculate some of the needed boundary conditions is explained in detail.

Chapter 5 will include the description of the conceptualisation of the groundwater model for Al-Najaf region by using Visual MODFLOW program in detail; step by step, with the method of building the 3-dimensional groundwater model. It will apply the boundary conditions and does the calibration and validation processes for the model.

Chapter 6 explains the results of the current situation of groundwater resources in Al-Najaf region. In addition, it will illustrate and explain the results that are resulted from the Visual MOFLOW analysis for Al-Najaf region groundwater model in detail for each case/scenario which is considered and applied to the model.

Chapter 7 summaries of the outcomes of the research study. According to the consequences, it will put the recommendations for the decision-maker that should be taken into consideration for the future well planning.

1.5 Publications

- **Conferences**

- Kareem, H. H. and Pan, S. 2016. Modelling of groundwater resources for Al-Najaf City, Iraq presented at ICWES 2016: 18th International Conference on Water and Environmental Sciences, Kuala Lumpur, Malaysia, 11-12 February 2016. urn:dai:10.1999/1307-6892/10003691.

- Kareem, H. H. and Pan, S. 2018. Impact of interface soil layer on groundwater aquifer behaviour presented at ICGMTA 2018: 20th International Conference on Groundwater Monitoring Technologies and Applications, London, United Kingdom, 15-16 February 2018. urn:dai:10.1999/1307-6892/10008558.

Chapter Two
Literature Review

2.1 Introduction

The fundamental development for the quantitative description of groundwater flow was in the 19th century as the first two scientists Hagen (1839) and Poiseuille (1840) were the only researchers who derived the equations deal with viscous flow through capillary tubes. Then, Henry Darcy (1856) derived the well-known flow law which can simulate water flow or groundwater movement in a porous medium and known as Darcy Law. Most groundwater studies have used this law as a base to identify the true results in either the experimental or numerical simulations. Many researchers have dealt with groundwater flow and groundwater-surface water interactions because groundwater issue represents an important source of fresh water that can help to support various life aspects. The connection of this source with the over-ground sources (Rivers, Streams, or Lakes) will affect each other geologically, hydro-geologically, and environmentally.

Although there are many aquifers in Iraq collecting groundwater, such as Dibdibba formation, Umm Er Radhuma Formation, Dammam formation, Injana formation, Fat'ha formation, Nfayil formation, and Euphrates formation (most of them are in the Iraqi Western Desert), but the groundwater studies at the Iraqi level are still very few. The reasons for that are sometimes the complexities of data access, financial support of those studies need for experiments to improve data required, less experience in the field of groundwater analyses, and difficulties in assigning the correct boundary conditions for the area intended to be under study. Therefore, the only Iraqi groundwater studies were conducted by Al-Salim and Khattab (2004), Al-Sadiq and Akulaims (2005), Al-Samma'a et al. (2008), and Al-Muqdadi and Merkel (2011). In those studies, MODFLOW and GMS "Groundwater Modelling System" program have been used to investigate the groundwater aquifers' behaviours in terms of estimating the groundwater quantities in those areas and its suitability for use. The weakness in these studies is, those studies were not taken into account the parameters that affect the quantity or quality of this source like the contaminant, recharge, discharge, the impact of pumping wells-field, and the future prediction of this source. However, Dibdibba aquifer located in the area under study in this research lacks for any study that deals with the behaviour of this aquifer under external impacts such as pumping schedule or climate change although the presence of pumping wells used for agricultural purposes.

Groundwater modelling represents the management tool that helps to provide a decision about the groundwater system behaviour and the future response of that system due to the several impacts applied on aquifers. Modelling process has three important objectives (Anderson and Woessner 1992):

- Predicting the behaviour for certain events which may the system be exposed for;
- Gaining an overview of the dominant parameters by interpreting the dynamics of the system so that if the data is insufficient, it will provide the appropriate guides for data collection activities; and
- Formulating the regulatory guidelines for the area under study by generating the appropriate geological conditions for flow analysis.

To meet these objectives, several groundwater models have been developed to deal with the problem of groundwater which can generally be classified into two categories, physical and mathematical models. In order to assess the groundwater and groundwater-surface water interaction, several studies on groundwater flow, its relationship/connection and its affect/effect on/with surface water will be reviewed in this chapter. These studies will provide a comprehensive insightful on the deficiencies or weaknesses of previous works to identify the appropriate requirements of treatment.

2.2 Groundwater models

Generally, a model is a device designed to represent an approximation to simplify the modelling process of complex physical processes. It may represent the groundwater model by an electric model or a scale model or a real groundwater aquifer model. A groundwater model, if it is constructed by a proper way, can be considered as an effective and valuable predictive tool for the groundwater resources management. The groundwater flow issues in the environment can be simulated using groundwater models (Anderson and Woessner 1992). In addition, it can consider the groundwater model more powerful if this model simply quantifies the groundwater heads and time for the complex hydrogeological conditions (Anderson et al. 2015). Poeter and Hill (1997) divided the groundwater models into two categories, the first one is the groundwater flow models which solve the head distribution over a domain and can predict the hydrological changes (such as irrigation developments or groundwater abstraction), while the second one is the solute transport models that solve the concentration of solute which is affected by dispersion, advection, and chemical reactions. Generally, groundwater models can be classified into two types, physical models and mathematical models. Physical models are those constructed in the laboratory by using the porous material (usually sand) to identify the

groundwater heads and flows directly (Anderson et al. 2015). Mathematical groundwater models are generally those models depended upon the equations of groundwater flow, which are the partial differential equations. These equations often can be solved by either the analytical or numerical methods; therefore, it can call the mathematical models as numerical, mathematical, or computational groundwater models. Analytical models are typically using the structure of mathematics to simplify the complex geometry of the groundwater domain to get a quick answer. Numerical or mathematical models are generally based on the real physics (real geological, hydrogeological, and boundary conditions) of the groundwater flow through deriving the appropriate mathematical equations. These mathematical equations are solved by various numerical solutions techniques or methods such as the finite difference method, the finite element method, and many more (Anderson et al. 2015).

2.2.1 Physical models

As physical models are those constructed in the laboratory, it can be using these experimental models to understand the groundwater flow and transport processes. The widely spread model is named as the "SandBox Model", which represents a reduced scale of the natural porous medium domain. This model type has been used in many applications in groundwater flow and transport phenomena. Series of laboratory experiments have been made by Oswald and Kinzelbach (2000) to study the phenomenon of the variable-density flow of the subsurface flow in a saturated medium to use the results of these experiments in verifying the reliability of some numerical codes. Therefore, Sand Box models can be used to obtain the information required for elaborating of the benchmark examples (Loudyi 2005). In addition, these kinds of models can be used to study the groundwater contamination and remediation movement under different site field conditions (Hoopes and Harleman 1967; Ishaq and Ajward 1993). However, there are significant differences between the phenomena measured in the sandbox model and those observed in the field resulting from the small size of the laboratory model compared to the actual dimensions of the field site. Therefore, conclusions obtained from such models need to be re-examined when applied and translated into the field situation (Loudyi 2005).

2.2.2 Mathematical models

Groundwater flow mathematical models have been in use since the late of the eighteenth century. The fundamental concept of these models to deal with the behaviour of the aquifer system is represented by a set of mathematical expressions, such as linear algebraic equations or partial differential equations. Broadly, these models can be classified as either deterministic or stochastic (Loudyi 2005).

Deterministic methods/models assume that the whole system works on the principle that the occurrence of a given set of events will lead to a specific definable outcome, whereas stochastic methods assume in advance that inputs are uncertain and accordingly it is designated to record of this uncertainty. Although there is an intended trend in research to develop the using of the stochastic methods, but deterministic methods are still more widely used than stochastic methods. Depending upon the assumptions which are made for the flow problem in terms of the partial differential equations, initial conditions, and boundary conditions, the governing equations in the deterministic approach will be almost solved numerically (Loudyi 2005).

The more realistic field situations for the constructed mathematical models of a regional flow is almost analysed by approximated numerical techniques. Since the 1960s, numerical models have remained in continuous development where it becomes the preferred modelling approach to the sophisticated groundwater problems, especially the recent development of the high-speed digital computers. Numerical models have provided many advantages which included the ability of:

1. Simulating the complex physical systems;
2. Simulating the multidimensional groundwater systems;
3. Simulating both temporal and spatial distributions of various model output;
4. Incorporating the complex boundary conditions;
5. Harmonizing the spatial variability of the inputted parameters; and
6. Harmonizing both steady-state and transient conditions.

Consequently, numerical groundwater models are better for simulating those problems of the real flow field. Where in fact, conceptualisation of a groundwater model into a mathematical model in the form of defined the field governing equations with the associated boundary conditions could have more complexity than that for constructing an analytical model. The solution of a mathematical model can be obtained through transferring those kinds of models into numerical models and then writing a computer code for solving the partial differential equations of the numerical model. The partial differential equations can be replaced by a set of algebraic equations which must be solved simultaneously as various numerical techniques and codes are existing for solving numerical models (Loudyi 2005).

Numerical methods/techniques solve the partial differential equations, which are stated in the mathematical models, by an approximated solution. The hydraulic heads resulted from the approximate solution represent the numerical values at specified points in space and time domains defined for the groundwater problem. Where, as mentioned earlier, a set of algebraic

equations in terms of discrete piezometric heads will replace the partial differential equations at discrete points within the model domain (Loudyi 2005).

Fluid applications have been solved by many numerical methods for various combinations of diffusion-advection problems. Generally, pure diffusion equation can describe the groundwater problems (i.e. flow problems), while diffusion-advection equation can represent the solute transport and the variable density flow. In this study, flow problems which mostly dominated by diffusion have been emphasised to investigate the worldwide techniques which have been used for this type of mechanism. The current principal methods which are nowadays in use for those equations integrated within the fluid applications are the finite difference method; finite element method; integrated finite difference method; boundary element method; and finite volume method (Abott 1989).

The most extensively important and widely used methods in the groundwater flow problems are the finite difference method and the finite element method. Where the classic codes which have been used widely in these techniques have proven the strength of these methods in certain applications, but sometimes showed weakness in others. The three later methods are newer in their applications in the groundwater flow problems and still under investigation.

2.3 Existing groundwater codes and limitations

Various codes have recently been developed for most problems classes which are accounted in the field of groundwater management. Some of these codes are comprehensive for some extent and have the ability to handle various specific problems, whilst others are like tailor-made designed for particular problems. Most of these codes are developed or adapted to be used in the microcomputers through benefitting from the development of computer speed, graphical capacities, and high memory storages. Groundwater flow codes are structured to formulate the numerical algorithms to be able for tackling fluid flow problems where these algorithms called solvers. In addition, many codes offer great accessibility to access their code solving power. Nowadays, all the commercial CFD "Computational Fluid Dynamics" packages have a complex user interfaces for inputting parameters and examining outputs where most of these codes are containing three main elements, a pre-processor of the input parameters, a solver that can approximate the unknown variables, and a post-processor computer program that can offer graphic capabilities for inputs and outputs visualizations (Loudyi 2005).

Generally, some public domain programs have less user-friendly facilities because those programs are more concentrated on solver performances than other facilities. Therefore, such

high capabilities represent a part of the selection criteria of the groundwater flow modeller who should choose the related code carefully. Table A.1 in Appendix A summarizes the most widely used existing codes in the field of groundwater flow simulations in the saturated zones. The performance of each modelling code, its applicability and functionality, stability, accuracy, data preparation or execution of each flow problem can be analysed depending on the programme documentation or manuals (Loudyi 2005).

Over 500 computer programs currently exist for analysing groundwater or surface water problems (Van der Heijde 1996) where although this number has increased dramatically as many codes are newly created and developed to address the various research purposes, but this field remains need for development. For instance, one of the problems, evaluation of groundwater model applications remains without a common agreed methodology to evaluate these applications. In the face of decision-making based on model applications in many water quality issues, organizational staff needs guidance to evaluate the objective from building a model. The system of experts for selecting the appropriate computer software to analyze groundwater problems could be a very useful and helpful tool for promoting their use among local communities. For specific objectives, some authors have already proposed such systems, for instance, groundwater protection programs, pumping test experts system (Ouazar et al. 1996), groundwater management has focused on the assessment and clean-up activities for hazardous waste site risk (Chowdhury and Canter 1998), or wellhead protection program (Wang 1997). Some governments have published their handbook on the selection and application of mathematical models for either flow or solute transport processes (USEPA 1994; NGWCL 2001). More generally, selection of the appropriate model's code for a specific field problem will depend upon the modelling objectives and the criteria that are describing the related code for a specific site.

A computer programming language represents the numerical technique that will create a code for a specific problem. Therefore, limitations and capabilities of a code will depend on the performance of the numerical method used and the efficiency of computer platform. It became more important to evaluate the limitations of a selected code for the improvement purposes. Generally, a brief description of code limitations are broadly classified as follows (Loudyi 2005):

- Conceptualisation related: geological and hydrogeological features that can simulate the problem. These assumptions are needed when developing a model such as (model dimensions, boundary conditions, confined or unconfined, isotropic or anisotropic, steady or transient flow, heat considerations, transport considerations, etc.).

- Mathematical solution needed: It depends on the solution method selected, if a numerical technique is used in the selected code, the solution will be either in FD "Finite Difference", FE "Finite Element", FV "Finite Volume", or BE "Boundary Element" method where the solution method will identify the limitations of the problem. Therefore, the accuracy and efficiency of the code will be affected by this type of limitations.

- Hardware needed: In the programming language, the number of cells, model size, time steps, the amounts of data that can conceptualise the problem, and the numerical precision of calculations, are restricted to storage capacity and computer speed.

2.4 Numerical models

The world has recently proceeded the development use of groundwater rapidly, often outside the control of the governments. As a result, the uninterrupted pumping and pollution have threatened the sustainability of groundwater aquifers. Therefore, in many countries, awareness has emerged the need to improve groundwater management because, in many regions, the sustainability of groundwater resource is exposed to the daily shrinkage due to the excessive daily use (Groundwater Governance 2015). Generally, groundwater is controlled by three problems: depletion resulted from overdraft; submerged regions with water which will lead to increase the salinization due to insufficient drainage system; and pollution resulted from industrial, agricultural and other human activities (Shah et al. 2000). Overdraft is a process of extracting groundwater beyond the equilibrium or safe yield of groundwater aquifer, which could cause some consequences such as drying up some sub-surface groundwater aquifers, as this problem has led to drying up some of the natural streams and springs during the eighties of the last century (Shah et al. 2000). Due to the lack or sometimes absence of the drainage system and the lack of water management, some of the saturated irrigation fields have significantly affected by the occurrence of salinization. The increase in the irrigation process for agriculture has led to double the risk of waterlogging and salinization (Kbrom 2017). The quality of groundwater is threatened by degradation either due to the seawater intrusion (in coastal areas) or by the anthropogenic pollution resulted from the variety of contaminants which are existing in industrial or urban or even agricultural areas, so pollution represents sometimes a great issue in groundwater management (Groundwater Governance 2015).

Iraq has suffered from a severe shortage in groundwater studies due to the need of such studies for many data and a good knowledge of the nature of spatial and temporal characteristics, as well as sometimes required to conduct some laboratory tests to get some important characteristics in the modelling process. At the local level (in Al-Najaf City and the surrounding area), properties of soils of groundwater aquifers have been studied by Al-Aboodi (2008), Ali

(2012), Jalut et al. (2013), Abojassim (2014), and Omran et al. (2014). Those studies have investigated the chemical concentrations in Bahr Al-Najaf's groundwater aquifers, hydrological properties for the area extended between Al-Najaf and Karbala provinces, uncertainty of parameters effect on the head as a dependent variable in Bahr Al-Najaf, the concentrations of uranium in the groundwater and soil in some areas of Al-Najaf province, and estimated the quantity of surface water in the groundwater source in Bahr Al-Najaf as well as how are these kinds of waters are distributed in the groundwater resource respectively. These research still without a confidence because the materials which those researchers have been used still have the weakness of confidential results although these studies still contain the minimum amount of information and data necessary to initiate comprehensive and complex studies.

In the same context, the other groundwater aquifers' properties studies in other areas at the country level, the Western Sahara has motivated lots of researchers to consider that area as it has some important regional groundwater aquifers with huge amounts of water. Where, Parsons (1957), Ingra Yugoslavian Company (1961-1967), Consortium-Yugoslavia (1977), AlFurat (1989), AlFurat (1995), Al-Jiburi and Al-Basrawi (2009), Al-Fatlawi and Jawad (2011), Al-Muqdadi and Merkel (2012), Ali et al. (2013), and Al-Mussawy (2014) have studied different areas in Iraq to investigate the deep fractured aquifers properties, chemical analysis and pumping test, hydrogeological conditions in the Mutable blocks, Umm Er Radhuma aquifer properties, wadis specifications in the Iraqi western desert, geochemical parameters in Tigris river's water in Baghdad province. Still the focusing of all of the mentioned studies is on the geological, hydrogeological, and environmental properties of the Iraqi groundwater aquifers without taking into account the benefits of this available groundwater source.

Groundwater flow analysis represents the fundamental aspect of many researchers who looking for how to extract groundwater and treat it so that can consider it as a new source of water which can be used for different life purposes such as agriculture, industry, domestic use, and others. In the same context, many researchers have studied the effect of different kinds of pollutants on groundwater which resulted from factories, after being buried under the earth's surface in order to evaluate the effect of these contaminants on the groundwater quality and how it spreads. In other words, find the time and mass which the contaminant needs to spread through the groundwater system in order to keep this source as far as from pollution. This is because the groundwater source in an area has the ability to feed different fields of human life's needs.

The Iraqi regions which have been under study by the international researchers are very limited. Groundwater flow and contaminant studies are many where each researcher has the choice to choose the appropriate program that can simulate the intended area for study. The codes which are used to analyse the groundwater/surface water bodies' behaviours are many (as illustrated in Table A.1 in Appendix A), where the selection of the appropriate code depends upon the aim of the study and the characterization of the study site. A review on the groundwater flow studies and groundwater-surface water interaction studies that have been used Visual MODFLOW program will be presented.

Mace et al. (2000) who developed a three-dimensional groundwater model to estimate the groundwater availability and levels of water for the purpose of pumping and future use for the upper and middle Trinity aquifer in Hill Country Area, USA. MODFLOW software was used to simulate the model for the steady-state (when the water levels in the aquifer near equilibrium) and transient (when climates are transitioned from a dry to wet period). The steady state calibration process was carried out for the year 1975 for the water table levels and the results were good as it is shown in Figure 2.6. Recharge and the horizontal hydraulic conductivity were effected the water levels of the middle Trinity aquifer, while the water levels of the upper Trinity aquifer were most sensitive to the vertical hydraulic conductivity.
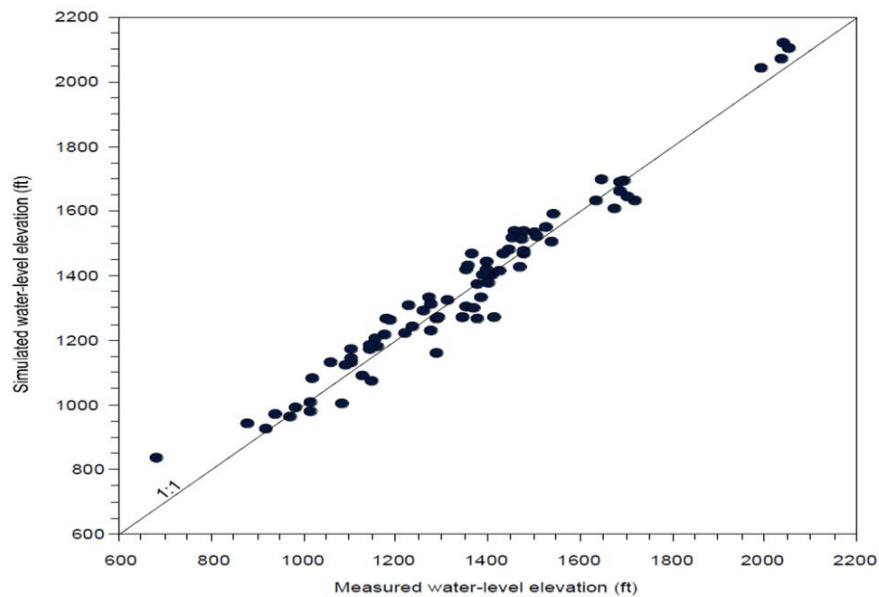
Figure 2.1: Simulated water levels for the middle Trinity aquifer for the 1975 steady-state model (Adopted from Mace et al. 2000)

CEDARE (2002) developed a groundwater flow model for the Egypt Nubian sandstone aquifer system in order to simulate the system of groundwater flow for this area for the last 8000 years due to climatic changes.

Andrews and Neville (2003) studied the amount of chromium released in the valley which is near to Mojave River in California, USA. This study was presented to understand the methods that controll migration and fate of chromium in groundwater in order to be used as a tracer to investigate and study the dynamics of the basin. MODFLOW and MT3D were used for simulating the groundwater and chromium transport, respectively. Developments and modifications to MODFLOW resulted in a new well package that guesses pumping rates from wells for each time step depending upon the available drawdown. MT3D was modified to account for mass trapped and to redistribute mass to the system when the water table descends under non-irrigated areas and when water levels rise above.

Leighton and Phillips (2003) built a numerical groundwater flow model for the Antelope Valley ground-water basin in California, USA by using geohydrology data. The system of groundwater flow comprises of three aquifers: the Upper, Middle, and Lower one. The model of groundwater flow of the basin was divided horizontally into a grid which consists of 43 rows and 60 columns of square cells one mile on each side and vertically for the three aquifers as which represented above. The results of model simulation showed that groundwater storage was declined for an approximately of 8.5 million acre-ft (10.5×10^9 m^3) from 1915-1995 and the water level to about 150ft in the south-central part of the groundwater basin and this was with an extra 5ft of subsidence was simulated in the central part of the basin.

Scanlon et al. (2003) used various approaches to simulate the groundwater flow in karst system. These approaches were equivalent to porous media distributed parameter, lumped parameter and dual porosity approaches, as well as discrete fracture or conduit approaches. The study was to simulate the regional groundwater flow in karst aquifer by using two different equivalents porous media approaches: lumped and distributed parameter as well as to evaluate the adequacy of these two approaches. The results showed that the Karst aquifer was very sensitive for the recharge than the pumping rate and this means that it needs to enhance recharge as well as to keep the conservation measures in order to improve the spring flow.

A groundwater numerical model was built for a multi-aquifer and unconsolidated complex system in Swidnica area, southwestern Poland by Jacek and Maciek (2004). MODFLOW program integrated within GMS software was used to develop and calibrate the conceptual model depending upon the investigations from several hundred boreholes using the steady state condition. This study was to analyse the impact of wells abstractions 53000 m^3/day on the groundwater level. Results showed that the abstractions' impact on the multi-aquifer system was well (the groundwater decline was very slight) and the aquifer system was working efficiently

because the aquifer was received recharges from rainfall, Sudety Mountains which were existing along the boundary fault zone, and some lakes infiltrations. In addition, the aquifer system showed the ability for increasing the abstractions from wells.

Al-Siba′ai (2005) has built a mathematical model for modelling the movement of groundwater in the lower basin of the Euphrates (Sector Six) in Syria by using MODFLOW program. The results of the study showed that the area in case of bad drainage, and the basin in general suffered from the problem of bad drainage process, which led to a gradual rise in the underground water level.

Blegen (2005) accomplished both analytical and numerical groundwater flow models for the aquifers in delta structures (Trandum delta) in eastern Norway. This study has carried out the analytical and numerical solutions for the steady state head in those confined aquifers and unconfined aquifers in the area and after that, the results of these models were compared with each other. The analytical model was simplified to a one-dimensional flow so that it can use Poisson's equation to get the solution. While, MODFLOW was used to make the numerical solution. Results were similar for a wide range between both analytical and numerical models.

Karamouz et al. (2005) developed a method to conjunct of using the groundwater and surface water with emphasis on the quality of water by using the ANNs and GAs (Artificial Neural Networks and Genetic Algorithms), respectively. The objectives of the study were to control the groundwater table fluctuations, reduce pumping cost, and supply an acceptable water quality. This model was applied to the irrigation networks in the southern part of Tehran, Iran. Results of the proposed model showed the importance of an incorporated systems approach to allocating the surface and groundwater resources in the study area.

Abdulla and Al-Assa'd (2006) studied the groundwater flow for Mujib aquifer, Jordan. The groundwater in Mujib area is the main source of water because Jordan is an arid country with a very little amount of water. The groundwater model was built to simulate the aquifer system under different stresses. The results of this model showed that this model was very sensitive to the anisotropy, horizontal hydraulic conductivity, and specific yield even when the recharge rates were low.

Sefelnasr (2007) has developed a three-dimensional transient groundwater flow model by using FEFLOW program (Finite Element Flow) for the Nubian Sandstone Aquifer System (NSAS) by depending upon the GIS-Database integration. This model was suggested to do three things, the

1st was to standardize a define regional boundary conditions of the NSAS, the 2nd was to simulate the management options of the groundwater for a various stressed areas within the aquifer, and the 3rd one was to predict the environmental effect which results from the extraction projects on the present and future groundwater extraction on the various exploitation locations. In addition, this study was used to predict the economic lifting depth through the simulation until 2100. Therefore, five scenarios of extraction were proposed to detect the practical option of groundwater management. Through the results, scenario 3 was the optimal one that meets the optimal groundwater management option and the economic lifting depth, while scenario 5 gave a lifting depth after the 100m and this represents faraway the economic lifting depth in both the Kufra oasis and the East Oweinat area.

MODFLOW and MT3D have been used to simulate the groundwater flow and solute transport in the subsurface systems in the Azraq basin, Jordan by Wa'il and Randa (2007). The model simulated five scenarios to control the effect of the pumping rate on the groundwater systems as well as estimating the TDS (Total Dissolved Solids) results from the pumping schedule through finding the EC (Electrical Conductivity). The study reported that the scenarios which have been applied have an impact on the drawdown values. In addition, these scenarios have an impact on the EC values less than the impact on the drawdown.

Humphrey (2008) developed a new numerical groundwater flow model for the southern portion of Honey Lake Valley in Lassen County, California County, Nevada to simulate the drawdown in the interbasin transfer across the California-Nevada state line. The people in this area and the SIAD (Sierra Army Depot) were worried about the reduction in the groundwater in the interbasin transfer. This was because of the prior models' predictions which presented for this area by others which resulted in a large range of drawdown. The values 1.4m and 0.8m were the results of model simulation for the drawdown across the California-Nevada state line and the SIAD, respectively.

Fouépé et al. (2009) built a groundwater model to simulate the groundwater flow and particle migration in an unconfined and shallow aquifer in the south-east of Yaounde City, Cameroon by using Visual MODFLOW. A steady-state simulation was carried out after calibrating the model using 18 observation wells. The calibration gave good agreement between the calculated and observed heads after excluding one observation well because of the errors in measuring this value. The results reported good trend for the contours levels which were corresponding to the observed ones.

Montenegro and Odenwald (2009) tested a three-dimensional saturated/unsaturated groundwater flow model for an excavation pit in Minden, Germany in order to overcome on the water table difference which is currently about 13m beside of this excavation pit. This study was to assess the design parameters like the elevation of seepage face, head distribution, and discharge to the pit. The study was depended upon the difference between 3D model and a conventional vertical-plane approach. Calculations of the 3D pit model led to a higher head distribution than any vertical plane model in the area close to the upper and lower head of the pit as well as vertical-plane approach cannot apply for the radial flow. The 3D model results showed a seepage face slightly above the pit bottom while higher levels of seepage were estimated from the vertical-plane model.

Tesfaye (2009) studied the groundwater flow and contaminant transport for Akaki wellfield and its surrounding catchments in Addis Ababa, Ethiopia by using steady-state groundwater modelling. One layer aquifer (100m thick) was presented in this study. This aquifer was simulated by using PMWIN (Chiang and Kinzelbach 1998) software (pre and post processor for MODFLOW) (McDonald and Harbaugh 1998) under confined and unconfined conditions. Furthermore, PMPATH has been used to find the path lines and times of travel of the contaminant. By using the trial and error method, the model was calibrated by comparing the observed and calculated heads. Recharge and base flow values which resulted from modelling were approximately indicating good agreement between different models. In addition, hydraulic conductivity and recharge that represent the optimized parameters were distributed spatially over the area of the model. Flow lines were converging toward of the Akaki wellfield from all directions and this means that any water contaminant from the upper aquifer part will end in the wells and cause the pollution for all the wellfield.

Nasrin et al. (2013) performed a mathematical groundwater model using Visual MODFLOW (v. 3.1) to evaluate the current and future development effects quantitatively and qualitatively in the Narmab aquifer located in Golestan province, Iran. Water level data from 15 wells for the period from October 2003 to October 2004 were used to calibrate the model of the study area and the results showed a good agreement with the calculated head values. Results showed that the groundwater level remains acceptable with the current pumping schedule during the complex climate change. While, for the future prediction in the next few years, the groundwater level will decline in the aquifer, especially when the pumping rate was increased.

A steady state, finite difference, two aquifers groundwater model was developed by using MODFLOW to estimate the quantity of the groundwater in the Choutuppal Mandal, Nalgonda,

India by Kumar and Kumar (2014). The observation heads from 19 observation wells were used to calibrate the model and the result of the calculated heads gives a good agreement as it is shown in Figure 2.7 after excluding 7 wells which do not match the calculated ones. Results showed that the aquifers are suffering from low storage and needs for an immediate arrangement for the groundwater recharge to save this source for future usage.
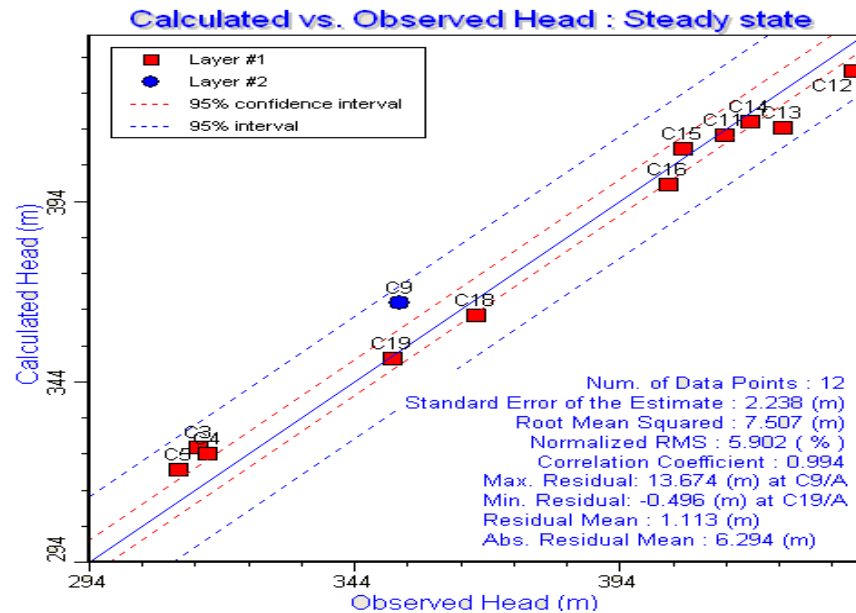
Figure 2.2: Computed groundwater level contours in groundwater flow model (Adopted from Kumar and Kumar 2014)

The MODFLOW code which is integrated within GMS software (Groundwater Modelling System) was used by Manouchehr and Ali (2015) to simulate Gotvand plain aquifer in Iran and assess of Abbid-Sarbishe area, which is located to the north of Gotvand in case of applying an artificial recharge. The model was calibrated and validated from September 2009 to August 2010 and then used to assess the artificial recharge applied on this area. Through the results, it was found that the western areas of the project were highly affected by the artificial recharge during the period from 2005 to 2007 around the piezometer G19 which was located on the northern part of Gotvand plain. In addition, the artificial recharge has a positive effect on the study area aquifer, but this effect was not sufficient because of the sedimentation, drought in the past years, and the seasonal water flood.

By using the GMS program, a numerical groundwater flow model was established by Shuwei et al. (2015) to evaluate the groundwater resources systems in the Jilin Urban Area (JUA) in China based on the collected data from 190 boreholes. Stages of the river were calibrated to control the groundwater flow in the field. The input for the model in terms of the hydraulic conductivity and specific yield were extracted from the results of 290 pumping tests. The model was calibrated using the trial and error method and gives a good agreement with a root mean square

of 0.66 m. Recharge was the most important sensitive factor on this model. Results reported that there was a decline in the groundwater level along the river valley in the Songhua. The model provided a scientific basis for using the groundwater source sustainably based on the demand and supply for the water resources in the JUA.

In Iraq, the groundwater aquifers in general include the formations of Dibdibba, Umm Er Radhuma, Dammam, Injana, Fat'ha, Nfayil, and the Euphrates where most of these formations are located in the Iraqi Western Desert. Although these formations have huge quantities of groundwater, but the groundwater studies that deal with this vital source are lacking, especially Dibdibba formation which has not been studied before despite the presence of pumping wells in this formation used for agricultural purposes. The reasons for that are sometimes the complexities of data access, financial support of those studies need for experiments to improve data required, less experience in the field of groundwater analyses, and difficulties in assigning the correct boundary conditions for the area intended to be studied. Therefore, the only Iraqi groundwater studies were conducted by Al-Salim and Khattab (2004), Al-Sadiq and Akulaims (2005), Al-Samma'a et al. (2008), and Al-Muqdadi and Merkel (2011). Bashiqa and Al-Hamdaniya regions in the northern part of Iraq and Umm Er Radhuma and Dammam formations in the Iraqi Western Sahara were the undertaken areas being studied. Some of those researchers have used MODFLOW and the others have used GMS to investigate the groundwater aquifers behaviours in terms of its availability in those areas and the ability to use this source. The weakness in these studies is that those studies were not taken into account the parameters that affect the quantity or quality of this source like contaminants, recharges, discharges, the impact of pumping wells-field, and the future prediction of this source.

One of the most important processes for any groundwater model is the calibration process where it needs to make a comparison between the simulated heads or fluxes with the field measurements during the adjustment of the aquifer's parameters. Typically, groundwater models are calibrated either to steady-state conditions only or transient conditions only or for a steady state followed by a transient calibration (Anderson and Woessner 1992). When the calibration has conducted using trial-and-error calibration, the calibration process is considered to be completed when the residuals errors values between the simulated and calibrated values can subjectively judge it as "acceptable" (Philip 1980).

All of the above reviewed studies were calibrating the groundwater models either using the transient calibration only or using the steady state one when there are no pumping conditions applied over the studied area (this type of calibration called "Static Calibration"). When there

are pumping conditions applied on the study site, the calibration will be called "Dynamic Calibration". The name of Static or Dynamic comes from the behaviour of groundwater heads over the whole study area which is affected by the groundwater parameters such as recharge, pumping rates variation, evapotranspiration quantities, and others. The Static and Dynamic heads are shown in Figure 2.9, where the observed water table levels inside the pumping wells when the pumping wells are out of work or operation represent the "Static Heads" and when the pumping wells are in operation, the heads will be "Dynamic".
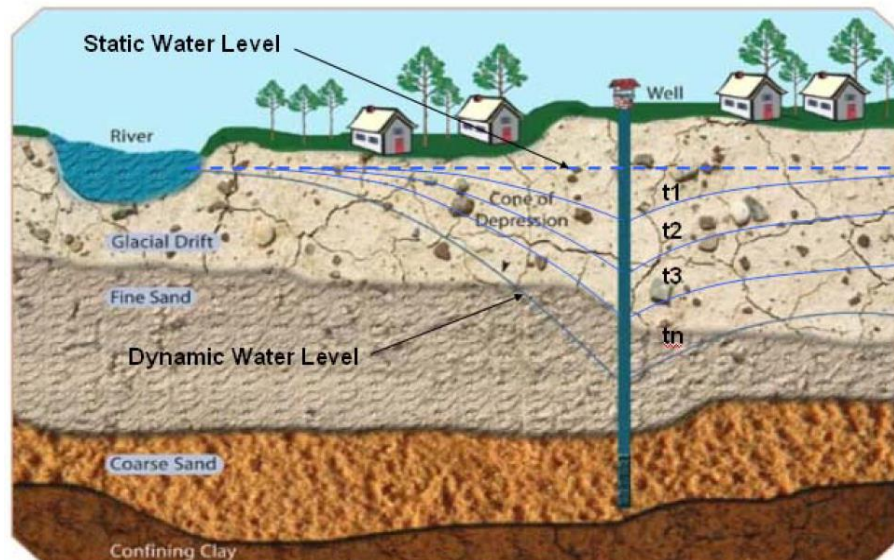
Figure 2.3: A cone of groundwater table depression generating by the effect of pumping schedule (Adopted from Fletcher 1995)

In fact, often due to the unavailability of groundwater heads observations over intermittent intervals of a study site, the transient flow calibration is difficult to carry out and only the steady state calibration (Static Calibration) has been used. The steady state calibration when the pumping schedule is under operation (Dynamic Calibration) has not applied yet in the research. Where, the steady state "Static" calibration without pumping schedule applied will remain untrusted for the following reasons:

1. Static heads are measured before running the pumping wells, but in the reality, this measure is done during the operation of the neighbouring wells so that this will give an inaccurate level of the measured heads.

2. Measuring the dynamic heads is always done after running the pumping well and reaching the steady state condition where at this point, the level of water inside the pumping well (dynamic head) is measured. Therefore, dynamic heads are more reasonable to deal with in the calibration process.

3. Dynamic heads are measured during the operation of all the neighbouring wells in the study area or at least most of the wells in the vicinity around the pumping well intended

to be measured where this will enhance the confidence of the Dynamic calibration greater than the Static calibration.

2.5 Groundwater-surface water interaction

Traditionally, water resources management has usually focused on either groundwater or surface water as separate entities. However, due to the development of both land and water resources, it is apparent that there is an effect on the quantity and quality of the groundwater and surface water due to the interaction between them where this connection affects each other. All surface water resources like lakes, wetlands, streams, reservoirs, rivers, and estuaries are interacting with groundwater resources. The interaction between the surface water and groundwater leads to exchanging water and solutes between them. Therefore, it needs a clear understanding of this connection to get an effective land and water management (Winter et al. 1998). In Iraq, studies which are belonging to the relationship between groundwater and surface water are have not considered yet, especially those studies dealing with the direct or indirect relationship between the river and groundwater. Some of the previous world studies which have been studied the relation of groundwater-surface water will be presented.

In 2002, a two-dimensional theoretical groundwater model of unconnected alluvial aquifer was modelled by Yassin and Michael (2002) to assess the quantity of seepage from a stream or a river through the streambed (Clogging Layer) into a subsurface aquifer. This assessment was carried out by modifying the saturated MODFLOW Code with a saturated/unsaturated code called "MOBFLOW". Results of both Codes MOBFLOW and MODFLOW were compared with a variably saturated model, SWMS_2D to evaluate the widely used groundwater–river interactions MODFLOW models.

Stream or River package in MODFLOW (McDonald and Harbaugh 1996) is considered to be connected with the underlying aquifer by a model cell. In addition, the seepage between the channel and the aquifer is assumed to be proportional to the difference between the river's heads and aquifer's water tables, if the groundwater table level was connected to the river water level. But, once the groundwater table of an aquifer drops below the riverbed level, the assumed exchange between the river and the aquifer which was dependence on the difference between them, it will become proportional of the river water level alone when the system becomes disconnected. Therefore, in the disconnected (either shallow or deep groundwater table) system, the seepage from the river toward the aquifer will become constant.

Bouwer (1969), Rovey (1975), and Dillon and Liggett (1983) developed new equations/models to address the exchange quantity when the system is disconnected. All the three models were not capable to estimate the variable seepage for the shallow water table where with the third model, there was an ignoring for some aquifer properties which led to overestimating the exchange values. In MOBFLOW model which was improved by Yassin and Michael (2002), an equation was used to overcome the disconnection problem. The newly suggested MOBFLOW code and the original MODFLOW code were compared with the SWMS_2D code. The results showed that the quantity of seepage for the disconnected river-aquifer system of MOBFLOW and SWMS_2D were very close to each other, whilst with the MODFLOW code, the seepage was 67.5% underestimated than those values for the other two codes where this is because MODFLOW cannot dressed of the unsaturated situation.

The arguments of the research done by Yassin and Michael (2002) are:

- The Yassin and Michael (2002) study have treated the disconnected river-aquifer system which already does not address in MODFLOW as the Schlumberger Water Services Company (who innovative this software) has stated that the program is dedicated to the study of saturated conditions.

- It was a two dimensional study and for a theoretical case study, not for a real case study as the field has many climatic, geological and hydrographic changes that may change many of the physical properties of the model instantly or simultaneously and therefore the results may be true but do not reflect the real field's situation.

- It can conclude from this study the accuracy of the MODFLOW program in cases where there is a connection between the river and groundwater and this promotes the widespread use of this code in solving the problems of groundwater models.

Philip et al. (2010) studied the accuracy of MODFLOW software for simulating the groundwater-surface water interaction for a connected/disconnected losing river and compared that accuracy with the HydroGeoSphere program results. HydroGeoSphere is a program that can simulate the saturated and unsaturated groundwater-surface water flows. The study focused on four MODFLOW aspects to be under accuracy evaluation, which were:

- MODFLOW inability to simulate the negative pressures underneath the riverbed when the groundwater table become disconnected with the river;

- As stated by Schlumberger Water Services Company, MODFLOW can simulate the river-groundwater interaction with either fully connected river or fully disconnected river, this point was under evaluation where as Philip et al. (2010) stated that in the reality the situation is transitional;

- The mismatch between the river's and cell's widths during the model horizontal discretization which will result in a groundwater table position error under the river; and
- Due to the coarse vertical discretization to avoid drying cells out, the simulation will have an error in the height of groundwater table.

To evaluate these four aspects, a small scale model was built by Philip et al. (2010) with a homogeneous layer 120m depth, 250m width, 10m thickness and a river of 10m length, 10m width, and 0.5m depth in both of MODFLOW and HydroGeoSphere programs. The river was assigned for single straight cells' line. The vertical layer was divided into 12 sub-layers with 10m thickness each. Comparison of the MODFLOW results with those of HydroGeoSphere showed that:

- When the groundwater table level was underneath the riverbed, the infiltration flux was an underestimation and the under-river layer was unsaturated.
- If the river remains connected, but losing water into the subsurface aquifer, the difference in the infiltration flux was not affected too much by the groundwater table level change because the pressure head in both of MODFLOW and HydroGeoSphere programs were close to each other in their values. Therefore, the underestimation of infiltration flux was affected by the disconnected situation only.
- When the river's width was greater than the cell's width, the groundwater table level was overestimated and vice versa, this was indicated for the connected system. For the unconnected system, the horizontal discretization was affected the groundwater head.
- If a vertical discretization was applied to the model, dry cells were found as this has affected the model's consequence during the simulation process.

The argument for Philip et al.'s (2010) study, for each point is illustrated below:

- It is already noticed and mentioned by Schlumberger Water Services Company (who innovative this software) that this software is applied for the saturated flows with a high accuracy so the researcher should collect the right code for the site under study to be the results more trusty.
- It needs to check the situation of the groundwater-river interaction through all the simulating processes to be ensured that the connection between the two systems still exists and there is no mismatch in the river seepage or aquifer discharge.
- In MODFLOW, there is a high capability to manipulate by the cells' sizes to be corresponding exactly to the river's width through the refining cells process where this will raise the accuracy and efficiency of the groundwater-surface water interaction simulations.

- There is no need for the vertical discretization in simulating the real case studies as this will mislead the simulation process to give results do not correspond to the real situation in the real field.

Therefore, all the above statements mentioned by Philip et al. (2010) are, either it can deal with them within the MODFLOW program and overcome them directly, or may not need them to be existed originally within the groundwater model prepared for the considered study site.

Globally there are many studies dealt with the relationship between the groundwater and surface water resources to be under the microscope for the purpose of studying and investigating the factors that affect each other.

To quantify the relationship between the groundwater and surface water in the habitat restoration along riparian, a groundwater model was built by Tain-Shing et al. (2001) using MODFLOW and applied along the San Joaquin River from the Merced River to the Friant Dam, Nevada, USA. Calibration was done using the available data. The model was used to demonstrate the sensitivity of the groundwater elevations to the river seepage rates and regional boundary conditions. Results illustrated the nature dynamic and transient interactions between the groundwater and surface water.

An overview of different methods for estimating the exchange fluxes in the transition zone between the surface water and groundwater was involved by Kalbus et al. (2006) to choose the appropriate one. Results concluded that when combining different measuring methods together, this will considerably complex the estimated fluxes values between the groundwater and surface water.

A three-dimensional groundwater flow model with eight aquifers was established by Li-Tang et al. (2007) for simulating the regional groundwater-surface water flow connection among the springs, rivers, and groundwater in the Heihe river basin in China. The model was calibrated with the investigated base flow as well as the historical groundwater level and gives a good reasonable correspondence. The modelling results reported that there were a coupling and decoupling between the groundwater and surface water represented by the Heihe River in some reaches. In addition, the study results were suggested to reduce the groundwater schedule pumping to maintain and sustain the development of the groundwater in the study area.

Tomohiro et al. (2007) used the isotope data to study the interaction between the groundwater and surface water in the Heihe River basin, North-Western of China, particularly in the lower desert reaches during the irrigation and non-irrigation periods. Results reported that in the non-irrigation period the river water will feed the groundwater in both the desert riparian fringe area and the riparian forest region. While in the irrigation period, the lower desert reaches of the river was usually dried up. In addition, in the riparian forest region, the groundwater level has to rise rapidly after the short-term releases water from the middle reaches but it will return to decline after the short-term releases finished. Therefore, the short-term releases discharged water will not contribute in recharging the groundwater in the desert-riparian fringe region during the irrigation period.

Safavi and Bahreini (2009) developed a groundwater model to examine the interactions between the groundwater and surface water in Najafabad semiarid plain region in Iran through the steady-state and transient conditions by using MODFLOW-2000. The results of the study showed that water budget was completely depending upon the seepage from Zayandehrood River and return flows from irrigated lands components, while boundary conditions were playing as a minor component in the total balance mass.

Allison et al. (2010) developed a link between MODFLOW and RiverWare to provide a model which can be used to incorporate the critical features through modelling the low flow of river periods in the semi-arid riparian environments in the south-western of United States. The critical features were such as the local variations in seepage rates, riparian evapotranspiration, distributed water based on the rule of allocations to users and/or environmental flows and irrigation flows. The performance of this link was applied on the Rio Grande in the vicinity of Albuquerque, New Mexico and illustrated that the excessive reliance of human water use gave an adverse impact through endangering the Rio Grande silvery minnow. In addition, the linked model prediction showed that the flows in the Rio Grande Basin were reasonably accurate except when the flow was very low during few periods.

Alphonce and Thomas (2010) developed a coupled model through integrating MODFLOW and TOPNET with these models which are integrating through the exchange of base-flow and recharge and river-aquifer connections and applied this model in the Big Darby Watershed in Ohio, USA. Generally, the coupled model gave good agreement results for calibration and validation processes between the measured stream-flow and water table depths, and the simulated results. Therefore, the good matching between the measured and simulated values

illustrated that the coupled model was adequate and can simulate the study area as well as capturing the effect of temporal and spatial variation in the recharge parameter.

To gain an insight into the potential climate changes in the Western United States, an integrated groundwater-surface water model were used by Justin and Richard (2012) through using 12 circulation model projections for rainfall and temperature from 2010-2100. This model was to evaluate the interaction between the hydrologic variables such as storage, groundwater recharge, streamflow, evapotranspiration, groundwater discharge, and snowmelt timing. The changing in rainfalls and temperatures over the period 2010-2100 resulted in more than 30% reduction in streamflow through the summertime and this highlighted the impacts of the climate changes on the groundwater resources.

An investigation for the spatial and temporal variations in water chemistry which were affected by humans has been done by Yang et al. (2012) to characterise the relationships between the surface water resources such as rivers, lakes, and reservoirs and the groundwater source near the river in a shallow aquifer in Jialu River, a branch of Huaihe River in China. Results showed that the excessive domestic use has affected the groundwater source chemically in the north of Zhengzhou City and Fugou County. In addition, approximately 60-70% of river water was composed of the groundwater in the close vicinity.

A developed interface tool has integrated with the MODFLOW software to determine the nature and extent of the groundwater-surface water connection to finally manage the water supply was carried out by Ruopu et al. (2016). This tool can be applied in other areas when the settings were similar and need for a water management. Applying of this tool on the State of Nebraska, USA gave utility and robustness for the results. Therefore, with some appropriate adjustments and precautions, this program can be used for managing and planning the water resources in terms of studying the connection between the groundwater and surface water.

Despite the existence of the Tigris and Euphrates rivers, and many groundwater aquifers in Iraq particularly in Al-Najaf province, studies that deal the relationship between groundwater sources and surface water (rivers or lakes) are missing and unavailable. Even at the level of the Arab, studying the river's relationship with groundwater is rare.

Most the previous studies were either focused on the effect of climate changes (weather), or geological and hydrological characteristics of either system, or studied of the effect of contaminants on each of them due to the connection exists between them, or studied the

chemical elements in groundwater and their effect on surface water. While none of those studies have studied the effect of pumping schedule on the interaction between these two systems. It is also not clear that those studies were conducted in the residential or non- residential areas.

2.6 Hydraulic conductivity

Generally, in the environmental and water regimes protection, hydraulic conductivity represents the key role that affecting these regimes. In addition, it is necessary to know how can determine (approximate) the hydraulic conductivity value (K) to explain, analyse, and describe the surface and subsurface flows in various regions such as urban, rural, and even landscape areas. Many methods have been used to estimate K, some of laboratory methods and some others are field methods (Jakub 2014). Where, K-value has the ability to change from place to place horizontally and vertically due to the internal or external impacts (Oosterbaan and Nijland 1994).

Generally, two types of groundwater water flow models are available right now, the forward and inverse models. The basic stand of the forward model is for the solution of the hydraulic head of an aquifer at any time and any point of the aquifer. When the aquifer parameters like storativity, transmissivity, hydraulic conductivity, stresses on the aquifer, and the initial and boundary conditions are known, the forward solution will be easily obtained. But, in reality, the entire aquifer parameters are rarely found complete or represent the whole area of interest, as in most cases those parameters are found to be as scattered measurements in the study area. Therefore, in order to develop a reliable groundwater flow model that can be used to predict the behaviour of an aquifer, the aquifer criteria or parameters should be interpolated (Sefelnasr 2007). Typically, inverse model is standing to solve the groundwater aquifer parameters through using the head observations as a dependent variable in the governing equation of flow (Laplace equation), where usually the field-measured values of fluxes and heads are having a higher degree of confidence (Anderson et al. 2015).

Inverse models or problems are usually solved by history matching. History matching is a term originated from the petroleum industry field and refers to the matching process between the outputs of a model and the historical time series of measured values (field measurements) after adjusting the model inputs in both of steady-state and transient simulations (Anderson et al. 2015). The procedure that is used to estimate the aquifer parameters is called the calibration. Model calibration is the process of adjusting one or more aquifer's parameters to reach the best matching between the simulated results and the measured data (Sefelnasr 2007). The goal of history matching is to produce a satisfactory match to the field measurements (observations) by

identifying a set of parameters that promote the satisfactory matching. These parameters are adjusted within reasonable ranges in successive forward runs of the model until that model can produce an acceptable match. The term historical matching includes (Anderson et al. 2015):

1. Identify the calibration targets from a set of field observations (which parameter needs to calibrate with the observations that available);
2. Run the model after estimating the input parameters by the best way (hydrologic and material property parameters);
3. Compare model outputs with the field observations;
4. Adjust the input parameter values to obtain a better fit of the outputs to observations; and
5. Select the model with the best possible fit that corresponds the field limitations and resources.

When the correspondence between the observed and calculated heads or fluxes resulted from a groundwater model does not reach the sufficient accuracy, a little confidence of the calibrated model will be generated which will affect the future forecasting; therefore, history matching is very important for the model's fit evaluation. There are two phases for history matching to solve the inverse model, the first is the manual trial-and-error approach, and the second is the automated trial-and-error approach which is performed using software (Anderson et al. 2015).

2.6.1 Manual trial-and-error approach

The base of this approach starts with selecting an initial value of the unknown parameters; then, the forward model will run, and the model outputs represented by the calculated hydraulic heads will be compared to the field-measured heads. This approach depends upon repeating the running process multiple-times where the modeller will manually change some parameters' values and then evaluate the outputs after each parameter's adjustment until a satisfactory matching is obtained (Sefelnasr 2007). The manual adjustment method has some advantages such as improving the modeller experience on how changes of the number, magnitude, and location of the adjusted parameters influence the matching fit of the simulated and observed values, providing a wide insight on how the groundwater simulation and groundwater aquifer behave, and enable the modeller to identify the sensitive and insensitive parameters that influence the model outputs effectively or less effective. Although the manual approach helps largely in developing the modeller's hydro-sense, but it remains imperfect process because sometimes the parameters that affect the model are large and thus it is impossible to track each one in the calibration process (Anderson et al. 2015). The deficiencies and inherent subjectivity

of this approach are: it is expensive because it needs strenuous work, it is disappointing because it remains all the time needs for an improvement, and it is subjective because its results will be biased and this makes it difficult to evaluate the project under study (Carrera and Neuman 1986).

In addition, manual trial-and-error approach even with a rigorous procedure of manual parameters changes may still having some untested sets of parameters that might give a better model, where the lack of guarantee to present the best fit of a model, especially groundwater models that are used in the regulatory and legal areas, is undesirable (Bair and Metheny 2011). Therefore, automated trial-and-error rigorous mathematical methodologies are developed.

2.6.2 Automated trial-and-error approach

The automated trial-and-error approach includes two types of methods which can estimate the parameters of groundwater flow in the inverse models (problems): the direct and indirect methods.

A. The direct method

Stallman (1956a, b) has suggested a direct solution to the inverse problem of the groundwater flow modelling. This method assumes that the model's groundwater hydraulic head is known in space and time over the model's domain, but in fact, field-measured head sometimes requires interpolation. In this case, the partial differential equation of the groundwater flow will be written with the hydraulic conductivity as a dependent variable. Solving this equation will specify hydraulic conductivity. Due to the heads' interpolation even with small values, solving the partial differential equation will lead to large errors in the hydraulic conductivity of the inverse model. Therefore, although the direct method is attractive due to mathematical elegance and computational efficiency, but it found to be unstable to the most realistic problems (Anderson et al. 2015).

B. The indirect method

The indirect method is essentially automating the manual trial-and-error method where the hydraulic properties of a groundwater model will be estimated by using computer algorithms and statistical regression. This method has been advocated by many researchers, Yeh and Tauxe (1971), Cooley and Sinclair (1976), and Cooley (1979) to solve groundwater parameters and now it's called "PEST" "Parameter Estimation Method". The inverse code of this method has been developed by Cooley (1979) and Cooley and Naff (1990) and then extended to MODINV

(Doherty 1990), MODFLOWP (Hill 1992), and UCODE (Poeter et al. 2005). PEST (*Parameter EST*imation) that recently developed by Doherty (2014a, b) has replaced MODINV in 1994 to become currently widely used in the applications of groundwater modellings. The mechanism of this method depends upon using an algorithm of (Yeh 1986) that involves and accomplishes this loop of orders: find or guess an initial value of a specific parameter, compare the calculated outputs of the forward model to the observed field data, and repeat the last step until the value of the considered parameter (the considered objective function) will reach the minimal difference as compared to the observed data (Sefelnasr 2007). This method is considered to be a valuable and essential tool for groundwater modelling where it can estimate the groundwater parameters for complex models through the calibration process. Nowadays, automated methods are still evolving and finding better ways to solve the partial differential equation in the inverse models or problems and become active methods in the research area (Zhou et al. 2014).

Groundwater aquifers are classified into two categories, simple or complex, based on the aquifer thickness and the spatial variation of the hydraulic conductivity. If these two parameters are not varied over the study site, the study site will consider having simple aquifer conditions; otherwise, aquifer conditions will be complex. The most important target of any groundwater flow model is the hydraulic head behaviour's prediction over a groundwater aquifer, where the spatial and temporal variation of the aquifer boundary conditions, aquifer parameters, and stresses will have the greatest impact on the response of any groundwater aquifer (Sefelnasr 2007).

Various hydro-stratigraphic units of an aquifer can be identified and distinguished from the pumping tests calculations through calculating hydraulic conductivities and storativities. It is impossible in the real world to obtain comprehensive values of data at every desired point due to partial constraints (Sefelnasr 2007). In Iraq, particularly in Al-Najaf region (the study site), due to the difficult circumstances that the country has suffered from for at least a half-century, there was a scarcity of the data sets collected from various sources.

To account this scarcity and discontinuity of the data needed, and to establish an accurate 3D groundwater model for the area under study. A novel third approach called "Distributed Value Property Zones Approach" rather than the manual and automated trial-and-error approaches is available in Visual MODFLOW, is applied to Al-Najaf region groundwater model to reach for the best representation of the real field where although this novel approach is easy to access and apply through using Visual MODFLOW, but there is no one has applied it. Therefore, a great effort is given to apply this novelty through the spatially interpolating the hydraulic conductivity

in order to approximate the aquifer hydraulic conductivity to help in producing the best matching of the simulated and observed data. The methodology and application of this process are available in detail in section 5.7. Where, the "Optimal Prediction" method that refers to the synonymous of the word "Kriging" (Kriging method) is applied to predict the best underneath groundwater aquifer that gives the best matching for a high extent with the real field. This method uses the appropriate Variogram to analyse the spatial variation parameters and the roughness and continuity of various surfaces (Barnes 1991; Zimmerman 1991). It reduces the error of the expected values estimated by the spatial distribution. Therefore, accurate aquifer parameters will result in more efficient groundwater models.

2.7 Interface soil layer

A good conceptualisation of a groundwater model is the most important step that is needed to represent the real-modelled field that in turn will result in good predictions (Spiliotopoulos and Andrews 2006). As a result of accurate modelling and models of groundwater, decision-makers will be able to manage groundwater resource, assess the impacts on aquifers, issue the appropriate plan to negotiate local and regional groundwater supply, evaluate dewatering due to ecological systems, design and control pumping schedules needed, assess drought impact during dry seasons, predict the effects of climate changes and issue the scenarios to control those effects in advance, and many more advantages will be available under consideration for decision-makers through these developed groundwater models (Jeff et al. 2017).

In most populated areas of the world, groundwater collected in the geological formations constitutes an important component of water supply for agriculture, industry, and domestic use. Withdrawal waters from pumps are supplied by those geological environments capable for yielding large amounts of water where these geological formations are existing underneath the ground surface and called aquifers. An aquifer is defined as that geological environment, saturated and permeable enough to provide an economic quantity of water for extraction process as it is commonly composed of unconsolidated sand or gravels and sometimes from permeable limestone and sandstone which represents rocky sediments (Kruseman et al. 2000). These aquifers may be confined or unconfined, depending upon the geological and lithological characteristics of the subsurface layers. There may also be more than one aquifer carrying water as this will be called by layered aquifer systems or multi-layered aquifer systems (Hemker 1999). Layered aquifer system consists of either two or more aquifers separated by aquitards or aquicludes as shown in Figure 2.4. Typically, aquitard geological unit has limited ability to transmit water vertically as this makes aquitard's water production is not sufficient to meet pumping wells demand, where as it consists of loams or clays, sometimes aquitard can be

considered as an impermeable layer. Aquiclude is classified as a completely impermeable geological unit, consists of unfractured dense metamorphic or igneous layers (Kruseman et al. 2000).
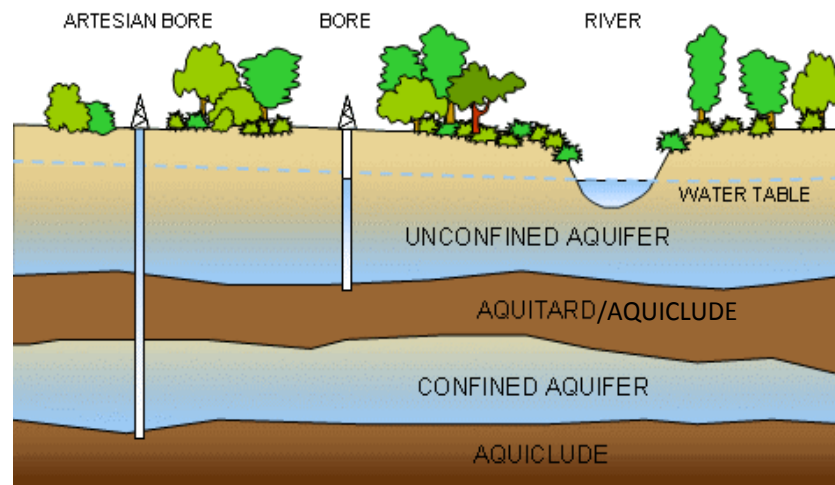
Figure 2. 4: Impermeable layers (AQUITARD/AQUICLIDE) along an aquifer which zero vertical flows occurs (Adopted from Kruseman et al. 2000)

Whilst, sometimes, layered aquifer system consists of two or more aquifers or layers, each has its own geological and hydrogeological characteristics and is separated by interfaces which allow for crossflow as shown in Figure 2.5. The interface between layers is considered as an open boundary for transmitting water and stresses applied on the aquifer (Kruseman et al. 2000).

(a)   (b)
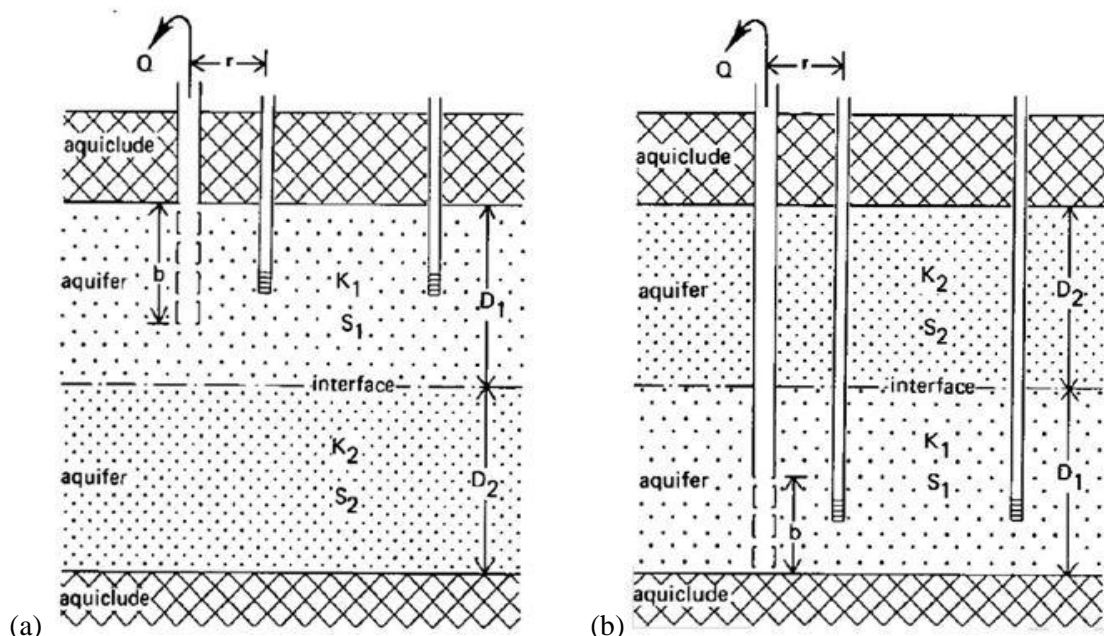
Figure 2. 5: A confined layered aquifer system showing the partially penetrating well, either in the upper layer (a) or in the lower layer (b) (Adopted from Kruseman et al. 2000)

Most studies are either dealing with a layered aquifer system that having either aquitards or aquicludes (Blegen 2005; Wa'il and Randa 2007; Abdulla and Al-Assa'd 2006; Al-Muqdadi

2012), or dealing with a single aquifer single soil layer (confined/unconfined) (Al-Salim and Khattab 2004; Al-Siba′ai 2005; Shuwei et al. 2015), while sometimes it may have single aquifer with layered soils separated by interfaces.

In Figure 2.5, it can be seen that there are two layers of soil separated by an interface soil layer, each of which has its own hydraulic conductivity, transmissivity, and storativity coefficients. Because the interface soil layer allows the water to move vertically, which layer will provide the water to the pump is not of considerable importance. The sequence of the layers in Figure 2.5a and b will not affect the pumping well because both of these layers will contribute by providing the required amount of pumping water. Thus, it is clear that both layers act as a single groundwater aquifer, even though these two layers are separated by the presence of the interface soil layer. This means that the interface soil layer must be represented in the mathematical model for the region under study to be the model conceptualises the real field (Kruseman et al. 2000).

The numerical representation of the interface soil layers in the groundwater models will certainly affect the uncertainty tests that are applied to the groundwater models to reach to the accepted model. Therefore, it is necessary to represent those interface soil layers mathematically/numerically, especially if that interface exists in the area. The reaction of the layered groundwater aquifer systems separated by an interface soil layer to the pumping process will be similar to those of the single-layer groundwater systems. Where, the hydraulic conductivity of the stratified groundwater systems separated by an interface soil layer depends on the equivalent value of the hydraulic conductivities of the entire system. If the layered groundwater aquifer system was confined, as shown in Figure 2.5a and b, then the equivalent value of the hydraulic conductivity for the whole system will be calculated using the analytical method that was develped by Javandel and Witherspoon (1983). Otherwise, if the entire domain of the groundwater system was unconfined; then, the equivalent hydraulic conductivity of the system will be calculated according to Darcy Law/Method (Kruseman et al. 2000). The full description of Javandel and Witherspoon (1983) with the boundary conditions and limitations to be able to apply for a layered aquifer system is presented in detail in Kruseman et al. (2000).

The study area in this research is Al-Najaf region of Iraq, which has two soil layers with various geological and lithological characteristics for each layer. These two layers comprise the groundwater aquifer in this region (Dibdibba aquifer). These two soil layers are separated by an interface soil layer, which does not prevent the groundwater from the vertically movement between these two soils. Therefore, the impact of existing of an interface soil layer separating

the single unconfined Dibdibba-aquifer into two soil layers on Dibdibba aquifer behaviour is studied for the first time in this work. It will also explore the effect of the interface soil layer on the model's results and calibration if it does not conceptualise in the constructed model for Al-Najaf region. The calibration will compare the results of the models with and without an interface soil layer. All of the geological, lithological, hydrological, and boundary conditions related with Al-Najaf region study area will be explained in detail in Chapter Four.

2.8 Summary

Mnay studies in different regions around the world have dealt with the problem of groundwater and groundwater-surface water, chemically, physically, and hydraulically. But, the particular groundwater-river interaction has been dealt with in a few manner because this overlap needs to build complex groundwater models and complex analyzes in which accurate results can be obtained for this interaction process. This interaction will be under investigation for Al-Najaf region. Calibration of groundwater models is commonly classified into two well-known methods, the steady-state and transient calibrations. The steady state-dynamic calibration is used in this study and gave acceptable correspondence between the calculated and observed collected data with the assistance of applying the new approach "Distributed Value Property Zones" which is used to improve Al-Najaf region model through conceptualising the entire hydraulic conductivity of the study area to be very close to the real entire domain in the field. The impact of the interface soil layer which is located between the two layers of Dibdibba aquifer on the conceptualisation process and model results is studied to assess whether or not its conceptualisation will affect the behaviour and results of the groundwater model. In addition, the study area is completely new and it is under study for the assessment and investigation purposes for the first time.

Chapter Three
Methodology

3.1 Introduction

According to the increase of the awareness and understanding of the interaction between the surface water and groundwater, mathematical and conceptual models' ability must be increased to efficiently and accurately reproduce the complex and difficult exchanges between these two types of water resources. The complexity in simulating the interaction difficulty is caused due to the temporal variations in surface water and groundwater diffusion phenomena (Constantz 2008; Bunner et al. 2009). The spatial range between groundwater (GW), surface water (SW) features and the mechanism interaction of the mathematical models' representation is an attempt to close the interactions scale of SW/GW from approximately simple analytical methods to complex and difficult numerical solutions (Konrad 2006; Rushton 2007).

Good management of groundwater aquifers requires the ability to predict the groundwater system movement and salt situation of that system as well as predict the changes which are implemented on the groundwater system by the nature and human activities (Al-Siba'ai 2005).

3.2 Flow simulation

The general equation of flow (Laplace equation) is developed on the assumption of the flow in the porous medium is transient. But when the storage term of the aquifer system becomes zero, the flow will change to steady state. The difference between these two types of flow, the steady-state and transient flows, is the time. In the steady state system, water particle enters the flow domain from the inflow boundary will continue flow straightforward to the outflow boundary in a direction parallel to the pathlines, which are coinciding with the flowlines without paying any attention for the time as shown in Figure 3.1a. Whilst, in a transient flow system, the flowlines and pathlines do not coincide with each other as shown in Figure 3.1b. Where, the flowlines are changing over time; thus, these flowlines will represent the direction movements of the water particle at a specific instant in time and cannot in themselves estimate the complete path water particle. Consequently, groundwater hydrologists should understand the flow simulation techniques to analyze both the steady-state and transient flows accurately by using the appropriate mathematical equations (Freeze and Cherry 1979). A description of the flow simulation techniques is illustrated.
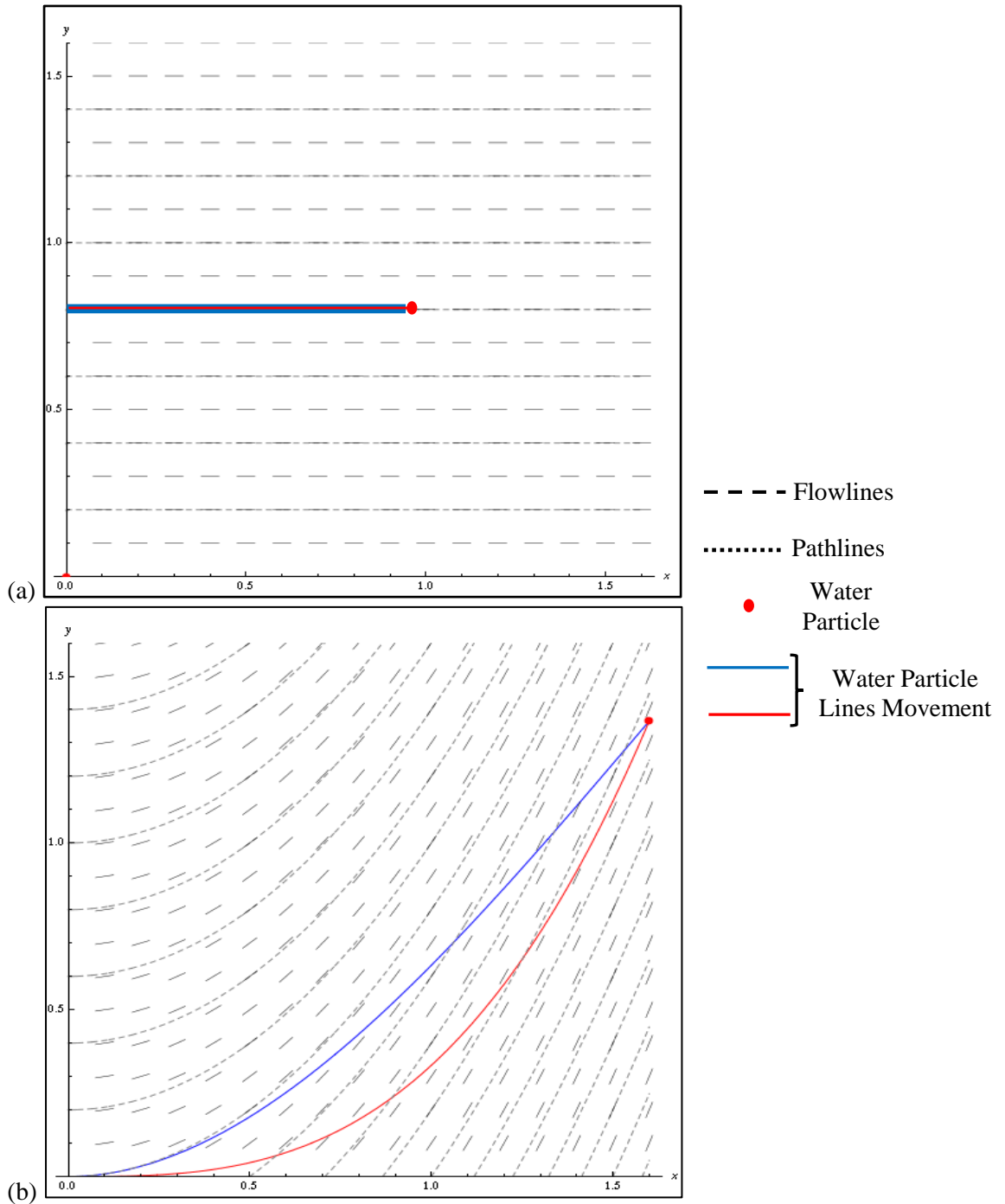
Figure 3. 1: Water particle movement in: a) Steady state flow, and b) Transient flow (Adopted from Faber 2001)

3.2.1 Steady-state simulation

In the steady state flow model, the variation of head with time in Laplace flow governing equation will be equal to zero which will result in constant computed heads and fluxes with time interval. Often many modelling objectives are addressed through the steady-state solution alone, such as analysis of various groundwater flow patterns, estimate leakage losses from surface water bodies, calculate the water table gradients for regional problems, simulate flow directions

pattern affected by the long-term pumping schedule, and forecast the time-averaged stress effects such as drought or projected long-term extractions. In addition, the initial conditions of transient modelling in transient flow models use the solution resulted from the steady-state modelling. In any graphical user interface software (GUI), the default simulation option used to specify inputs is usually representing the initial steady-state simulation process of a groundwater flow model (Anderson et al. 2015).

3.2.2 Transient simulation

Transient simulation begins by introducing individual stresses such as defining the change in recharge rate or pumping extraction, or by combining both of recharge rate and pumping schedule at the same time to identify the initial conditions represented by specifying the distributed starting heads. The boundary conditions located on the model's circumference are usually affected the steady-state solution, but in case of the transient simulation, the transient solution will be affected by those stresses defined at the beginning of the simulation process when those stresses reach the perimeter boundary. Typically, a flow model will reach for a new steady state condition when new stressed conditions are continued for a sufficient period. Some factors are required to be considered by transient simulation (Anderson et al. 2015):

1. Storage parameter values for all hydrogeologic units as well as to the hydraulic conductivity that should be set in the model.
2. The initial conditions of the model shall be formulated.
3. The hydrologic stresses should not be propagated to reach the perimeter boundary of the model, because this may affect the simulated field conditions.
4. An appropriate discretization of time and space should be done for the model.
5. In the model calibration process, field observations should represent the length of the simulated time period.
6. Longer running time is required for transient simulation than the steady-state one because the transient model must solve the problem at each time step, which requires several iterative trial solutions, as each model needs for multiple time steps to terminate.
7. Head results are only one set in steady-state simulation, while in the transient simulation, each time step has its calculated head results which mean transient model will produce more outputs.

3.3 Governing equations

Groundwater flow is mostly representative by Darcy law wherein the flow rate is proportional of the hydraulic gradient and the hydraulic conductivity which describes the characteristics of the hydraulic media which represents the area where the groundwater flows (Bouwer 1978). Hydraulic conductivity is always changing through the distance according to the changes in geological characteristics (Lent and Kitanidis 1989). It can be expressed this in Eq. (3.1):

$$V = -Ki = -K_C \frac{dh}{dL}$$ (3.1)

where, V is the velocity of groundwater (L/T); K_C is the hydraulic conductivity of the soil (L/T); h is the water table of the groundwater (L); and L is the length of flow of the soil particle through the soil media (L).

The general representation of the conservation of fluid mass equation (Continuity Equation) can be expressed in Eq. (3.2). Eq. (3.2) represents the flow discharge which represented by, Q is the discharge (L^3/T), i is the hydraulic gradient (dh/dL) (dimensionless), and a is the area of flow (L^2).

$$Q = -Kia$$ (3.2)

Negative signs in both equations 3.1 and 3.2 refer to the convention for the relation between the flow direction and head gradient.

Whereas the equations of groundwater movement in general are based on two famous equations which are Darcy equation and energy conservation equation as the integration of these equations will give the public and general partial differential equation (Konikow et al. 2006). Therefore, the 3-D equation of groundwater movement of constant density through porous media can be described in Eq. (3.3):

$$\frac{\partial}{\partial x}\left(K_{xx}\frac{\partial h}{\partial x}\right) + \frac{\partial}{\partial y}\left(K_{yy}\frac{\partial h}{\partial y}\right) + \frac{\partial}{\partial z}\left(K_{zz}\frac{\partial h}{\partial z}\right) \mp W = S_s \frac{\partial h}{\partial t}$$ (3.3)

where, K_{xx}, K_{yy}, and K_{zz} are hydraulic conductivities along x, y, and z coordinates (L/T); h is the potentiometric head (L); W is the volumetric flux per unit volume which representing sinks and/or sources of water. It's value less than (zero) when flow out of the groundwater system, and it will be greater than (zero) when flow is into the system (T^{-1}); S_s is the specific storage of the porous media (L^{-1}); and t is the time (T).

Eq. (3.3) describes the non-equilibrium, heterogeneous and anisotropic groundwater flow conditions that provide the principal axes of the hydraulic conductivity aligned with the

direction of coordinates. Moreover, Eq. (3.3), together with the specification of flow and/or head conditions and initial head conditions will constitute a groundwater flow mathematical representation of an aquifer system (Harbaugh 2005).

Equation 3.3 is complex and cannot be solved analytically through its general boundary conditions despite the presence of some analytical solutions for special cases. To obtain the appropriate solution of groundwater governing flow equations, a set of boundary, initial, and constraint conditions is required to compute groundwater flow. Continuity equation is classified as a non-linear equation which makes the analytical solution of this equation has some complexity; therefore, numerical methods are the most appropriate ones to solve these formulas. Where numerical methods have more flexibility in their processes for the solution of partial equations, but it should firstly prepare for the discretization of the model domain, which represents the most important technique to solve the partial differential equations (Yeh 1981). Mostly the finite element method (FEM) and the finite difference method (FDM) are the most used techniques due to their great clarity. In groundwater field, the FDM is the well-known method where in this method, the partial differential equation is solved through divided the problem into network of cells represented by network of points at the centres of these cells, which called "Nodes "(McDonald and Harbaugh 1988). Generally, each cell in the network system is connected with six neighbouring cells around it with a centred point called "Node" where the head will be calculated. The flow between every two cells will equal to the hydraulic conductivity between them multiplied by the perpendicular area on the direction of flow between these two cells multiplied by the hydraulic gradient, this is according to Darcy's law. The water budget for each cell is given by Eq. (3.4), which depends upon the equation of continuity, and it is represented by the parameter ($\sum Q_i$) "the sum of all flows into and out of the whole cells system", ($\sum q_i$) "the sum of all flows from the external sources or stresses which affecting a single cell such as rivers, drains, recharge, evapotranspiration, and wells", (N) "number of cells neighbouring to the centre cell", and $\left(S_S \dfrac{\partial h}{\partial t} \Delta V \right)$ "the rate of change in storage within the cell for the whole system" (Harbaugh 2005).

$$\sum_{i=1}^{N} Q_i + \sum_{i=1}^{N} q_i = S_S \frac{\partial h}{\partial t} \Delta V \tag{3.4}$$

Eq. (3.4) represents the exact flow from one of the neighbouring cells to the central one as well as the flows from external sources. The numerical solution of Eq. (3.4) according to the finite difference method is explained in detail in MODFLOW manual as well as the discretization of flow domain (Harbaugh 2005). Also, Eq. (3.4) represents the unknown pressure heads at time (t) for one of the six neighbouring cells in the network system surrounding the central one. So, it

is impossible to solve the previous equation individually, but must be resolved in conjunction it with the neighbouring cells associated in the network system and this needs to solve (n) equation simultaneously for each time step interval. The final simultaneous solution will give the values of head at various nodes through specific times.

3.4 The simultaneous solution of linear algebraic equations

The linear algebraic equations solution is mostly done by using the iteration methods whereas the iterations are used at each time interval of the mathematical model run. Firstly, assume the initial values of heads in each cell at the beginning of the model run and after running the model will get other values which are closer to the actual solution for these equations. These values will be taken as a new basis for the initial values of heads for the next model run, and repeat the solution until becomes the difference between the values entered and the resulting values is very small and within the acceptable limit, thus these values of heads will give the closest solution of the linear algebraic equations.

The developer has been adopted the Visual MODFLOW program developed by U.S. Geological Survey (McDonald and Harbaugh 1988) to resolve the main equations governing the movement of groundwater flow because this software has a high reliability and flexibility to build and analyze the mathematical and conceptual models to meet the studied case.

The development of a conceptual model represents one the most important processes or steps used in the modelling of groundwater flow. The conceptual model which describes, explains, expects and controls on the hydrogeological conditions is composed of two determinants which are physical and chemical (Toth 1970). Through these determinants, it can be developed the conceptual model by building a simplified representation to the required study area and then defines the location and movement of groundwater in the study area, lithology of area of study, and identify the properties and boundaries of the aqueous formations within the study area so that it can apply the numerical model correctly and accurately to find the results.

3.5 Conceptual Model

To construct a conceptual model, it requires identifying a set of assumptions that can describe the composition of the system, the relevant flow domain properties, and the mechanism of flow process. Therefore, an extensive exploration to investigate the natural behaviour of the system and the right collection and interpretation of field data are fundamentally crucial to understand the system's behaviour and help to prepare the correct definition and representation of the flow

problems. The objective of problem management, level of accuracy, type of the investigated problem (either flow or contaminant), and the use of the model whether for exploration the system only or for future forecasting, are the most important features used to identify the appropriate conceptual model selection and its simplification. A schematic pattern for the construction of a conceptual model is illustrated in Figure 3.2. This schematic shows the common essential requirements needed to start building a conceptual model such as model domain geometry, flow characteristics, fluid properties, sources and sinks, processes of simulation, geological and hydrogeological data required, and initial and boundary conditions (Loudyi 2005).

Large models which simulate large areas need more details and crucial objectives, which mean more cost needed with more complex/accurate codes and larger capacity of computers. However, a simple conceptual model for reasonable areas that can facilitate modeller efforts should be considered, but not too simple to that extent leads to exclude some important features which dominate the groundwater problem being investigated. In conclusion, the conceptual model will be good when it constructs to meet the exact objective need, as possible as low cost, and use the adequate available data to develop and calibrate the model professionally with an acceptable manner. Ultimately, the final constructed conceptual model would not be definitive as it can always be adjusted with any updates resulting from the calibration process (Loudyi 2005).
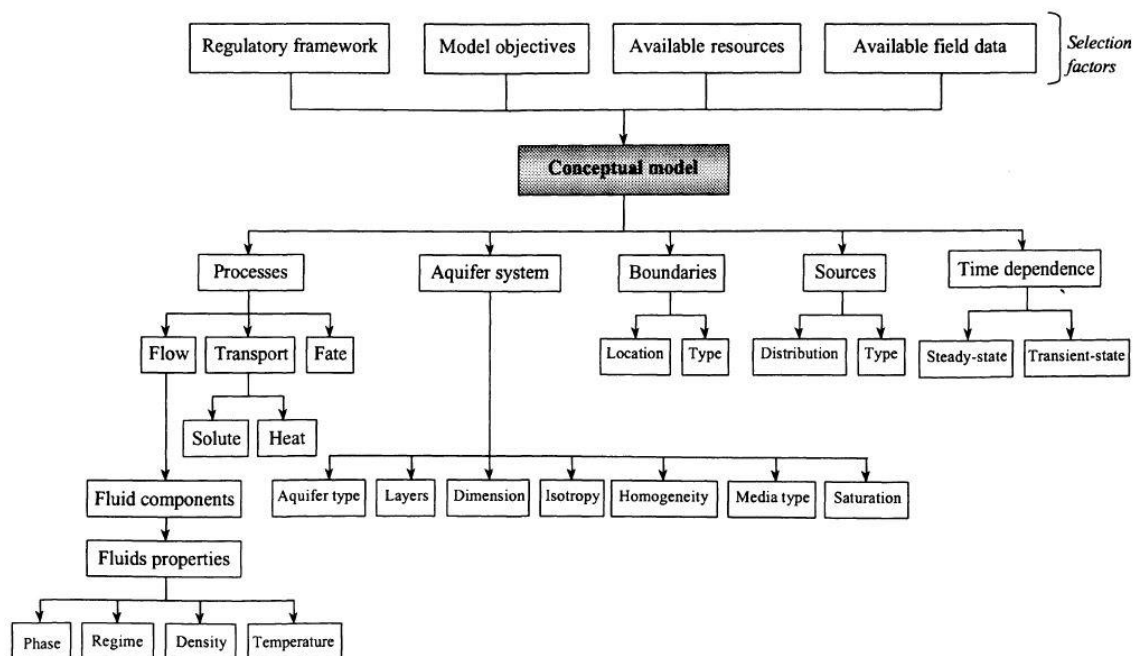
Figure 3.2: Schematic pattern used to build a conceptual groundwater model (Adopted from Loudyi 2005)

3.6 Boundary conditions

Groundwater model boundaries are generally represented by the underground or over ground domains or points at which the head (dependent variable) or the derivation of the head (flux) is known, where these boundaries could be outer and/or inner. According to Franke et al. (1987), it is completely critical to select the right or appropriate boundary conditions through the model's construction process. The presence of large surface water or impermeable rocky bodies will form the physical boundary of groundwater flow systems. In respect of the hydraulic boundaries of groundwater flow systems, the groundwater or surface water divides as well as to the streamlines, river-lines, and lakes will be the potentiometric boundaries of these systems (Anderson and Woessner 1992; Diersch 1998; Anderson et al. 2015). Mathematically, the hydrogeological boundary conditions of a groundwater flow system can be explained by four types of boundaries as illustrated below:

1. **Dirichlet Boundary Condition (Head Boundary):**

    In this type of boundary, the key assumption is to neglect the groundwater flow within the flow domain. In addition, at the flow domain boundary, the outside water bodies have no influence at that boundary which means that the assigned potentials at the boundary will remain fixed and constant (Diersch 1998). The hydraulic head at the domain boundary is known, such as lakes, rivers, streams, or occasional water bodies which are in contact with an aquifer. If such these boundaries do not have a connection with an aquifer, it will remain a boundary through applying a fixed or specified head in a specific cell or cells which have known heads.

2. **Neuman Boundary Condition (Flow or Flux Boundary):**

    Regardless the state of flow and groundwater movement inside the flow domain, the flux boundary condition is fixed by the external flow boundaries which are effected on domain boundaries. The domain flux boundaries are specified by either no flow boundary which presents naturally between geological units (normally assigned by zero) or by a specific value such as in the interactions between surface water and groundwater bodies, underneath flow, spring-flow, and seepage between bedrock and alluvium. The commonly Neuman boundary which is applied widely is the no-flow boundary which occurring between those units of higher and lowers permeability or at the water divide boundary where the movement of groundwater flow takes two opposite directions at a specific boundary (Delleur 1999).

The variation in soil permeability between two adjacent soil units causes refraction of flow lines, especially when the difference reaches two orders of magnitude or higher, where, in general, the flow movement in the high conductivity layers is horizontal and essentially vertical in those lower conductivity layers; therefore, this can be considered enough to rationalize a no-flow boundary (Freeze and Witherspoon 1967; Neuman and Witherspoon 1969). Examples of the no-flow boundary can be found at faults, saltwater interface located close to coastal aquifers, low permeability layer results in little flow quantities, and divides located at regional groundwater aquifers (Zheng et al. 1988).

3. **Cauchy Boundary Condition (A dependent Head Flow Boundary):**

When there is a difference in the heads values over a specific boundary (one greater than the other), there will a flux crossing that boundary by a magnitude equals to that heads' difference multiplied by the transferred unit's hydraulic conductivity. Cauchy boundary condition is applied for surface water bodies' leakages where the fluxes quantities seeped into the subsurface bodies will be dependent on the hydraulic head difference between the surface water and groundwater levels and the hydraulic conductivity which separates these two bodies vertically, and sometime evapotranspiration parameter because flux quantity in the unconfined aquifer is proportional of the subsurface water table (Diersch 1998).

4. **Injection and/or Pumping Wells Boundary Condition:**

Groundwater aquifer is mostly exposed for stresses by undergoing extraction schedules or sometimes by injection schemes, which are leading to changing the groundwater table level, where it can consider the locations where those schemes are applied as a boundary condition for the aquifer (Diersch 1998).

3.6.1 Recharge rate

Recharge is one the most important factor affecting the behaviour and levels of regional groundwater aquifer systems, especially in those environments classified as arid and semi-arid, and unfortunately, its quantity is often difficult to estimate (Wood and Sanford 1995). Natural recharge flowing to the saturated area of the groundwater reservoir results from the vertical percolation of rainfall over an area and also from the leakage losses of rivers, lakes, and streams after a heavy rainfall is falling in the upper part of a catchment. Direct recharge refers to large amounts of rainfall, some of which contribute to the provision of sufficient moisture content of the soil, and the remaining part crosses the groundwater table to become part of the groundwater

flow system. In groundwater modelling, the natural assumption of recharge is to be spatially distributed to include all areas if these regions are all recharged from precipitation. The recharge value used in the groundwater system is usually positive to indicate that there is a quantity of water leaking into the groundwater system. Most recharge to groundwater usually occurs in wet seasons such as the winter season and some occurs during those seasons with intermittent rainfall. In dry seasons, often in arid and semi-arid areas, the effect of recharge is often neglected because it is too small to be sufficient even for soil moisture. For the purpose of estimating the recharge value of groundwater system, several methods have been developed which can be divided for chemical (**Tracers)**, physical (Water Balance Method) and isotopic methods (Simmers 1988).

3.6.2 Constant head and specified head

The word "Constant" refers to a uniform value distributed over an area (points) through time. In groundwater system, constant hydraulic head (line or surface) represents the sum of the pressure head (comes from gage pressure divided by the unit weight of water) and elevation head (water particle's potential energy located above a datum). Physically, the water level above a specific datum in an observation well or a piezometer is the constant hydraulic head. Although it may be imaginary, but sometimes the head over a surface may distribute equally at all points. Consequently, all the observation wells located on a surface of equal hydraulic head will have the same heads; therefore, it can be assigned all of those points with an equal or constant head boundary. Commonly, when a part of a boundary of a surface of an aquifer system coincides with another essentially constant head surface, the constant head boundary will occur (Lehn et al. 1987).

Regarding to the specified head boundary which represents a general boundary condition type as compared with constant head boundary type, it occurs wherever it can specify the head as a function of position and time over a specific boundary part of a groundwater system. An example of this boundary type is an aquifer connected with a stream/river and there is a seepage from that stream downward into the aquifer, the boundary condition between them will depend upon the change in heads in the aquifer and the stream as a function with time. Where, it can be specified that boundary as a constant head boundary if no significant changes occur and in this case, the boundary will be a function of position alone, otherwise the boundary will be as a function of position and time. In other word, streambed heads are assigned as specified heads over a groundwater system depending upon the circumstances external to that system where these specified heads will remain the same during the simulation process of the groundwater

system problem, regardless the real stresses that may the groundwater system will be subjected for during the simulation process (Lehn et al. 1987).

Both constant head and specified head boundaries have an important physical characteristic in the simulation analysis process in aquifer systems models. Where, it actually represents an inexhaustible source of water during the analysis process of groundwater model even if the quantity of water provided by these boundaries is not reasonable in the real field. Therefore, it should be carefully defined the right head boundaries in each simulation of the groundwater system because these boundaries affect significantly and effectively in evaluating the results and predictions of groundwater system (Lehn et al. 1987).

3.6.3 Groundwater-surface water (river) interaction

Traditionally, water resources management has usually focused on either groundwater or surface water as separate entities. All surface water resources like lakes, wetlands, streams, reservoirs, rivers, and estuaries are interacting with groundwater resources. The interaction between the surface water and groundwater leads to exchanging water and solutes between them. Therefore, it needs for a clear understanding of this connection to get an effective land and water management (Winter et al. 1998).

There is a dynamic interaction between the groundwater and surface water where this interaction is continuous in the hydrological cycle (Winter et al. 1998; Sophocleus 2002). In either system, the quality and quantity of water will practically be affected due to these dynamic interactions. Traditionally, groundwater and stream or river have been treated by hydrologists as distinct, or independent resources. However, due to the development of land and water resources, it became apparent that this development has affected the quantity and quality of both systems (Winter et al. 1998). For instance, contaminated aquifers that discharging water into a river may lead to long-term pollution of surface water source, or, on the other hand, bodies of surface water may be considered as the major pollution source to groundwater aquifers. Understanding the connection relationship between surface water and groundwater has been nowadays receiving a growing attention from the research community. The European Union Water Framework Directive (2000) have recognised the groundwater-surface water interactions' importance and the real need for integrating the management of both these two bodies.

Recharge into the groundwater aquifers is provided by the surface water bodies and not only from precipitation. The exchange zone in streams (hyporheic zone) is existing where it can be found a mixture of surface water and groundwater (Kazezyilmaz and Medina 2006). The

hyporheic zone is a very complex biochemical, hydrological, and geological zone (Conant 2004). Hyporheic zone has the ability of affecting the groundwater source quality and quantity due to the connection with the surface water source, where any effect affects these sources, it will move to the other through this zone (Kazezyilmaz and Medina 2006). This effect will become more pronounced when abstraction from wells-field takes place in or close to hyporheic zone. Fluxes direction between groundwater and surface water bodies depends upon the hydraulic gradients' variation which depends on the flows balance and topography of surface in the whole hydrological system, where the flows between these two systems are controlled by the hydraulic properties of them (Townley 1998).

Actually, aquifer-stream connection happens through various scales both in space and time (Schaller and Fan 2009). Three patterns of spatial scales are shown in Figure 3.3 that corresponding to the direction of movement of water, which has three types of movements away, toward, and parallel to the water table surface (Toth 1963). Additionally, the geology and topography of the field considered to be under study will also control the groundwater-surface water interaction (Woessner 2000).
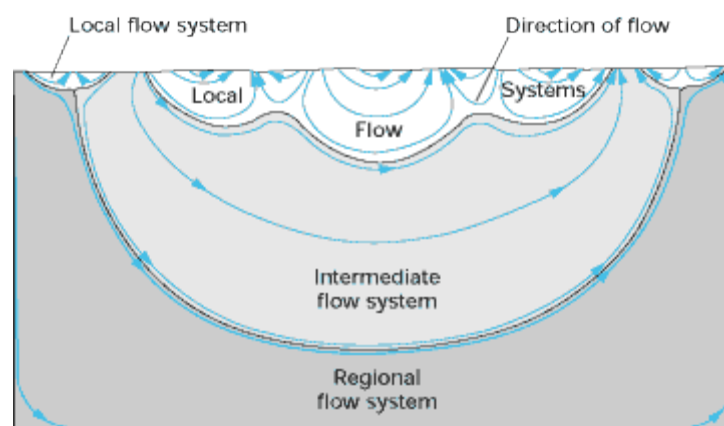
Figure 3.3: Groundwater flow systems can be local, intermediate, and regional in scale
(Modified and adopted by Toth 1963)

Streams usually feed on the groundwater in most climatic settings and physiographic. Even when streams are foremost losing surface water to groundwater, certain reaches or springs may be received a groundwater inflow through some seasons. The stream water proportion which is derived from groundwater inflow varies across climatic setting and physiographic (Winter et al. 1998). According to Winter et al. (1998), it is classified that there are three kinds of interaction between groundwater and streams or rivers: 1) gaining stream, 2) losing stream, and 3) stable stream flow (no flow across streambed).

When the water table elevation which is adjacent to the streambed is greater than the stream water level, streambed will allow to groundwater to percolate through it and this will lead to

increasing the stream water level through groundwater as shown in Figure 3.4 (Pattle Delamore Partners and Environment Canterbury 2000).
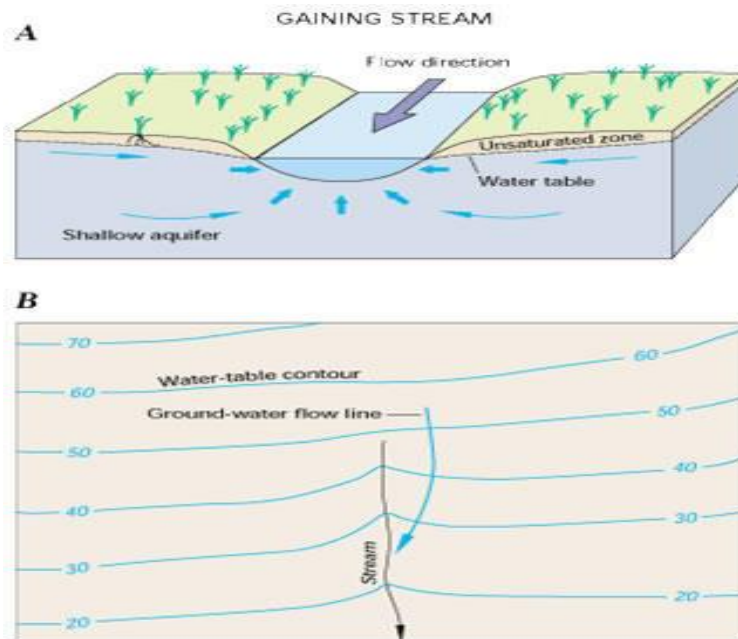
Figure 3.4: (A) Receive water from the groundwater system, (B) Contour lines on the upstream crosses the stream (Adopted from Winter et al. 1998)

If the water table, which is adjacent to the streambed, was below or lesser than the stream water level, this will lead to losing water from the stream into the groundwater by the outflow through the streambed as shown in Figure 3.5 (Pattle Delamore Partners and Environment Canterbury 2000).
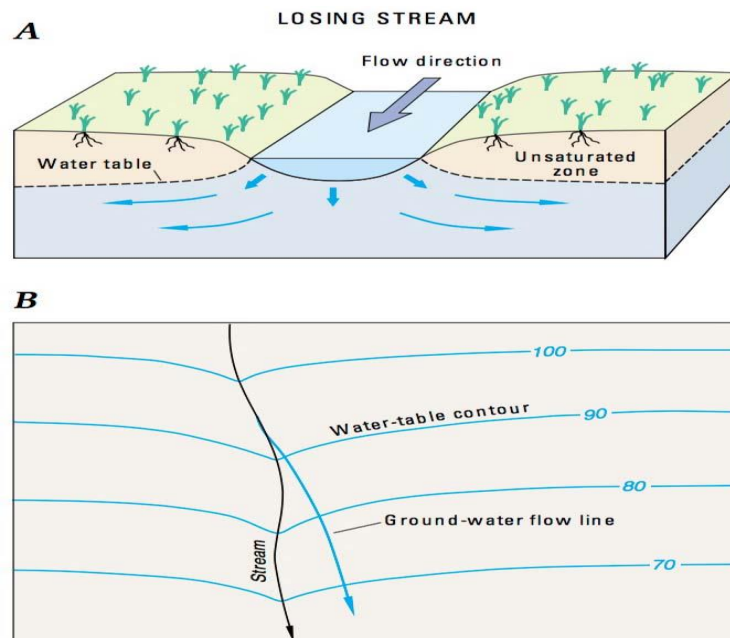
Figure 3.5: (A) Lose water to the groundwater system, (B) Contour lines on the downstream direction leaves the stream (Adopted from Winter et al. 1998)

When the groundwater and stream levels are exactly the same, this means that there is no flow across the streambed. However, it is relatively rare to occur like this case over long reaches for prolonged periods (Pattle Delamore Partners and Environment Canterbury 2000).

It can also the streams or rivers be separated from the groundwater system by an unsaturated zone. This zone will be located between the riverbed and the groundwater table level where the stream in this situation will be known as a disconnected stream as shown in Figure 3.6.
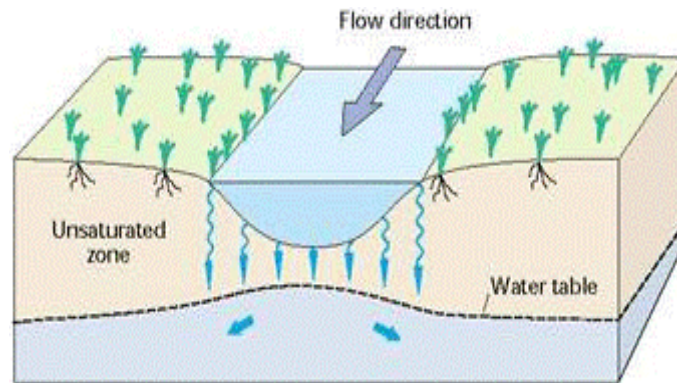
Figure 3.6: Schematic representation of a disconnected river (Adopted from Winter et al. 1998)

Sometimes streams or rivers have suffered from rapid water stage's rise due to storm precipitation, or release water from reservoirs, or rapid snowmelt which may cause water to move from the stream or rivers into the stream-banks where this process is known as bank storage (Winter et al. 1998), as shown in Figure 3.7.
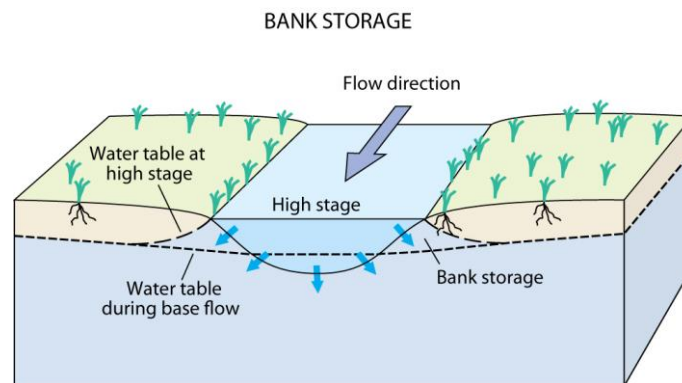
Figure 3.7: Stream water moves into the stream-banks as bank storage (Adopted from Winter et al. 1998)

In respect of the interaction between the groundwater and lakes, there are three basic ways of interactions between groundwater and lakes as illustrated in Figure 3.8. These are some lakes receive groundwater inflow from its entire bed, some loss water into the groundwater through the seepage from the entire bed, but actually most lakes loss its surface water into the groundwater by the seepage from some parts of the bed and receive groundwater inflow from the other parts of the bed and this is the third basic interaction way (Winter et al. 1998).
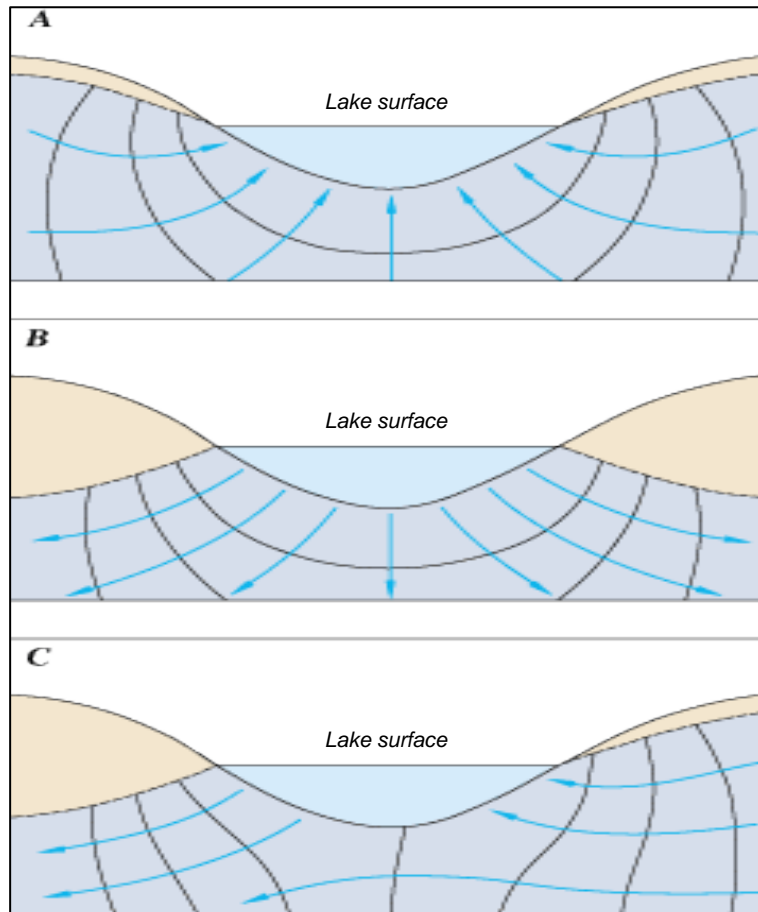
Figure 3.8: (A) Lakes receives groundwater inflow, (B) Lakes loses water as seepage to groundwater, (C) Both (Adopted from Winter et al. 1998)

Despite of these basic interactions are approximately the same for streams, but it is still different in several ways. The level of water for natural lakes, which are not controlled by dams, generally does not vary as quickly as the level of water in streams; therefore, the importance of bank storage for lakes is lesser than those for streams. Evaporation has a lesser effect on stream levels than lake levels because the lakes surface area is generally bigger and less shaded than many reaches of streams. This is because the water of the lake is not replenished as easily as the reach of a stream. Furthermore, lakes can be found widely spread in the landscape with a complex groundwater flow system than streams. Also, commonly, lake sediments have larger bulks of organic deposits with a very poor permeability than those for streams. These deposits can affect more on the seepage from the lakebed and biogeochemical exchanges of solute and water of lakes than on streams (Winter et al. 1998).

Hydrogeological properties of the riverbed have a significant impact on the degree of groundwater-surface water interaction. It is reported by Fox and Durnford (2003) that the streambed/riverbed of the stream/river has a hydraulic conductivity with some orders of magnitude less than the surrounding aquifer as this explains the hydraulic head loss that occurs

in this less conductive layer. Also, Fox and Durnford (2003) have assumed that due to the continuous supply of water to the surface water bodies (streams or rivers) and in turns to the streambed, the streambed layer will remain fully saturated, so the geology of this layer will control the determination of the hydraulic conductivity of streambed. Often the materials that much form the streambed layer are deposited suspended sediment from the river water. These suspended materials are often solids and unable to infiltrate the streambed into groundwater aquifer, and will be removed from the river's water and deposited in the upper surface of the streambed layer in a process known as mechanical clogging. This clogging is unable to protect itself in the situations when there is an abstraction process from the groundwater aquifer to be filtered through the riverbed. Mechanical clogging could be reduced normally by the quantity of bed-load transported by the river when whirl up and remove the sediments from the bed's river (Schubert 2002). It is highly predicted by Schubert (2002) to happen a chemical clogging when there are high loads of biodegradable substances in the river water that can strongly cause a change in the redox potential and pH, which will cause sedimentation of materials in the pore spaces of the streambed and aquifer. Therefore, there is an important role for the quality of the river's water that can affect strongly the degree of clogging, degree of groundwater-surface water interaction, and all in turn will affect the groundwater quality.

Groundwater gains water from rivers or streams and vice versa depending upon the head gradient difference between the groundwater regime and the water level of the river. River package (RIV) exists within Visual MODFLOW program is designed to simulate the flow effects between groundwater and surface water systems. According to that, there is a term must be added to the equation of flow Eq. (3.4) represents the seepage between the surface water and groundwater for each cell in the blocked centred system.

The general equation of flow between the river and the groundwater system is presented in Eq. (3.5). Some assumptions are made for this equation, the first one is, all model cells underlying the riverbed are fully saturated and this means that the level of water table should not drop below the riverbed layer bottom, and the second is, head losses that measured between the aquifer and the river are limited and depending upon those that across the riverbed layer, that is, no intrinsic head loss occurs between the underlying model cell node and the riverbed layer bottom as illustrated in Figure 3.9A & B.

$$(Q_b)_{riv} = (C_b)_{riv}\left(H_{riv} - h_g\right) \tag{3.5}$$

where, $(Q_b)_{riv}$ is the river-aquifer exchange flow, positive if it seeped into the aquifer (L^3T^{-1}); H_{riv} is the river water level (stage) (L); h_g is the groundwater head beneath the river (L); and $(C_b)_{riv}$ is the riverbed hydraulic conductance (L^2T^{-1}) and it equals:

$$(C_b)_{riv} = \frac{(K_b)_{riv} L_{riv} W_{riv}}{M_{riv}} \tag{3.6}$$

where, $(K_b)_{riv}$, L_{riv}, W_{riv} and M_{riv} are the hydraulic conductivity of the riverbed, river length that crosses the node of the cell, the width of the river within the cell, and thickness of the riverbed layer, respectively and all of them can be shown in Figure 3.9C.
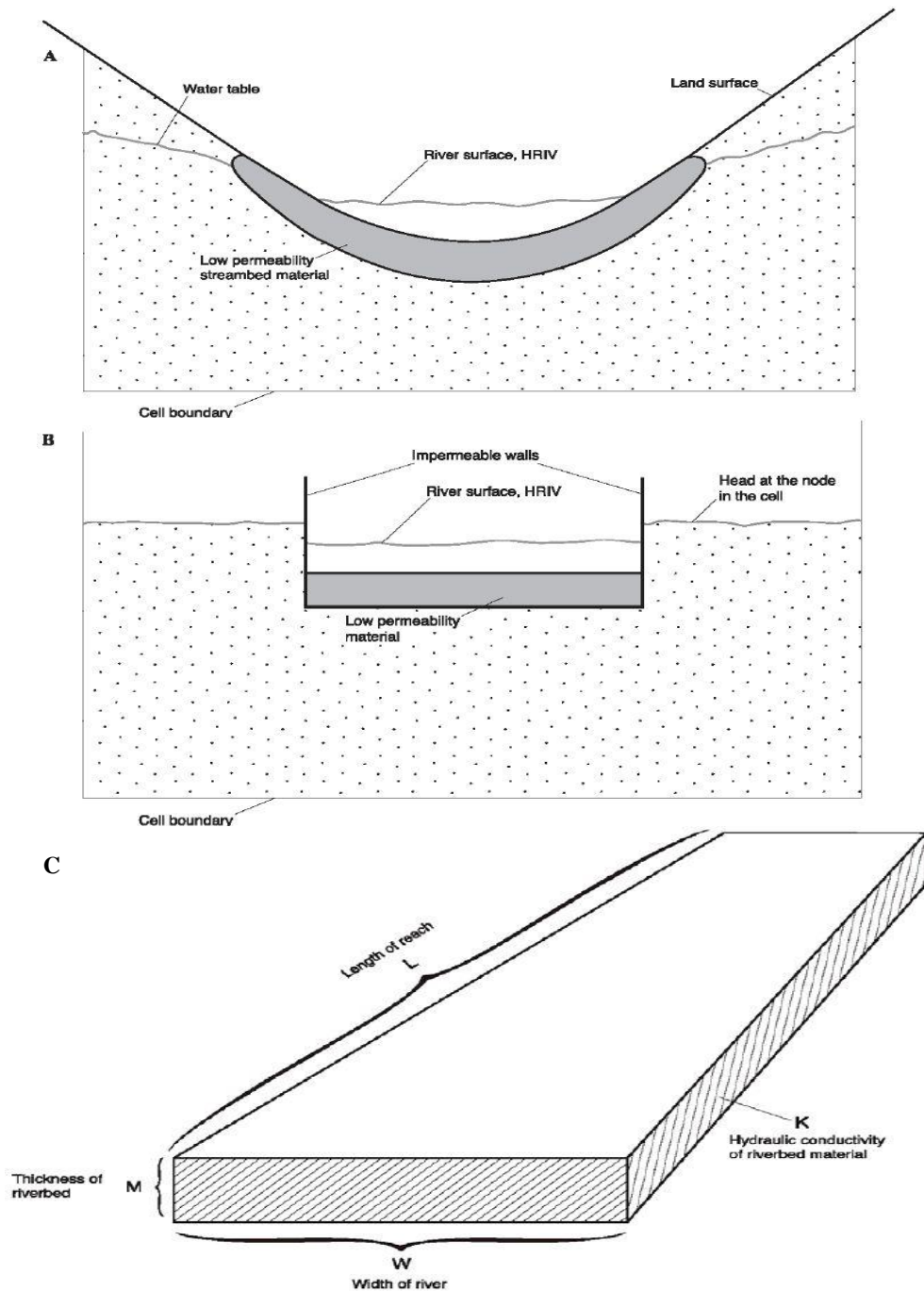
Figure 3.9: (A) An aquifer shows a river cross-section, (B) River-Aquifer conceptualisation through a simulation, and (C) Individual cell of idealized riverbed conductance (Modified and adopted by McDonald and Harbaugh 1988)

Indeed, Eq. (3.5) gives acceptable values of flow between the river and the aquifer over a certain range of aquifer heads. However, if the groundwater table (W.T.) level in the aquifer falls below the riverbed bottom leaving an unsaturated space underlying this layer, the seepage from the river into the groundwater in this case will depend on the head in the aquifer as it can be seen in Figure 3.10. In addition, whether it is assumed that the riverbed layer will remain saturated, this will lead to considering the head at the riverbed base to represent the elevation of water table at this point and this means it will be equal to B_{riv}. According to that assumption, the seepage flow from the riverbed bottom (the river) into the groundwater will be represented in Eq. (3.7):

$$(Q_b)_{riv} = C_{riv}(H_{riv} - B_{riv}) \qquad (3.7)$$

where, B_{riv} is the riverbed elevation.
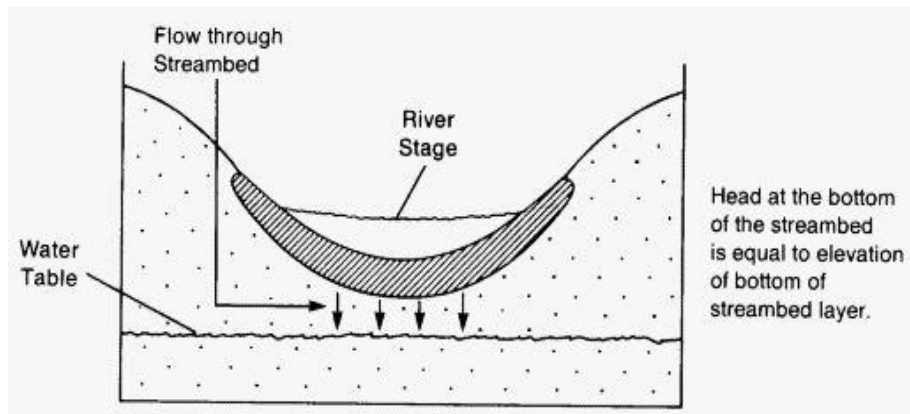
Figure 3.10: Water table falling beneath the riverbed bottom (Modified and adopted by McDonald and Harbaugh 1988)

It can rewrite Eqs. (3.5) and (3.7) by depending upon the riverbed elevation (B_{riv}) which represents the Visual MODFLOW simulation concept of groundwater-surface water interaction as below:

$$(Q_b)_{riv} = (C_b)_{riv}(H_{riv} - h_g) \qquad\qquad h_g \succ B_{riv}$$

$$(Q_b)_{riv} = (C_b)_{riv}(H_{riv} - B_{riv}) \qquad\qquad h_g \leq B_{riv}$$

Indeed, in general, the flow seepage between the aquifer and river is a three-dimensional process and it is just an approximation when representing the flow between them by a single conductance term and the elevation of the riverbed. This is because the riverbed is much various from the confining layer in the idealized situation (McDonald and Harhaugh 1988). This means the flow between these two parameters (river and aquifer) is considered to be one dimensional because the flow exchange is just through the riverbed.

3.7 Hydraulic conductivity

Hydraulic conductivity or transmissivity are the most important parameters which are required for a steady-state groundwater flow modelling to be distributed over the grid cells of a groundwater model. Specifically, hydraulic conductivity represents a tool to measure water transmit capacity and it is defined as a constant of proportionality that discharges a certain amount of water in a specific porous medium under a unit of hydraulic gradient and it can be expressed by Darcy law (V=−Ki), which is illustrated in detail in Eq. (3.1). As transmitted water is controlled by hydraulic conductivity, this means that the hydraulic conductivity has the ability to control the rate of groundwater movement under a given hydraulic gradient in the saturated zone and also control the containment degree of pollution. Coefficient of permeability is also represented the hydraulic conductivity term and it refers to the soil behaviour which is either can transmit water "Permeable" or cannot transmit it "Impermeable". If the hydraulic conductivity distributed over an area is constant with an equal value, the aquifer soil hydraulic conductivity in that area is said to be "Homogeneous", but if its value was different from place to place over an area, it will call the aquifer soil hydraulic conductivity as "Heterogeneous". In a specific place, if the hydraulic conductivity is essentially the same in all directions within the aquifer, that aquifer will be called as "Isotropic", otherwise, it will be called as "Anisotropic" (Tesfaye 2009). In groundwater modelling process, it is general to assume that the aquifers are homogeneous and isotropic to convenience the simulation process although this situation is completely rare. However, the modellers need to simulate the aquifers as possible as close to reality (Sefelnasr 2007).

3.8 Pumping

Pumping water from aquifers which are connected to the bodies of surface water will have a crucial effect on water movement between these two bodies of water. The effect of withdrawal wells on the regime will be local in scale if the withdrawals were presented by a single well or a small group of wells. However, when the withdrawing wells are many over large areas, the effect will be regional in scale (Winter et al. 1998). If the diversions of spring flow or the groundwater withdrawals are affecting the system of the groundwater by the negative way, the one option of management is to limit the withdrawals for an established safe yield and specifying the location of the new wells in order to minimize or overcome on the negative impacts as illustrated in Figure 3.11. Drawdown (water level decline) may still happen at large distances from the pumping wells until establishing new equilibrium conditions even when the levels of water near the pumping wells can recover its level relatively quickly (USDA 2007).
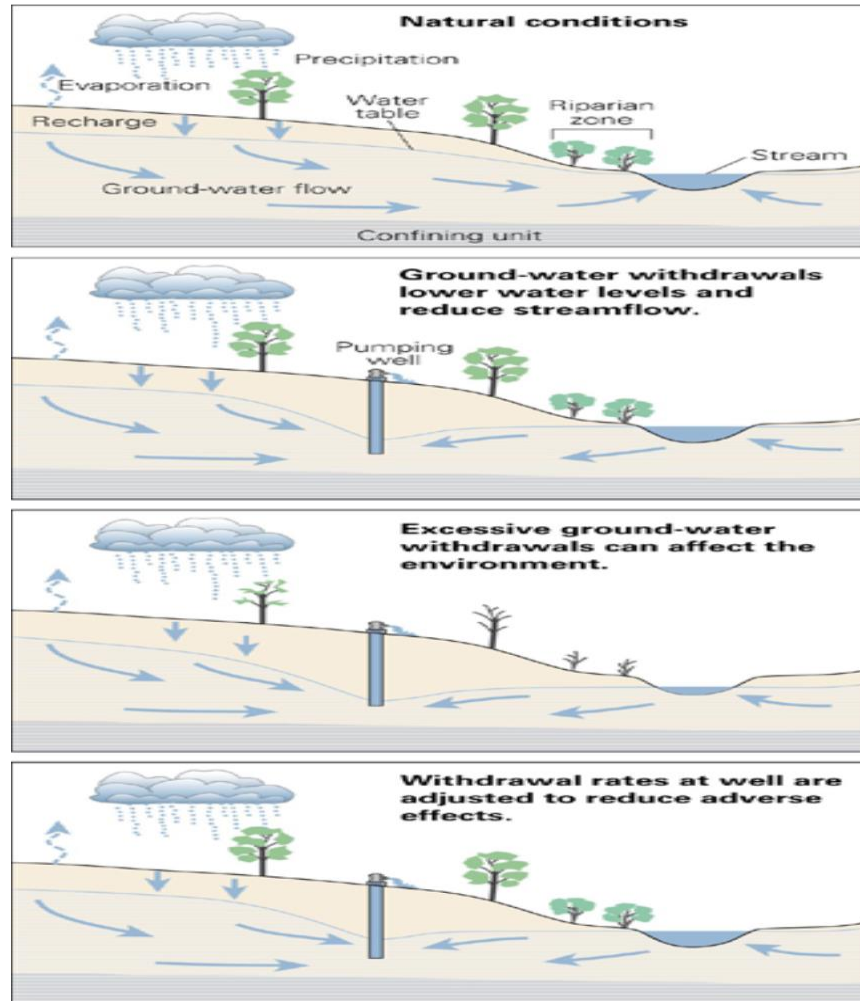
Figure 3.11: Effects of pumping from a hypothetical groundwater system that discharges to a stream (Adopted from Heath 1983)

Fox and Durnford (2003) discuss the three regimes which are describing the river-aquifer interaction when there is an abstraction process. It is reported that in case of the groundwater level in the aquifer is within the elevation of the river bed, the interacting regime is dominated to be fully saturated with flow. This situation happens when water pressures are not sufficiently negative enough to make the subsoil unsaturated, where this means, the rate of abstraction from the aquifer is less than the aquifer's recharge seeping from the river. Hence, the specific discharge (q) (L/T) through the stream or river bed into aquifer can be described in Eq. (3.8):

$$q = -K_b \frac{S_w}{S_w - H_{riv}} \tag{3.8}$$

where, K_b is the saturated hydraulic conductivity of the streambed, S_w is the drawdown that represents the distance between the water level in the river (H_{riv}) and the water table in the groundwater aquifer (Fox and Durnford 2003).

The negative sign refers to the downward flux seeping from the river toward the groundwater aquifer.

3.9 Evapotranspiration

As groundwater represents of strategic importance, it needs for an accurate estimation of groundwater recharge. In addition, protection of groundwater systems requires an assessing of the fundamental controlling factors that affect these systems' protection (Zomlot et al. 2015). The actual evapotranspiration process represents a major process in the hydrological cycle where it plays an important role in simulating the hydrological effect of climate change (Zhao et al. 2013). As Al-Najaf province is classified as an arid area (Ahmed et al. 2013), thus the most important parameter that highly affects the groundwater recharge is the actual evaporation. To estimation this parameter, an experimental (using measurement instruments) and mathematical techniques have been investigated by many researchers as detailed below.

3.9.1 Measurement techniques

A variety of instruments have been used to estimate the actual evaporation, such as pan-measurement, Bowen ratio (BR), using of weighing lysimeters, and Eddy covariance techniques (Li et al. 2009). The description of each experimental method is available in detail in Bosman (1990), Bausch and Bernard (1992), Edwards (1986), and Leuning et al. (1990), respectively.

3.9.2 Mathematical methods

The widely used mathematical methods are categorized into either empirical methods or analytical methods (Verstraeten 2008). In the empirical methods, the actual evaporation is estimated by depending upon the meteorological data for the site under consideration through using empirical relationships. By depending upon the direct and indirect measurements such using remote sensing technology or ground-based instruments, complex analytical physical processes methods are established to estimate the potential evaporation and then either use it as it is, or corrected it to estimate the actual evaporation (Li et al. 2009), so these methods are rarely used. The commonly applied empirical methods that estimating the potential evaporation are Penman equation, Penman-Monteith equation, Blaney-Criddle method, Turc's formula, and Thornthwaite method. Penman equation needs for lots of parameters which are not available through the data that have been collected for the study site. For instance, one of these parameters that are used in Penman equation is (Δ) which represents the slope of saturated vapour pressure curve with respect to temperature and this is unavailable in the data collected. Therefore, it cannot use it to find the potential evaporation (PE). In Penman-Monteith equation, a lot of parameters are not available through the collected data where this makes this equation more difficult to apply. Blaney-Criddle method depends upon various coefficients such as k (the

crop coefficient consumptive use for monthly period) and K (the crop coefficient for irrigation season or growing period of the evapotranspiration consumptive use). Indeed, these coefficients are not available for the crop cover in the study site; therefore, it is unable to use this formula. Turc's formula needs values of 10 days of rainfall and temperature as well as the mean of the short wave radiation to calculate the potential evaporation over 10 days. However, these data may not available through the collected data of a particular site. Therefore, it is not possible to use this formula to calculate the potential evaporation parameter. The formula proposed by Thornthwaite equation (1948) is the only method which can be used because all of its parameters are more likely be available. It is mainly based on the monthly temperature mean with an adjustment for the daily number of daylight hours. The potential evaporation for each month of the year, according to this method, can be estimated as:

$$PE = 16 \left[\frac{10T_i}{I} \right]^a \tag{3.9}$$

where, PE is the monthly potential evaporation (mm); T_i is the average monthly temperature (°C); and I is the annual heat index (°C), which can be calculated as over a 12-month (or a year) period:

$$I = \sum_{i=1}^{12} \left(\frac{T_i}{5} \right)^{1.514} \tag{3.10}$$

and constant **a** can be calculated as:

$$a = 0.016I + 0.5 \tag{3.11}$$

The corrected potential evaporation PEc (in mm) can be estimated as

$$PEc = PE * K \tag{3.12}$$

where, K is the constant factor expressing the daylight hours and the latitude for the selected study region.

Values of monthly main potential evaporation that result from Thornthwaite's (1948) equation need to be corrected using (K) based on latitude geographical position for an area and the daylight hours in that area. K-values are illustrated in Table B.1 in Appendix B.

Table B.1 in Appendix B has provided the K-values that should be used to correct the calculated potential evaporation to get the actual evaporation value. The only parameter needed to apply Thornthwaite's formula is the mean monthly temperature values. In addition, the latitude and longitude directions of the considered study site with the daylight hours that this study site exposed for, are the only needed parameters to correct the potential evaporation values. Applying of Thornthwaite equation (1948) for wet areas (or rainy months) will give very well

results, but it needs to use the adjustment coefficient "16" in the beginning of the equation in dry months or areas (Bautista et al. 2009).

3.10 Accuracy of numerical models

Minimizing the uncertainties and errors represent the most important issues that controlling the accuracy and reliability of numerical models. Errors in the applications of groundwater modelling are sourced from (Konikow and Bredehoeft 1992):

- Conceptual errors: represent theoretical misconceptions about the basic processes that have been introduced into the model.
- Numerical errors: generate in the equation-solving algorithm where these errors include round-off errors, numerical dispersion, and truncation errors, especially in transport models.
- Inadequacies and uncertainties of the input data will lead to arising errors which in turn will affect the comprehensive description of stresses, aquifer properties, and domain boundaries.

The most common sources of most groundwater modelling errors are arising from the conceptualisation and uncertainty problems. Recent studies emphasise on how it can incorporate uncertainties in numerical modelling. A stochastic program was presented by Yangxiao and Van Geer (1992) to reduce and quantify the groundwater flow uncertainty for the input data processed by a numerical model called MODFLOW. Linking of numerical and stochastic models was suggested by many researchers (Anderson and Woessner 1992; Karakostas and Manolis 1998).

In the model development, groundwater modelling errors occur at the stage of the mathematical treatment of the generating accuracy, governing equations, consistency, convergence or stability problems. As groundwater numerical models are almost approximations, modelling errors are generally generated while subdividing the model domain by a set of grids, either while differentiating or integrating the governing equations (i.e. the mass balance equations), or while interpolating the various model parameters, or while solving the resulted system set of equations. In the present work, a high attention is paid to apply accurate boundary conditions and accurate geological and hydrogeological properties to arrive for the best construction of the groundwater model for the considered study site.

In Visual MODFLOW program, in order to define River Package data, it needs to input six entries which are layer, row, and column of the cell which containing the river reach, width of

the river, river stages at the start and end points, riverbed layer thickness, riverbed layer conductance, and riverbed bottom at the start and end points. In the simulation process for the River Package, river seepage term which is entered at the beginning of each iteration will be added to the equation of flow for each cell in the system. According to the comparing between the last recent values of head at the cell that containing the river reach and the value of $RBOT_n$ for the reach, Visual MODFLOW program will choose which equation will use either Eq. (3.5) or Eq. (3.7) to calculate the flow seepage. This means that the value of head (h) at a specific cell from the previous iteration will be used to the next one and because the program will check this value again at the beginning of the new iteration to take a decision of which river seepage equation will use, this will lead to lagging by one iteration behind the calculations of seepage.

3.11 Visual MODFLOW description

Visual MODFLOW (v.4.6) used in this research has been presented to modelling and assessing of groundwater flow in one, two, or three dimensions, heterogeneous, and anisotropic (aligned with grid) aquifers by U.S. Geological Survey Institute. This software is produced by McDonald and Harbaugh (1988) using the programming language of Fortran 77. It is dealing with the saturated flow, block centred cells, and steady-state or transient flow. This program uses the finite difference method to solve set of equations by depending upon Eq. (3.3) which is presented previously in this chapter and it is supported by various options/solvers to solve matrix equations like (SIP, SOR, LMG, PCG2, PCG4, and WHS). In addition, the possibility to develop this software makes it an easy and complete one to conceptualise the environment practically such as groundwater flow and contaminant transport, so that, this program has been developing constantly since 1988 to date. Moreover, advantages of Visual MODFLOW model comprise of many facilities such as adjust information and data entry and exit, exchange data between various standard form within of it, source code availability, ability to simulate groundwater-surface water interactions, sediment transport, simulation of water quality and protection initiatives of water source, involving many packages that simulate the hydrological stresses of groundwater and contaminant systems, and many more as well as the low price comparatively to other software (Kumar 2002).

Visual MODFLOW accuracy with regard to spatial discretisation has been explored by Haitjema et al. (2001). The accuracy of the boundary conditions for the groundwater regime and the appropriate cell sizes were the most important issues founded by Haitjema et al. (2001) to get an accurate groundwater model. The regions that having singular velocities near corners, zones or layers with contrasting transmissivity levels, or regions with strongly diverging or converging flows, need for a large number of cells to be accurately modelled. It should notice

that the nature of the finite difference grid as well as cell sizes is restrictively depending upon the cells' number (number of rectilinear rows and columns).

In 1997, Barrash and Dougherty have found that the finite difference formulation which is used in MODFLOW gives underestimated results for large head gradients occur in the pumping vicinity closed to wells. Generally, relative small grid spacing is required for flow field in the vicinity of irregular hydro-geologic units (e.g. discontinuities, or very little data). Moreover, an accurate velocity is needed due to the accuracy of the contaminant transport models which is represented by the advection dominated transport where using small cell sizes represent often a condition to reach the model's stability and accuracy. It can reduce or eliminate these limitations through refining the system's gird by using a more flexible grid structure. A local grid refinement method was presented by Mehl and Hill (2002) and (2004) in a 2-dimensional and then 3-dimensional block-centred finite difference grids by using shared nodes with good accuracy results. Others three programs (MODTMR, TMRDIFF, and RIVGRID) were developed by Leake and Claar (1999) using a telescopic mesh refinement method within MODFLOW program. Another method was presented by Spitz et al. (2001) for refining a model grid. In MODFLOW and MODPATH, the nested re-discretisation method is used to improve the resolution of path-lines by eliminating weak sinks. However, it may need for a long execution time to run the model when fine grids are used where this will lead to understand the system dynamics and calibrate the model accurately. Alternatively of the grid refinement, an analytical element model has been suggested by Kelson (2002) to extract the aquifer properties, boundary conditions, and parameter values for those sub-regions to be then applied in Visual MODFLOW regional model to get an accurate local modelling.

A finite element package was presented in Jones (1997) as an alternative method to solve the equation of groundwater flow within the model layer, while a finite difference method was used to simulate the vertical flow. The input data was consistent with MODFLOW modules with a capability for manipulating of the designed grid. In fact, no other works deal with the flexibility of the grid structure in MODFLOW that have been investigated so far. Where, it was suggested by Hill (2002) that in the future, MODFLOW will be developed to improve the local grid's refinement which will make the model grids less structured. In 1990, a higher-order finite volume method has been developed by Zheng (1990) for transport simulation which is represented by the MT3D code integrated within MODFLOW where this method was based on the finite difference method for dividing grid cells so that can drive the interstitial fluid velocity components.

Different interpolation techniques errors and performance through approximating the hydraulic parameters and gradient terms in each cell on the surface of a model in MODFLOW have not been investigated so far. Matrix solvers potential inaccuracies of old MODFLOW version, SIP, SSOR and PCG2 were fully addressed and discussed by Osiensky and Williams (1997). In the recent MODFLOW version, Mehl and Hill (2001) have compared the added solver AMG with the previous solvers through two simple tests. Another comparison was made by Wilson and Naff (2004) to the newly solver GMG. The latest achieved WHS solver added to MODFLOW can implement conjugate gradient algorithms called the Bi-Conjugate Gradient Stabilized (Bi-CGSTAB) acceleration routine efficiently with Stone incomplete decomposition for the partial differential equations of groundwater flow (Obretch 1994). Where, due to the initial "ill-conditioned" of the groundwater flow matrices equations, an effective pre-conditioning for these matrices is necessary to be the solution more efficient. This solver works on a two-tier approach to reach the solution at each one time step. To approach the solution, the factorized parameter matrix is varying due to the effect of the outer iterations. When the hydrogeologic parameters of the flow are updated, such as (saturated thickness, transmissivity, storativity) in the factorized matrices' equations set, then the outer iteration will be completed. Various factorization levels are allowed for matrices to be initialized differently to improve the stability and efficiency of the model's solution. The outer iterations matrices are solved iteratively by the inner iterations.

3.12 Discretization

Discretization is a phenomenon concerned by the temporal and spatial transformations of the groundwater model's geometric and time-dependent components through transforming these components into discrete elements. Geometry discretization represents a crucial element to distribute the boundary conditions and stresses which need to be applied. Model geometry cells should be small enough to express clearly the details of the geologic and hydrogeologic parameters, demonstrate as smoothly as possible the curvature of the hydraulic gradient and groundwater table, and show the effects on the hydrogeological system come from point stresses such as nodes pumping wells, recharge, and evapotranspiration (Sefelnasr 2007).

Mesh or grid size in the discretization process should be chosen to be appropriated to describe evidently the spatially distributed aquifer properties and aquifer heterogeneity, where almost it needs to refine the model grids as much as possible to meet the large variation of aquifer properties. In contrast, less variation of the distributed data of aquifer properties will need for large sizes of mesh or grid cells. Sizes (Refinement) of grid cells will lead to achieving the objectives of groundwater modelling as all aquifer properties will be spatially distributed over the hydrogeological system. Therefore, for the purpose of groundwater management and

sustainability, a great attention should be paid for simulating the hydrogeological systems when specifying the sizes of grid cells of groundwater flow system. It is not always practical to use comparable grids or cells in size and dimension to the cells where the pumping wells are located, although the predicted head or drawdown in the area close to pumping well is almost high even in case of applying groundwater management and sustainability schemes. Where, typically, as in the finite difference models, the pumping rate is applied to the cell where the pumping point (well) is assigned, the pumping well diameter will remain much smaller than the cell size, which means it cannot refine the grid size by depending upon the well diameter (Sefelnasr 2007). Visual MODFLOW finite difference technique depends upon block centred formulation of groundwater model discretization, as shown in Figure 3.12, as a well-known method to distribute the geological and hydrogeological parameters over the discretised model domain (Harbaugh 2005).
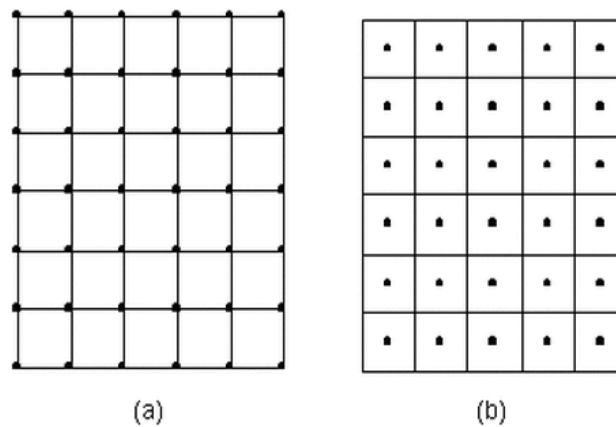
Figure 3. 12: Finite difference grid conventions in two dimensions: (a) Mesh-centred grid system, and (b) Block centred grid system (Adopted from McDonald and Harbaugh 1988)

3.13 Calibration

Many hydrological problems that the groundwater model exposed for should be addressed in the calibration process. The accurate definition of "Calibration" in groundwater science is the manipulating of model input data to be the results of the model (heads or flows) as closely as to the observed field information. An automatic or manual model parameter adjustment can be done and check the effects through using some statistical techniques as this step of adjustment represents one of model calibration aspects. Where there are some other key aspects have the capability to control model results and can produce a good matching with the field data, such as the conceptualisation process of the groundwater flow system, discretisation, recharge rate, and many more. The basic concepts that identify the model acceptability are the closeness between the simulated and observed collected data, and some other important parameters need to be incorporated in the model, both are crucial in evaluating the final calibrated model. It can be

seen some of the conducted calibrations with various methods according to each investigator in detail in Anderson and Woessner (1992).

Several techniques are employed to assess the calibration process without paying any attention to the calibration method used, either trial and error (Manual) or automated. The most well-known technique is by calculating the difference between the measured and calculated heads (called residuals) which will assist in clear quantification of the calibration process through either graphical or statistical comparisons. The calibrated model should have as minimum as residual value and standard deviation through comparing them with the acceptable threshold values. The standard statistics which are used to evaluate the model calibration process are the Standard Error of the Estimate (SEE) (m), Root Mean Squared Error (RMSE) (m), Normalized RMSE (%), and the Correlation Coefficient (CC) (dimensionless). Equations used for these statistics are illustrated below.

$$SEE = \sqrt{\frac{1}{n(n-1)}\sum_{i=1}^{n}(R_i - R)^2} \qquad (3.13)$$

$$RMSE = \sqrt{\frac{1}{n}\sum_{i=1}^{n}R_i^2} \qquad (3.14)$$

$$\text{Normalized RMSE} = \frac{RMSE}{(X_{obs})_{max} - (X_{obs})_{min}} \qquad (3.15)$$

$$CC = \frac{Cov(X_{cal}, X_{obs})}{\sigma_{cal}.\sigma_{obs}} \qquad (3.16)$$

where, $R_i = X_{cal} - X_{obs}$; $R = \frac{1}{n}\sum_{i=1}^{n}R_i$; X_{cal} and X_{obs} are the calculated and observed results of a specific parameter, respectively, $Cov(X_{cal}, X_{obs})$ is the covariance between the calculated and observed results, and (σ_{cal} . σ_{obs}) are the standard deviations results of the calculated and observed values of a specific parameter. Formulas of the covariance and standard deviations are illustrated in detail in Visual MODFLOW 2011.1 user's manual designed by Schlumberger Water Services.

Groundwater models need to be calibrated to ensure the forecasting results as each model either be calibrated under steady state condition or under transient condition. Usually, it needs to perform water levels in the steady state calibration which are represented by the mean of either the monthly long-term water levels, or the annual water levels, or the seasonal water levels for a specific season. At a particular point exposed for certain stresses with a specific time, a new calibration approach called quasi-steady state calibration is used to explore the behaviour of an

aquifer. Transient calibration is considered to explore water levels and aquifer behaviour under changeable stresses with time such as changing recharge rate and extraction quantity over time. Consequently, transient calibration requires some handle control for these fluxes during the modelling process period to achieve the model with an accurate calibration (Anderson and Woessner 1992).

3.14 Validation

In practice, the process of validating the model's aquifer is very similar to that of the well-known process called calibration. The International Atomic Energy Agency (IAEA) defined "Validation" as the process of comparing the calculations produced by the modelling process with those of field observations and experimental measurements. However, the multiplicity of attempts of the supposed solutions and the uniqueness of model solutions means providing good comparison with inadequate or erroneous models simulated previously. Also, because the expression "good" is objective and compatible with the operational definitions used in the validation process, any competent scientist may declare that the model validation result is acceptable while another scientist may use the same field data and prove that the model is not valid and cannot consider it as acceptable. Therefore; in science and engineering, the operational definition of "good" does not seem to be meaningful.

The sampling division method is one of the attempts that could make the model validation process more rigorous as this approach is patterned in groundwater studies after it was applied in the verification process in watershed modelling. Using this procedure, the model is calibrated using one part of the historical recorded data of the study site, which contains more than one referenced event which can through it characterize or distinguish the system response. Then the other part of the historical recorded data will be inserted into the calibrated model to verify the response of the model through comparing its results with the observations as this process called the verification process.

The application of division sampling approach in groundwater is usually a weak procedure. Generally, groundwater systems have a long time scale to response for the external events much longer than the surface water systems, as it is rare for a historical record to be long enough to be divided into independent data sets during groundwater analysis. Therefore, it is necessary to take into consideration when considering split sampling that the model response does not be influenced by stresses during the verification process period. Since the data of groundwater models are rare to presence independently, it is difficult to apply these spilt data widely in groundwater systems (Leonard and John 1992).

3.15 Uncertainty

Uncertainty in the hydrological modelling may be a result of either inaccurate model conceptualisation or incomplete input parameters or natural inherited processes. Due to the incomplete understanding of the model simulation process and the inaccurate hydrologic processes reproduction by using either mathematical or statistical techniques, the model uncertainty has arisen (Das and Lewis 2007). In each modelling process, it should be reported the uncertainties which are influenced on model results to be accurately taken into account in input parameter values (either the geological or hydrogeological properties). A further detailed description is provided by McMahon et al. (2001). When a system of continuous interest to society has referred for predictions of a problem, the roles of uncertainty analysis will include improving the design of the simulated model to monitor the predicted trends and changes in the aquifer system. The model should then be periodically reviewed and evaluated by re-calibrating it through inserting new and necessary information (such as changes in stresses), where the model predictions then can be validated by comparing its results with field observations and accordingly revised the presumed conceptual model. When the predictions/results of a model are matching the field data, it can be considered the constructed model as a satisfactory model, otherwise, it will need to made changes for some model parameters to reach for an acceptable adjusted model (Taylor 1985).

3.16 Summary

An investigation of flow simulation process with its methods applied on groundwater models whether it is steady state or transient simulations is explained. The procedure to initiate building a conceptual model for an area with the boundary conditions and aquifer properties needed is explored with a schematic pattern that shows the steps required to reach the acceptable groundwater model. The basic equation of groundwater flow in the porous medium, unconfined aquifer, and heterogeneous and anisotropic groundwater flow conditions is mathematically described. Due to the presence of the Euphrates River in the study area, river package (RIV) equations and the river connection with the groundwater aquifer are also described. The interaction between the river and groundwater reserviour when there is a pumping process in-operation is illustrated. The basic well-known equations of potential evaporation estimation and its requirements to apply are illustrated with the appropriate equation (Thornthwaite equation) for the current study. An explanation of Visual MODFLOW with its accuracy in modelling groundwater problems are reviewed to highlight the advantage from using this software. The related crucial techniques such as calibration, validation, and uncertainty analyses which are required to assess groundwater models to be acceptable and represent the real studied region,

are investigated to highlight the benefits from these techniques on how can assist to reach the final acceptable models.

Chapter Four
Study Area

4.1 Introduction

Reliable and accurate information for any study area is needed. Any modelling study is depending on the collected measured data which are required to success the modelling process (Kumar 2015). However, most of the groundwater resource available in Al-Najaf region is either used inefficiently by a way led to drying it or it left to gather underneath the ground surface without using it which in turns led to either damaging the agricultural areas, or damaging buildings' foundations, or submerging some of the desert areas. In Iraq, there are few aquifers having a huge quantity of groundwater. Dibdibba aquifer located within the boundaries of Al-Najaf region (the study site in this research) is considered to be under investigation because there is no availability for the good management of groundwater resource in this region.

The study area has the Euphrates River passing through the eastern part of it after bifurcating itself into two branches. The first branch called Al-Kufa (on the western side of the eastern part of the study area) and the second branch called Al-Abbasiyah (on the eastern side of the eastern part of the study area). The study area contains some of the populated areas like Al-Najaf central, Al-Kufa, Al-Abbasiyah, Al-Hurryah, Maysan, Al-Haidariyah, Al-Manathirah and many more where the total number of population in these regions is approximately 1.25 million Iraqi citizens. It can be seen the location of Al-Najaf region which represents the study area with some details in Figure 4.1. The study area is about 25.25 km in longitude direction and 38.7 km in latitude direction respectively, enclosing a model area of approximately 976 km^2.

In Figure 4.1, it can be seen that there is Tar Al-Najaf, which is located on the lower west side of the study area. This geological formation represents a cliff on the ground surface with a level reach to 90 m where on the foot of this cliff, there is a transferal fault called Abu-Jir fault.
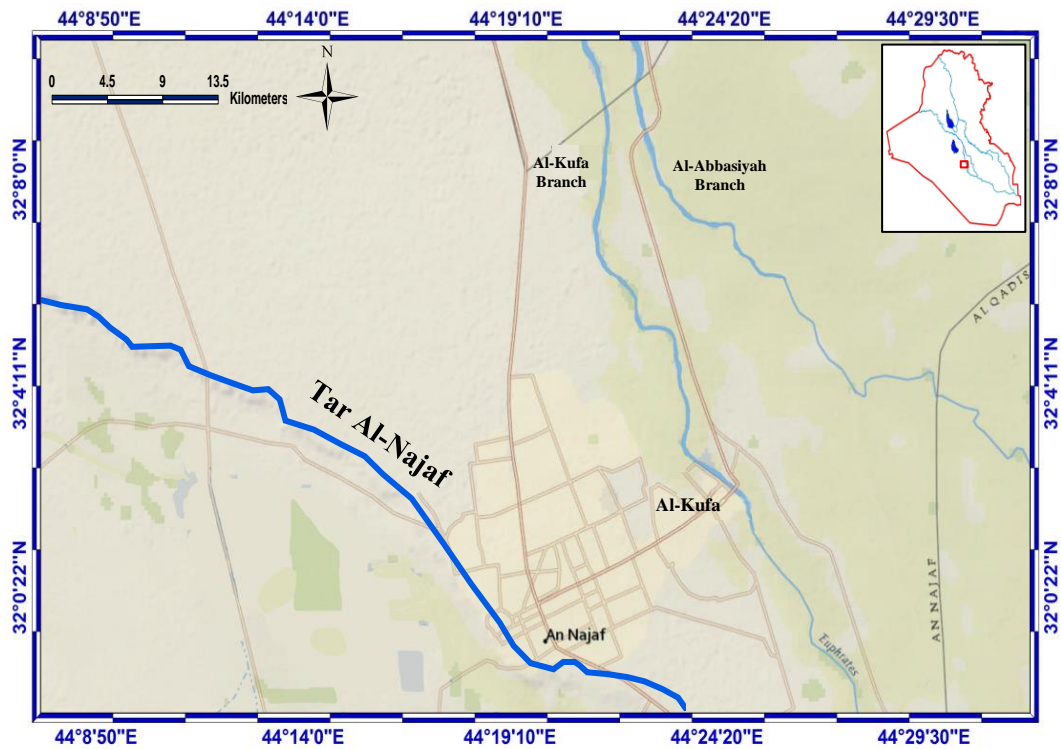
Figure 4.1: The study site with natural geological boundary conditions

4.2 Field data

The numerical models of groundwater need for intensive, accurate, complete data sets which are covering the whole region of the modelled area. But, with the development of GIS techniques and the complicated statistical methods, it should largely no longer be a problem to model the interested area even with a data gap. In order to develop the model of the groundwater, the following information and data should be completely prepared: (a) the complete layer discretization and slice elevations over the whole interested area, (b) aquifer parameters, and (c) the boundary conditions. Generally, the required data for a groundwater model can be listed below (Moore 1979).

- DEM (Digital Elevation Model) for the area of interest.
- Geological settings and cross-sections of the aquifer layers.
- Contour maps and the topographic map of the terrain surface.
- Hydrological parameters of the aquifer system.
- Water table and potentiometric maps for the whole aquifer.
- The thickness of each layer of the aquifer.
- Transmissivity and hydraulic conductivity data.
- Collimation beds information.

- Well extraction strategy.
- A description on the aquifer layers such as which one is confined and which one is not.
- Temporal and spatial information about rates of evapotranspiration, recharge into groundwater, discharge from groundwater into the surface water, and climate situation.

Data sets which are related to the area under study are collected from various offices and ministries in Iraq, including the cross-sections of the Euphrates River, upstream and downstream levels of water for the Euphrates River, bed elevation for the Euphrates River. Data related with wells that are injected in the study area, and those related with the geology and the hydrology of the area of study are also collected. Some of the most important offices and ministries are:

1. Ministry of water resources (MOWR 2015).
2. Ministry of industry and minerals, general commission for geological survey and mining (GEOSURV 2015).
3. Ministry of transportation, Iraqi meteorological organization and seismology (MOTRANS 2015).
4. Ministry of science and technology (MOST 2015).
5. General commission for groundwater.
6. General company for drilling wells irrigation.
7. Baghdad University.
8. Some geologists in the geology of soil and groundwater in the MOWR.
9. Al-Najaf Meteorological station.

The data obtained need for processing and checking to find the geological and hydrogeological properties as well as the boundary conditions related to the study area so that it can build a model of the study area by a careful and accurate way.

4.3 Digital Elevation Model (DEM)

To build a groundwater model to represent the area of study with a high accuracy, one of the information that need to be known accurately is, the natural levels of ground to find the terrain in the right form. To address that, it can use either the GPS device or the aerial satellite images. The use of GPS device represents a complex process where the user needs to be present in most of the locations of the study area. In addition, the collected coordinates need for an adjustment process, therefore; ground levels collected by the GPS device could have inaccurate coordinates with a high proportion of error. The other method is by using the aerial satellite images such as DEM-Digital Elevation Model or DTM-Digital Terrain Model whereas these images have a

very accurate ground level coordinates as well as containing another data, which are very interesting (Khemiri et al. 2013).

Therefore, one of the most important data, which should be prepared for the area of study is, the DEM-Digital Elevation Model because this satellite image has much information such as terrain elevations, contour lines, and much more that can be obtained through processing of this image.

The Digital Elevation Model (DEM) is a digital representation of the terrain, which is varying in height, and it is one of the basic outputs of the geographic information systems (GIS). Digital Elevation Model, in particular, is an estimation tool for the distributed surface and subsurface characteristics. It can also show the characteristics of flow as well as illustrating the control on the water movement that is exerted by topography in the landscape and the prediction of the flow characteristics for these regions (Khemiri et al. 2013). Moreover, one of the important advantages of the digital elevation model is, its ability to store large amounts of spatial data on a regular basis and easy to handle as a database (Al-Faris 2002).

GIS provides an opportunity to show the study area as a digital representation in two dimensions and in three dimensions through extracting (x, y, z) coordinates. X and Y of these coordinates represent the horizontal directions, while Z represents the vertical direction (height) as well as to other facilities, which are built by a computer through the GIS software (Seeruttun and Crossley 1997; Jazmani and Al-Maqdisi 2002). Moreover, Geographical Information System (GIS) has allowed users for a better and effective understanding use of water cycle through processing of contours, radar and optical images downloaded from the satellite. Indeed, the use of DEM is growing impressively with the GIS use and this leads to the improvement of the extracted information from the elevation data such as forest regions, lineaments, erosion, and floods mapping (Khemiri et al. 2013).

One of key elements to start this research is, to find the elevations of the ground surface of the study area to be adopted in the analysis of groundwater model and this can be done by using the aerial digital photographs which are called Digital Elevation Models (DEM). GLCF "Global Land Cover Facility" http://www.landcover.org/data/srtm/ website is used to download the aerial photograph "Downloaded Image" with 90m accuracy that is representing the DEM of Al-Najaf province as shown in Figure 4.2.

To process the downloaded image, it needs to open it by using the GIS program. The study area can be extracted from the downloaded DEM after processing it through the GIS software. The final extracted DEM for the study site is illustrated in Figure 4.3.
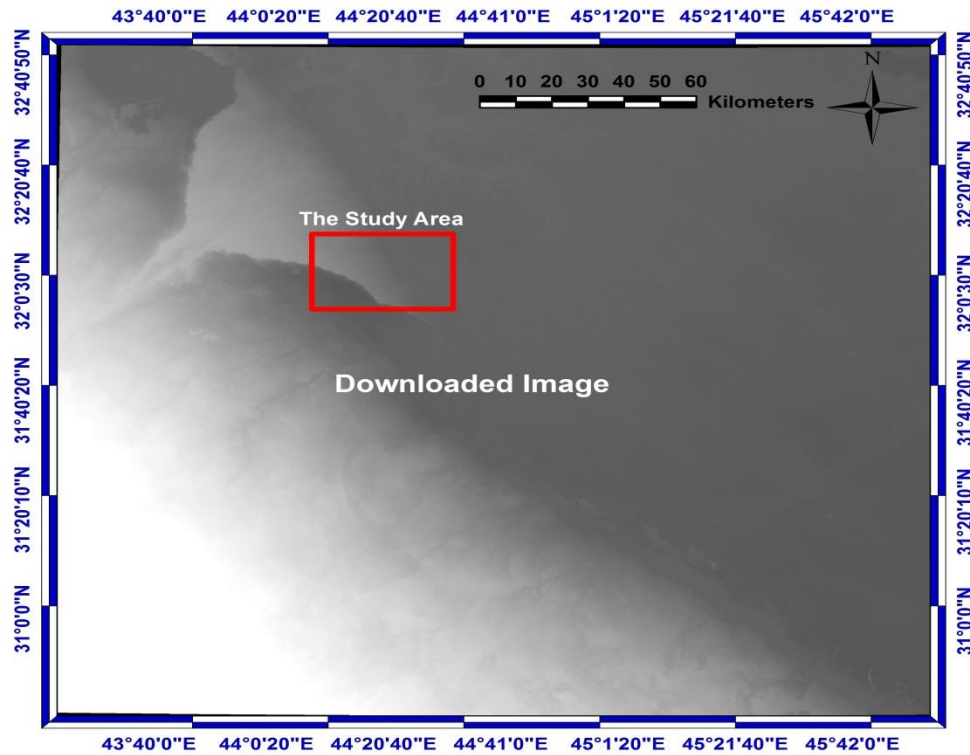
Figure 4.2: DEM as downloaded from GLCF website
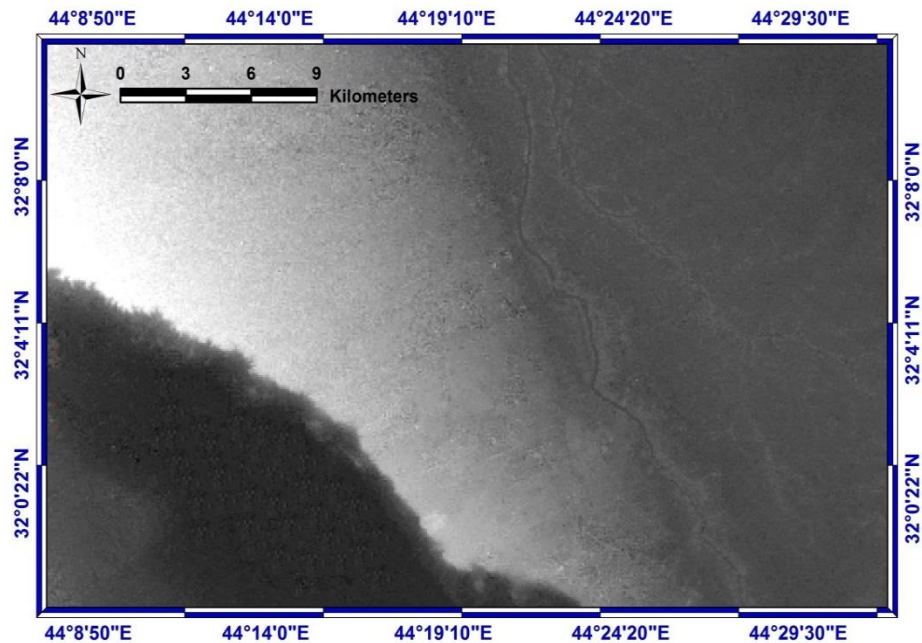
Figure 4.3: Final DEM of the study area after extracting from the downloaded image

The elevations of the top ground surface of the study area shown in Figure 4.3 is extracted from the GIS-program as an ASCII file and then plotted in 3D as shown in Figure 4.4.
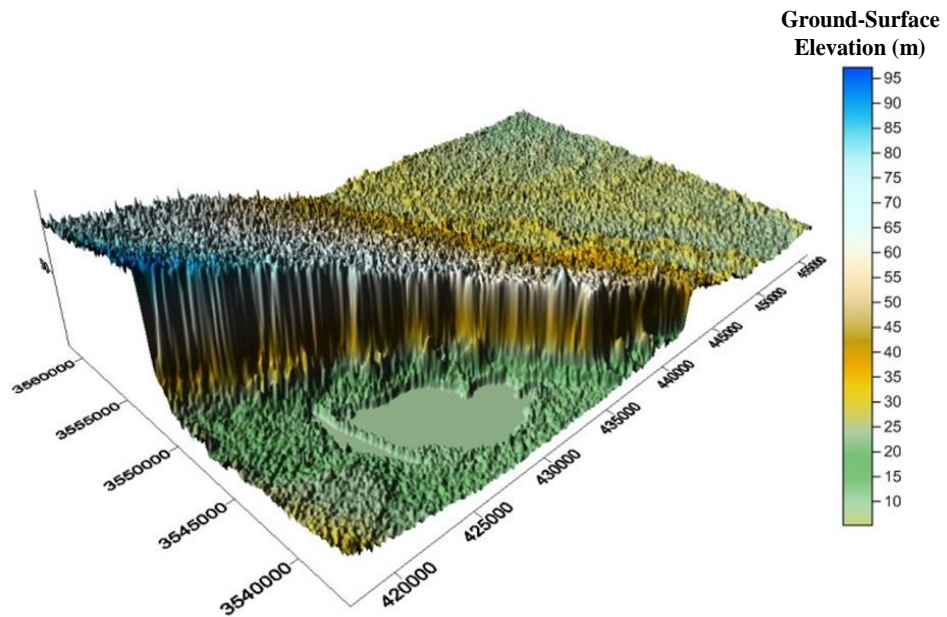
Figure 4.4: Topology or terrain of the study area extracted from DEM

Using the downloaded 90m DEM for the study site shown in Figure 4.3, the Elevation Contour map by using the ARC MAP program can be produced as shown in Figure 4.5. It is obvious that the elevation of the ground surface is higher on the western side and gradually decreases into the eastern side direction. According to that elevation, the movement of groundwater depends sometimes on the slope of the ground surface and this means that the movement is from the west side to east side for the whole region of the study site. The general slope of the study area according to Quinn et al. (1991) method is 0.0018.
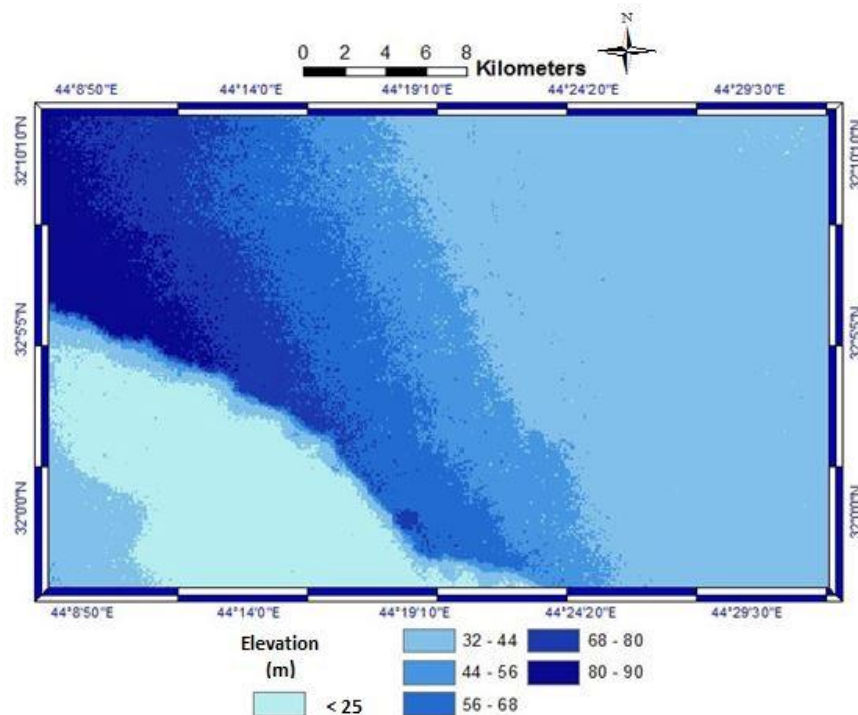
Figure 4.5: Topographic contour map of the area of study

4.4 Geological properties of the study site

According to the data collected, there is a fault (transversal fault) located on the south-west of the study area right underneath the cliff (Tar Al-Najaf) as illustrated in Figure 4.1. The groundwater in this area does not have any connection with the groundwater on the eastern side and the groundwater that comes from the western part of the desert will emerge at this fault. According to that, it means that this area needs to be inactive or removed when building the groundwater model in order to remove the results of this area from the simulation of the groundwater modelling results. The fault in the study area is illustrated on the geological map shown in Figure 4.6. The fault in the area of study called Abu Jir Fault. The upper part (ground surface area) of the fracture called Tar Al-Najaf.
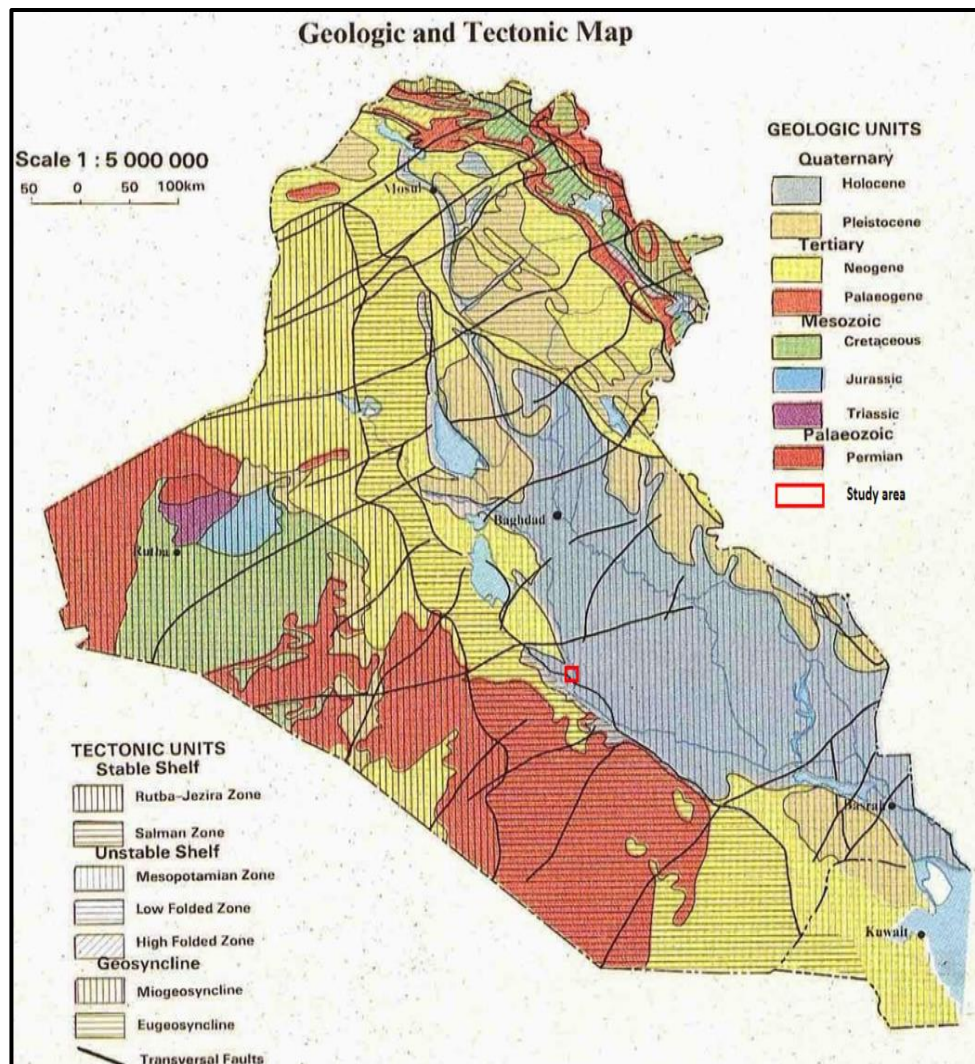
Figure 4.6: Geological map shows the locations of faults in Iraq and Al-Najaf province
(Adopted from GEOSURV 2015)

4.4.1 Tar Al-Najaf

Tar Al-Najaf is represented by a high cliff whereas at the foot of that cliff, the Abu Jir fault is located. In the Western side/part of Al-Najaf province, there is the urban city of Al-Najaf as well as a large depression, which is called Al-Najaf Sea. Al-Atia (2006), as it is cited in Al-Shemmari (2012), Tar Al-Najaf represents one of the limits of the study area on the southwest part. There are a number of formations located on both sides of Tar Al-Najaf. Figure 4.7 shows a picture of this cliff, it forms a sequence of sharp rocky cliffs, which are composed of claystone and sandstone. The depth of this cliff reaches to approximately 100m (Al-Shemmari 2012).
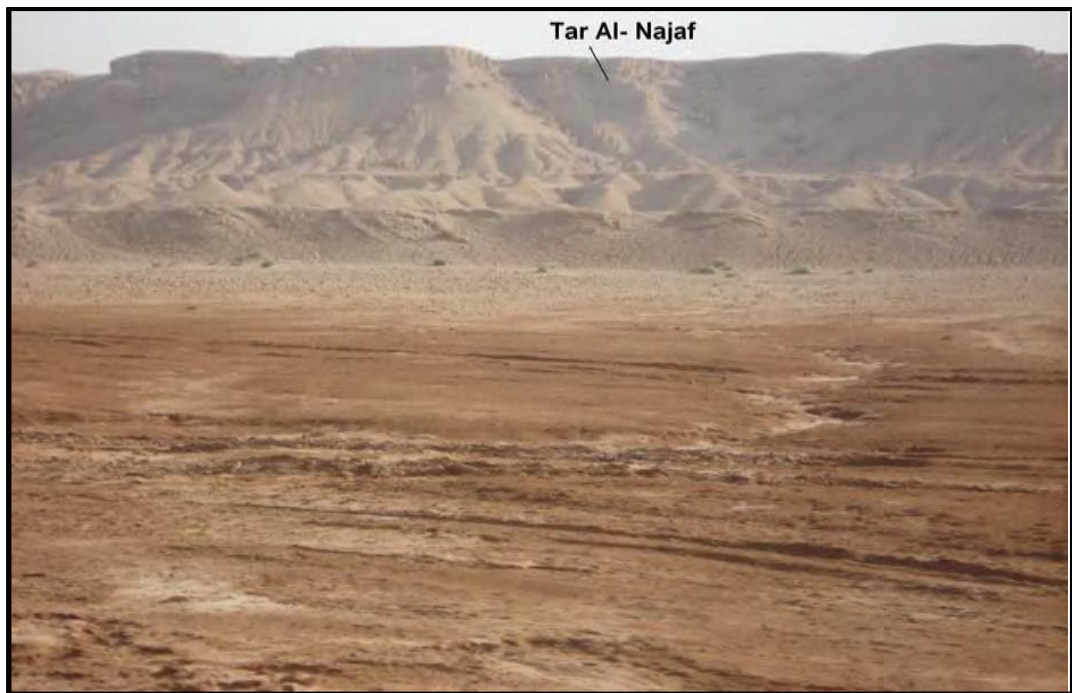
Figure 4.7: Tar Al-Najaf (Adopted by Al-Shemmari 2012)

4.4.2 Stratigraphic features of the study area

Indeed, the formations that constitute the aquifers in the region of the study area can be illustrated in Figure 4.8. According to Figure 4.8, the stratification of aquifers is formed by the old ages of soils (ancient geological epochs) and depending upon the erosion that is happened in ancient times (Barwary and Nasira 1996). Figure 4.9 will show a section that illustrates the aquifers in the study area. It will explain most of these aquifers separately.
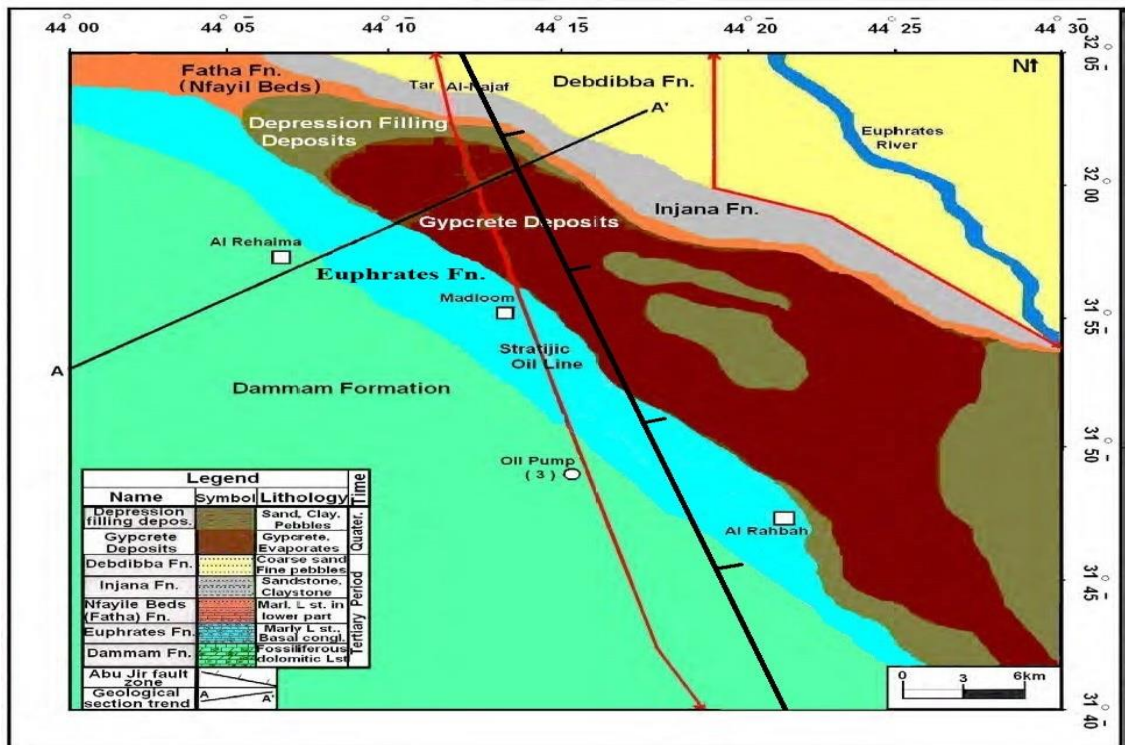
Figure 4.8: A section of the geological map of a part of the study area (Al-Najaf) (Adopted from Barwary and Nasira 1996)
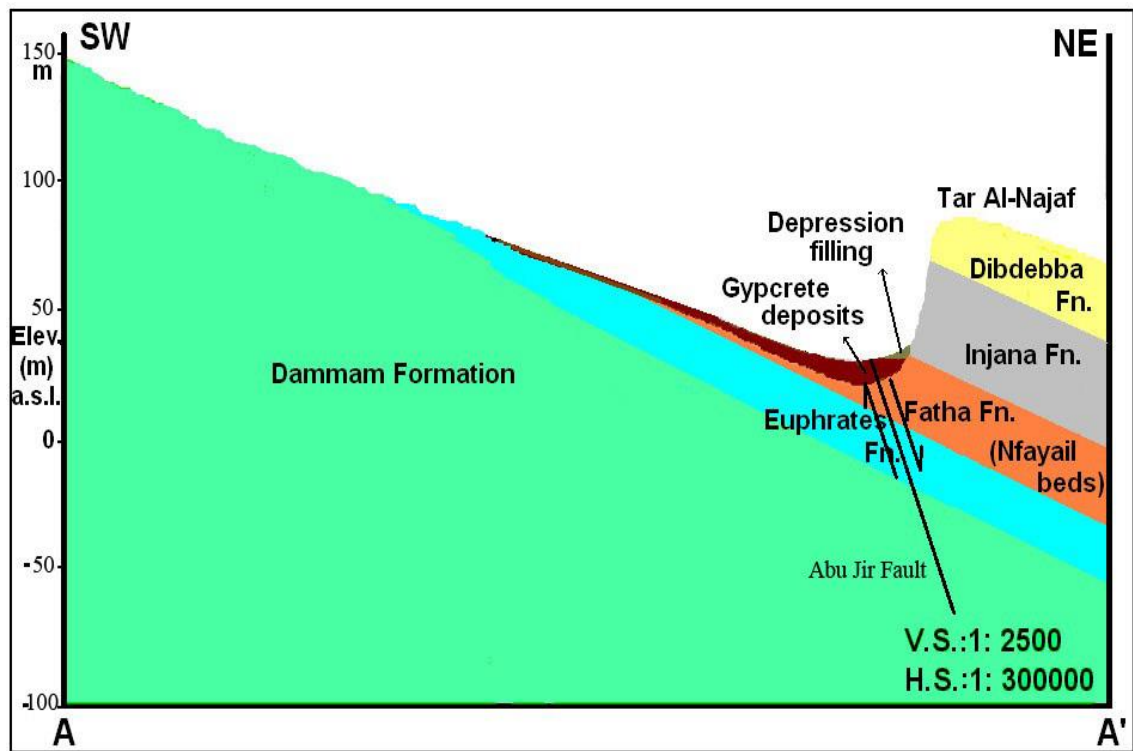
Figure 4.9: Geological cross-section along AA' in a part of the study area developed by (Adopted from Barwary and Nasira 1996)

4.4.2.1 Dibdibba formation (Pliocene – Pleistocene)

Al-Jawad et al. (2002), as it is cited in Al-Mussawy and Khalaf (2013), the main soils of this formation that are composed it, are coarse sandstone and pebbly fine sandstone. The thickness of this formation is approximately 85m. It is exposed along the ridge of Tar Al-Najaf and represents the top most part of the exposed series, so making up the area between Karbala and Al-Najaf. This formation appears again in Al-Basra and Al-Muthana Cities which are located in the southern part of Iraq with a maximum thickness reaches to about 350m (Jassim and Goff 2006).

This formation forms a large area between Al-Najaf and Karbala, it is about 29800×10^6 m^2, 3400×10^6 m^2 of this area is between Al-Najaf and Karbala provinces and 26400×10^6 m^2 is in the southern desert. The underneath formation of Dibdibba is Injana, but the upper of it is with Quaternary sediments (Jassim et al. 1984; Al-Mussawy and Khalaf 2013).

4.4.2.2 Injana formation (Late Miocene)

Barwary and Slewa (1995), as cited in Al-Mussawy and Khalaf (2013), Injana represents the second formation below Dibdibba and it generally consists of sandstone and claystone with some other soils like partly greenish silty, lenticls of grey, brownish, and yellowish sandstone. In addition, it contains thin beds of about 0.3m of marly and chalky limestone which occasionally present in the sequence. The thickness of this formation is up to 35m.

4.4.2.3 Fat'ha formation and Nfayil formation (Middle Miocene)

The lower part of Injana formation consists of two formations which are called Fat'ha formation and Nfayil formation. The thickness of both of them is up to 25m and between (15-30)m, respectively. Fat'ha formation represents one of the aerially and economically important formations in Iraq. Fat'ha formation consists of a sequence of reddish sandy calcareous claystone and brownish coarse grained sandstone, with limestone intercalations (0.2-2.0)m (Barwary and Slewa 1995). While Nfayil formation consists of green, partly reddish in sandy places, dolomaitic and gypseous marl with interbedded calcareous, partly sandy claystone and fossiliferous limestone (Al-Jaf and Al-Saady 2010).

4.4.2.4 Euphrates formation (Early Miocene)

It represents one of the most widespread formations in Iraq and belongs to the early Miocene sequence. It consists of olitic to chalky limestone which locally contains corals and shell coquinas (Jassim and Goff 2006).

4.4.2.5 Dammam formation

Dammam formation comprises of dolomites, shales, limestone (chalky, dolomitic or organodetrital), and marls. The thickness of this formation reaches to 250m. Indeed, it represents the most important aquifer in the south west part of Iraq. Jassim and Gaff (2006) characterized this formation as one of the formations which have a highest transmissivity and permeability in most area of it because of the presence of karastified and cavities canals, joints and fissures, as well as fractures.

4.4.3 Aquifer of groundwater in the study area

As a consequental of the previous information, Dibdibba, Injana, Euphrates, and Dammam formations are considered the main geological aquifers in the study area which are containing groundwater. According to the data collected, indeed, the deepest boreholes (Wells) in the study area from the whole number of the wells which are injected in the study area are used to find the thickness, extension, and stratigraphy of the aquifer which will be used as the aquifer that will provide groundwater in Al-Najaf study area.

Figure 4.10 shows the locations of the deepest boreholes in the study area and the direction of the geological section which is (A-A'). Figure 4.11 demonstrates the stratigraphy of aquifers, thicknesses of each aquifer, elevations of boreholes, and the distance between boreholes.
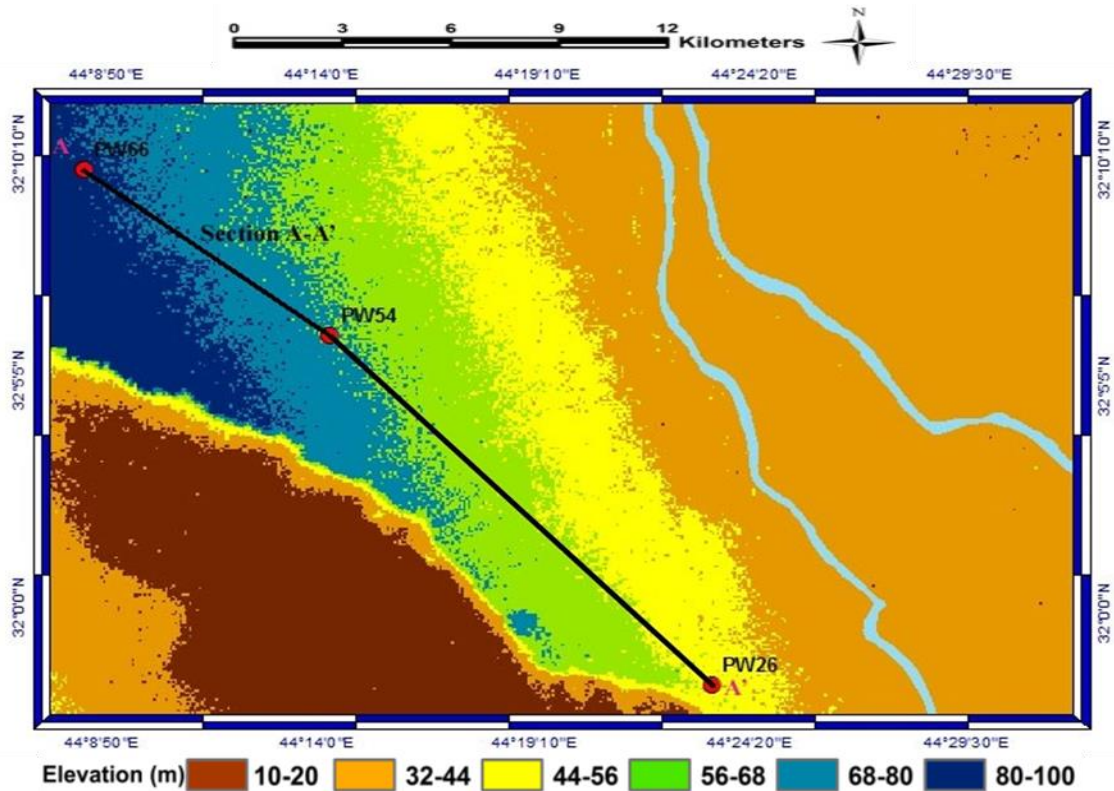
Figure 4.10: Locations of the deepest boreholes in the study area
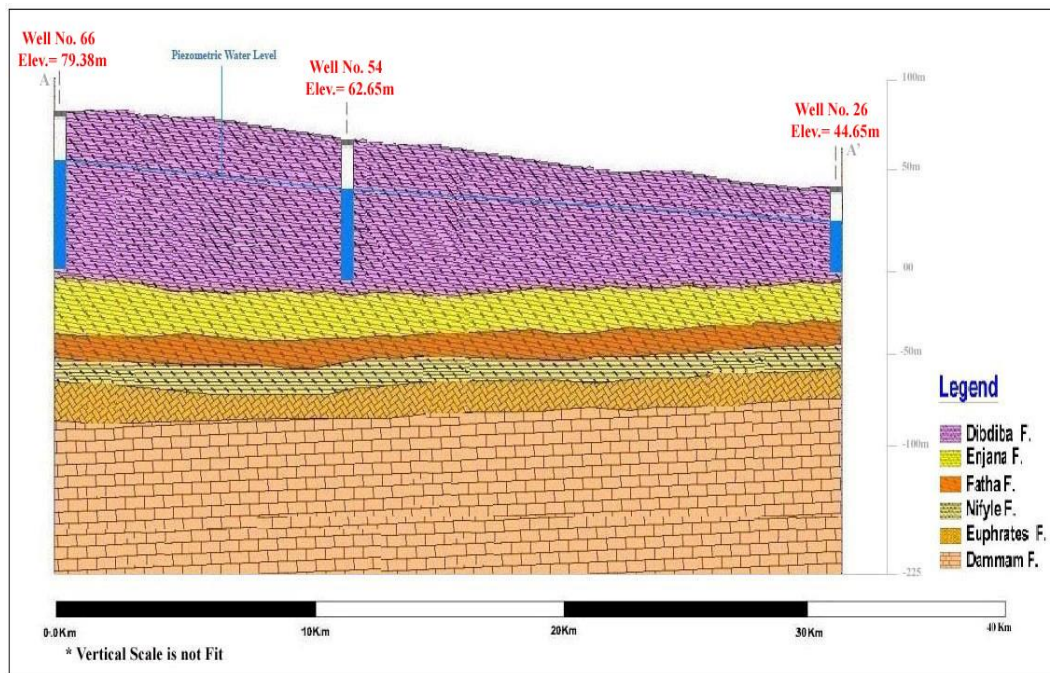
Figure 4.11: Cross-section A-A' through the deepest boreholes in the study area (GEOSURV 2015)

According to section (A-A'), which is illustrated in Figure 4.11, boreholes (Well No. 26, Well No. 54, and Well No. 66) are representing the deepest wells. Therefore, this means that the aquifer that will be presented or considered to be the aquifer that should be studied within the

study area is Dibdibba aquifer or Dibdibba formation. Collected data shows that Dibdibba formation comprises of two layers and it is considered as unconfined aquifer. These layers are coarse sand (Top layer) and fine pebbles (Bottom layer) with conductivities equal to 1.67e-4 m/s and 1.98e-4 m/s, respectively (GEOSURV 2015).

4.4.4 Dibdibba aquifer soil properties

The layers of the groundwater Dibdibba aquifer in the study area are two. The first one (Top) is coarse sand, with a conductivity equals to 1.67e-4 m/s, and the second (Bottom) one is fine pebbles, with a conductivity equals to 1.98e-4 m/s. The hydraulic conductivities which are corresponding to these values in m/day are 14.43 m/day and 17.1 m/day for the Top and Bottom layers of the aquifer respectively (GEOSURV 2015).

4.5 Hydrogeological properties of the study area

The movement of groundwater in all the regions in Iraq as well as to the groundwater levels can be shown in the hydrogeological map in Figure 4.12. The hydrogeological map illustrates that the movement of the groundwater for the whole area of Al-Najaf province is from the western part to the eastern part as it is illustrated in the hydrogeological map shown in Figure 4.12 and it is the same for the area of study. The movement of groundwater over the study area is longitudinally with levels of 50 m and 20 m on the western and eastern sides respectively; therefore, the boundary conditions represented by the constant heads over the study area will be represented by these levels. The other hydrogeological data such as temperature, rainfall, daily rainfall, soil moisture, change in soil moisture, sunshine duration, radiation, potential evaporation totals, wind speed, and relative humidity which are related to Al-Najaf province are collected from the Iraqi Ministry of Transportation (MOTRANS 2015) for the period (1980 – 2014) and inserted in Appendix C in the Tables C.2 through C.11. Some of these data need to be processed to find other factors that affected the study area such as finding the recharge rate that should be implemented on the area of study.
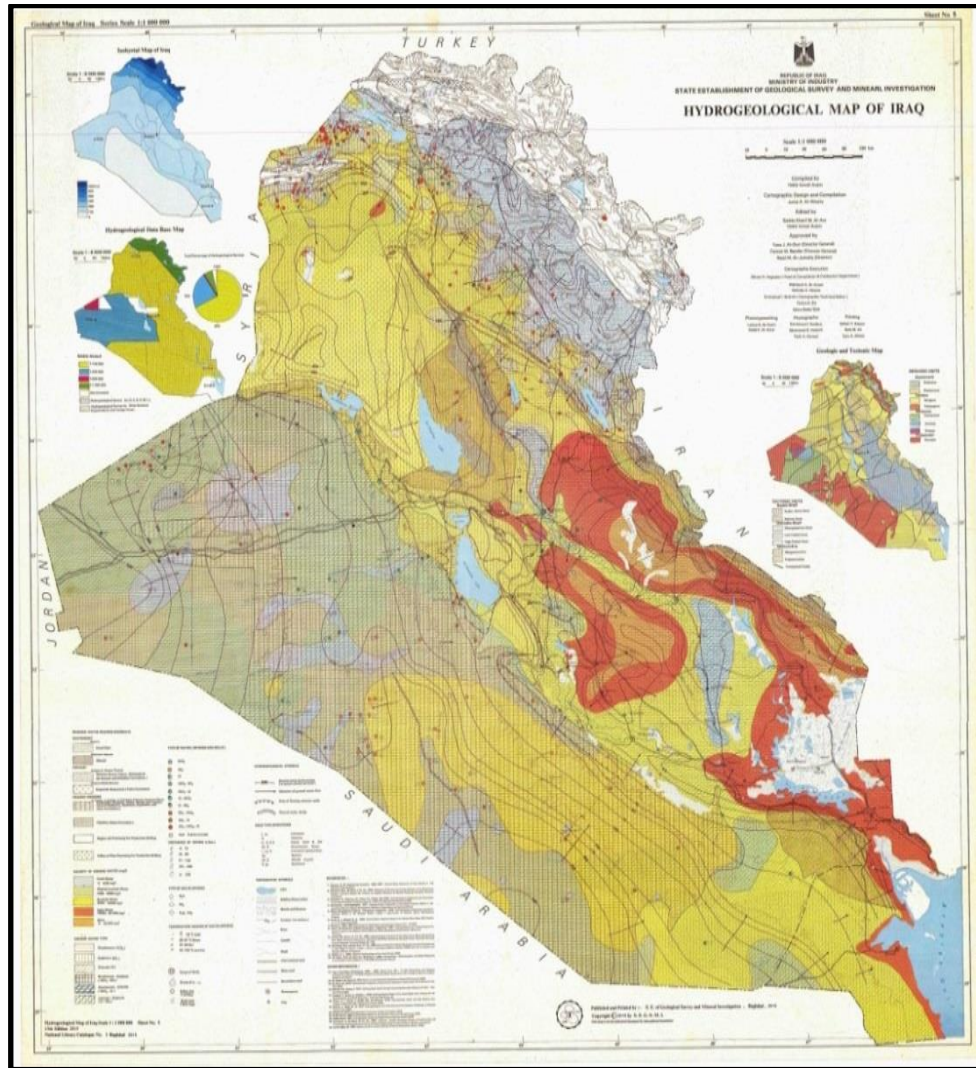
Figure 4.12: Hydrogeological map shows the elevations of groundwater in Iraq (Adopted from GEOSURV 2015)

4.5.1 The Euphrates River

It was mentioned that the Euphrates River passes through the eastern side of the study area with two branches. Therefore, due to the bifurcation of Euphrates River in the study area, it requires the boundary conditions at both sections to be specified separately. The details of those conditions are given in TABLE 4.1 for both branches of Euphrates River (MOWR 2015).

Table 4.1: Conditions for Euphrates River used in the model

Branch	Water Elevation		Bed Elevation (m)	Bed layer Thickness (m)	Width (m)	Hydraulic Conductivity (m/d)
	Northern end (m)	Southern end (m)				
Western	24.65	21.05	19.2	0.6	174	0.364
Eastern	24.55	21.35	19.2	0.6	99	0.300

4.5.2 Observation and pumping wells

The total number of the observation and pumping wells in the study area is 69 wells and these wells imported into the model using an excel sheet file with all the information needed (well number, easting, northing, well ID, pumping rates, and dynamic and static water levels). The details of these wells are illustrated in Appendix C in Table C.1 (GEOSURV 2015).

4.5.3 Meteorological data

Most of the meteorological data collected to address the groundwater system in Al-Najaf region study area is provided by the ministry of transportation, Iraqi meteorological organization and seismology (MOTRANS 2015). The only station available in Al-Najaf province is Al-Najaf province meteorological station which is located in the Western Sahara of Al-Najaf province at a distance of about 40 km from the western border of the study area. The analyses of the collected data shown in Tables C.2 through C.11 in Appendix C will be briefly described in this part.

4.5.3.1 Rainfall

Rainfall data analysis represents an important issue for different domains such as water resources planning and management, agricultural planning, steam flow estimation, runoff prediction, climatological studies, and environmental studies (Subramaya 1984; Hatzzian et al. 2007). Where, the quantity, distribution, and intensity of rainfall are representing the most crucial parameters in many hydrologic studies (Mutreja 1990; Juny et al. 2001). Figure 4.13 shows the mean monthly and yearly values of rainfall which falls on Al-Najaf province for the period 1980-2014. Clearly, it can be seen from Figure 4.13, the rainfall is always enclosed between January and April period, and, October and December period, where the highest values are in January, February, March, November, and December, while the lowest values of rainfall are in April and October. The other months from May to September (some of Spring and Summer season months), there is no rainfall in these seasons or completely rare. In addition, Figure 4.13 shows that the average rainfall value is oscillating over the period 1980-2014 where the lowest and highest values were in 1990 and 2006 respectively. Moreover, most values of rainfall are ranged between 5mm and 10mm yearly except for some years which are higher or lower, where this represents that Al-Najaf province was suffering from the lack of rainfall.
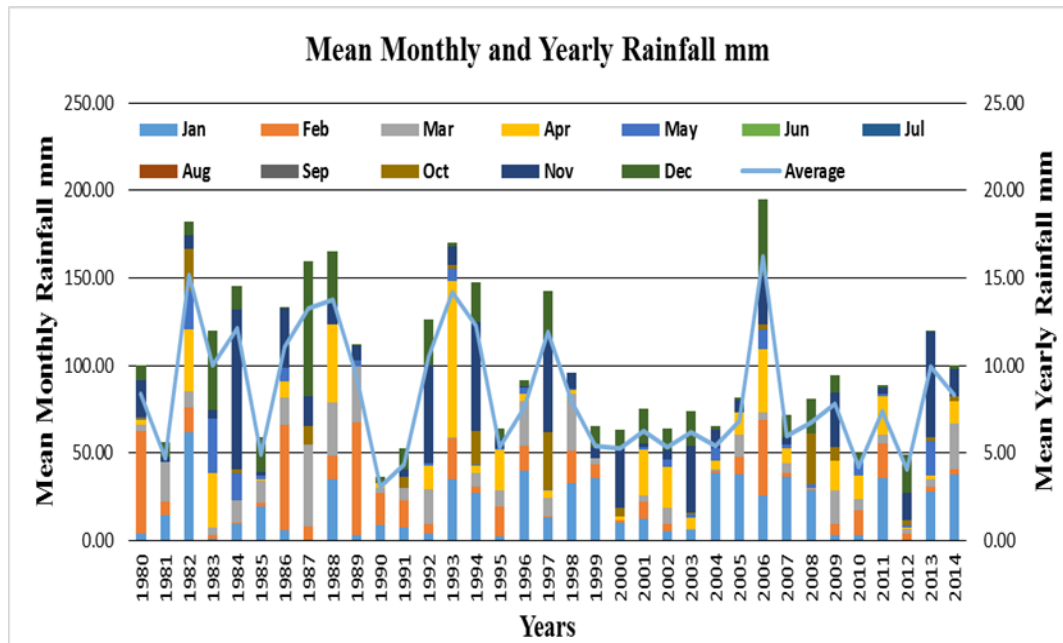
Figure 4.13: Monthly and yearly mean values of rainfall for the period 1980-2014

4.5.3.2 Temperature

Figure 4.14 shows the average monthly temperature ^{0}C over the period 1980-2014. It can be obviously seen that July and August temperatures are ranged between 40 ^{0}C and 50 ^{0}C and sometimes become very close to 50 ^{0}C. Where in the reality these values are the monthly mean and this explains that the daily temperatures maybe reach greater than 50 ^{0}C so this will add a great impact on the study area in terms of evapotranspiration increase which in turns lead to an impact on the groundwater resource. In addition, from Figure 4.14, April, May, June, September, and October have a temperature between 30 ^{0}C and 40 ^{0}C where sometimes become below this range in April and October. While the other months January, February, March, November, and December are ranged approximately between 8 ^{0}C and 25 ^{0}C. Overall, the average temperatures over the period 1980-2014 for all months is approximately 30 ^{0}C per year where this value is high and will affect the study area through increasing the evapotranspiration which will lead to increasing the dryness.
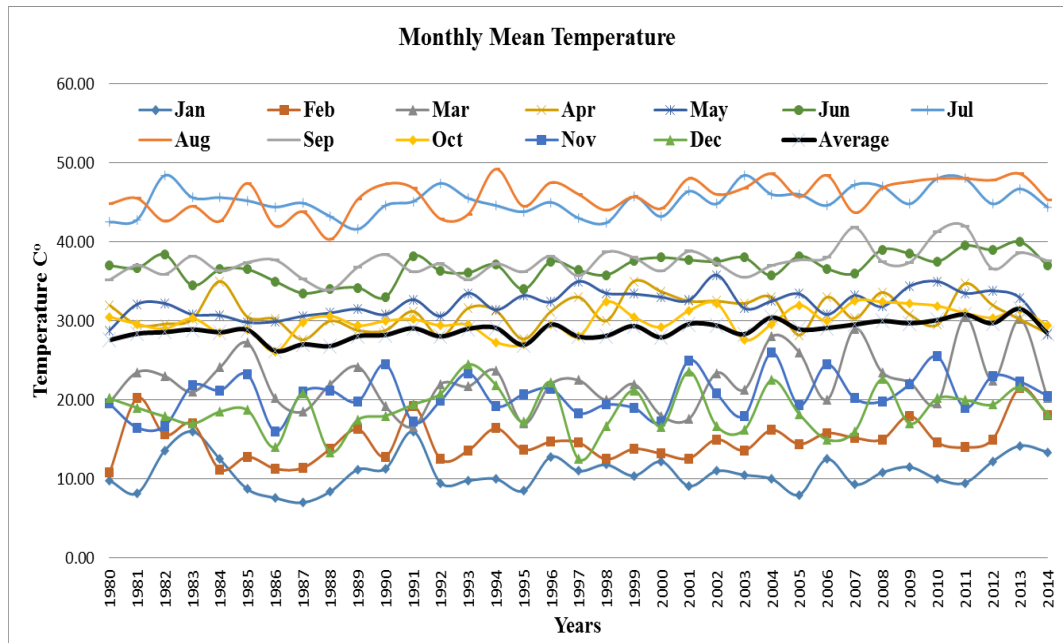
Figure 4.14: Mean monthly temperature over the period 1980-2014

4.5.3.3 Potential evaporation

Evaporation is the most important parameter in the hydrological cycle where any increase in the temperature will lead to increasing the evaporation rate. However, evaporation parameter is also affected by wind speed, humidity, radiation, and water availability (Thompson and Perry 1997; Al-Muqdadi 2012). In addition, evaporation represents the quantity of water which is actually evaporated on a normal day and this means if the soil emerged the water out, the actual evaporation will be the quantity of water which has been evaporated and not that quantity which could be evaporated when the soil has an infinite quantity of water to evaporate daily (Zahraa 2016). For many years, there were difficulties in measuring the evaporation and transpiration from the open water surface which led to misunderstanding the hydrological cycle. However, these difficulties together with the ambiguous results from different types of instruments led to developing empirical techniques which can easily estimate the evaporation by using the available climatic data (Dawod et al. 2006). According to the (MOTRANS 2015), potential evaporation is measured by using Pan Class A. Figure 4.15 illustrates the mean monthly and yearly evaporation for the period 1980-2014. It can be seen that the monthly evaporation in June, July, August, and September has the largest values as compared with the other months. In addition, overall values of evaporation over the year's months are too large where the least and highest values over the period 1980-2014 are approximately 2400mm (2.4m) and 4250mm (4.25m) yearly respectively where this means that there is a high impact on the groundwater and surface water resources. In respect of the mean yearly evaporation, Figure 4.15 shows that the evaporation is increased significantly in the last 9 years (2006-2014) as compared with the

previous ones. Where, it is increased from about 200mm in 1980 to be greater than 350mm in the period 2006-2014. Over the period 1980-2005, the peak evaporation events were only three events in 1985, 1990, and 1996 and were approximately 325mm, while the peak events over the period 2006-2014 have been happened each year when compared the evaporation values of these years with the previous peaks, where the least evaporation of these years was equal to 325mm.
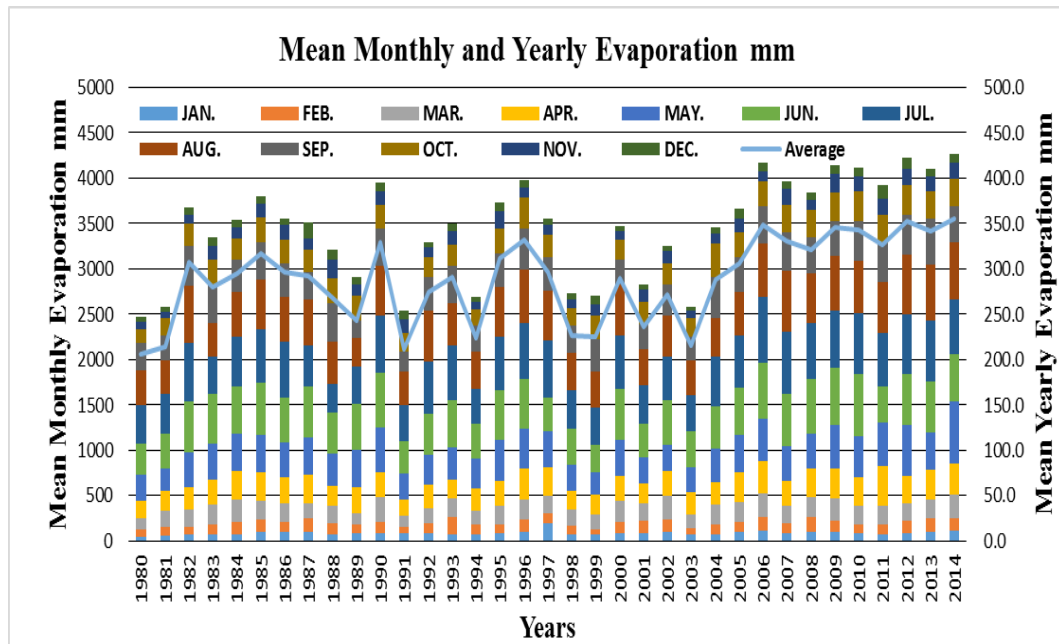
Figure 4.15: Mean monthly and yearly potential evaporation over the period 1980-2014

4.5.3.4 Soil moisture

Soil moisture content represents the ratio of the present water weight of soil to the dry weight of soil, this is if it is expressed by weight, but if it is expressed by volume, it will be the ratio of water volume in the soil mass to the total volume of the soil mass. The variable key in the climatic system is the soil moisture where it represents an important parameter for water and energy storage in the regional climatic system (Seneviratne et al. 2006). In addition, due to the spatial and temporal variations in the soil moisture, the attention in the climate studies is increased because soil moisture represents an essential element that can effect the biogeochemical and ecosystem cycles in the land atmosphere system through participating in the derivation of energy fluxes and land water surface (Xi and Qi 2004). Figure 4.16 and Figure 4.17 show the values of the soil moisture in Al-Najaf province and the change in the soil moisture in each month over the period 1980-2014 respectively. From Figure 4.16, it can be seen that the soil moisture values are oscillating over the year's months through the period 1980-2014 and this is because soil moisture has affected by other parameters such as rainfall, temperature, evapotranspiration rate, and others. In addition, the overall trend of soil moisture is

declined dramatically over the period 1980-2014 where in 2014 the soil moisture values did not exceed 30mm as compared with the beginning values which were greater than 60mm. Moreover, from Figure 4.16 seen that there are only two peaks for soil moisture, both of them were in 1983 in March and April months.
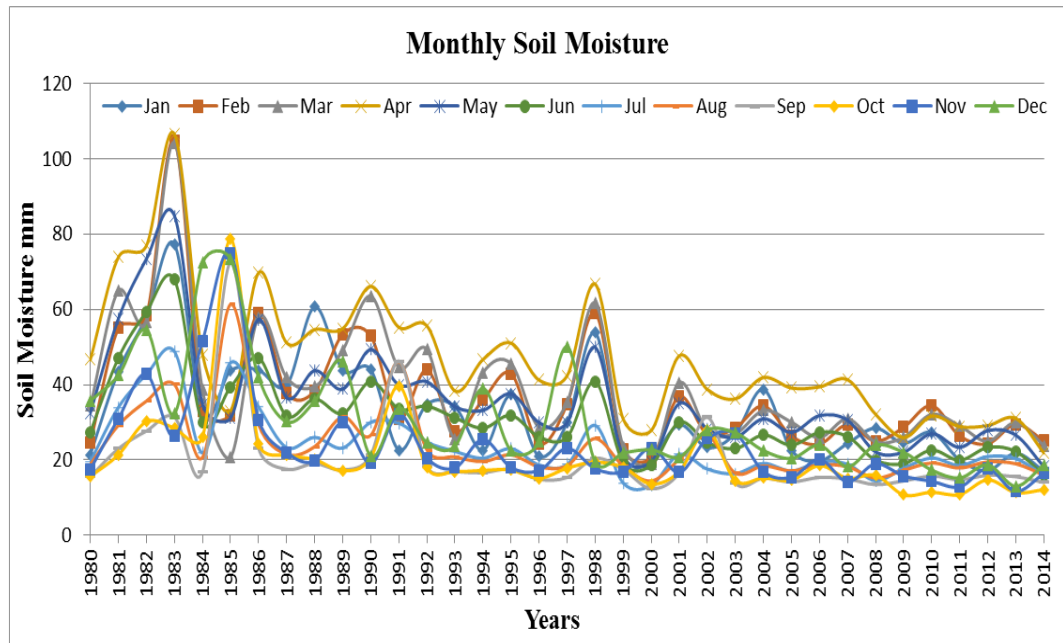
Figure 4.16: Monthly soil moisture over the period 1980-2014

Figure 4.17 shows the change in monthly average and yearly total soil moisture values for the period 1980-2014. Clearly from this figure, it can be seen that there are some values of soil moisture are negative and some are positive for a specific year. The negative value of soil moisture means that the soil mass will feed itself from the groundwater system during the dry seasons, while the positive value means that there is an abundance or surplus water in the soil mass that can move to feed the groundwater system during the wet seasons. In addition, Figure 4.17 shows that the trend of the soil moisture summation curve is declining significantly in the last decade 2004-2014 to give approximately the least values of soil moisture. Moreover, from the summation curve of the soil moisture seen that only 18 years have been fed the groundwater aquifer in Al-Najaf province as compared with the others which were consuming some of the aquifer's water to compensate the drought in soil mass.
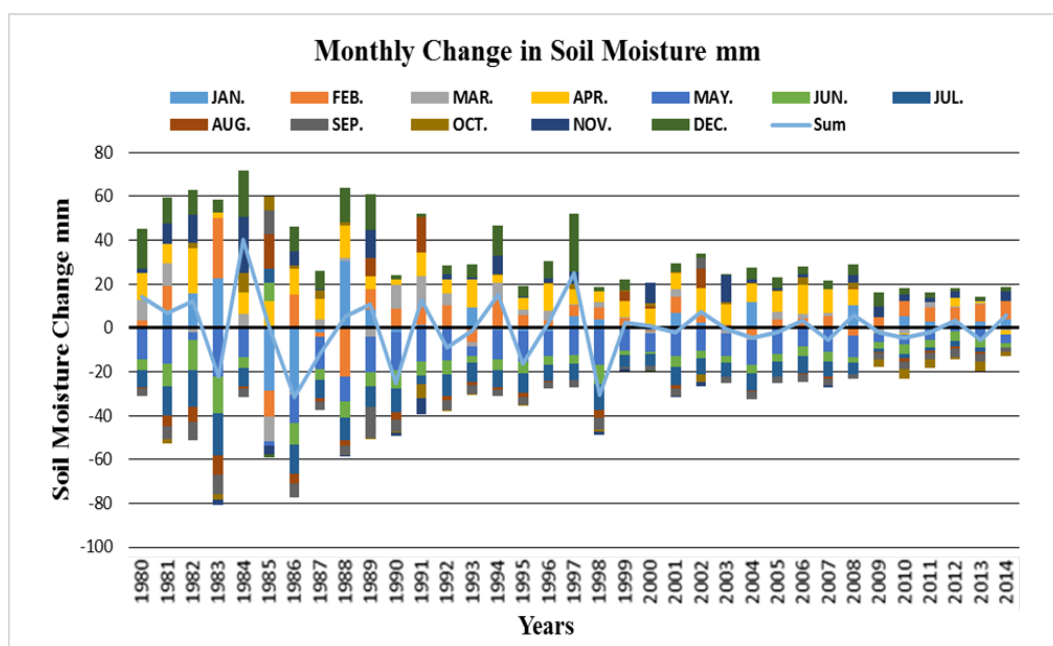
Figure 4.17: Monthly soil moisture change with the total summation over the period 1980-2014

4.5.3.5 Relative humidity

Relative humidity represents the ratio of the actual water vapour quantity in the air to the maximum required water vapour quantity which can saturate at the particular temperature or it is the air water vapour content to its capacity ratio (Ahrens 2007; Al-Muqdadi 2012). Figures 4.18 and 4.19 show the mean annually and monthly values of relative humidity over the period 1980-2014, respectively. From the annual average values shown in Figure 4.18, it can be seen that most values of relative humidity are low (less than 50%) and this explains that the atmosphere of the area of study is dry for some extent where only one year 2009 exceeds the 50%. Where, the maximum and minimum values are in 2009 (51.42%) and in 1984 (36.17%) respectively. From the monthly mean values shown in Figure 4.19, it can be seen that when the temperature increased during the Spring (April, May, June) and Summer (July, August, September) seasons, the relative humidity is decreased dramatically from approximately 70% to be 25% in July. This indicates why the study area is classified as an arid area where when temperature increases, the relative humidity decreases and this will dry the climate and add an impact on the sources of water through increasing the evapotranspiration.

Mean Yearly RH %
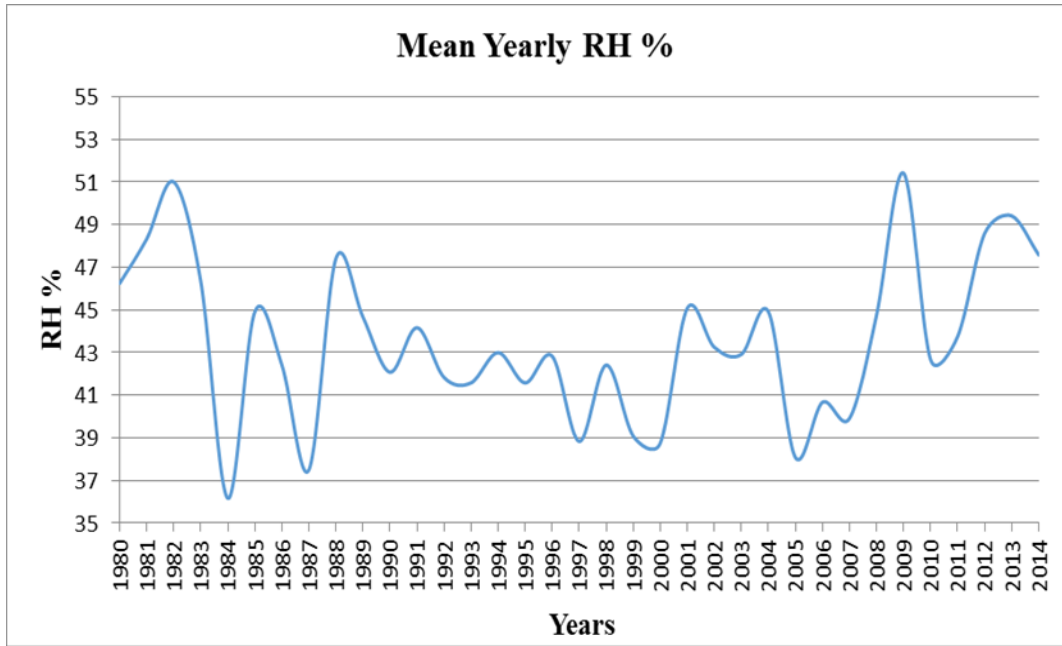
Figure 4.18: Annual mean of the relative humidity over the periods 1980-2014

Mean Monthly RH %
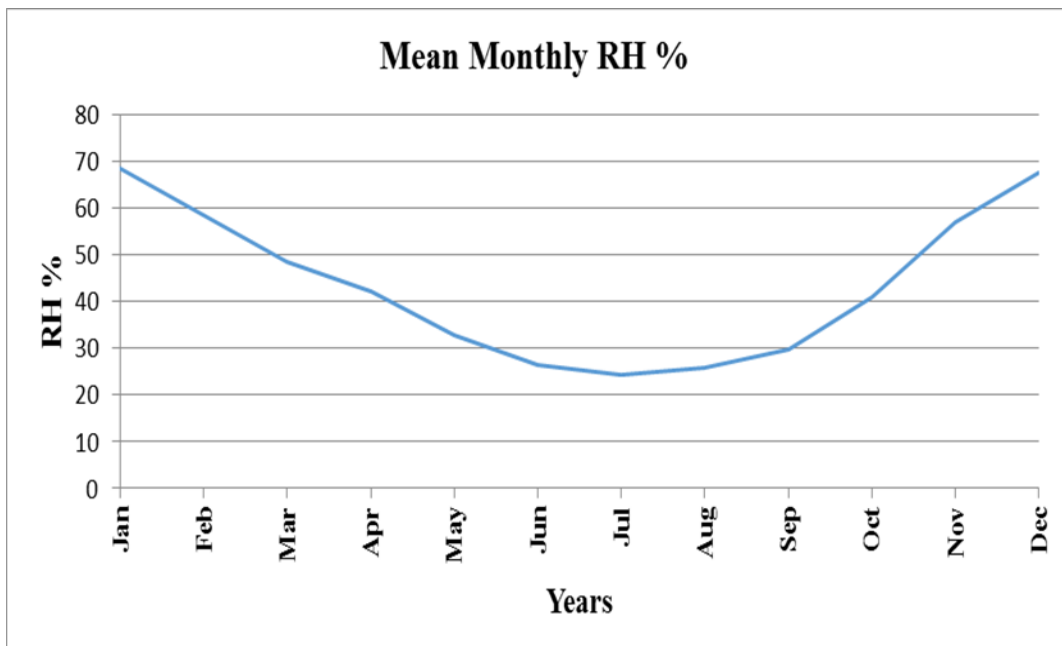
Figure 4.19: Monthly mean of the relative humidity over the periods 1980-2014

4.5.3.6 Wind speed

Wind is a natural three-dimensional vector which has different directions. Where, it represents one of the well-known and crucial factors that causing erosion (Ahrens 2007; Al-Muqdadi 2012). Around the study area and during the year, wind is blowing from north, north-west, and west directions (Consortium-Yugoslavia 1977). Figure 4.20 and Figure 4.21 are showing the annually and monthly mean wind speeds over the period 1980-2014 respectively. From Figure

4.20 seen that the average range of wind speed for the period 1980-2014 is approximately between 1.5 m/s and 3 m/s where the overall trend shows that wind speed is reduced in its intensity in the last decade. It is obvious from Figure 4.21 that again in Spring and Summer seasons, the wind speed is higher than the other seasons as a result of the drought and high temperatures.
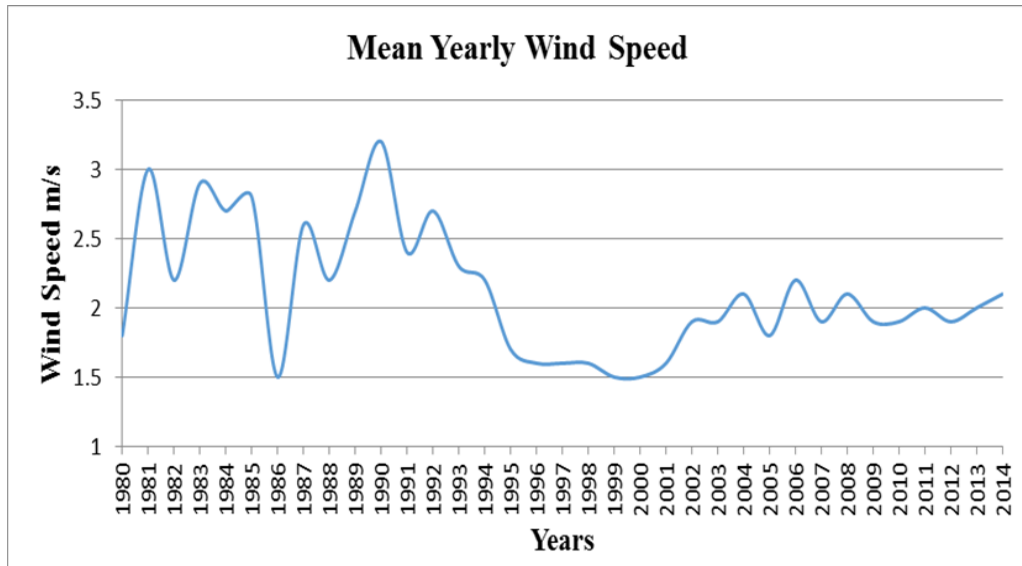
Figure 4.20: Annual mean of wind speed in m/s over the period 1980-2014
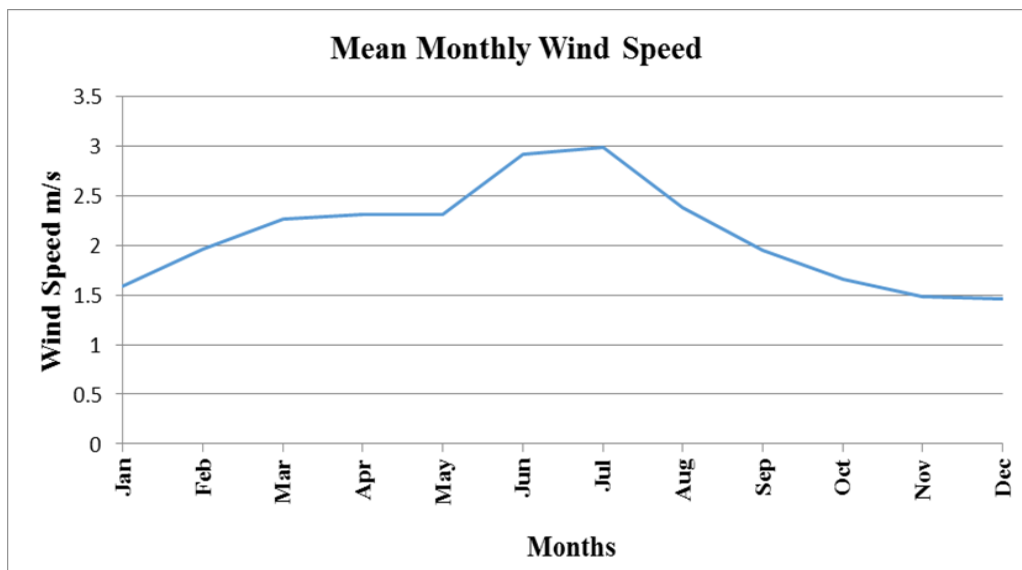
Figure 4.21: Monthly mean of wind speed in m/s over the period 1980-2014

4.5.3.7 Radiation

Earth's surface sunlight or solar radiation represents the main source of energy in the climate system as well as the key component for the life on the planet where it plays an important role in the Global Energy Balance (Trenberth et al. 2009). Radiation quantity arrives the earth surface various dramatically due to the position change of the sun during the day and the change

in the atmosphere conditions (Kurt and Frank 2006). Because of the solar radiation power represents an alternative way to produce photovoltaic cells and electricity, it becomes rapidly common method (Chandal et al. 2005). In Iraq, the stations that are measuring the global solar energy are few and need to increase the pyrometers at many locations of a given area to record more data (Tadros et al. 2014). Figure 4.22 and Figure 4.23 illustrate the solar radiation values per year and month respectively for the period 1980-2014. Most yearly values of the solar radiation shown in Figure 4.22 are significantly high where it ranges between 400 Mw/cm^2 and 575 Mw/cm^2 except for year 2000 which was 368 Mw/cm^2. The peak value as shown in Figure 4.22 was in 2004 and it was 566.5 Mw/cm^2. From Figure 4.23, it can be shown that in Spring season, Summer season, last month on Winter season, and first month on Autumn season, solar radiation produced large values because of the long exposure to sunlight and heat power in solar radiation, which produces a huge amount of solar energy.
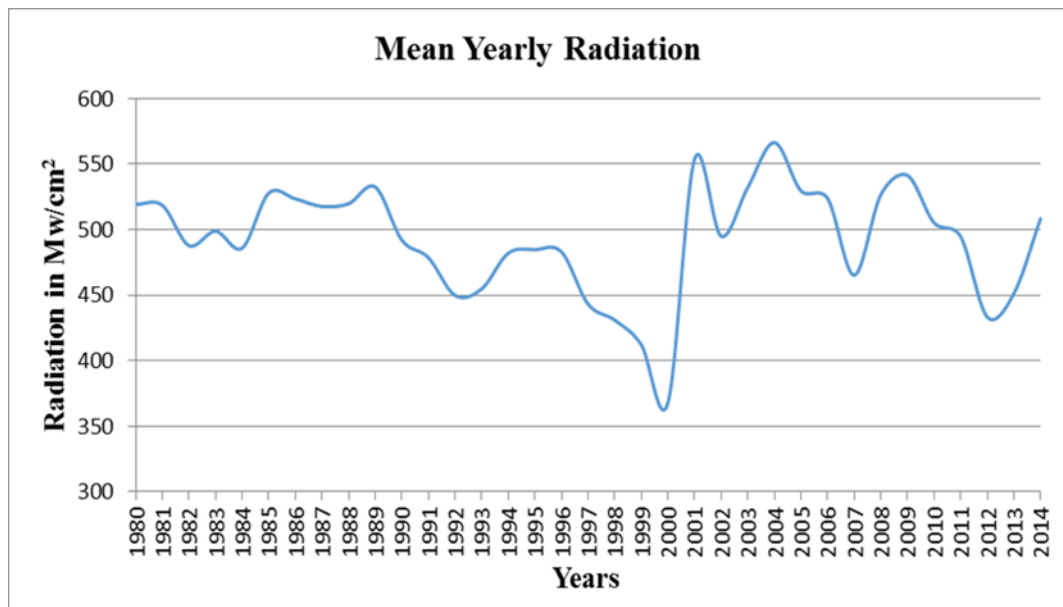
Figure 4.22: Annual mean radiation in Mw/cm^2 over the period 1980-2014
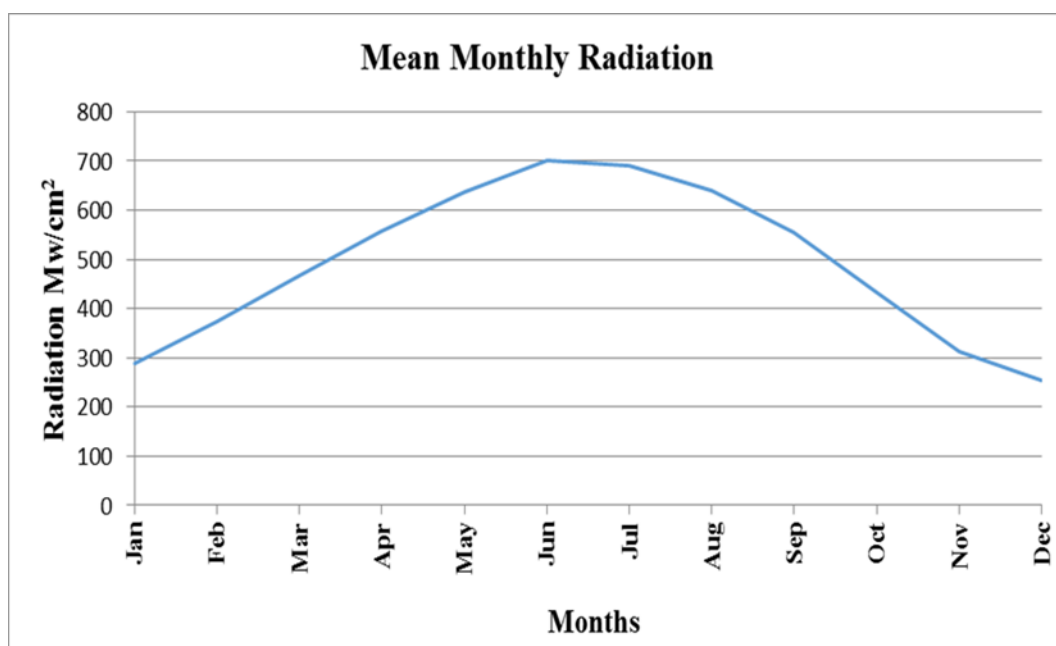
Figure 4.23: Monthly mean radiation in Mw/cm^2 over the year's months for the period 1980-2014

4.5.3.8 Sunshine duration

According to GAW (Global Atmosphere Watch) and WMO (World Meteorological Organization) (2003), sunshine is defined as the period in which the direct solar radiance exceeds the threshold value which is 120 W/m^2. Where, to estimate the potential solar energy, it needs to collect the information about the solar radiation data which is essential for designing the system of the solar energy conversion (Bekele 2009). When the solar radiance averages 1 kw/m^2, the peak sun hour (PSH) will be considered and it will be equivalent to the number of hours per day that have been exposed to sunshine at the averaged point (MOST 2006). Figure 4.24 and Figure 4.25 show the average values of sunshine per year and month respectively. Sunshine ranges between approximately 7.5 h/d and 9.5 h/d over the period 1980-2014, as shown in Figure 4.24. The peak values were in 1985, 1990, and 1998 and it was 9.3 h/d, while the minimum value was in 1992 and it was 7.4 h/d, as it is illustrated in Figure 4.24. From Figure 4.25, it can be seen that the maximum values of the monthly mean sunshine hours are in Spring and Summer seasons (greater than 8 h/d) where in these seasons the daytime is longer than the night as compared with the other seasons, Winter and Autumn. Exposure to long periods of sunlight will lead to increasing the impact on the existing sources of water such as surface water and groundwater.
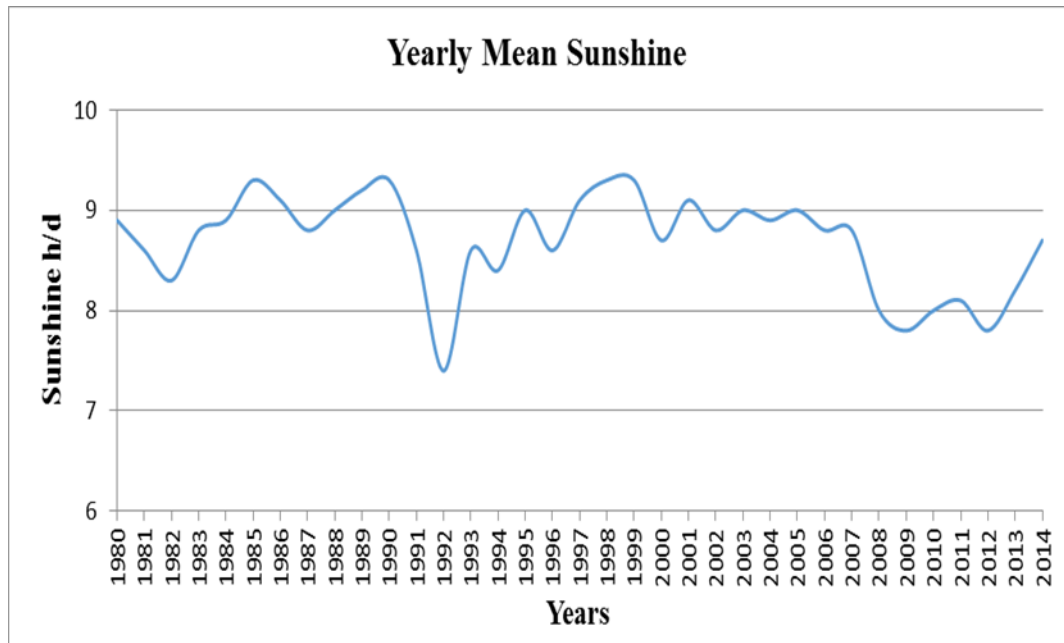
Figure 4.24: Annual mean sunshine duration in h/d over the period 1980-2014
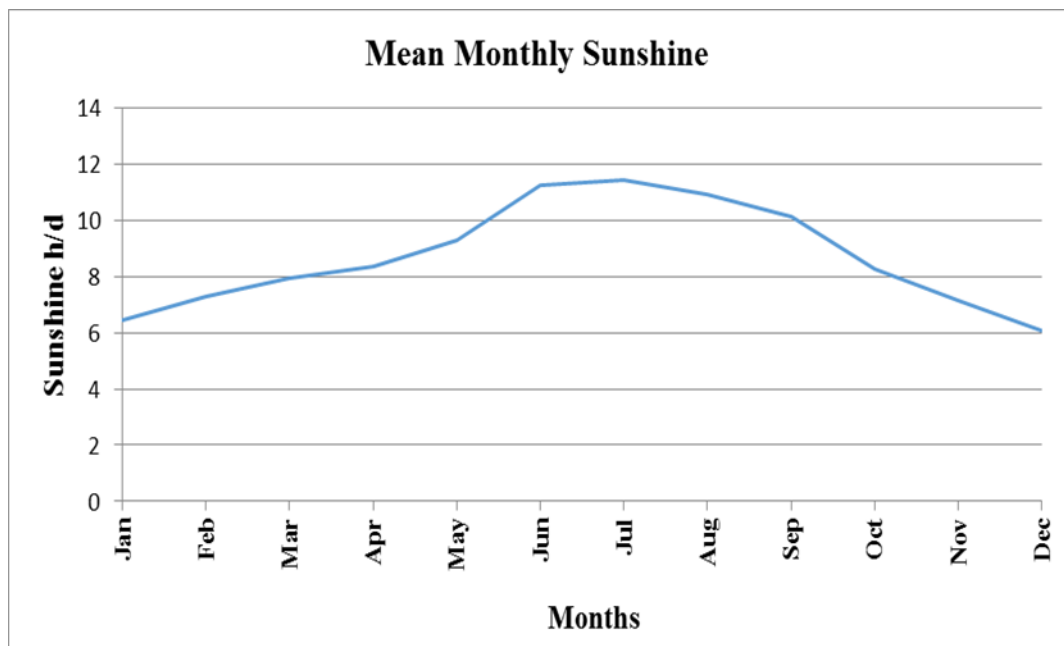
Figure 4.25: Monthly mean sunshine duration in h/d over the year's months for the period 1980-2014

4.5.4 Water balance and recharge rate

Water balance describes the quantity of water flow IN and OUT from an aquifer which are produced through the zone budget. The budget of a zone can be considered as a column of soil or a drainage basin. Water balance has assumed that the input and output are equal and any change for one of the parameters that represented by the input or output will lead to a change in storage (ΔS) as shown in Eq. (4.1) (Al-Muqdadi 2012).

$$\text{Input (R) } - \text{ Output (PET + RO + } \Delta\text{SM)} = \text{Storage change (} \Delta\text{S)} \qquad (4.1)$$

Rainfall (R) is considered as the only input over the study area, while Potential Evapotranspiration (PET), Runoff (RO), and change in soil moisture content (ΔSM) will be the outputs. The aquifer in the study area relies only on the precipitation or rainfall as the main recharge for it. An accurate estimation of this parameter is very important for different hydrologic type's assessments such as modelling of groundwater flow, contaminant or solute transport, protection of water quality, and many more. The estimated recharge represents the key for understanding various development effects in industrial, urban, and agricultural areas. Recently, the hydrologic assessment demand is increased to support the decisions of management in different aspects of life and this leads to increasing the need for practical methods and ways to estimate recharge rates and finding zones with the similar value of recharge (Scanlon et al. 2002).

Generally, there is a net groundwater recharge (RGW) that can be extracted through making the balance between the quantity of water that input to the groundwater system and the output water from it. First of all, it needs to classify the area of study in respect of climate to identify whether the area of study is arid or semiarid area. Where, Aridity Index represents the parameter which can be used to classify the study area.

4.5.4.1 Aridity Index

According to the United Nations Environment Programme (Middleton and Arnold 1997) that has adopted an aridity index which is defined by the Eq. (4.2) and shown in Table 4.2:

$$I_i = R/PET \qquad (4.2)$$

where, PET is the potential evapotranspiration; and R: average monthly precipitation or rainfall.

Table 4.2: Index of Aridity (Middleton and Arnold 1997)

Climate Type	Aridity index range
Hyper-arid	< 0.05
arid	0.05 – 0.2
Semi-arid	0.2 – 0.5
Dry sub-humid	0.5 – 0.65

According to the collected data which are illustrated in Tables C.3 and C.9 in Appendix C (Rainfall and Potential Evaporation Totals respectively), it is noticed that the area of study is considered as an arid climate type.

4.5.4.2 Recharge into groundwater calculations (RGW)

Calculated the net groundwater recharge represents a crucial point of the parameter inputs for the groundwater model especially for the areas depending only on rainfall. Therefore, to calculate this parameter, it needs to find and calculate four parameters, which are vegetation index, actual evapotranspiration, soil moisture, and runoff as shown in the network frame Figure 4.26.
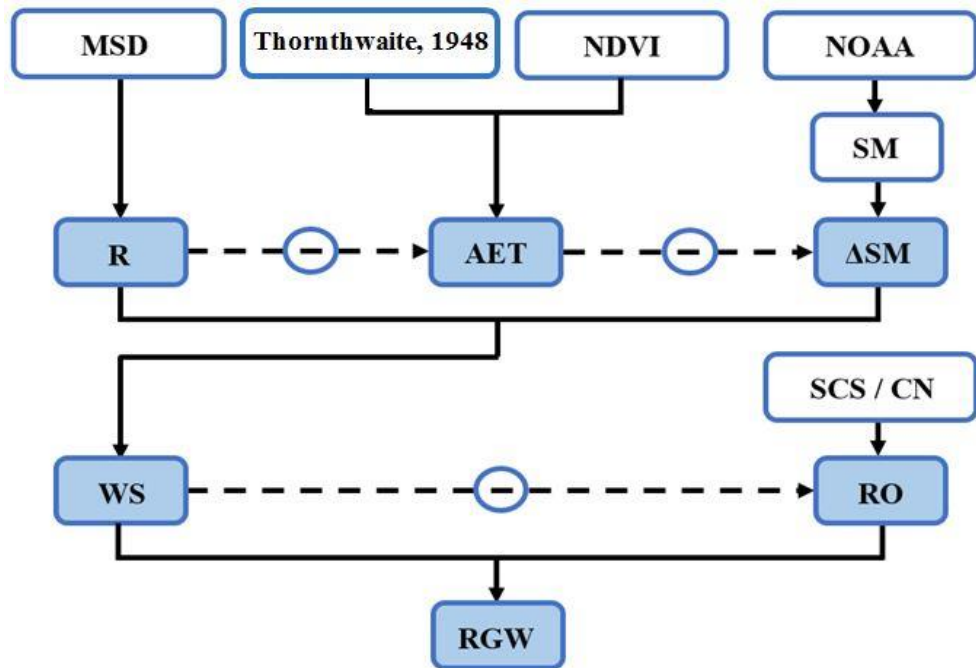
Figure 4.26: Frame for calculating groundwater recharge

where, MSD: meteorological station data (Al-Najaf meteorological station); NDVI: normalized difference vegetation index; NOAA: National Oceanic and Atmospheric Administration; SM: soil moisture content; R: Rainfall; AET: actual evaporation and evapotranspiration; ΔSM: change in soil moisture content; SCS: soil conservation service; CN: curve number; WS: water surplus; RO: runoff; and RGW: groundwater recharge.

1. Vegetation Index

To assess water use, biomass, plant stress, crop production, and plant health, it needs to calculate the vegetation indices through using the remote sensing technique because nowadays these indices are widely used and have numerous benefits in different disciplines (Jackson and Huete 1991). The Normalized Difference Vegetation Index (NDVI) represents a good measure for the vegetation cover over the ground surface for wide regions. NDVI is also recognizing the water and ice for the areas without vegetation cover (Reading University 2002).

To calculate the NDVI, it needs to download Thematic Mapper (TM) data with band 3 (Red) and band 4 (Near Infrared, NIR) and then processing it by using the GIS program through using the following Eq. (4.3):

$$NDVI = \frac{NIR - Red}{NIR + Red} \qquad (4.3)$$

The Thematic Mapper of the study area has been downloaded from the "Global Land Cover Facility" GLCF http://www.landcover.org/data/landsat/ website as a "Landsat Imagery" and processed using the GIS software. Results show that the minimum NDVI was (-0.6363) and the maximum was (0.4473) while the mean was (0.00588). Since the mean NDVI value was less than (0.1), this means, generally between (-0.1 – 0.1) corresponds to barren areas of sand, snow, or rock (Cohen and Shoshany 2002). Therefore, the impact of evapotranspiration from the crops in the study area has been neglected because the study area shows that it lacks for vegetation cover or has a very small transpiration value does not constitute a significant effect so it can be neglected. Consequently, transpiration from the crops' cover land will be neglected because its effect on the calculations will be very small and imperceptible.

Actually, in arid areas, rainfall is not meeting the water demand for growing plants because it is insufficient whereas the rainfall to transpiration ratio may be less than (0.1) (Domenico and Schwartz 1998). Due to no vegetation cover in the study area is investigated (NDVI-less than 0.1), thus, the parameters of the total evaporation (PET) = actual evaporation (AE), the runoff (RO), and the change in soil moisture content (ΔSM) shown in Eq. (4.1) will represent the only output quantities from the model.

2. Actual evaporation (AE)

Due to the increasing use of the irrigation over farmlands and also discharging water from the soils with high levels of groundwater, estimating evaporation has become a crucial parameter during the recent decades. An accurate estimation of evaporation represents a very hard process either due to unsecure parameters that should be considered into account or unavailability of these parameters. Indeed, most of the calculations of the evaporation parameter depend upon empirical models in estimation and this leads to resulting in inaccurate values (Karlsson and Pomade 2005).

To calculate the (AE), it needs to find the potential evaporation (PE) first for the purpose of using it to calculate the actual value of evaporation. There are several and different equations that could be used to calculate the potential evaporation (PE) as described in chapter Three. The most appropriate formula that can apply to Al-Najaf region is Thornthwaite's formula (1948).

This equation is described in detail in chapter Three. As mentioned, potential evaporation values which are resulted from this equation need for an adjustment. The calculations of the potential evaporation values are illustrated in Table D.1 in Appendix D. When the value of the temperature is equal or exceeds 26.5 ^{O}C, it cannot use Thornthwaite's formula to calculate the PE and it will use Table 4.3 to find PE directly from this table (Thornthwaite 1948):

Table 4.3: Values of PE for temperature rates ≥ 26.5 C° (Thornthwaite 1948)

T(C^o)	PE (mm)
26.5	135.0
27.0	139.5
27.5	143.7
28.0	147.8
28.5	151.7
29.0	155.4
29.5	158.9
30.0	162.1
30.5	165.2
31.0	168.0
31.5	170.7
32.0	173.1
32.5	175.3
33.0	177.2
33.5	179.0
34.0	180.5
34.5	181.8
35.0	182.9
35.5	183.7
36.0	184.3
36.5	184.7
37.0	184.9
37.5	185.0
38.0	185.0

The value of the potential evaporation is calculated and corrected (PEc) as illustrated in Table D.1 in Appendix D, so it is ready to use it to calculate the actual evaporation (AE) as bellow (Bryson et al. 2008):

$$AE = \begin{cases} R - PEc \geq 0 & THEN & AE = PEc \\ R - PEc \prec 0 & THEN & AE = R \end{cases} \tag{4.4}$$

where, R is the monthly mean rainfall (mm).

3. Soil moisture (SM)

The Climate Prediction Centre (CPC) and National Oceanic and Atmospheric Admiration (Noaa 2009) are providing the modelled monthly mean soil moisture water height as equivalent values with a curve for a selected region. The soil moisture values for the study area are downloaded

from this website www.esrl.noaa.gov/psd/cgi-bin/db_search/SearchMenus.pl for the period from 1980 to 2014 as illustrated in Table C.5 in Appendix C.

The collected data represents the values of the soil moisture (SM), while to calculate the groundwater recharge, it needs to find the change in soil moisture (ΔSM). The change in soil moisture for a specific month can be calculated through subtracting the soil moisture content value for the previous month from that specific month's value of soil moisture. After obtaining the values of change in soil moisture (ΔSM), it can calculate the values of water surplus (WS) as shown in Eq. (4.5) below:

$$WS = R - (AE + \Delta SM) \qquad (4.5)$$

Three assumptions are considered with respect to R and AE to estimate water surplus (WS) value, if considering that there is no change in soil moisture content (Domenico and Schwartz 1998):

1. R = AE: Theoretically this means that Water Surplus equals to zero (WS=0) because rainfall will satisfy the evaporation completely without residual.
2. R < AE: Rainfall will be available to participate or satisfy the evaporation partially.
3. R > AE: Practically Water Surplus in this case is existing and will rebuilding the component of soil moisture to be ready for the recharge that may be happened later.

4. Runoff (RO)

Subtracting of the Runoff (RO) value from the water surplus (WS) will result the groundwater recharge (RGW). Where there is no data available or collected from Iraq which can be used to calculate the value of runoff (RO) for the study area, so it needs to find an easy way or formula to estimate this parameter. Thus, the Runoff Curve Number (Simply CN) represents a hydrology empirical parameter that can be used to predict runoff from the value of rainfall. This curve number was developed by the USDA (United States Department of Agriculture 2007) and formerly called the SCS-Approach (Soil Conservation Service Curve Number Approach). This Number is widely used because it represents an efficient method for calculating approximately the runoff through using the rainfall for a specific area. According to the infiltration rate, it can be classified the type of soil in the study area depending on the hydrology soil groups and also find the Curve Number (CN). Tables 4.4 and 4.5 show the hydrology soil groups and the values of CN.

Table 4.4: Hydrologic soil groups according to infiltration rates (Maidment 1993)

Group	Infiltration rate cm/h	Runoff rate	Soil Description
A	≥ 0.76	Low	Sands or gravels
B	0.38 – 0.76	Moderate - Fine	Silt loam and loam
C	0.13 – 0.38	Fine - High	Sandy clay loam
D	0.0 – 0.13	High	Clay loam, silty clay loam, sandy clay, silty clay and clay

Table 4.5: CN according to the hydrologic soil group (Maidment 1993)

Cover description		Curve numbers for hydrologic soil group			
		A	B	C	D
Open space (lawns, parks, golf courses, cemeteries, etc.)	Poor condition (grass cover <50%)	68	79	86	89
	Fair condition (grass cover 50 to 75%)	49	69	79	84
	Good condition (grass cover >75%)	39	61	74	80
Impervious areas	Paved parking lots, roofs, driveways, etc. (excluding right of way)	98	98	98	98
	Paved; curbs and storm sewers (excluding right-of-way)	98	98	98	98
Streets and roads	Paved; open ditches (including right-of-way)	83	89	92	93
	Gravel (including right of way)	76	85	89	91
	Dirt (including right-of-way)	72	82	87	89
Western desert urban areas	Natural desert landscaping (previous area only)	63	77	85	88
	Artificial desert landscaping (impervious weed barrier, desert shrub with 1- to 2-inch sand or gravel mulch and basin borders)	96	96	96	96
Urban districts	Commercial and business (85% imp.)	89	92	94	95
	Industrial (72% imp.)	81	88	91	93
	$\frac{1}{8}$ acre or less (town houses) (65% imp.)	77	85	90	92
Residential districts by average lot size	$\frac{1}{4}$ acre (38% imp.)	61	75	83	87
	$\frac{1}{3}$ acre (30% imp.)	57	72	81	86
	$\frac{1}{2}$ acre (25% imp.)	54	70	80	85
	1 acre (20% imp.)	51	68	79	84
	2 acres (12% imp.)	46	65	77	82

From Tables 4.4 and 4.5, the area of study belongs to hydrologic soil group A and Curve Number equals to (63) for a natural desert (Maidment 1993). The study area has a maximum daily rainfall equals to (1.16 in) (29mm) as shown in Appendix C in Table C.4. This means that the value of Runoff is equal to zero or very close to zero as it can be found from the SCS relation curve between storm runoff and rainfall that illustrated in Figure 4.27.
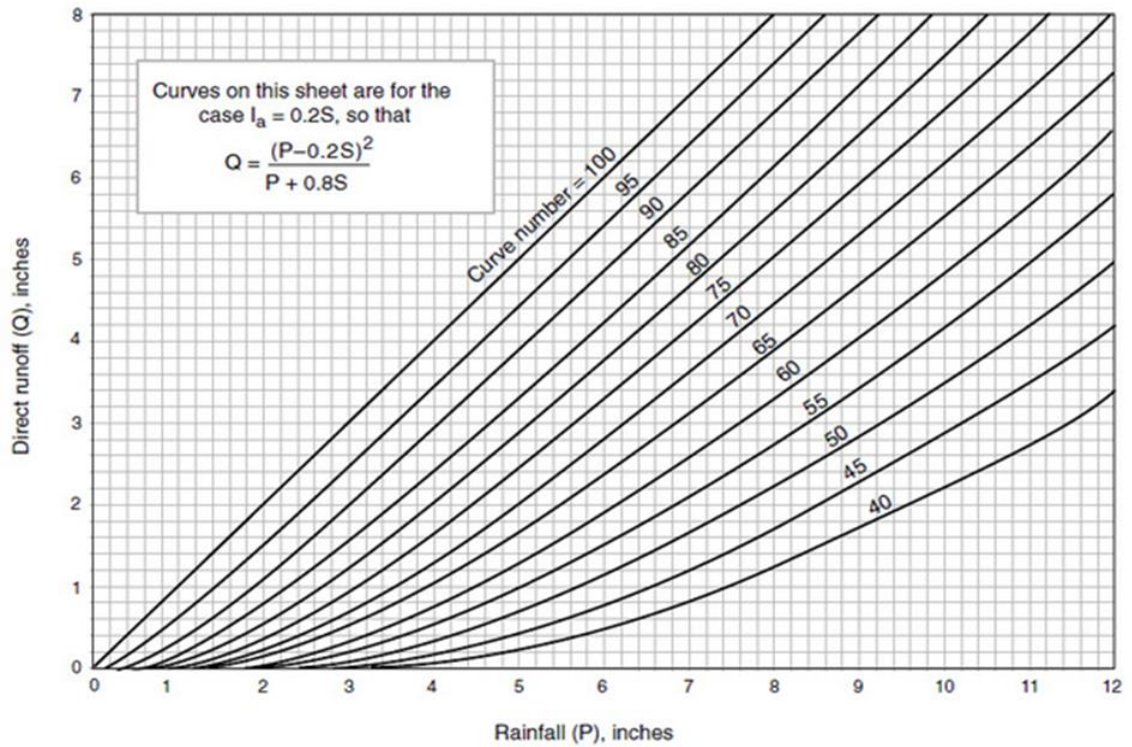
Figure 4.27: SCS relation between storm runoff and rainfall (Maidment 1993)

Finally, after finding the value of runoff which was equal to zero, now it can be found the value of the recharge rate for the groundwater system which is needed to be implemented into the conceptual model of the study area in Al-Najaf region as below:

$$RGW = WS - RO \qquad (4.6)$$

All the calculations of the recharge rate into the groundwater (RGW) are illustrated in detail in Table D.1 in Appendix D. A brief description of these calculations is also explained in Table 4.6. The calculations showed that the mean value of recharge rate for 35 years (1980-2014) is (40.32 mm/year). Actually, 70% of this recharge happened in January, May, June, July, August, and September, while 30% in February, March, April, October, November, and December, as an overall trend as shown in Table 4.6. Sometimes, the groundwater recharge is negative in some months for a specific year as illustrated in the calculations in Table D.1 in Appendix D, where this means that the groundwater aquifer in some months of a year is losing water upward into the soil to substitute the dryness in that soil.

Table 4.6: Values of groundwater recharge for the period (1980 – 2014)

Year	Total R mm	Monthly WS	RGW mm
1980	100.4	Jan, Feb, May, Jun, Jul, Aug, Sep	42.52
1981	56	Jan, May, Jun, Jul, Aug, Sep, Oct	6.56
1982	182.5	Jan, Feb, Mar, May, Jun, Jul, Aug, Sep	48.93
1983	119.9	Mar, May, Jun, Jul, Aug, Sep, Oct, Nov, Dec	55.96
1984	145.4	Jan, May, Jun, Jul, Aug, Sep, Nov	30.32
1985	58.8	Jan, Feb, Mar, May, Nov, Dec	21.81
1986	132.6	Jan, Feb, Mar, May, Jun, Jul, Aug, Sep, Nov	111.23
1987	159.3	Jan, Feb, Mar, May, Jun, Jul, Aug, Sep, Dec	86.7
1988	165.1	Jan, Feb, May, Jun, Jul, Aug, Sep, Nov, Dec	54.06
1989	112.3	Feb, Mar, May, Jun, Jul, Sep, Oct	42.25
1990	36.4	Jan, Feb, May, Jun, Jul, Aug, Sep, Oct, Nov	43.96
1991	52.5	May, Jun, Jul, Oct, Nov	-12.7
1992	116	Jan, May, Jun, Jul, Aug, Sep, Oct, Nov	46.7
1993	170	Jan, Feb, Mar, May, Jun, Jul, Aug, Sep, Oct	52.21
1994	147.6	Jan, May, Jun, Jul, Aug, Sep, Nov	55.44
1995	64.1	Jan, Feb, May, Jun, Jul, Aug, Sep, Oct	26.54
1996	91.3	Jan, Feb, May, Jun, Jul, Aug, Sep	41.96
1997	142.9	Jan, May, Jun, Jul, Aug, Sep, Nov	44.02
1998	95.7	Jan, Feb, Mar, May, Jun, Jul, Aug, Sep, Oct, Nov	79.64
1999	54.8	Jan, May, Jun, Jul, Sep, Nov	34.33
2000	62.9	Jan, Feb, Mar, May, Jun, Jul, Sep, Nov, Dec	24.41
2001	75	Jan, May, Jun, Jul, Aug, Sep, Nov	19.46
2002	64.2	Jan, May, Jun, Jul, Oct, Nov, Dec	-1.68
2003	74.1	Jan, Mar, May, Jun, Jul, Sep, Nov, Dec	38.15
2004	65.2	Jan, Feb, Mar, May, Jun, Jul, Aug, Sep	42.02
2005	71.7	Jan, May, Jun, Jul, Sep	42.76
2006	194.9	Jan, Feb, May, Jun, Jul, Aug, Sep, Dec	90.2
2007	71.9	Jan, May, Jun, Jul, Aug, Sep, Nov, Dec	45.29
2008	81.2	Jan, Feb, May, Jun, Jul, Sep	20.71
2009	94.1	Jan, Mar, Apr, May, Jun, Jul, Aug, Sep, Oct, Nov	9.72
2010	50.3	Feb, Mar, Apr, May, Jun, Jul, Aug, Sep, Oct	15.69
2011	78.2	Jan, Feb, Apr, May, Jun, Jul, Aug, Sep, Oct	52.93
2012	48.8	May, Jun, Jul, Aug, Sep, Oct, Dec	2.95
2013	119.5	Jan, May, Jun, Jul, Aug, Sep, Oct, Nov	70.07
2014	99.9	Jan, Mar, Apr, May, Jun, Jul, Sep, Oct	26.02
Mean	**98.7**	**70% Jan, May, Jun, Jul, Aug, & Sep**	**40.32**

In addition, Table 4.6 shows that the values of the recharge rates leaking to the groundwater aquifer (RGW) are very large, as most of them have exceeded 25% of the rainfall value and sometimes exceeded 50% as in the years 1987, 1999, 2004, 2005, 2007, 2011, and 2013. It can also be noticed in the years 1986 and 1998 that the value of recharge rate received by the groundwater aquifer in Al-Najaf region exceeded 80% of the rainfall value. In 1990, it is noticed that the value of recharge rate 43.96 mm/year leaking into the aquifer was greater than the value of the rainfall 36.4 mm/year for this year. It can; therefore, be concluded that most of the recharge rate values shown in Table 4.6 are illogical because Al-Najaf province is classified as: 1) an arid area, 2) the amount of rainfall received in this province is very low, and 3) it is subjected to high degrees of temperatures sometimes reaching 55 ^{0}C, which leads to high evaporation amounts. All of these problems will prevent the arrival of large quantities of rainwater to the aquifers available in this province, as this is enhanced by the presence of some negative quantities of recharge rates, which indicate that the soil sometimes moisturizes itself depending on the groundwater through the capillary phenomenon. In addition, from Table 4.6, the quantity of recharge rate (RGW) into the groundwater aquifer in the years 1981, 2009, and 2012 can be considered logical and acceptable because, after subtracting the losses (evapotranspiration, soil moisture, and others) from the rainfall amount, the remaining rainfall that will recharge the aquifer will be within these values, as shown in Table 4.6, for these years.

4.6 Summary

The study site is selected to be under assessment for groundwater and surface water sources. On the eastern side of the study area, the surface source of water represented by the Euphrates River is located. All the geological and hydrogeological characteristics of the study site collected from either GEOSURV (2015) or MOWR (2015) or MOTRANS (2015) are illustrated in detail. The meteorological collected data related with the climatology of the study site such as Temperature, Rainfall, Daily Rainfall, Soil Moisture, Change in Soil Moisture, Sunshine duration, Radiation, Potential Evaporation Totals, Wind speed, and Relative humidity are also analysed in detail to understand clearly the weather of this province. It is found that this province is exposed for an arid climate. In addition, to estimate the recharge rate that the study site exposed for, Thornthwaite formula is used and it is found that the study area has 40.32 mm/year recharge rate. The DEM-Digital Elevation Model is downloaded from the GLCF "Global Land Cover Facility" from the website http://www.landcover.org/data/srtm/ and by using the GIS-Geographical Information Systems software, the ground surface elevations are extracted. In addition, analysis of the DEM results in the topographic contour map of the study site and this map shows a general eastern slope of the study area equals to 0.0018.

Chapter Five
Model Setup and Validation

5.1 Introduction

The definition of the groundwater model as modified by Anderson and Woessner (1992) is the computational method that needs for an approximation for an underground water system to simplify the more sophisticated reality. Natural processes and human activities are usually affected the groundwater systems so it requires to manage and maintain the groundwater resources within the acceptable limits to provide the economic and social advantages from this source. Therefore, the past and present knowledge behaviours of the groundwater systems should represent the base of modelling to understand the future changes and uncertainties (Kumar 2015).

Groundwater modelling represents a powerful tool for groundwater prediction, management, and protection and remediation. Where using these models will help the decision-makers to prior predict the behaviour of the groundwater system. Groundwater models are classified into three categories: analogue, physical, and mathematical models. The category which the most popular nowadays is the mathematical models where these models can be solved by either analytical or numerical methods. Analytical solution methods do not require much data, but the application of these methods is limited to simple problems. While, the numerical solution methods have the ability to handle the more complex problems, where these models have become more effective and simple to use because of the rapid development for the computer processors and speeds. The most well-known approaches of groundwater modelling are the "Finite Difference" and "Finite Element" methods where each method has its limitations and advantages. Where, according to the problem concern and the objectives of modelling, the appropriate approach of modelling method can be selected. The results of any groundwater problem are affected by the modelling approach chosen, initial conditions, boundary conditions, space and time of discretization, and quality and quantity of prepared data (Husam 2009).

There are main stages for a numerical groundwater model setup (Kresic 2007):
1. Development of the conceptual model, which represents the crucial part of modelling and the basis for all further simulation activities.
2. Computer model code selection that can effectively simulate the problem and prepare the purposes of simulation.

3. Definition of the geometrical properties such as the grid layout, boundaries of the model, position, and layers number.

4. Input of the geological and hydrogeological properties such as the hydraulic conductivities, storage, porosity, and others.

5. Definition of the boundary conditions of the model that influence the simulation process such as the internal and external constant heads stresses which affecting the system, recharge applied to the model, wells pumping, springs outflow, evapotranspiration, drains, rivers, and others.

The next step after completing the model setup is, running the simulation process and then calibrating the model to match the hydraulic heads or the hydraulic chemical or contaminant data which is collected from the field.

5.2 Groundwater modelling process

There are several steps should be done to get a complete and correct groundwater model that can predict the future changes of climate accurately (Merz and National Centre for Groundwater Research and Training 2012). The modeller needs to have a wide knowledge about the geology of the study site and about the hydrogeology which is related to the groundwater flow processes, description of groundwater flow mathematical equations, flow and solute movement, solving techniques of the differential equations either by the "Analytical" or "Numerical" solutions, and checking the reliability of the results (Kumar 2015). The groundwater modelling process steps are shown in Figure 5.1 and the description of some important steps are illustrated below (Merz and National Centre for Groundwater Research and Training 2012).

1. **Planning:** It needs in this step to know clearly the objective from designing the model to provide the appropriate data which is related to the objective and can use it to build the model.

2. **Conceptualisation:** It comprises of many activities, such as defining the geometry of the model, geological and hydrogeological properties of the model, and boundary conditions which are needed to design the groundwater model.

3. **Calibration and Sensitivity analysis:** It represents an important process and it is an iterative process to simulate the hydrogeological properties and boundary conditions in order to be the model's results as closely as the historical and collected observations.

4. **Prediction:** It provides the results of the modelled equations which are simulating the objective of the modelling study. In addition, these results show the state of the study site and provide a description and prediction for the future events that may happen and

what will be the effect of these events through comparing that effect with the original state and decide whether the effect is acceptable or not.
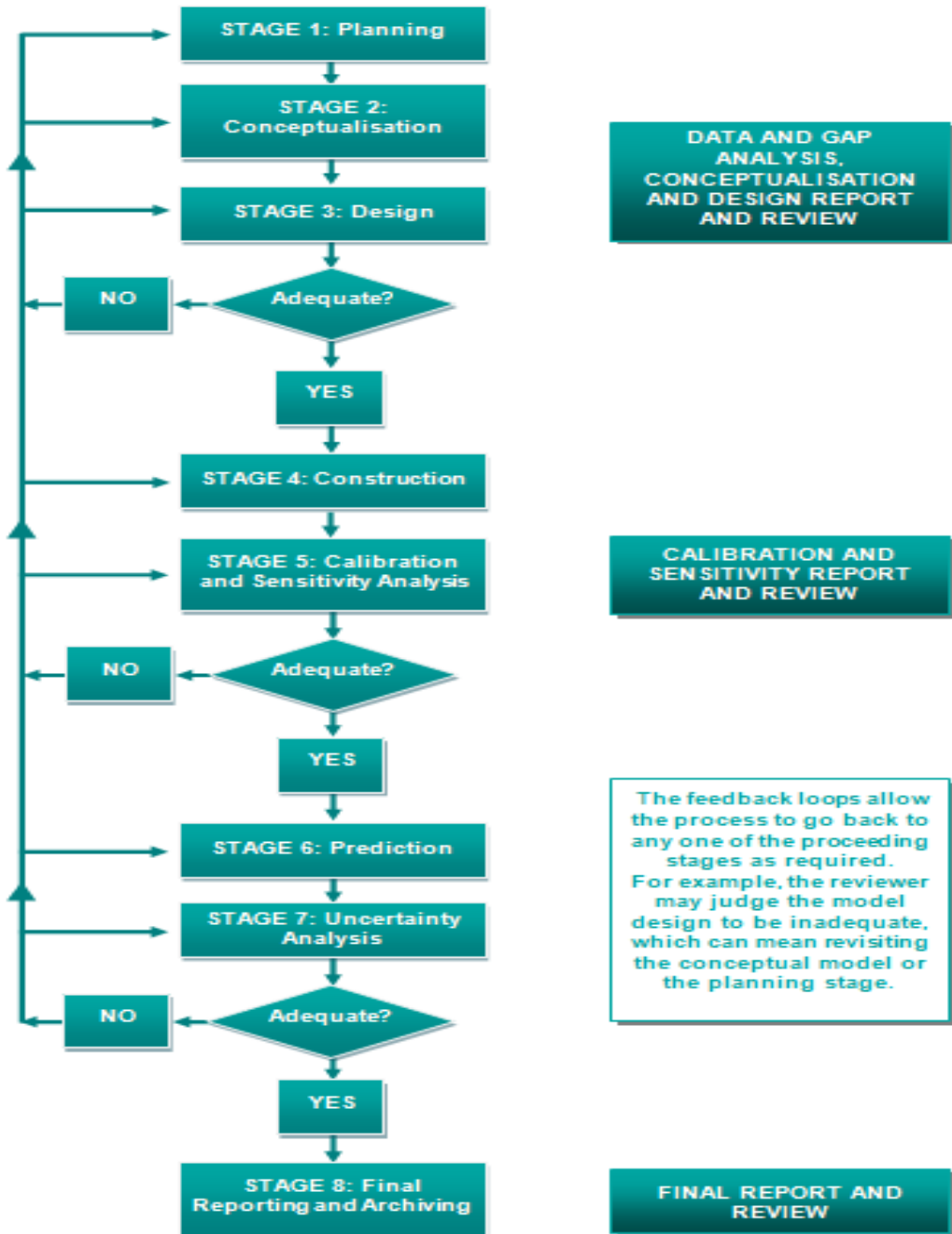
Figure 5.1: Groundwater modelling process (Modified after MDBC 2001; Yan et al. 2010)

After defining and knowing the appropriate information which is needed to start building the conceptual model, the next step is represented by creating the conceptual model that represents the study area. In general, to build the groundwater model, it should prepare the data or information that governs the analysis system, building the conceptual model and defining the boundary conditions, and the final step is choosing the numerical type of model analysis

whether by the finite difference or finite element method. In this study, Visual MODFLOW represents an accurate and good software to analyse the groundwater models by using the finite difference method and it is important here to mention that grid refinement is not required due to the huge area of study.

Creating a model needs mainly for five steps, inserting the input files of the study area with all the boundary conditions, running the model, visualizing and checking the outputs, calibrating the model through manipulating the input parameters and boundary conditions, and finally finding the final predictive model and doing the sensitivity analysis if needed (Al-Muqdadi 2012). Figure 5.2 represents the methodology that considered in this research.
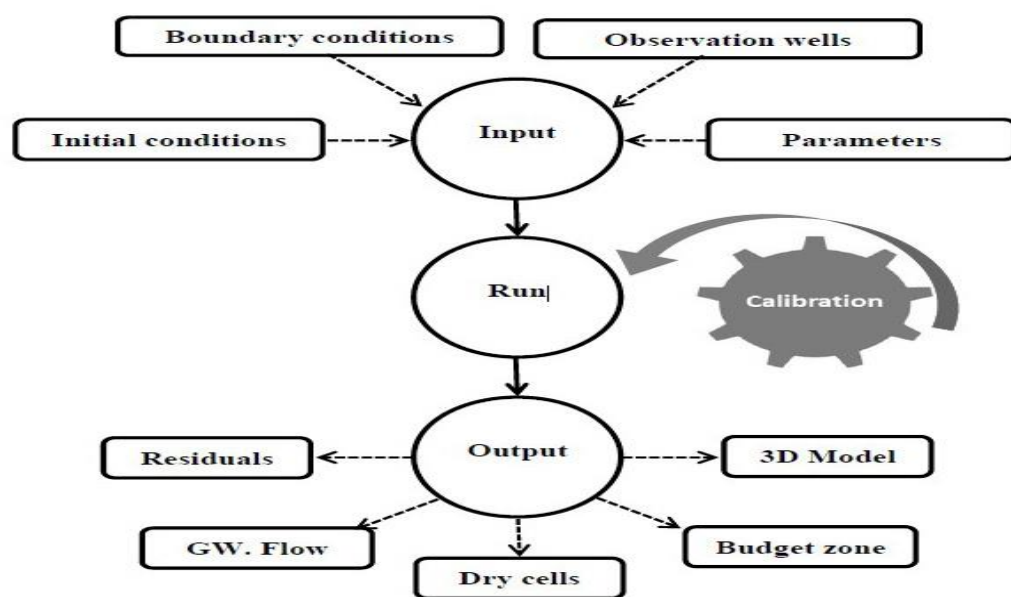
Figure 5.2: Groundwater flow Model by Visual MODFLOW (Adopted from Al-Muqdadi 2012)

5.3 Conceptual model of the study area

To simulate the groundwater system in the study area, it needs for software that can deal with the simulation process accurately and efficiently. Therefore, Visual MODFLOW program which is designed by Waterloo Hydro-geologic Company is used because the software deals with the environmental processes effectively. Visual MODFLOW has six solvers which are PCG, SIP, SOR, WHS, SAMG, and GMG). WHS represents the most suitable one that can be running the model as compared with the others, which are failed to run the model.

Visual MODFLOW software is set up for the study area to get the initial forward model. The computational mesh for the study area consists of 194 columns by 127 rows with two layers as shown in Figure 5.3, Figure 5.4A and B, with a 3D view. The size of the cells used is

approximately 200m by 200m, covering an area equals to 38676m by 25234m with average 19499 active and 5139 inactive cells. Based on the geological and hydrogeological analyses illustrated in chapter 4, it can build the groundwater model with two layers with a known permeability. The elevation of the ground surface is imported from the 90m SRTM data according to the downloaded DEM. The bottom elevations of each layer are extracted from the wells that are injected in the study area. In addition, as it is illustrated in the geological data, there is a fault in the western part of the study area so this part is considered as an inactive area. The model's aquifer is unconfined with two layers to represent the geological features of the study area. The hydraulic conductivities are set to 14.43 m/day and 17.1 m/day for the Top and Bottom layers respectively as stated by GEOSURV (2015). As suggested by the field observations, the movement of groundwater is also eastward in general. Therefore, constant heads along the western and eastern boundaries are set to 50m and 20m respectively (MOWR 2015). To run the model, the recharge rate into the groundwater needs to be adopted, from the calculations illustrated in chapter 4, the recharge rate value is 40.32 mm/year.
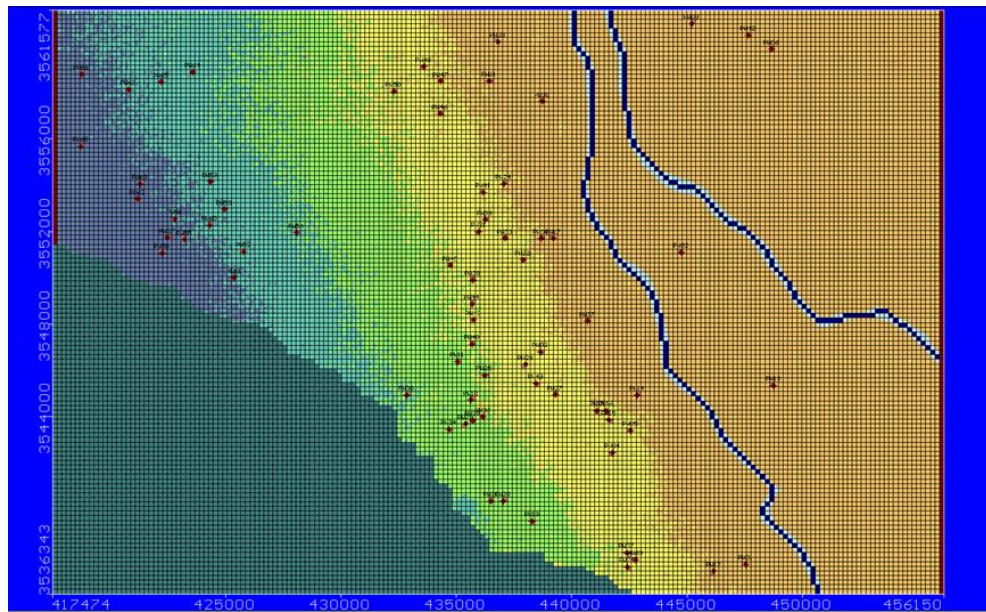
Figure 5.3: Computational mesh and location of pumping wells with the specification of boundary conditions
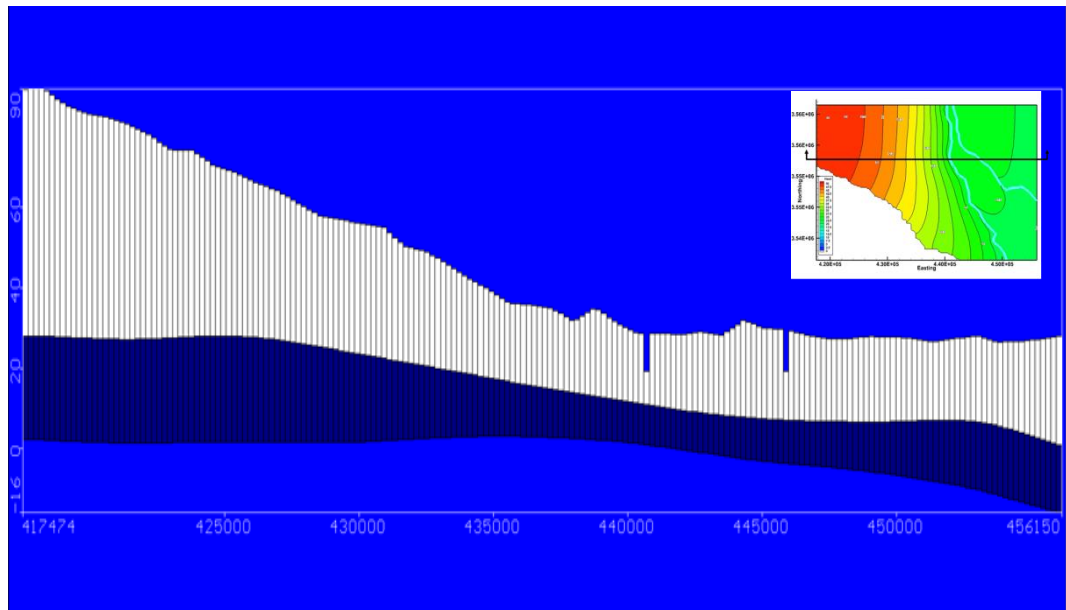
A
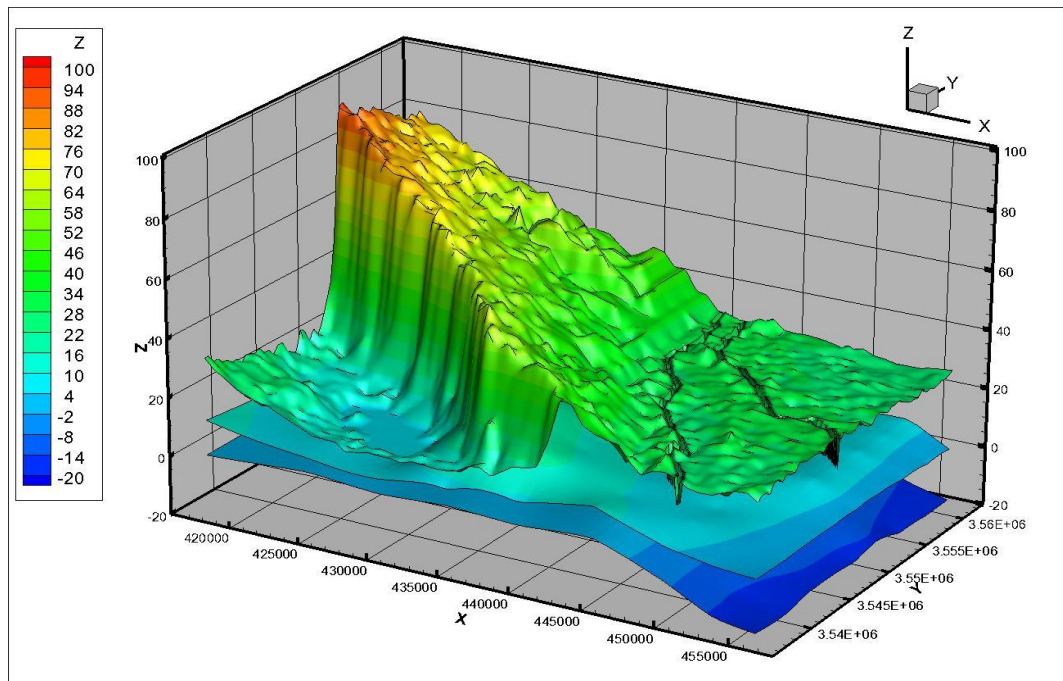
B

Figure 5.4: Vertical cross-section shows the layers of the study area, (A) Typical cross-section of the study area layers, and (B) 3D view of the topography of the study area forward model with layers composition

5.4 Model calibration

Model calibration represents an important part of any groundwater modelling process. Before implementing the groundwater model in any type of role management, it must be proved that the groundwater model can successfully simulate the observed aquifer behaviour. To make the

114

calibration process, there are certain parameters such as the recharge rate and hydraulic conductivity need to be changed in a systematic way and leave the model to repeatedly run until the computed values corresponding the field observed values with an acceptable level of accuracy (Al-Mussawy and Khalaf 2013).

The calibration process in this part will comprise of two types through using 69 observation wells that injected in the Al-Najaf region study area with values of static heads (when there are no pumping conditions) and dynamic heads (when there are pumping conditions).

5.4.1 Static calibration (Steady State without Pumping Conditions)

In this part will run Visual MODFLOW with a steady-state condition. Pumping rates in this step of calibration of the model will not be implemented. Static term means that in this part of calibration, it will use the values of observed heads in the steady state condition for the observation wells which are measured when there is no pumping schedule implemented in the area of study. Running Visual MODFLOW model without pumping from the wells has given the groundwater table shown in Figure 5.5. It is clear that there is a flooded area toward the end of slope from the west. Comparing the computed heads with the static observed heads taken from 69 wells is shown in Figure 5.6, which indicates an overestimation from the model in general.
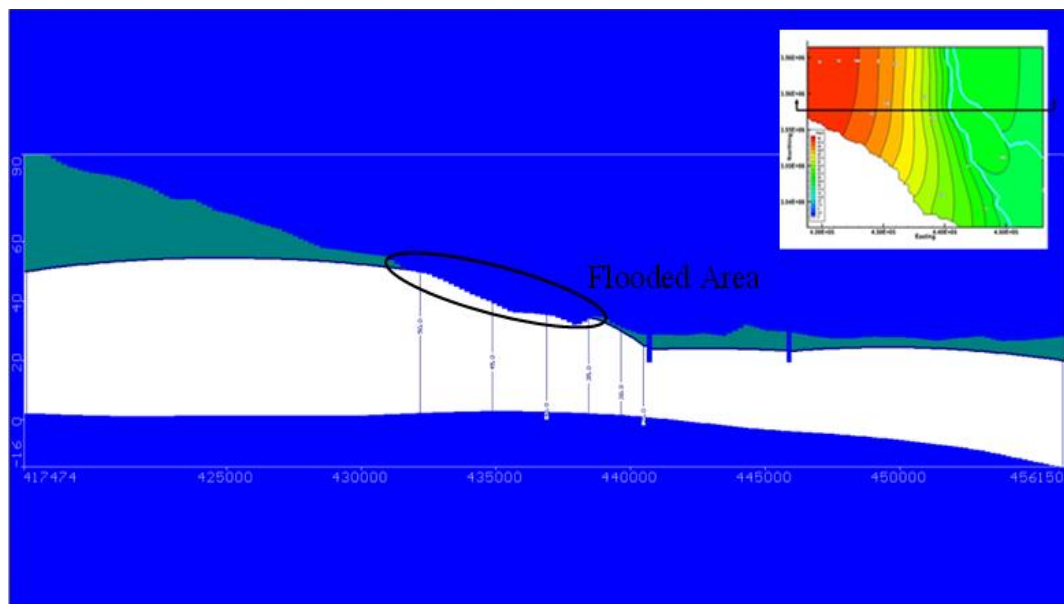
Figure 5.5: The water table with a flooded area in Al-Najaf province model for a recharge R=40.32 mm/year
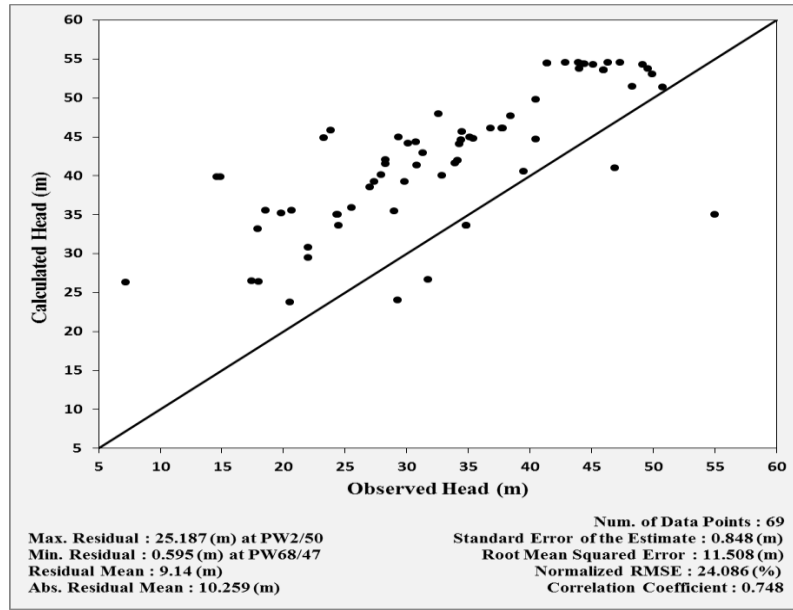
Figure 5.6: The relation between the calculated and observed heads for a recharge R=40.32 mm/year and 69 wells

From the results shown in Figures 5.5 and 5.6, it is suggested that the recharge value (it is a large value) used in the model be excessively larger than that is required. Since the calculated recharge is regarded as the potential recharge, and in reality the study area has never been found to be flooded in the past, rather suffered from the water scarcity due to the high temperature leading to high evaporation, the over-estimate might be due to the inaccuracy in data collection, for instance, the soil moisture which has a great impact on the recharge value in terms of increasing or decreasing it. Where, soil moisture values are provided by The Climate Prediction Centre (CPC) and National Oceanic and Atmospheric Admiration (NOAA 2009) as equivalent modelled values for the monthly mean soil moisture water height. Therefore, these values represent potential values measured by a model and not actual field measurements measured in the field. In addition, it may not be for the actual study area, it may be creeping for the adjacent areas which are close to the study area and not within the accurate boundaries of the study area.

To further determine realistic recharge value, a further sensitivity test is carried out using the static heads measured from 69 wells in the study area, by varying the recharge value. To quantify the sensitivity test, the Normalized Root Mean Squared Error (Normalized RMSE%), and the Residual Sum of Squares (RSS) m^2 shown in Eq. (5.1), are used.

$$RSS = \sum_{i=1}^{N} (h_c - h_o)^2 \qquad (5.1)$$

where, RSS is the total residual sum of squares (summation of the squared difference between the calculated and observed heads); h_c is the calculated head; h_o is the observed head; and, N is the number of wells (69 wells).

116

Visual MODFLOW results for the sensitivity test are illustrated in Table 5.1. As it can be seen from Table 5.1, the minimum value of the Normalized RMSE% and the minimum squared difference between the calculated and observed heads are corresponding to a value of a recharge equals to 7.55 mm/year. Therefore, this value will be used as a recharge for the static calibration because it gives the best fitting between the calculated and observed heads (Figure 5.7) as well as there is no flood with this value as it is illustrated in Figures 5.8. From both figures, the fitting can be considered acceptable and also there is no flooding in the study area.

Table 5.1: Results of Visual MODFLOW program for the Static case with different values of recharge over the study area

Iteration No.	Recharge mm/year	Normalized RMSE %	RSS m^2
1	40.32	24.086	9139
2	37.5	22.825	8207
3	35	21.738	7444
4	32.5	20.675	6733
5	30	19.647	6081
6	27.5	18.651	5480
7	25	17.703	4937
8	22.5	15.567	3817
9	20	15.967	4016
10	17.5	15.207	3643
11	15	14.014	3094
12	14.5	13.943	3062
13	14	13.875	3033
14	11	13.590	2909
15	10.5	13.561	2897
16	9	13.551	2892
17	7.55	13.517	2878
18	6	13.582	2906
19	5	13.659	2939
20	4	13.760	2982
21	2.5	13.967	3073
22	2	14.049	3109
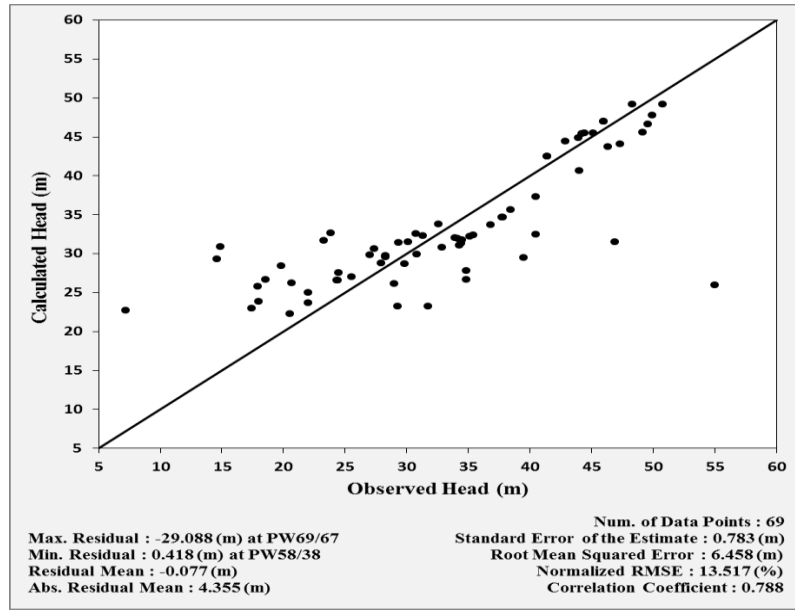
Figure 5.7: Relation between the calculated and observed heads for a recharge = 7.55 mm/year
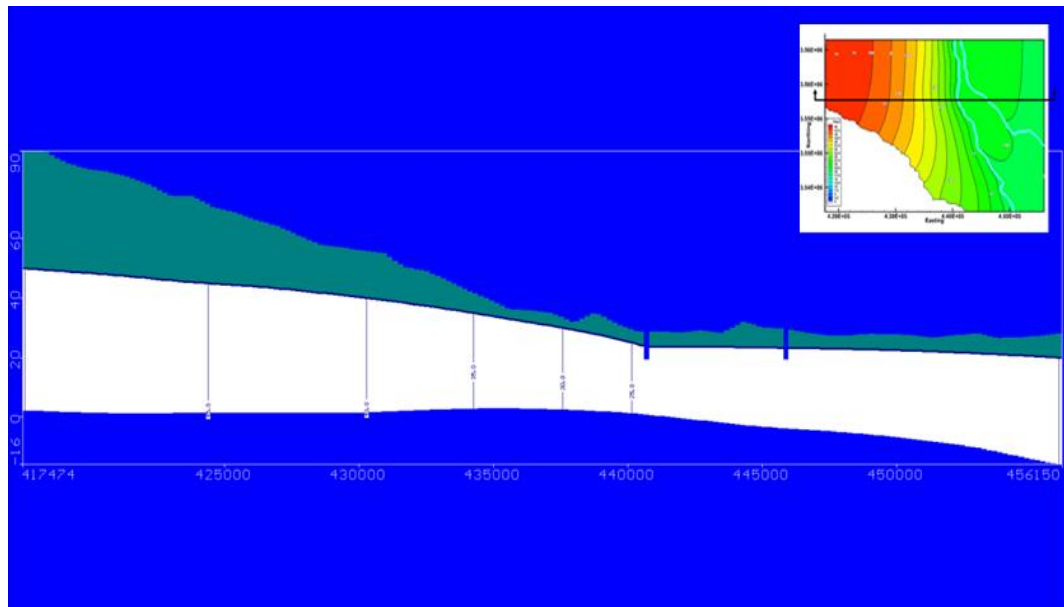
Figure 5.8: Water table elevation with a recharge R=7.55 mm/year

5.4.2 Dynamic calibration (Steady State with Pumping Conditions)

Following the calibration of the model on the static heads, it will now consider the dynamic heads of the pumping wells to calibrate the study area model under a steady state condition when there are pumping conditions. Dynamic heads are the observed groundwater levels inside the pumping wells which are measured during the operation of all the pumping wells after reaching the steady state (equilibrium) condition. When applying the optimal recharge 7.55 mm/year obtained from the static calibration to the case when all 69 pumps are operating, Figure 5.9 shows the comparison between the calculated and observed dynamic heads. It is clear

that most of the calculated heads are underestimated when the pumping wells are under the operation process, indicating that the specified recharge of 7.55 mm/year is too low for this case. Therefore, the recharge needs to be increased.
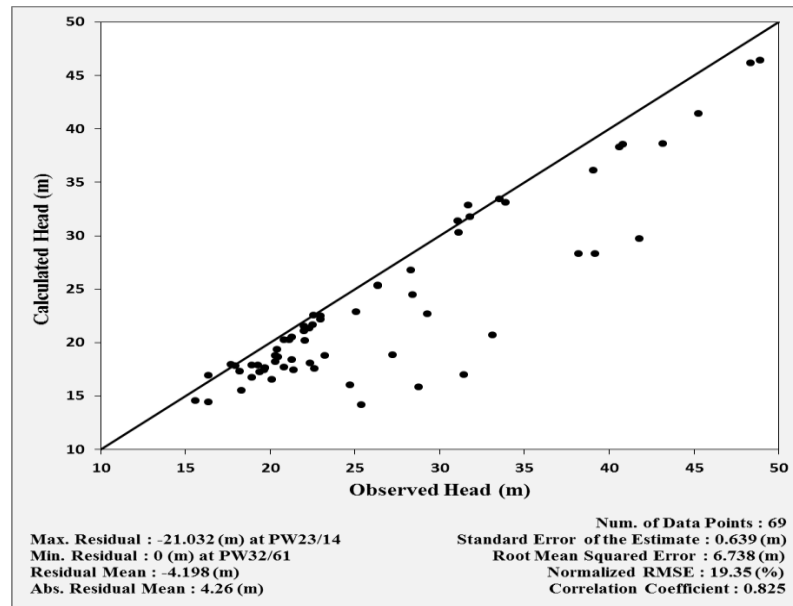
Figure 5.9: Relation between the dynamic calculated and observed heads for a recharge = 7.55 mm/year with 69 wells

By using the potential recharge rate calculated based on the main monthly data collected during the period (1980 - 2014), 40.32 mm/year, it will calibrate the model under a steady state case with pumping conditions. Figure 5.10 shows the relationship between the calculated and observed dynamic heads when all pumps are operating where although the study area does not subject for a flooded area, but it can be seen that most of the calculated heads are still overestimated due to the large recharge rate value exerted on the area. Therefore, it is clear that the recharge value 40.32 mm/year is too high and needs to be reduced to get the optimal recharge value and it should be between 7.55 mm/year and 40.32 mm/year.
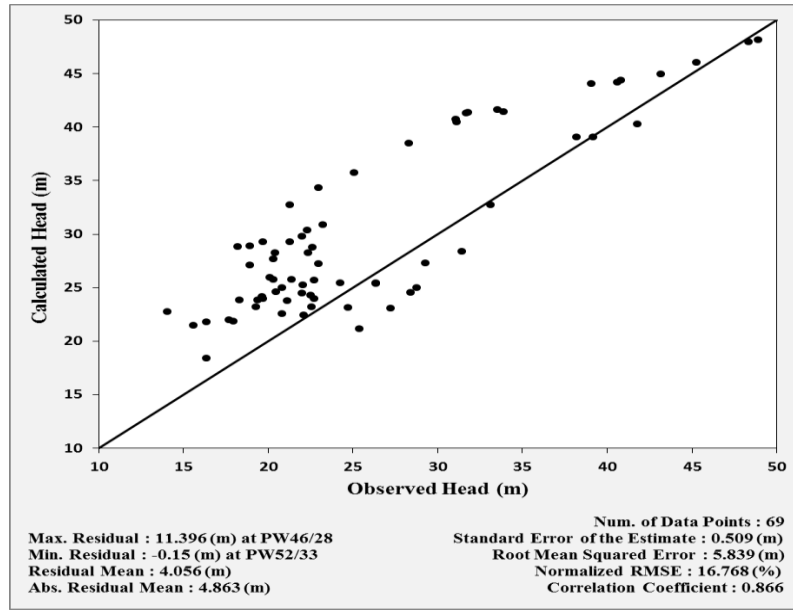
Figure 5.10: Relation between the dynamic calculated and observed heads for a recharge = 40.32 mm/year with 69 wells

According to that, by starting from the recharge value 7.55 mm/year, it will increase the value of the recharge rate for the dynamic condition when the pumping wells are under operation until getting the best fit between the calculated and observed dynamic heads. Table 5.2 illustrates the key parameter values which give the indication for the best fit between the calculated and the observed heads, which are Normalized RMSE (%), and Residual Sum of Squares RSS which is defined in Eq. (5.1).

Table 5.2: Results of Visual MODFLOW program for the Dynamic case with different values of recharge

Iteration No.	Recharge mm/year	Normalized RMSE %	RSS m²
1	7.55	19.35	3132
2	9	16.845	2374
3	10.5	16.783	2356
4	12	14.2	1687
5	13.5	12.467	1300
6	15	11.611	1128
7	16.4	11.007	1014
8	16.5	10.969	1006
9	16.6	11.694	1144
10	18	12.616	1332

In Table 5.2, the value of the recharge has been increased by an increment of approximately 1.5 mm/year in the range from 7.55 mm/year to 18.0 mm/year, with an increment of 0.1 mm/year more and less around the optimal recharge value to be more accurate in assigning the optimum

recharge rate value. It is found clearly from Table 5.2 that the recharge 16.5 mm/year gives the best values of fitting, with the Normalized RMSE 10.969 % and least value of RSS = 1006 m^2. This value of recharge with these parameters values indicates that when the recharge value equals to R= 16.5 mm/year, the calculated dynamic heads will be the closest to the observed ones. Figure 5.11 shows the relationship between the calculated and the observed heads when there are pumping conditions. In this figure, it can be shown that most of the calculated heads are close to the observed heads except some wells which having underestimated values of the head.
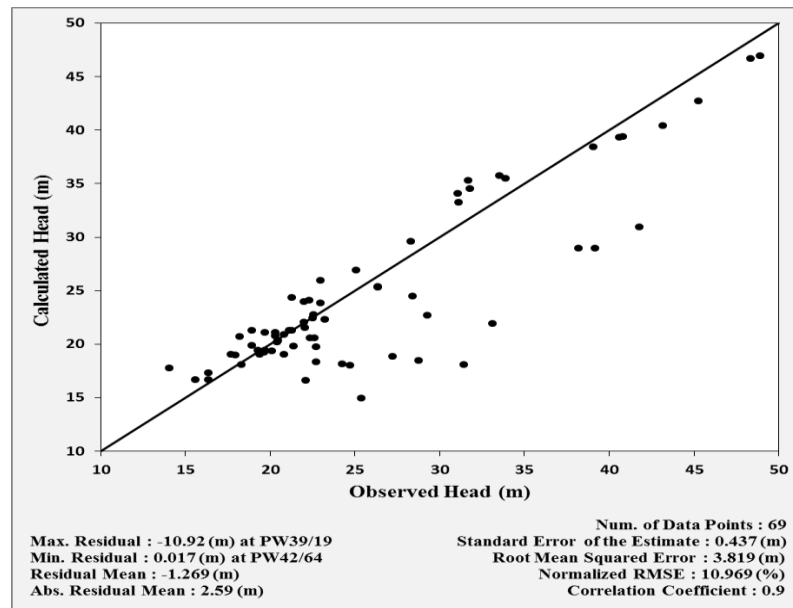
Figure 5.11: Relationship between the dynamic calculated and observed heads for a recharge = 16.5 mm/year with 69 wells

5.5 Applying the vertical discretization for Al-Najaf model

Groundwater flow field discretization is essential to either improve the numerical model or provide an agreeable representation of the hydrogeologic physical system that is represented by the constructed mathematical models (Philip 1994). The discretization of model grids is divided into horizontal and vertical. The uniform horizontal discretization is commonly applied to the top surface of a model to improve the model's results. However, to minimize the perturbations in the vertical direction of flow, it is sometimes necessary to consider vertical discretization (Philip et al. 2010).

In this section, it will perform the vertical discretization for the Forward model obtained from the static and dynamic calibration processes at the recharge rates of 7.55 mm/year and 16.5 mm/year respectively. The model for the Al-Najaf region consists of two layers with a constant hydraulic conductivity for each (GEOSURV 2015). It will subdivide the top and bottom layers

into two layers each, so that the model will comprise of four layers as shown in Figure 5.12. It will then perform the calibration process for the model statically and dynamically through Visual MODFLOW. Finally, the calculated heads' results will be compared with those observed in the field.
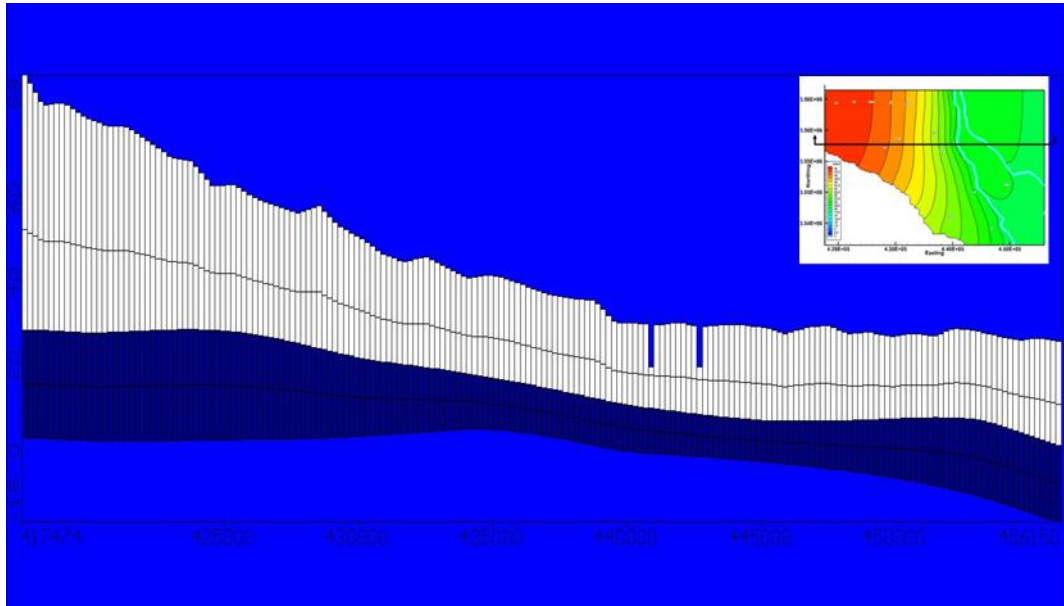
Figure 5. 12: Vertical cross-section shows the vertical discretization applied for the top and bottom layers of Al-Najaf region model

Tables 5.3 and 5.4 illustrate the comparison between the key parameters values (SEE, RMSE, Normalised RMSE, CC, and RSS) obtained from the four-layer model after running it twice: once without pumping conditions (Static-Table 5.3) and again with pumping conditions (Dynamic-Table 5.4). From Tables 5.3 and 5.4, applying the vertical discretization to Al-Najaf model leads to be the calculated head results worsen, where the difference between the calculated and observed heads becomes larger. This has led to the key parameters being greater than those values obtained when the model was run with two layers (as it is in the real field). Vertical discretization indicates the unacceptability of the model results. Figures 5.13 and 5.14 show the difference between the calculated and observed heads for the Forward Model, both without and with the vertical discretization, respectively, after applying the static and dynamic calibration for both models, respectively. Figures 5.13 and 5.14 indicate that Al-Najaf model (without vertical discretization) has given acceptable results for the corresponding calculated and observed heads as compared with those poor and dispersed calculated heads that resulted from the Forward Model with the vertical discretization (four layers) which are remarked as unacceptable.

Table 5. 3: A comparison of the static calibration results between the Forward Model Without Discretization and the Forward Model With Discretization

Calibration Case	Recharge mm/year	SEE m	RMSE m	Normalized RMSE %	CC	RSS m^2
*Static	7.55	0.783	6.458	13.517	0.788	2878
**Static	7.55	0.803	7.728	16.174	0.778	4121

* Forward Model Without Discretization
** Forward Model With Discretization
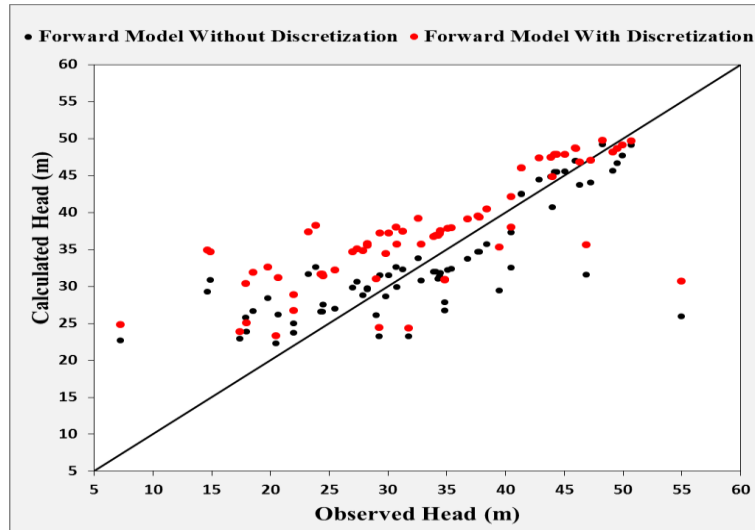
Figure 5. 13: Comparison of the static computed and observed heads for the Forward Model Without Discretization and the Forward Model With Discretization when applying a recharge rate of 7.55 mm/year

Table 5. 4: A comparison of the dynamic calibration results between the Forward Model Without Discretization and the Forward Model With Discretization

Calibration Case	Recharge mm/year	SEE m	RMSE m	Normalized RMSE %	CC	RSS m^2
*Dynamic	16.5	0.437	3.82	10.969	0.900	1006
**Dynamic	16.5	0.466	4.566	13.114	0.88	1439
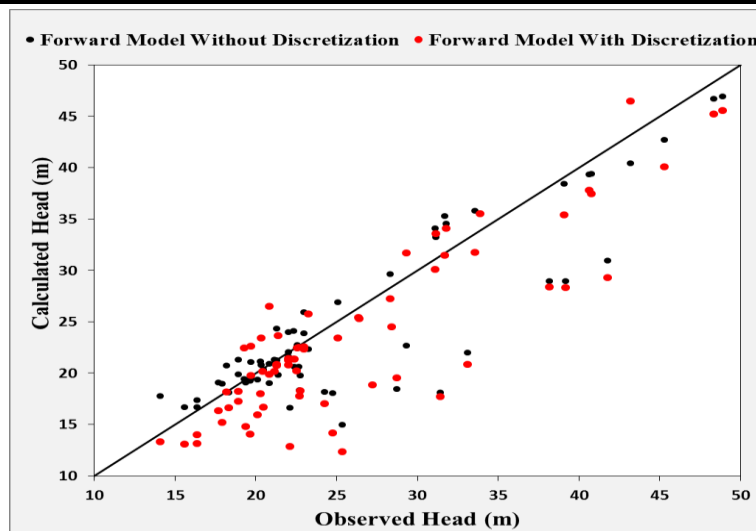
Figure 5. 14: Comparison of the dynamic computed and observed heads for the Forward Model Without Discretization and the Forward Model With Discretization when applying a recharge rate of 16.5 mm/year

The vertical discretization that is used in Visual MODFLOW through the finite difference method is computationally convenient when the layers of a model are distributed horizontally with regular rectangular cells. Most of the finite difference numerical codes, particularly MODFLOW, assume that the layers of a model are distributed horizontally (in the vertical direction) with a uniform shape of the rectangular cells to compute the flow. Due to the sophisticated configuration of the distributed hydrogeologic units in three-dimensions, it is sometimes necessary to create an accurate numerical model through the refinement in the vertical direction of flow (Philip 1994).

However, Al-Najaf model results (Forward Model with Discretization-Four Layers) were unacceptable. Philip et al. (2010) stated that the vertical discretization of the aquifer in Visual MODFLOW will influence the groundwater levels due to some cells falling under the dryness problem. Therefore, it will use Al-Najaf model with two layers only. In many cases, it is often very convenient to set up the groundwater model with a single layer only (Philip et al. 2010). However, because the provided/collected information show that Al-Najaf groundwater aquifer comprises of two types of soil layers, the constructed model has depended on these information where the calibration results for the dynamic heads were excellent and acceptable. Therefore, it will consider that model of two types of soil layers to be Al-Najaf region model.

5.6 Model sensitivity

Sensitivity criterion is a good measure for the uncertainty of any groundwater model and it is caused by the uncertainty of the aquifer parameters and sometimes the model boundary conditions. The fundamental concept from implementing sensitivity analysis is to understand the influence that caused by the variation of model parameters and the hydrogeological stresses on the groundwater aquifer system through changing the calibrated values systematically to finally identify which parameter needs to a special attention in the future studies (Anderson and Woessner 1992). In this study, the approach of sensitivity is performed through using a systemic change in the value of recharge. Model sensitivity to the hydraulic conductivity in the aquifer is also examined.

Figure 5.15a and b show the relationship between the Root Mean Squared Error RMSE (m) and recharge rate when implemented the static and dynamic heads in the model respectively. The result indicates that the model is less sensitive when the recharge rate is less than 16.5 mm/year and significantly sensitive for the recharge values higher than 16.5 mm/year as an overall trend. Values of RMSE are decreased slightly when the values of recharge rate increase either up to 7.55 mm/year (For Static Sensitivity) or up to 16.5 mm/year (For Dynamic Sensitivity). With

higher recharge rates (more than 16.5 mm/year), the RMSE values increase dramatically. This indicates that the model is more sensitive for recharge values greater than (16.5 mm/year) and less sensitive for recharge values less than that value. In addition, values of RMSE are ranged between (6.45-8.65) m and (3.82 -7.49) m for the static and dynamic heads respectively where with the dynamic heads, there is a dramatic variation in the RMSE values and also the values of the RMSE for the dynamic heads are often less than those for the static heads. As the error is reduced with the dynamic heads, this indicates that with the dynamic observation heads, the values of the calculated heads for the dynamic calibration are more closed to the observation heads as compared with those calculated heads resulted from applying the static observation heads. The least values of RMSE for the static and dynamic heads were at the recharge rates 7.55 mm/year and 16.5 mm/year respectively as this enhances the confidence in the calibration results obtained from the Forward model which were showing that the best matching between the calculated and observed heads are at the recharge rates of 7.55 mm/year and 16.5 mm/year for the static and dynamic calibrations respectively.

(a)

(b)
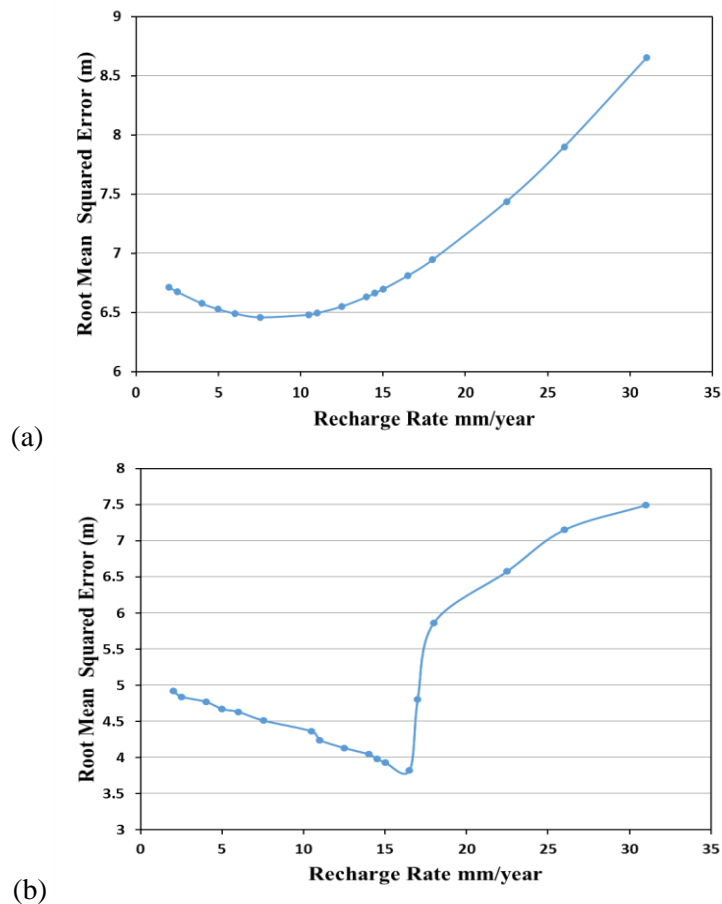
Figure 5.15: Relationship between the Root Mean Squared Error (RMSE) and recharge rate when implementing: (a) Static head and (b) Dynamic head

For the model sensitivity to the hydraulic conductivity, a series of tests are carried out with a wide range of variation of the hydraulic conductivity. The logarithmic relationship between the

hydraulic conductivity and the Normalized Root Mean Squared Error (RMSE %) is shown in Figure 5.16 for the static and dynamic heads which are implemented in the model. It can be noticed from Figure 5.16 that all values of the hydraulic conductivity which are greater than approximately 14 m/day have a little effect on the values of the Normalized RMSE and this means that the model is less sensitive for the increase in the hydraulic conductivities more than this value. However, the sensitivity for decreasing the hydraulic conductivity values to be less than 14 m/day is found to be very large and resulted in high values of the Normalized RMSE. This suggests that more careful consideration should be given when the hydraulic conductivity is determined, in particular when it is less than 14 m/day because the results can be dramatically changed. In addition, values of the Normalized RMSE resulted from applying the dynamic heads are smaller than those resulting from applying the static heads and this clearly indicates that again the values of the calculated dynamic heads are better than the calculated static heads.
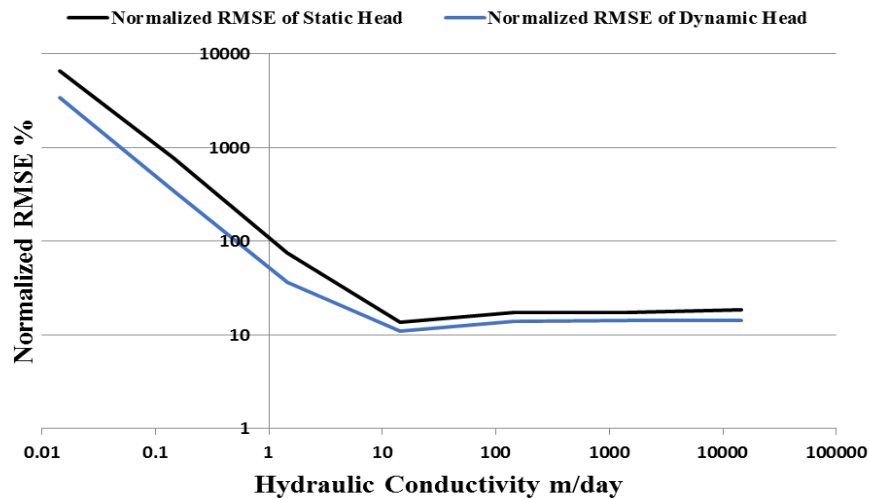
Figure 5.16: The logarithmic relationship between the hydraulic conductivity and Normalized RMSE

As demonstrated, the values 7.55 mm/year and 16.5 mm/year are considered to be the best values of the recharge rate which give acceptable results between the calculated and observed heads for static and dynamic calibrations respectively. In addition, the model was sensitive for the change in the hydraulic conductivity as an overall trend and this situation needs to be considered into account to reach for the accurate model that can be represented the real entire domain of the study area.

5.7 PEST-automatic parameter estimation approach

A good conceptualisation of a groundwater model is the most important step that is needed to represent the real-modelled field that in turn will result in good predictions (Spiliotopoulos and

Andrews 2006). Due to the general lack of the estimation of the hydraulic conductivity and dispersivity, the groundwater model has sometimes untrusted results; therefore, at least, one of these parameters should be estimated accurately to be the conceptualisation process more efficient and the results more reasonable (Takounjou et al. 2012). In the real field, the entire aquifer's parameters are rarely found complete or represent the whole area of interest, as in most cases those parameters are found to be as scattered measurements in the area under study. Therefore, in order to develop a reliable groundwater flow model that can be used to predict the behaviour of an aquifer, the aquifer criteria or parameters should be interpolated (Sefelnasr 2007). Typically, inverse model is standing to solve the groundwater aquifer parameters through using the head observations as a dependent variable in the governing equation of flow (Laplace equation), where usually the field-measured values of fluxes and heads are having a higher degree of confidence (Anderson et al. 2015). The method used to solve inverse model has been advocated by many researchers (Yeh and Tauxe 1971; Cooley and Sinclair 1976; Cooley 1979) to solve groundwater parameters automatically and now it's called "PEST" "Parameter ESTimation Approach". The PEST (Parameter ESTimation) technique has the capability to optimize the hydraulic conductivity of an aquifer through a process called "Calibration Process". In this parameter estimation approach, minimizing the difference between the observed and calculated groundwater heads represent the main objective function where when this objective is achieved, the parameter estimation approach will terminate (Ganesan and Isabella 2013).

In this section, it will apply the parameter estimation approach which is integrated within Visual MODFLOW to interpolate the hydraulic conductivity of the study site. Two constant hydraulic conductivities and 69 field observations are inserted into the PEST approach as the model is run under these constraints to achieve the calculated heads to be close to the observed ones. PEST approach is run for two cases, the first case is when there is no pumping schedule applied on the model and the recharge rate equals to 7.55 mm/year (Static Calibration), and the second is when all the 69 pumping wells are in-operation and the recharge rate equals 16.5 mm/year (Dynamic Calibration). Figures 5.17 and 5.18 resulted from Visual-MODFLOW-PEST running approach are representing of those two cases respectively. Where, Figures 5.17 and 5.18 illustrate the relationship between the calculated and observed heads after reaching the best estimation of the hydraulic conductivity of the study site. As illustrated in Figure 5.17, applying PEST approach has improved the Static calibration through improving the values of the Standard Error of the Estimate SEE, Root Mean Squared Error RMSE, and Normalized RMSE by reducing of these values as well as to increase the Correlation Coefficient (CC), as compared with the same values shown in Figure 5. 7. The value of RSS is also reduced to become 2855 m^2.
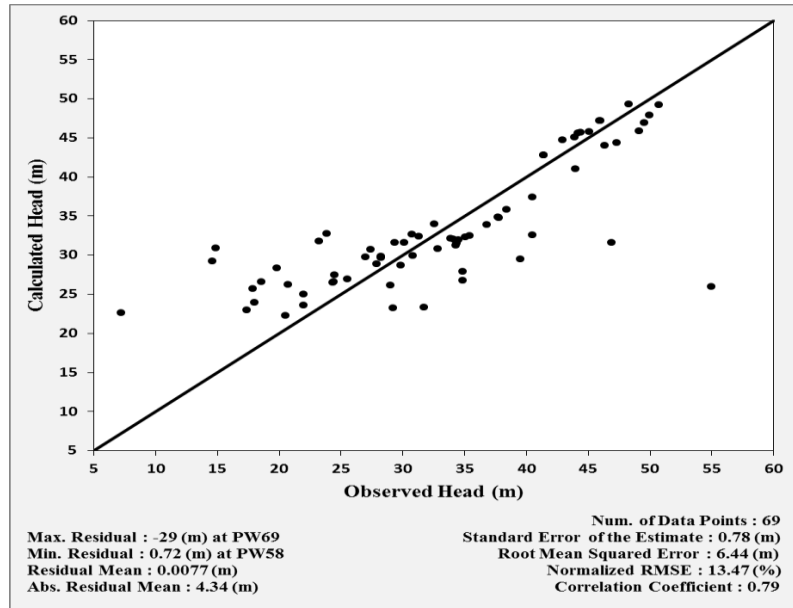
Figure 5.17: PEST result of the calculated and observed heads for a recharge = 7.55 mm/year

In respect of the PEST approach results for the Dynamic calibration shown in Figure 5.18, it has been noticed that the values of SEE, RMSE, Normalized RMSE, and RSS are increased referring to unacceptable matching between the calculated and observed heads as compared with those results shown in Figure 5.11, which were better. Even the CC is reduced as shown in Figure 5.18.
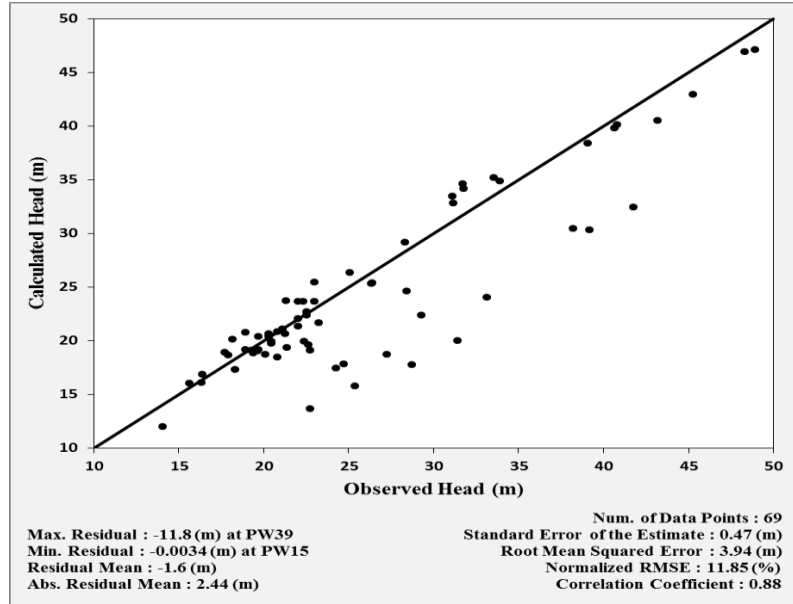
Figure 5.18: PEST result of the dynamic calculated and observed heads for a recharge = 16.5 mm/year with 69 wells

In conclusion, the PEST approach applied on the study area has slightly improved the Static calibration, but with respect of the Dynamic calibration, the results of the SEE, RMSE, Normalized RMSE, and RSS are increased where this means that when the pumping wells are

in-operation, PEST approach failed to improve the model domain to result acceptable head values close to the field observations. Where, as the Dynamic calibration is the one that should be used because of its logic where it takes into account the impact of pumping wells while these wells are in-operation; therefore, it will apply the new approach "Distributed Value Property Zones" to see whether it can improve the subsurface domain or not through getting the best fitting between the calculated and observed heads.

5.8 Distributed value property zones approach

Any groundwater flow model requires assigning the initial heads, storage, conductivity, and transporting parameter property values for each active cell in the finite difference grid to be able to run either the flow or transport simulation. Although these property values are sometimes distributed uniformly, in most situations, these property values are non-uniformly distributed throughout the entire domain of a model. Hence, it is necessary to assign different property values for different regions of the model. In Visual MODFLOW, there is an approach called "Distributed Value Property Zones" that is available only for scattered observation points such as conductivity, initial heads, storage, dispersion properties, and initial concentrations. In this approach, the property of the zone is linked to one or more parameter distribution arrays containing discrete scattered points. This linkage will lead to the need to recalculate the zone parameter depending upon an interpolation process that is called Kriging, which in turns will result in a new property parameter for each cell or zone of the model. The Kriging interpolation process needs an appropriate Variogram which is a three-dimensional function that is used to correspond the spatial correlation of the observed variables of a model (Schlumberger Water Services 2011). The Kriging and Variogram processes will be explained in detail.

5.8.1 Kriging interpolation of discrete points

The methods of interpolation are an important part of many different fields and can be used them for modelling various discrete properties, such as an elevation dataset. These methods are crucial to the visualization process, either in 2D or 3D, due to converting data from scattered points to raster (surfaces) to better understand or identify bad samples. Usually, interpolation methods produce a surface that represents the real domain, so it should be as accurate as possible because it will often form the basis for spatial analysis. Although three-dimensional surfaces are created from the interpolation process, in reality this process is a two-dimensional process because it considers only x and y coordinates while the elevation is considered as an attribute (Ledoux and Gold 2005). Therefore, the definition of the interpolation is a process of constructing, estimating, intermediating, and filling new data values in some locations of

unmeasured parameters from a discrete set of known data points that are collected from those regions in the same surrounding vicinity (Sefelnasr 2007). Visual MODFLOW has a set of interpolation methods that can be used for interpolating discrete data and producing surfaces. These methods are: Inverse Distance, Kriging, and Natural Neighbours. The most well-known and representative geostatistical method that accounts for the hydrogeological information is the Kriging method which was firstly developed by the geologist Krige (1951 and 1952), who originated from South Africa (Sefelnasr 2007).

The geostatistical Kriging technique has the capability of the visual appealing maps for the irregular discrete data interpolation, so that the anisotropy of the data can be incorporated by an efficient manner through Kriging. Bohling (2005) has illustrated the mechanism of the interpolation process that is adopted by Kriging method through Eq. (5.2):

$$Z^*(u) - m(u) = \sum_{\alpha=1}^{n(u)} \lambda_\alpha \left[Z(u_\alpha) - m(u_\alpha) \right] \tag{5.2}$$

where, $Z^*(u)$, and $Z(u_a)$ are the estimated property value and the known neighbouring property value that are distributed over the region respectively; u, and u_a are the location vectors of the estimated point and the neighbouring data points that are distributed over the region respectively; $m(u)$, and $m(u_a)$ are the expected trend components of $Z^*(u)$ and $Z(u_a)$ respectively; $n(u)$ is the number of data values at n locations $\alpha = 1, \ldots, n$; and λ_a is Kriging weights. An example is available in Bohling (2005) showing the application of Eq. (5.2) in detail.

Kriging method incorporates the anisotropy in an efficient and natural manner, where by specifying the appropriate model of Variogram, Kriging method will have the capability to be custom-fit to a dataset (Sefelnasr 2007). Covariance function represents the basis derivation of the Kriging weights as this covariance will be represented by the appropriate Variogram (Bohling 2005).

5.8.2 Variogram

A Variogram represents a three-dimensional function that is used to correspond the spatial correlation of the observed variables of a model. It represents a change of parameters or variables on the average measure basis. The fundamental principle of a Variogram is that, on the average, the similarity of each two points or observations closer together will be better than two points or observations that are further apart. In addition, a Variogram is a directional function because the fundamental processes of the data often have preferred orientations. This leads to changing values quickly in one specific direction more than other directions (Sefelnasr 2007). As shown in Figure 5.19, it will be assumed that there are two independent $Z(x)$ and $Z(x+h)$

random variables with a distance between them that equals the lag distance *h*. The equation that represents the variogram (*γ(h)*) function will be written as the average squared difference of those quantities located at the corners of the lag distance (Debashish 2014).

$$\gamma(h) = \frac{1}{2} n * \sum_{1}^{n} (Z_n - Z_{n+h})^2$$ (5.3)

where: n: number of variables.
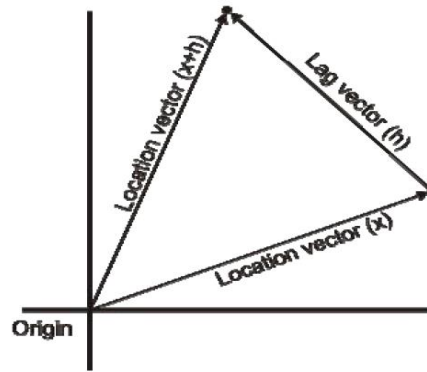
Figure 5. 19: The spatially distribution of two independent random variables separated by a lag distance (Adopted from Sefelnasr 2007)

Visual MODFLOW has various Variogram models that are available to the user to choose the appropriate one, which are: Spherical, Exponential, Gaussian, Power, and Hole Effect.

Aquifer parameters such as hydraulic conductivity, transmissivity and storativity can be measured through the well tests during the pumping period as these obtained parameters may be appropriate for site-scale spatial variation in either small-scale or regional scale depending on the extension of cone depression during the pumping period (Anderson et al. 2015). A new method called "Distributed Value Property Zones" rather than the forward (the constructed model with two constant hydraulic conductivities) or automated methods (PEST model) is available in Visual MODFLOW, is applied to Al-Najaf region groundwater model to reach for the best representation of the real field. Changing some certain parameters such as recharge or hydraulic conductivity represents an altered systematic fashion process which leads to computing the best matched solution between the field's observed data and the model's calculated data which is resulting in an acceptable level of accuracy (EMRL 1999).

The results presented in the previous sections (5.6 and 5.7) clearly show that the hydraulic conductivity is one of the key parameters to affect the model accuracy. Using a constant hydraulic conductivity for each layer (Forward Model) may not be desirable. In addition, the automated parameter estimation method (PEST Model) has not given acceptable results for the dynamic calibration where even the results for the static calibration were not changed too much in the matching of the calculated and observed heads. Therefore, the data collected from the

field are further analysed to generate a map of spatially interpolating the hydraulic conductivity through using the "Distributed Value Property Zones" approach integrated within Visual MODFLOW. In total, hydraulic conductivity values were extracted from 55 out of 69 wells. These 55 wells are located in the middle, western and northern-east areas. In order to cover all the entire computational area, 5 additional points around the computational domain using the hydraulic conductivity values to their closest points are used as shown in Figure 5.20.

An interpolation process using Kriging method is applied to predict the best interpolation for the underneath hydraulic conductivity of the groundwater aquifer that gives the best matching for a high extent with the real field observations. This method uses the appropriate Variogram (Power one) to analyse the spatial variation parameters and the roughness and continuity of various surfaces (Barnes 1991; Zimmerman and Zimmerman 1991). Figure 5.21 shows the Power variogram of the hydraulic conductivity distribution over the study site. Figure 5.22 shows the spatially interpolating the hydraulic conductivity resulted from applying the "Distributed Value Property Zones" approach (integrated within Visual MODFLOW) on the study site. It can be seen that larger values of the hydraulic conductivity comprise of small area from the study site. Most the central part of the computational domain is ranged between 13 m/day and 17 m/day, while the overall range of the hydraulic conductivity is between 11 and 25 m/day. This interpolation is incorporated in order to reach a better representation of the sub-surface soil formation for Dibdibba aquifer, which is located within the study site. To assess all of these approaches which are resulted from the Forward, Automated, and Distributed Value Property Zones models, it will recalculate the heads from the latest one "Distributed Value Property Zones Approach" and compare these heads with the field observations to ultimately choose the model with the best correspondence between the calculated and observed data.
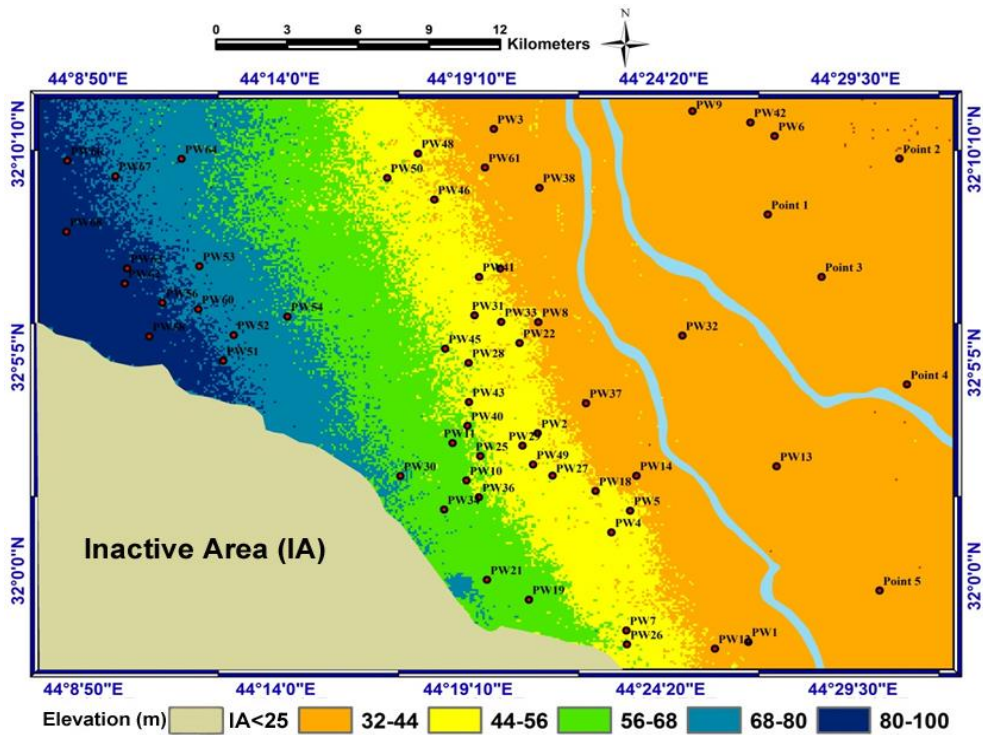
Figure 5.20: Names and locations of the 60 wells having hydraulic conductivities
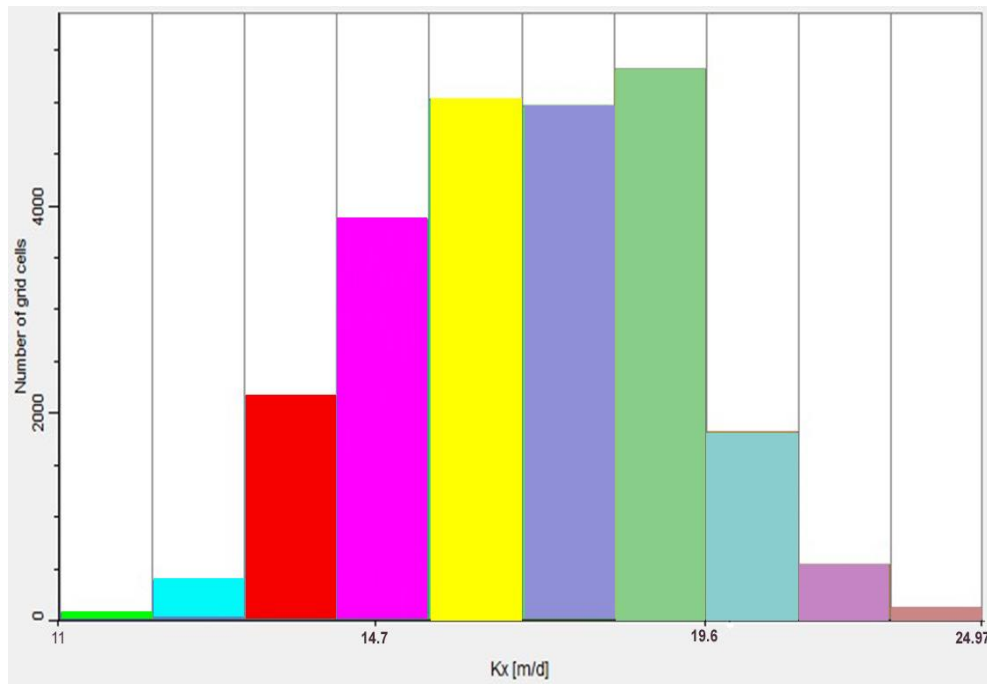
Figure 5.21: Variogram shows the zones of the spatial hydraulic conductivity distribution

■ 11.000 – 12.051 m/day	■ 12.051 – 13.070 m/day	■ 13.070 – 14.176 m/day
■ 14.176 – 15.365 m/day	■ 15.365 – 16.654 m/day	■ 16.654 – 18.051 m/day
■ 18.051 – 19.578 m/day	■ 19.578 – 21.220 m/day	■ 21.220 – 23.015 m/day
	■ 23.015 – 24.965 m/day	■ Inactive Area
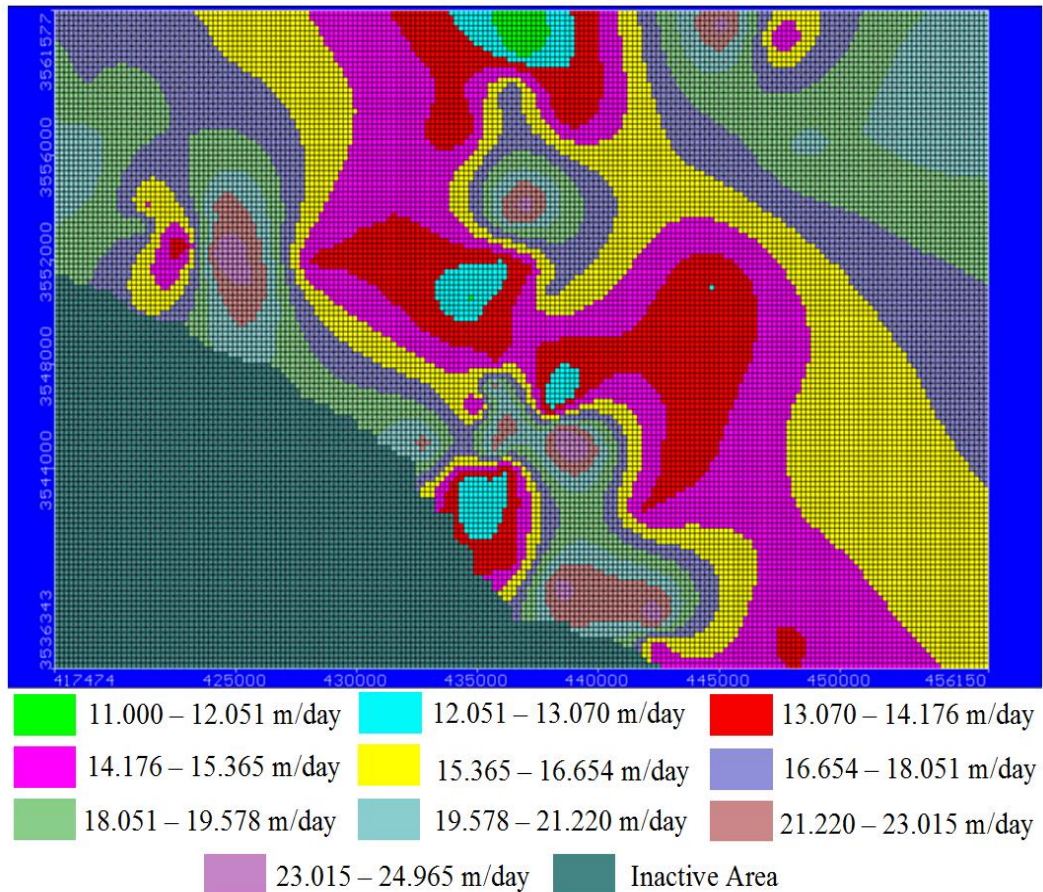
Figure 5.22: Map of spatially interpolating the hydraulic conductivity

5.9 Applying distributed value property zones approach

With the spatially interpolating the hydraulic conductivity map resulted from applying the "Distributed Value Property Zones Approach" shown in Figure 5.22, the head distribution is re-calculated for both the static and dynamic calibrations. The re-calculated heads for the static and dynamic calibrations are illustrated in Figures 5.23 and 5.24 respectively where these figures show the relationship between the calculated and observed heads for three calibrations, 1) the Forward model when there are only two layers with a constant hydraulic conductivity for each, 2) after applying the automated parameter estimation approach (PEST Model), and 3) after applying the spatially interpolating the hydraulic conductivity using the "Distributed Value Property Zones" approach (Distributed Value Property Zones Model). Clearly, it can be seen that with the Distributed Value Property Zones approach and with the dynamic calibration (Figure 5.24), the values of the calculated heads resulted from the Distributed Value Property Zones Model are more reliable and acceptable than those heads resulted from the other approaches (Forward Model and PEST Model) for both the static and dynamic calibrations. In addition, it can be seen in Figures 5.23 and 5.24 that there are some observations are not matching the calculated heads and cannot be considered these heads as acceptable heads.
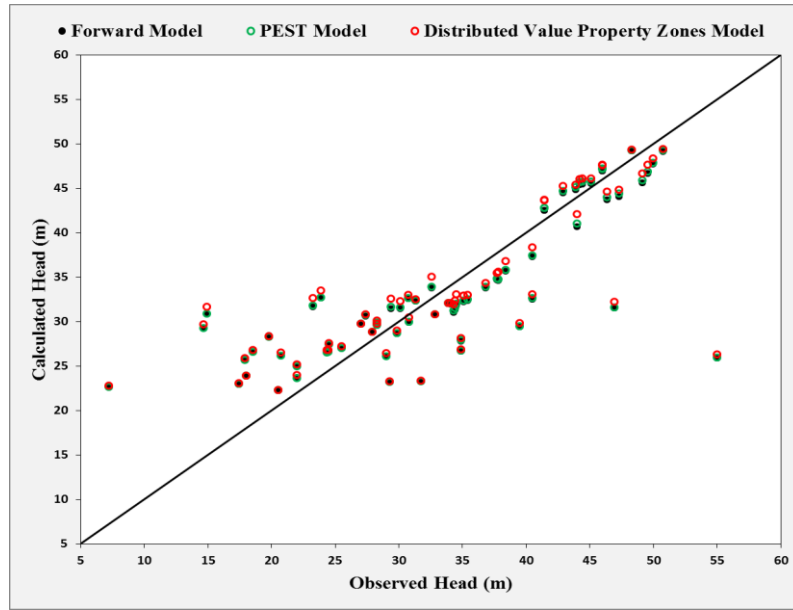
Figure 5.23: Comparison of the static computed and observed heads for three models when applying a recharge rate of 7.55 mm/year
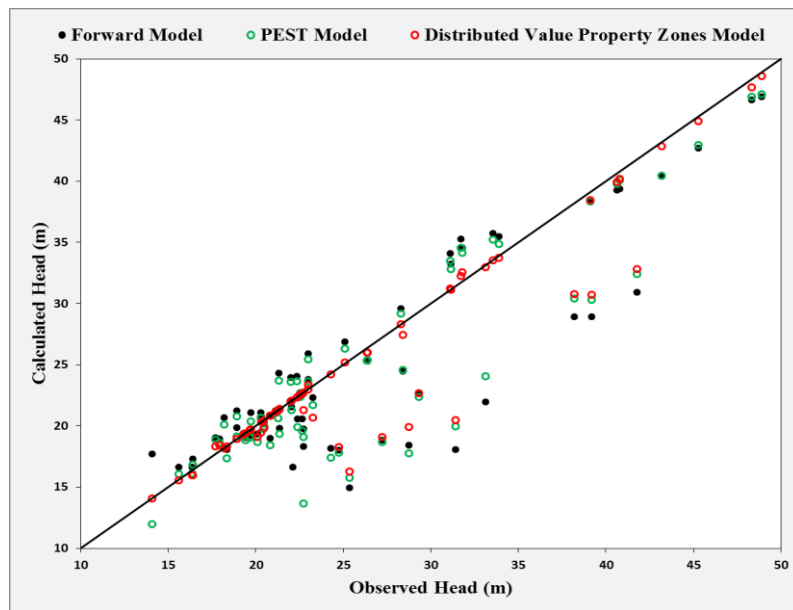
Figure 5.24: Comparison of the dynamic computed and observed heads for three models when applying a recharge of 16.5 mm/year

Table 5.5 shows a comparison between the SEE, RMSE, Normalised RMSE, CC, and RSS for the three approaches applied to Al-Najaf study site for both the static and dynamic calibrations to help in assessing the most reliable approach that achieving the matching between the calculated and observed heads.

Table 5.5: A comparison between the final static and dynamic calibration parameters for three models with different approaches applied

Calibration Case	Recharge mm/year	SEE m	RMSE m	Normalized RMSE %	CC	RSS m²
*Static	7.55	0.783	6.458	13.517	0.788	2878
**Static	7.55	0.78	6.44	13.47	0.79	2855
***Static	7.55	0.779	6.435	13.468	0.79	2857
*Dynamic	16.5	0.437	3.82	10.969	0.900	1006
**Dynamic	16.5	0.47	3.94	11.85	0.88	1315
***Dynamic	16.5	0.398	3.694	10.609	0.917	941

* Forward Model
** PEST-Parameter ESTimation Model
*** Distributed Value Property Zones Model

Clearly from Table 5.5, it can be noticed that the values of the SEE, RMSE, Normalised RMSE, and RSS for the Distributed Value Property Zones Model with a recharge value R= 16.5 mm/year are the least with the highest magnitude of CC where this indicates that the calculated heads are the closest to the observed ones. Ultimately, the dynamic calibrated model with the spatially interpolating for the hydraulic conductivities observed in 60 wells and recharge value of 16.5 mm/year will be the groundwater model of Al-Najaf region that will be considered in this study. Therefore, if the unacceptable observations shown in Figure 5.24 for the Distributed Value Property Zones Model are excluded, the SEE, RMSE, Normalised RMSE, and RSS will become 0.106m, 0.866m, 2.487%, and 42m² with the best value of CC 0.996.

5.10 Model validation

In this section, as it has been proved in the current research that the Dynamic calibration is the best method to calibrate the model, it will use the data collected for year 2013 for 56 pumping wells for the study area for the purpose of comparing the calculated heads, resulted from Visual MODFLOW program through the steady-state simulation when there are pumping conditions (Dynamic Heads), with the observed heads (Dynamic Heads). 13 wells (10 on far west and 3 on far east) of the 69 wells are removed from the simulation process because these wells are not there in 2013. The groundwater recharge used for the validation process will be 16.5 mm/year where this value has resulted in the best corresponding between the calculated and observed data as the dynamic calibration shows.

Figure 5.25 demonstrates the fitting of the validation process for the calculated and observed dynamic heads resulted from Visual MODFLOW simulation when all of the 56 pumping wells are under operation. A good fitting can be seen from Figure 5.25 between the calculated and observed dynamic heads which can be considered acceptable.
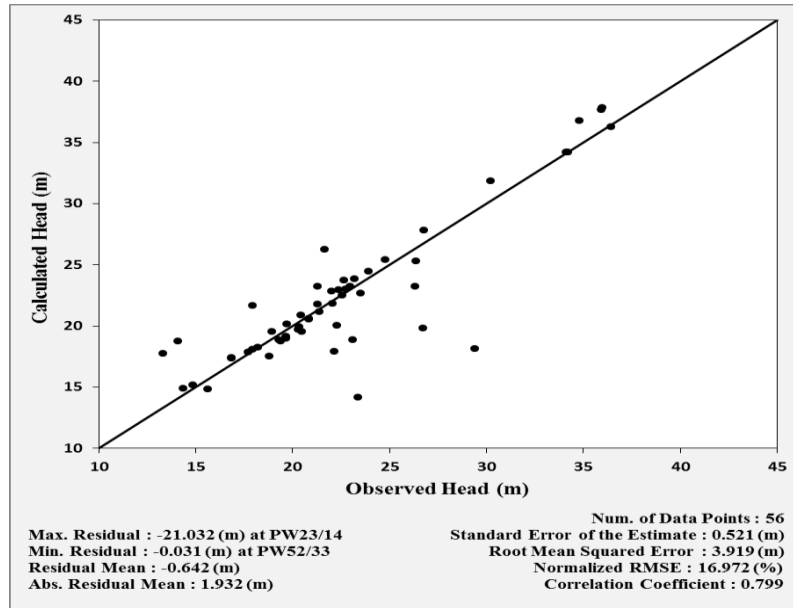
Figure 5.25: Comparison of the calculated and observed heads for 56 wells with a recharge rate of 16.5 mm/year

5.11 Interface soil layer effect

At this point, the final groundwater model of Al-Najaf region is considered to consist of two heterogeneous layers as a result of the interpolation of the collected hydraulic conductivities by using the "Distributed Value Property Zones Approach" with an interface soil layer separating these two layers as shown in Figure 5.26. To assess the impact of that interface soil layer on the behaviour of Al-Najaf Dibdibba aquifer, it will remove that interface from the considered model of Al-Najaf region to comprise of one unconfined aquifer with one heterogeneous soil layer as shown in Figure 5.27. The behaviour of these two models under the current applied pumping schedule and the interaction of Dibdibba aquifer-the Euphrates River, will be examined in results section (Chapter Six) to evaluate Dibdibba aquifer behaviour for the impact of that interface soil layer.
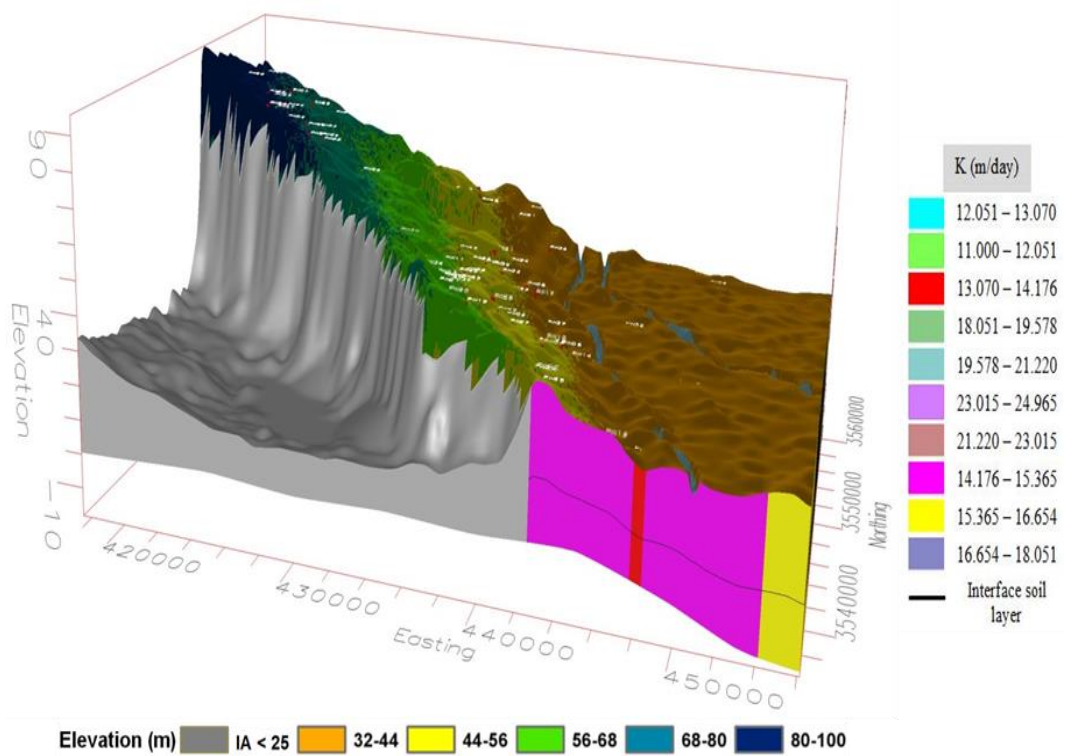
Figure 5.26: 3D view of Al-Najaf considered model with two heterogeneous soil layers separated by an interface soil layer
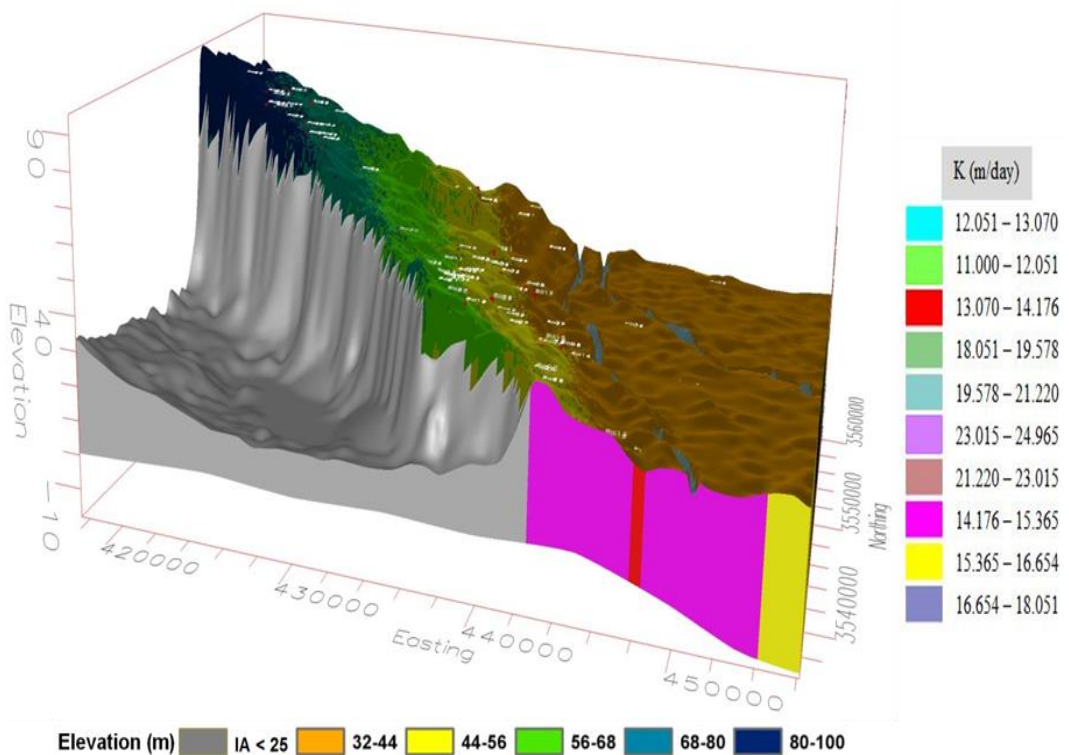
Figure 5.27: 3D view of Al-Najaf considered model with one heterogeneous soil layer after removing the separated interface soil layer

5.12 Summary

A three-dimensional conceptual groundwater model, Forward Model with two homogeneous layers, has been constructed for Al-Najaf region by using Visual MODFLOW (version 4.6). The total area of the study site is 976 km^2. An area of approximately 205 km^2 is marked as inactive area because of this area was not represented part of the Dibdibba groundwater aquifer which is the aquifer considered under study in this research. Sensitivity analysis for the recharge rate and hydraulic conductivity has been examined. The 40.32 mm/year recharge rate applied on the study site has flooded the study area which has never been found to be flooded in the past, rather suffered from the water scarcity. Static and Dynamic calibrations are tested and it is found that the Dynamic one (when all pumping wells are in-operation) is the best as it gives a 16.5 mm/year as the best recharge rate that achieves the fitting between the dynamic calculated and observed heads. PEST "Parameter ESTimation" and the "Distributed Value Property Zones" of hydraulic conductivity approaches are applied to improve the model to reach the best representation of the hydraulic conductivity that represents the entire domain of the study site. The "Distributed Value Property Zones" approach by using Kriging method with the appropriate variogram gave the best model of Al-Najaf region with two heterogeneous layers separated by an interface soil layer. Validation process has also carried out where the results gave an acceptable agreement. To assess the impact of an interface soil layer presents in an aquifer, it will remove that interface soil layer from the aquifer of Dibdibba for Al-Najaf region model and assess the results of the model (with and without) interface soil layer in the results' chapter.

Chapter Six
Results and Discussions

6.1 Introduction

By using Visual MODFLOW (version 4.6), it will explore the current state of the Al-Najaf region groundwater aquifer as well as the interaction between the Euphrates River and groundwater system under various approaches of hydraulic conductivity estimation to investigate the importance of the novel approach "Distributed Value Property Zones" through comparing its results with the others results of the constant hydraulic conductivity and Parameter ESTimation approaches (Forward and PEST models). Where, according to the calibration process, it is found that the Distributed Value Property Zones Approach has resulted in the best model of the study site. The impact of the interface soil layer located between the two soil layers of Al-Najaf region aquifer will be investigated through comparing the results of the model with interface soil layer with those ones of the model without interface soil layer. In addition, study how can overcome the current impact of the pumping process on the study area in terms of declining the groundwater table level (appearing the dry area) and keeping the Euphrates River without losing water from its current water. More than that, study the impact of different dry climates scenarios on both the groundwater aquifer and the Euphrates River through predicting the effect of these future dry climates scenarios to be under consideration for the decision-makers.

In addition, studying the impact of different dry climates cases on both the groundwater aquifer and the Euphrates River through predicting the effect of these future dry climates to be under consideration for the decision-makers. Where it will keep the current pumping schedule as it is now and change the boundary conditions in the first three cases, such as reducing the recharge rate by 25% and 50%, reducing the western head for 45m as well as the recharge rate, and reducing the Euphrates River level by 0.5m and 1m as well as the recharge rate and the western head all at the same time. It will increase the current pumping rate up to 50% with the current boundary conditions in the fourth case. In the rest cases from 5 to 8 and through the increasing the current pumping rate up to 50%, it will reduce the recharge rate, then the western constant head, then the level of Euphrates River, and finally all of them at the same time respectively.

6.2 Current state of Al-Najaf study area

Figure 6.1 shows the results of the computed groundwater table in the top and bottom layers of the groundwater model for each approach after applying the best recharge rate 16.5 mm/year and Al-Najaf region boundary conditions. Running Visual MODFLOW program with a steady state condition over a one year period for the case when the current pumping schedule is in operation, articulates dry areas in the top and bottom layers with various volumes. However, with the current applied pumping schedule, the resulted dry area as indicated by Grey in the top and bottom layers of the model for the constant hydraulic conductivity approach (Forward Model) were 54.1 km^2 and 4 km^2 respectively (Figure 6.1-top), 56.24 km^2 and 6.16 km^2, for the Parameter ESTimation of hydraulic conductivity approach (PEST-Model) (Figure 6.1-middle), and 32 km^2 and 1.32 km^2 for the Distributed Value Property Zones approach (the Distributed Value Property Zones Model) (Figure 6.1-bottom) respectively. Clearly from Figure 6.1, it can be seen that the third model with the spatially interpolated of the hydraulic conductivity resulted from the Distributed Value Property Zones approach has the least dry areas, with the best fitting (as illustrated in Chapter Five in detail). Therefore, it will consider the Distributed Value Property Zones model as the corresponding model of Al-Najaf region study site.
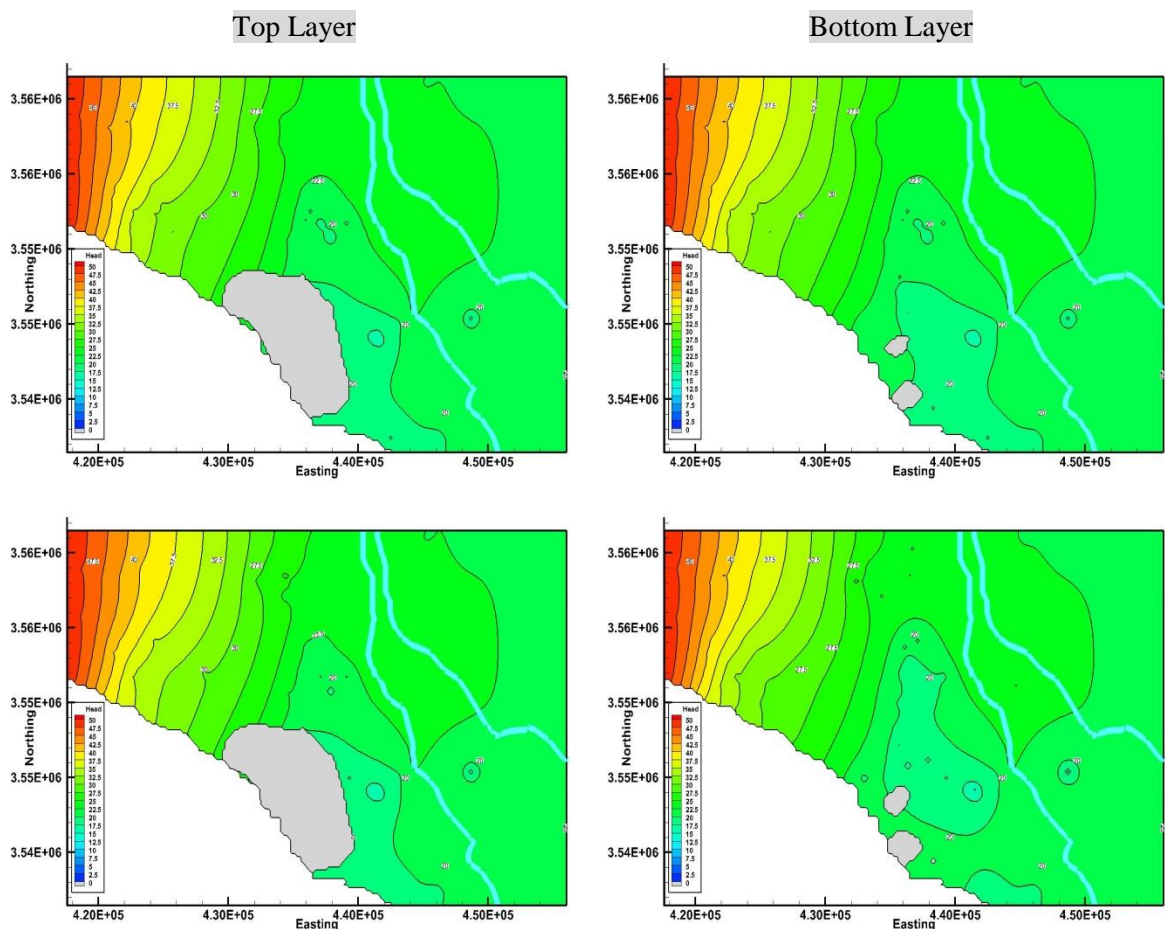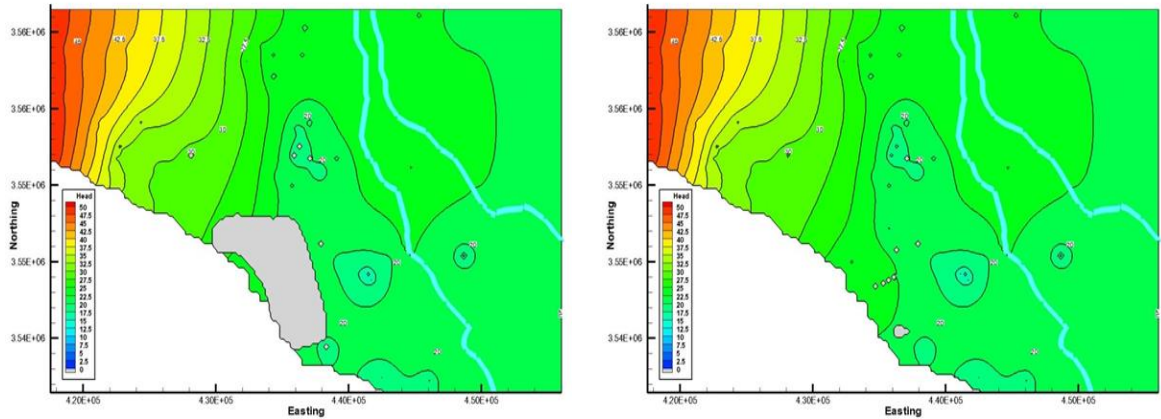
Figure 6.1: Computed groundwater table with 16.5 mm/year recharge rate: (top) Forward Model, (middle) PEST Model, and (bottom) Distributed Value Property Zones model

To explore the Euphrates River status, an important leakage quantity is resulting from the impact of the pumping schedule on the groundwater aquifer as resulted from groundwater balance. The groundwater balance illustrates that the Euphrates River leaks 8035 m^3/day (inflow into the river: 1521 m^3/day and outflow from the river: 9556 m^3/day), 7358 m^3/day (inflow into the river: 1723 m^3/day and outflow from the river: 9081 m^3/day), and 5354 m^3/day (inflow into the river: 1951 m^3/day and outflow from the river: 7305 m^3/day) in to the groundwater aquifer for the Forward Model, PEST Model, and Distributed Value Property Zones model respectively.

Running Visual MODFLOW in a steady state condition over a one year period with the current pumping schedule results in a significant decline in the groundwater level. Cross-sections of groundwater level decline over the study site are selected in the most affected sites and shown in Figure 6.2. An important issue can be seen in Figure 6.2 where when the groundwater level decreases and become below the bottom elevation of the top layer (Head Upper shown in Figure 6.2a) or bottom layer (Head Lower shown in Figure 6.2b) of the model, that layer falls under the influence of drought. Moreover from the cross-sectional figure, even with that significant decline in the groundwater level, it can be seen that there is a connection between the groundwater table and the Euphrates River level due to the saturation with water at the downstream area of the study site. Therefore, it can be trusted the results of Visual MODFLOW when it is running as a saturated model.
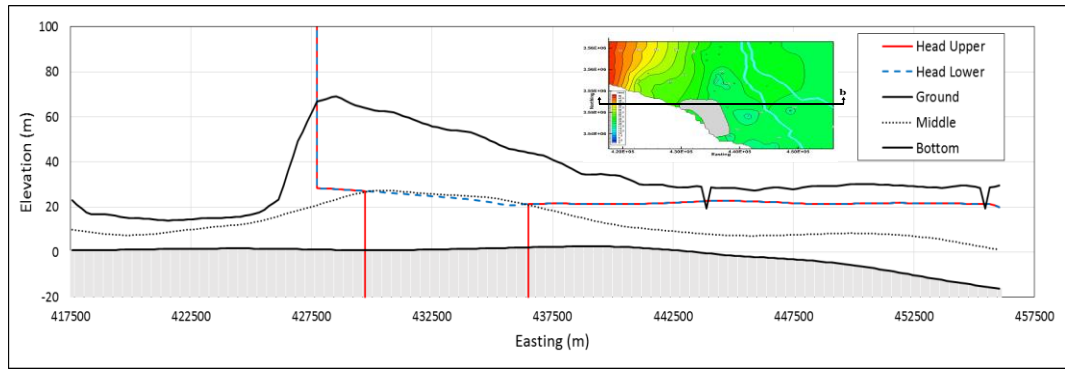
(a)
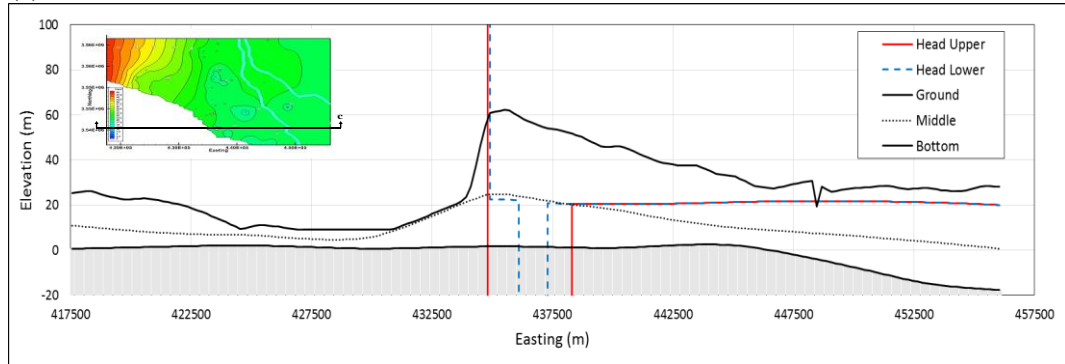
(b)

Figure 6.2: Groundwater level decline for the Distributed Value Property Zones model: (a) Top layer and (b) Bottom layer

The results of running Visual MODFLOW over a one year period with a steady state condition when there is no pumping schedule applied are shown in Figure 6.3. Figure 6.3 shows (a) groundwater movement over the study site, (b) computed groundwater table with 16.5 mm/year recharge rate, and (c) groundwater level decline at the worst location. The results illustrate an eastward groundwater movement in general as predicted from field observations (Figure 6.3a), no dry areas either in the top or bottom layers of the model are generated (Figure 6.3b), and according to the latitudinal cross-section over the study site shown in Figure 6.3c, the connection between the groundwater-Euphrates River is existing where the Euphrates River gains water from the groundwater aquifer reach to 23527 m^3/day (inflow into the river: 27035 m^3/day and outflow from the river: 3508 m^3/day) as the groundwater balance illustrates.
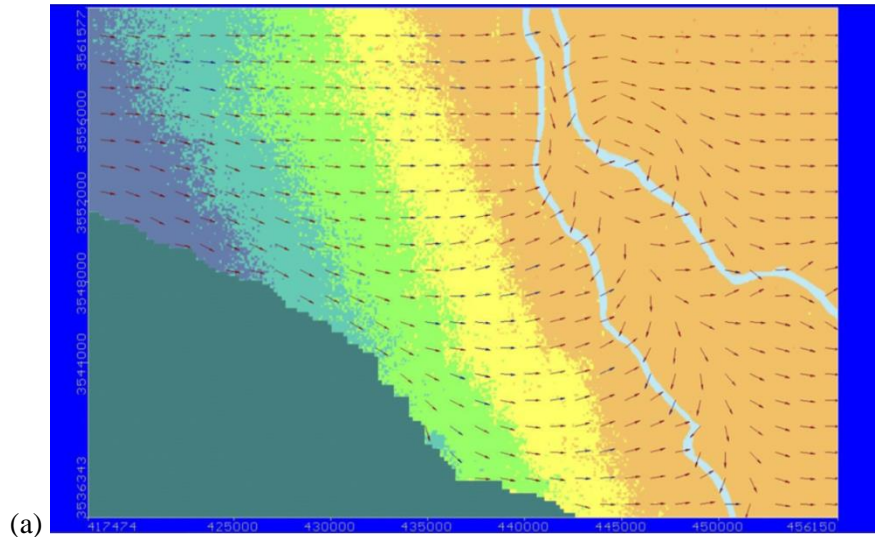
(a)
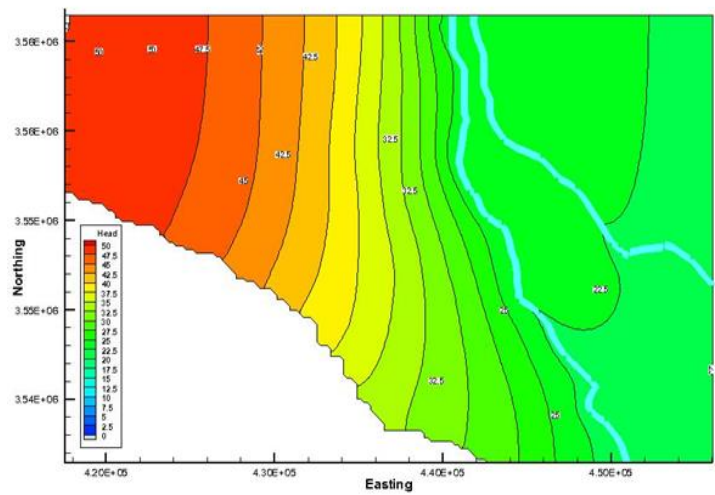
(b)
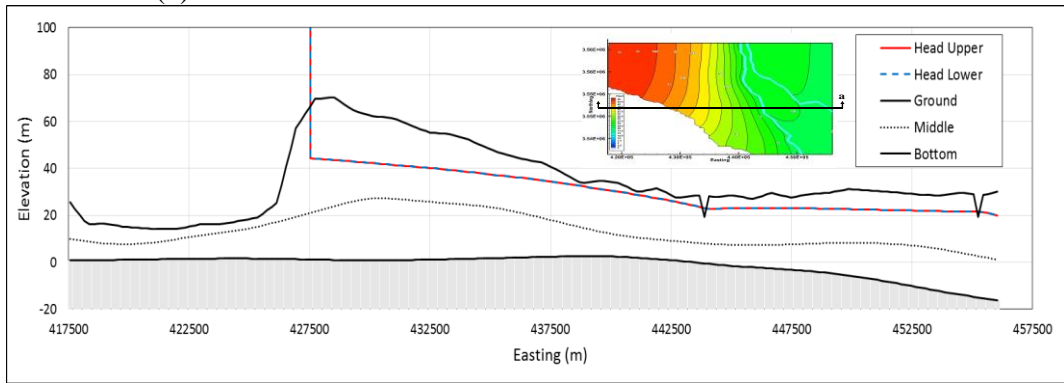
(c)

Figure 6.3: Results of the Distributed Value Property Zones model when there is no pumping schedule applied: (a) Groundwater movement over the study site, (b) Computed groundwater table with 16.5 mm/year recharge rate, and (c) Groundwater level decline

Ultimately, from the Distributed Value Property Zones model, the groundwater aquifer in the study site does not supply the required or applied pumping rate (52454 m^3/day) and supplying only 44263 m^3/day where this quantity represents only 84% of the required pumping rate and this indicates the weakness of groundwater aquifer in providing the required pumping rate as

well as the pressure added to the surface water source represented by the Euphrates River. In addition, due to the over-pumping and the impact of dryness, nine wells are stopped working which led to losing the pumping quantities pumped from these wells. In conclusion, the province of Al-Najaf and its surrounding regions represented by the groundwater aquifer (Dibdibba Aquifer) is suffering from the great pressure resulted from the current pumping schedule which in turns led to adding a significant impact on the Euphrates River through losing its water into the groundwater aquifer by the seepage phenomenon.

6.3 Impact of the interface soil layer

It will explore and assess the impact of the interface soil layer located between the layers of Dibdibba aquifer (the Distributed Value Property Zones model) on the groundwater table and the exchange between the groundwater and surface water represented by the Euphrates River after removing that interface soil layer and compare the results with the original model. The computed groundwater table in the top and bottom layers of the Distributed Value Property Zones model (without interface soil layer) when applying a recharge rate of 16.5 mm/year is shown in Figure 6.4a. The results of the Distributed Value Property Zones model with two layers separated by an interface soil layer in respect of the dry area and the Euphrates River leakage are illustrated previously in section 6.2. However, when ignoring the interface soil layer from the conceptualisation process, Figure 6.4a shows that the dry area is only 0.16 km^2. In addition, the Euphrates River was losing 7994 m^3/day (inflow into the river: 1522 m^3/day and outflow from the river: 9516 m^3/day). Moreover, the Dibdibba aquifer is supplied only 48533 m^3/day of total extracted water 52454 m^3/day. Where, due to the over-pumping applied on the study area, four wells are stopped to pump water for the required pumping schedule as compared with nine stopped wells when the interface soil layer is modelled. It is obvious that there is a significant difference between the results of the model whether there is an interface soil layer or not. Consequently, in case of there is an interface soil layer in the real field domain, but it is not adopted in the model's conceptualisation, the behaviour of the aquifer will greatly affect the groundwater table results and its interaction with the surface water bodies as this means that the model's current behaviour and future impacts predictions results will not represent the field in the reality. Therefore, it will consider the Dibdibba aquifer model (the Distributed Value Property Zones model) with two types of soil layers with an interpolation of their hydraulic conductivities as a final model for Al-Najaf region to be examined for the future climate changes. Figure 6.4b shows a comparison between the calculated heads resulted from Al-Najaf model with and without interface soil layer and the observed heads. It is obvious from Figure 6.4b that the correspondence between the calculated and observed heads for that model without interface soil layer is unacceptable for some extent. Where, the large values of the SEE

(0.449 m), RMSE (3.875 m), Normalised RMSE (11.129%), and RSS (1037 m^2) for the model without interface soil layer as compared with those values highlighted in Table 5.5 mean that the correspondence between calculated head values and field observation values is very large. Even the correlation coefficient for the model without interface soil layer, which is equal to 0.902, has become lower than that highlighted value shown in Table 5.5. It is very clear that there is an impact affecting the behaviour of Al-Najaf model; where, ignoring the interface soil layer from the conceptualisation process has led to resulting in large values of the SEE, RMSE, Normalised RMSE, and RSS, as this will affect the calibration process of the model to become very complex due to the calculation of unrealized head values, which in turn will complicate the process of obtaining the required/accepted matching between the calculated and observed collected data.

(a)

(b)
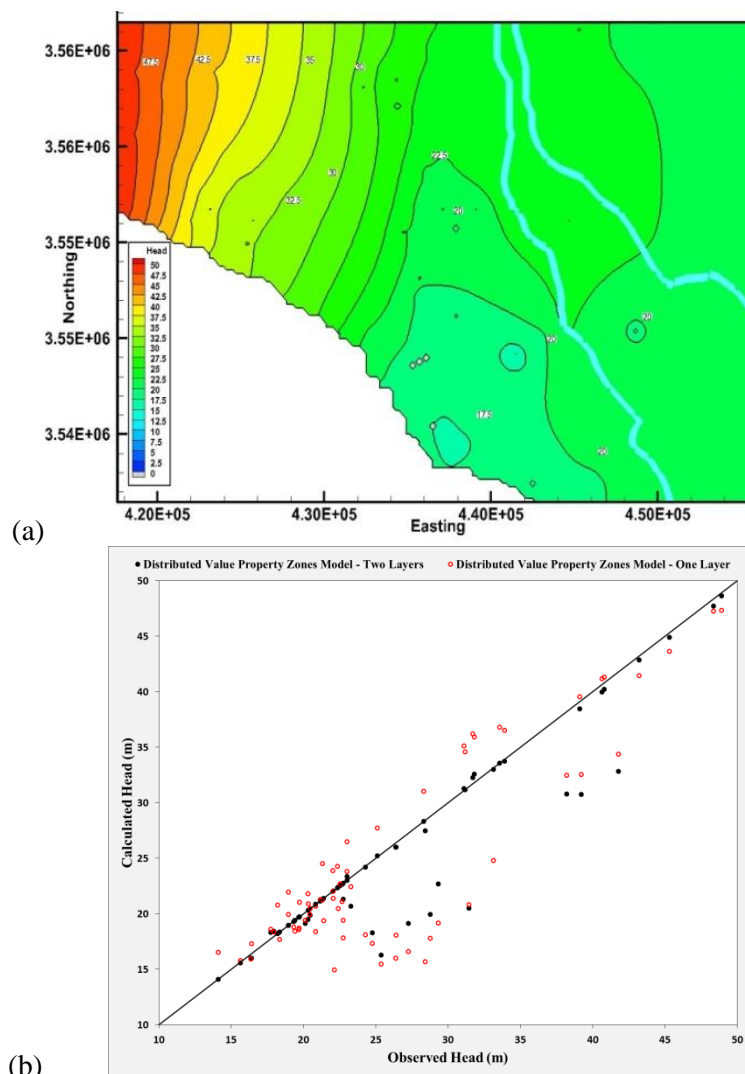
Figure 6.4: (a) Computed groundwater table of the Distributed Value Property Zones model without interface soil layer, with 16.5 mm/year recharge rate, and (b) Calibration comparison's results of the Distributed Value Property Zones model with and without interface soil layer

146

6.4 Simulations for future climate conditions

The effect of various dry climates cases will be examined to monitor and assess the groundwater system efficiency, firstly in the case of keeping the current pumping schedule as it is now and change some boundary conditions, and secondly when increasing the current pumping schedule up to 50% and change some boundary conditions at the same time.

With the present annual pumping schedule 19.15 million cubic meters, three proposed dry climates cases were simulated in Visual MODFLOW to evaluate the predicted effect on the groundwater aquifer (Dibdibba aquifer) and the Euphrates River-groundwater aquifer interaction. In the first case (Case 1) will reduce the current recharge value 16.5 mm/year by 25% to be 12.375 mm/year and 50% to be 8.25 mm/year. The second case (Case 2) will deal with the reduction in the recharge value by 25% and 50% as well as the reduction in the west constant head from 50 m to 45 m. In the third case (Case 3) will reduce three parameters at the same time which are the recharge rate by 50%, reduce the west constant head to become 45 m, and reduce the Euphrates River level by 0.5 m and 1 m.

When increasing the pumping schedule from 10% up to 50%, five proposed dry climates cases will be simulated in MODFLOW. The first case (Case 4) will examine the current state of the study area but when increasing the pumping schedule up to 50%. The second case (Case 5) will deal with the reduction in the recharge rate by 50% to become 8.25 mm/year through various increments in the pumping rate value. With the various increments in the pumping schedule will reduce the west constant head to be 45 m in the third case (Case 6). In the fourth case (Case 7) will reduce the Euphrates River level by 1 m through the various increments in the pumping rate. In the final fifth case (Case 8) will reduce all of, recharge rate by 50%, the west constant head to be 45 m, and the Euphrates River level by 1 m with the various increments in the pumping schedule. Table 6.1 shows the cases' details to be more obvious.

Table 6.1: Cases of dry climates examined in MODFLOW

Cases	Recharge mm/year	Western Constant Head (CH) m	River Level Reduction m	Applied Pumping Rate m^3/day
Case 1	Reduced by 25% and 50%	Not Change	Not Change	Current
Case 2	Reduced by 25% and 50%	Reduced to be 45 m	Not Change	Current
Case 3	Reduced by 25% and 50%	Reduced to be 45 m	Reduced by 0.5m and 1m	Current
Case 4	Not Change	Not Change	Not Change	Increased up to 50%
Case 5	Reduced by 50%	Not Change	Not Change	Increased up to 50%
Case 6	Not Change	Reduced to be 45 m	Not Change	Increased up to 50%
Case 7	Not Change	Not Change	Reduced by 1m	Increased up to 50%
Case 8	Reduced by 50%	Reduced to be 45 m	Reduced by 1m	Increased up to 50%

It will mention some of the justifications which called for taking into account these cases to be under consideration as these cases may happen and affect the study site in the future. As the study area is located in the Middle East region and this region suffers from high temperatures, low precipitations, high evapotranspiration, and dry climates (Middleton and Arnold 1997), the study area in turns classified as an arid climate type. Where, this gives an indication for the possibility of rainfall reduction (as enhanced by the rainfall, temperature, and soil moisture analyses shown in Chapter 4), and this leads to a decrease in the amount of recharge, which is considered a major source of groundwater recharge in the study site. Therefore, the value of recharge will be reduced by either 25% or 50% at a higher level where even in cases of severe dryness in the area of study, still there is a possibility of precipitation fall, so this decrease is sufficient for the purpose of investigating its impact. The range of reduction of the recharge rate by 25% (4.125 mm/year) and 50% (8.25 mm/year) to become either 12.375 mm/year or 8.25 mm/year, respectively, is considering to be satisfactory because even in areas with very dry climates, the study area will remain collecting for a recharge value either from the Euphrates River leakage or those wet seasons with little rainfall intensities.

In respect of the groundwater level (constant head boundary condition) on the western side of the study area which is equal to 50m, this level has been reduced to 45m while maintaining the eastern side level at 20m. The reason for reducing the water level on the western side only is because the western side represents the source of water input the groundwater aquifer and since the movement of water is eastward of the study area, this means that any decrease in the level of groundwater on the western side will negatively affect the performance of the groundwater aquifer on the downstream side. In addition, since the study area is classified as a dry climate, this will exclude the possibility of increasing the groundwater level boundary on the west side to be in the future more than 50m. Therefore, there is no need to explore the effect of increasing this level on the study area where even when it is likely to increase, this will reduce the risks and potential disadvantages to which the study area may be exposed because its impact will be positive. In respect of the eastern side (constant head on the eastern side), the groundwater level has been stabilized at 20m because: 1) the eastern area is saturated with water flowing from the west region and terminated exactly on the eastern area, and 2) there are huge quantities of water leaking from the Euphrates River into the groundwater aquifer on the eastern side and this will raise the groundwater level at the bottom of the reservoir. Where the reduction of groundwater level on the eastern side to be lower than 20m will have almost no effect on the central and western regions of the study site because these regions are far from the point of impact, even the eastern area will not affected by the reduction of the eastern boundary level as it is completely saturated. Now, the reason for reducing the western groundwater level (constant head boundary

condition) by only 5m is that the value of the reduction 5m is significantly large, where although it has not occurred for a long time (maybe 35 years ago or more), but it remains considered as a potential value in the future. However, the decrease in the value of the western groundwater table to a value of more than 5m is not feasible because it is not expected to occur in the future or very rare. Where, the results that will appear to the value of the decrease of 5m can be used to predict the effect in the event of a decline in the level of groundwater for less than 45m. Therefore the risk for the groundwater reduction to be less than 45m can be deduced from the groundwater aquifer or it can predict the behaviour of the aquifer when that event occurs in the future. Although the range between the constant heads of 50m and 45m is considered to be large but still largely to happen in the future in those very arid climates, where predicting the results for this reduction value (5m) will help in estimating the risks that may happen and can help to develop the necessary treatments for these risks. This will help to predict the groundwater resource, either from drought or from damage.

In regards to the level of the Euphrates River, this level has been reduced by either by 0.5m or 1m as a maximum value to study the effect of this decrease on the groundwater aquifer, as well as on the amounts of water exchanged between the Euphrates River and the aquifer, so there is no need to reduce the level of the river more where the total maximum (upstream) and minimum (downstream) depths of water in the Euphrates River are 5.45m and 1.85m respectively. Where, the reduction of the river level by 1m can give the satisfying indication for the purpose of assessment to the exchange relationship between surface water and groundwater in the study site. In addition, the range of reductions of 0.5m or 1m will reduce the Euphrates River levels on the upstream and downstream sides to 4.45m and 0.85m (if the reduction was 1m), respectively. Where, it can be seen that the downstream level has reduced considerably. These values of level reduction are considered to be satisfactory to estimate the impact of the Euphrates River's level on the groundwater aquifer.

6.4.1 Case 1

In this case, it will reduce the groundwater recharge, which is originally 16.5 mm/year, by 25% (12.375 mm/year) and 50% (8.25 mm/year). The applied pumping schedule 52454 m^3/day remains constant in this case. Groundwater table is affected by the quantity of recharge which is relying mainly on the precipitation intensity (Todd 1958). The groundwater recharge on the Al-Najaf region Dibdibba aquifer which is resulted from the calibration process 16.5 mm/year will be reduced to investigate the effect of this reduction on the study site for the purpose of future dry climates. Figure 6.5 shows the computed groundwater table and the dry areas in the top and

bottom layers of the study site with the current recharge rate and when the recharge rate is reduced by 25% (R= 12.375 mm/year) and 50% (R= 8.25 mm/year).

From Figure 6.5, a great impact resulted from reducing the recharge rate can be seen wherein in the top layer, the dry area increased from 39 km^2 with the current recharge rate to 83.68 km^2 and 90.28 ^{km2} for the recharge reduction of 25% and 50% respectively. The same impact can be noticed in the bottom layer where the dry area was 1.32 km^2 for the current recharge rate, but it becomes 3.84 km^2 and 26.52 km^2 for these reductions respectively. It is obvious in Figure 6.5 that the dry area in the top or bottom layers is increased and spread from the lower central region to the west of the study site where this confirms that the western side is more affected by the decrease in the recharge rate and overall this indicates the effect of the future dry climate.
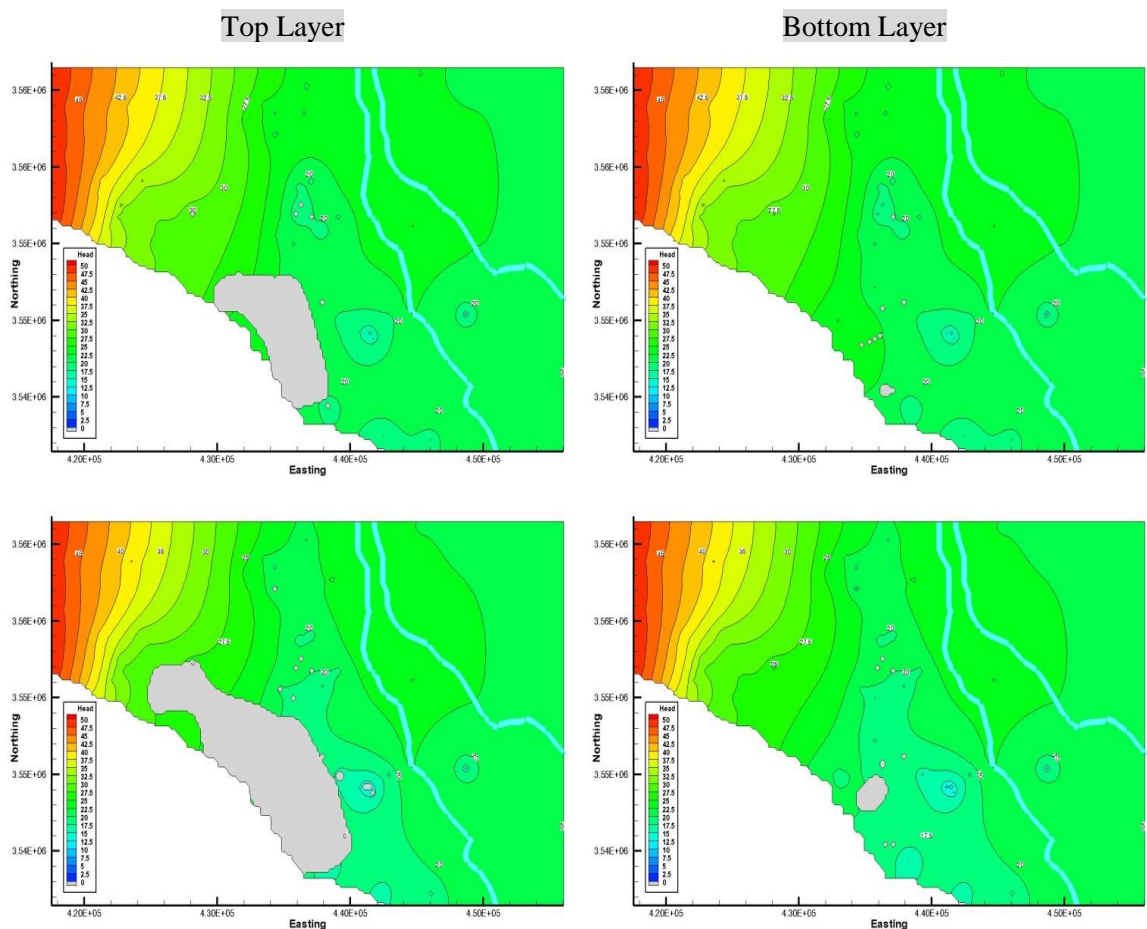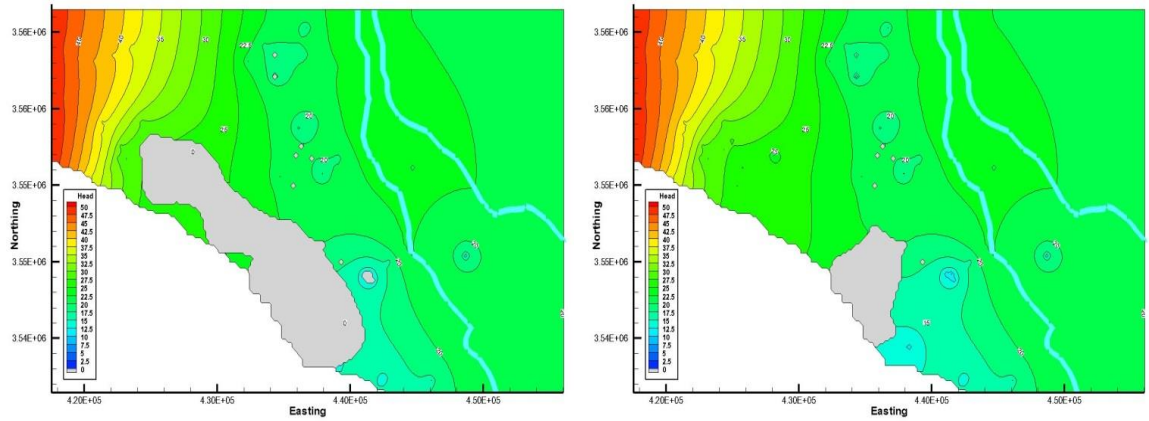
Figure 6.5: Computed groundwater table with the current pumping rate and current recharge (top), 25% recharge reduction (middle), and 50% recharge reduction (bottom)

In addition, it is needed to mention that the problem of dry area appears when the level of groundwater table becomes below the bottom elevation of the top or the bottom layers of the model and this happened due to the over-pumping schedule. In addition, some wells are stopped working due to the over-design pumping and thus these wells will become as dry wells and shown as Grey.

To see how the effect of dry climate, which is influenced by the recharge rate, affects the groundwater table in the study site, Figure 6.6 shows the vertical cross-sections of the groundwater decline in the worst locations of dryness for the current recharge rate and for the reductions of the current recharge rate. These cross-sections are selected in the regions where the effects are maximum. Figure 6.6 illustrates that the groundwater table declines more when the recharge rate reduced. With the current recharge rate, the decline in the groundwater table is having a slight distance Figure 6.6a as compared with those distances shown in Figure 6.6b and 6.6c for a recharge reduction of 25% and 50% respectively, particularly for the lower head (bottom layer) which is increased dramatically. However, overall trend, the connection between the groundwater level and the Euphrates River level remains there and does not affected more by this reduction and this enhanced the expectation that the eastern region is saturated with water and is not significantly affected by the climate changes.
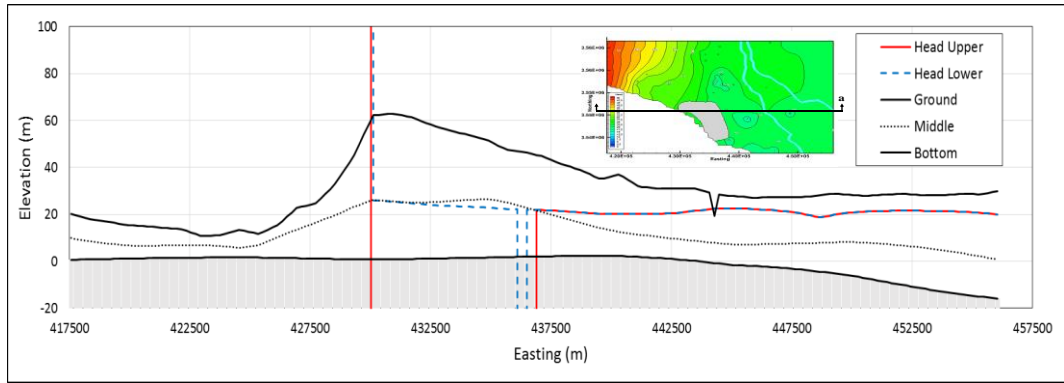
(a)
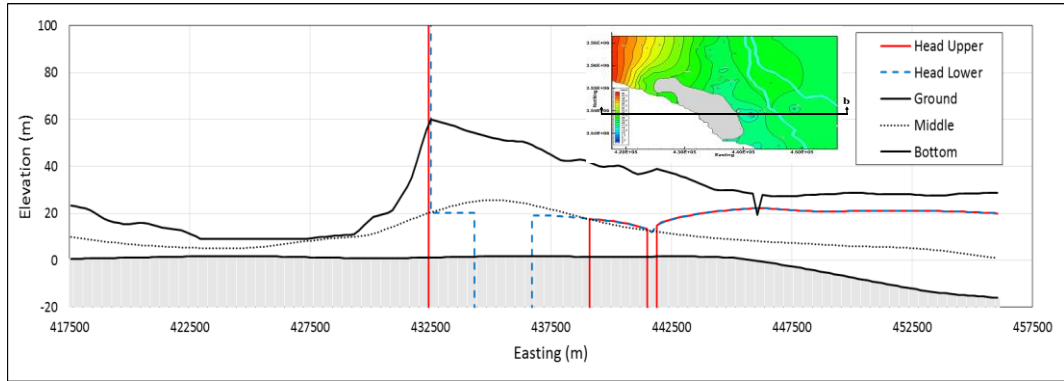
(b)
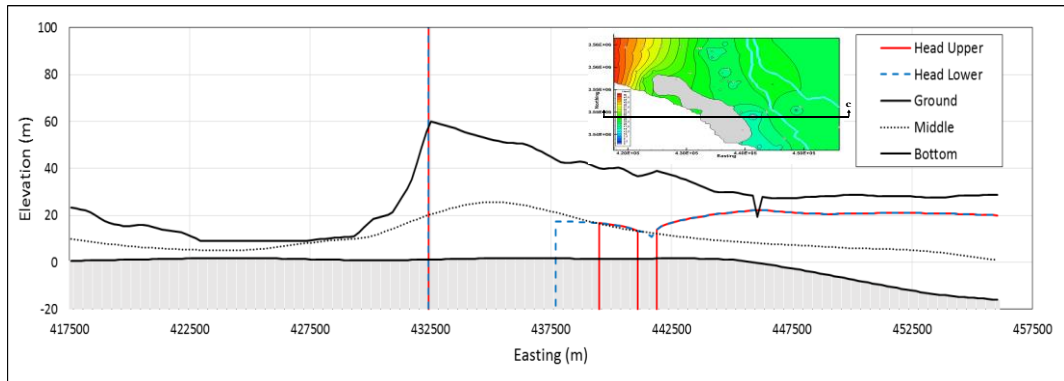
(c)

Figure 6.6: Effect of reducing the current recharge rate by 25% and 50%, on the groundwater level with the current pumping rate in some selected worst locations

To examine and assess the connection between the groundwater and surface water represented by the Euphrates River, Figure 6.7 shows the quantities of water exchanged between the Euphrates River and groundwater aquifer due to the recharge reduction. River leakage IN and OUT demonstrates the quantities of water in m^3/day which are entering and leaving the groundwater aquifer respectively. In addition, Figure 6.7 shows the net water value lost by the Euphrates River in m^3/day, which is resulted from subtracting the entering value (IN) from the leaving value (OUT). From Figure 6.7 and as the groundwater balance illustrates, with the current recharge rate (as a benchmark case), the Euphrates River was losing 5354 m^3/day, while it loses of 10145 m^3/day and 14100 m^3/day when the recharge rate is reduced by 25% and 50% respectively. By comparing the quantities of water lost by the river with the benchmark case

152

(current situation), it indicates that the Euphrates River will lose of approximately 2 times and 2.6 times from its water to feed the groundwater aquifer during the dry climates. If the future climate has become worsen and affected the recharge rate value through reducing it, then the impact of the pumping schedule will increase the pressure on both the study site and the Euphrates River.
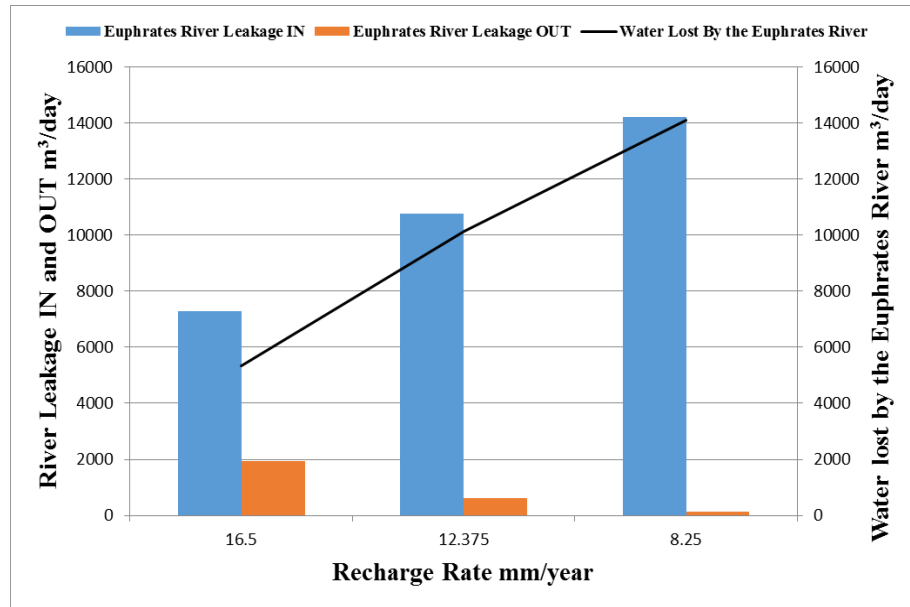
Figure 6.7: The leakage of Euphrates River with the reduction of recharge rates

With the current required/applied pumping rate 52454 m³/day and through the recharge rate reductions, Figure 6.8 illustrates the quantities of water which are actually pumped from the groundwater aquifer and the net lost water by the Euphrates River. By comparing the actual pumped water with the required quantity, Figure 6.8 shows that even with the current recharge value, the groundwater aquifer cannot provide the required pumping rate. Therefore reducing the recharge rate has added another impact on the aquifer to meet the applied quantity where by reducing the recharge value due to the dry climate by 25% and 50%, the actual pumped water has been decreased. In addition, it can be seen from Figure 6.8 that, the waters of the Euphrates River have been participated by a significant part of the actual pumped water where with the current recharge rate, the Euphrates River participates by approximately 12%, while it participates by 24% and 36% when the recharge rate reduces by 25% and 50%. By comparing the participation percentage of the Euphrates River waters with the required pumping rate through the various recharge rates, it is found that these percentages are equivalent to 10%, 20%, and 27% when the recharge rate is the current and when it is reduced by 25% and 50% respectively.
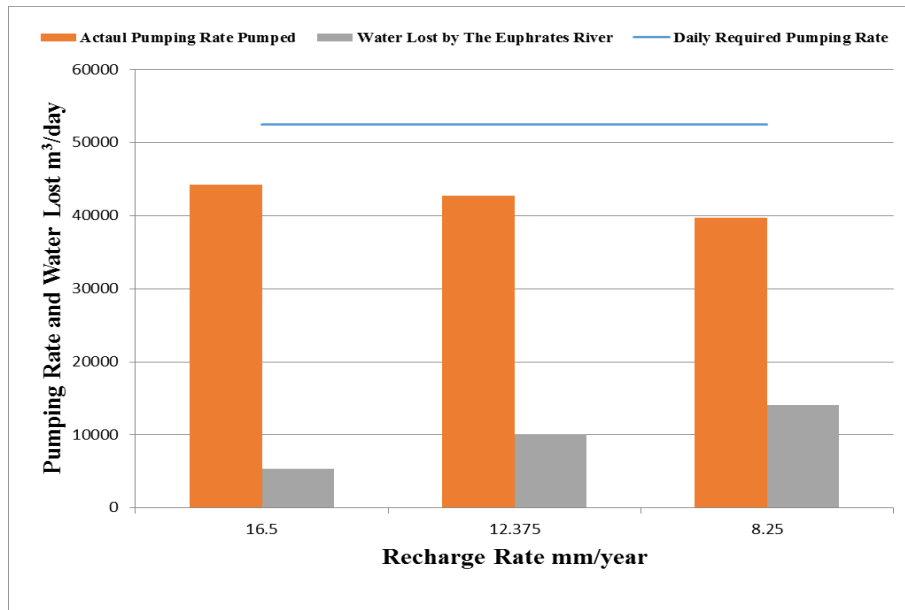
Figure 6.8: The actual pumped water and the Euphrates River leakage with the reduction of recharge rates

Ultimately, to evaluate the current case, it is clearly obvious that reducing the recharge rate that may happen due to the climate changes impact will affect the groundwater aquifer in the study site dramatically through increasing the volume of the appearing dry areas and preventing the aquifer to provide the required pumping schedule. In addition, the impact of reducing the recharge rate will reach the Euphrates River and make it losing part of its water into the subsurface aquifer to reduce the pressure on groundwater source.

6.4.2 Case 2

The effect of reducing the western constant head by 5m to be 45m with the reduction of the recharge rate by 25% and 50% at the same time is studied in this case. The applied pumping schedule 52454 m^3/day remains constant in this case. Climate change can affect the recharge rate and this in turn can affect some boundaries of the aquifer. One of these boundaries is the constant head. As previously described, a constant head of 50m is used in the model along of the western boundary for both the top and bottom layers. The west side represents the water input for the groundwater aquifer where as the groundwater movement is eastward, so any reduction in the groundwater level on this side will completely affect groundwater aquifer. Therefore, it is decided to examine the impact of reducing the west constant head imposed along the west boundary to 45m as well as reducing the recharge rate by 25% and 50% at the same time since the climate changes can affect both.

Running Visual MODFLOW with the steady state condition and with the 45m boundary condition resulted in some issues will discuss them in detail. Figure 6.9 shows a comparison of

the computed groundwater table and the dry areas in the top (Figure 6.9a) and bottom (Figure 6.9b) layers of the of the study site when the constant head on the west side is 50m and 45m respectively with a reduction of 25% and 50% in the recharge rate value.

With the current recharge rate, and due to the constant head reduction to be 45m, it is noticed that the dry area has increased dramatically in the top layer as compared with the slight increase in the bottom layer as illustrated in Figure 6.9. By comparing the computed dry areas in the top and bottom layers of the model when reducing the west constant head to 45m as well as reducing the recharge rate by 25% and 50% with those dry areas for the constant head of 50m, it is obvious that the increase in the dry areas are crucial and this indicates the importance of the west constant head. In addition, Figure 6.9 shows that the dry area is again increased toward the western part of the study site due to the constant head reduction and influenced the groundwater equipotential lines pattern through pushing these equipotential lines toward the west side.

a. Top layer

50m

45m

Current Recharge Rate

25% Reduction

155
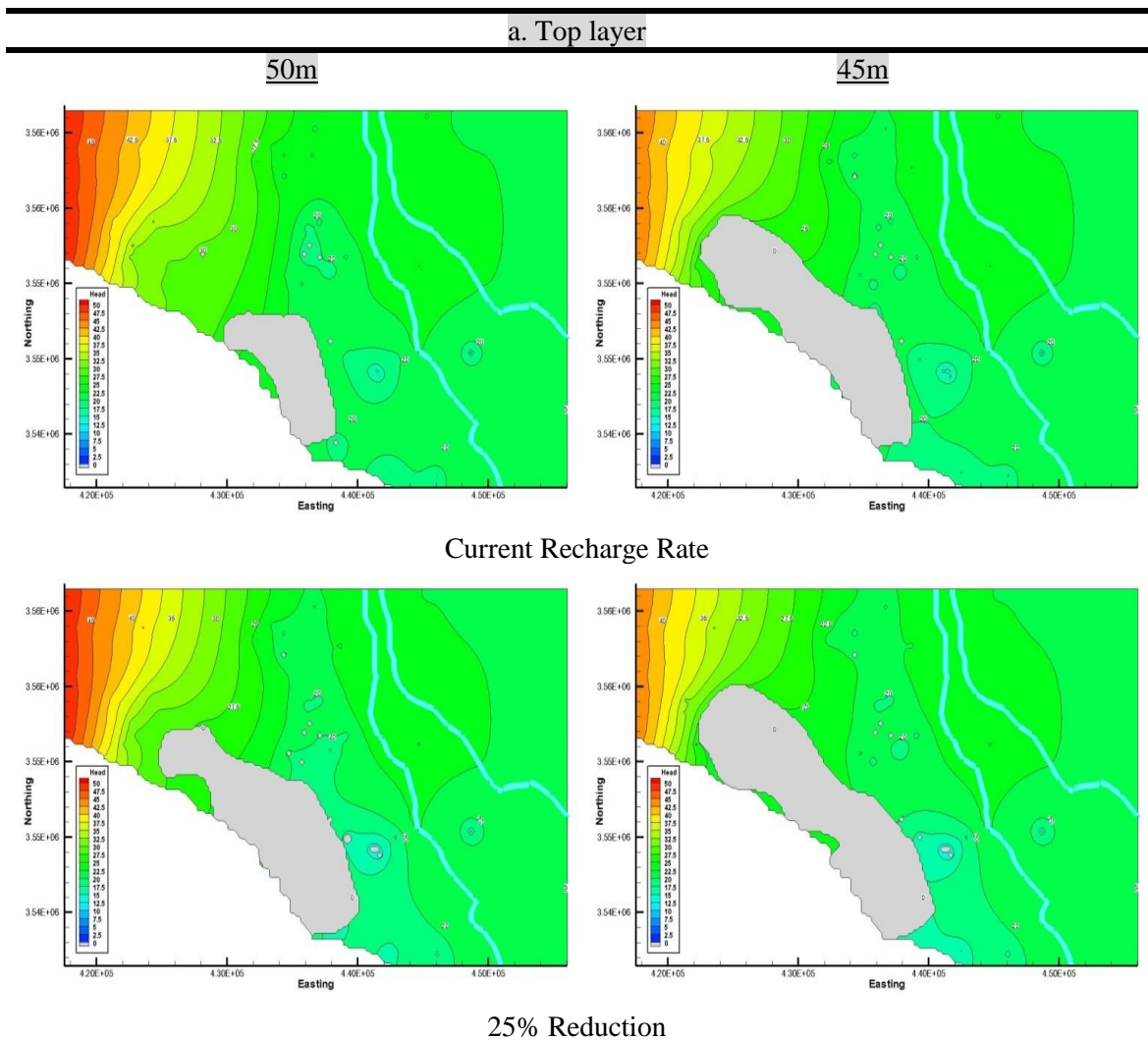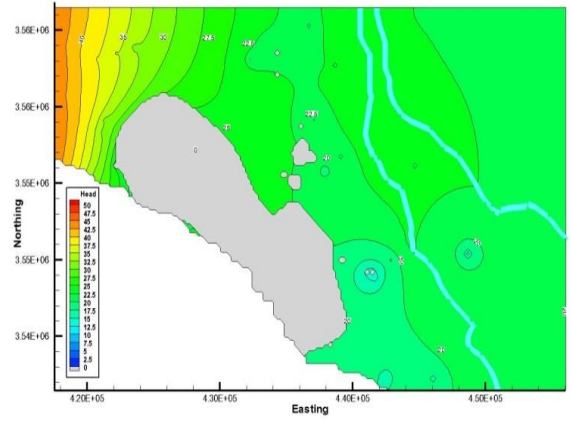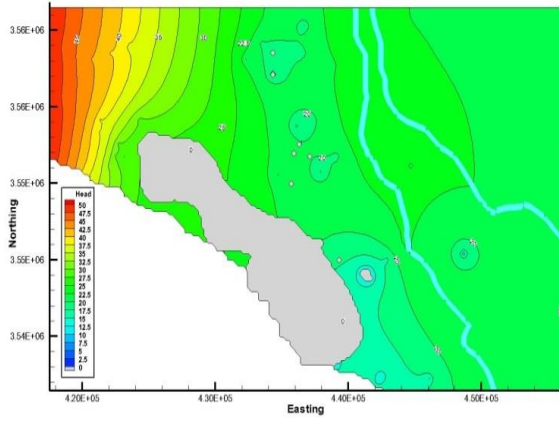
50% Reduction

50m   45m
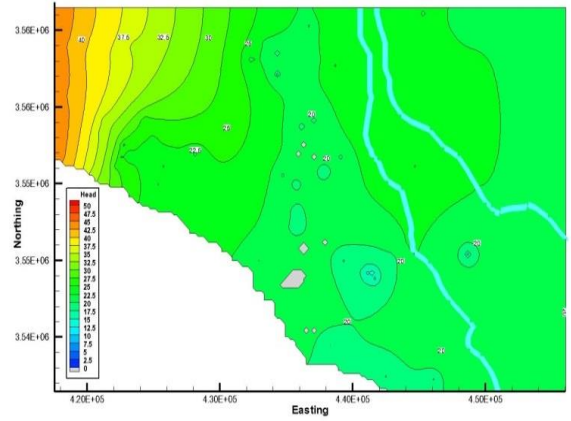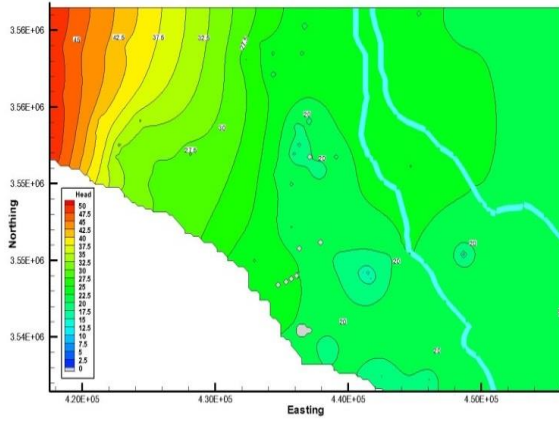
Current Recharge Rate
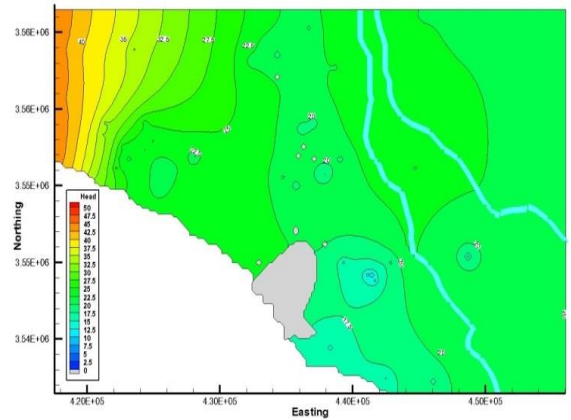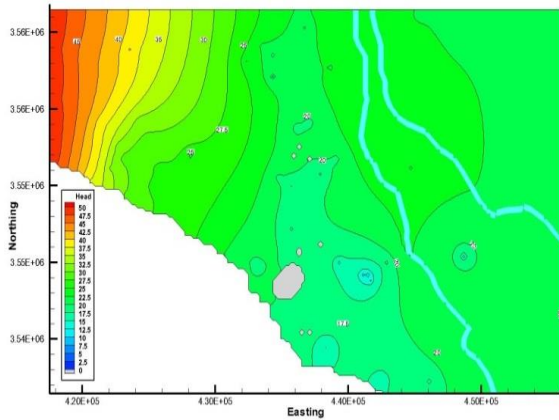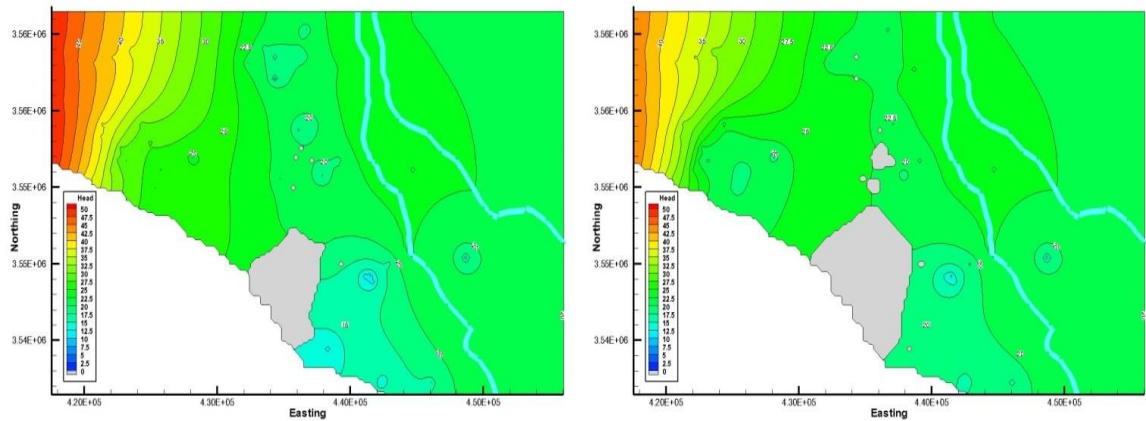
25% Reduction

50% Reduction

Figure 6.9: Comparison of the computed groundwater table and dry areas in a) Top Layer, and b) Bottom Layer, with the current recharge rate (top), 25% reduction of recharge rate (middle), and 50% reduction of recharge rate (bottom), when the constant head equals 50m and 45m

To investigate the effect of reducing the constant head (CH) from 50m to 45m in more detail, Figure 6.10 illustrates the volumes of the dry areas which are resulted due to that reduction. From Figure 6.10, there is a significant increase in the dry area in the top layer of the model due to the constant head effect for all recharge rate values. Similarly, the same significant impact can be seen in the bottom layer of the model for the recharge rates of 12.375 mm/year and 8.25 mm/year as compared with that impact for the recharge rate of 16.5 mm/year which is very slight.
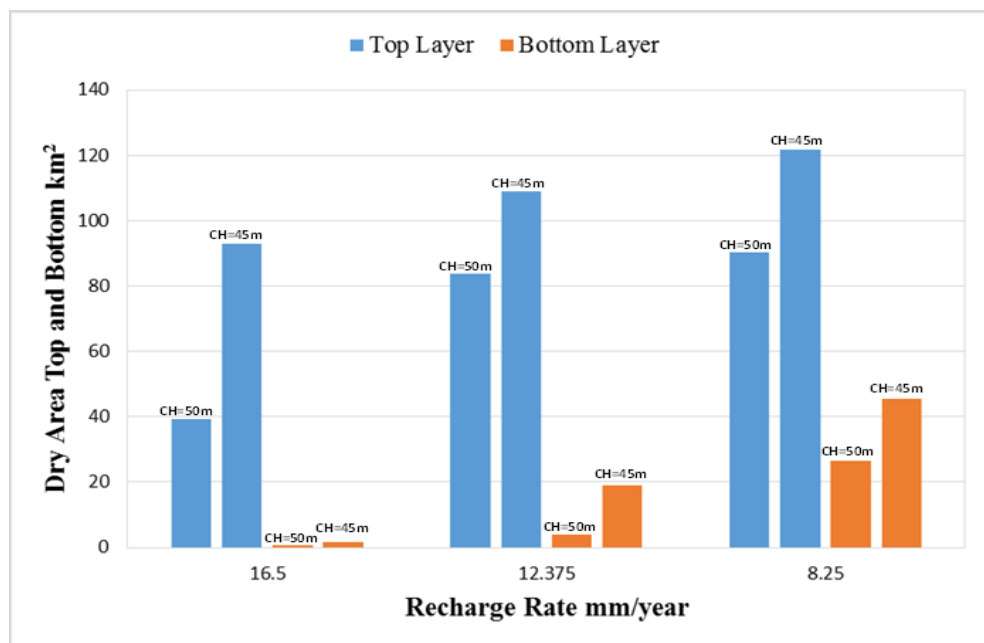
Figure 6.10: Dry area volumes in the top and bottom layers with different values of recharge rates when the western constant head equals 50m and 45m

To explore whether the Euphrates River remains connected with the groundwater table or not, Figure 6.11 will illustrate the worst vertical cross-sections, which are selected in those regions having the greatest dry areas and affected more than the others by the constant head reduction. These cross-sections will show the decline in the computed groundwater level affected by reducing the constant head to 45m and recharge rate by 25% and 50%.

(a)

(b)

(c)
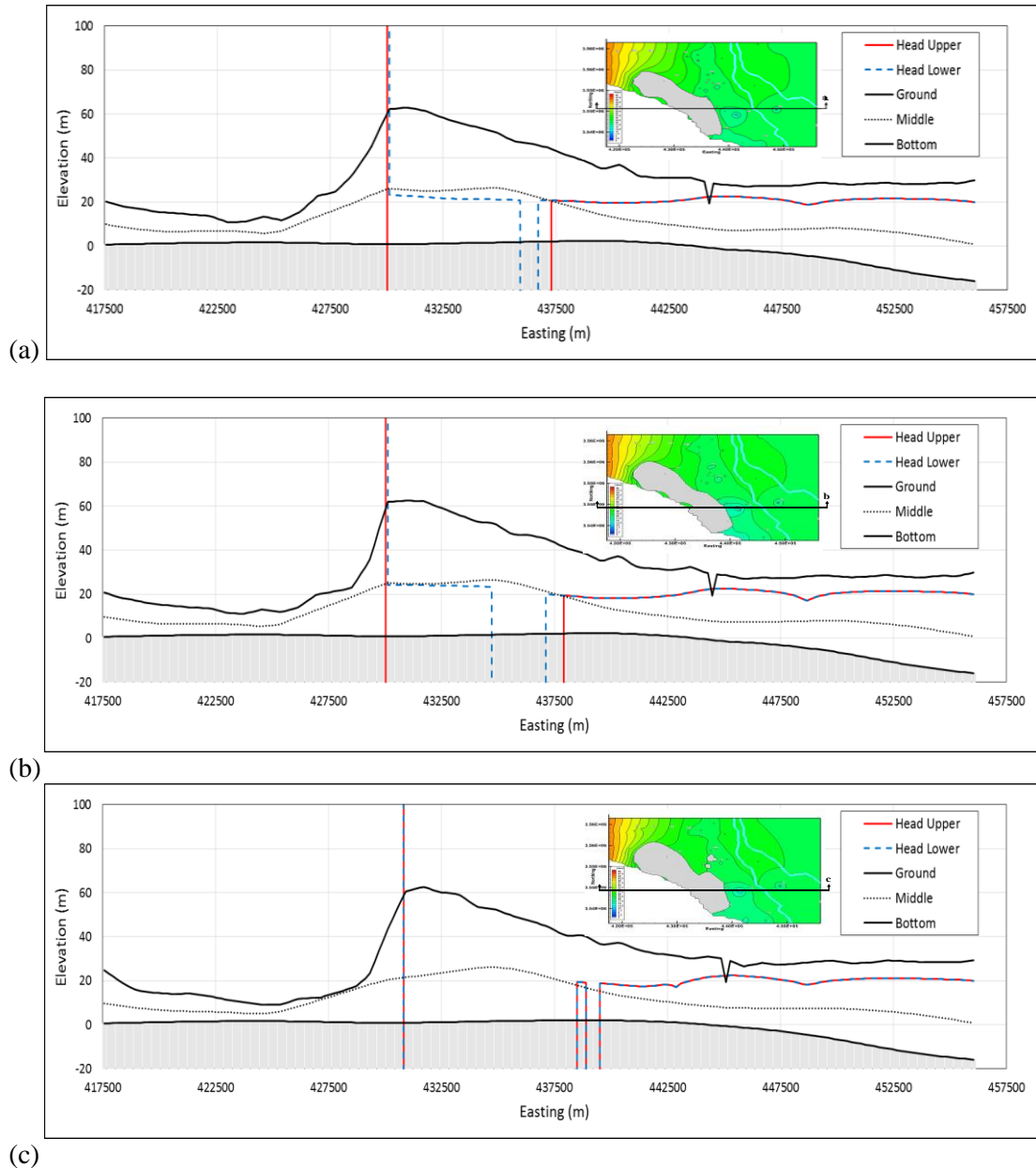
Figure 6.11: Worst locations of water table decline when reducing the western constant head to 45m with: a) the current recharge rate, b) 25% reduction of recharge rate, and c) 50% reduction of recharge rate

It can be seen that all cross-sections shown in Figure 6.11 are connected with the Euphrates River although the huge impact on the study site. Where this impact has been lowered the groundwater table below the bottom elevation of the upper or lower layers, but it does not affect the saturated area on the eastern side of the study area.

158

To explore the Euphrates River leakage due to the reduction of the western constant head to 45m and the recharge rate value by 25% and 50%, the quantities of water exchanged between the Euphrates River and groundwater aquifer due to the connection between them is shown in Figure 6.12. Figure 6.12 shows the comparison between the values of the Euphrates River leakage for the values of the constant heads 50m and 45m when the recharge values are 16.5 mm/year, 12.375 mm/year, and 8.25 mm/year. The exchange quantities of water are resulted from enabling the groundwater balance results. From Figure 6.12, it can be seen that the effect of reducing the constant head to 45m does not have a significant impact on the Euphrates River leakage either the IN or OUT quantities and either in the top or bottom layers of the model if excluding the IN quantities for the recharge rates 16.5 mm/year and 8.25 mm/year which are increased and decreased slightly respectively. The overall effect of the constant head reduction to 45m shows that the Euphrates River will lose water lowers than that quantity when the constant head equals 50m because the difference between the Euphrates River level and groundwater table is reduced. Where the quantity of water lost by any surface water source through the seepage phenomenon toward the groundwater source depends upon the difference of the heads between these two sources, if the difference was big then the water quantity will be big, and vice versa on the assumptions that these two sources will remain directly connected without forming a separating zone between them such as the hyporheic zone and the groundwater head will remain lower than the head of the surface water source.
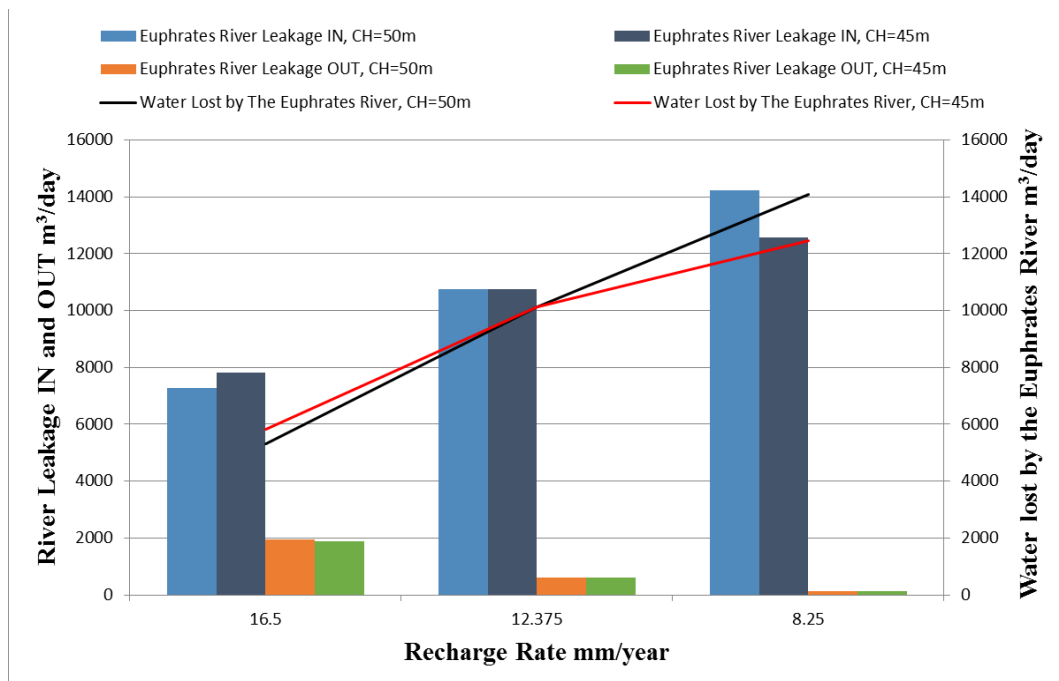
Figure 6.12: The leakage of Euphrates River with the reductions of recharge rate and constant head

Figure 6.13 illustrates the quantities of water which are actually pumped from the groundwater aquifer and the net lost water by the Euphrates River for various recharge rates and constant

heads. It is shown by Figure 6.13 that the actual pumping rates have been decreased due to the constant head reduction as compared with those quantities resulted when the constant head was 50m. Same effect can be seen for the water lost by the Euphrates River where it is either still constant or reduced as shown in Figure 6.13 when both the recharge rate and the constant head are reduced to 12.375 mm/year or 8.25 mm/year and 45m respectively. The interpretation of the reduction of the water lost by the Euphrates River is that because the actual pumping rate is reduced and this reduces the impact on the connection between the Euphrates River and groundwater aquifer. To compare the quantities of water lost by the Euphrates River to the actual pumping rate to assess how much the Euphrates River participates in that quantity, it is found that with the current recharge rate, the Euphrates River participates by approximately 13%, while it participates by 25.5% and 35.5% when the recharge rate reduces by 25% and 50%. While when comparing the water lost by the Euphrates River to the required pumping rate, it will be 10.5%, 19% and 24% when the recharge rate is the current and when it is reduced by 25% and 50% respectively.
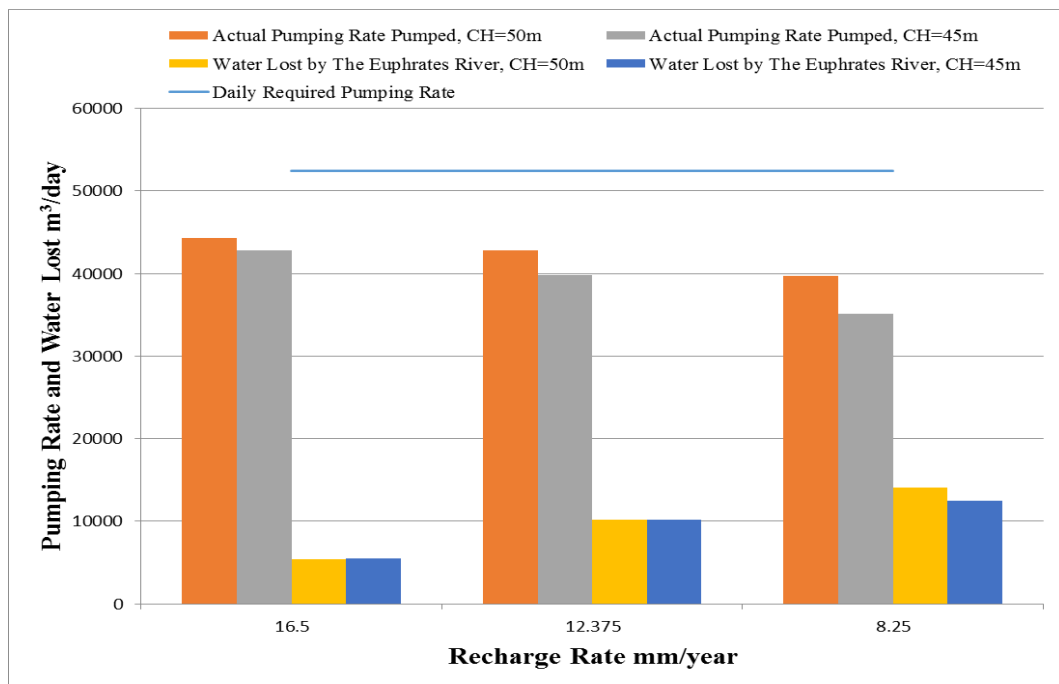
Figure 6.13: The actual pumped water and the Euphrates River leakage with the reduction of recharge rates and constant head

As a result from this case, reducing the constant head boundary condition from 50m to 45m with a reduction in the recharge rate value will add an impact on the study site in terms of increasing the dry area which in turn means increasing the declining in the groundwater table level. However, the impact on the Euphrates River leakage (net leakage) will be less. In addition, in respect of the actual pumping rate quantity, it is also affected less when reducing the constant head to 45m as compared with those quantities for the constant head of 50m. Also, it

should mention here that the impact of decreasing the recharge rate on the study site is greater than the decreasing of the constant head.

6.4.3 Case 3

The effect of reducing all of the western constant head by 5m to be 45m, the recharge rate by 50%, and the Euphrates River level by 0.5m and 1m at the same time is studied in this case. The applied pumping schedule 52454 m^3/day remains constant in this case. Due to the climate change, an impact may happen on the water level in a river particularly in the arid and semi-arid areas. As the study site is classified as an arid area (Middleton and Arnold 1997), this means the potentiality for this impact to happen is large. Increasing the river level will lead to reducing the overall expected impact. However, in general, decreasing the river water level will complicate the expected damage on the river and the surrounding areas. In this case, it will focus on the effect which may happen due to the Euphrates River level reduction.

It will investigate the Euphrates River level reduction in two scenarios, the first scenario will deal with the Euphrates River level reductions when only reducing the recharge rate by 50% and keep the western constant head as the same as the current now 50m. In the second scenario, it will reduce the recharge rate by 50% and also the western constant head by 5m to become 45m, this will be in the addition to the Euphrates River level reductions. In each scenario will decrease the Euphrates River level by 0.5m and 1m. The pumping rates will remain constant 52454 m^3/day for both scenarios.

The results of Visual MODFLOW for both scenarios are illustrated in Figures 6.14 and 6.15. Both figures show the computed groundwater table patterns and the dry areas in the top and bottom layers of the study site when the Euphrates river level has been reduced by 0.5m and 1m as compared with the current level, the recharge rate is reduced by 50%, and when the western constant head equals 50m and 45m respectively.

When keeping the western constant head at 50m, and reducing both the recharge rate by 50% and the Euphrates River level by 0.5m and 1m, this will affect the study site. Focusing on the Euphrates River level reduction effect, the impact of reducing the Euphrates River level by 0.5m has a slight effect on the study site in terms of affecting the groundwater table pattern and appearing the dry areas in the top and bottom layers of the model as it is shown in Figure 6.14 where there is a slight increase in the dry areas in the top and bottom layers of the model as compared with those results of the current level of the Euphrates River. However with a 1m reduction in the Euphrates River level, the effect can be considered significant where the increase in the dry areas in the top and bottom layers of the model is increased significantly as

compared with case when there is no reduction in the Euphrates River level (Current Level of the Euphrates River) as Figure 6.14 illustrates. Also, it is obvious that the increase in the dry area is either influenced the westward or the northward regions of the study site. Exactly the same effect can be seen in Figure 6.15 when reducing all of the recharge rate by 50%, western constant head to be 45m, and the Euphrates River level by 0.5m and 1m.
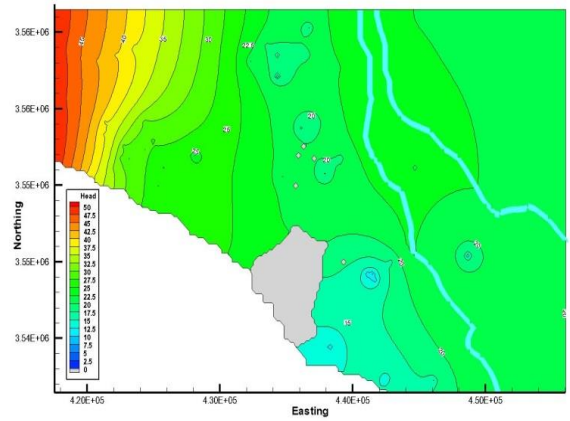
Current Level of the Euphrates River

0.5m reduction of the Euphrates River Level

1m reduction of the Euphrates River Level

Figure 6.14: Comparison of the computed groundwater table and dry areas with 0.5m and 1m reductions of the Euphrates River level when the recharge rate reduction is 50% and the western constant head is 50m

Top Layer   Bottom Layer

Current Level of the Euphrates River

0.5m reduction of the Euphrates River Level

1m reduction of the Euphrates River Level
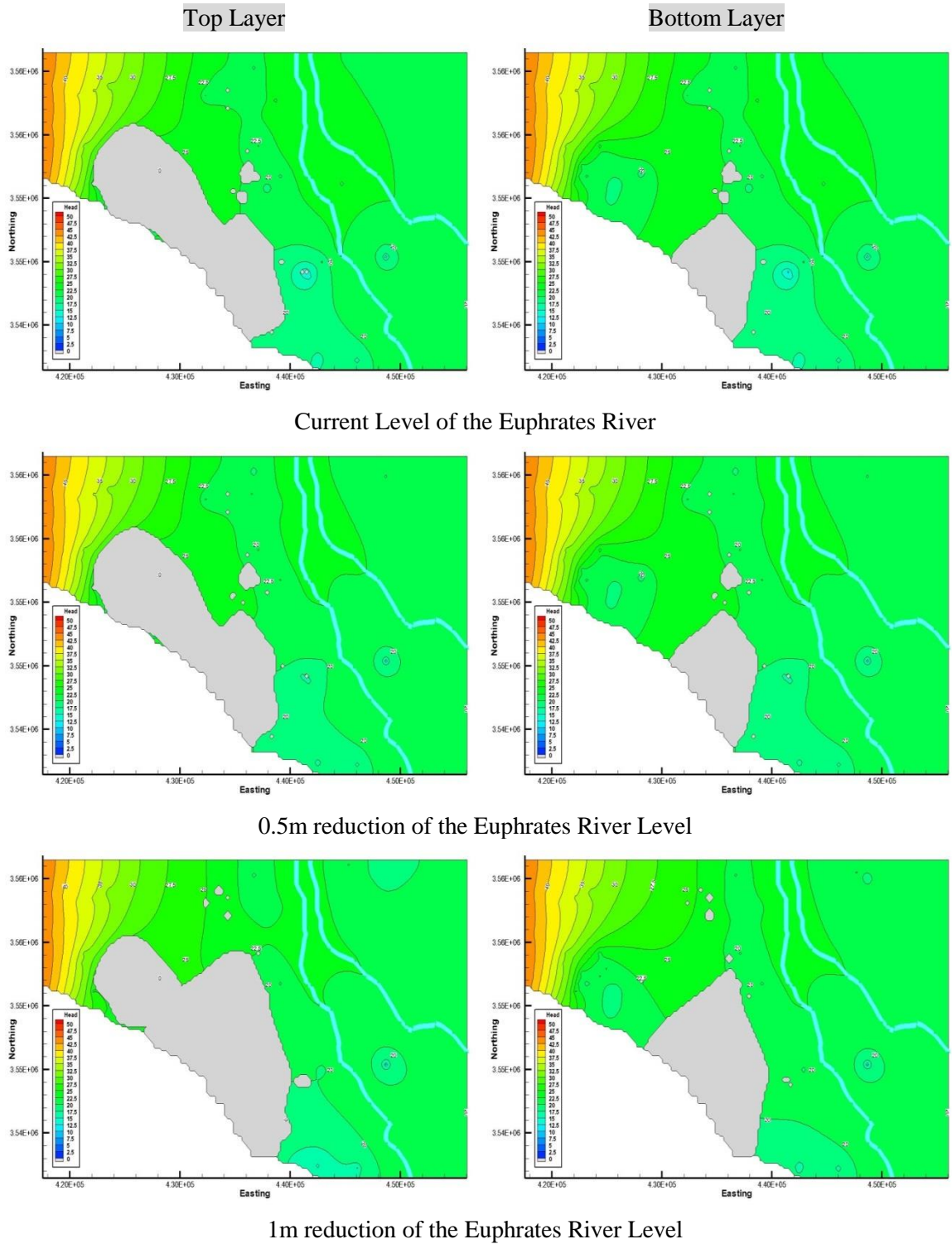
Figure 6.15: Comparison of the computed groundwater table and dry areas with 0.5m and 1m reductions of the Euphrates River level when the recharge reduction is 50% and the western constant head is 45m

To investigate the worst case in regarding of the connection between the surface water represented by the Euphrates River and the groundwater aquifer to see whether the Euphrates River remains connected or not, Figure 6.16 will show the cross-section of the case when

reducing the recharge rate by 50%, the western constant head to be 45m, and the Euphrates River water level by 1m.
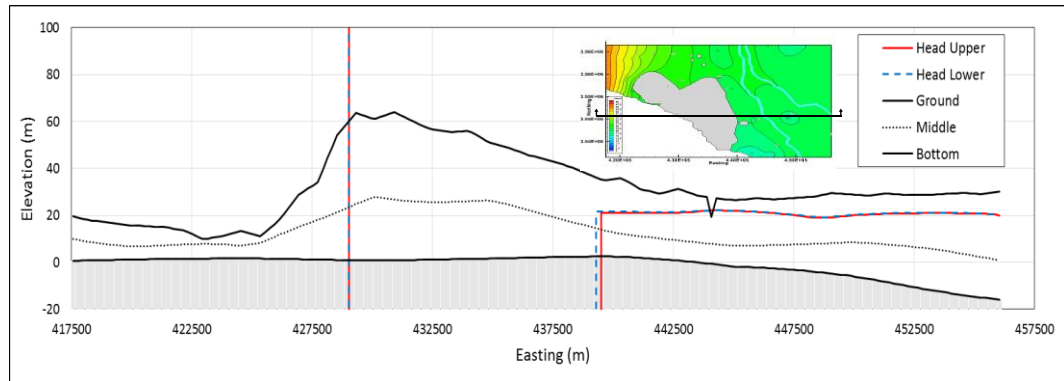
Figure 6.16: Cross-section of groundwater table decline when reducing the recharge rate by 50%, western constant head by 5m (45m), and the Euphrates River level by 1m

It is obvious from Figure 6.16 that the Euphrates River level remains having the connection with the groundwater aquifer water table and does not fall down to be below the bed elevation of the Euphrates River. This ensures the assumption which says that the eastern part of the study site is completely saturated with waters with high levels.

To explore the effect of the Euphrates River level reduction which is related to the dry areas in the top and bottom layers of the model in numbers, Figure 6.17 will demonstrate that effect. When reducing the recharge rate by 50% and keep the western constant head as the same as now (CH=50m), the dry areas in the top and bottom layers of the model were 90.28 km^2 and 26.52 km^2 with the current water level of the Euphrates River. Reducing the level of the Euphrates River by 0.5m and 1m leads to a slight increase in the dray areas in the top and bottom layers where the dry areas become 91.76 km^2 (Top), 28.6 km^2 (Bottom) and 95.36 km^2 (Top), 38.48 km^2 (Bottom) respectively. However, when decreasing the western constant head by 5m to become 45m (CH=45m) and the recharge rate by 50%, the Euphrates River water level reduction has affected the study site significantly. Where with the current level, the dry areas in the top and bottom layers of the model were 124.8 km^2 and 45.6 km^2 respectively, while it becomes 148.44 km^2, 71.72 km^2 and 156.48 km^2, 86.96 km^2 for the 0.5m and 1m reductions of the Euphrates River level respectively.
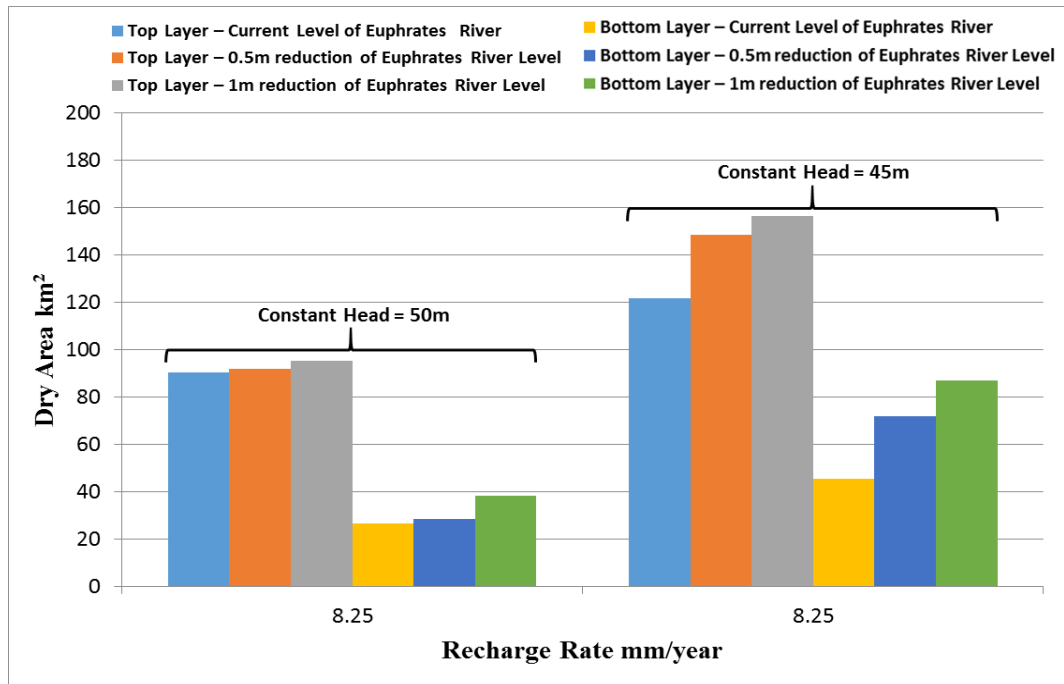
Figure 6.17: Dry area volumes in the top and bottom layers of the model for 0.5m and 1m levels' reduction of the Euphrates River when the recharge rate reduced by 50% and the western constant head equals 50m and 45m

It is very important to investigate the exchanged amounts of water between the Euphrates River and the groundwater aquifer during the various reductions in the Euphrates River level and when the recharge rate is 8.25 mm/year. Figure 6.18 shows the quantities of water lost from the Euphrates River when reducing its level by 0.5m and 1m. The overall effect for the Euphrates River level reduction is reducing the seeping water from the Euphrates River into the subsurface aquifer when the western constant head is 50m. The same effect can be seen in Figure 6.18 for the situation when decreasing the western constant head to 45m except for that quantity when reducing the water level by 1m which led to increasing the water lost from the Euphrates River. It should be noticed here that the leakage of the Euphrates River is affected completely by: 1) the difference between the water levels of the river and the aquifer which is implicitly affected by the actual extracted quantities of water, and 2) by the actual quantities of pumped water, not the demanded extractions, where if those quantities were large, the Euphrates River will lose more water and vice versa.

Actual pumping rate has been affected by the Euphrates River level so any change in this level will either decrease or increase the actual pumping quantity. Figure 6.19 illustrates the amounts of actual pumping rates which are pumped from the groundwater aquifer as well as the amounts of Euphrates River leakage waters which are participating partially in the actual pumped water as compared to the daily required pumping rates through the various water levels of the Euphrates River and when the recharge rate is 8.25 mm/year. With both values of constant head

(CH=50m, CH=45m), it can be seen from Figure 6.19 that the actual pumped water has been decreased when decreasing the water level of the Euphrates River except for that value when the Euphrates River level reduced by 1m and the constant head was equal 45m where the actual pumped water has been increased. As the Euphrates River leakage has completely affected by the actual pumped water, Figure 6.19 shows that all values of waters lost from the Euphrates River have been decreased, except that value when the actual pumped water which is increased when the Euphrates River level is reduced by 1m as compared with a 0.5m reduction, where the water lost from the Euphrates River has been increased.
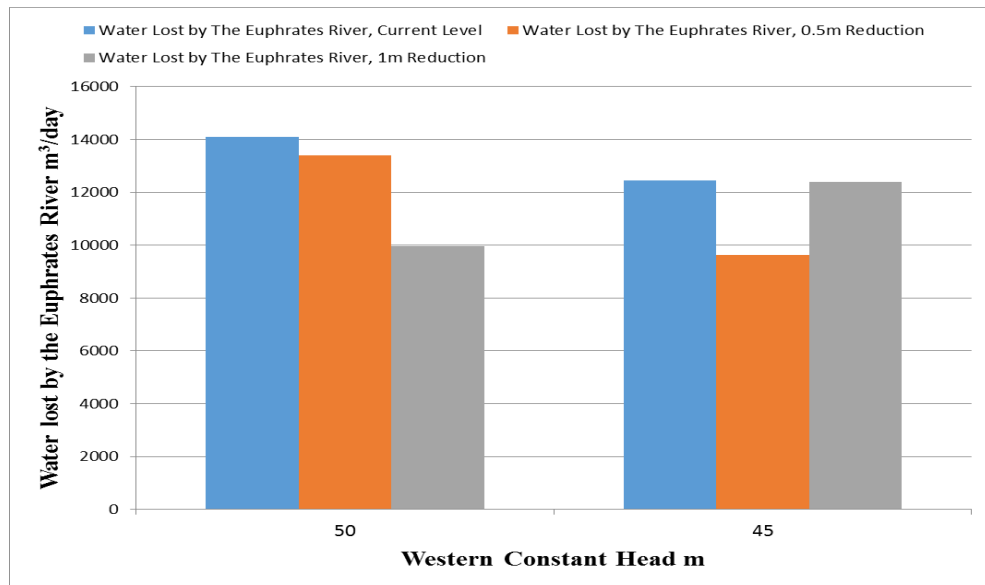
Figure 6.18: The water lost by the Euphrates River through the various reductions in its level when the western constant head equals 50m and 45m and the recharge rate is 8.25 mm/year
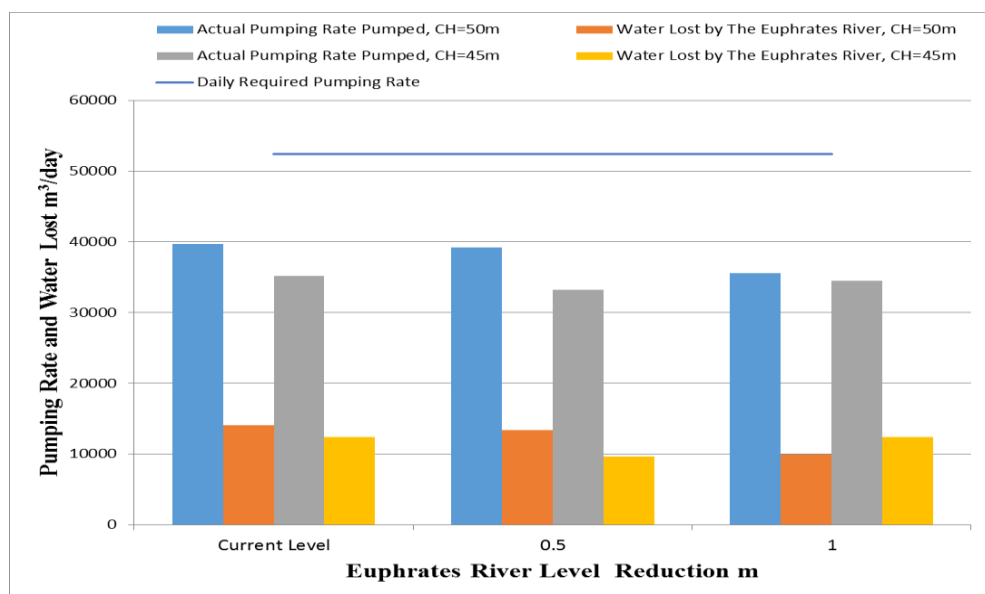
Figure 6.19: The actual pumped water and the water lost by the Euphrates River through the various reductions in its level when the western constant head equals 50m and 45m and the recharge rate is 8.25 mm/year

167

The percentage of participation of waters lost from the Euphrates River to the actual pumped water and the daily required water is ranging between (28 – 36)% and (18.5 – 27)% respectively and do not forget that all the actual pumped waters do not meet the required pumping schedules.

The results from Case 3 clearly show that the effect of climate change on the Euphrates River level has been added an impact on the river in terms of losing its water into the subsurface aquifer. Where the declining in the Euphrates River water level by 0.5m does not affect the quantity of water lost by the river too much as compared with that declining around 1m or more where the waters lost from the Euphrates River were significantly large. Therefore it needs to monitor and control the exchange process between the Euphrates River and the groundwater aquifer. In respect of the daily required pumping schedule, through all the simulated scenarios of the groundwater aquifer in Case 3, the aquifer could not supply those quantities and provide only part of those pumping schedules which are represented by the actual pumping rates. In addition, the connection between the Euphrates River and the aquifer remains available in the worst and most dangerous scenario when reducing all of the recharge rate by 50%, the constant head to 45m, and the Euphrates River water level by 1m.

The examination for the impact of dry climate is explored in the study site in Cases 1, 2, and 3 with the current pumping schedule (without change). However, often low rainfall in the regions suffered from climate changes is solved by the water provided by the groundwater through the pumping schedule although there are many of the negative effects which are created from the pumping such as the seawater intrusion, aquifers pollution, and many more (Lenntech 1993; Stollenwerka et al. 2007). Excessive pumping rates lead to various effects on the groundwater-surface water interaction's aquifers. Where, groundwater levels depletion represents nowadays the most important global phenomenon which is associated with the issue of pumping water from the subsurface aquifers in many countries (Konikow and Kendy 2005). Alley et al. (2007) have been defined the groundwater level depletion as the long-term declination in the groundwater level which is caused by the groundwater pumping sustainability over time. The groundwater depletion has been affected many of major areas in the South and Central of Asia, North of America, Middle East, Australia, and North of China (Konikow 2005).

Consequently, the situation of groundwater aquifer in the study site with various increments in the current schedule of pumping rates will be investigated through exploring the effect of increasing the pumping schedule up to 50% on the groundwater aquifer.

6.4.4 Case 4

This case will study the effect of increasing the current pumping schedule by 10% increment up to 50% to assess the impact on the study area that may result from these increments. As illustrated previously, the study site is affected by the current pumping schedule. For the future predictions and due to the study area development, it may need to increase the pumping rates, therefore it will apply an increment of 10% for the required pumping schedule up to 50% to investigate the impact of these increments on the study site. Figure 6.20 shows the computed water tables and dry areas in the top and bottom layers of the study site for the current pumping rate and the various increments of the pumping rate for the current boundary conditions of the study site.

Figure 6.20 shows that with the current required pumping schedule, there is an impact on the study site resulting in declining the groundwater table and in turns appearing dry areas in the top and bottom layers of the groundwater aquifer. In addition, the groundwater aquifer has pumped only 44263 m^3/day. Due to the increase in the required pumping schedule to 10%, the dry areas in the top and bottom layers have been increased which means increasing the impact on the study site as shown in Figure 6.20. Although the actual pumping rate has been increased to become 47053 m^3/day, but this increase leads to a slight decrease in the pumping wells number where due to the over-designing pumping water, some wells are stopped pumping water for the pumping schedule. With the 20% increment of the required pumping rate shown in Figure 6.20, there was a significant decrease in the pumping wells where approximately 19 wells are stopped working due to the over-designing pumping. This leads to being the dry area in the top layer decreases, but in the bottom layer increases. The explanation of that is, it can be seen that the area located in the middle of the study site has been dried for both the top and bottom layers of the model due to the impact of the pumping schedule, while the area on the western side which was dried previously, now become non-dry due to the suspension of some wells (stopping) to pump water due to over-pumping. Where, the actual pumped water from the groundwater aquifer has been deceased to become 40892 m^3/day. The same effect of the 20% increment happens with the 30% increment of the pumping schedule as illustrated in Figure 6.20. Where, the dry area in the middle of the study site in the top and bottom layers of the model is increased dramatically due to the impact of the required pumping schedule, while on the western side decreased as a result of stopping some pumping wells. In addition, the reduction in the number of pumping wells and the actual pumped water becomes 25 wells and 37700 m^3/day respectively. The increasing of the required pumping schedule to 40% has been affected the study site as shown in Figure 6.20 by stopping one well more from pumping water where this leads to decreasing the dry area in both the top and bottom layers of the model although the

actual pumped water has been increased to become 39518 m³/day. In addition, with the increment of 40%, it can be seen that the wells on the western side have been affected the western area through increasing the dryness in the top layer as compared with the previous increments. Finally, the increment of 50% of the required pumping schedule has followed the same behaviour of the 40% increment where the dry areas in the top and bottom layers of the model have been increased and the actual pumped water is increased to 42275 m³/day, where the pumping wells are still the same as those for the case of 40% increment of the pumping schedule, without change. In Figure 6.20 with the increment of 50%, an important issue needs to be noticed which is the dry areas in the top and bottom layers of the model in the middle of the study site have been dried vertically as compared with all of those studied cases which were dried to the western side, where this supports the expectation that the area on the eastern side is saturated with water and does not affect too much by the issue of the dryness.

Top Layer   Bottom Layer

Current Pumping Rate

10% Increment

170
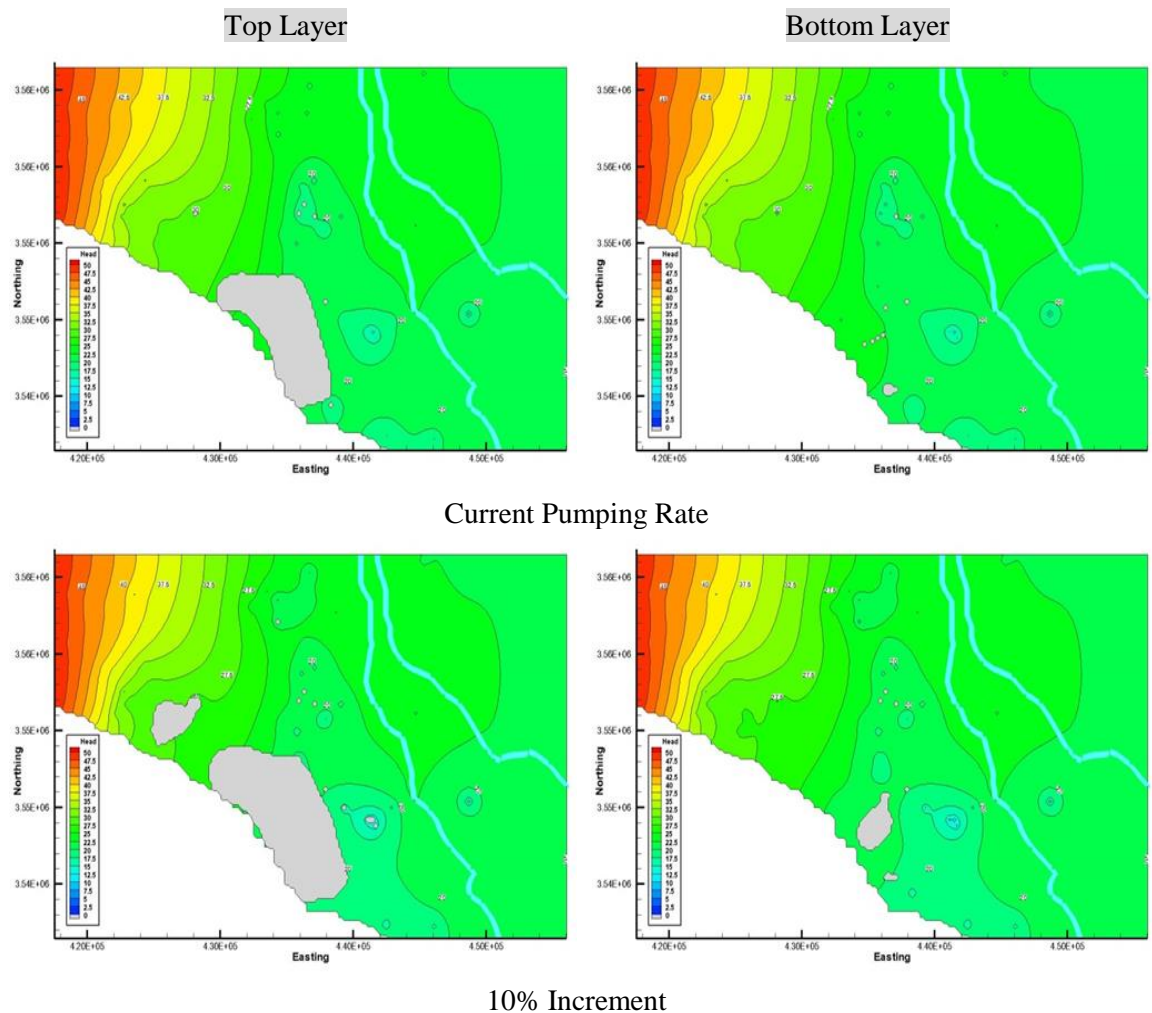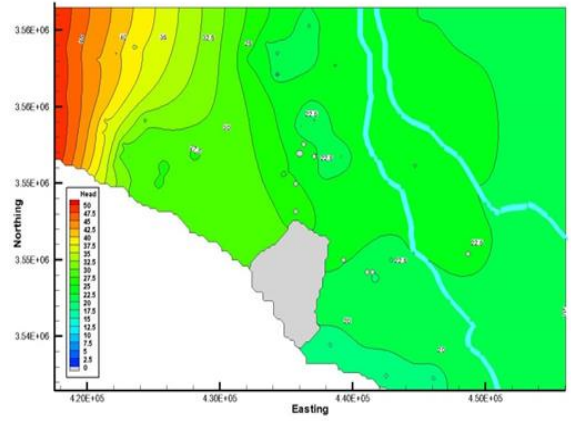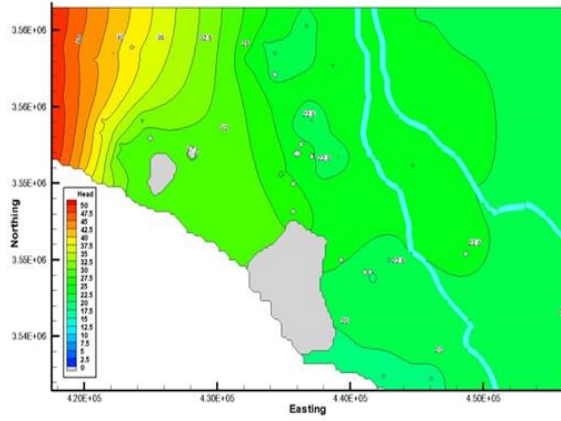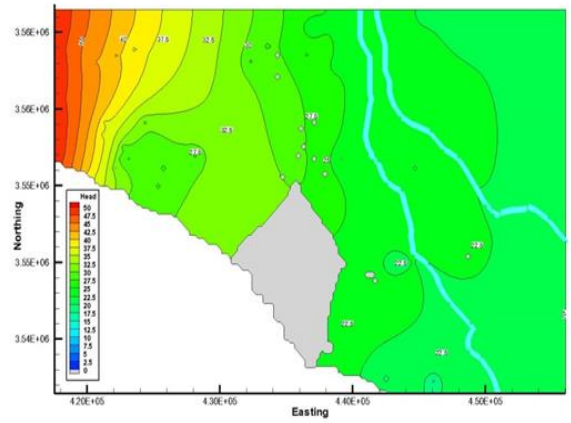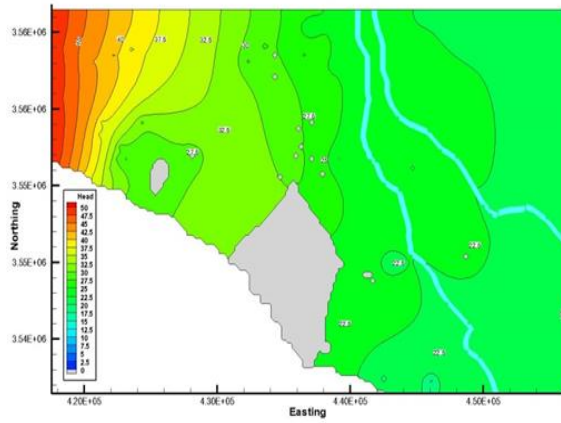
20% Increment
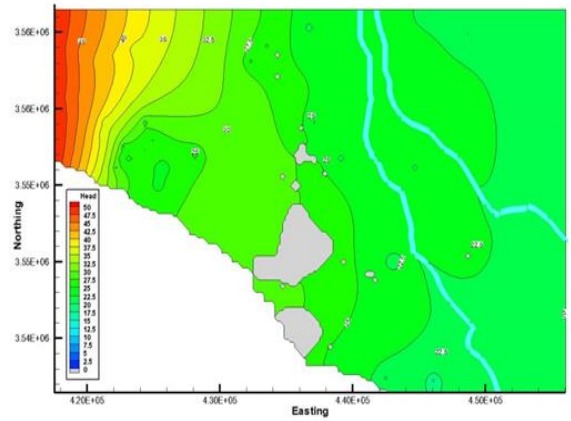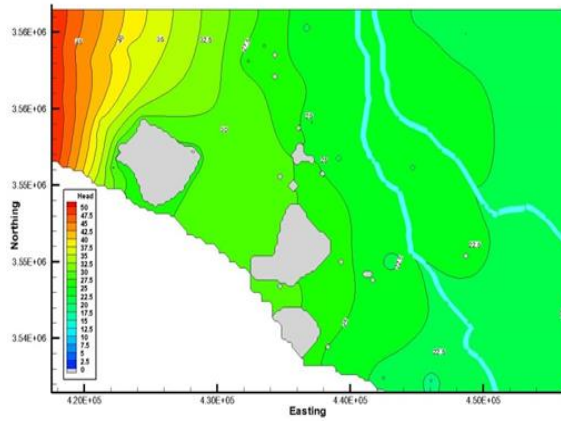
30% Increment
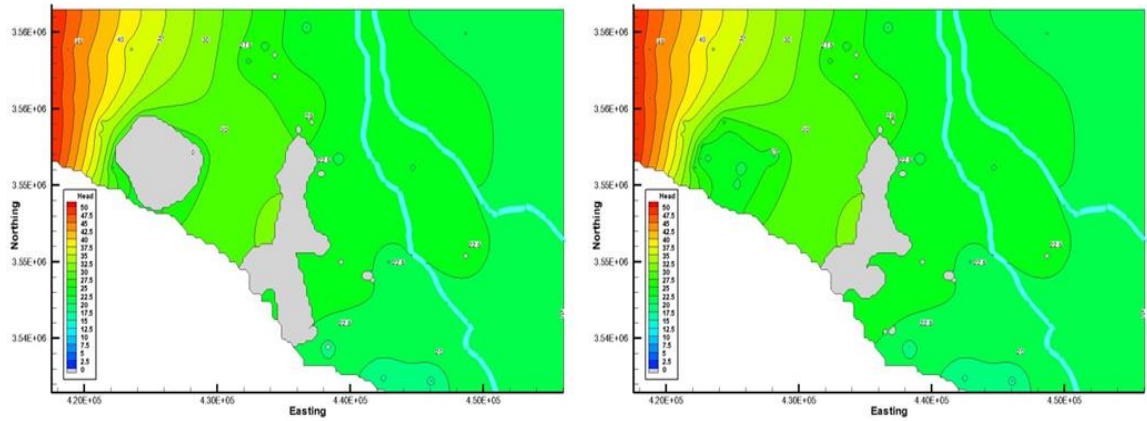
40% Increment

50% Increment

Figure 6.20: Computed groundwater table levels in the top and bottom layers of the model through various increments of the pumping rate

To explore the effect of increasing the current pumping schedule up to 50% on the study site dry area and on the total number of working wells in numbers for the current status of the study site (current boundary conditions), Figure 6.21 will demonstrate that effect. As demonstrated in Figure 6.21, with the current pumping schedule, the dry areas in the top and bottom layers of the model are 39 km^2 and 1.32 km^2 respectively. Different dry area values have been resulted due to the pumping rate increase where in the top layer, the dry area values become 62.64 km^2, 38.44 km^2, 54.28 km^2, 43.68 km^2, and 63.48 km^2 for each 10% increment up to 50% respectively. While in the bottom layer, the dry area values become 5.76 km^2, 29.36 km^2, 52.32 km^2, 24.56 km^2, and 28.80 km^2 for each 10% increment up to 50% respectively. The total number of pumping wells is 69 wells according to the collected data. This number has reduced with the current pumping rate to become 60 wells while for each 10% increment of the current pumping schedule, it becomes 58 wells, 50 wells, 44 wells, 43 wells, and 43 wells respectively. Clearly from Figure 6.21, it can be noticed that the worst case in the top and bottom layers of the model were for the increments of 50% and 30% of the current pumping rate respectively as these increments have affected the study site more than the others through increasing the dryness significantly.
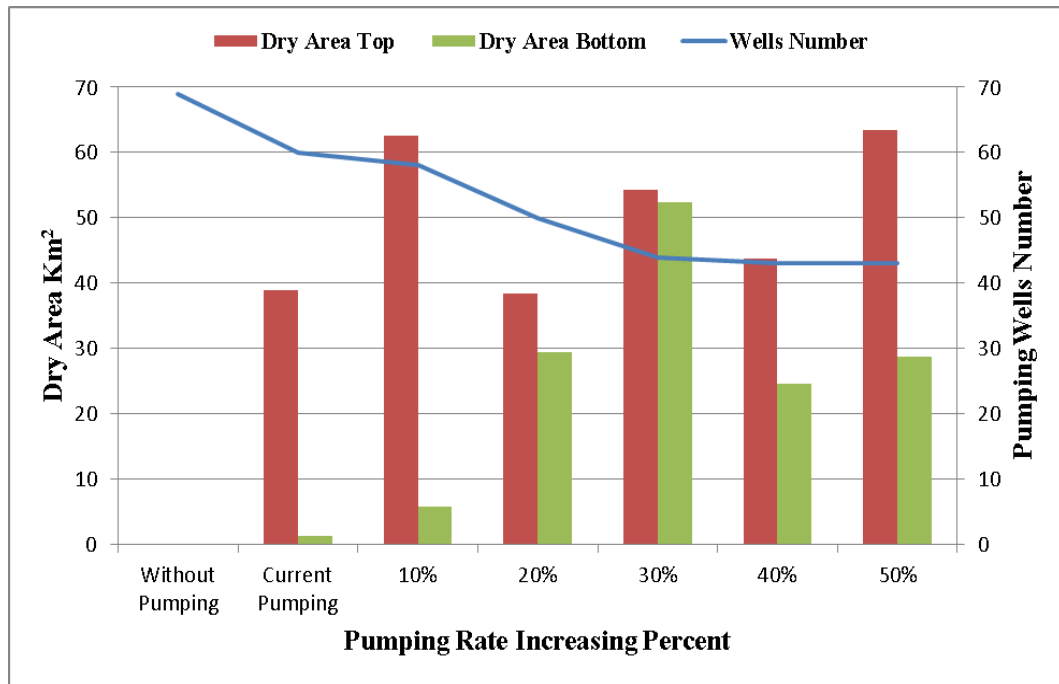
Figure 6.21: Dry area volumes in the top and bottom layers of the model with various increments of the current pumping schedule for the current status of the study site

In respect of the Euphrates River leakage, Figure 6.22 shows the river leakage IN, OUT, (OUT-IN), and the actual pumping rates pumped during the various increments in the pumping schedule for the current status of the boundary conditions. Figure 6.22 illustrates that when there is no pumping schedule applied, the Euphrates River was gaining water by a huge quantity (greater than 20000 m³/day) because of the OUT leakage (water leaves the groundwater aquifer toward the Euphrates River) is greater than the IN leakage (water leaves the Euphrates River toward the groundwater aquifer). However, with the current pumping schedule and the various increments in the pumping rates, noticed that the Euphrates River leakages IN and OUT are various in values depending upon the actual pumped water quantities. Where, the net water gains by the Euphrates River (OUT-IN) is increased and decreased during the decreasing and increasing in the actual pumped water respectively. Therefore, the only parameter affected the river leakage is the quantity of actual pumped water from the aquifer and not the applied/required pumping schedule. Where sometimes the applied pumping schedule is large and because the aquifer cannot provide the applied quantity, some wells will stop working, so in this case the quantity of water pumped will be less than the applied. From Figure 6.22, it can be noticed that the Euphrates River starts for gaining water at 30% increment of pumping rate, but at 40% and 50% increments, the water gains by the river is declining again due to the impact of the pumping rates increase. All the minus values shown in Figure 6.22 represent that the Euphrates River was losing water into the groundwater aquifer.
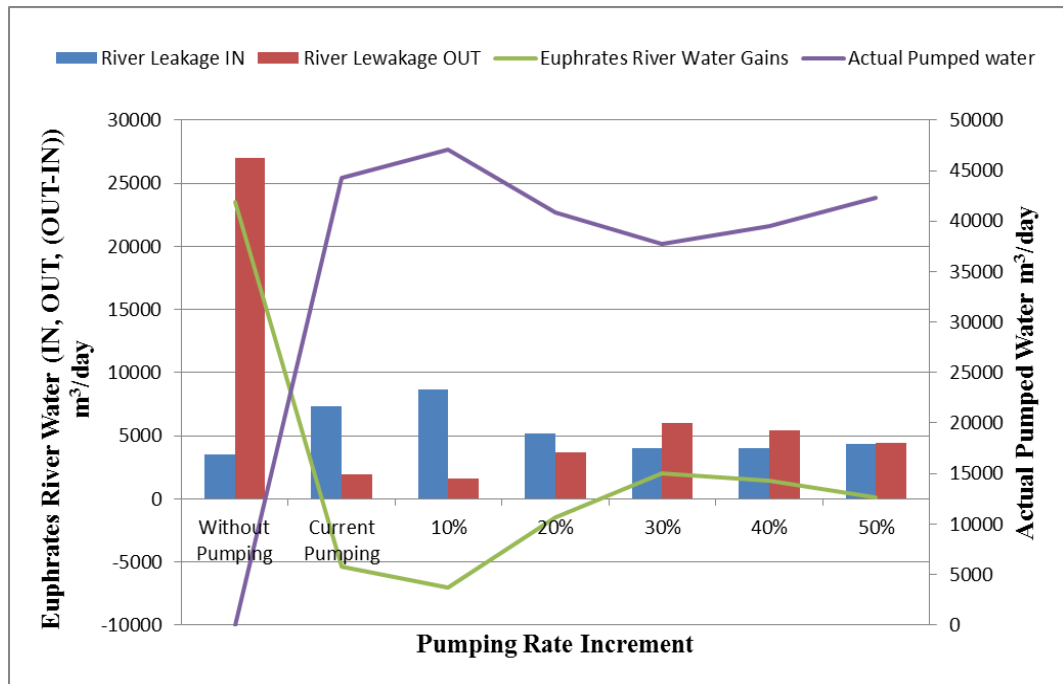
Figure 6.22: Actual pumped water and Euphrates River leakage IN, OUT, and water gains by river (OUT-IN) with the various increments in the applied pumping rates with the current boundary conditions

Actual pumped water has affected by the total actual number of working pumping wells and the quantity of pumping rate for each well individually. Figure 6.23 illustrates the amounts of actual pumping rates which are pumped from the groundwater aquifer as well as the amounts of Euphrates River leakage waters which are participating partially in the actual pumped water as compared to each increment. It can be seen from Figure 6.23 that with all of the increments in the required pumping rates and even with the current pumping schedule, the groundwater aquifer does not supply the required/applied quantities of pumping rates where all of the quantities of the actual pumped water were less than the intended need. As the Euphrates River leakage has completely affected by the actual pumped water, Figure 6.23 shows that the maximum participation water from the Euphrates River was at the increment of 10% of the required pumping schedule while for the increments from 30% and up to 50%, the Euphrates River does not lose water from its flowing water and does not participate by the actual pumped water.
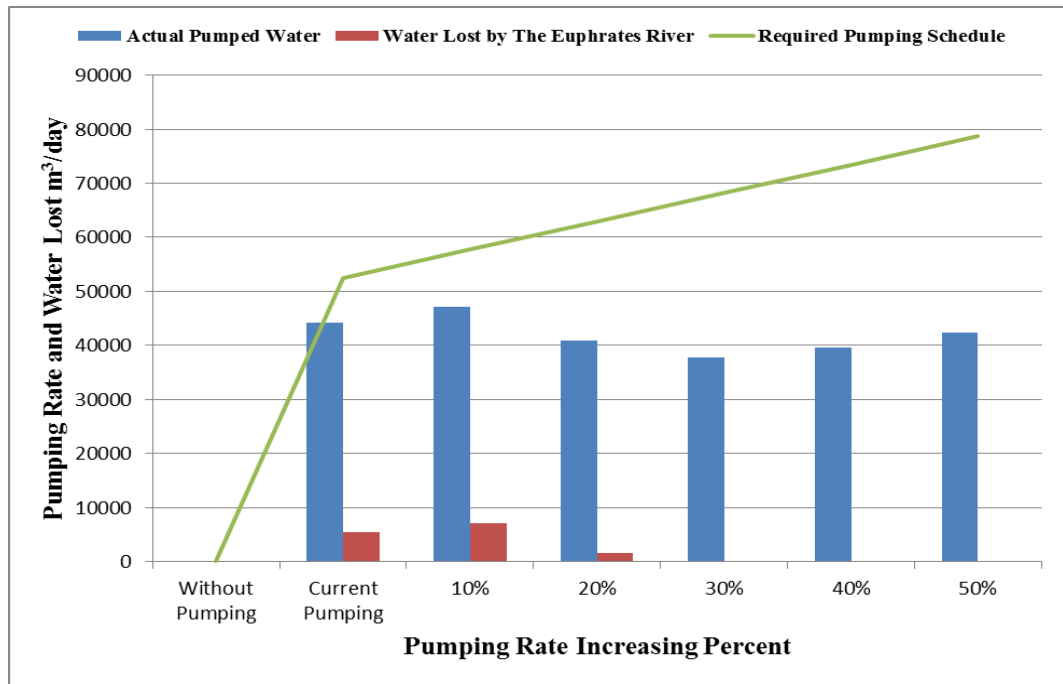
Figure 6.23: The actual pumped water and the water lost by the Euphrates River with various increments of the current pumping schedule for the current status of the study site

6.4.5 Case 5

In this case, it will explore the effect of increasing the pumping schedule up to 50% on the study area when reducing the recharge rate by 50% to become 8.25 mm/year. The computed water tables in the top and bottom layers of the aquifer for the current pumping rate and those intended increments when reducing the recharge rate applied on the study site by 50% are shown in Figure E.1 in Appendix E.

To investigate the behaviour of the groundwater aquifer, Figure E.1 is converted into numbers and illustrated in Figure 6.24, which shows the impact on the groundwater aquifer on both layers (top and bottom) when increasing the pumping rate up to 50% and reducing the recharge rate by half. In Figure E.1, It can be noticed that with all the increments of the pumping schedule, the dry areas in the top and bottom layers of the model are either creep toward the west or towards the top of the study site as these two regions are always affected more as compared with the eastern side, which is benefiting from either the Euphrates River seepage or from that water flowed toward it.

As shown in Figure 6.24, with the current required pumping schedule, an impact on the study site has resulted in declining the groundwater table hugely and in turns appearing dry areas in the top and bottom layers of the aquifer. Overall, in some increments, the impact on the aquifer

in terms of declining the groundwater table was less as compared with the case when pumping the current schedule as illustrated in the increments 10%, 40%, and 50% in the top layer (due to stopping of some wells from pumping water because of the over-pumping), but in respect of the impact on the bottom layer, Figure 6.24 shows that through the increments (10%, 20%, and 30%)of the pumping rate, the dry area is increased as compared with the current applied pumping rate (due to the increase in applied pumping rate) and decreased in the 40% and 50% increments. While in the 20% and 30% increments, the effect on the top layer in terms of declining the groundwater table and appearing the dry area was very significant and very large. Reducing the recharge rate to become 8.25 mm/year with the current pumping schedule caused in appearing top and bottom dry regions in the study site equal to 90.48 km^2 and 26.52 km^2 respectively. While with the increments of 10% up to 50%, the dry areas in the top layer were 66.48 km^2, 109.24 km^2, 108.6 km^2, 78.92 km^2, and 68.72 km^2 for each increment respectively and in the bottom layer were 51.6 km^2, 64.4 km^2, 78.2 km^2, 50.36 km^2, and 64.6 km^2 for each increment respectively as shown in Figure 6.24. The number of working pumping wells is reduced to 54 wells with the current pumping rate due to the over-pumping resulted from reducing the recharge rate. The impact on the pumping wells has increased when increasing the required pumping schedule up to 50% and decreasing the recharge rate to 8.25 mm/year at the same time. Where, the number of wells which are still working for each increment was 44 wells, 43 wells, 41 wells, 39 wells, and 34 wells for each of 10% successive increment as shown in Figure 6.24. Figure 6.24 shows that the worst case in the top and bottom layers of the model were for the increments of 20% and 30% of the current pumping rate respectively as the dryness was bigger than the other increments.
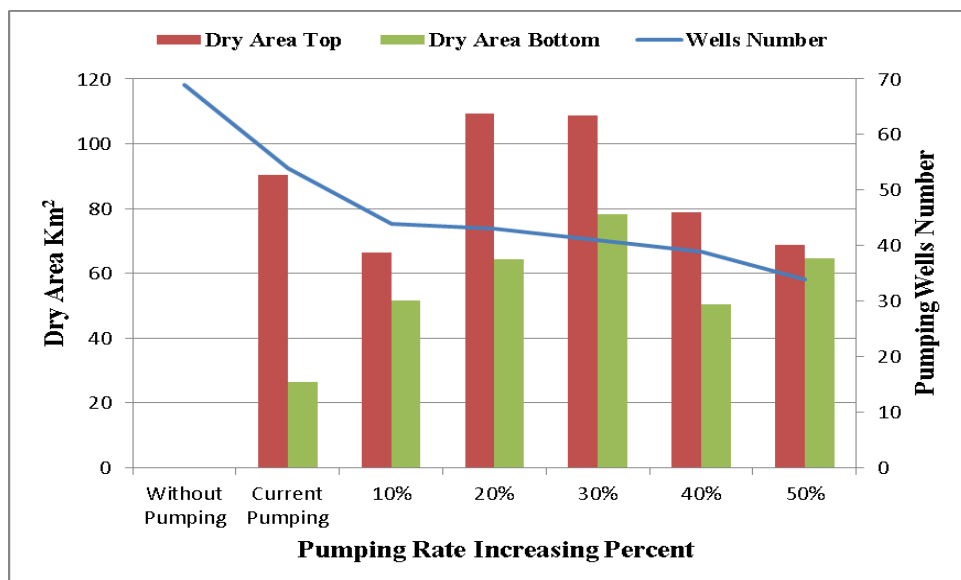
Figure 6.24: Dry area volumes in the top and bottom layers of the model with various increments of the current pumping schedule when reducing the recharge rate by 50%

The Euphrates River leakage shown in Figure 6.25 illustrates the river water lose (IN), the river water gain (OUT), the net river water lose (OUT-IN), and the actual pumping rates pumped during the various increments in the pumping schedule and when the recharge boundary condition is reduced to 8.25 mm/year. When there is no pumping schedule applied, the value of river leakage OUT shown in Figure 6.25 illustrates that the Euphrates River was gaining water by a huge quantity because the OUT leakage is greater than the IN leakage. However, with the current pumping schedule and the various increments in the pumping rates, noticed that the Euphrates River leakages IN are much greater than the OUT leakage values. Where, the net water gain by the Euphrates River (OUT-IN) is completely negative so the Euphrates River was losing water through all the pumping rate increments. Therefore, the impact of recharge reduction has a great impact on the study area in terms of losing the Euphrates River for a part of its water during the dry climates.
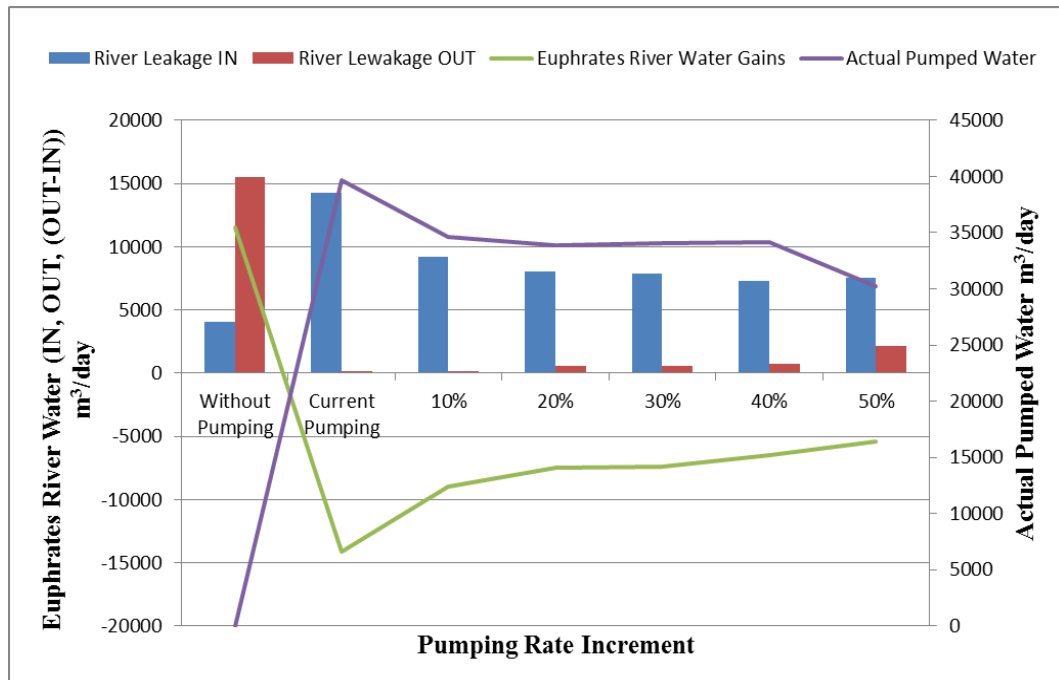
Figure 6.25: Actual pumped water and Euphrates River leakage IN, OUT, and water gains by the river (OUT-IN) with the various increments in the applied pumping rates when the recharge rate is 8.25 mm/year

The total actual number of working pumping wells and the quantity of pumping rate for each well are affected the actual pumped water. The amounts of the actual pumped waters which are pumped from the groundwater aquifer as well as the amounts of Euphrates River leakage waters which are participating in the pumping schedule, are shown in Figure 6.26. From Figure 6.26, it can be noticed that all the pumping rates applied on the groundwater aquifer in the study site are affected the study area and the groundwater aquifer again cannot provide the intended quantities. Where, the actual pumped waters were 39702 m³/day, 34609 m³/day, 33848 m³/day, 33030 m³/day, 34143 m³/day, 30278 m³/day for the current applied pumping rate 52454 m³/day

and those increments from 10% to 50% respectively. The Euphrates River is also suffered through all of these pumping schedules through losing a part from its flowing water into the groundwater aquifer to participate by a part of all of these schedules as shown by Figure 6.26. Also, it can be seen in Figure 6.26 that the maximum participation water by the Euphrates River through the actual pumped water was at the current pumping schedule by greater than 14000 m^3/day and decreased gradually through the 10% increments up to 50%. For the increments from 10% to 50%, the Euphrates River participation in the actual pumped water was ranged between 5400 m^3/day – 9000 m^3/day as illustrated in Figure 6.26.
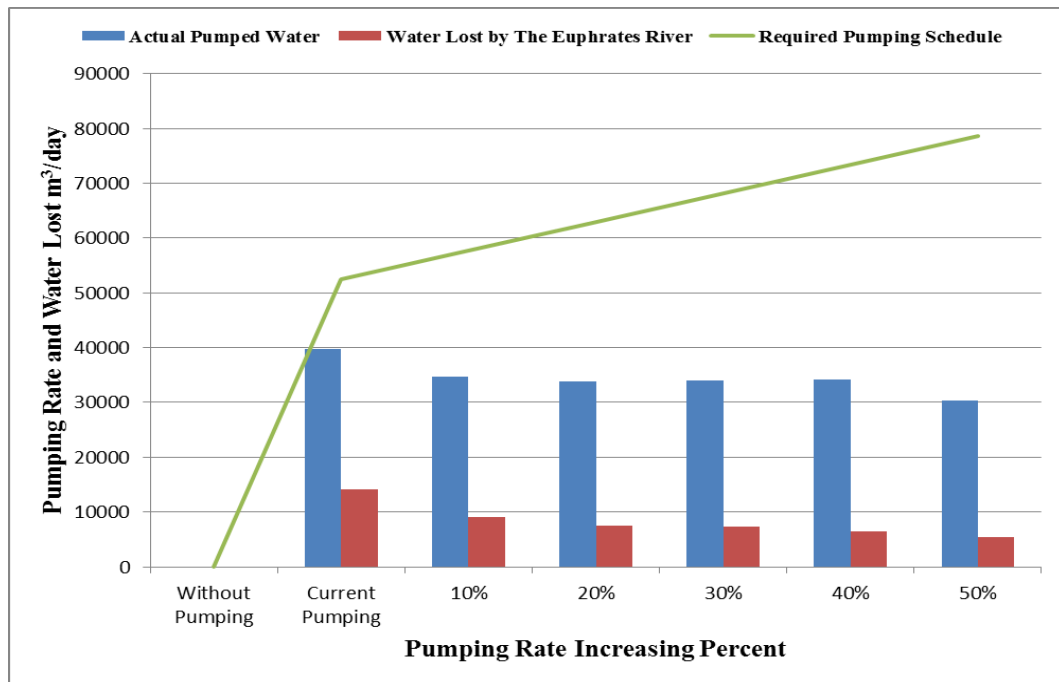
Figure 6.26: The actual pumped water and the water lost by the Euphrates River with various increments of the current pumping schedule when reducing the recharge rate by 50%

6.4.6 Case 6

It will explore in this case the effect of decreasing the western constant head by 5m to become 45m through the increase in the current pumping rate up to 50%. Reducing this parameter is completely expected in the future due to the effect of climate change in the area under study and due to the high temperatures which lead to high evaporation rates. The computed water tables and dry areas in the top and bottom layers of the groundwater aquifer for the current pumping rate and the various increments of the pumping rates when reducing the western constant head for 45m are shown in Figure E.2 in Appendix E. To assess the impact of reducing the western constant head to 45m, Figure E.2 shown in Appendix E is converted into numbers to be clear and can be easily discussed as shown in Figure 6.27. Figure 6.27 shows the impact on the top

and bottom layers of the groundwater aquifer when the western constant head has reduced to 45m and the scheduled pumping rate has increased up to 50%.

From Figure 6.27, in general, the impact of decreasing the western constant head's boundary condition to 45m with the increase of the pumping schedule up to 50% in Case 6 has led to being the behaviour of the aquifer as similar as of that behaviour of Case 4, but with a significant increase in the dry area volumes in the aquifer's layers and the wells number which are stop to pump water due to over-pumping. Increasing the applied/required pumping rate through decreasing the western constant head from 50m to 45m at the same time will affect the groundwater level distribution over the whole study area and in turns this will add an impact on the groundwater aquifer to provide the required water. When reducing the western constant head and keep the current pumping schedule as the same as now, it is found that the study area will have a dry area problem in the top and bottom layers of 93.84 km^2 and 3.24 km^2 respectively. With the increments of 10% up to 50% of the required pumping schedule, the dry areas in the top layer were 100.56 km^2, 87.52 km^2, 127.28 km^2, 62.92 km^2, and 87.68 km^2 for each increment respectively and in the bottom layer were 21.32 km^2, 46.2 km^2, 64 km^2, 62.92 km^2, and 87.68 km^2 for each increment respectively as shown in Figure 6.27. With the current pumping rate, when reducing the western constant head to 45m, it is noticed that the number of working wells are reduced to 58 wells where 11 wells are stopped to pump water due to the over-pumping. With the 10% increments up to 50% of the current pumping schedule, the only still working wells are reduced to 56 wells, 45 wells, 43 wells, 38 wells, and 34 wells for each increment as illustrated in Figure 6.27. Overall the most worsen situation was at 30% increment and 50% increment of the current pumping rate in the top and bottom layers of the model respectively.

Figure 6.28 illustrates the Euphrates River leakage IN, OUT, (OUT-IN), and the actual pumping rates pumped during the various increments in the pumping schedule and when the western constant head boundary condition is reduced to 45m. The Euphrates River gains water from the groundwater aquifer by a huge quantity when there is no pumping rate applied on the groundwater system. However, reducing the head to 45m with the current pumping rate and when the pumping rate increased by 10%, the Euphrates River leakage IN will be greater than the OUT leakage which will lead to losing the Euphrates River for its water into the groundwater aquifer. On the contrary, small quantities have been gained by the Euphrates River in the increments 20%, 30%, 40%, and 50% of the current pumping rate due to the decrease in the actual pumped water. Overall, it can be considered that the reduction in the constant head

level during the dry climates has almost a slight impact on the Euphrates River leakage as compared with Case 4.
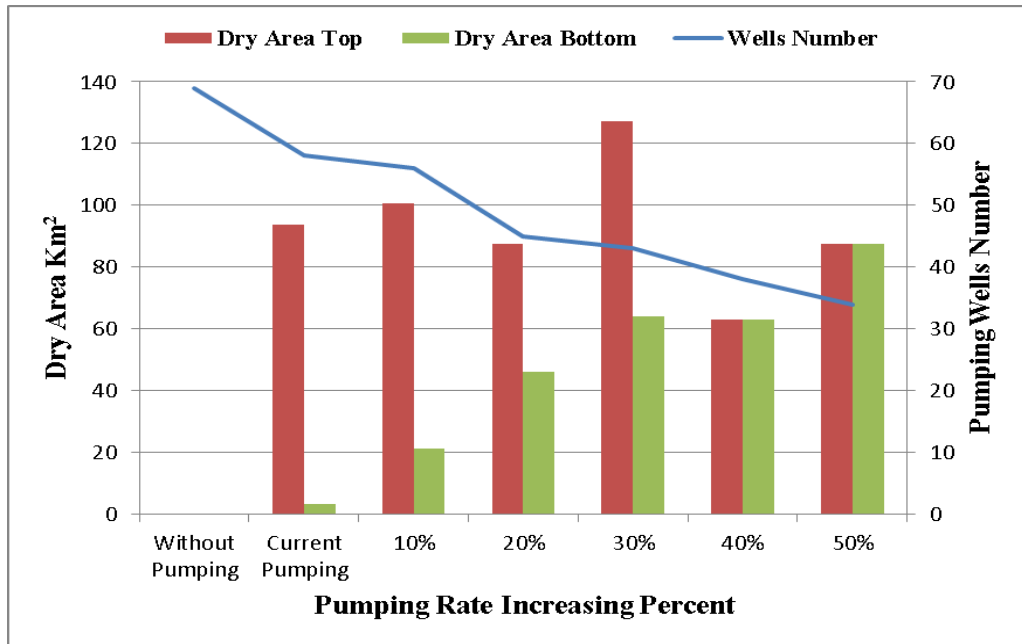
Figure 6.27: Dry area volumes in the top and bottom layers of the model with various increments of the current pumping schedule when reducing the western constant head to 45m
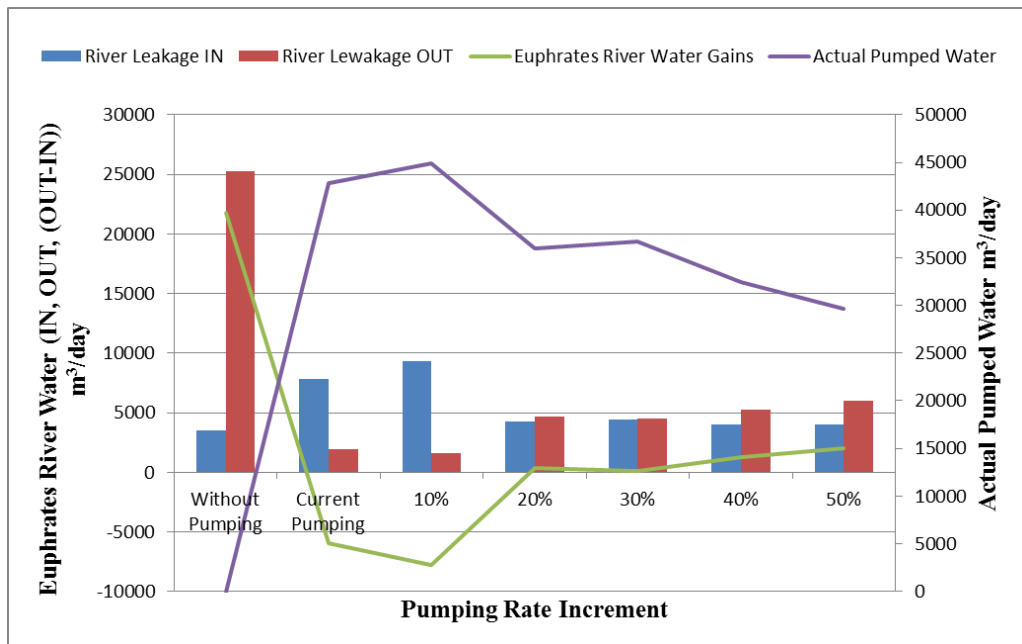
Figure 6.28: Actual pumped water and Euphrates River leakage IN, OUT, and water gains by the river (OUT-IN) with the various increments in the applied pumping rates for the west constant head 45m

Figure 6.29 illustrates the actual amounts of water pumped from the groundwater aquifer as well as the amounts of water gained by the groundwater aquifer from the Euphrates River which are

participating in a part of the pumping schedule. The study area cannot supply the applied pumping quantities where even the actual pumped water is not completely supplied by the groundwater aquifer. The Euphrates River have shared by a part in most of the pumped quantities through most of the increments of pumping rates. The Euphrates River is participating in the actual pumped waters through the increment of 10% as well as the current pumping schedule. Where, it was on its maximum participation when the current pumping schedule increased by 10% and equals 7750 m³/day. For the increments from 20% to 50%, the Euphrates River was not participating with the groundwater aquifer by a part of its water because the impact of the pumping schedules was big and the groundwater aquifer already provides very little quantities. The most effected parameter on the Euphrates River leakage is the actual pumped water where when this quantity reduces, the participation will already be reduced as it is demonstrated in Figure 6.29 and vice versa.
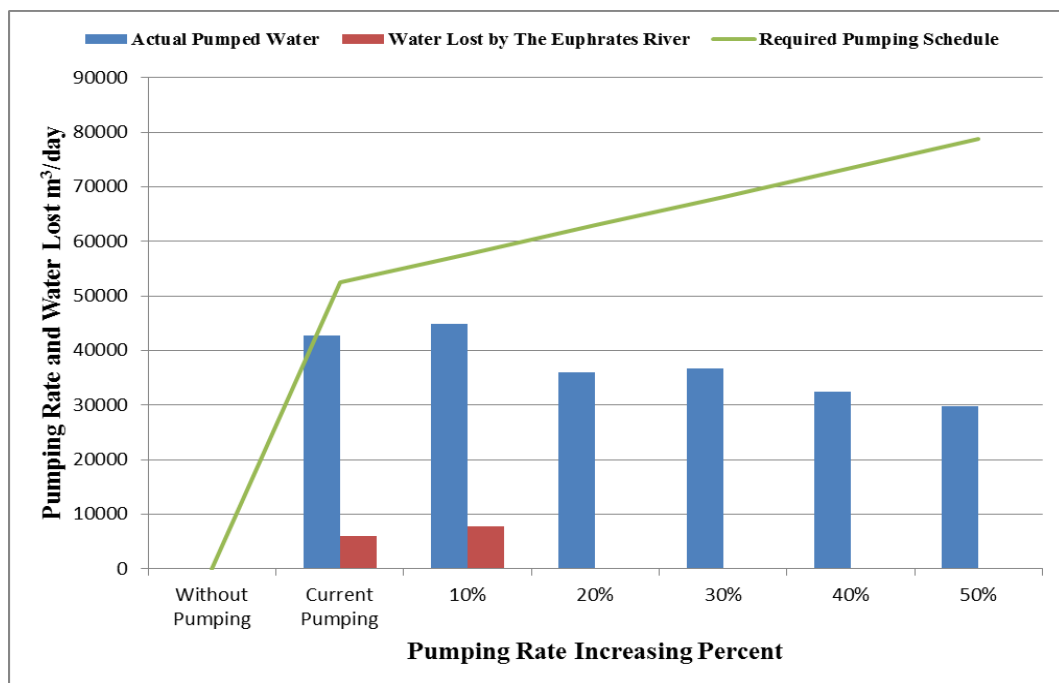
Figure 6.29: The actual pumped water and the water lost by the Euphrates River with various increments of the current pumping schedule when reducing the western constant head to 45m

6.4.7 Case 7

The impact of reducing the Euphrates River level by 1m through the increase in the current pumping rate up to 50% is explored in this case. Due to the water exchange phenomenon between the groundwater and surface water represented by the Euphrates River, the rainfall shortage in the study area, and many issues as mentioned in Chapter 1, it will highly be expected to have a reduction in the level of the Euphrates River. Therefore, it will investigate the impact of reducing the Euphrates River level by 1m through the various increments in the

required pumping schedule on both the groundwater aquifer and the Euphrates River. Figure E.3 in Appendix E shows the computed water tables and the dry areas in the top and bottom layers of the groundwater aquifer for the current pumping rate and the various increments of the pumping rates when reducing the Euphrates River level by 1m. To review the effect of reducing the Euphrates River level by 1m with the various increments of the pumping rate, the dry area volumes and wells number (the working ones) are extracted and illustrated in Figure 6.30. Figure 6.30 shows the dry area volumes in the top and bottom layers of study site as well as the remaining working wells number when reducing the Euphrates River level by 1m and increasing the current pumping rate up to 50%.

When reducing the Euphrates River level by 1m with the increase in the pumping schedule, it is found that the groundwater tables will be suffered more where it can be seen that dry areas have appeared in the top and bottom layers of the model equal to 43.24 km^2 and 1.68 km^2 with a little increase as compared with Case 4 (current pumping rate). With the 10% increments up to 50% in the current pumping rate, the dry areas in the top layer become 51.44 km^2, 38 km^2, 52.12 km^2, 54.28 km^2, and 78.5 km^2 for each increment respectively and in the bottom layer were 7.84 km^2, 32.32 km^2, 43.32 km^2, 36.36 km^2, and 36.44 km^2 for each increment respectively as shown in Figure 6.30. The impact on the pumping wells has increased when increasing the required pumping schedule up to 50% and decreasing the Euphrates River level by 1m. Where, the number of wells which are still working for each 10% increment was 57 wells, 47 wells, 44 wells, 43 wells, and 43 wells for each increment respectively as compared with the current pumping rate which has 60 wells able to pump water as shown in Figure 6.30. In addition, Figure 6.30 shows that the worst case in the top and bottom layers of the model is for the increments of 50% and 30% of the current pumping rate respectively as the dryness was bigger than the other increments.

The Euphrates River leakage IN, OUT, (OUT-IN), and the actual pumping rates pumped during the various increments in the pumping schedule and when the Euphrates River level is reduced by 1m are illustrated in Figure 6.31. Again when there is no pumping from the groundwater aquifer, the Euphrates River will gain water of over 20000 m^3/day. With the current pumping rate and when the current pumping rate is increased by 10%, Figure 6.31 shows that the actual pumped water is increased and thus the water gains by the Euphrates River is decreased where in both of these cases, the Euphrates River was defined as a losing river because it was losing its water into the groundwater aquifer. At 20% increment of the current pumping rate, the actual pumped water is reduced significantly and the Euphrates River situation is converted to the gaining state. At 30%, 40%, and 50% increments of the current pumping rate, the actual

pumped water is increased slightly with a slight reduction effect on the Euphrates River gaining water to keep the river with the gaining situation as Figure 6.31 showed. It is obvious from the results shown in Figure 6.31 that the impact of reducing the Euphrates River level is not significantly large as the results were highly closed to Case 4 with some changes coming from this reduction.
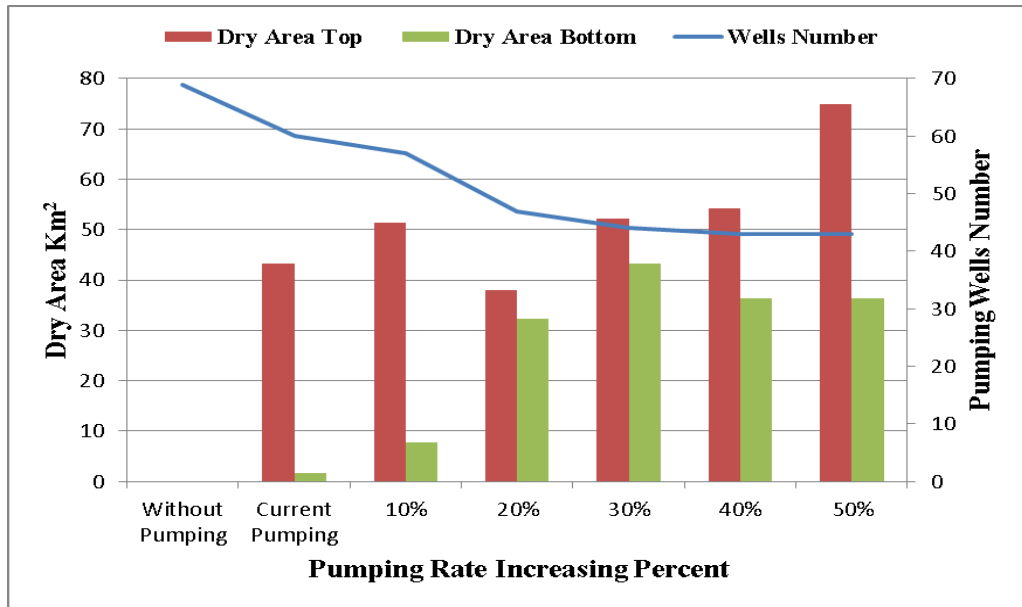
Figure 6.30: Dry area volumes in the top and bottom layers of the model with various increments of the current pumping schedule when reducing the Euphrates River level by 1m
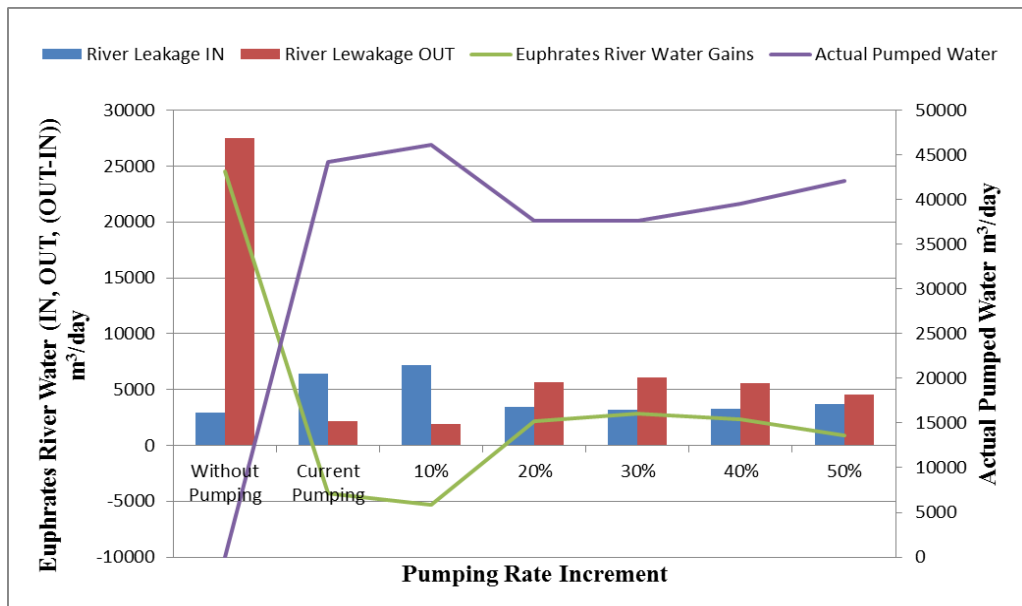
Figure 6.31: Actual pumped water and the Euphrates River leakage IN, OUT, and water gains by the river (OUT-IN) with the various increments in the applied pumping rates when reducing in the Euphrates River level by 1m

Figure 6.32 shows the amounts of the actual pumped waters from the groundwater aquifer as well as the amounts of the Euphrates River leakage waters which are participating in the

pumping schedule when reducing the Euphrates River level by 1m and increasing the current pumping schedule up to 50%. It can be noticed from Figure 6.32 that the study area has affected by all of the pumping rates applied on the groundwater aquifer where it does not supply the required quantities. The Euphrates River is suffered only with the current pumping schedule and with the increment of 10% of the current pumping schedule. The required/applied pumping rates were ranging between 52454 m^3/day and 78681 m^3/day while the actual pumped waters were ranging from 42162 m^3/day to 44263 m^3/day where it can be seen that the groundwater aquifer does not supply all of the required pumping in a complete quantity as Figure 6.32 shown. The Euphrates River participates only in the current pumping rate and when increasing the pumping schedule by 10% while for the increment from 20% to 50%, it does not participate in any quantity of water. Where the maximum participation water by the Euphrates River was for the 10% increment and equals 5280 m^3/day.
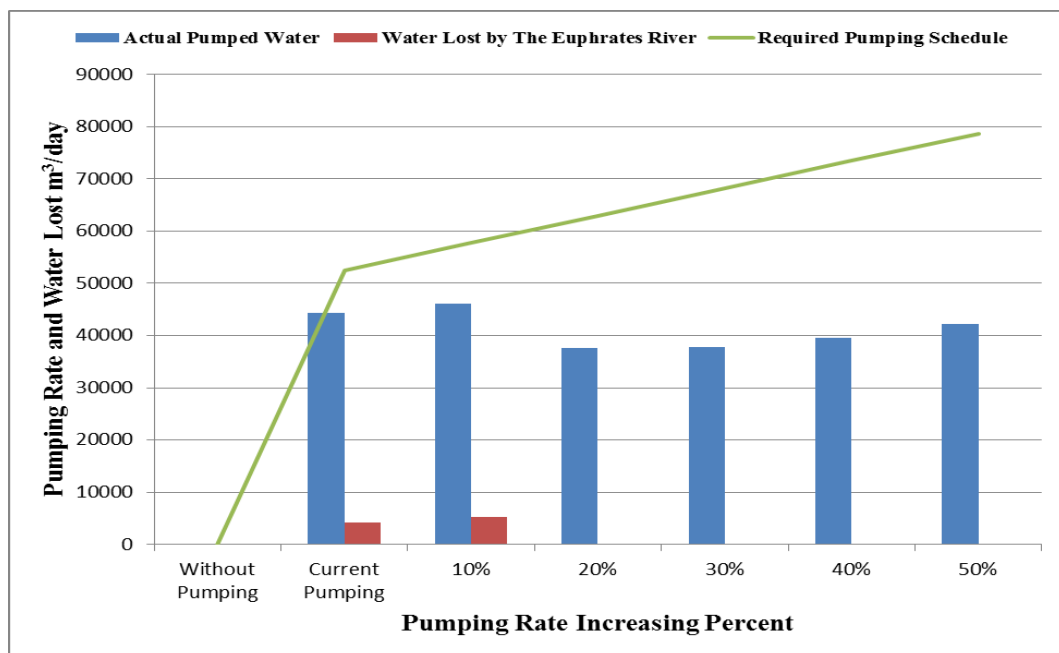
Figure 6.32: The actual pumped water and the water lost by the Euphrates River with various increments of the current pumping schedule when reducing the Euphrates River level by 1m

6.4.8 Case 8

The impact of reducing all of the recharge rate by 50%, the western constant head to be 45m, and the Euphrates River level by 1m, through the increase in the current pumping rate up to 50% is explored in this case. It is highly expected that any area will experience severe drought, especially in areas that are exposed to high temperatures and poor rainfall. The study area is classified as having a dry climate. Therefore in this case, it will reduce various parameters all together that may the study site will face in the future to explore the behaviour of the study site

and the expected effect that may apply. These parameters are the recharge rate (will reduce it by 50% to become 8.25 mm/year), western constant head by 5m (to become 45m), and the Euphrates River level by 1m. Figure E.4 in Appendix E shows the computed water tables and the dry areas in the top and bottom layers of the groundwater aquifer for the current pumping rate and the various increments of the pumping rates when reducing various boundary conditions all together at the same time. Figure 6.33 will show the volumes of dry areas and the wells number which are still working to pump water numerously when applying the reduction of some boundary conditions.

The effect of reducing the recharge rate by 50%, reducing the western constant head to 45m, reducing the Euphrates River level by 1m, and increasing the current pumping rate up to 50% in numbers on the groundwater aquifer is illustrated in Figure 6.33. Clearly, it can be seen that reducing of the recharge rate by 50%, the western constant head to 45m, and the Euphrates River level by 1m have affected the study site when increasing the pumping schedule through increasing the dry areas in the top and bottom layers of the model by various percentages. Where, with the current pumping schedule, the dry areas in the top and bottom layers of the model were 121.16 km^2 and 49.96 km^2 respectively. While with the 10% increments up to 50%, the top dry areas became 150.32 km^2, 96.56 km^2, 125.32 km^2, 97.76 km^2, and 100.2 km^2 for each increment respectively and in the bottom layer became 85.28 km^2, 84.12 km^2, 117.16 km^2, 92.92 km^2, and 96.56 km^2 for each increment respectively as shown in Figure 6.33. The pumping wells are also affected by reducing these parameters when increasing the current pumping rate where with the current pumping rate, the wells which were still pumping water reduced from 69 wells to 46 wells while with the 10% increments up to 50%, the running pumping wells which are still pumping water become 43 wells, 37 wells, 31 wells, 30 wells, and 30 wells for each of 10% increment as shown in Figure 6.33. In addition, Figure 6.33 shows that the worst case in the top and bottom layers of the model were for the increments of 10% and 30% of the current pumping rate respectively as the dryness was bigger than the other increments. It is clear that this Case (8) is the worse because it leads to affecting the study site critically.
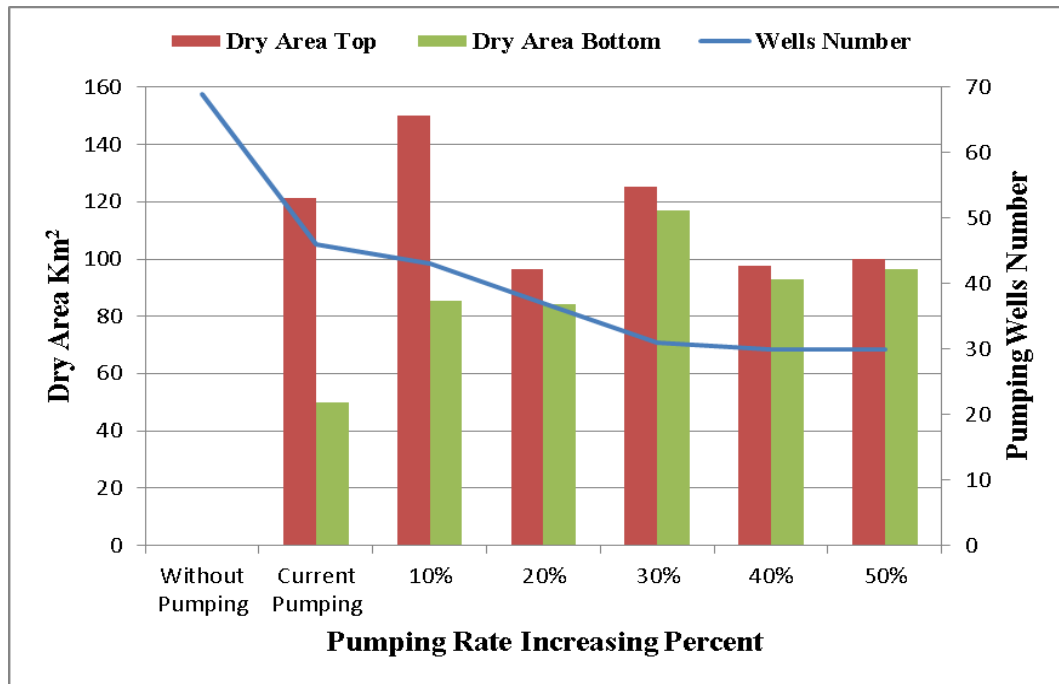
Figure 6.33: Dry area volumes in the top and bottom layers of the model with various increments of the current pumping schedule when reducing the recharge rate by half, the western constant head to be 45m, and the Euphrates River level by 1m

The Euphrates River leakage IN, OUT, (OUT-IN), and the actual pumping rates pumped during the various increments in the pumping schedule and when the recharge rate R=8.25 mm/year, western constant head boundary condition = 45m, and the Euphrates River level is reduced by 1m are illustrated in Figure 6.34. Overall, with the current pumping rate and all the increments in the pumping schedule, the Euphrates River remains losing its water into the groundwater aquifer to substitute the reduction in the groundwater quantity that should be provided to the required/applied pumping schedules. In addition, Figure 6.34 shows that there is a shortage in the availability of the groundwater in the aquifer during the critical dry climates which are affected the whole pumping schedule and in turn the actual pumped water. Where for all the pumping schedules applied on the groundwater aquifer, it can be seen that the actual pumped water averages between approximately 22000 m^3/day and 33000 m^3/day and these quantities are very little as compared to the applied quantities 52454 m^3/day (current) and those quantities of 10% increment each up to 50%.
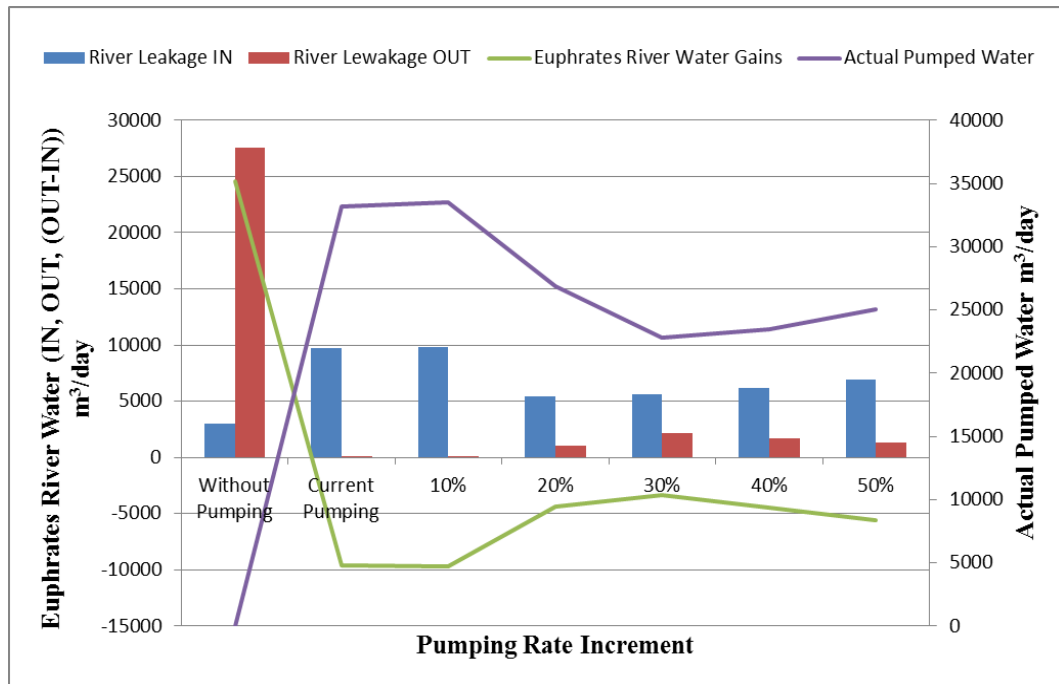
Figure 6.34: Actual pumped water and Euphrates River leakage IN, OUT, and water gains by river (OUT-IN) with the various increments in the applied pumping rates for R=8.25 mm/year, west constant head = 45m, and a reduction in the Euphrates River level of 1m

Figure 6.35 demonstrates the total actual pumped waters which are pumped from the remaining working pumping wells after excluding those wells affected by the over-pumping and stop pumping water, and the amounts of the Euphrates River leakages which are participating in the pumping schedule after reducing some boundary conditions that control the study site. It can be seen from Figure 6.35 that the groundwater aquifer cannot provide the applied/required pumping schedules due to the impact on the aquifer where for the current pumping rate and all the increments of the current pumping rates, the actual pumped waters were not satisfying the required schedules. Therefore it can be noticed that these actual pumped waters are too little to compare with the required schedules where this reflects the huge impact exerted on the groundwater aquifer during the future predicted climate changes (if happened). The Euphrates River has exposed for the impact of the climate changes where it was losing for a part of its water into the pumping schedule where the water which was losing ranged between 3392 m^3/day and 9686 m^3/day through all of those 10% increments of the current pumping rate as illustrated in Figure 6.35.
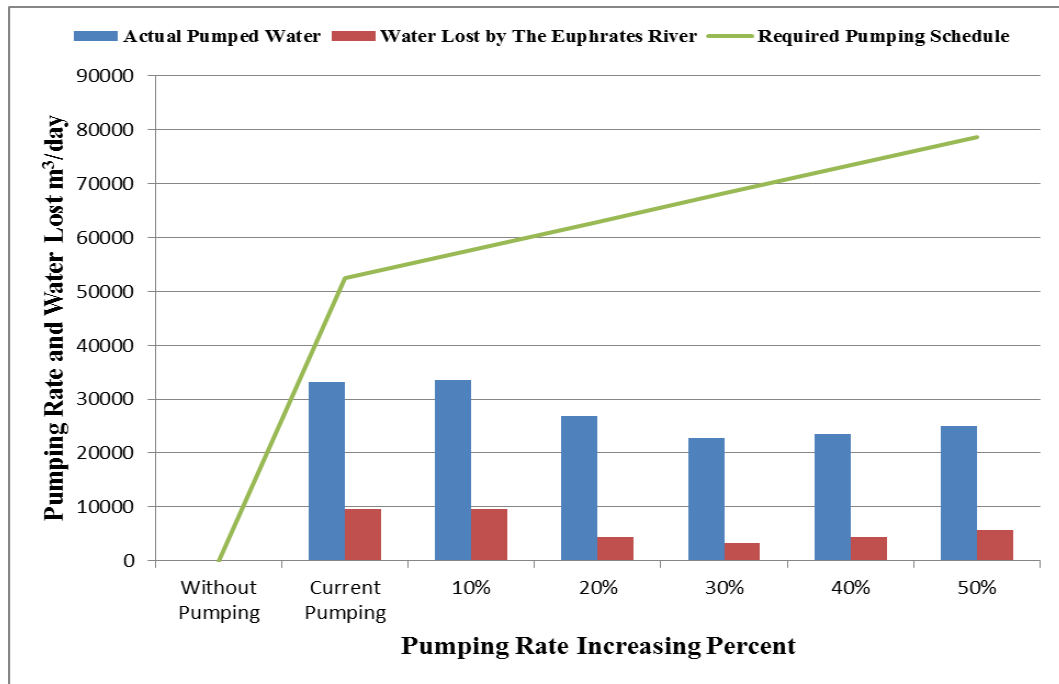
Figure 6.35: The actual pumped water and the water lost by the Euphrates River with various increments of the current pumping schedule when reducing the recharge rate to 8.25 mm/year, the western constant head to 45m, and the Euphrates River level by 1m

In order to conclude the effect of various climate changes (Cases 4, 5, 6, 7, and 8) as well as the effect of increasing the applied/required pumping rates on the groundwater table level and the Euphrates River leakage in Al-Najaf region groundwater model, Figure 6.36 and Figure 6.37 will conclude these effects. These figures are illustrating the effect on the study site in terms of the dry area (km^2) and the actual pumped water (m^3/day) through the current pumping rate 52454 m^3/day and with each of 10% increment in the current pumping rate up to 50%.

The dry area volumes through the current and the different increments of the required pumping rate in all of the five cases (4, 5, 6, 7, and 8) shown in Figure 6.36 and Figure 6.37 are resulting from the decline in groundwater table which is affected completely by the number of working pumping wells and the actual pumped water from the only working pumping wells during the system operation process. Where increasing the applied pumping rate on the groundwater aquifer will add a great impact on the groundwater aquifer especially when the climate changes have negatively affected the quantity of groundwater where this will lead to decreasing the number of working pumping wells which should still run to pump the required pumping rate. The impact on the groundwater system represented by the dry area issue is depending upon the quantity of the actual pumped water, where it may increase or decrease followed the actual pumped quantity behaviour. Where sometimes the actual pumped water quantity will increase and sometimes decrease during the various increments in the applied pumping rates due the

various pressures exerted on the aquifer. The explanation of the increase and the decrease issues will be discussed in detail.

In case of the actual pumped water is increased, generally, the dry area will be increased, but sometimes the dry area will be decreased. The interpretation of this case is firstly the stopped working pumping wells which were affecting the study area and causing the declining in the water table and in turn causing the dry area are stopped to work (due to over-pumping) so the resulted dry area is reduced. Secondly, the remaining working pumping wells will pump more water due to the increasing in the applied pumping schedule where these wells will not have a great impact on the study area in terms of declining the water table and causing the dry area because the pumped water from these wells are still within the capacity of those wells or those wells are installed in an area with a very high groundwater table. Therefore, the effect of increasing the applied pumping rate will either does not have any impact on the aquifer or the impact will be too small.

On the other hand, generally, the decrease in the actual pumped water will result in decreasing in the dry area. However, in some cases will lead to increasing the dry area. The reasons for this are, 1) some of the pumping wells which were working in the previous increment of the current pumping rate (any increment) will stop to pump water in the successive increment due to the over-pumping where the over-pumped wells (stopped to pump water) did not have a significant impact on the groundwater table and thus the dry area, 2) the extra quantity in the applied pumping rate due to the successive increment which should be pumped from the remaining working pumping wells will have a significant influence on the groundwater aquifer and thus on increasing the dry area although the total actual pumped water from all the remaining working wells is decreased. Where when comparing the effect of the wells that have stopped to pump water with those wells that have remained working and pumping water on the dry area (groundwater table) will find that the effect of the wells that have remained working is much more, so the dry area increased.

From Figure 6.36, it can be identified the most influential case on the study area, which causes the largest dry areas in the top layer of the model. Cases 5, 6, and 8 represent the most dangerous future predicted cases where the study site will be suffered from the impact generated from these cases particularly Case 8 which highly affected Dibdibba aquifer, especially when the daily need for water is increased. Similarly, it can be seen the same effect in Figure 6.37 for the same case but in the bottom layer.

With the current applied pumping rate and the various increments of the current pumping rates, the impact on the groundwater table was very high through declining the level of the groundwater and appearing hugely dry areas especially in the top layer of the model as illustrated in Figures 6.36 and 6.37. The reduction in the recharge rate boundary condition is also showed a significant impact on the study area as this parameter is highly predicted to happen because the area is suffered from a shortage in the precipitation intensities. In addition, the dry area problem has led to affecting the actual pumped water from the groundwater aquifer which should be supplied for the daily's need. Where, it can be seen in Figure 6.36 and Figure 6.37 that the groundwater aquifer supplied quantities lesser than the required/applied ones where the maximum and minimum quantities were approximately 47050 m^3/day and 22800 m^3/day. The shortage in providing the required pumping rates is because: 1) the over-pumping which led to damaging some pumping wells, and 2) the unsustainability of the groundwater aquifer to provide the required pumping rates.
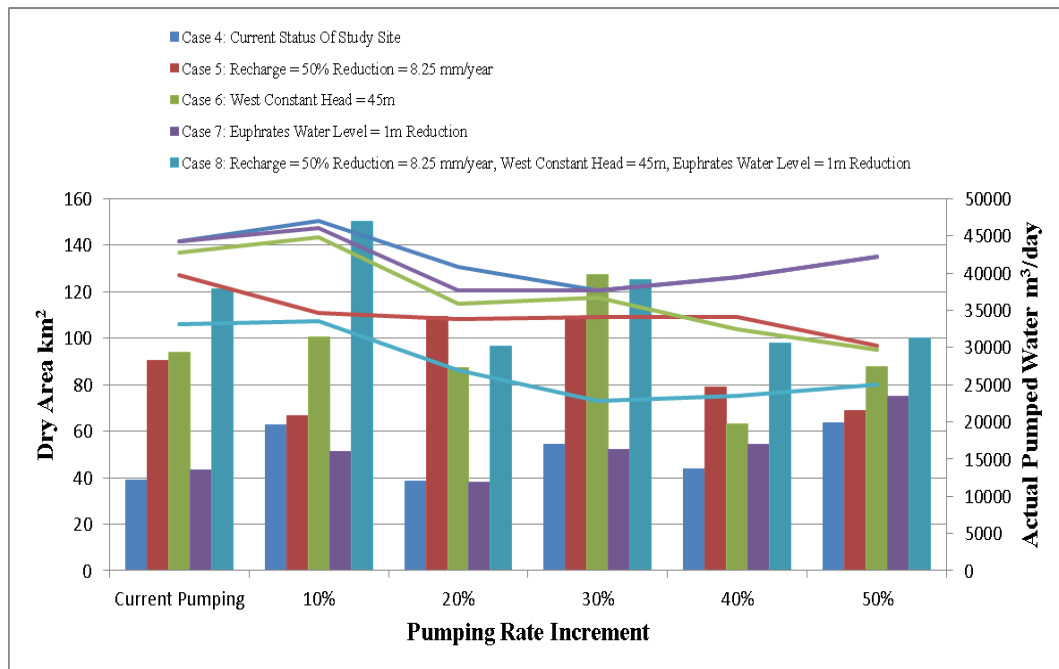
Figure 6.36: Dry areas in top layer in km^2 and the actual pumped water, with the various increments in the applied pumping rates for Cases 4, 5, 6, 7, and 8
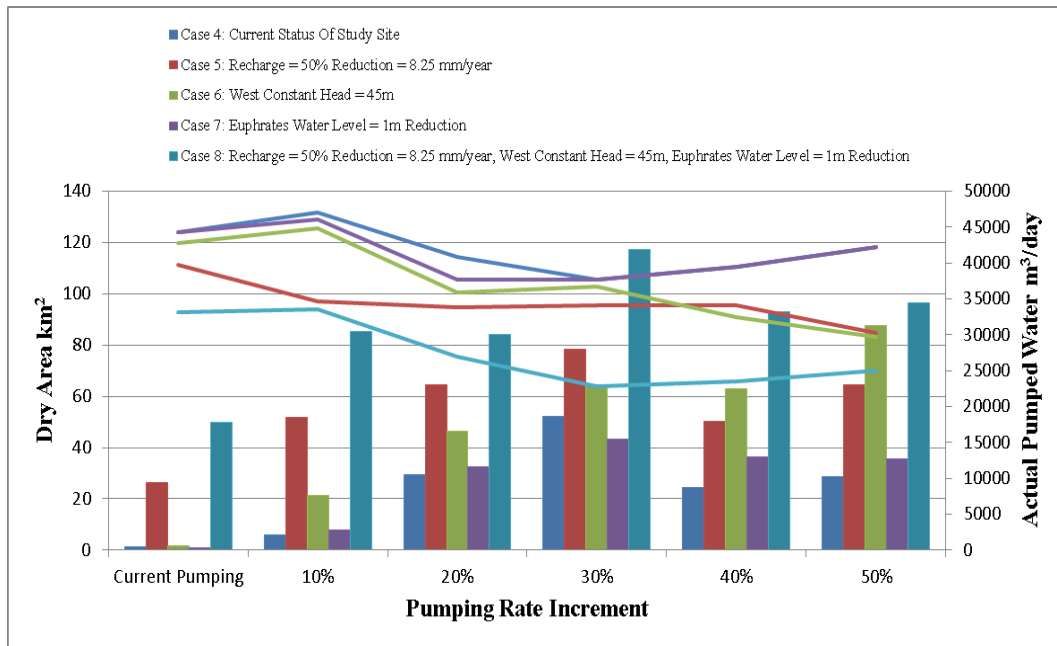
Figure 6.37: Dry areas in bottom layer in km^2 and the actual pumped water, with the various increments in the applied pumping rates for Cases 4, 5, 6, 7, and 8

Figure 6.38 shows the actual number of working pumping wells which are actually pumped water through the current pumping schedule and the various increments in the current pumping schedule up to 50% through the various predicted climate changes. The total number of pumping wells in Al-Najaf region is 69 from the field observations. Overall, clearly from Figure 6.38, it can be seen that the change in one of the boundary condition with any increment in the pumping schedule will affect the pumping wells number and lead to stop working some of them. With the current pumping schedule from the wells 52454 m^3/day and through the various changes of boundary conditions, the total number of pumping wells that pumping the actual water is reduced and this reduction was significant and critical for both of Cases 5 and 8. In Case 4, Case 6, and Case 7, the reduction in the pumping wells number is little during the various increments in the pumping schedule, except for the Case when the western constant head is reduced to 45m (Case 6) with an increment in the pumping schedule of 40% and 50%, where the reduction in the pumping wells number is more significant and should be taken into account. In conclusion, reducing the actual working pumping wells number will affect the actual pumped water through increasing it or decreasing it, depends upon: 1) the quantity of pumped water from each individual well, and 2) for which extent this well will be affected by the external impact which may lead to either damaging it or affecting its pumping rate's quantity.
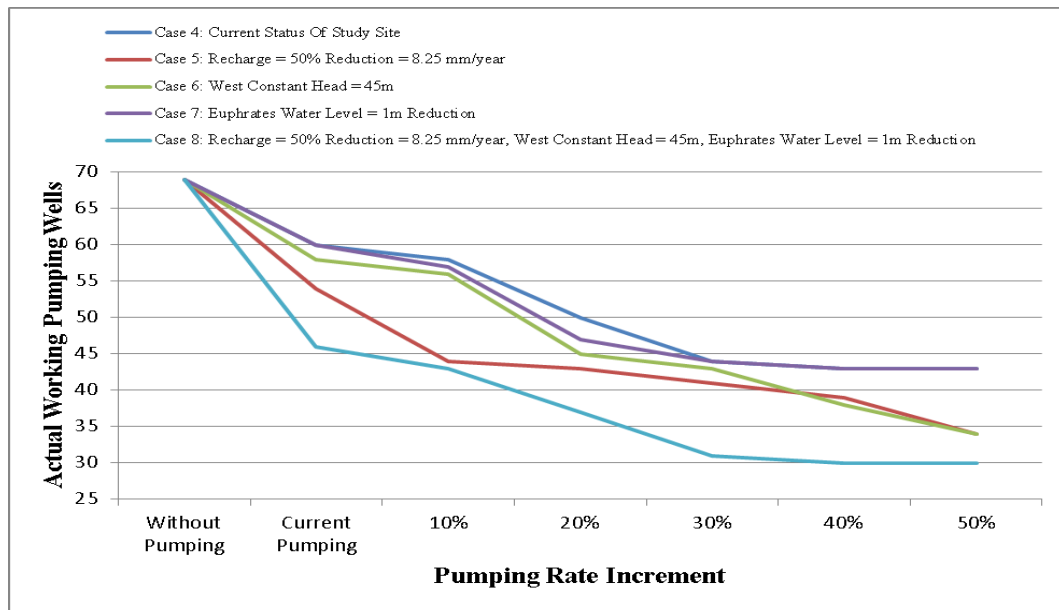
Figure 6.38: The relation between the actual working pumping wells number and the various increments in the current pumping rate for Cases 4, 5, 6, 7, and 8

In respect of the effect of the cases 4, 5, 6, 7, and 8 on the Euphrates River flowing water, Figure 6.39 shows the conclusion of these five applied/predicted cases. Figure 6.39 shows the relationship between the quantities of water lost by the Euphrates River into the groundwater aquifer through the various predicted cases when increasing the current pumping schedule by 10% increments up to 50%. As it can be shown in Figure 6.39 that the Euphrates River was losing water into the groundwater aquifer through the various cases, but all the cases of the current pumping schedule and the 10% increment in the current pumping schedule, the Euphrates River was participating by a part of the actual pumped water from the groundwater aquifer larger than the other increments, as it reaches sometimes to approximately 14000 m^3/day. In addition, it can be noticed from Figure 6.39 that the Cases 5 and 8 are still the most important and effected cases on the groundwater aquifer as compared with others which have less impact. Therefore, the decision-makers should be taken into account these two cases for the future predictions to be ready for planning and controlling the impacts coming from changing the boundary conditions identified in these cases.
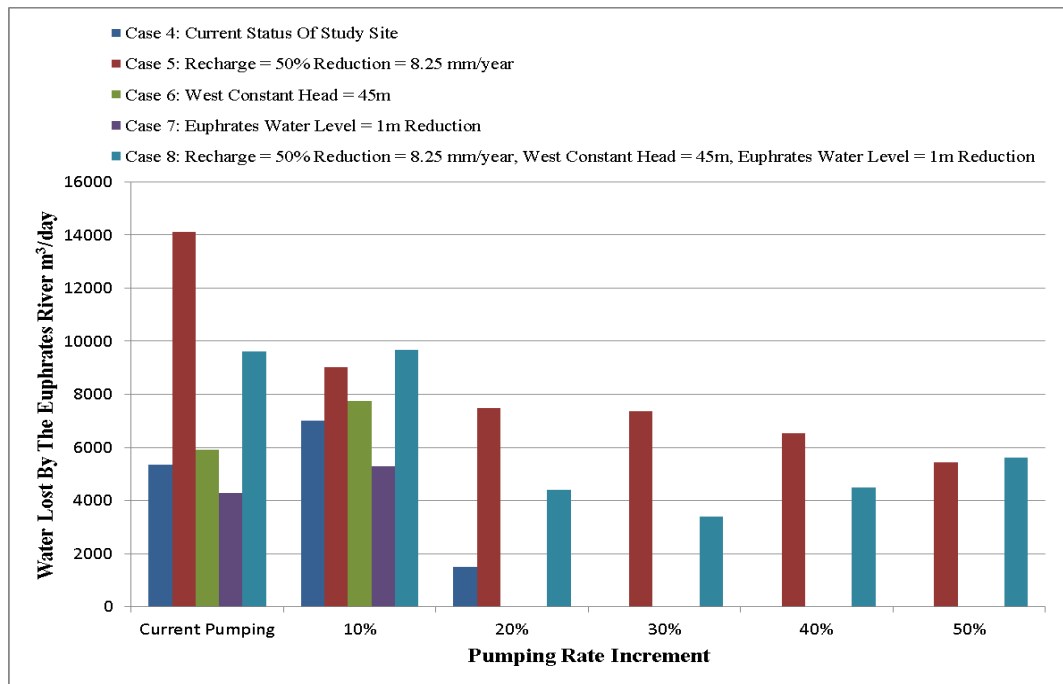
Figure 6.39: The relation between the water lost by the Euphrates River and the various increments in the current pumping rate for Cases 4, 5, 6, 7, and 8

According to the largely affected cases, it is needed to explore the connection between the groundwater table and the Euphrates River level to see whether these two levels are still connected to each other or not. Therefore, it will take a vertical cross-section in the most dangerous cases with the most dangerous pumping rate increments in the top and bottom layers of the model to investigate that connection. The biggest dry areas in the top and bottom layers of the model represent those statuses which may affect the groundwater-the Euphrates River levels' connection. Figure 6.40 shows some cross-sections of groundwater level decline due to the highest dry areas over the study site selected in the most affected locations for Case 8 through the increments of 10% and 30% of the current pumping schedule in the top and bottom layers of the model respectively, because this case has resulted in the largest effects on the study site.

It is noticed that although climatic changes and the increases in the amounts of pumping schedule can significantly affected the groundwater table in the central and western regions, but the level of groundwater in the eastern region is not affected too much, where the connection between the groundwater and the Euphrates River levels is remaining there, as shown in Figure 6.40. The connection between the levels of the groundwater and the Euphrates River will make the estimated results for the amounts of water lost or depleted from the Euphrates River into groundwater are acceptable. Where, if the groundwater level was below the bottom elevation of the Euphrates River, then the estimated leakages will not be the real and will be underestimated leakage results, as Visual MODFLOW deals with the saturated mediums so when the level of

193

groundwater decline below the bed of a river, this will generate a hyporheic unsaturated zone between the groundwater and the Euphrates River levels which in turn will affect the river leakage results by the underestimation problem.
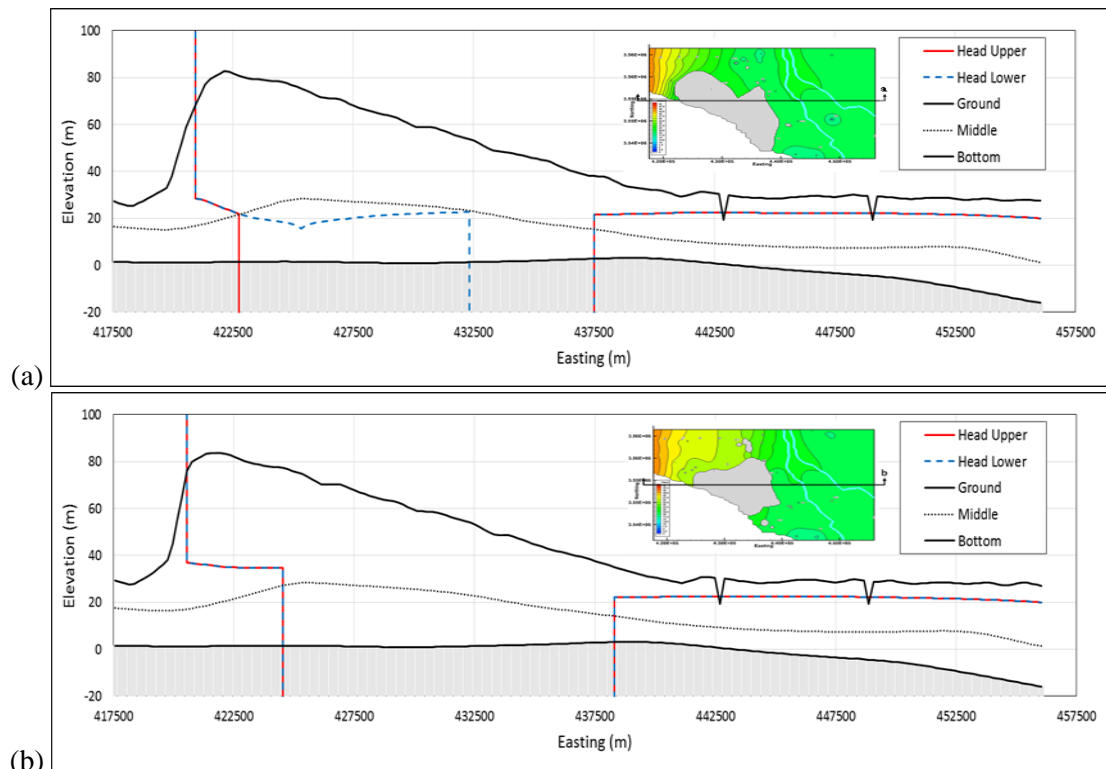
Figure 6.40: Groundwater level decline in the most effected situations of Case 8: (a) Top layer, and (b) Bottom layer

From all the cases that have been carried out (Case 4-8), it is clearly found that the pressure exerted on the groundwater aquifer, no matter how large, it will dry the central and western regions of the model and does not affect significantly on the eastern region of the model as this area is completely saturated with water and the level of groundwater is very high. Therefore any external influences are not able to influence the connection between the groundwater level and the Euphrates River. Consequently, all the results of the Euphrates River leakage resulting from the groundwater model of Al-Najaf City and the surrounding area are valid/correct and reliable to determine the impact on the Euphrates River which is resulting from the expected climatic changes or the current and future extra quantities of pumping schedule.

6.5 Management the current problem in Al-Najaf region

Sustainable management of groundwater and surface water resources requires concerted efforts to produce good planning. The response to acute resource degradation will be insufficient if there is no attention from all users is paid for these sources, particularly the source of groundwater, to be well protected. Because the source of groundwater is not visible, it requires

an understanding of groundwater systems, groundwater flows, basic hydrogeology, groundwater depth, and groundwater revenues so that the sustainable principle will be implemented as required (Chevalking et al. 2008). To overcome the current pumping schedule problems in Al-Najaf region groundwater aquifer which are related with the dry areas in the top and bottom layers of the groundwater aquifer and the Euphrates River leakage, it will examine two scenarios in which it is possible to provide a vision for the decision-makers to use both of these sources in an efficient manner that preserves them without causing collateral damage on both of them.

6.5.1 Scenario 1: Reducing the current pumping schedule

It will reduce the current value of the pumping rate 52454 m^3/day until getting a case with no dry area and no river leakage (the Euphrates River does not lose its water into the subsurface aquifer). Visual MODFLOW program will run for each percentage reduction over one year to get a steady state. Results show that at a percentage of reduction of 60% and 40% of the current pumping rate will sustain the groundwater aquifer in the top and bottom layers of the model respectively and in turn will remove the impact of dry areas as it can be seen that in Figure 6.41, which shows the groundwater tables and dry areas after applying various reductions of the current pumping schedule. While the impact on the Euphrates River will be sorted at a percentage of reduction of 35% of the current pumping rate, where the Euphrates River will gain water from the groundwater aquifer if the percentage of reduction becomes greater than this percentage as shown in Figures 6.42 and 6.43.

Figure 6.41 shows the computed groundwater table at the top and bottom layers of the model with various conditions/reductions of pumping rate ratios. The impact of the pumping/extracting the water from the wells caused significant changes in water head around the wells as shown by Figure 6.41. The dry areas in the top and bottom layers of the model have been reduced through decreasing the extraction schedule ratios until the impact of the dry areas is disappeared at a reduction percentage of pumping rate of 60% and 40% respectively.

Top Layer
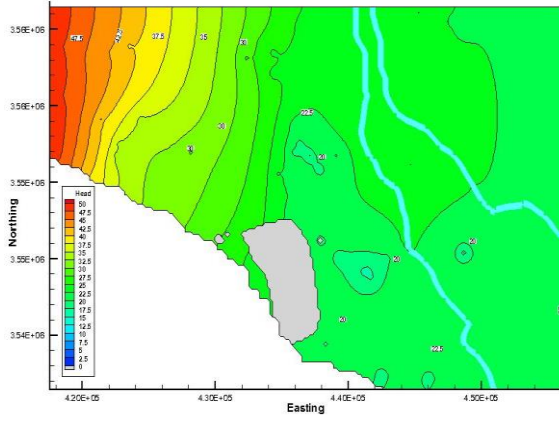
Bottom Layer
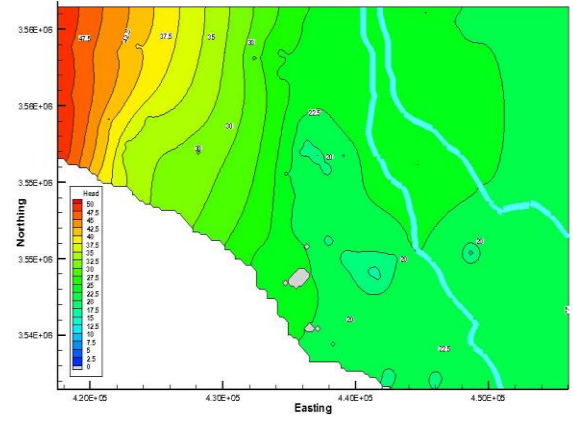
10% - Reduction
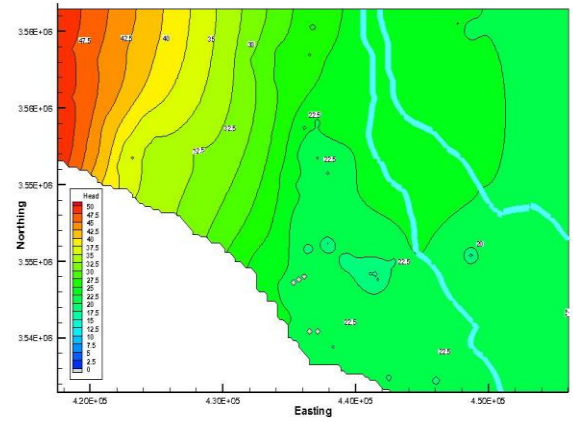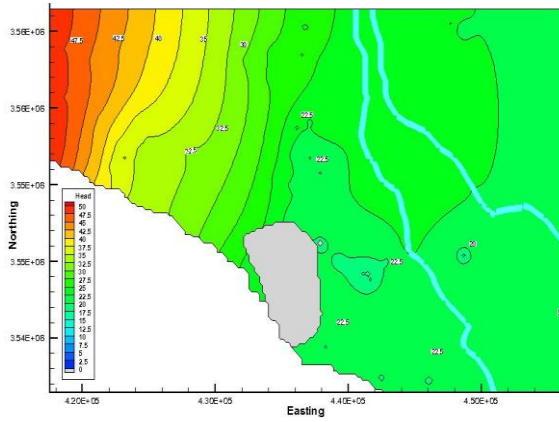
20% - Reduction
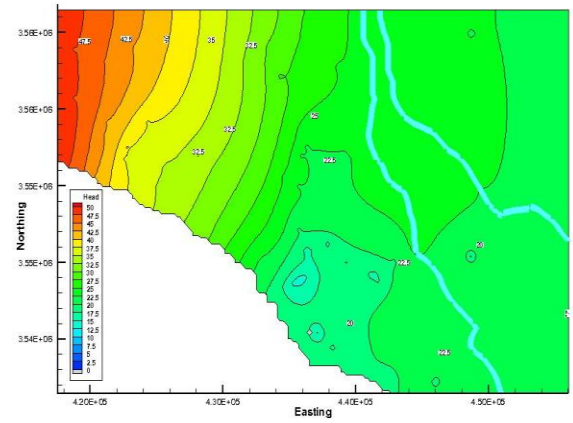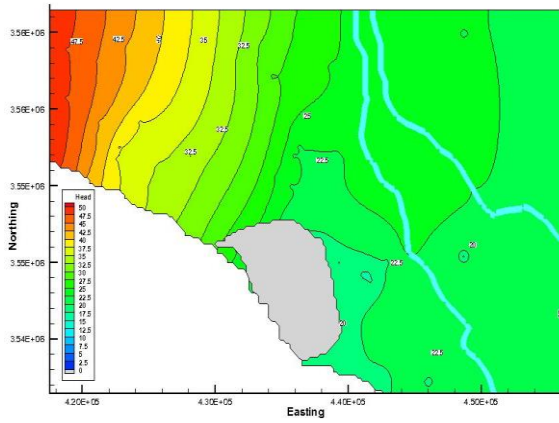
30% - Reduction
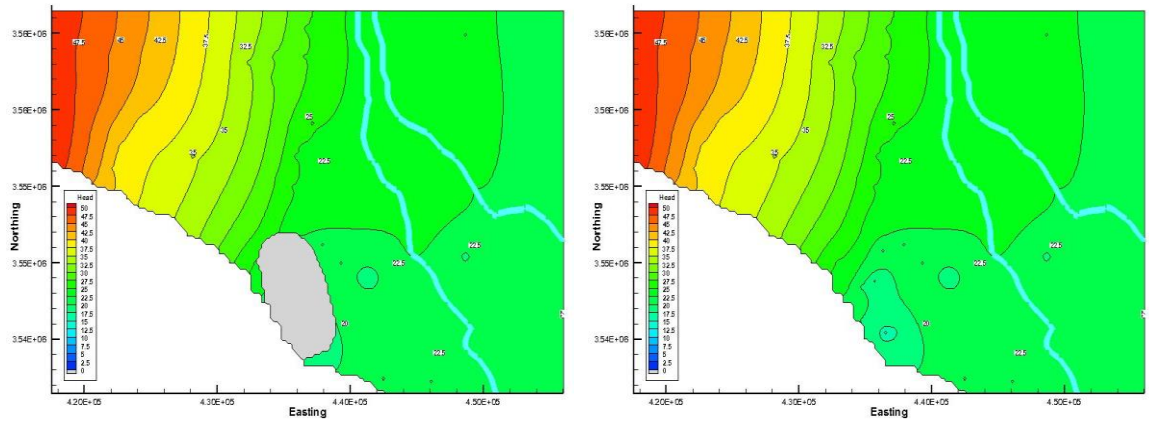
40% - Reduction
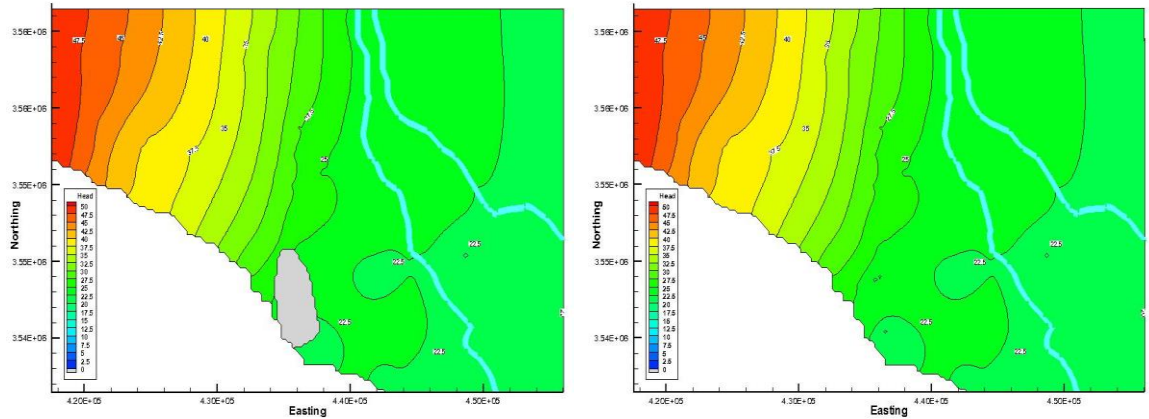
50% - Reduction
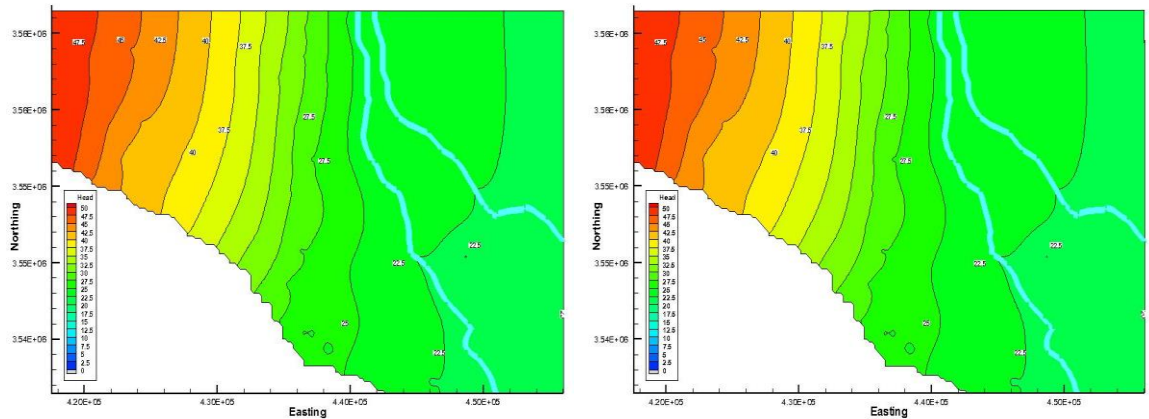
60% - Reduction

Figure 6.41: Computed groundwater table with 16.5 mm/year recharge rate and various pumping rate reduction ratios in the Top and Bottom layers of the model

In respect of the Euphrates River leakage, Figure 6.42 shows the relationship between the pumping rates reduction ratios and the Euphrates River leakage IN and OUT as extracted from the water balance given by Visual MODFLOW. River leakage IN gives the quantity of water which is entering into the groundwater aquifer and leaving the Euphrates River. While river leakage OUT gives the quantity of water which is leaving the groundwater aquifer and entering into the Euphrates River. It can be seen clearly from Figure 6.42 that the decrease of the

quantity of pumping rate leads to converting the Euphrates River from losing river to gaining river when the reduction percentage of the current pumping rate is equal to or exceeding about 35% (intersecting point between the River Leakage IN and OUT) whereas the quantity of water entering the river is more than that which is leaving it by approximately 77 m^3/day. Figure 6.43 shows the relationship between the net leakages of the Euphrates River (OUT-IN) with the decrease in the pumping rate value by various percentages. From Figure 6.43, it can be seen that there is a significant effect for the decrease of the pumping rates ratios when these ratios are 34% or less on the quantities of water leaving the Euphrates River. However, the quantities of water which are leaving the Euphrates River are reduced by a large value to be converted from losing quantities to gaining quantities at a 35% reduction of the current pumping rate or greater than this percentage to add water to the Euphrates River from the groundwater system.
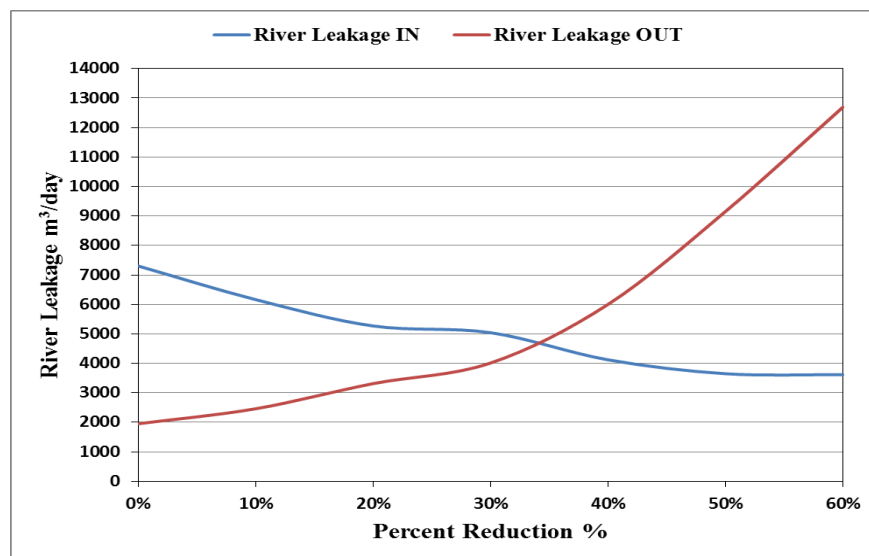
Figure 6.42: The relation between the reduction percentage of the pumping rate and the Euphrates River leakage IN and OUT
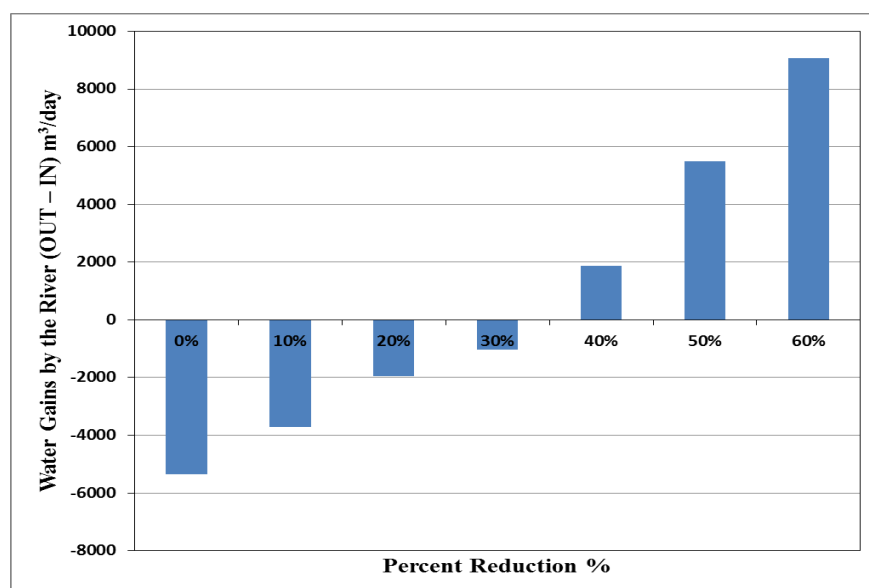
Figure 6.43: The relation between the reduction percentage of the current pumping rate and the net water quantity (OUT-IN) entering the Euphrates River

Briefly, it can be concluded that, pumping schedule needs to be reduced by 60% to remove the impact of extraction represented by the dry area from the top layer of the aquifer and by 40% from the bottom layer, so it needs to make a balance for the withdrawal value of water to secure the aquifer from the dryness. On the other hand, to overcome on the Euphrates River leakage and convert the situation of this river from a losing river to a gaining river, it needs to reduce the pumping schedule to 35% or more.

Eventually, in this Scenario, it is impossible to apply different pumping rate reduction values at the same time to overcome the dry area in the top layer (60%), bottom layer (40%), and (35%) to convert the Euphrates River to become as a gaining river. Therefore, the 60% of pumping rate reduction is possible to overcome all where reducing the pumping schedule to 60% to be (20982 m^3/day) will lead to removing the dry area from the top and bottom layers of the groundwater aquifer and also converting the Euphrates River from a losing river to a gaining river to get 9077 m^3/day.

6.5.2 Scenario 2: Removal of pumping wells

The process of reducing the total pumping rate that was made in Scenario 1 to be 60% for the top layer and 40% for the bottom layer for the purpose of getting rid of the low water table, and, reducing the pumping rate to 35% for the purpose of converting the Euphrates River from the lose water resulted from the large pumping rate, considers as an inefficient and non-useful process. Even more than that, reducing the pumping schedule by 60% to cover all problems remains illogical because the bottom layer does not need this much reduction of the pumping rate and also the river, which needs to reduce the amount of pumping by only 35%.

Therefore, in Scenario 2, it will address the problems of the study area in a sequential manner, i.e., it will address the dry area problem as a first step, and then it will look to the leakage problem of the Euphrates River whether it is already sorted or not to move to the second step which is addressing the Euphrates River leakage problem if it stills affected the Euphrates River.

To address the dry area problem, it is found that when cancelling/removing the wells that affected the groundwater table from the pumping schedule (those wells caused the dry area issue) and relying only on the rest of the pumping wells, this process will get rid of the dry area problem. Therefore, the pumping wells PW20, PW21, PW23, PW30, PW34, PW35, PW36, PW51, PW52, PW55, PW57, PW58, and PW60 are ignored from the pumping schedule and the wells PW25 and PW56 are reduced to be pumped -125 m^3/day and -15 m^3/day instead of -1120

m^3/day and -1129 m^3/day respectively. As a result of that, Figure 6.44 shows the computed groundwater table over the study site after ignoring 13 pumping wells from the pumping schedule and reducing the pumping rate of 2 pumping wells where the groundwater table distribution is the same in the top and bottom layers of the model. In addition, it can be seen from Figure 6.44 that the dry area impact in the study site disappeared after cancelling the wells that affecting the study area to be the total pumping rate equals 38171 m^3/day instead of the current applied pumping rate 52454 m^3/day. After solving the first issue in the study site which is the dry area, then it will be needed to check the Euphrates River leakage, whether it loses its water or acquires water from groundwater aquifer.
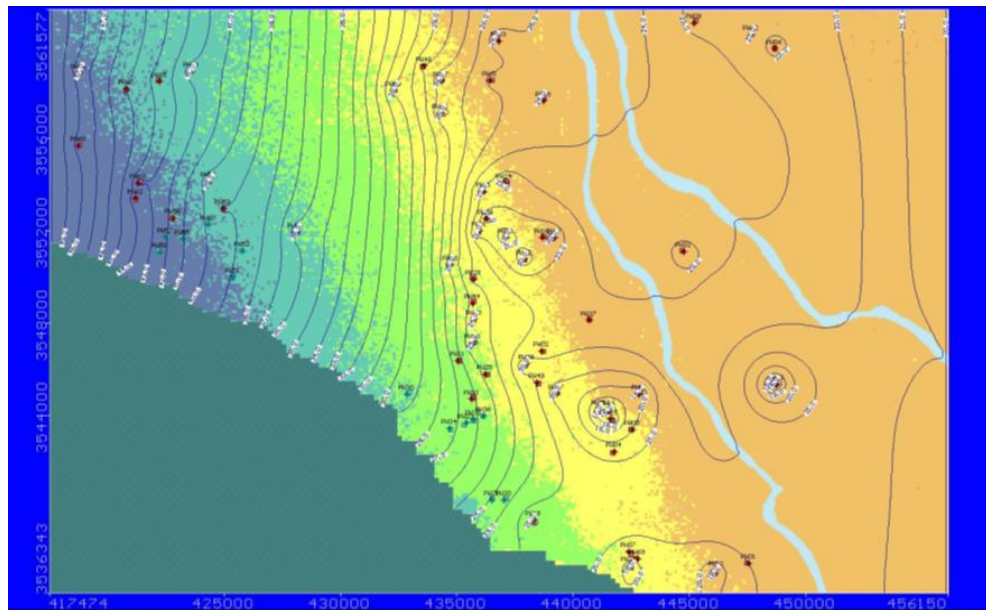
Figure 6.44: Computed groundwater table with 16.5 mm/year recharge rate after ignoring 13 pumping wells from the pumping schedule and reducing the pumping rate of 2 wells

In regarding of the Euphrates River leakage, the water budget results after removing 13 pumping wells and reducing the pumping rate for 2 wells shows that the Euphrates River is losing for a part of its water toward the groundwater aquifer by approximately 3291 m^3/day, which indicates the need to apply the second step. Therefore, in order to overcome the problem of the Euphrates River leakage, it needs to reduce again the value of the pumping rate 38171 m^3/day until converting the river from losing to gaining river. Table 6.2 illustrates the MODFLOW water budget results after running the program over a one year period for each percentage reduction of the pumping rate 38171 m^3/day. Figure 6.45 shows the values of the river leakage IN, OUT, and net (OUT – IN) lost by the Euphrates River for various percentage reduction of the 38171 m^3/day which has been obtained from the first step after removing 13 wells and reducing the pumping rate of 2 wells.

Table 6.2: MODFLOW water budget results for Scenario 2 – step 2 after reducing the pumping rate by some percentage

Percentage Reduction	Pumping Rate m³/day	River Leakage IN m³/day	River Leakage OUT m³/day	River Leakage (OUT – IN) m³/day	Dry Area (Top Layer) Km²	Dry Area (Bottom Layer) Km²
0%	38171	5909	2618	-3291	0	0
5%	36263	5246	3299	-1947	0	0
10%	34354	4747	4161	-586	0	0
15%	32445	4409	5163	754	0	0
20%	30537	4145	6235	2090	0	0
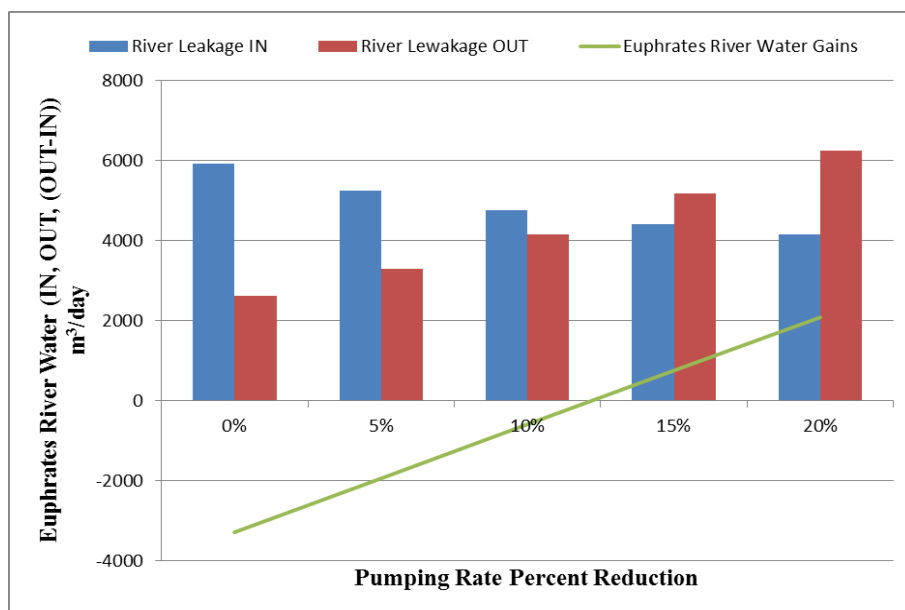
Figure 6.45: The relation between the reduction percentage of the pumping rate and the Euphrates River leakage IN and OUT after ignoring 13 pumping wells from the pumping schedule and reducing the pumping rate of 2 wells

From Figure 6.45, at the percentage reduction of 13%, the Euphrates River state is converted to a gaining river and becomes gaining water from the groundwater aquifer by approximately 225 m³/day when the pumping rate reduces to 33209 m³/day. Indeed, to be in the safe side, in the future, if it needs to dig a new pumping well somewhere or increasing the pumping schedule 33209 m³/day from the current reduced pumping wells (second step), it should be ensured that the Euphrates River will never lose its water into the subsurface aquifer. Where the Euphrates River gaining quantity 225 m³/day is very little as any increase in the pumping schedule 33209 m³/day will lead to changing the situation of the Euphrates River back to the losing river state. Consequently, it should be always making the Euphrates River gaining water from the groundwater aquifer by more than 2000 m³/day. Therefore, reducing the pumping rate to 20% to be 30537 m³/day results in making the Euphrates River gaining water by 2090 m³/day as it is

illustrated in Table 6.2. The value of the pumping rate 30537 m³/day does not affect the study area in terms of declining the groundwater table (appearing the dry area) or making the Euphrates River losing for its water.

Now, the obtained pumping rate of the 20% reduction of the 38171 m³/day value 30537 m³/day represents about 58% of the current required pumping rate 52454 m³/day without having any impact either on the groundwater aquifer or the Euphrates River as compared with the 60% reduction of Scenario 1 which was 20982 m³/day. Table 6.3 illustrates the final reduction percentage for each pumping well with the pumping rate value that should be pumped from each well in the future to keep the study area far from appearing the problem of the dry area or losing the Euphrates River for its water.

Table 6.3: The new daily pumping rate for the pumping wells in the Al-Najaf region

Well No.	Well Name	Current Pumping Rate m³/day	Reduction Percentage	New Pumping Rate m³/day
1	PW01	0	20%	0
2	PW02	0	20%	0
3	PW03	-785	20%	-628
4	PW04	0	20%	0
5	PW05	0	20%	0
6	PW06	-860	20%	-688
7	PW07	0	20%	0
8	PW08	0	20%	0
9	PW09	-750	20%	-600
10	PW10	0	20%	0
11	PW11	0	20%	0
12	PW12	-1020	20%	-816
13	PW13	-3256	20%	-2605
14	PW14	-977	20%	-782
15	PW15	-940	20%	-752
16	PW16	-1029	20%	-823
17	PW17	-1085	20%	-868
18	PW18	-800	20%	-640
19	PW19	-940	20%	-752
20	PW20	-840	Cancelled	0
21	PW21	-1100	Cancelled	0
22	PW22	-912	20%	-730

Well No.	Well Name	Current Pumping Rate m³/day	Reduction Percentage	New Pumping Rate m³/day
23	PW23	-760	Cancelled	0
24	PW24	-1020	20%	-816
25	PW25	-1120-125	20% of -125	-100
26	PW26	-985	20%	-788
27	PW27	-645	20%	-516
28	PW28	-435	20%	-348
29	PW29	-870	20%	-696
30	PW30	-1153	Cancelled	0
31	PW31	-746	20%	-597
32	PW32	-442	20%	-354
33	PW33	-640	20%	-512
34	PW34	-800	Cancelled	0
35	PW35	-1140	Cancelled	0
36	PW36	-921	Cancelled	0
37	PW37	0	20%	0
38	PW38	-355	20%	-284
39	PW39	-742	20%	-594
40	PW40	-840	20%	-672
41	PW41	-873	20%	-698
42	PW42	-302	20%	-242
43	PW43	-540	20%	-432
44	PW44	0	20%	0
45	PW45	-470	20%	-376
46	PW46	-942	20%	-754
47	PW47	-793	20%	-634
48	PW48	-622	20%	-498
49	PW49	0	20%	0
50	PW50	-1185	20%	-948
51	PW51	-924	Cancelled	0
52	PW52	-1030	Cancelled	0
53	PW53	-1200	20%	-960
54	PW54	-1010	20%	-808
55	PW55	-976	Cancelled	0
56	PW56	-1129-15	20% 0f -15	-12

Well No.	Well Name	Current Pumping Rate m^3/day	Reduction Percentage	New Pumping Rate m^3/day
57	PW57	-837	Cancelled	0
58	PW58	-1043	Cancelled	0
59	PW59	-866	20%	-693
60	PW60	-650	Cancelled	0
61	PW61	-470	20%	-376
62	PW62	-869	20%	-695
63	PW63	-992	20%	-794
64	PW64	-1163	20%	-930
65	PW65	-1089	20%	-871
66	PW66	-1197	20%	-958
67	PW67	-1152	20%	-922
68	PW68	-1222	20%	-978
69	PW69	0	20%	0
Sum				**30537**

The results obtained in Scenarios 1 and 2 show the management process of the groundwater reservoir in Al-Najaf region. Scenario 2 gave more acceptable results than Scenario 1. In Scenario 1, the total amount of the current pumping rate installed on the study site is reduced by 60% to become 20982 m^3/day, as this is insufficient and impractical because the problems of drought (dry area) and the Euphrates River leakage will always appear if the pumping quantity is increased even with a little percentage greater than 20982 m^3/day. While in Scenario 2, these wells which were the main cause of the dryness of the layers of the model and the loss of the Euphrates River for its water are removed. Where, removing 13 pumping wells with their impact on the aquifer, reducing the pumping rate of two wells, and maintaining/keeping the current pumping amounts of the other pumping wells with a reduction of 20% of their pumping rates (54 wells) will maintain the sustainability and durability of the aquifer. Therefore, Scenario 2 represents the optimum and the best one that should the decision-makers commitment it in order to sustain Al-Najaf region Dibdibba groundwater aquifer.

6.6 Development areas in Al-Najaf region

In 2013, the number of pumping wells which were supplied water for the Al-Najaf region and the surrounding areas was 56 wells as it can be seen in Figure 6.46. This number has been increased to become 69 wells in 2014 and these wells were spread on the west and east sides of

the study area. This means that in the year 2014, 13 pumping wells only are injected into the area of study where it can be seen the locations of these 13 wells in Figure 6.47.
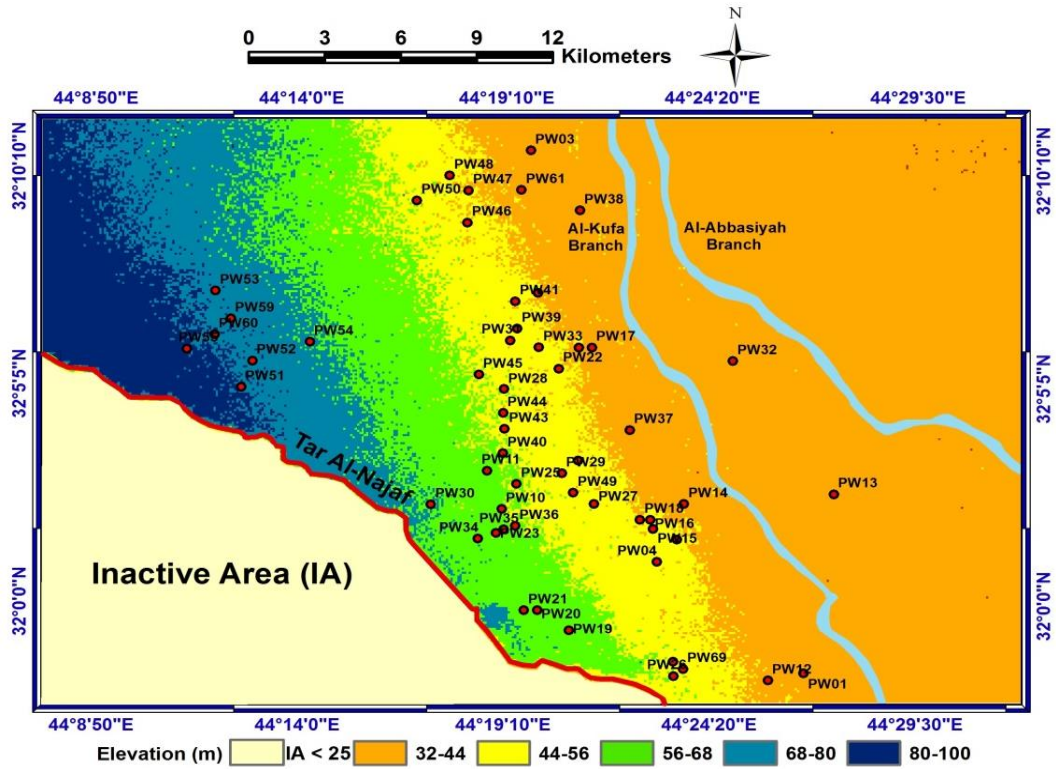
Figure 6.46: Locations of the 56 wells in the year 2013
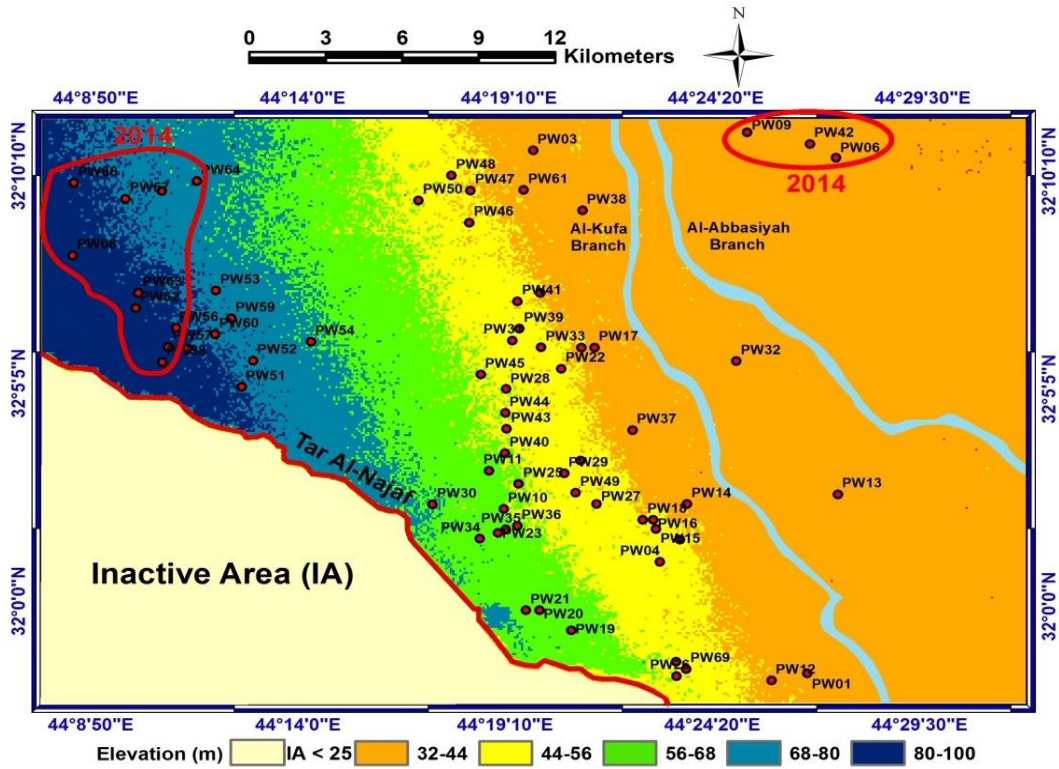
Figure 6.47: Locations of the new 13 wells in the year 2014 as well as the 56 wells in the

From Figure 6.47, it can be seen that the new 13 injected pumping wells are on the west and east sides of the study area, so it can consider that the areas on the west and east sides of the study site and so on as the development areas as shown in Figure 6.48. The purpose of knowing the development areas is to study the effect of injection new pumping wells for the agricultural purposes in these areas and to provide a map for the right locations of the scheduled pumping wells which should be injected in the future through exploring the impacts of the new injected wells in these new locations on the groundwater aquifer and the Euphrates River.
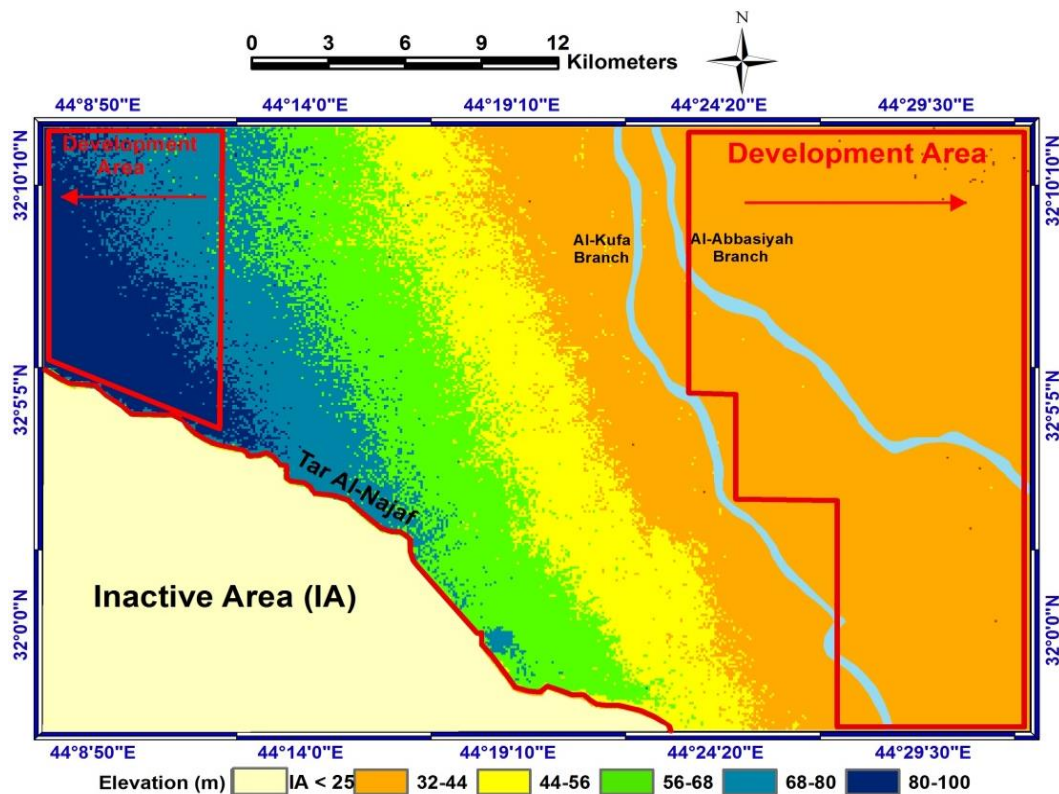
Figure 6.48: Locations of the development areas in the study site

6.7 Getting the current annual daily pumping schedule

As the development areas in the study area are known and these areas are on the west and east sides of the study area model. Now, it needs to provide the reduced quantity 21917 m^3/day, which has been reduced from current annual daily pumping rate 52454 m^3/day to become 30537 m^3/day in Scenario 2 after ignoring 13 pumping wells from the pumping schedule and reducing the pumping rate of 2 wells to become the total pumping wells equal 56 wells.

Therefore, it will study how can get the current annual daily pumping rate without affecting the study area in terms of appearing the dry area or losing water from the Euphrates River. It is already having a pumping rate equals to 30537 m^3/day obtained from the 56 wells in Scenario 2 shown in Table 6.3. Where some new pumping wells will be added or injected in the study area

in the satisfying and development areas to pump the rest quantity of the current pumping rate which is approximately equal to 22000 m³/day. In order to get this quantity of water from the groundwater aquifer system, 11 pumping wells are added to the study site (5 of them on the far west, 6 of them on the top far east (divided into two groups of 3 wells)). The vertical distance between each of the 11 pumping wells equals to 0.6 km and the pumping rate for each equals to 2000 m³/day as shown in Figure 6.49, where these distances are identified to keep each well far from the effect coming from the wells around.
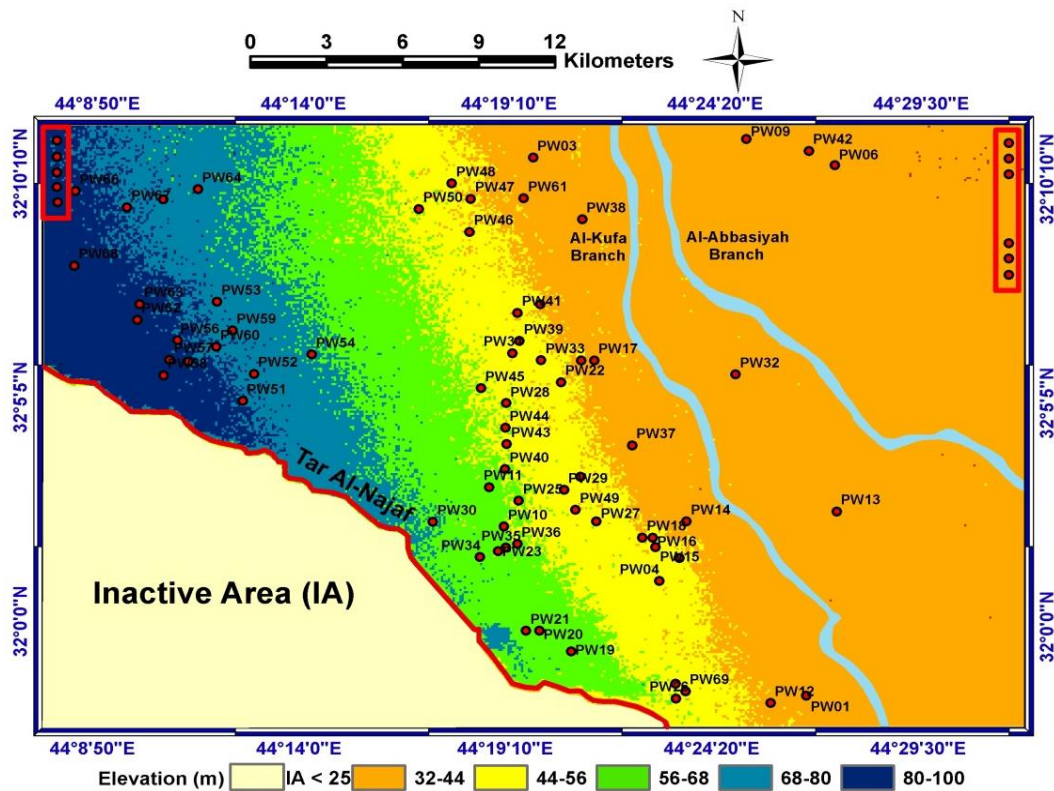
Figure 6.49: Location of the new 11 pumping wells added in Al-Najaf region Model

Visual MODFLOW model is run for a steady state condition over a period of one year with a recharge rate of 16.5 mm/year for the case when there are 56 pumping wells with a total pumping rate equals to 30537 m³/day and the new 11 pumping wells that having a pumping rate equals to 22000 m³/day to be the total pumping rate from all the 67 wells equals to 52537 m³/day. The results are shown in Figure 6.50 which represents the computed groundwater table for 67 pumping wells and in Table 6.4 which represents the water zone budget results.

It is obvious from Figure 6.50 that there is no dry area resulted from the impact of the pumping schedule on the groundwater system in the study site. This means that there is no stress applied to the study area from the extraction process even when the pumping rate is equal to 52537 m³/day as compared with the previous situation shown in Figure 6.1 (the Distributed Value Property Zones model). The water zone budget results illustrated in Table 6.4 shows that the

quantity of water leaving the groundwater system toward the Euphrates River (the Euphrates River Leakage OUT) is greater than the quantity of water leaving the Euphrates River toward the groundwater system (the Euphrates River Leakage IN) by 1512 m^3/day. In addition, it can be seen from Table 6.4 that there is no dry area in the top or bottom layers of groundwater model resulted from the pumping schedule.
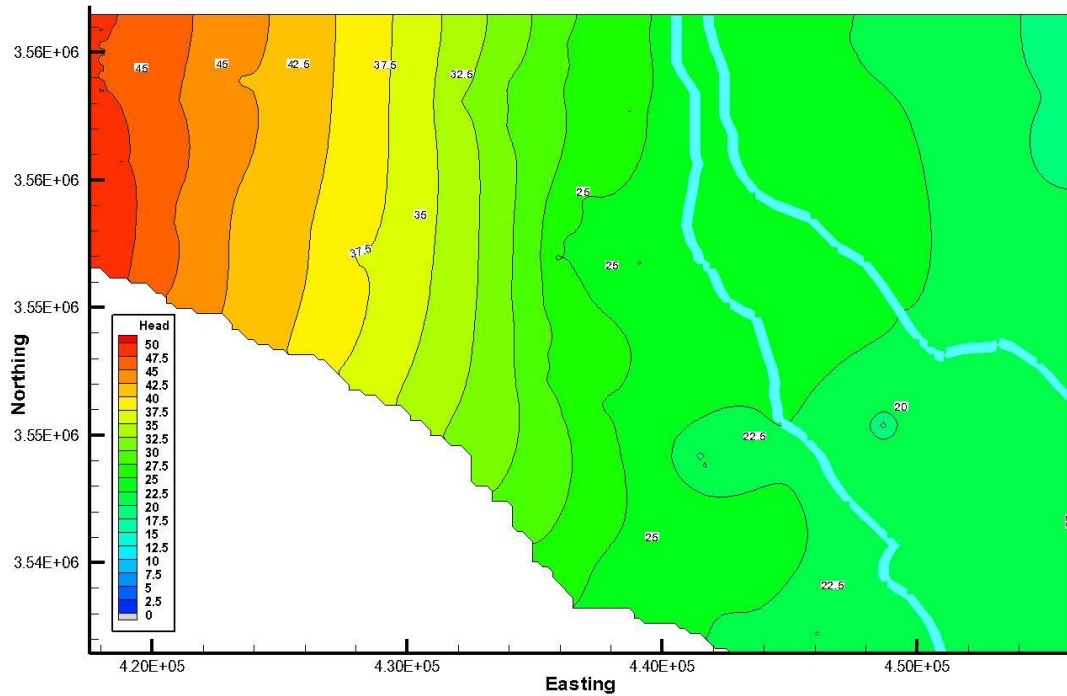
Figure 6.50: Computed groundwater table resulted from Visual MODFLOW for 67 pumping wells

Table 6.4: Water zone budget resulted from Visual MODFLOW for the 67 pumping wells

Total Pumping Rate Required m^3/day	Total Pumping Rate Pumped m^3/day	Euphrates River Leakage IN m^3/day	Euphrates River Leakage OUT m^3/day	Euphrates River Leakage OUT – IN m^3/day	Dry Area Top Layer km^2	Dry Area Bottom Layer km^2
52454	52537	4231	5743	1512	0	0

Eventually, running Visual MODFLOW program with the current situation gives perfect results whereas all the pumping rate required is pumped, no dry area resulted from the impact of the pumping process, and the Euphrates River is gaining water by approximately 1512 m^3/day as this means that it can be considered the Euphrates River as a gaining river.

6.8 Future plan for Al-Najaf region

According to the results mentioned in part 6.7, digging pumping wells in the development areas will give an excellent result through supplying all the required pumping schedule with no dry area and without losing water from the Euphrates River. In addition, the Euphrates River will gain water from the groundwater system although the pumping wells are in-operation. Therefore, in this section, it will add another 9 pumping wells in the study area (2 of them on the far west, 3 of them on the far mid east, and 4 of them on the far bottom east). The vertical distance between each of the 9 pumping wells equals to 0.6 km and the pumping rate for each equals to 2000 m^3/day as shown in Figure 6.51. Again these distances are considered into account to keep each well far from the effect which comes from the other wells around. These 9 pumping wells will be injected in the development areas in order to keep the study area far from the impact of the pumping schedule which may result in declining the groundwater table (forming a dry area) or losing the Euphrates River water.

The total number of pumping wells will be 67 pumping wells with a pumping rate of 52537 m^3/day and 9 pumping wells with a pumping rate of 18000 m^3/day to be the total equals to 70537 m^3/day as shown in Figure 6.51.
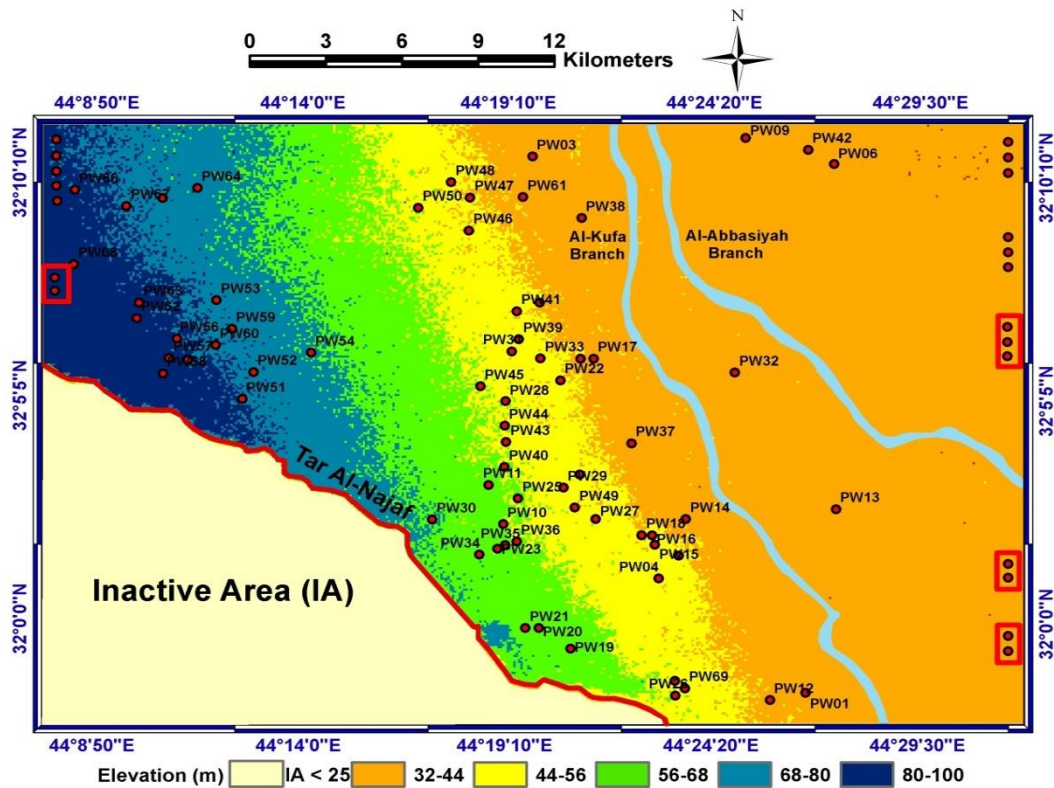
Figure 6.51: Location of the new 9 pumping wells added in Al-Najaf province study area

The Visual MODFLOW program is run with a steady state condition over a period of one year with a recharge value of 16.5 mm/year. The results are shown in Figure 6.52 and Table 6.5.

Figure 6.52 shows the computed groundwater table pattern after applying a value of a pumping rate equals to 70537 m^3/day which means by an increment value equal to approximately 34.32% of the current pumping rate of 52454 m^3/day. It can be seen from Figure 6.52 that there is no effect on the study area in respect of forming a dry area or losing the Euphrates River for its water. Moreover, as shown in Table 6.5 which represents the Visual MODFLOW water zone budget results, the required pumping rate pumped from the 76 wells is completely pumped with the acquisition of the Euphrates River on an amount of water estimated by 595 m^3/day.
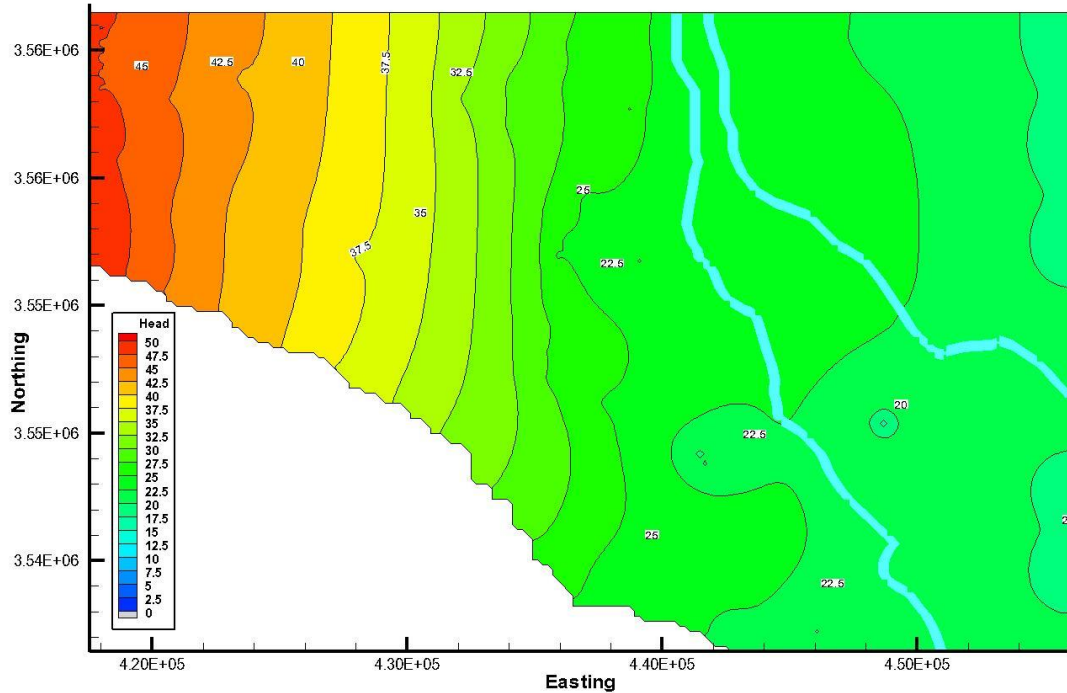
Figure 6.52: Computed groundwater table resulted from Visual MODFLOW for 76 pumping wells

Table 6.5: Water zone budget resulted from Visual MODFLOW for the 76 pumping wells

Total Pumping Rate Required m^3/day	Total Pumping Rate Pumped m^3/day	Euphrates River Leakage IN m^3/day	Euphrates River Leakage OUT m^3/day	Euphrates River Leakage OUT – IN m^3/day	Dry Area Top Layer km^2	Dry Area Bottom Layer km^2
70537	70537	4609	5204	595	0	0

6.9 Keys for decision-makers for sustainable management

Ultimately the decision-makers in Al-Najaf province should understand the seriousness of the current situation on the groundwater aquifer and the Euphrates River and work real and very hard to maintain the continuity of these sources for the future uses. Where, these sources are crucial resources for the irrigation and agricultural processes, economic processes, and domestic

uses, particularly at the present time of Al-Najaf region which suffers from the scarcity of water for all purposes. So, it should apply any advice to secure these sources for the purpose of the sustainability and durability.

The management process shows that Scenario 2 is the best and practical one to apply. Where, because there are some pumping wells are already injected in the wrong places without knowing that these locations will affect both the groundwater aquifer and the Euphrates River, so it needs to remove these wells to get rid of their effects. Generally, adding a pumping well at any place of an area should be located carefully with a precise study for its impact on the surrounding features and boundaries and an accurate estimation for the designed and operated amount of pumping that should not be exceeded by the users. Removing or cancelling 13 pumping wells, reducing the pumping rate for 2 wells, and reducing the pumping rate of the remaining 54 wells by 20% lead to keeping the groundwater aquifer and the Euphrates River far from the declining in the groundwater table and the leakage from the Euphrates River respectively, but if the pumping process is increased again, the problems will come over again. Therefore, in the future, any increment of that pumping schedule identified in Scenario 2 or any new pumping well needs to be injected somewhere in the study area should follow the keys obtained from the current research results which are:

1. The decision-makers in Al-Najaf province should follow the results illustrated in Scenario 2 in this research to manage Dibdibba aquifer to be more sustainable and durable under the future uses and also taking the future impacts of the future predicted cases seriously in their attention to success the management process.

2. Checking the location of the new pumping wells where it should be in the satisfying locations or in the development places which are identified in the current research because these areas do not have a great impact on the groundwater system and the Euphrates River leakage.

3. The pumping rate 30537 m^3/day which is obtained from Scenario 2 (the 56 pumping wells) in this research is suitable to overcome the dryness in the study area and the Euphrates River exodus, but it may need to reduce this extraction when adding a new pumping well. Where it needs to check the dryness and river leakage again after being all the pumping wells are in-operation.

4. Do not add any pumping well close to the Euphrates River because this well will reduce the water gaining by the river to the least value, and not in the middle lower location of the study area because the top elevation of the bottom layer is very high and close to the

groundwater table where any pumping rate in this location even it was very little will lead to appearing a dry area in the top layer.

6.10 Summary

A groundwater model has been built for Al-Najaf region, Iraq by using Visual MODFLOW. To obtain the best model which can represent the study site, three approaches are explored, Manual Trial and Error (the Forward Model), Automatic Trial and Error which known as PEST (the PEST Model), and Distributed Value Property Zones (the Distributed Value Property Zones Model). Results show that the third approach gives the best results. In addition, the effect of the real field representation of the groundwater aquifer is studied where, as Al-Najaf region groundwater aquifer contains an interface separating the two soil layers, sometimes this interface is neglected by modellers and considered an aquifer with one unconfined layer only. Comparing the results obtained from the single layer-one aquifer and two layers-one aquifer groundwater models with each other show various responses for the applied impact of extractions, sensitivity behaviour, and calibration results. Therefore, this enhances how important the existence of the interface in the conceptualisation process of the groundwater models in case of those interfaces are existing in the real field to be the constructed model as close as to the reality, especially as groundwater models are originally adopted to explore/predict the behaviour of the aquifer for the current and future climate impacts.

The current situation of Al-Najaf region is affected greatly by the exerted pumping schedule, which led to adding a significant impact on the groundwater aquifer and the Euphrates River. As a foreseeable future action, the effect of reducing of various parameters (recharge rate, groundwater level on the western side of the study area, and the Euphrates River level) on both the groundwater aquifer and the Euphrates River leakage is studied in 8 cases when the current pumping rate is constant (Cases 1, 2, and 3) and when it is increased up to 50% (Cases 4, 5, 6, 7, and 8) to anticipate the effect that will occur and prepare the kit to avoid those damages in advance. Overall, it is noticed that the decrease in one parameter, which is the recharge rate (Cases 1, and 5) or all parameters (Cases 3, and 8) has the greatest effects either on the study site or the Euphrates River leakage as compared with the reduction impact coming from the other parameters/cases (the western groundwater level and the Euphrates River level). In addition, increasing pumping quantities from the groundwater aquifer have also affected the study site and the Euphrates River leakage greatly.

To manage/solve the current problem in Al-Najaf region, two scenarios have been applied/studied, where it is found that Scenario 2 is the best. In this scenario, some pumping

wells are removed and some others are reduced of their pumping rates, while 54 wells are still pumping the current extractions to overcome the dryness problem. Then all of the pumping wells are reduced by 20% to overcome the Euphrates River leakage. More than that, this research study how can provide an extra pumping water for the future development need that can be used for various purposes as well as proving sites that can provide water without any side effects either on the groundwater aquifer or on the Euphrates River.

Installing pumping wells on the far west or far east (top or bottom) of the study site (the development areas) will keep the groundwater aquifer in Al-Najaf region far from declining the groundwater level and this will, in turn, keep the groundwater aquifer from the dryness and also keep the Euphrates River from declining its level and losing its flowing water. Finally, some important keys for the decision-makers are established to know how can control the groundwater aquifer as well as the Euphrates River in Al-Najaf region to be sustainable and durable as well as to control the connection between the surface water represented by the Euphrates River and the groundwater system available in Al-Najaf City and the surrounding area.

Chapter Seven

Conclusions and Recommendations

7.1 Conclusions

Al-Najaf region, which is located in the south-west of Iraq, is considered to be the study area in this research. The groundwater aquifer based in this region is called Dibdibba aquifer. The main source for Al-Najaf region groundwater aquifer comes from the surface water represented by the Euphrates River and the precipitation as the decline in both of these sources will negatively influence on the amount of water available in Dibdibba aquifer. The study area has 69 pumping wells installed in the region with a total pumping of 52454 m^3/day.

The conceptual model is built using the geologic and hydrogeologic conditions collected for the region, together with the Digital Elevation Model (DEM) data. The spatial interpolation for the hydraulic conductivities of 60 wells is applied on the study site by using the "Distributed Value Property Zones" approach, where this approach has resulted in the best model with the best representation of Dibdibba subsurface soils. The computer model is also implemented with the distributions of 69 pumping wells in the area and with the steady pro-defined hydraulic head along its boundaries.

The model is applied with the recharge rate of 16.5 mm/year, where the model is calibrated with the measured hydraulic heads at the locations of 69 wells in the domain. The model is calibrated both statically and dynamically. The dynamic calibration has shown a better corresponding to the field observations as compared with the static calibration.

From this study, the following conclusions can be drawn:

1. The value of the recharge rate 40.32 mm/year, which is calculated for the collected data over the period 1980-2014, is found to be too high when it is applied to the study area because it has flooded it and given overestimated calculated heads as compared to the observations. Whereas, since the calculated recharge is regarded as the potential recharge, and in reality the study area has never been found to be flooded in the past, rather suffered from the water scarcity due to the high temperature leading to high evaporation, the over-estimate might be due to the inaccuracy in data collection such as soil moisture values. Therefore, the recharge rate value has been reduced to meet the observation heads data through the calibration process. Sensitivity analysis is also carried out, and it is found that

the model is sensitive to recharge rate, particularly when the rate is greater than (16.5 mm/year). Hydraulic conductivity is also found to affect the results significantly. Therefore, the hydraulic conductivity from the measurements at the locations of wells is interpolated for model use by using Kriging method with the best Variogram.

2. The novel approach "Distributed Value Property Zones" that is integrated within Visual MODFLOW is used in this study for interpolating the subsurface domain of hydraulic conductivity. This approach has greatly improved Al-Najaf region model as compared with the traditional approaches which are the Manual and Automated approaches. The results from the present model shows that the study area (Dibdibba groundwater aquifer) is suffering from the dryness in the top and bottom layers of the constructed model (appearing dry areas) due to the impact of the excessive extractions (52454 m^3/day). This leads to declining the groundwater tables. The dry area resulting from the Distributed Value Property Zones Model as compared with those Forward Model (Manual hydraulic conductivity approach) and the PEST Model (Parameter ESTimation approach) are found to be much lower than those dry areas that resulted from these models. The Distributed Value Property Zones Approach improves the calibration process where the results of the calculated heads are now more consistent with the field observations for this model. In addition, it is found that the Euphrates River is also suffering from the excessive extractions where it loses some of its water toward the groundwater aquifer to compensate the shortage of the pumping's supplied quantity.

3. Another novelty is represented by exploring the impact of the interface soil layer. Usually, groundwater researchers have neglected the conceptualisation of the interface soil layer, especially when this interface is located within the aquifer soil layers. The Dibdibba aquifer in Al-Najaf region has two soil types that are separated by an interface soil layer. It is found that the interface soil layer located between the two soil types of Dibdibba aquifer has also affected the results of Al-Najaf region aquifer. When Dibdibba aquifer is modelled as a one layer, the dry area and the Euphrates River leakage resulted from Visual MODFLOW have shown different values to those when the interface soil layer is modelled within Al-Najaf region model with two soil layers, as illustrated in detail in Section 6.3. In addition, a comparison is made for the calculated heads that result from the calibration process for the Distributed Value Property Zones Model when the interface soil layer is modelled and the same model without an interface soil layer after recalculating the model's heads. It is found different results of the calculated heads for that model without interface soil layer, which makes that calibrated model has unacceptable calculated heads for an extent and this in turn will affect the model acceptability. Therefore, the real conceptualisation for field domain is

crucial to be the current and forecasted behaviours of the aquifer are correct and can be considered by decision-makers for successful sustainability and management.

4. It is found that there is no connection between the Euphrates River and the groundwater aquifers on the Western Sahara, where the connection is only with the groundwater aquifer close to the Euphrates River which is Dibdibba aquifer. Consequently, the western lower part of Al-Najaf region model is not considered in the conceptualised model area and it is assigned as inactive area.

5. According to the hydrogeological map, the general flow pattern is from the west to east in the study area where this agrees well with the revealed model results, the observations, and the gradient of the ground surface. It is found that with the current operational pumping rates in the area, a dry area is resulted in the lower central part of Al-Najaf City (adjacent to Tar Al-Najaf cliff) and its surrounding area due to the large quantity of groundwater being withdrawn. The computed water balance with the current operational pumping schedule shows that the Euphrates River supplies water into the groundwater at approximately 5354 m^3/day, instead of gaining water of 23527 m^3/day from the groundwater if there is no pumping from the wells. In addition, the current pumping schedule leads to declining the groundwater tables significantly and this led to dry areas appearing in the top and bottom layers of the model, equal to 39 km^2 and 1.32 km^2, respectively. For the future predictions when it needs to increase the current pumping schedule from 10% up to 50% with a 10% increasing increment, it is found that the study site will suffer more from the dryness in both of its layers (i.e. the top and bottom layers). Where the maximum dry areas in the top and bottom layers of the model will happen at the 50% (63.48 km^2-Case 4) and 30% (52.32 km^2-Case 4) increments of the current pumping rate, respectively. The maximum quantity of water lost by the Euphrates River will be 7020 m^3/day for Case 4 at a 10% increment of the current pumping rate.

6. The impact of reduction of varies parameters are studied in this research for the purpose of forecasting the future aquifer behaviour, such as reducing the recharge rate of 16.5 mm/year either by 25% or 50%, or reducing the western constant head to 45m, or reducing the Euphrates River level by either 0.5m or 1m, or reducing all of these parameters together. The reduction in all of these parameters either reduced individually or all together is explored (i) with the current pumping schedule of 52454 m^3/day and (ii) when increasing the current pumping schedule by 10% up to 50%. Eight cases are investigated to assess the impact of reducing of these parameters. The conclusion of those eight cases are:

a. With the current pumping schedule and when increasing the current pumping schedule by up to 50%, there is a crucial and critical impact on the groundwater aquifer resulting from reducing the recharge rate (either by 25% or 50%) or the western constant head value to be 45m individually or both together at the same time on the groundwater heads. These two parameters will significantly decline the equipotential head levels over the study site and this will lead to dry areas appearing in the top and bottom layers of the aquifer as well as losing huge quantities from the Euphrates River's water into the subsurface (Dibdibba) aquifer. In the same context, appearing dry areas in the study area indicate that these regions cannot provide the required/applied pumping rate and this will lead to stopping some pumping wells from pumping water. Those stopped wells are resulting from the over-designing pumping process applied on those wells.

b. With either the current pumping schedule or when increasing the pumping schedule from 10% up to 50%, the reduction in the Euphrates River level by either 0.5m or 1m does not have a significant impact on the groundwater aquifer. Meanwhile, reducing the river level leads to a slight change in the computed groundwater heads over the study area. However, it could have an effect on the river leakage because the river leakage depends upon the difference of the groundwater-river levels as well as the actual pumped water from the groundwater aquifer.

c. In respect of the pumping rate, with the current required pumping schedule or with those extra pumping rates (up to 50% increase of the current schedule), all the predicted cases do not supply the required pumping rate by a complete quantity because of the over-pumping and dry areas problems where this means that there are some pumping wells are stopped to pump water due to the over-pumping problem. Therefore, the actual pumped water does not satisfy the current needs of Al-Najaf region so the groundwater aquifer compensates for a part of the missed water from the Euphrates River and this will affect the groundwater-surface water sources interaction.

7. For the purpose of sustainable management of water resources in the region to control the current problem of the groundwater aquifer in Al-Najaf region in terms of appearing dry areas in the top and bottom layers of the aquifer (water table decline) and seeping water from the Euphrates River into the aquifer, two scenarios are explored. This research shows the following:

a. In addition to the removal of those wells that affect the aquifer (13 wells), it is found that the current pumping schedule pumped by the other wells (56 wells) needs to be reduced by approximately 20% to keep the groundwater head over the study area within

the sustainable head and control on the Euphrates River's water without losing it toward the subsurface source (i.e. the groundwater aquifer).

b. It needs to cancel/remove some of the pumping wells in the lower middle and lower west regions of the study area which are affecting the groundwater heads even if these wells are having small quantities of pumping rates. In addition, cancelling/removing those pumping wells which are very close to the Euphrates River will help in keeping the quantity of water lost by the Euphrates River toward the groundwater. Where those wells are always taking for a part of the Euphrates River's water through the actual pumped water supplied by the aquifer.

c. The future development within the study area should be restricted in the development areas, which are specified in this research and located on the far east or far west as these regions have no big impact (sometimes rare) on the groundwater head and the Euphrates River leakage.

d. To compensate for the current reduced pumping schedule or to pump extra water from the aquifer for future agricultural, economical, or domestic use developments, new pumping wells may need to be dug. Where, it is found that digging or injecting new pumping wells in the development areas which are specified in the current research will be the only choice for decision-makers in Al-Najaf province to keep the Euphrates River-groundwater interaction as far away as possible from the external effect. In addition, these areas have high levels of groundwater table and can provide more water for the pumping schedule without affecting the groundwater levels in the middle regions and will also keep the Euphrates River away from the pumping schedule impact.

7.2 Recommendations

This study has achieved all the significant issues found in Al-Najaf region, such as the dry areas problem, the seepage from the Euphrates River, and the problem of the non-scientific and unstudied pumping schedule, which has been affected both groundwater and surface water resources. Despite this achievement, this research can be further improved by considering the following, which are not fully implemented in this study, particularly there are many aquifers in Al-Najaf province carrying large quantities of groundwater in their formations. The further improvements can be made with the following recommendations:

7.2.1 Recommendations for water management in the study area

1. Using the other aquifers in the province of Al-Najaf (Injana formation, Fat'ha formation, Euphrates formation, and Dammam formation) for the purpose of participating in providing the needed water to reduce the impact on the aquifer used now (Dibdibba formation). This will positively affect the level and quantity of water of the Euphrates River when reducing the usage of its water.

2. Drilling more observation wells distributed over the whole area to cover all aquifers of Al-Najaf region could significantly improve the model calibration both in short and long terms as well as to explore the groundwater levels in the short and long terms for the purpose of taking the advantage of these wells to know the influences that affected groundwater levels. In addition, through these wells will provide the groundwater database which will provide the ability to run the current model and any future groundwater model by a transient flow.

3. All aquifers in the province of Al-Najaf should be continuously monitored to maintain the durability of this water resource for future uses, particularly Al-Najaf province and those provinces located southern of Iraq and depend on the Euphrates River water. Where due to the severe suffering of the harsh climatic conditions (temperature increase, high evaporation, and low rainfall) which are likely to be worse in the future, but it will remain need to use the groundwater resources available/located in the lower soil layers, even when these quantities of water are few or limited due to the climate change effect.

7.2.2 Recommendations for future work

1. Indicating and identifying the agricultural land-use where pumping wells are needed would significantly help in warding the potential risk to the aquifer and providing a future vision helps in the sustainability of this resource. So, it must be chosen the sites of these wells as well as the pumping quantities more carefully to keep the aquifer safe from impacts through maintaining the groundwater durability in the aquifer and keep the impact far from the surface water levels represented by the Euphrates River.

2. Continuously monitoring of groundwater levels in all aquifers in the province of Al-Najaf for the purpose of maintaining the durability of that water resource for future uses particularly Al-Najaf province and those provinces located southern of Iraq and depended on the Euphrates River water. Where due to the severe suffering of the harsh climatic conditions (temperature increase, high evaporation, and low rainfall) which are likely to be worse in the future, but it will remain need to use the groundwater resources

available/located in the lower soil layers, even when these quantities of water are few or limited due to the climate change effect.

3. Including the water quality for the aquifers in Al-Najaf province chemically and physically to investigate its suitability for drinking purposes in addition to the agricultural and industrial uses, to reduce the dependence on the surface water source through the maximum benefit from the available groundwater source. In addition, study the impact of various pollutants either on Dibdibba aquifer or on those aquifers located in the Western Sahara of Al-Najaf province and what is the speed of transmission of these pollutants through the aquifers because there are a cement factory and treatment plant in this province.

References

Abbott, M. B. 1989. *Computational fluid dynamics: an introduction for engineers*. London: Longman Pub Group.

Abdulla, F. and Al-Assa'd, T. 2006. Modelling of groundwater flow for Mujib aquifer, Jordan. *Journal of Earth System Science* 115, pp. 289-298.

Abdullah, E. 2008. *The water crisis in Iraq, and the reasons for that* [Online]. Available at: http://www.alukah.net/culture/0/3948/ [Accessed: 27 October 2014].

Abojassim, A. A. 2014. Uranium concentrations measurement for Ground Water and Soil Samples in Al-Najaf/Iraq. *IOSR Journal of Applied Chemistry* 6, pp. 61-65.

Aesh, M.H. 2009. Groundwater resources [Online]. Available at: https://ar.wikipedia.org/wiki/%D9%85%D9%8A%D8%A7%D9%87_%D8%AC%D9%88%D9%81%D9%8A%D8%A9 [Accessed: 14 December 2015].

Aherns, C. D. 2007. *Meteorology today: an introduction to weather, climate, and the environment*. USA, Belmont: Brooks/Cole, Cengage Learning.

Ahmed, A. R., Mukdad, H. A. and Rafea, K. K. 2013. Assessment of groundwater recharge in arid and semi-arid areas: a case study of the composition of the Dibdibba aquifer in the Karbala-Najaf plateau. *Iraqi Journal of Science* 54(4), pp. 902-910.

Al-Aboodi, A. H. 2008. Hydrochemical classification of groundwater in Bahr Al-Najaf, western desert, Iraq. *Journal of Basrah Researches (Sciences)* 34(2), pp. 23-32.

Al-Atia, M. J. 2006. *History of AL-Najaf earth, geological legacy and natural wealth's*. Iraq: AL-Nbras Institution for advertising and Publishing, P. 159.

Al-Faris, I. A. 2002. Estimation the accuracy of digital elevation model resulted from contour lines. Journal of the Iraqi Association of Remote Sensing 1, pp. 15-25.

Al-Fatlawi, A. N. and Jawad, S. B. 2011. Water surplus for Umm Er Radhuma aquifer – west of Iraq. *Euphrates Journal of Agriculture Science* 3(4), pp. 1-10.

Al-Furat, C. 1989. General Scheme of water resources and Land development in Iraq. *Ministry of Agriculture and Irrigation*, Iraq, stage III (Unpublished).

Al-Furat, C. 1995. Groundwater recharge, Al-Haidaria area, Karblla. *Ministry of Agriculture and Irrigation, Iraq*, (Unpublished).

Ali, B. M. 2012. Hydrogeological study of area between Najaf – Karbala'a cities. *Iraqi Journal for Science* 2(53), pp. 353-361.

Ali, S. M., Al-Tawash, B. S. and Al-Bassam, K. S. 2013. Geochemical modelling and isotope analysis of the shallow groundwater aquifer of Baghdad Area. *Arab Journal for Geoscience* 7, pp. 1811–1827.

Al-Jaf, A. A. and Al-Saady, Y. I. 2010. *Report of land use –land cover maps of Iraq, Karbala quadrangle sheet NI-38-14, scale 1:250000*. Iraq: General Commission for Geological Survey and Mining.

Al-Jawad, S. B., Al-Dabagh, R. H., Mussa, M. S. and Al-Hady, H. A. 2002. *Hydrogeology of the Aquifers In the Western Desert -west and south of the Euphrates River, sections I and II*. Iraq: The National Program, Unpublished.

Al-Jiburi, H. K. and Al-Basrawi, N. H. 2009. Hydrogeology. *Iraqi Bulletin of Geology and Mining Journal* 3, pp. 77-91.

Alley, W. M., Reilly, T. E. and Franke, O. L. 2007. Effects of ground water development on ground water flow to and from surface water bodies. Retrieved January 2008, from http://pubs.usgs.gov/circ/circ1186/html/gw_effect.html

Allison, V., Harihar, R. and Edith, Z. 2010. Incorporating groundwater-surface water interaction into river management models. *Ground Water Journal* 48(5), pp. 661-673.

Al-Muqdadi, S. W. 2012. *Groundwater investigation and modeling - western desert of Iraq*. PhD Thesis, Technische University.

Al-Muqdadi, S. W. and Merkel, B. J. 2011. Automated Watershed Evaluation of Flat Terrain. *Journal of Water Resource and Protection* 03, pp. 892-903.

Al-Muqdadi, S. W. and Merkel, B. J. 2012. Interpretation of Groundwater Flow into Fractured Aquifer. *International Journal of Geosciences* 03, pp. 357-364.

Al-Mussawy, W. H. 2014. Assessment of groundwater quality in UMM ER Radhuma aquifer (Iraqi Western Desert) by integration between irrigation water quality index and GIS. *Journal of Babylon University* 1(22), pp. 201-217.

Al-Mussawy, W. H. and Khalaf, R. M. 2013. *Optimum management models for groundwater use in Karbala desert area*. PhD Thesis, Al-Mustansiriyah University.

Alphonce, C. G. and Thomas, B. H. 2010. Simulating stream flow and water table depth with a coupled hydrological model. *Water Science and Engineering Journal* 3(3), pp. 241-256.

Al-Sadiq, A. A. H. and Akulaims, Y. F. 2005. The possibility of using groundwater modeling system program to prepare the geological profiles of Al-Hamdaniya area, northern Iraq. *Journal of Al-Rafidain Sciences* 16(2), pp. 176-190.

Al-Salim, T. H. and Khattab, M. F. A. 2004. Mathematical model of ground water flow of Bashiqa area, northern Iraq. *Iraqi National Journal of Earth Sciences* 4(2), pp. 84-98.

Al-Shamma'a, A. M., Saud, Q. J. and Al-Jawad, S. B. 2008. Mathematical model for groundwater flow west Al-Razzazah Lake, Iraqi western desert. *Journal Iraqi Bulletin of Geology and Mining* 4, pp. 29-42.

Al-Shemmari, A. N. H. 2012. Establishing relations between hydraulic parameters and geoelectrical properties for fractured rock aquifer in Dammam formation at Bahr Al-Najaf basin. PhD Thesis, Baghdad University.

Al-Siba′ai, M. 2005. Modeling of groundwater movement (Euphrates lower basin). *Journal of Damascus University for Basic Sciences* 21(2), pp. 91-114.

Al-Talua, H. M. 2013. Using of geographic information systems (GIS) to interpret the hydrogeological data in Kikla aquifer in the Nafusa mountain in Libya. *Journal of Remote Sensing and GIS* 1(1), PP. 23-29.

Anderson, M. and Woessner, W. 1992. *Applied groundwater modeling: Simulation of Flow and advective transport*. San Diego, California: Academic Press Inc.

Anderson, M. P., Woessner W. W. and Hunt R. J. 2015. *Applied groundwater modeling, simulation of flow and advective transport.* London: Academic Press.

Andrews, C. B. and Neville, C. J. 2003. Ground Water Flow in a Desert Basin: Challenges of Simulating Transport of Dissolved Chromium. *Ground Water* 41(2), pp. 219-226.

Bair, E. S. and Metheny, M. A. 2011. Lessons learned from the landmark "A Civil Action" trial. *Groundwater* 49(5), pp. 764–769.

Barnes, R. 1991. The variogram sill and the sample variance. *Mathematical Geology* 23(4), pp. 673-678.

Barrash, W. and Dougherty, M. E. 1997. Modeling axially symmetric and non-symmetric flow to a well with MODFLOW, and Application to Goddard2 well test, Boise, Idaho. *Ground Water* 35(4), pp. 602-611.

Barwary A. M. and Nasira, A. S. 1996. *Geological map of Al-Najaf quadrangle sheet NH-38-2 of scale 1:250 000*. 1st. ed. Iraq: General Commission for Geological Survey and Mining.

Barwary, A. M. and Slewa, N. A. 1995. *Report on the regional geological mapping of Karbala quadrangle - sheet NI-38-14*. Iraq: General Commission for Geological Survey and Mining.

Bausch, W. C. and Bernard, T. M. 1992. Spatial averaging Bowen ratio system: Description and lysimeter calibration. *Transactions of the ASAE* 35, pp. 121-128.

Bautista, F., Bautista, D. and Delgado-Carranza, C. 2009. Calibration of the equations of hargreaves and thornthwaite to estimate the potential evapotranspiration in semi-arid and subhumid tropical climates for regional applications. *Atmosphera* 22(4), pp. 331-348.

Bekele, G. 2009. Study into the potential and feasibility of a standalone solar-wind hybrid electric energy supply system, for application in Ethiopia. PhD Thesis, Royal Institute of Technology, KTH.

Blegen, J. T. K. 2005. *Numerical and analytical modelling of ground water flow in delta structures*. University Of Oslo. http://urn.nb.no/URN:NBN:no-10725.

Bohling, G. 2005. *Introduction to geostatistics and variogram analysis* [Online]. Available at: http://people.ku.edu/~gbohling/cpe940/Variograms.pdf.

Bosman, H. H. 1987. The influence of installation practices on evaporation from symon's tank and american class a-pan evaporimeters. *Agricultural and Forest Meteorology* 41, pp. 307 323.

Bouwer, H. 1969. Theory of seepage from open channel. *Advances in Hydroscience* 5, New York: Academic Press.

Bouwer, H. 1978. *Groundwater hydrology*. McGraw-Hill, New York, p. 480.

Brunner, P., Simmons, C. T. and Cook, P. G. 2009. Spatial and temporal aspects of the transition from connection to disconnection between rivers, lakes and groundwater. *Journal of Hydrology* 376, pp. 159-169.

Bryson, B., Zbigniew, W. K., Shaohong, W. and Jean, P. 2008. Climate change and water. Intergovernmental Panel on Climate Change, IPCC. Geneva, pp. 210.

Carrera, J. and Neuman, S. P. 1986. Estimation of aquifer parameters under transient and steady state conditions: maximum likelihood method incorporating prior information. *Water Resources Research* 22(2), pp. 199–210.

CEDARE, 2002. *Final draft report on the regional strategy for the utilization of the Nubian sandstone aquifer system*. Cairo, Egypt: Centre for Environment and Development for the Arab Region and Europe, pp. 22-82.

Chandal, S. S., Agarwal, R. K. and Pandey, A. N. 2005. New correlation to estimate global solar radiation on horizontal surface using sunshine hours and temperature data for Indian cities. *Journal of Solar Energy Engineering* 127(3), pp. 417-420.

Chevalking, S., Knoop, L. and Van Steenbergen, F. 2008. *Ideas for Groundwater Management*. Wageningen, The Netherlands: MetaMeta and IUCN.

Chiang, W. H. and Kinzelbach, W. W. 1998. Processing MODFLOW: a simulation system for modeling groundwater flow and pollution. Hamburg, Zürich: Germany.

Chowdhury, A. K. M. M. and Canter, L. W. 1998. Expert systems for ground water management. *Journal of Environmental Systems* 26(1), pp. 89-110.

Cohen, Y. and Shoshany, M. 2002. A national knowledge-based crop recognition in Mediterranean environment. International Journal of Applied Earth Observation and Geo-information 4(1), PP. 75-87.

Conant, B. 2004. Delineating and quantifying ground water discharge zones using streambed temperatures. *Ground Water* 42(2), pp. 243-257.

Consortium-Yugoslavia 1977. Hydrogeological explorations and hydro-technical work-Western Desert of IRAQ. *Blook7, Directorate of western desert development projects*. Republic of Iraq (Unpublished).

Constantz, J. 2008. Heat as a tracer to determine streambed water exchanges. *Water Resources Research* 44, pp. 1-20.

Cooley, R. L. 1979. A method of estimating parameters and assessing reliability for models of steady state groundwater flow, 2. Application of statistical analysis. *Water Resources Research* 15(3), pp. 603– 617.

Cooley, R. L. and Naff, R. L. 1990. *Regression modeling of ground-water flow*. U.S. Geological Survey Techniques of Water- Resources Investigations, 03–B4, pp. 232.

Cooley, R. L. and Sinclair, P. J. 1976. Uniqueness of a model of steady-state groundwater flow. *Journal of Hydrology* 31(3–4), pp. 245–269.

Darcy, H. 1958. *Les Fontains Publiques de la Ville de Dijon*. Victor Dalmont: Paris.

Das, D. B. and Lewis, M. 2007. Dynamics of fluid circulation in coupled free and heterogeneous porous domains. *Chemical Engineering Science* 62(13), pp. 3549-3573.

Dawod, M. A. A., El-Rafy, M. A. and Alaa EL-Din, H. A. 2006. New empirical formula for estimate the evaporation from Nasser lake in Egypt. *Meteorological Research Bulletin – the Egyptian Meteorological Authority* 21, pp. 1-13.

Debashish, S. 2014. *Recent trends in modelling environmental contaminants*. New Delhi: Springer.

Delleur, J. W. 1999. The handbook of groundwater engineering. 1st ed., Boca Raton and Heidelberg: CRC Press and Springer, pp. 949.

Diersch, H. J. G. and Kolditz, O. 1998. Coupled groundwater flow and transport: 2. Thermohaline and 3D convection systems. *Advances in Water Resources*, 21(5), pp. 401-425.

Dillon, P. J. and Liggett, J. A. 1983. An ephemeral stream–aquifer interaction model. *Water Resources Research* 19(3), pp. 621–626.

Doherty, J. 1990. *MODINV – suite of software for MODFLOW preprocessing, postprocessing, and parameter optimization-user's manual*. Australia: Australian Centre for Tropical Freshwater Research.

Doherty, J. 2014a. *PEST, model-independent parameter estimation—user manual*. Australia: Watermark Numerical Computing.

Doherty, J. 2014b. *Addendum to the PEST Manual*. Australia: Watermark Numerical Computing.

Domenico, P. A. and Schwartz, F. W. 1998. Physical and chemical hydrogeology. New York: Wiley.

Edwards, W. R. N. 1986. Precision weighing lysimetry for trees, using a simplified tarred-balance design. *Tree Physiology* 1(2), pp. 145-150.

El-Baz, F. 2013. *Remote sensing to explore the groundwater in the Arab world* [Online]. Available at: http://www.arsco.org/detailed/73f28ecc-5abf-463a-802c-b3aeba044afa [Accessed: 5 November 2014], (In Arabic).

EMRL, Environmental Modelling Research Laboratory 1999. *Groundwater Modelling System – GMS Reference Manual*. Birmingham Young University, Birmingham.

European Union Water Framework Directive: European Commission 2000. European parliament and commission. *Official Journal* (OJ L 327) on 22 December 2000.

Faber, T. E. 2001. *Fluid dynamics for physicists*. Cambridge: Cambridge University Press, United Kingdom.

Fletcher, G. D. 1995. *Groundwater and wells*. USA, Minnesota: Johnson Screens.

Fouépé, A. T., Rao, V. V. S. G., Ngoupayou, J. N., Nkamdjou, L. S. and Ekodeck, G. E. 2009. Groundwater flow modelling in the upper Anga'a river watershed, Yaounde, Cameroon. *African Journal of Environmental Science and Technology* 3(10), pp. 341-352.

Fox, G. and Durnford, D. 2003. Unsaturated hyporheic zone flow in stream/aquifer conjunctive systems. *Advances in Water Resources* 26, pp. 989-1000.

Franke, O. L., Reilly, T. E. and Bennett, G. D. 1987. *Definition of boundary and initial conditions in the analysis of saturated groundwater flow systems; an introduction*. Techniques of Water Resources Investigations, 03-B5, USGS, pp. 15-56.

Freeze, A. and Cherry, J. 1979. *Groundwater*. Englewood Cliffs, New Jersey: Prentice-Hall, p. 604.

Freeze, R. A. and Witherspoon, P. A. 1967. Theoretical analysis of regional groundwater flow: 2. effect of water table configuration and subsurface permeability variation. *Water Resources Research* 3, pp. 623-624.

Ganesan, M. and Isabella, M. M. 2013. Estimation of hydraulic conductivity and dispersivity through numeric modelling. *Journal of Groundwater Research* 2(1), pp. 79-90.

GAW (Global Atmosphere Watch) and WMO (World Meteorological Organization) 2011. *Quality assurance in monitoring solar ultraviolet radiation: the state of the art*. Geneva, Switzerland: WMO.

GEOSURV, 2015. Geological and hydrogeological data of Al-Najaf province. The Iraqi Ministry of Industry and Minerals, General Commission for Geological Survey and Mining.

Groundwater Governance 2015. *Global diagnostic on groundwater governance*. Rome, Groundwater Governance: A Global Framework for Action.

Hagen, G. 1839. Ueber die bewegung des wassers in engen cylindrischen röhren. *Annalen der Physik und Chemie* **122**(3), pp. 423–442.

Haitjema, H. M., Kelson, V. A. and de Lange, W. 2001. Selecting MODFLOW cell sizes for accurate flow fields. *Ground Water* 39(6), pp. 931-938.

Harbaugh, A. W. 2005. *MODFLOW-2005, The U.S. Geological Survey modular groundwater model—the ground-water flow process*. U.S. Geological Survey Techniques and Methods 6-A16, Ch.2, p. 1.

Hatzzian, A. N., Katsoulis, B., Pnevmatikos, J. and Antakis, V. 2007. Spatial and temporal variation of precipitation in Greece and surrounding regions based on global precipitation climatology project data. *Journal of Climate* 21, pp. 1349-1370.

Heath, R. C. 1983. *Basic Ground-Water Hydrology: U.S. Geological Survey Water-Supply Paper 2220*. U.S. Dept. of the Interior, U.S. Geological Survey, pp. 33.

Hemker, C. J. 1999. Transient well flow in layered aquifers systems: the uniform well-face drawdown solution. *Hydrology Journal* 225, pp. 19-44.

Hill, M. C. 1992. *A computer program (MODFLOWP) for Estimating Parameters of a transient, three-dimensional, ground- water flow model using nonlinear regression*. U.S. Geological Survey, Open-File Report 91-484, pp. 358.

Hill, M. C. 2002. *The U.S. geological survey modular ground-water flow model*. A MARGINS Education and Planning Workshop: Developing a Community Sediment Model. The Institute of Arctic and Alpine Research (INSTAAR), Boulder, Colorado.

Hoopes, J. A. and Harleman, D. R. F. 1967. Waste water recharge and dispersion in porous media. *ASCE Journal of the Hydraulics Division* 93 (5), pp. 51-71.

Humphrey, S. 2008. A stochastic approach to a groundwater flow model of southern Honey Lake Valley in Lassen County, CA and Washoe County, NV. MSc Thesis, University of Nevada, Reno.

Husam, B. 2009. Fundamentals of groundwater modelling. In: Luka, F. K. and Jonas, L. W. eds. *Groundwater: modelling, management and contamination.* USA: Nova Science Publishers, Ch. 4, pp. 149-166.

Igor, S. Z. and Lorne, G. E. 2004. *Groundwater resources of the world and their use*. The United Nations Educational, Scientific and Cultural Organization, Saint-Denis.

Ingra Yugoslavian Company, 1961-1967. Russain company to investigate groundwater in the Western Sahara of Iraq.

Ishaq, A. M. and Ajward, M. H. 1993. Investigation of chloroform plumes in a porous media. *Proceedings of the Symposium on Engineering Hydrology*, pp. 970-976.

Jacek, G. and Maciek, L. 2004. Modeling of complex multi-aquifer systems for groundwater resources evaluation—Swidnica study case (Poland). *Hydrogeology Journal* 13, pp. 627–639.

Jackson, R. D. and Huete, A. R. 1991. Interpreting vegetation indices. Preventive Veterinary Medicine Journal, 11, pp. 185-200.

Jakub, S. 2014. Examples of determining the hydraulic conductivity of soils: theory and applications of selected basic methods. Faculty of the Environment, Handbook on Soil Hydraulics, Jan Evangelista Purkyně University.

Jalut, Q. H., Khalaf, R. M. and Abdul-Mehdi, T. R. 2013. Modeling of Transient Groundwater Flow Using Fuzzy Approach. *Modern Applied Science* 7(4), pp. 77-94.

Jassim, S. Z. and Goff, J. C. 2006. *Geology of Iraq*. 1st ed. Brno: Doline, Prague and Moravian Museum.

Jassim, S. Z., Karim, S. A., Basi, M. A., Al-Mubarak, M. and Munir, J. 1984. *Final report on the regional geological survey of Iraq*. Iraq: General Commission for Geological Survey and Mining, No. 1447.

Javandel, I. and Witherspoon, P. A. 1983. Analytical solution of a partially penetrating well in a two-layer aquifer. *Water Resources Research Journal* 19(2), pp. 567-578.

Jazmani, S. and Al-Maqdisi, S. 2002. Geographical information systems (GIS). *Arab Orient House, Beirut, Lebanon,* pp. 150-153.

Jeff, D., Sean, K., Jim, F., Mary, H., Jill, V. D., David, B. and Mohsen, M. 2017. *Applications of groundwater modeling for decision-making in water management and engineering with water supply and remediation case studies*. National Ground Water Association Press: U.S.A.

Jones, M. A. 1997. NCF: a finite-element computer program to simulate ground-water flow within the U.S. geological survey modular ground-water flow model (MODFLOW). *Ground Water* 35(4), pp. 721-723.

Juny, H. S., Gyu, H. L. and Jai, H. O. 2001. Interpretation of the transient variation of precipitation amount in Seoul l, Korea, Part I: Diurnal Variation. *American Meteorological Society Journal* 14(13), pp. 2989-3004.

Justin, L. H. and Richard, G. N. 2012. Role of surface-water and groundwater interactions on projected summertime streamflow in snow dominated regions: An integrated modeling approach. *Journal of Water Resources Research* 48(W11524), pp. 1-20.

Kalbus, E., Reinstorf, F. and Schirmer, M. 2006. Measuring methods for groundwater? surface water interactions: a review. *Hydrology and Earth System Sciences Discussions* 10, pp. 873-887.

Karakostas, C. Z. and Manolis, G. D. 1998. Stochastic boundary element solution applied to groundwater flow. *Engineering Analysis with Boundary Elements* 21(1), pp. 9-21.

Karamouz, M., Tabari, R. M., Kerachian, R. and Zahraie, B. 2005. Conjunctive use of surface and groundwater resources with emphasis on water quality. *Impacts of Global Climate Change:* pp. 1-12.

Karlsson, E. and Pomade, L. 2005. *Methods of estimating potential and actual evaporation*. [online] Department of Water Resources Engineering, pp. 1-11. Available at: http://www.civil.utah.edu/~mizukami/coursework/cveen7920/ETMeasurement.pdf [Accessed 9 December 2015].

Kazezyilmaz-Alhan, C. and Medina, M. 2006. Stream solute transport incorporating hyporheic zone processes. *Journal of Hydrology* 329, pp. 26-38.

Kbrom, A. G. 2017. A review on waterlogging, salinization and drainage in Ethiopian irrigated agriculture. *Sustainable Water Resources Management Journal*, pp. 1-8.

Kbrom, A. G. 2017. A review on waterlogging, salinization and drainage in Ethiopian irrigated agriculture. *Sustainable Water Resources Management Journal*, pp. 1-8.

Kelson, V. A. 2002. *Using MODFLOW as an analytic element pre-processor*. The Geological Society of America, Denver Annual Meeting, paper no. 44-6.

Khemiri, S., Chenini, I., Saidi, S., Baamar, B., Mammou, A., B. and Zargouni, F. 2013. Dem-based GIS algorithms and 3D geospatial mapping for creation of hydrogeological models data in Foussana basin (Central Tunisia). *Journal of Water Resource and Protection* 5, pp. 801-815.

Konikow, L. F. 2005. Ground water depletion across the nation. Retrieved January 2008, from USGS: http://pubs.usgs.gov/fs/fs-103-03/

Konikow, L. F. and Bredehoeft, J. D. 1992. Groundwater models cannot be validated. *Advances in Water Resources* 15(1), pp. 75-83.

Konikow, L. F. and Kendy, E. 2005. Groundwater depletion: a global problem. *Hydrogeology Journal* 13, pp. 317-320.

Konikow, L. F., Reilly, T. E., Barlow, P. M. and Voss, C. I. 2006. Groundwater modeling. In: Delleur, J. W. eds. *The Handbook of Groundwater Engineering*. 2nd ed. USA: CRC press.

Konrad, C. P. 2006. Longitudinal hydraulic analysis of river-aquifer exchanges. *Water Resources Research* 42, pp. 1-14.

Kresic, N. 2007. Hydrogeology and groundwater modelling. 2nd ed. New York: CRC Press, Taylor and Francis Group.

Krige, D. G. 1951. A statistical approach to some basic mine valuation problems on the Witwatersrand. *Journal of Chemistry Metals and Mining Society*, 52 (6), pp. 119-139.

Krige, D. G. 1952. A statistical analysis of some of the borehole values in the orange free state goldfield. *Journal of Chemistry Metals and Mining Society*, 53 (3), pp. 47–64.

Kruseman, G. P., de Ridder, N. A. and Verweij, J. M. 2000. *Analysis and evaluation of pumping test data*. Amsterdam: ILRI Publication 47.

Kumar, C. P. 2002. Groundwater flow models. *Technical Notes*, pp. 1-27.

Kumar, C. P. 2015. Modelling of groundwater flow and data requirements. *International Journal of Modern Sciences and Engineering Technology* 2(2), pp. 18-27.

Kumar, G. N. P. and Kumar, P. A. 2014. Development of groundwater flow model using Visual MODFLOW. *International Journal of Advanced Research* 2(6), pp. 649-656.

Kurt, S. and Frank, F. 2006. Estimating hourly incoming solar radiation from limited meteorological data. *Weed Science Journal* 54, pp. 182-189.

Leake S. A. and Claar D. V. 1999. *Procedures and computer programs for telescopic mesh refinement using MODFLOW*. U.S. Geological Survey: Open-File Report, pp. 99-238.

Ledoux, H. and Gold, C. 2005. Interpolation as a tool for the modelling of 3D geoscientific datasets. *In: Proc. 4th ISPRS Workshop on Dynamic and Multi-dimensional GIS*, pp. 79–84.

Lehn, F., Thomas, E. R. and Gordon, D. B. 1987. *Definition of boundary and initial conditions in the analysis of saturated ground-water flow systems-an introduction*. Techniques Of Water Resources Investigations of the United States Geological Survey, Department of The Interior. USA: Washington.

Leighton, D. A. and Phillips, S. P. 2003. *Simulation of ground-water flow and land subsidence in the Antelope Valley ground-water basin, California*. Sacramento, Calif, U.S. Dept. of the Interior, U.S. Geological Survey. http://purl.access.gpo.gov/GPO/LPS31370.

Lenntech, 1993. Seawater intrusions in groundwater. http://www.lenntech.com/About-Lenntech.htm , was created in 1993 by Alumni from the Technical University of Delft, the Netherlands.

Lent, T. and Kitanidis, P. K. 1989. Numerical spectral approach for the derivation of piezometric head covariance function. *Water Resources Research* 25(11), pp. 2287-2298.

Leuning, R. and Moncrieff, J. 1990. Eddy covariance CO_2 flux measurements using open-path and closed-path CO_2 analyzers-corrections for analyzer water vapor sensitivity and damping of fluctuations in air sampling tubes. *Boundary-Layer Meteorology* 53, pp. 63-76.

Li, L., Yu, Q., Su, Z. and Tol, C. V. 2009. A simple method using climatic variables to estimate canopy temperature, sensible and latent heat fluxes in a winter wheat field on the north china plain. *Hydrol. Process* 23, pp. 665-674.

Li-Tang, H., Chong-Xi, C., Jiu, J. J. and Zhong-Jing, W. 2007. Simulated groundwater interaction with rivers and springs in the Heihe river basin. *Hydrological Processes Journal* 21, pp. 2794-2806.

Loudyi, D. 2005. *A 2d finite volume model for groundwater flow simulations: integrating non-orthogonal grid capability into MODFLOW*. PhD Thesis, Cardiff University.

Mace, R. E., Chowdhury, A. H., Anaya, R. and Way. S. 2000. *A numerical groundwater flow model of the upper and middle Trinity Aquifer, Hill Country area*. Austin, Texas Water Development Board.

Maidment, D. R. 1993. Handbook of hydrology. New York.

Manouchehr, C. and Ali, M. 2015. Evaluation of artificial recharge on groundwater using MODFLOW model (Case Study: Gotvand plain-Iran). *Journal of Geoscience and Environment Protection* 3, pp. 122-132.

McDonald, M. G. and Harbaugh, A. W. 1988. A modular three-dimension finite-difference groundwater flow model. *Techniques of Water Resources Investigations of the U.S. Geological Survey*, USA.

McMahon, A., Heathcote, J., Carey, M. and Erskine, A. 2001. *Guide to good practice for the development of conceptual models and selection and application of mathematical models of contaminant transport processes in subsurface*. NC/99/38/2, National Groundwater and Contaminated Land Centre (NGWCL), Environment Agency, U.K.

MDBC - Murray–Darling Basin Commission 2001. *Groundwater Flow Modelling Guideline*. Report prepared by Aquaterra.

Mehl, S. and Hill, M. C. 2002. Development and evaluation of a local grid refinement method for block-centered finite-difference groundwater models using shared nodes. *Advances in Water Resources* 25(5), pp. 497-511.

Mehl, S. E. and Hill, M. C., 2001. *MODFLOW-2000, the U.S. geological survey modular ground-water model — user guide to the link-AMG (LMG) package for solving matrix equations using an algebraic multi-grid solver*. U.S. Geological Survey Open-File Report 01-177.

Merz, S. K. and National Centre for Groundwater Research and Training 2012. *Australian groundwater modelling guidelines*, No. 82. Australian Government, Canberra: The National Water Commission.

Middleton, N. J. and Arnold, D. S. G. T. 1997. *World atlas of desertification*. 2nd ed. United Nations Environment Programme.

Montenegro, H. and Odenwald, B. 2009. *Analysis of spatial groundwater flow for the design of the excavation pit for a ship lock in Minden Germany*. 2nd International FEFLOW User Conference. 14-18 September, Potsdam, Germany.

Moore, J. E. 1979. Contributions of groundwater modeling to planning. *Journal of Hydrology* 43, pp. 121-128.

MOST, (Ministry of Science and Technology) 2006. *Solar Electric System*. Ministry of Science and Technology-Republic of the Union of Myanmar, pp. 16. (Unpublished).

MOST, 2015. Ministry of Science and Technology in Iraq.

MOTRANS, (Ministry of Transportation) 2015. Meteorological data of Al-Najaf province station. Ministry of Transportation - Iraqi Meteorological Organization and Seismology – Iraq.

MOWR, (Ministry of Water Resources) 2015. Water crisis reasons. Ministry of Water Resources. *Al-Rafidain Journal.* (Un-Published).

Mutreja, K. N. 1990. *Applied Hydrology*. New Delhi: Tata McGraw-Hill Publishing Company Limited.

Nasrin, K., Mehdi, M. H. and Amir, A. D. 2013. Numerical simulation of groundwater level using MODFLOW software (a case study: Narmab watershed, Golestan province). *International Journal of Advanced Biological and Biomedical Research* 1(8), pp. 858-873.

National Groundwater and contaminated Land Centre (NGWCL) 2001. *Guidance on assigning values to uncertain parameters in subsurface analytical contaminant fate and transport models*. NGWCLC Report NC/99/38/3, Environment Agency, U.K.

Neuman, S. P. and Witherspoon, P. A. 1969. Applicability of current theories of flow in leaky aquifers. *Water Resources Research* 5, pp. 817-829.

Noaa, U. S. 2009. National Oceanic and Atmospheric Administration.

Obrecht, M. 1994. *WHS solver documentation*. Report to Water Loo Hydrologic, Inc.

Omran, H. A., Mahmood M. S. and Kadhem A. A. 2014. Quantity and distribution of the current surface and ground water resources in Bahr An-Najaf in Iraq. *International Journal of Scientific and Engineering Research* 5(8), pp. 79-83.

Oosterbaan, R. J. and Nijland, H. J. 1994. Determining the saturated hydraulic conductivity. In: Ritzema, H. P. *Drainage principles and applications*. International Institute for Land Reclamation and Improvement (ILRI), Publication 16, pp. 1-38.

Osiensky, J. L. and Williams, R. E. 1997. Potential inaccuracies in MODFLOW simulations involving the sip and ssor methods for matrix solution. *Ground Water* 35(2), pp. 229-232.

Oswald, S. E. and Kinzelbach, W. 2000. Three-dimensional physical model for verification of variable-density flow codes. *IAHS Publication (International Association of Hydrological Sciences)* 265, pp. 399-404.

Ouazar, D., Cheng, A. H. D. and Kizamou, A. D. 1996. Object-oriented pumping-test expert system. *Journal of Computing in Civil Engineering* 10(1), pp. 4-9.

Parsons, R. M. 1957. *Groundwater resources of Iraq, mesopotamian plain*. Development Board, Ministry of development, Government of Iraq, Baghdad 11, pp. 157.

Pattle Delamore Partners, and Canterbury, N. Z. 2000. *Guidelines for the assessment of groundwater abstraction effects on stream flow*. Christchurch [N.Z.], Environment Canterbury.

Philip, B., Craig, T. S., Peter, G. C. and Rene', T. 2010. Modelling surface water-groundwater interaction with MODFLOW: some considerations. *Ground Water* 48(2), pp. 174-180.

Philip, J. G. 1980: Field heterogeneity: some basic issues. *Water Resources Research* 16(2), pp. 443-448.

Philip, T. H. 1994. *Comparison of vertical discretization techniques in finite-difference models of ground-water flow: example from a hypothetical New England setting*. U.S. Geological Survey Open-File Report 94-343, Denver.

Poeter, E. and Hill, M. 1997. Inverse Models - a necessary next step in groundwater modeling. *Journal of Groundwater* 35(2), pp. 250-260.

Poeter, E. P., Hill, M. C., Banta, E. R., Mehl, S. and Christensen, S. 2005. *UCODE_2005 and six other computer codes for universal sensitivity analysis, calibration, and uncertainty evaluation*. U.S. Geological Survey Techniques and Methods, 6 A11, 47 pp. 283.

Poiseuille, J. L. M. 1840. Recherches experimentales sur Ie mouvement des liquids dans les tubes de tres petits diametres; Influence de la pression sur la quantite de Iiquide qui traverse les tubes de tres petits diametres. *C. R. Acad. Sci.* 1l, pp. 961-67.

Quevauviller, P. 2008. General introduction: the need to protect groundwater. In: *Groundwater Science and Policy – An international overview*. The Royal Society of Chemistry: 3-18.

Quinn, P., Beven, K., Chevallier, P. and Planchon, O. 1991. The prediction of hillslope flow paths for distributed hydrological modelling using digital terrain models. Hydrological Processes 5(1), pp. 59-79.

Reading University 2002. Normalised Difference Vegetation Index (NDVI) [Online]. Available at: http://www.pvts.net/pdfs/ndvi/3_3_ndvi.PDF [Accessed: 29 Oct 2015].

Rovey, C. E. K. 1975. Numerical model of flow in stream aquifer system. *Hydrology* 74, Colorado State University, Fort Collins, Colorado.

Ruopu, L., Mahesh, P., Jesse, B., Gengxin, O., Jim, S., Brandi, F., Jessie, W. and Sudhansh, C. 2016. Evaluating hydrologically connected surface water and groundwater using a groundwater model. *Journal of the American Water Resources Association* 52(3), pp. 799-805.

Rushton, K. R. 2007. Representation in regional models of saturated river-aquifer interaction for gaining/losing rivers. *Journal of Hydrology* 334 (12), pp. 262-281.

Safavi, H. R. and Bahreini, G. R. 2009. Conjunctive simulation of surface water and groundwater resources under uncertainty. *Iranian Journal of Science and Technology, Transaction B, Engineering* 33(B1), pp. 79-94.

Scanlon, B. R., Healy, R. W. and Cook, P. G. 2002. Choosing appropriate techniques for quantifying groundwater recharge. Hydrogeology Journal, 10(1), pp. 18-39.

Scanlon, B. R., Mace, R. E., Barrett, M. E. and Smith, B. 2003. Can we simulate regional groundwater flow in a karst system using equivalent porous media models? Case study, Barton Springs Edwards aquifer, USA. *Journal of Hydrology -Amsterdam* 276, pp. 137-158.

Schaller, M. F. and Fan, Y. 2009. River basins as groundwater exporters and importers: Implications for water cycle and climate modeling. *Journal of Geophysical Research* 114, pp. 1-21.

Schlumberger Water Services 2011. *Visual MODFLOW 2011.1 user's manual: for professional applications in three-dimensional groundwater flow and contaminant transport modelling*. Ontario: Schlumberger Water Services.

Schubert, J. 2002. Hydraulic aspects of riverbank filtration - field studies. *Journal of Hydrology* 266, pp. 145-161.

Seeruttun, S. and Crossley, C. 1997. Use of digital terrain modelling for farm planning for mechanical harvest of sugar cane in Mauritius. *Computers and Electronics in Agriculture* 18, pp. 29-42.

Sefelnasr, A. M. 2007. *Development of groundwater flow model for water resources management in the development areas of the western desert, Egypt*. PhD Thesis, Martin Luther University, Germany.

Seneviratne, Daniel, L., Michael, L. and Christoph S. 2006. Land-atmosphere coupling and climate change in Europe. *Nature, International Weekly Journal of Science* 443(14), pp. 205-209.

Shah, T., Molden, D., Sakthivadivel, R. and Seckler, D. 2000. *The global groundwater situation: Overview of opportunities and challenges.* Colombo, Sri Lanka: International Water Management Institute.

Shuwei, Q., Xiujuan, L., Changlai, X., He, H., Zhang, F. and Fengchao, L. 2015. Numerical simulation of groundwater flow in a river valley basin in Jilin urban area, China. *Water Journal* 7, pp. 5768-5787.

Siebert, S., Burke, J., Faures, J. M., Frenken, K., Hoogeveen, J., D¨oll, P. and Portmann, F. T. 2010. Groundwater use for irrigation – a global inventory. *Hydrology Earth System Sciences* 14, pp. 1863-1880.

Simmers, I. 1988. *Estimation of natural groundwater recharge*.: Boston, MA: D. Reidel Publishing Co, pp. 510.

Sophocleous, M. 2002. Interactions between groundwater and surface water: the state of the science. *Hydrogeology Journal* 10(1), pp. 52-67.

Sour, I. 2013. *12 Million visitors going to Al-Najaf annually* [Online]. Available at: http://sourlb.com/newsview.aspx?id=4652&c=0 [Accessed: 25 October 2014].

Spiliotopoulos, A. and Andrews, C. B. 2006. Analysis of aquifer test data – MODFLOW and PEST. *Conference of Managing Ground-Water Systems*, pp. 569-573.

Spitz, F. J., Nicholson, R. S. and Daryll, A. P. 2001. A nested re-discretization method to improve pathline resolution by eleminating weak sinks representing wells. *Ground Water* 39(5), pp. 778-785.

Stallman, R. W. 1956a. Numerical analysis of regional water levels to define aquifer hydrology. *Transactions American Geophysical Union* 37(4), pp. 451–460.

Stallman, R. W. 1956b. Use of numerical methods for analysing data on groundwater levels. *International Association of Scientific Hydrology* 41(2), pp. 227–331.

Stollenwerka, K. G., Breitb, G. N., Welchc, A. H., Yountd, J. C., Whitneyd, J. W., Fostere, A. L., Uddinf, M. N., Majumderg, R. K. and Ahmedg, N. 2007. Arsenic attenuation by oxidized aquifer sediments in Bangladesh. Science of the Total Environment 379 (2-3), pp. 133-150.

Subramaya, k. 1984. *Engineering hydrology*. New Delhi: Tata McGraw-Hill Publishing Company Limited.

Tadros, M. T. Y., Mustafa, M. A. M. and Abdel-Wahab, M. 2014. Estimation of the global horizontal solar radiation in Iraq. *International Journal of Emerging Technology and Advanced Engineerin*g 4(8), pp. 587-605.

Tain-Shing, M., Deborah, L. H. and Adam, N. H. 2001. MODFLOW simulation of transient surface water/Groundwater interactions in a shallow Riparian zone using HEC-2-based water surface profiles. *Proceedings of the Conference on MODFLOW 2001 and Other Modeling Odysseys*. Australia, 11-14 September, 2001. Germany: Hannover, pp. 397-823.

Takounjou, A. F., Fantong, W., Ngoupayou, J. N. and Nkamdjou, L. S. 2012. Comparative analysis for estimating hydraulic conductivity values to improve the estimation of groundwater recharge in Yaoundé-Cameroon. *British Journal of Environment and Climate Change* 2(4), pp. 391-409.

Taylor, J. K. 1985. What is Quality Assurance. In: Taylor, J. K. and Stanley, T. W. (eds.), *Quality Assurance For Environmental Measurements*. American Society for Testing and Materials (ASTM), Special Technical Publication 867, pp. 5-11.

Tesfaye, A. 2009. Steady-state groundwater flow and contaminant transport modeling of Akaki wellfield and its surrounding catchment (Addis Ababa, Ethiopia). MSc Thesis, International Institute for Geo-Information Science and Earth Observation Enschede, The Netherlands.

Thompson, R. D. and Perry, A. H. 1997. *Applied climatology: principles and practice*. New York: Psychology Press.

Thornthwaite, C. W. 1948. An approach toward a rational classification of climate. *Geographical Review* 38(1), pp. 55-94.

Tomohiro, A., Akiko, S., Yusuke, Y., Genxu, W., Koji, F., Masayoshi, N., Jumpei, K. and Yuki, K. 2007. Surface water-groundwater interaction in the Heihe River basin, Northwestern China. *Bulletin of Glaciological Research* 24, pp. 87-94.

Toth, J. 1963. A theoretical analysis of groundwater flow in small drainage basins. *Journal of Geophysical Research* 68(16), pp. 4785-4812.

Toth, J. 1970. A conceptual model of the groundwater regime and the hydrogeologic environment. *Journal Hydrology* 10, pp. 164-176.

Townley, L. 1998. Shallow groundwater systems. In: Dillon, P. and Simmers, I. *Shallow groundwater systems*. Rotterdam: A.A. Balkema, pp. 3-12.

Trenberth, K. E., Fasullo, J. T. and Kiehl, J. 2009. Earth's global energy budget. *Bulletin of the American Meteorological Society Journal* 90(3), pp. 311–323.

U.S. Environmental Protection Agency (USEPA) 1994. *A technical guide to ground-water model selection at sites contaminated with radioactive substances*. EPA/402/R-94/012, Office of Solid Waste and Emergency Response, U.S. Environmental Protection Agency, Washington, D.C.

USDA - United States Department of Agriculture 2007. *Technical guide to managing ground water resources*. [Washington, D.C.], U.S. Dept. of Agriculture, Forest Service, Minerals and Geology Management, Watershed, Fish, Wildlife, Air, and Rare Plants, Engineering.

Van der Heijde, P. K. M. 1996. *Compilation of saturated and unsaturated zone modelling software*. EPA/600/SR-96/009, National Risk Management Research Laboratory, Ada: U.S. Environmental Protection Agency.

Verstraeten, W. W., Veroustraete, F. and Feyen, J. 2008. Assessment of evapotranspiration and soil moisture content across different scales of observation. *Sensors* 8(1), pp. 70–117.

Wa'il, Y. A. S. and Randa, I. H. 2007. Using MODFLOW and MT3D groundwater flow and transport models as a management tool for the Azraq groundwater system. *Jordan Journal of Civil Engineering* 1(2), pp. 153-172.

Wang, X. 1997. Conceptual design of a system for selecting appropriate groundwater models in groundwater protection programs. *Environmental Management* 21(4), pp. 607-615.

Wilson, J. D. and Naff, R. L., 2004. *MODFLOW-2000, the U.S. geological survey modular ground-water model - GMG linear equation solver package documentation*. U.S. Geological Survey Open-File Report 2004-1261.

Winter, T. C., Harvey, J. W., Franke, O., L. and Alley, W. M. 1998. *Ground water and surface water: a single resource*. Denver, Colo, U.S. Geological Survey.

Woessner, W. W. 2000. Stream and fluvial plain ground water interactions: rescaling hydrogeologic thought. *Ground Water* 38 (3), pp. 423-429.

Wood, W. W. and Sanford, W. E. 1995. Chemical and isotopic methods for quantifying ground-water recharge in a regional, semiarid environment. *Groundwater* 33, pp. 458–468.

Xi, C. and Qi, H. 2004. Groundwater influences on soil moisture and surface evaporation. Journal of Hydrology 297, pp. 285–300.

Yan, W., Alcoe, D., Morgan, L., Li C. and Howles, S. 2010. *Protocol for Development of Numerical Groundwater Model*. Version 1, Report prepared for the Government of South Australia, Department for Water.

Yang, L., Song, X., Zhang, Y., Han, D., Zhang, B. and Long, D. 2012. Characterizing interactions between surface water and groundwater in the Jialu River basin using major ion chemistry and stable isotopes. *Hydrology and Earth System Sciences Journal* 16, pp. 4265-4277.

Yangxiao, Z. and Van Geer, F. C. 1992. KALMOD, a stochastic-deterministic model for simulating groundwater flow with kalman filtering. *Hydrological Sciences Journal* 37(4), pp. 375-389.

Yassin, Z. O. and Michael, P. B. 2002. Modelling stream–aquifer seepage in an alluvial aquifer: an improved loosing-stream package for MODFLOW. *Journal of Hydrology* 264, pp. 69–86.

Yeh, G. T. 1981. On the computation of Darcian velocity and mass balance in the finite element modeling of groundwater flow. *Water Resources Research* 17(5), pp. 1529-1534.

Yeh, W. W. 1986. Review of parameter identification procedures in groundwater hydrology: The inverse problem. *Water Resourced Research* 22 (2), pp. 95-108.

Yeh, W. W. G. and Tauxe, G. W. 1971. Optimal identification of aquifer diffusivity using quasilinearization. *Water Resources Research* 7(4), pp. 955–962.

Zahraa, N. M. 2016. Estimation daily evaporation employing neural network for Abu-Garib station, Baghdad, Iraq. *International Journal of Scientific and Research Publications* 6(2), pp. 322-325.

Zhao, L., Xia, J., Xu, C., Wang, Z., Sobkowiak, L. and Long, C. 2013. Evapotranspiration estimation methods in hydrological models. *Journal of Geographical Sciences* 23(2), pp. 359-369.

Zheng, C. 1990. *MT3D, a modular three-dimensional transport model for simulation of advection, dispersion, and chemical reactions of contaminants in groundwater systems*. Report to the Kerr Environmental Research Laboratory, U.S. Environmental Protection Agency, Ada, Oklahoma.

Zheng, C., Bradbury, K. R. and Anderson M. P. 1988. Role of interceptor ditches in limiting the spread of contaminants in ground water. *Groundwater* 26(6), pp. 734–742.

Zhou, H., Gómez-Hernández, J. J. and Liangping, L. 2014. Inverse methods in hydrogeology: Evolution and recent trends. Advances in Water Resources 63, pp. 22–37.

Zimmerman, D. L. and Zimmerman, M. B. 1991. A comparison of spatial semivariogram estimators and corresponding ordinary kriging predictors. *Technometrics* 33(1), pp. 77-91.

Zomlot, Z., Verbeiren, B., Huysmans, M. and Batelaan, O. 2015. Spatial distribution of groundwater recharge and base flow:assessment of controlling factors. *Journal of Hydrology* 4, pp. 349–368.

Appendix A

TABLE A.1: Compilation of few numerical groundwater flow models (Adopted from Dalila 2005)

Name of Software	Model Description/Process Simulation	Type of Solution	Site Conditions for Model Application	References/Sources
3DFATMIC*	3-D subsurface flow, transport and fate	FE	Transient or steady-state density-dependent flow field in heterogeneous and anisotropic media with variable boundary conditions	Yeh, G.T., USEPA
3DFEMFAT	3-D flow groundwater and transport	FE	Saturated/unsaturated media, heterogeneous and anisotropic, transient or steady-state, variable boundary conditions	Yeh, G.T., Scientific Software Group
ABCFEM	2-D groundwater flow and transport	FE	Steady state or transient flow, pumping or injection wells. Variety of boundary conditions. Confined/unconfined systems	Brown, A., and Hertzman, R. Adrian Brown Consultants Inc.
AQUA3D	3-D ground flow, heat and solute transport	FE	Inhomogeneous and anisotropic flow conditions, variable boundary conditions, steady or transient flow	Scientific Software Group
AQUIFEM	2 and 3-D groundwater flow	FE	Anisotropic, heterogeneous, phreatic or confined, leaky or non-leaky aquifers under transient or steady state conditions	Townley, L.R., et al., Scientific Software Group
BEAVERSOFT	2-D groundwater flow and transport	FD and FE	Steady and unsteady 2-D flow in nonhomogeneous aquifers, flow through dams.	Veiniijt, A., and Bear, J. Delft University of Technology
BEMLAP	2 or 3-D Laplace problems	BEM	Steady state, homogeneous and isotropic media, subject to any type of the domain boundary conditions, no sources/sink can be considered	Kirkup, S. Integrated Sound Software
BIGFLOW	3-D groundwater flow	ED or FV	Saturated/unsaturated, heterogeneous and anisotropic media, transient and/or steady- state, variable boundary conditions	Ababou, R. U.S.Nuclear Regulatory Commission
BioF&T	3-D biodegradation, ground-water flow and transport	FE	Saturated/unsaturated, heterogeneous, anisotropic porous media or fractured media, variable boundary conditions, steady or transient flow	Scientific Software Group
BIOSLURP	2-D groundwater flow and vapor transport	FE	Multiphase flow in saturated/unsaturated zones, heterogeneous, anisotropic porous media or fractured media 1st and 2nd type boundary source/sink boundary	Scientific Software Group
CFEST*	2 and 3-D coupled fluid, energy and solute transport	FE	Accounts for heterogeneity and anisotropy, steady and transient -state flow, multilayered s stem and time- dependent or constant source/sinks	Gupta, S.K., and Cole, C.R. USDOE
DSTRAM	3-D groundwater flow and transport	FE	Density-dependent flow and transport in hilly saturated porous media, steady/transient simulations, heterogeneous and anisotropic media, a wide range of boundary conditions	Huyakom, P.S. HydiGeoLogic, Inc
DYNFLOW	3-D groundwater flow	FE	Transient and/or steady-state flow, heterogeneous anisotropic saturated media, confined- unconfined flow conditions allows a wide range of stresses and boundary conditions	Riordan, P.J., et al. Camp Dresser&McKee

FACT	3-D groundwater flow and contaminant transport	FE	Saturated/unsaturated, porous media, highly heterogeneous, multi-layer aquifer system with different options for boundary conditions implementation	Aleman, S. USDOE
FEFLOW	2 and 3-D groundwater flow and transport	FE	Transient or steady-state flow, density-dependent flow, variable boundary conditions	Durbin, T.J., and Bond, L.D. Waterloo Hydrogeologic, Inc.
FEMWATER*	3-D saturated/unsaturated Ground flow	FE	Heterogeneous and anisotropic media, transient and/or steady-state, variable boundary conditions	Yeh, G. T. USEPA and USNRC
FLONET	2-D groundwater flow	FE	Steady-state, confined or unconfined aquifer, heterogeneous and anisotropic porous media with complex boundary	Frind, E., et al. Waterloo HydroGeologic Software
FLOWPATH	2-D groundwater flow	FD	Steady-state, confined, leaky or unconfined flow in heterogeneous *and* anisotropic porous media. Variable boundaries	Franz, T., and Guiguer, N. Waterloo HydroGeologic Software
FTWORK	1, 2 and 3-D groundwater flow and solute transport	FD	Steady-state and transient flow in saturated media under confined and unconfined conditions. The model handles heterogeneities and anisotropy for flow	Faust, C.R., et al. GeoTrans, Inc.
GGU-SS FLOW2D GGU-TRANSIENT GGU-SS FLOW 3D	2 -D groundwater flow 3 -D groundwater flow	FE	Steady state. Considerations of seepage lines and unsaturated zones apply. The transient state flow model. Steady state only	GGU-Software
Golder Groundwater Computer Package	2 and 3-D groundwater flow and solute transport	FE	Steady-state or transient simulation, in anisotropic, heterogeneous, multi-layered aquifer systems, for confined, leaky-confined and unconfined flow problems	Miller, I., and Marlon-Larabert, J. Golder Associates, Inc.
HMS (SHM, THM, GHM, CGI)	3-D hydrolgic model system	FD	The sub-model GHM simulates saturated flow for confined-unconfined aquifers, restrictions on boundary conditions	Yu, Z. Earth System Science Center, Penn State University
HST3D*	3-D groundwater flow, heat and solute transport	FD	Saturated groundwater flow, confined or unconfined aquifer, heterogeneous and anisotropic with variable boundary conditions	Kipp, J.K.L. USGS
JDB2D/3D*	2-D groundwater flow quasi-3D flow	FD	2D, single-aquifer (JDB2D) and quasi-3D, multi-aquifer (JDB3D), transient flow for confined and leaky-confined aquifer systems	Bredehoeft, J.D. USGS
MARS	2 or 3-D groundwater flow and solute transport	FE	Multiphase flow in unconfined heterogeneous, anisotropic aquifers, in saturated or unsaturated zones	Scientific Software Group
MicroFEM	2-D groundwater flow	FE	Confined, leaky and unconfined conditions, heterogeneous aquifers and aquitards steady-state and transient flow, anisotropic aquifers, spatially and temporally - varying wells and boundary conditions, Precipitation, evaporation, drain, rivers, saturated single-density flow, multiple-aquifer systems and stratified aquifers	Hemker, C J and Boer, R.G. Scientific Software Group

240

MikeSHE	2 or 3-D groundwater flow and hydrologic processes	FD	Saturated/unsaturated zones, heterogeneous and isotropic media, steady/unsteady state confined/unconfined aquifer, variables boundary conditions, link to surface water models	DHI Software
MODFE*	2-D groundwater flow	FE	Transient or steady state conditions; nonhomogeneous and anisotropic flow, confined and unconfined, the three types of boundary conditions	Torak, L.J., et al. USGS
MODFLOW*	3-D groundwater flow	FD	Transient or steady state conditions; nonhomogeneous and anisotropic flow, confined and unconfined, variable boundary conditions	McDonald, M.G., and Harbaugh, A.W. USGS
MOFAT*	2-D groundwater flow and solute transport	FE	Multiphase flow in variably-saturated porous media, heterogeneous, anisotropic porous media, boundary type 1 and 2 can be simulated	Katyal. A.K., et al. USEPA
MOTIF	1, 2 or 3-D groundwater flow, heat and solute transport	FE	Variably saturated flow in fractured, deformable or porous media, steady/transient state heterogeneous and anisotropic media	Guvanasen V., et al. Atomic Energy of Canada, Ltd.
MOVER	2-D groundwater flow	FE	Multiphase flow, saturated/unsaturated zones, heterogeneous, anisotropic porous or fractured flow systems, with specified head and flux conditions and source/sink	Scientific Software Group
PLASM	2-D groundwater flow	FD	Non-steady flow of ground-water in heterogeneous anisotropic aquifers under water table, nonleaky, and leaky confined conditions, Include rampage from wells	Prickett, T.A., and Lonnquist, C.G. Thomas A. Prickett & Associates, Inc
PORFLOW	2 or 3-D groundwater flow, heat and mass transport	FV	Multiphase fluid flow, variably saturated, fractured or porous media, anisotropic and heterogeneous, arbitrary sources of sinks and varied boundary conditions	Runchal, A.K.. Analytic & computational research Inc.
ROCKFLOW*	2-D groundwater flow heat and mass transport	FE	Variable density flow, porous or fractured media, confuted/unconfined aquifers, anisotropy and heterogeneity, variable boundary conditions	Krohn, K..P., et al. Institute of Fluid Mechanics, Hannover.
SEEP2D	2-D groundwater flow	FE	A steady state, confined or unconfined, saturated and unsaturated flow model with non-homogeneous and anisotropic soil. It is designed to compute seepage on profile models	Tracy, F. USACE
SEEP/W	2-D groundwater flow	FE	Saturated/unsaturated conditions, steady/transient state flow , wells, a variety of boundary conditions, confined/phreatic heterogeneity and anisotropy may be analyzed	Krahn, J., et al. GeoSlope International, Inc.
SUTRA*	2 and 3-D groundwater flow. solute or energy transport	FE and IFD	Saturated/unsaturated, constant or variable-density fluid flow, steady-state or transient flow, variables flow boundary conditions	Voss, C.I., USGS
SWICHA	3-D groundwater flow and solute transport	FE	Simulates variable density fluid flow and solute transport processes in fully-saturated porous media, steady-state or transient field problems	Huyakom, P.S., et al. GeoTrans, Inc
SWIFT	3-D groundwater flow and transport	FD	Flow and transport of fluid, heat, brine, and radionuclide chains in porous and fractured geologic media. Heterogeneity, anisotropy and a variety of boundary condition and sources may be modeled	Cranwcll,R.M., et al. GeoTrans, In

TARGET	2, 3-D groundwater flow and chemical-species transport	IFD	2-D confined/unconfined, transient ground-water flow, 3-D saturated, density coupled, transient ground-water flow	Shaima, D., et al. IGWMC
VS2DT	1 and 2-D groundwater flow and solute transport	FD	Variable saturated flow, confined/unconfined aquifers, anisotropy and heterogeneity may be modelled, varied boundary conditions	Healy, R.W. USGS

Appendix B

TABLE B.1: Values of corrected factor K for PE calculated by Thornthwaite (1948)

Lat. North	Jan	Feb	Mar	Apr	May	June	July	Aug	Sep	Oct	Nov	Dec
0	1.04	.94	1.04	1.01	1.04	1.01	1.04	1.04	1.01	1.04	1.01	1.04
5	1.02	.93	1.03	1.02	1.06	1.03	1.06	1.05	1.01	1.03	.99	1.02
10	1.00	.91	1.03	1.03	1.08	1.06	1.08	1.07	1.02	1.02	.98	.99
15	.97	.91	1.03	1.04	1.11	1.08	1.12	1.08	1.02	1.01	.95	.97
20	.95	.90	1.03	1.05	1.13	1.11	1.14	1.11	1.02	1.00	.93	.94
25	.93	.89	1.03	1.06	1.15	1.14	1.17	1.12	1.02	.99	.91	.91
26	.92	.88	1.03	1.06	1.15	1.15	1.17	1.12	1.02	.99	.91	.91
27	.92	.88	1.03	1.07	1.16	1.15	1.18	1.13	1.02	.99	.90	.90
28	.91	.88	1.03	1.07	1.16	1.16	1.18	1.13	1.02	.98	.90	.90
29	.91	.87	1.03	1.07	1.17	1.16	1.19	1.13	1.03	.98	.90	.89
30	.90	.87	1.03	1.08	1.18	1.17	1.20	1.14	1.03	.98	.89	.88
31	.90	.87	1.03	1.08	1.18	1.18	1.20	1.14	1.03	.98	.89	.88
32	.89	.86	1.03	1.08	1.19	1.19	1.21	1.15	1.03	.98	.88	.87
33	.88	.86	1.03	1.09	1.19	1.20	1.22	1.15	1.03	.97	.88	.86
34	.88	.85	1.03	1.09	1.20	1.20	1.22	1.16	1.03	.97	.87	.86
35	.87	.85	1.03	1.09	1.21	1.21	1.23	1.16	1.03	.97	.86	.85
36	.87	.85	1.03	1.10	1.21	1.22	1.24	1.16	1.03	.97	.86	.84
37	.86	.84	1.03	1.10	1.22	1.23	1.25	1.17	1.03	.97	.85	.83
38	.85	.84	1.03	1.10	1.23	1.24	1.25	1.17	1.04	.96	.84	.83
39	.85	.84	1.03	1.11	1.23	1.24	1.26	1.18	1.04	.96	.84	.82
40	.84	.83	1.03	1.11	1.24	1.25	1.27	1.18	1.04	.96	.83	.81
41	.83	.83	1.03	1.11	1.25	1.26	1.27	1.19	1.04	.96	.82	.80
42	.82	.83	1.03	1.12	1.26	1.27	1.28	1.19	1.04	.95	.82	.79
43	.81	.82	1.02	1.12	1.26	1.28	1.29	1.20	1.04	.95	.81	.77
44	.81	.82	1.02	1.13	1.27	1.29	1.30	1.20	1.04	.95	.80	.76
45	.80	.81	1.02	1.13	1.28	1.29	1.31	1.21	1.04	.94	.79	.75
46	.79	.81	1.02	1.13	1.29	1.31	1.32	1.22	1.04	.94	.79	.74
47	.77	.80	1.02	1.14	1.30	1.32	1.33	1.22	1.04	.93	.78	.73
48	.76	.80	1.02	1.14	1.31	1.33	1.34	1.23	1.05	.93	.77	.72
49	.75	.79	1.02	1.14	1.32	1.34	1.35	1.24	1.05	.93	.76	.71
50	.74	.78	1.02	1.15	1.33	1.36	1.37	1.25	1.06	.92	.76	.70

Lat. South	Jan	Feb	Mar	Apr	May	June	July	Aug	Sep	Oct	Nov	Dec
5	1.06	.95	1.04	1.00	1.02	.99	1.02	1.03	1.00	1.05	1.03	1.06
10	1.08	.97	1.05	.99	1.01	.96	1.00	1.01	1.00	1.06	1.05	1.10
15	1.12	.98	1.05	.98	.98	.94	.97	1.00	1.00	1.07	1.07	1.12
20	1.14	1.00	1.05	.97	.96	.91	.95	.99	1.00	1.08	1.09	1.15
25	1.17	1.01	1.05	.96	.94	.88	.93	.98	1.00	1.10	1.11	1.18
30	1.20	1.03	1.06	.95	.92	.85	.90	.96	1.00	1.12	1.14	1.12
35	1.23	1.04	1.06	.94	.89	.82	.87	.94	1.00	1.13	1.17	1.25
40	1.27	1.06	1.07	.93	.86	.78	.84	.92	1.00	1.15	1.20	1.29
42	1.28	1.07	1.07	.92	.85	.76	.82	.92	1.00	1.16	1.22	1.31
44	1.30	1.08	1.07	.92	.83	.74	.81	.91	.99	1.17	1.23	1.33
46	1.32	1.10	1.07	.91	.82	.72	.79	.90	.99	1.17	1.25	1.35
48	1.34	1.11	1.08	.90	.80	.70	.76	.89	.99	1.18	1.27	1.37
50	1.37	1.12	1.08	.89	.77	.67	.74	.88	.99	1.19	1.29	1.41

Appendix C

TABLE C.1: Observation Head Values

Well No.	EAST	NORTH	*SWL (m)	**DWL (m)	Q (m³/d)
PW01	447551.366	3537632.56	7.22	20.84	0
PW02	438640.327	3546815.877	14.64	21.38	0
PW03	436785.632	3560209.296	14.9	22.02	785
PW04	441762.6	3542449.2	18.55	19.69	0
PW05	442554.659	3543406.153	17.9	19.31	0
PW06	448666.605	3559894.631	17.4	21.15	860
PW07	442394.1	3538134.9	20.7	19.67	0
PW08	438670.2	3551704.9	19.8	20.33	0
PW09	445189.974	3560990.008	18	22.53	750
PW10	435627.913	3544733.975	23.26	22.75	0
PW11	435045.828	3546384.979	23.86	22.39	0
PW12	446143.188	3537330.807	22	17.72	1020
PW13	448748.837	3545362.224	20.5	16.39	3256
PW14	442825.528	3544944.134	22	17.95	977
PW15	441604.4	3543869.5	24.32	15.62	940
PW16	441500.2	3544269.8	24.42	25.37	1029
PW17	439194.4	3551704.9	24.5	20.47	1085
PW18	441091	3544269.8	25.51	16.36	800
PW19	438276.6	3539489.4	27.9	27.24	940
PW20	437027.038	3540359.743	28.27	14.09	840
PW21	436502.306	3540362.992	28.26	22.14	1100
PW22	437878.2	3550785.9	27	20.11	912
PW23	435395.016	3543695.302	29.35	22.74	760
PW24	437059.313	3554061.335	27.4	20.3	1020
PW25	436213.8	3545809.9	30.1	24.28	1120
PW26	442416.9	3537518.9	29	24.75	985
PW27	439272.8	3544952.2	29.85	18.34	645
PW28	435722.833	3549911.704	30.74	19.71	435
PW29	438000.5	3546267.1	30.8	28.76	870
PW30	432833.5	3544931.4	32.56	22.65	1153
PW31	435971.949	3552005.139	31.3	18.2	746
PW32	444762.174	3551112.563	29.25	22.56	442
PW33	437097.6	3551714.5	32.85	18.94	640
PW34	434685.209	3543453.501	34.5	26.39	800
PW35	435710.818	3543847.261	34.4	26.37	1140
PW36	436157.676	3543998.408	34.3	28.42	921
PW37	440687.582	3548135.994	34.85	22.05	0
PW38	438716.432	3557621.326	34.85	22.99	355
PW39	436241.4976	3552520.179	34.1	31.42	742
PW40	435679.105	3547142.048	35.1	29.31	840
PW41	436166.005	3553697.419	33.9	18.94	873

Well No.	EAST	NORTH	*SWL (m)	**DWL (m)	Q (m³/d)
PW42	447646.138	3560492.061	31.75	22.02	302
PW43	435738.195	3548188.563	35.4	20.44	540
PW44	435686.947	3548876.829	40.5	21.3	0
PW45	434730.588	3550535.07	36.8	23.26	470
PW46	434275.5448	3557097.545	37.7	21.31	942
PW47	434327.1396	3558483.846	37.8	33.13	793
PW48	433580.234	3559130.347	38.4	23	622
PW49	438451.849	3545437.239	39.5	20.84	0
PW50	432282.2334	3558052.808	40.5	25.1	1185
PW51	425346.3281	3550000.78	41.4	38.2	924
PW52	425784.8048	3551136.833	41.4	39.19	1030
PW53	424329.859	3554166.309	42.9	31.8	1200
PW54	428056.9118	3551953.994	44	28.31	1010
PW55	423193.8057	3551655.033	43.9	31.1	976
PW56	422775.2597	3552551.917	44.2	31.71	1129
PW57	422456.3675	3551734.756	44.4	33.9	837
PW58	422217.1983	3551077.041	45.1	33.56	1043
PW59	424927.3508	3552961.273	46.35	41.77	866
PW60	424289.9976	3552272.887	47.3	31.16	650
PW61	436414.553	3558507.682	46.9	22.34	470
PW62	421180.7987	3553408.94	46	40.64	869
PW63	421280.4525	3554066.655	45.95	40.8	992
PW64	423578.0839	3558889.9	49.13	39.1	1163
PW65	422205.8175	3558459.719	49.54	43.2	1089
PW66	418749.2457	3558810.177	48.3	48.91	1197
PW67	420782.1834	3558132.531	49.95	45.3	1152
PW68	418709.3841	3555681.047	50.75	48.34	1222
PW69	442786	3537824.7	55	19.41	0

*SWL: Static Water Level

**DWL: Dynamic Water Level

TABLE C.2: Temperature Totals (C°)

Year	Jan	Feb	Mar	Apr	May	Jun	Jul	Aug	Sep	Oct	Nov	Dec
1980	9.8	10.8	19.7	32	28.8	37	42.5	44.8	35.2	30.5	19.5	20.2
1981	8.2	20.2	23.5	29.5	32.1	36.7	42.8	45.5	37	29.6	16.5	19
1982	13.6	15.6	23	29.6	32.2	38.4	48.4	42.6	35.9	29	16.7	17.9
1983	16	17	21	30.2	30.8	34.5	45.6	44.5	38.2	30.3	21.8	17
1984	12.5	11.2	24.1	35	30.7	36.5	45.6	42.6	36.3	28.5	21.2	18.5
1985	8.7	12.8	27.2	30.5	29.8	36.5	45.2	47.4	37.4	28.9	23.2	18.7
1986	7.6	11.3	20.2	30.2	29.9	35	44.4	42	37.7	26.1	16	14
1987	7	11.4	18.5	27.6	30.6	33.5	44.9	43.8	35.3	29.8	21	20.8
1988	8.4	13.8	22	30	31	34	43.2	40.3	33.9	30.6	21.2	13.4
1989	11.2	16.3	24.2	28.8	31.5	34.2	41.6	45.4	36.8	29.4	19.8	17.5
1990	11.3	12.8	19.2	28.8	30.8	33	44.6	47.3	38.4	30	24.5	18
1991	16	19.2	16.6	31.2	32.7	38.2	45.1	46.8	36.2	30.2	17.2	19.4
1992	9.5	12.5	22	28	30.6	36.3	47.4	42.9	37.2	29.4	19.9	20.8
1993	9.8	13.6	21.7	31.6	33.5	36.1	45.5	43.5	35.2	29.5	23.4	24.5
1994	10	16.4	23.7	31.3	31.4	37.1	44.6	49.2	37.2	27.3	19.2	21.9
1995	8.5	13.7	17	27.7	33.2	34	43.8	44.5	36.2	27	20.7	17.2
1996	12.8	14.7	22	31.2	32.4	37.5	45	47.5	38.2	29.6	21.4	22.2
1997	11	14.6	22.5	33	35	36.4	43	46	35.7	28	18.3	12.5
1998	11.8	12.5	20	30	33.5	35.8	42.4	44	38.7	32.4	19.4	16.7
1999	10.4	13.8	22	35	33.4	37.6	45.7	45.7	38	30.5	19	21.2
2000	12.2	13.2	18	33.7	33	38	43.2	44.2	36.3	29.2	17.3	16.6
2001	9.1	12.6	17.6	32.5	32.6	37.7	46.4	48	38.8	31.3	25	23.6
2002	11	15	23.4	32.5	35.8	37.5	44.8	46	37.3	32.2	20.8	16.7
2003	10.5	13.6	21.3	32.2	31.6	38	48.4	46.8	35.5	27.6	18	16.2
2004	10	16.2	28	33	32.5	35.7	46	48.6	37	29.6	26	22.5
2005	8	14.4	26	28.2	33.4	38.2	46	45.7	37.7	32	19.3	18.2
2006	12.5	15.8	20	33	30.8	36.6	44.6	48.4	38	30	24.5	15
2007	9.3	15.2	29	30.3	33.2	36	47.2	43.7	41.8	32.5	20.2	16
2008	10.8	15	23.5	33.6	31.8	39	47	46.8	37.5	32.4	19.8	22.6
2009	11.5	18	22.2	30.8	34.4	38.5	44.8	47.6	37.4	32.2	22	17
2010	10	14.6	19.6	29.5	35	37.5	48	48	41.3	31.9	25.5	20.2
2011	9.5	14	30.5	34.7	33.5	39.5	48	48	42	31	19	20
2012	12.2	15	22.4	32	33.8	39	44.8	47.8	36.6	30.4	23	19.4
2013	14.2	21.5	30.2	30.2	32.9	40	46.7	48.6	38.6	31.4	22.3	21.6
2014	13.4	18.1	20.2	28.4	28.3	37	44.4	45.3	37.6	29.4	20.5	18.2

TABLE C.3: Monthly Rainfall Totals (mm)

Year	Jan	Feb	Mar	Apr	May	Jun	Jul	Aug	Sep	Oct	Nov	Dec	Total
1980	4.1	58.4	3.7	2.4	1.0	0.0	0.0	0.0	0.0	0.4	21.4	9.0	100.4
1981	14.5	7.5	22.9	0.0	0.0	0.0	0.0	0.0	0.0	0.0	2.5	8.6	56.0
1982	61.5	14.4	9.5	35.1	22.1	0.0	0.0	0.0	0.0	23.8	8.3	7.8	182.5
1983	1.0	2.1	4.3	31.0	31.0	0.0	0.0	0.0	0.0	0.0	5.1	45.4	119.9
1984	9.3	0.7	12.6	0.5	15.5	0.0	0.0	0.0	0.0	1.8	91.3	13.7	145.4
1985	19.5	1.7	13.2	0.4	2.3	0.0	0.0	0.0	0.0	0.0	1.8	19.9	58.8
1986	6.0	60.3	15.4	9.2	7.5	0.0	0.0	0.0	0.0	0.0	34.0	0.2	132.6
1987	0.0	7.8	46.6	0.0	0.0	0.0	0.0	0.0	0.0	11.3	16.5	77.1	159.3
1988	34.6	13.5	30.7	44.7	0.0	0.0	0.0	0.0	0.0	0.0	12.1	29.5	165.1
1989	3.2	64.5	31.6	0.0	3.8	0.0	0.0	0.0	0.0	0.0	8.6	0.6	112.3
1990	8.9	18.1	3.1	2.5	0.0	0.0	0.0	0.0	0.0	0.0	0.2	3.6	36.4
1991	7.6	15.4	6.7	0.0	0.0	0.0	0.0	0.0	0.0	6.6	4.0	12.2	52.5
1992	3.5	6.2	19.5	13.7	1.2	0.0	0.0	0.0	0.0	0.0	56.3	25.9	126.3
1993	34.7	23.5	0.5	89.8	7.1	0.0	0.0	0.0	0.0	1.8	10.5	2.1	170.0
1994	27.0	3.5	8.1	4.2	0.6	0.0	0.0	0.0	0.0	18.9	62.2	23.1	147.6
1995	2.6	17.0	8.7	23.8	0.3	0.0	0.0	0.0	0.0	0.0	6.2	5.5	64.1
1996	40.0	14.3	25.1	4.7	3.2	0.0	0.0	0.0	0.0	0.0	0.8	3.2	91.3
1997	12.8	0.7	10.9	4.1	0.6	0.0	0.0	0.0	0.0	33.0	53.9	26.9	142.9
1998	32.5	18.4	32.9	2.1	0.8	0.0	0.0	0.0	0.0	0.0	9.0	0.0	95.7
1999	35.5	7.8	3.7	0.0	0.0	0.0	0.0	0.0	0.0	0.0	6.0	12.1	65.1
2000	10.0	1.6	0.3	1.5	0.0	0.0	0.0	0.0	0.0	5.4	34.09	10.0	62.9
2001	12.1	9.9	4.0	25.7	1.4	0.0	0.0	0.0	0.0	0.4	2.2	19.3	75.0
2002	5.0	4.5	9.3	23.3	4.0	0.0	0.0	0.0	0.0	0.4	5.3	12.4	64.2
2003	6.1	0.0	0.4	6.8	2.0	0.0	0.0	0.0	0.0	0.5	37.93	20.4	74.1
2004	38.6	1.2	1.0	4.4	7.2	0.0	0.0	0.0	0.0	0.0	11.1	1.7	65.2
2005	38	9.7	12.8	12.4	0.2	0.0	0.0	0.0	0.0	0.3	6.6	2.0	82.0
2006	25.5	43.3	4.2	36.6	11.3	0.0	0.0	0.0	0.0	2.8	27.1	44.1	194.9
2007	36.0	2.4	5.6	8.3	2.3	0.0	0.0	0.0	0.0	0	4.5	12.8	71.9
2008	28.4	1.0	0.5	0.2	2.0	0.0	0.0	0.0	0.0	28.8	0.5	19.8	81.2
2009	3.4	5.8	19.5	16.8	0.2	0.0	0.0	0.0	0.0	7.4	31.5	9.5	94.1
2010	2.7	14.8	5.9	13.4	8.6	0.0	0.0	0.0	0.0	0.0	0.0	4.9	50.3
2011	35.6	19.8	4.8	21.9	1.6	0.0	0.0	0.0	0.0	0.3	3.400	1.1	88.5
2012	0.2	3.9	2.8	0.2	1.7	0.0	0.0	0.0	0.0	2.4	15.7	21.9	48.8
2013	27.6	3.2	4	2.1	20.0	0.0	0.0	0.0	0.0	1.9	60.6	0.1	119.5
2014	37.7	2.6	26.3	12.6	0.001	0.001	0.0	0.0	0.0	2.9	16.0	1.8	99.9
Mean	19.0	13.7	11.7	13.0	4.6	0.0	0.0	0.0	0.0	4.3	19.1	14.5	99.9

TABLE C.4: Daily Rainfall (mm)

Days	Jan	Feb	Mar	Apr	May	Jun	Jul	Aug	Sep	Oct	Nov	Dec
											Year: 2009	
1			0.001								1.0	
2												
3												
4					0.001							
5					0.001							
6				0.2								
7				2.5								
8				12.6								0.001
9			6.4		0.001							
10	0.001	5.8										
11	0.001											
12												9.5
13			0.001		0.200						10.1	
14					0.001							
15												
16					0.001						3.5	0.001
17											0.001	
18											3.600	
19	3.4											
20												
21												
22												
23		0.001										
24		0.001								7.4	0.6	
25										0.001	7.300	
26												
27				1.5							5.4	
28												
29			6.8									
30			6.3							0.001		
31										0.001		
SUM	3.4	5.8	19.5	16.8	0.2	0.0	0.0	0.0	0.0	7.4	31.5	9.5
No. of Storms	3	3	5	4	6	0	0	0	0	4	8	3
MAX. / Day	3.4	5.8	6.8	12.6	0.2	0.0	0.0	0.0	0.0	7.4	10.1	9.5

248

Days	Jan	Feb	Mar	Apr	May	Jun	Jul	Aug	Sep	Oct	Nov	Dec
1					8.6							
2												
3		1.0										
4												
5		0.3										
6		1.5										
7				3.7								
8												
9												
10												
11												0.4
12				7.6								1.1
13				0.7	0.001							
14												
15												
16		0.001		0.001								
17												
18	0.001	0.5	0.001									0.001
19												
20	2.7											
21				0.001								
22				1.4								
23			0.8									0.001
24			0.7									
25	0.001	0.6										
26		0.001	4.4									
27			0.001									
28		10.9										
29												
30	0.001		0.001									3.3
31												0.1
SUM	2.7	14.8	5.9	13.4	8.6	0.0	0.0	0.0	0.0	0.0	0.0	4.9
No. of Storms	4	8	6	6	2	0	0	0	0	0	0	6
MAX. / Day	2.7	10.9	4.4	7.6	8.6	0.0	0.0	0.0	0.0	0.0	0.0	3.3

Year: 2010

249

Days	Jan	Feb	Mar	Apr	May	Jun	Jul	Aug	Sep	Oct	Nov	Dec
Year: 2011												
1		9.8										
2		0.3										
3	1.5											
4	0.001	2.8									0.001	
5		1.7										
6					1.6							
7		4.8										
8	5.400	0.3										
9	3.700											
10												
11											1.4	
12			0.001									
13												
14	5.2											
15	2.8											0.001
16												
17												
18												
19				0.001								
20				0.001								
21			0.001	2.3							2.000	
22			3.1									
23												
24			0.7	3.0								
25	8.0	0.1	1.0									
26	4.4			2.8						0.001		
27										0.1		
28				0.001						0.2		
29	1.5			0.001								
30	3.1			13.8								0.1
31												1.0
SUM	35.6	19.8	4.8	21.9	1.6	0.0	0.0	0.0	0.0	0.3	3.4	1.1
No. of Storms	10	7	5	8	1	0	0	0	0	3	3	3
MAX. / Day	8.0	9.8	3.1	13.8	1.6	0.0	0.0	0.0	0.0	0.2	2.0	1.0

					Year: 2012							
Days	Jan	Feb	Mar	Apr	May	Jun	Jul	Aug	Sep	Oct	Nov	Dec
1												
2			0.2									
3					1.7							
4			0.001									0.001
5												
6		0.001										
7	0.001											
8	0.001											
9										0.001		
10				0.2							0.001	
11				0.001							1.0	
12												
13											0.5	
14		0.3										
15		0.1										
16												
17											0.1	
18											2.0	0.4
19	0.001									0.001	0.3	3.3
20												
21												
22											5.8	
23											1.0	
24		0.5								0.001		0.001
25	0.001	3.0								0.7	5.0	18.2
26										1.7		
27												
28												
29			2.6									
30	0.1		0.001									
31	0.1											
SUM	0.2	3.9	2.8	0.2	1.7	0.0	0.0	0.0	0.0	2.4	15.7	21.9
No. of Storms	6	5	4	2	1	0	0	0	0	5	9	5
MAX. / Day	0.1	3.0	2.6	0.2	1.7	0.0	0.0	0.0	0.0	1.7	5.8	18.2

Days	Jan	Feb	Mar	Apr	May	Jun	Jul	Aug	Sep	Oct	Nov	Dec
Year: 2013												
1		0.1			2.2						12.4	
2					3.3						3.0	
3					9.1							0.001
4				0.001	3.0							0.001
5												
6		3.0										
7			2.2									
8		0.1									7.7	
9	0.5		0.001								0.1	
10											0.001	
11												
12				0.8	1.2						0.001	
13			0.7									
14					0.001							
15				0.001	1.2					1.9		
16												
17											4.0	
18	0.001										4.2	0.001
19												
20				1.3							0.2	
21												
22	0.4	0.001										
23											29.0	
24												
25	0.001		1.1									
26	0.5									0.001		
27	1.2											
28	24.1											
29	0.8											0.001
30				0.001								0.1
31	0.1											
SUM	27.6	3.2	4.0	2.1	20.0	0.0	0.0	0.0	0.0	1.9	60.6	0.1
No. of Storms	9	4	4	5	7	0	0	0	0	2	10	5
MAX. / Day	24.1	3.0	2.200	1.3	9.1	0.0	0.0	0.0	0.0	1.9	29.0	0.1

Days	Jan	Feb	Mar	Apr	May	Jun	Jul	Aug	Sep	Oct	Nov	Dec
Year: 2014												
1				0.001	0.001	0.001						
2		0.001	0.001	12.0								
3		2.6	2.1									
4	1.2											
5	2.5											
6												
7				0.001								
8			1.1		0.001							
9	2.1		0.2			0.001						0.6
10	2.7		0.001									
11			2.7									
12			2.9	0.4						0.2		
13												0.6
14			13.3	0.001						0.001		0.001
15	1.1	0.001	3.8							1.7		
16		0.001									0.001	
17	22.2											
18												
19			0.2							0.7		
20										0.3	0.001	
21											6.1	
22												
23												
24											8.9	
25											1.0	
26	0.6			0.001								
27	5.3									0.001		0.001
28	0.001			0.2							0.001	0.6
29			0.001									
30			0.001									
31												
SUM	37.7	2.6	26.3	12.6	0.0	0.0	0.0	0.0	0.0	2.9	16.0	1.8
No. of Storms	9	4	12	7	2	2	0	0	0	6	6	5
MAX. / Day	22.2	2.6	13.3	12	0.0	0.0	0.0	0.0	0.0	1.7	8.9	0.6

TABLE C.5: Monthly Soil Moisture (mm)

Year	Jan	Feb	Mar	Apr	May	Jun	Jul	Aug	Sep	Oct	Nov	Dec
1980	21.46	24.62	34.36	46.65	32.51	27.45	19.59	18.87	15.57	15.64	17.5	35.72
1981	43.56	55.07	65.01	73.9	57.56	47.1	34.01	29.22	23.02	21.39	31.02	42.52
1982	58.16	58.37	56.56	76.98	73.46	59.45	42.74	35.67	27.72	30.19	42.83	54.57
1983	77.31	104.77	104.26	106.6	84.91	67.9	48.84	40.07	31.37	28.54	26.35	32.32
1984	32.06	33.12	38.56	48.05	34.76	29.95	21.89	20.72	16.87	26.04	51.7	72.42
1985	43.71	31.92	20.76	33.15	31.06	39.35	45.89	61.37	72.47	78.74	75	73.42
1986	43.86	59.17	57.96	69.75	57.36	47.15	34.09	29.32	23.07	24.39	30.75	42.02
1987	39.86	37.92	41.91	51.15	36.56	31.7	23.29	21.52	17.57	21.34	22	30.17
1988	60.71	38.32	39.56	54.7	43.76	36.25	26.04	23.57	19.07	20.14	19.8	35.67
1989	43.91	53.37	49.21	54.95	38.86	32.35	23.19	31.52	17.37	17.14	30	46.22
1990	43.96	52.92	63.56	66.15	49.36	40.9	30.04	26.57	21.32	20.64	19.1	21.02
1991	22.66	31.02	44.66	55.3	39.96	33.6	29.79	46.17	46.32	39.74	32.2	33.72
1992	34.81	43.97	49.36	55.65	40.81	34.3	24.74	22.67	18.32	17.89	20.45	24.67
1993	34.16	27.72	25.66	38.35	34.16	31.25	22.29	20.82	16.97	16.94	17.9	23.72
1994	22.61	36.02	43.26	46.7	33.21	28.45	20.49	19.62	16.67	17.24	25.5	39.02
1995	37.36	43.02	45.61	51.1	37.61	31.9	23.04	21.37	17.57	17.34	18	22.52
1996	21.01	24.42	28.66	41.25	29.96	26.15	18.69	18.22	14.87	15.14	17.2	24.82
1997	29.96	34.92	35.36	42.4	29.96	26.1	18.79	18.47	15.37	17.84	23.13	50.07
1998	53.81	59.12	61.66	66.75	49.96	40.85	29.19	25.72	20.47	19.44	17.7	19.52
1999	18.79	22.92	23.56	30.85	20.96	19.35	13.89	18.42	17.47	18.04	16.9	21.82
2000	20.61	20.42	19.06	27.85	19.56	18.65	13.29	14.42	12.37	13.64	23.25	22.72
2001	29.36	36.87	40.56	47.7	35.06	30.05	21.49	20.17	16.57	16.94	16.7	20.82
2002	23.31	26.82	27.76	38.75	28.26	24.65	17.59	26.52	31.37	27.84	25.7	28.02
2003	27.11	28.62	27.06	36.25	26.06	23.05	16.39	16.52	13.87	14.54	27.05	27.22
2004	38.76	34.42	33.16	41.95	30.96	26.65	19.09	18.42	15.17	15.24	16.9	22.52
2005	22.61	26.32	30.06	39.15	27.36	23.95	17.09	17.12	14.17	14.64	15.4	20.42
2006	19.81	24.24	25.96	39.45	31.81	27.35	19.49	18.72	15.37	18.54	20.2	23.92
2007	24.41	29.42	30.96	41.35	30.56	26.25	18.89	18.22	14.97	15.14	14.2	18.22
2008	28.48	25.02	24.86	32.15	22.16	19.95	14.49	15.22	13.47	15.94	19	23.92
2009	24.48	28.7	26.06	25.96	22.09	19.05	17.84	17.3	14.45	10.74	15.75	22.04
2010	27.38	34.5	32.16	31.66	26.99	22.65	20.54	19.2	15.75	11.44	14.35	17.34
2011	20.02	26.4	29.06	28.86	23.39	19.95	18.54	17.9	14.75	10.84	12.85	15.24
2012	17.18	24.32	24.96	29.16	27.84	23.35	20.94	19.5	15.95	14.74	17.65	18.74
2013	21.78	29.5	29.96	31.06	26.59	22.25	20.34	19	15.55	11.34	11.65	13.04
2014	17.08	25.1	23.86	21.86	18.19	15.95	15.94	16	14.05	12.14	16.45	18.74

TABLE C.6: Monthly Change in Soil Moisture (mm)

Year	Jan	Feb	Mar	Apr	May	Jun	Jul	Aug	Sep	Oct	Nov	Dec	Sum
1980	0	3.16	9.74	12.29	-14.14	-5.06	-7.86	-0.72	-3.3	0.07	1.86	18.22	14.26
1981	7.84	11.51	9.94	8.89	-16.34	-10.46	-13.09	-4.79	-6.2	-1.63	9.63	11.5	6.8
1982	15.64	0.21	-1.81	20.42	-3.52	-14.01	-16.71	-7.07	-7.95	2.47	12.64	11.74	12.05
1983	22.74	27.46	-0.51	2.34	-21.69	-17.01	-19.06	-8.77	-8.7	-2.83	-2.19	5.97	-22.25
1984	-0.26	1.06	5.44	9.49	-13.29	-4.81	-8.06	-1.17	-3.85	9.17	25.66	20.72	40.1
1985	-28.71	-11.79	-11.16	12.39	-2.09	8.29	6.54	15.48	11.1	6.27	-3.74	-1.58	1
1986	-29.56	15.31	-1.21	11.79	-12.39	-10.21	-13.06	-4.77	-6.25	1.32	6.36	11.27	-31.4
1987	-2.16	-1.94	3.99	9.24	-14.59	-4.86	-8.41	-1.77	-3.95	3.77	0.66	8.17	-11.85
1988	30.54	-22.39	1.24	15.14	-10.94	-7.51	-10.21	-2.47	-4.5	1.07	-0.34	15.87	5.5
1989	8.24	9.46	-4.16	5.74	-16.09	-6.51	-9.16	8.33	-14.15	-0.23	12.86	16.22	10.55
1990	-2.26	8.96	10.64	2.59	-16.79	-8.46	-10.86	-3.47	-5.25	-0.68	-1.54	1.92	-25.2
1991	1.64	8.36	13.64	10.64	-15.34	-6.36	-3.81	16.38	0.15	-6.58	-7.54	1.52	12.7
1992	1.09	9.16	5.39	6.29	-14.84	-6.51	-9.56	-2.07	-4.35	-0.43	2.56	4.22	-9.05
1993	9.49	-6.44	-2.06	12.69	-4.19	-2.91	-8.96	-1.47	-3.85	-0.03	0.96	5.82	-0.95
1994	-1.11	13.41	7.24	3.44	-13.49	-4.76	-7.96	-0.87	-2.95	0.57	8.26	13.52	15.3
1995	-1.66	5.66	2.59	5.49	-13.49	-5.71	-8.86	-1.67	-3.8	-0.23	0.66	4.52	-16.5
1996	-1.51	3.41	4.24	12.59	-11.29	-3.81	-7.46	-0.47	-3.35	0.27	2.06	7.62	2.3
1997	5.14	4.96	0.44	7.04	-12.44	-3.86	-7.31	-0.32	-3.1	2.47	5.29	26.94	25.25
1998	3.74	5.31	2.54	5.09	-16.79	-9.11	-11.66	-3.47	-5.25	-1.03	-1.74	1.82	-30.55
1999	-0.73	4.13	0.64	7.29	-9.89	-1.61	-5.46	4.53	-0.95	0.57	-1.14	4.92	2.3
2000	-1.21	-0.19	-1.36	8.79	-8.29	-0.91	-5.36	1.13	-2.05	1.27	9.61	-0.53	0.9
2001	6.64	7.51	3.69	7.14	-12.64	-5.01	-8.56	-1.32	-3.6	0.37	-0.24	4.12	-1.9
2002	2.49	3.51	0.94	10.99	-10.49	-3.61	-7.06	8.93	4.85	-3.53	-2.14	2.32	7.2
2003	-0.91	1.51	-1.56	9.19	-10.19	-3.01	-6.66	0.13	-2.65	0.67	12.51	0.17	-0.8
2004	11.54	-4.34	-1.26	8.79	-10.99	-4.31	-7.56	-0.67	-3.25	0.07	1.66	5.62	-4.7
2005	0.09	3.71	3.74	9.09	-11.79	-3.41	-6.86	0.03	-2.95	0.47	0.76	5.02	-2.1
2006	-0.61	4.43	1.72	13.49	-7.64	-4.46	-7.86	-0.77	-3.35	3.17	1.66	3.72	3.5
2007	0.49	5.01	1.54	10.39	-10.79	-4.31	-7.36	-0.67	-3.25	0.17	-0.94	4.02	-5.7
2008	10.26	-3.46	-0.16	7.29	-9.99	-2.21	-5.46	0.73	-1.75	2.47	3.06	4.92	5.7
2009	0.56	4.22	-2.64	-0.1	-3.87	-3.04	-1.21	-0.54	-2.85	-3.71	5.01	6.29	-1.88
2010	5.34	7.12	-2.34	-0.5	-4.67	-4.34	-2.11	-1.34	-3.45	-4.31	2.91	2.99	-4.7
2011	2.68	6.38	2.66	-0.2	-5.47	-3.44	-1.41	-0.64	-3.15	-3.91	2.01	2.39	-2.1
2012	1.94	7.14	0.64	4.2	-1.32	-4.49	-2.41	-1.44	-3.55	-1.21	2.91	1.09	3.5
2013	3.04	7.72	0.46	1.1	-4.47	-4.34	-1.91	-1.34	-3.45	-4.21	0.31	1.39	-5.7
2014	4.04	8.02	-1.24	-2	-3.67	-2.24	-0.01	0.06	-1.95	-1.91	4.31	2.29	5.7

TABLE C.7: Monthly Mean Sun Shine Duration in Hours / Day

Year	Jan	Feb	Mar	Apr	May	Jun	Jul	Aug	Sep	Oct	Nov	Dec	Mean
1980	6.8	7.0	7.5	8.7	9.8	11.8	11.5	11.3	10.2	8.3	7.2	6.6	8.9
1981	6.6	6.9	8.2	8.8	8.2	11.6	11.4	10.6	9.5	8.3	7.5	5.7	8.6
1982	5.4	5.9	7.9	6.8	8.1	11.6	11.5	11.1	9.2	8.5	7.6	5.7	8.3
1983	6.4	7.5	8.3	8.4	7.0	10.4	11.9	11.4	10.6	9.4	7.6	6.6	8.8
1984	7.2	7.9	6.6	9.1	9.8	11.9	10.6	11.5	10.4	7.8	6.4	7.5	8.9
1985	6.7	8.0	7.8	9.1	10.0	12.5	12.5	11.4	10.6	9.4	7.0	6.5	9.3
1986	6.7	7.6	8.6	8.7	10.0	12.2	12.0	11.4	10.5	7.7	6.7	7.0	9.1
1987	8.2	8.3	7.9	9.7	7.8	10.3	11.9	10.5	9.5	7.8	7.9	6.2	8.8
1988	6.8	7.2	7.8	7.1	11.4	12.1	12.4	11.3	10.4	8.4	6.6	6.0	9.0
1989	7.3	7.2	7.0	9.5	9.7	12.4	12.4	11.5	10.5	9.1	7.1	7.2	9.2
1990	6.4	7.5	8.6	8.6	10.6	12.2	12.0	11.5	10.7	8.4	7.7	7.0	9.3
1991	6.3	7.2	8.1	8.4	9.3	11.4	11.1	10.9	9.9	7.3	7.5	5.7	8.6
1992	6.1	5.8	7.2	8.1	7.9	10.1	10.8	10.7	9.7	9.4	6.9	5.7	7.4
1993	6.4	7.1	8.1	7.6	7.2	11.7	11.4	11.1	10.0	8.0	7.7	6.8	8.6
1994	5.7	7.9	7.2	7.9	8.9	11.2	11.5	11.3	9.4	7.4	6.6	6.2	8.4
1995	6.4	7.6	8.8	8.7	10.4	11.2	11.8	11.4	10.4	9.1	8.4	3.3	9.0
1996	5.9	5.9	8.1	8.4	9.3	11.4	11.4	11.1	10.0	7.7	6.7	7.0	8.6
1997	6.7	7.6	8.6	7.1	11.4	12.1	12.4	11.5	10.7	8.4	6.6	6.0	9.1
1998	6.4	8.4	7.6	9.9	11.2	12.4	12.2	10.5	10.6	8.8	7.6	6.1	9.3
1999	6.7	6.4	8.9	10.5	10.7	12.2	12.0	10.9	10.7	8.8	8.3	5.7	9.3
2000	6.5	7.8	8.1	7.1	10.6	11.3	10.3	10.9	10.2	8.4	7.2	6.2	8.7
2001	6.7	8.0	8.2	9.0	10.2	12.0	11.9	10.5	10.1	9.5	7.7	5.3	9.1
2002	6.4	8.5	8.3	7.6	10.8	11.8	11.9	11.4	10.0	7.5	7.3	4.2	8.8
2003	7.3	7.2	7.6	10.5	10.7	10.8	11.9	11.4	11.0	8.5	6.3	5.1	9.0
2004	5.6	7.8	9.0	8.8	10.0	11.9	11.6	10.2	10.8	8.3	6.5	6.0	8.9
2005	6.4	7.3	8.3	9.4	10.2	10.7	10.9	10.7	10.6	8.5	8.0	6.5	9.0
2006	5.8	6.4	8.4	8.4	9.7	11.9	11.3	10.3	10.6	9.2	8.0	5.9	8.8
2007	5.9	7.1	8.0	6.7	9.2	11.7	11.9	11.2	10.5	8.5	8.0	6.8	8.8
2008	4.8	6.5	7.8	7.4	8.8	9.4	10.9	10.5	8.4	7.6	7.9	6.5	8.0
2009	6.9	6.0	7.1	7.7	8.2	9.1	10.2	10.2	9.8	7.3	5.5	5.1	7.8
2010	6.5	7.3	6.5	7.0	7.5	9.7	10.3	10.4	8.8	7.8	7.9	5.9	8.0
2011	5.2	6.0	8.0	6.7	8.3	9.7	10.3	10.5	9.7	8.3	7.1	6.8	8.1
2012	6.4	6.6	7.9	7.9	6.2	10.4	10.6	10.5	10.1	5.8	5.5	6.1	7.8
2013	5.8	7.5	7.3	8.8	7.5	10.4	10.9	10.7	9.8	8.5	5.0	6.0	8.2
2014	8.3	9.4	7.9	8.4	9.2	9.7	10.6	10.6	10.3	7.6	6.5	6.4	8.7

TABLE C.8: Monthly Mean of Incoming Radiation in *Mw/cm²

Year	Jan	Feb	Mar	Apr	May	Jun	Jul	Aug	Sep	Oct	Nov	Dec	Mean
1980	291.8	325.6	530.4	586.1	668.0	773.1	736.4	678.2	580.1	445.9	332.9	283.0	**519.3**
1981	295.8	371.5	493.0	600.0	654.4	751.2	751.2	685.5	576.8	439.2	330.6	274.3	**518.6**
1982	244.2	351.0	501.3	505.3	605.0	711.7	726.2	655.1	528.3	425.4	325.8	274.5	**487.8**
1983	303.4	400.2	477.2	558.6	557.4	687.9	693.1	651.6	579.4	475.8	336.4	264.3	**498.8**
1984	308.4	402.7	424.6	548.7	606.3	678.2	632.6	648.9	579.6	425.4	286.5	288.7	**485.9**
1985	289.4	398.9	498.7	550.6	637.1	740.4	719.6	689.9	634.7	510.7	358.0	306.7	**527.9**
1986	334.0	390.1	525.6	578.8	680.0	760.6	736.7	657.7	584.8	417.2	324.0	292.0	**523.5**
1987	359.3	451.0	499.9	633.0	605.9	699.0	714.7	648.7	555.5	418.8	360.0	266.1	**517.7**
1988	298.1	373.6	491.1	539.5	700.4	724.7	742.5	675.5	624.8	444.5	334.3	288.7	**519.8**
1989	351.0	419.7	467.2	617.8	667.7	752.5	748.0	673.7	602.8	468.6	330.5	291.4	**532.6**
1990	260.5	344.2	464.1	579.0	687.8	715.4	719.6	614.4	511.8	439.3	286.5	281.0	**492.0**
1991	308.4	402.7	424.6	548.7	680.0	760.6	736.7	569.5	492.6	330.8	268.6	219.7	**478.6**
1992	223.0	289.9	426.3	527.8	605.1	691.1	695.2	624.4	480.5	400.6	253.5	179.6	**449.8**
1993	238.9	289.8	430.4	511.6	500.5	656.1	606.0	673.7	602.8	468.6	276.7	200.7	**454.7**
1994	308.4	402.7	363.5	575.0	694.5	685.1	718.8	682.4	528.0	377.4	251.2	196.6	**482.0**
1995	239.7	355.4	485.3	551.9	700.2	692.7	638.3	640.3	480.5	441.4	340.5	250.5	**484.7**
1996	303.4	400.2	419.4	570.4	630.8	646.2	684.0	608.8	528.6	439.2	272.8	292.0	**483.0**
1997	254.4	366.9	434.9	502.7	617.4	606.1	663.9	591.5	489.3	334.4	253.5	201.8	**443.1**
1998	217.5	324.8	392.5	544.3	571.0	634.3	609.8	560.9	466.5	398.5	251.2	199.8	**430.9**
1999	213.6	311.9	431.2	513.9	547.8	562.8	551.1	513.7	462.6	350.8	282.3	202.3	**412.0**
2000	212.2	314.0	406.0	389.1	490.3	538.8	479.2	475.8	408.0	324.2	219.1	157.0	**367.8**
2001	263.8	391.9	545.8	573.4	754.8	816.3	772.6	741.2	639.1	517.1	325.7	302.4	**553.7**
2002	319.0	360.8	491.5	534.9	610.2	699.7	682.1	644.1	566.8	466.5	302.5	261.7	**495.0**
2003	311.7	405.3	458.2	602.2	674.4	709.9	767.3	676.7	630.9	455.5	393.0	300.8	**532.2**
2004	358.6	430.8	581.3	658.8	736.2	794.0	743.8	687.6	616.7	478.3	393.9	318.5	**566.5**
2005	295.2	366.0	459.1	622.1	717.4	804.5	734.7	684.6	552.5	473.6	377.7	267.3	**529.6**
2006	310.5	376.7	552.3	564.1	597.7	725.6	735.8	692.1	577.0	509.5	370.1	273.6	**523.8**
2007	313.4	371.2	357.3	478.8	590.5	695.1	679.3	619.3	524.1	391.0	335.7	226.4	**465.2**
2008	254.4	366.9	438.2	608.7	686.5	784.6	775.4	713.2	602.8	456.7	366.6	266.9	**526.7**
2009	323.3	425.9	592.3	617.3	716.4	761.2	723.2	705.1	554.6	449.9	362.7	264.4	**541.4**
2010	278.1	408.6	468.1	583.8	636.5	727.6	722.2	654.4	544.4	423.0	327.5	287.6	**505.2**
2011	239.7	400.2	434.9	544.3	694.5	685.1	718.8	676.7	630.9	456.7	251.2	202.3	**494.6**
2012	319.0	360.8	581.3	478.8	590.5	538.8	479.2	475.8	480.5	441.4	251.2	200.7	**433.2**
2013	358.6	289.8	430.4	511.6	500.5	656.1	606.0	475.8	528.0	377.4	377.7	302.4	**451.2**
2014	313.4	402.7	363.5	575.0	694.5	685.1	718.8	741.2	630.9	455.5	268.6	250.5	**508.3**

* Mw: MillWatt

TABLE C.9: Monthly Mean Potential Evaporation Totals mm

Year	Jan	Feb	Mar	Apr	May	Jun	Jul	Aug	Sep	Oct	Nov	Dec	Mean
1980	38.2	83.1	123.7	198.8	286.7	346.4	422	384.2	296.9	157.8	77.9	48.5	205.4
1981	55.6	88.8	181.9	216.8	246.5	391.3	435.9	375.7	276.9	190.5	67.3	48.0	214.6
1982	64.2	93.2	179.1	254.7	385.2	559.3	639.8	642.1	428.0	247.1	107.8	79.5	306.7
1983	66.3	110.1	219.6	271.6	407.0	546.4	414.8	370.2	415.1	277.9	148.8	103.1	279.2
1984	69.1	129.9	257.4	310.6	408.1	525.3	551.4	494.3	357.1	237.0	111.0	94.2	295.5
1985	92.1	142.5	208.9	312.9	416.0	563.5	597.7	551.2	410.6	267.3	148.6	85.6	316.4
1986	92.3	108.1	211.8	287.9	384.0	496.0	613.0	493.2	371.7	265.8	154.9	81.0	296.6
1987	95.1	147.6	172.9	311.2	415.8	556.2	460.7	500.6	302.8	247.8	124.5	176.1	292.6
1988	68.5	122.6	191.8	216.2	365.8	450.2	308.3	466.0	431.4	273.7	201.6	119.9	268.0
1989	82.3	97.6	123.4	286.0	411.2	515.3	402.9	317.0	188.5	277.8	124.2	85.0	242.6
1990	80.9	129.7	265.6	280.7	486.2	603.3	630.9	548.9	420.1	255.6	149.3	102.7	329.5
1991	83.2	68.8	116.1	187.8	283.1	358.3	400.4	370.6	212.0	214.0	151.4	90.9	211.4
1992	84.6	111.8	164.1	252.1	327.9	465.1	568.6	564.3	368.2	214.7	112.2	62.3	274.7
1993	64.8	199.3	205.8	208.9	351.6	516.1	606.9	473.4	402.1	236.4	148.8	83.6	291.5
1994	70.1	106.4	154.9	239.0	332.3	390.7	385.2	402.1	294.7	176.1	81.6	52.7	223.8
1995	77.1	106.8	195.4	274.2	460.7	546.6	586.2	548.3	370.4	279.3	184.8	101.0	310.9
1996	92.7	134.9	222.4	346.1	444.8	542.6	618.9	586.5	449.3	341.5	121.3	81.1	331.8
1997	188.3	111.7	192.8	310.5	409.5	368.2	622.4	553.7	370.8	253.8	103.8	64.2	295.8
1998	74.5	91.2	180.7	204.8	280.0	403.0	429.6	409.7	296.9	192.5	94.6	66.8	227.0
1999	68	56.1	167.8	212.5	252.7	301	407.3	397.3	357.2	266.0	126.6	90.8	225.3
2000	78.8	124.9	237.3	268.9	404.1	556.8	589.0	566.9	271.2	220.9	101.5	57.3	289.8
2001	82.4	132.0	190.4	219.5	295.6	369.0	425.1	397.3	269.4	253.5	139.4	54.5	235.7
2002	94.8	143.2	256.7	274.1	283.3	492.6	481.2	453.3	340.8	239.1	137.2	58.5	271.2
2003	75.3	66.2	150.2	240.0	279.0	397.1	401.0	374.0	263.9	211.0	78.9	44.9	215.1
2004	70.0	111.7	218.3	240.4	378.9	460.8	552.2	427.4	443.7	377.5	106.4	74.6	288.5
2005	92.5	109.7	217.3	340.7	411.5	510.3	579.0	480.7	387.1	277.4	144.5	117.1	305.7
2006	103.9	154.4	266.7	350.8	462.7	619.7	729.9	590.2	413.7	275.1	108.8	99.6	348.0
2007	80.9	109.8	192.2	278.8	382.6	578.0	687.2	667.2	425.1	297.5	187.5	75.6	330.2
2008	96.1	165.0	214.7	314.0	392.0	601.8	614.7	548.1	405.0	296.5	116.0	82.6	320.5
2009	96.6	128.0	237.8	336.9	472.3	638.5	624.7	603.6	389.5	310.0	209.5	99.4	345.6
2010	83.5	95.6	202.0	318.9	450.1	683.5	679.2	568.6	446.5	329.0	158.5	106.1	343.5
2011	71.8	113.2	198.3	438.1	487.8	390.1	593.3	560.0	422.2	312.7	178.5	154.3	326.7
2012	88.7	127.5	192.6	308.2	562.4	554.7	657.9	661.1	435.8	340.0	169.2	130.1	352.4
2013	102.2	138.8	211.3	324.4	416.5	560.1	671.2	625.9	508.8	291.8	164.3	85.1	341.7
2014	114.7	137.4	251.2	348.3	678.4	531.0	599.2	628.4	407.1	292.7	175.8	96.9	355.1

TABLE C.10: Monthly Mean Wind Speed (m/s)

Year	Jan	Feb	Mar	Apr	May	Jun	Jul	Aug	Sep	Oct	Nov	Dec	Mean
1980	1.2	1.1	1.5	1.9	2.2	2.4	2.9	2.3	1.6	1.5	1.5	1.3	**1.8**
1981	1.9	2.3	3.4	2.3	3.6	4.6	4.3	4	3	1.9	2.2	2.1	**3.0**
1982	1.9	2.2	2.5	2.6	2.4	3.5	2.9	2.3	1.4	1.5	1.5	1.5	**2.2**
1983	2.5	3.5	2.6	2.6	2.6	3.1	4.3	4	3.4	2.4	2.1	1.7	**2.9**
1984	2	1.9	2.5	2.3	2.9	4.4	4.1	2.9	3.4	2.3	2.2	1.8	**2.7**
1985	1.5	2	2.4	2.6	3.6	4.6	4.3	4	3	1.9	2.2	2	**2.8**
1986	1.2	1.1	1.5	1.9	1.7	1.5	2.9	1.5	1.9	1.2	1	0.6	**1.5**
1987	2.3	2.8	3.4	3.1	2.6	3.1	3.2	2.6	1.8	1.8	1.9	2	**2.6**
1988	2.0	1.9	2.5	2.3	2.5	2.2	3.4	2.0	1.7	2.2	1.9	2.0	**2.2**
1989	1.9	2.3	3.4	2.3	2.9	4.4	4.1	2.9	2.2	2.4	2.1	1.7	**2.7**
1990	2.3	2.8	3.4	3.1	3.6	4.6	4.3	4.0	3.4	2.3	2.2	1.8	**3.2**
1991	1.5	2	2.4	2.6	2.6	3.1	3.2	2.6	3.0	1.9	2.2	2.1	**2.4**
1992	2.5	3.5	2.6	3.0	2.9	3.0	4.3	2.6	1.8	1.8	1.9	2.0	**2.7**
1993	1.9	2.2	2.5	2.2	2.6	3.1	3.6	2.4	1.9	1.7	1.8	1.3	**2.3**
1994	1.5	2.0	2.4	2.6	2.4	3.5	3.2	2.6	1.6	1.5	1.5	1.5	**2.2**
1995	1.0	1.6	1.8	2.4	2.2	2.4	2.9	2.3	1.4	1.2	1.0	0.6	**1.7**
1996	1.2	1.1	1.5	1.9	1.6	2.1	2.2	1.5	1.9	1.7	0.9	1.2	**1.6**
1997	1.1	1.4	2.0	1.6	1.7	1.5	2.9	2.7	1.2	1.0	1.0	1.0	**1.6**
1998	1.2	1.2	1.8	1.9	2.1	2.2	2.1	1.6	1.7	1.3	0.7	1.0	**1.6**
1999	0.9	1.0	2.0	1.9	1.6	1.7	2.4	2.2	1.3	1.2	1.2	0.8	**1.5**
2000	1.3	1.4	1.8	2.1	1.5	2.5	1.7	1.5	1.6	1.1	0.5	0.9	**1.5**
2001	0.6	1.4	1.4	1.8	2.2	2.8	1.8	1.5	1.4	1.6	1.4	1.4	**1.6**
2002	1.0	2.0	2.1	2.5	1.9	2.5	1.7	2.4	2.3	1.4	1.4	1.1	**1.9**
2003	1.4	2.2	1.9	2.7	2.2	2.3	2.6	1.7	1.3	1.6	1.2	1.7	**1.9**
2004	1.6	2.1	2.4	2.5	2.6	3.3	3.0	1.9	1.3	1.7	1.4	1.1	**2.1**
2005	1.4	1.4	1.6	2.2	2.0	2.7	2.5	2.1	1.6	1.4	1.1	1.2	**1.8**
2006	1.6	1.7	2.2	2.1	1.9	3.2	3.4	3.0	2.0	1.8	1.9	1.1	**2.2**
2007	1.3	1.9	2.0	2.6	2.0	2.7	2.4	2.1	2.5	1.2	1.2	1.0	**1.9**
2008	1.4	2.2	1.9	2.7	2.2	3.7	2.5	1.8	1.7	1.9	1.1	2.0	**2.1**
2009	1.9	2.3	2.4	1.9	1.8	2.3	2.6	1.7	1.6	1.6	1.2	1.4	**1.9**
2010	1.8	2.1	2.0	1.7	2.0	2.3	2.9	1.8	1.6	1.6	1.6	1.6	**1.9**
2011	1.3	1.9	2.6	2.5	2.0	3.2	2.5	2.1	1.3	1.6	1.4	1.7	**2.0**
2012	1.9	2.5	2.3	2.1	2.1	2.4	2.1	1.8	1.7	1.3	1.2	1.7	**1.9**
2013	1.9	2.0	2.3	2.1	2.3	2.3	2.9	1.8	1.7	1.9	1.1	1.2	**2.0**
2014	1.6	1.7	2.2	2.1	2	2.7	2.4	3	2	1.8	1.1	2	**2.1**

TABLE C.11: RH. Totals %

Year	Jan	Feb	Mar	Apr	May	Jun	Jul	Aug	Sep	Oct	Nov	Dec	Total
1980	59	55	63	44	36	33	29	29	31	54	50	72	**555**
1981	72	64	48	43	31	35	34	33	37	45	63	75	**580**
1982	82	79	62	49	31	31	32	31	31	41	68	75	**612**
1983	70	66	55	47	35	27	25	28	27	33	75	68	**556**
1984	64	0	0	39	34	30	26	32	30	38	64	77	**434**
1985	74	58	52	51	31	28	27	27	28	40	52	71	**539**
1986	65	56	57	39	31	25	20	23	29	39	61	64	**509**
1987	63	59	39	35	24	20	19	20	29	38	46	58	**450**
1988	73	63	61	46	35	29	24	27	31	39	66	75	**569**
1989	75	67	49	56	40	24	20	25	28	37	49	66	**536**
1990	72	51	49	36	27	20	20	21	27	43	68	71	**505**
1991	77	70	54	43	27	25	23	22	28	42	52	67	**530**
1992	71	59	53	46	34	30	24	22	25	32	50	56	**502**
1993	63	45	43	34	25	23	22	25	29	42	69	79	**499**
1994	76	65	60	37	30	24	24	24	31	39	50	56	**516**
1995	69	57	42	34	29	27	26	24	33	38	50	70	**499**
1996	70	63	49	41	34	24	20	21	25	38	57	72	**514**
1997	70	57	51	43	34	17	17	18	22	33	41	63	**466**
1998	66	54	47	49	33	25	23	24	28	37	55	68	**509**
1999	66	52	37	36	32	27	23	31	26	30	54	55	**469**
2000	54	52	45	38	24	20	19	22	30	40	59	62	**465**
2001	69	61	47	47	34	25	27	24	33	47	54	73	**541**
2002	69	63	50	48	33	27	23	28	31	38	50	59	**519**
2003	63	54	40	35	33	26	24	27	37	52	63	61	**515**
2004	61	58	50	48	39	30	26	27	34	43	58	65	**539**
2005	57	53	44	43	31	27	22	21	27	36	41	55	**457**
2006	70	61	42	39	30	23	22	23	31	40	52	55	**488**
2007	62	52	39	31	26	21	22	25	27	41	65	68	**479**
2008	65	60	40	33	45	26	25	22	32	43	68	78	**537**
2009	75	68	65	49	33	30	29	29	35	50	78	76	**617**
2010	69	73	55	39	26	26	22	28	28	41	30	75	**512**
2011	66	66	64	42	34	24	27	25	25	25	72	55	**525**
2012	67	62	46	50	45	36	30	30	29	42	76	70	**583**
2013	84	60	50	40	39	32	27	33	41	60	45	82	**593**
2014	73	70	53	48	42	26	28	29	29	55	44	74	**571**
Mean	**68.6**	**58.65**	**48.6**	**42.22**	**32.77**	**26.37**	**24.31**	**25.71**	**29.82**	**40.88**	**57**	**67.6**	**522.57**

Appendix D

TABLE D.1: Calculations of water balance and net recharge

Year: 1980 , I = 169.42 , a = 3.21

Month	TC⁰	R (mm)	(T/5)	(T/5)^1.514	(T * 10)/I	[(T * 10)/I)]^a	PE (mm)	K	PEc (mm)	AE (mm)	SM (mm)	ΔSM (mm)	WS R - (AE + ΔSM) (mm)	RGW WS – RO (mm)
Jan	9.8	4.1	1.96	2.77	0.58	0.17	2.76	0.89	2.45	2.45	21.46	0.00	1.65	1.65
Feb	10.8	58.4	2.16	3.21	0.64	0.24	3.84	0.86	3.3	3.3	24.62	3.16	51.94	51.94
Mar	19.7	3.7	3.94	7.97	1.16	1.61	25.76	1.03	26.53	3.7	34.36	9.74	-9.74	-9.74
Apr	32	2.4	6.4	16.62	1.89	7.72	173.1	1.08	186.95	2.4	46.65	12.29	-12.29	-12.29
May	28.8	1.0	5.76	14.17	1.7	5.49	155.4	1.19	184.93	1	32.51	-14.14	14.14	14.14
June	37	0.0	7.4	20.7	2.18	12.2	184.9	1.19	220.03	0	27.45	-5.06	5.06	5.06
July	42.5	0.0	8.5	25.54	2.51	19.18	185	1.21	223.85	0	19.59	-7.86	7.86	7.86
Aug	44.8	0.0	8.96	27.66	2.64	22.56	185	1.15	212.75	0	18.87	-0.72	0.72	0.72
Sep	35.2	0.0	7.04	19.2	2.08	10.5	182.9	1.03	188.39	0	15.57	-3.30	3.3	3.3
Oct	30.5	0.4	6.1	15.45	1.8	6.6	165.2	0.98	161.9	0.4	15.64	0.07	-0.07	-0.07
Nov	19.5	21.4	3.9	7.85	1.15	1.57	25.12	0.88	22.11	21.4	17.5	1.86	-1.86	-1.86
Dec	20.2	9.0	4.04	8.28	1.19	1.75	28	0.87	24.36	9	35.72	18.22	-18.22	-18.22
SUM		100.4		169.42										42.49

Year: 1981 , I = 175.88 , a = 3.31

Month	TC⁰	R (mm)	(T/5)	(T/5)^1.514	(T * 10)/I	[(T * 10)/I)]^a	PE (mm)	K	PEc (mm)	AE (mm)	SM (mm)	ΔSM (mm)	WS R - (AE + ΔSM) (mm)	RGW WS – RO (mm)
Jan	8.2	14.5	1.64	2.11	0.47	0.08	1.28	0.89	1.14	1.14	43.56	7.84	5.52	5.52
Feb	20.2	7.5	4.04	8.28	1.15	1.59	25.44	0.86	21.88	7.5	55.07	11.51	-11.51	-11.51
Mar	23.5	22.9	4.7	10.41	1.34	2.63	42.08	1.03	43.34	22.9	65.01	9.94	-9.94	-9.94
Apr	29.5	0.0	5.9	14.69	1.68	5.57	158.9	1.08	171.61	0	73.9	8.89	-8.89	-8.89
May	32.1	0.000	6.42	16.7	1.83	7.39	173.1	1.19	205.99	0	57.56	-16.34	16.34	16.34
June	36.7	0.0	7.34	20.45	2.09	11.47	184.7	1.19	219.79	0	47.1	-10.46	10.46	10.46
July	42.8	0.0	8.56	25.81	2.43	18.9	185	1.21	223.85	0	34.01	-13.09	13.09	13.09
Aug	45.5	0.0	9.1	28.31	2.59	23.34	185	1.15	212.75	0	29.22	-4.79	4.79	4.79
Sep	37	0.0	7.4	20.7	2.1	11.66	184.9	1.03	190.45	0	23.02	-6.20	6.2	6.2
Oct	29.6	0.0	5.92	14.77	1.68	5.57	158.9	0.98	155.72	0	21.39	-1.63	1.63	1.63
Nov	16.5	2.5	3.3	6.1	0.94	0.81	12.96	0.88	11.4	2.5	31.02	9.63	-9.63	-9.63
Dec	19	8.6	3.8	7.55	1.08	1.29	20.64	0.87	17.96	8.6	42.52	11.50	-11.5	-11.5
SUM		56.0		175.88										6.56

Year: 1982 , I = 177.6 , a = 3.34

Month	TC^0	R (mm)	(T/5)	(T/5)^1.514	(T * 10)/I	[(T * 10)/I]^a	PE (mm)	K	PEc (mm)	AE (mm)	SM (mm)	ΔSM (mm)	WS R − (AE + ΔSM) (mm)	RGW WS − RO (mm)
Jan	13.6	61.5	2.72	4.55	0.77	0.42	6.72	0.89	5.98	5.98	58.16	15.64	39.88	39.88
Feb	15.6	14.4	3.12	5.6	0.88	0.65	10.4	0.86	8.94	8.94	58.37	0.21	5.25	5.25
Mar	23	9.5	4.6	10.08	1.3	2.4	38.4	1.03	39.55	9.5	56.56	-1.81	1.81	1.81
Apr	29.6	35.1	5.92	14.77	1.67	5.54	158.9	1.08	171.61	35.1	76.98	20.42	-20.42	-20.42
May	32.2	22.1	6.44	16.77	1.81	7.26	173.1	1.19	205.99	22.1	73.46	-3.52	3.52	3.52
June	38.4	0.0	7.68	21.9	2.16	13.09	185	1.19	220.15	0	59.45	-14.01	14.01	14.01
July	48.4	0.0	9.68	31.09	2.73	28.63	185	1.21	223.85	0	42.74	-16.71	16.71	16.71
Aug	42.6	0.0	8.52	25.63	2.4	18.62	185	1.15	212.75	0	35.67	-7.07	7.07	7.07
Sep	35.9	0.0	7.18	19.78	2.02	10.47	184.3	1.03	189.83	0	27.72	-7.95	7.95	7.95
Oct	29	23.8	5.8	14.32	1.63	5.11	155.4	0.98	152.29	23.8	30.19	2.47	-2.47	-2.47
Nov	16.7	8.3	3.34	6.21	0.94	0.81	12.96	0.88	11.4	8.3	42.83	12.64	-12.64	-12.64
Dec	17.9	7.8	3.58	6.9	1.01	1.03	16.48	0.87	14.34	7.8	54.57	11.74	-11.74	-11.74
SUM		182.5		177.6										48.93

Year: 1983 , I = 178.99 , a = 3.36

Month	TC^0	R (mm)	(T/5)	(T/5)^1.514	(T * 10)/I	[(T * 10)/I]^a	PE (mm)	K	PEc (mm)	AE (mm)	SM (mm)	ΔSM (mm)	WS R − (AE + ΔSM) (mm)	RGW WS − RO (mm)
Jan	16	1.0	3.2	5.82	0.89	0.68	10.88	0.89	9.68	1	77.31	22.74	-22.74	-22.74
Feb	17	2.1	3.4	6.38	0.95	0.84	13.44	0.86	11.56	2.1	104.77	27.46	-27.46	-27.46
Mar	21	4.3	4.2	8.78	1.17	1.69	27.04	1.03	27.85	4.3	104.26	-0.51	0.51	0.51
Apr	30.2	31.0	6.04	15.22	1.69	5.83	162.1	1.08	175.07	31	106.6	2.34	-2.34	-2.34
May	30.8	31.0	6.16	15.68	1.72	6.19	168	1.19	199.92	31	84.91	-21.69	21.69	21.69
June	34.5	0.0	6.9	18.62	1.93	9.11	181.8	1.19	216.34	0	67.9	-17.01	17.01	17.01
July	45.6	0.0	9.12	28.41	2.55	23.23	185	1.21	223.85	0	48.84	-19.06	19.06	19.06
Aug	44.5	0.0	8.9	27.38	2.49	21.44	185	1.15	212.75	0	40.07	-8.77	8.77	8.77
Sep	38.2	0.0	7.64	21.73	2.13	12.69	185	1.03	190.55	0	31.37	-8.70	8.7	8.7
Oct	30.3	0.0	6.06	15.3	1.69	5.83	165.2	0.98	161.9	0	28.54	-2.83	2.83	2.83
Nov	21.8	5.1	4.36	9.29	1.22	1.95	31.2	0.88	27.46	5.1	26.35	-2.19	2.19	2.19
Dec	17	45.4	3.4	6.38	0.95	0.84	13.44	0.87	11.69	11.69	32.32	5.97	27.74	27.74
SUM		119.9		178.99										55.96

Year: 1984 , I = 177.38, a = 3.34

Month	TC^0	R (mm)	(T/5)	(T/5)^1.514	(T * 10)/I	[(T * 10)/I]^a	PE (mm)	K	PEc (mm)	AE (mm)	SM (mm)	ΔSM (mm)	WS R - (AE + ΔSM) (mm)	RGW WS - RO (mm)
Jan	12.5	9.3	2.5	4	0.7	0.3	4.8	0.89	4.27	4.27	32.06	-0.26	5.29	5.29
Feb	11.2	0.7	2.24	3.39	0.63	0.21	3.36	0.86	2.89	0.7	33.12	1.06	-1.06	-1.06
Mar	24.1	12.6	4.82	10.82	1.36	2.79	44.64	1.03	45.98	12.6	38.56	5.44	-5.44	-5.44
Apr	35	0.5	7	19.03	1.97	9.63	182.9	1.08	197.53	0.5	48.05	9.49	-9.49	-9.49
May	30.7	15.5	6.14	15.61	1.73	6.24	165.2	1.19	196.59	15.5	34.76	-13.29	13.29	13.29
June	36.5	0.0	7.3	20.28	2.06	11.18	184.7	1.19	219.79	0	29.95	-4.81	4.81	4.81
July	45.6	0.0	9.12	28.41	2.57	23.4	185	1.21	223.85	0	21.89	-8.06	8.06	8.06
Aug	42.6	0.0	8.52	25.63	2.4	18.62	185	1.15	212.75	0	20.72	-1.17	1.17	1.17
Sep	36.3	0.0	7.26	20.11	2.05	11	184.7	1.03	190.24	0	16.87	-3.85	3.85	3.85
Oct	28.5	1.8	5.7	13.94	1.61	4.91	151.7	0.98	148.67	1.8	26.04	9.17	-9.17	-9.17
Nov	21.2	91.3	4.24	8.91	1.2	1.84	29.44	0.88	25.91	25.91	51.7	25.66	39.73	39.73
Dec	18.5	13.7	3.7	7.25	1.04	1.14	18.24	0.87	15.87	13.7	72.42	20.72	-20.72	-20.72
SUM		145.4		177.38										30.32

Year: 1985 , I = 181.11 , a = 3.4

Month	TC^0	R (mm)	(T/5)	(T/5)^1.514	(T * 10)/I	[(T * 10)/I]^a	PE (mm)	K	PEc (mm)	AE (mm)	SM (mm)	ΔSM (mm)	WS R - (AE + ΔSM) (mm)	RGW WS - RO (mm)
Jan	8.7	19.5	1.74	2.31	0.48	0.08	1.28	0.89	1.14	1.14	43.71	-28.71	47.07	47.07
Feb	12.8	1.7	2.56	4.15	0.71	0.31	4.96	0.86	4.27	1.7	31.92	-11.79	11.79	11.79
Mar	27.2	13.2	5.44	12.99	1.5	3.97	139.5	1.03	143.69	13.2	20.76	-11.16	11.16	11.16
Apr	30.5	0.4	6.1	15.45	1.68	5.84	165.2	1.08	178.42	0.4	33.15	12.39	-12.39	-12.39
May	29.8	2.3	5.96	14.92	1.65	5.49	162.1	1.19	192.9	2.3	31.06	-2.09	2.09	2.09
June	36.5	0.0	7.3	20.28	2.02	10.92	184.7	1.19	219.79	0	39.35	8.29	-8.29	-8.29
July	45.2	0.0	9.04	28.03	2.5	22.54	185	1.21	223.85	0	45.89	6.54	-6.54	-6.54
Aug	47.4	0.0	9.48	30.12	2.62	26.44	185	1.15	212.75	0	61.37	15.48	-15.48	-15.48
Sep	37.4	0.0	7.48	21.04	2.07	11.87	185	1.03	190.55	0	72.47	11.10	-11.1	-11.1
Oct	28.9	0.0	5.78	14.24	1.6	4.94	155.4	0.98	152.29	0	78.74	6.27	-6.27	-6.27
Nov	23.2	1.8	4.64	10.21	1.28	2.31	36.96	0.88	32.52	1.8	75	-3.74	3.74	3.74
Dec	18.7	19.9	3.74	7.37	1.03	1.11	17.76	0.87	15.45	15.45	73.42	-1.58	6.03	6.03
SUM		58.8		181.11										21.81

						PE		PEc	AE	SM	ΔSM	WS R − (AE + ΔSM)	RGW WS − RO
Year: 1986 , I = 159.28 , a = 3.05													
Month	TC⁰	R (mm)	(T/5)	(T/5)^1.514	(T * 10)/I	[(T * 10)/I]^a	PE (mm)	K	PEc (mm)	AE (mm)	SM (mm)	ΔSM (mm)	(mm)	(mm)
Jan	7.6	6.0	1.52	1.88	0.48	0.11	1.76	0.89	1.57	1.57	43.86	-29.56	33.99	33.99
Feb	11.3	60.3	2.26	3.44	0.71	0.35	5.6	0.86	4.82	4.82	59.17	15.31	40.17	40.17
Mar	20.2	15.4	4.04	8.28	1.27	2.07	33.12	1.03	34.11	15.4	57.96	-1.21	1.21	1.21
Apr	30.2	9.2	6.04	15.22	1.9	7.08	162.1	1.08	175.07	9.2	69.75	11.79	-11.79	-11.79
May	29.9	7.5	5.98	14.99	1.88	6.86	162.1	1.19	192.9	7.5	57.36	-12.39	12.39	12.39
June	35	0.0	7	19.03	2.2	11.08	182.9	1.19	217.65	0	47.15	-10.21	10.21	10.21
July	44.4	0.0	8.88	27.28	2.79	22.86	185	1.21	223.85	0	34.09	-13.06	13.06	13.06
Aug	42	0.0	8.4	25.08	2.64	19.31	185	1.15	212.75	0	29.32	-4.77	4.77	4.77
Sep	37.7	0.0	7.54	21.3	2.37	13.9	185	1.03	190.55	0	23.07	-6.25	6.25	6.25
Oct	26.1	0.0	5.22	12.21	1.64	4.52	72.32	0.98	70.87	0	24.39	1.32	-1.32	-1.32
Nov	16	34.0	3.2	5.82	1	1	16	0.88	14.08	14.08	30.75	6.36	13.56	13.56
Dec	14	0.2	2.8	4.75	0.88	0.68	10.88	0.87	9.47	0.2	42.02	11.27	-11.27	-11.27
SUM		132.6		159.28										111.23

						PE		PEc	AE	SM	ΔSM	WS R − (AE + ΔSM)	RGW WS − RO
Year: 1987 , I = 165.13 , a = 3.14													
Month	TC⁰	R (mm)	(T/5)	(T/5)^1.514	(T * 10)/I	[(T * 10)/I]^a	PE (mm)	K	PEc (mm)	AE (mm)	SM (mm)	ΔSM (mm)	(mm)	(mm)
Jan	7	0.0	1.4	1.66	0.42	0.07	1.12	0.89	1	0	39.86	-2.16	2.16	2.16
Feb	11.4	7.8	2.28	3.48	0.69	0.31	4.96	0.86	4.27	4.27	37.92	-1.94	5.47	5.47
Mar	18.5	46.6	3.7	7.25	1.12	1.43	22.88	1.03	23.57	23.57	41.91	3.99	19.04	19.04
Apr	27.6	0.0	5.52	13.28	1.67	5	143.7	1.08	155.2	0	51.15	9.24	-9.24	-9.24
May	30.6	0.0	6.12	15.53	1.85	6.9	165.2	1.19	196.59	0	36.56	-14.59	14.59	14.59
June	33.5	0.0	6.7	17.81	2.03	9.24	179	1.19	213.01	0	31.7	-4.86	4.86	4.86
July	44.9	0.0	8.98	27.75	2.72	23.15	185	1.21	223.85	0	23.29	-8.41	8.41	8.41
Aug	43.8	0.0	8.76	26.73	2.65	21.33	185	1.15	212.75	0	21.52	-1.77	1.77	1.77
Sep	35.3	0.0	7.06	19.28	2.14	10.9	183.7	1.03	189.21	0	17.57	-3.95	3.95	3.95
Oct	29.8	11.3	5.96	14.92	1.8	6.33	162.1	0.98	158.86	11.3	21.34	3.77	-3.77	-3.77
Nov	21	16.5	4.2	8.78	1.27	2.12	33.92	0.88	29.85	16.5	22	0.66	-0.66	-0.66
Dec	20.8	77.1	4.16	8.66	1.26	2.07	33.12	0.87	28.81	28.81	30.17	8.17	40.12	40.12
SUM		159.3		165.13										86.70

Year: 1988 , I = 162.13 , a = 3.09

Month	TC^0	R (mm)	(T/5)	(T/5)^1.514	(T * 10)/I	[(T * 10)/I]^a	PE (mm)	K	PEc (mm)	AE (mm)	SM (mm)	ΔSM (mm)	WS R - (AE + ΔSM) (mm)	RGW WS - RO (mm)
Jan	8.4	34.6	1.68	2.19	0.52	0.13	2.08	0.89	1.85	1.85	60.71	30.54	2.21	2.21
Feb	13.8	13.5	2.76	4.65	0.85	0.61	9.76	0.86	8.39	8.39	38.32	-22.39	27.5	27.5
Mar	22	30.7	4.4	9.42	1.36	2.59	41.44	1.03	42.68	30.7	39.56	1.24	-1.24	-1.24
Apr	30	44.7	6	15.07	1.85	6.69	162.1	1.08	175.07	44.7	54.7	15.14	-15.14	-15.14
May	31	0.0	6.2	15.84	1.91	7.39	168	1.19	199.92	0	43.76	-10.94	10.94	10.94
June	34	0.0	6.8	18.21	2.1	9.9	180.5	1.19	214.8	0	36.25	-7.51	7.51	7.51
July	43.2	0.0	8.64	26.17	2.66	20.55	185	1.21	223.85	0	26.04	-10.21	10.21	10.21
Aug	40.3	0.0	8.06	23.56	2.49	16.76	185	1.15	212.75	0	23.57	-2.47	2.47	2.47
Sep	33.9	0.000	6.78	18.13	2.09	9.76	180.5	1.03	185.92	0	19.07	-4.50	4.5	4.5
Oct	30.6	0	6.12	15.53	1.89	7.15	165.2	0.98	161.9	0	20.14	1.07	-1.07	-1.07
Nov	21.2	12.1	4.24	8.91	1.31	2.3	36.8	0.88	32.38	12.1	19.8	-0.34	0.34	0.34
Dec	13.4	29.5	2.68	4.45	0.83	0.56	8.96	0.87	7.8	7.8	35.67	15.87	5.83	5.83
SUM		165.1		162.13										54.06

Year: 1989 , I = 171.82 , a = 3.25

Month	TC^0	R (mm)	(T/5)	(T/5)^1.514	(T * 10)/I	[(T * 10)/I]^a	PE (mm)	K	PEc (mm)	AE (mm)	SM (mm)	ΔSM (mm)	WS R - (AE + ΔSM) (mm)	RGW WS - RO (mm)
Jan	11.2	3.2	2.24	3.39	0.65	0.25	4	0.89	3.56	3.2	43.91	8.24	-8.24	-8.24
Feb	16.3	64.5	3.26	5.98	0.95	0.85	13.6	0.86	11.7	11.7	53.37	9.46	43.34	43.34
Mar	24.2	31.6	4.84	10.89	1.41	3.05	48.8	1.03	50.26	31.6	49.21	-4.16	4.16	4.16
Apr	28.8	0.000	5.76	14.17	1.68	5.4	155.4	1.08	167.83	0	54.95	5.74	-5.74	-5.74
May	31.5	3.8	6.3	16.23	1.83	7.13	170.7	1.19	203.13	3.8	38.86	-16.09	16.09	16.09
June	34.2	0.0	6.84	18.38	1.99	9.36	180.5	1.19	214.8	0	32.35	-6.51	6.51	6.51
July	41.6	0.0	8.32	24.72	2.42	17.68	185	1.21	223.85	0	23.19	-9.16	9.16	9.16
Aug	45.4	0.0	9.08	28.22	2.64	23.45	185	1.15	212.75	0	31.52	8.33	-8.33	-8.33
Sep	36.8	0.0	7.36	20.53	2.14	11.85	184.9	1.03	190.45	0	17.37	-14.15	14.15	14.15
Oct	29.4	0	5.88	14.62	1.71	5.72	158.9	0.98	155.72	0	17.14	-0.23	0.23	0.23
Nov	19.8	8.6	3.96	8.03	1.15	1.57	25.12	0.88	22.11	8.6	30	12.86	-12.86	-12.86
Dec	17.5	0.6	3.5	6.66	1.02	1.07	17.12	0.87	14.89	0.6	46.22	16.22	-16.22	-16.22
SUM		112.3		171.82										42.25

													WS	RGW
Year: 1990 , I = 175.03 , a = 3.3							**PE**		**PEc**	**AE**	**SM**	**ΔSM**	**R − (AE+ΔSM)**	**WS − RO**
Month	**TC⁰**	**R (mm)**	**(T/5)**	**(T/5)^1.514**	**(T * 10)/I**	**[(T * 10)/I]^a**	**(mm)**	**K**	**(mm)**	**(mm)**	**(mm)**	**(mm)**	**(mm)**	**(mm)**
Jan	11.3	8.9	2.26	3.44	0.65	0.24	3.84	0.89	3.42	3.42	43.96	-2.26	7.74	7.74
Feb	12.8	18.1	2.56	4.15	0.73	0.35	5.6	0.86	4.82	4.82	52.92	8.96	4.32	4.32
Mar	19.2	3.1	3.84	7.67	1.1	1.37	21.92	1.03	22.58	3.1	63.56	10.64	-10.64	-10.64
Apr	28.8	2.500	5.76	14.17	1.65	5.22	155.4	1.08	167.83	2.5	66.15	2.59	-2.59	-2.59
May	30.8	0.0	6.16	15.68	1.76	6.46	168	1.19	199.92	0	49.36	-16.79	16.79	16.79
June	33	0.0	6.6	17.41	1.89	8.17	177.2	1.19	210.87	0	40.9	-8.46	8.46	8.46
July	44.6	0.0	8.92	27.47	2.55	21.96	185	1.21	223.85	0	30.04	-10.86	10.86	10.86
Aug	47.3	0.0	9.46	30.03	2.7	26.52	185	1.15	212.75	0	26.57	-3.47	3.47	3.47
Sep	38.4	0.0	7.68	21.9	2.19	13.29	185	1.03	190.55	0	21.32	-5.25	5.25	5.25
Oct	30	0.000	6	15.07	1.71	5.87	162.1	0.98	158.86	0	20.64	-0.68	0.68	0.68
Nov	24.5	0.2	4.9	11.09	1.4	3.04	48.64	0.88	42.8	0.2	19.1	-1.54	1.54	1.54
Dec	18	3.600	3.6	6.95	1.03	1.1	17.6	0.87	15.31	3.6	21.02	1.92	-1.92	-1.92
SUM		36.4		175.03										43.96
Year: 1991 , I = 181.55 , a = 3.4							**PE**		**PEc**	**AE**	**SM**	**ΔSM**	**R − (AE+ΔSM)**	**WS − RO**
Month	**TC⁰**	**R (mm)**	**(T/5)**	**(T/5)^1.514**	**(T * 10)/I**	**[(T * 10)/I]^a**	**(mm)**	**K**	**(mm)**	**(mm)**	**(mm)**	**(mm)**	**(mm)**	**(mm)**
Jan	16	7.6	3.2	5.82	0.88	0.65	10.4	0.89	9.26	7.6	22.66	1.64	-1.64	-1.64
Feb	19.2	15.4	3.84	7.67	1.06	1.22	19.52	0.86	16.79	15.4	31.02	8.36	-8.36	-8.36
Mar	16.6	6.7	3.32	6.15	0.91	0.73	11.68	1.03	12.03	6.7	44.66	13.64	-13.64	-13.64
Apr	31.2	0.0	6.24	15.99	1.72	6.32	168	1.08	181.44	0	55.3	10.64	-10.64	-10.64
May	32.7	0.0	6.54	17.17	1.8	7.38	175.3	1.19	208.61	0	39.96	-15.34	15.34	15.34
June	38.2	0.0	7.64	21.73	2.1	12.46	185	1.19	220.15	0	33.6	-6.36	6.36	6.36
July	45.1	0.0	9.02	27.94	2.48	21.93	185	1.21	223.85	0	29.79	-3.81	3.81	3.81
Aug	46.8	0.0	9.36	29.55	2.58	25.09	185	1.15	212.75	0	46.17	16.38	-16.38	-16.38
Sep	36.2	0.0	7.24	20.03	1.99	10.38	184.3	1.03	189.83	0	46.32	0.15	-0.15	-0.15
Oct	30.2	6.6	6.04	15.22	1.66	5.6	162.1	0.98	158.86	6.6	39.74	-6.58	6.58	6.58
Nov	17.2	4.0	3.44	6.49	0.95	0.84	13.44	0.88	11.83	4	32.2	-7.54	7.54	7.54
Dec	19.4	12.2	3.88	7.79	1.07	1.26	20.16	0.87	17.54	12.2	33.72	1.52	-1.52	-1.52
SUM		52.5		181.55										-12.70

| Year: 1992 , I = 173.55 , a = 3.28 | | | | | | | | | | | | | WS | RGW |
Month	TC⁰	R (mm)	(T/5)	(T/5)^1.514	(T * 10)/I	[(T * 10)/I]^a	PE (mm)	K	PEc (mm)	AE (mm)	SM (mm)	ΔSM (mm)	R - (AE + ΔSM) (mm)	WS - RO (mm)
Jan	9.5	3.5	1.9	2.64	0.55	0.14	2.24	0.89	1.99	1.99	34.81	1.09	0.42	0.42
Feb	12.5	6.2	2.5	4	0.72	0.34	5.44	0.86	4.68	4.68	43.97	9.16	-7.64	-7.64
Mar	22	19.5	4.4	9.42	1.27	2.19	35.04	1.03	36.09	19.5	49.36	5.39	-5.39	-5.39
Apr	28	13.7	5.6	13.58	1.61	4.77	147.8	1.08	159.62	13.7	55.65	6.29	-6.29	-6.29
May	30.6	1.2	6.12	15.53	1.76	6.39	165.2	1.19	196.59	1.2	40.81	-14.84	14.84	14.84
June	36.3	0.0	7.26	20.11	2.09	11.22	184.7	1.19	219.79	0	34.3	-6.51	6.51	6.51
July	47.4	0.0	9.48	30.12	2.73	26.95	185	1.21	223.85	0	24.74	-9.56	9.56	9.56
Aug	42.9	0.0	8.58	25.9	2.47	19.41	185	1.15	212.75	0	22.67	-2.07	2.07	2.07
Sep	37.2	0.0	7.44	20.87	2.14	12.13	184.9	1.03	190.45	0	18.32	-4.35	4.35	4.35
Oct	29.4	0.0	5.88	14.62	1.69	5.59	158.9	0.98	155.72	0	17.89	-0.43	0.43	0.43
Nov	19.9	56.3	3.98	8.1	1.15	1.58	25.28	0.88	22.25	22.25	20.45	2.56	31.49	31.49
Dec	20.8	25.9	4.16	8.66	1.2	1.82	29.12	0.87	25.33	25.33	24.67	4.22	-3.65	-3.65
SUM		116.0		173.55										46.70

| Year: 1993 , I = 180.69 , a = 3.39 | | | | | | | | | | | | | WS | RGW |
Month	TC⁰	R (mm)	(T/5)	(T/5)^1.514	(T * 10)/I	[(T * 10)/I]^a	PE (mm)	K	PEc (mm)	AE (mm)	SM (mm)	ΔSM (mm)	R - (AE + ΔSM) (mm)	WS - RO (mm)
Jan	9.8	34.7	1.96	2.77	0.54	0.12	1.92	0.89	1.71	1.71	34.16	9.49	23.5	23.5
Feb	13.6	23.5	2.72	4.55	0.75	0.38	6.08	0.86	5.23	5.23	27.72	-6.44	24.71	24.71
Mar	21.7	0.5	4.34	9.23	1.2	1.86	29.76	1.03	30.65	0.5	25.66	-2.06	2.06	2.06
Apr	31.6	89.8	6.32	16.3	1.75	6.67	170.7	1.08	184.36	89.8	38.35	12.69	-12.69	-12.69
May	33.5	7.1	6.7	17.81	1.85	8.05	179	1.19	213.01	7.1	34.16	-4.19	4.19	4.19
June	36.1	0.0	7.22	19.94	2	10.48	184.3	1.19	219.32	0	31.25	-2.91	2.91	2.91
July	45.5	0.0	9.1	28.31	2.52	22.95	185	1.21	223.85	0	22.29	-8.96	8.96	8.96
Aug	43.5	0.0	8.7	26.45	2.41	19.73	185	1.15	212.75	0	20.82	-1.47	1.47	1.47
Sep	35.2	0.0	7.04	19.2	1.95	9.62	182.9	1.03	188.39	0	16.97	-3.85	3.85	3.85
Oct	29.5	1.8	5.9	14.69	1.63	5.24	158.9	0.98	155.72	1.8	16.94	-0.03	0.03	0.03
Nov	23.4	10.5	4.68	10.35	1.3	2.43	38.88	0.88	34.21	10.5	17.9	0.96	-0.96	-0.96
Dec	24.5	2.1	4.9	11.09	1.36	2.84	45.44	0.87	39.53	2.1	23.72	5.82	-5.82	-5.82
SUM		170.0		180.69										52.21

Month	TC⁰	R (mm)	(T/5)	(T/5)^1.514	(T * 10)/I	[(T * 10)/I]^a	PE (mm)	K	PEc (mm)	AE (mm)	SM (mm)	ΔSM (mm)	WS R - (AE + ΔSM) (mm)	RGW WS - RO (mm)
Year: 1994 , I = 182.77 , a = 3.42														
Jan	10	27.0	2	2.86	0.55	0.13	2.08	0.89	1.85	1.85	22.61	-1.11	26.26	26.26
Feb	16.4	3.5	3.28	6.04	0.9	0.7	11.2	0.86	9.63	3.5	36.02	13.41	-13.41	-13.41
Mar	23.7	8.1	4.74	10.55	1.3	2.45	39.2	1.03	40.38	8.1	43.26	7.24	-7.24	-7.24
Apr	31.3	4.2	6.26	16.07	1.71	6.26	170.7	1.08	184.36	4.2	46.7	3.44	-3.44	-3.44
May	31.4	0.6	6.28	16.15	1.72	6.39	170.7	1.19	203.13	0.6	33.21	-13.49	13.49	13.49
June	37.1	0.0	7.42	20.79	2.03	11.26	184.9	1.19	220.03	0	28.45	-4.76	4.76	4.76
July	44.6	0.0	8.92	27.47	2.44	21.13	185	1.21	223.85	0	20.49	-7.96	7.96	7.96
Aug	49.2	0.0	9.84	31.87	2.69	29.5	185	1.15	212.75	0	19.62	-0.87	0.87	0.87
Sep	37.2	0.000	7.44	20.87	2.04	11.45	184.9	1.03	190.45	0	16.67	-2.95	2.95	2.95
Oct	27.3	18.9	5.46	13.07	1.49	3.91	143.7	0.98	140.83	18.9	17.24	0.57	-0.57	-0.57
Nov	19.2	62.2	3.84	7.67	1.05	1.18	18.88	0.88	16.61	16.61	25.5	8.26	37.33	37.33
Dec	21.9	23.1	4.38	9.36	1.2	1.87	29.92	0.87	26.03	23.1	39.02	13.52	-13.52	-13.52
SUM		147.6		182.77										55.44
Year: 1995 , I = 164.42 , a = 3.13														
Jan	8.5	2.6	1.7	2.23	0.52	0.13	2.08	0.89	1.85	1.85	37.36	-1.66	2.41	2.41
Feb	13.7	17.0	2.74	4.6	0.83	0.56	8.96	0.86	7.71	7.71	43.02	5.66	3.63	3.63
Mar	17	8.7	3.4	6.38	1.03	1.1	17.6	1.03	18.13	8.7	45.61	2.59	-2.59	-2.59
Apr	27.7	23.8	5.54	13.36	1.68	5.07	143.7	1.08	155.2	23.8	51.1	5.49	-5.49	-5.49
May	33.2	0.3	6.64	17.57	2.02	9.03	177.2	1.19	210.87	0.3	37.61	-13.49	13.49	13.49
June	34	0.0	6.8	18.21	2.07	9.75	180.5	1.19	214.8	0	31.9	-5.71	5.71	5.71
July	43.8	0.0	8.76	26.73	2.66	21.37	185	1.21	223.85	0	23.04	-8.86	8.86	8.86
Aug	44.5	0.0	8.9	27.38	2.71	22.66	185	1.15	212.75	0	21.37	-1.67	1.67	1.67
Sep	36.2	0.0	7.24	20.03	2.2	11.8	184.3	1.03	189.83	0	17.57	-3.80	3.8	3.8
Oct	27	0.0	5.4	12.85	1.64	4.7	139.5	0.98	136.71	0	17.34	-0.23	0.23	0.23
Nov	20.7	6.2	4.14	8.59	1.26	2.06	32.96	0.88	29	6.2	18	0.66	-0.66	-0.66
Dec	17.2	5.5	3.44	6.49	1.05	1.16	18.56	0.87	16.15	5.5	22.52	4.52	-4.52	-4.52
SUM		64.1		164.42										26.54

Year: 1996 , I = 185.89 , a = 3.47

Month	TC^0	R (mm)	(T/5)	(T/5)^1.514	(T * 10)/I	[(T * 10)/I]^a	PE (mm)	K	PEc (mm)	AE (mm)	SM (mm)	ΔSM (mm)	WS R - (AE + ΔSM) (mm)	RGW WS - RO (mm)
Jan	12.8	40.0	2.56	4.15	0.69	0.28	4.48	0.89	3.99	3.99	21.01	-1.51	37.52	37.52
Feb	14.7	14.3	2.94	5.12	0.79	0.44	7.04	0.86	6.05	6.05	24.42	3.41	4.84	4.84
Mar	22	25.1	4.4	9.42	1.18	1.78	28.48	1.03	29.33	25.1	28.66	4.24	-4.24	-4.24
Apr	31.2	4.7	6.24	15.99	1.68	6.05	168	1.08	181.44	4.7	41.25	12.59	-12.59	-12.59
May	32.4	3.2	6.48	16.93	1.74	6.83	175.3	1.19	208.61	3.2	29.96	-11.29	11.29	11.29
June	37.5	0.0	7.5	21.13	2.02	11.47	185	1.19	220.15	0	26.15	-3.81	3.81	3.81
July	45	0.0	9	27.84	2.42	21.47	185	1.21	223.85	0	18.69	-7.46	7.46	7.46
Aug	47.5	0.0	9.5	30.22	2.56	26.1	185	1.15	212.75	0	18.22	-0.47	0.47	0.47
Sep	38.2	0.0	7.64	21.73	2.05	12.07	185	1.03	190.55	0	14.87	-3.35	3.35	3.35
Oct	29.6	0.0	5.92	14.77	1.59	5	158.9	0.98	155.72	0	15.14	0.27	-0.27	-0.27
Nov	21.4	0.8	4.28	9.04	1.15	1.62	25.92	0.88	22.81	0.8	17.2	2.06	-2.06	-2.06
Dec	22.2	3.2	4.44	9.55	1.19	1.83	29.28	0.87	25.47	3.2	24.82	7.62	-7.62	-7.62
SUM		91.3		185.89										41.96

Year: 1997 , I = 173.86 , a = 3.28

Month	TC^0	R (mm)	(T/5)	(T/5)^1.514	(T * 10)/I	[(T * 10)/I]^a	PE (mm)	K	PEc (mm)	AE (mm)	SM (mm)	ΔSM (mm)	WS R - (AE + ΔSM) (mm)	RGW WS - RO (mm)
Jan	11	12.8	2.2	3.3	0.63	0.22	3.52	0.89	3.13	3.13	29.96	5.14	4.53	4.53
Feb	14.6	0.7	2.92	5.07	0.84	0.56	8.96	0.86	7.71	0.7	34.92	4.96	-4.96	-4.96
Mar	22.5	10.9	4.5	9.75	1.29	2.31	36.96	1.03	38.07	10.9	35.36	0.44	-0.44	-0.44
Apr	33	4.1	6.6	17.41	1.9	8.21	177.2	1.08	191.38	4.1	42.4	7.04	-7.04	-7.04
May	35	0.6	7	19.03	2.01	9.87	182.9	1.19	217.65	0.6	29.96	-12.44	12.44	12.44
June	36.4	0.000	7.28	20.2	2.09	11.22	184.7	1.19	219.79	0	26.1	-3.86	3.86	3.86
July	43	0.0	8.6	25.99	2.47	19.41	185	1.21	223.85	0	18.79	-7.31	7.31	7.31
Aug	46	0.0	9.2	28.79	2.65	24.45	185	1.15	212.75	0	18.47	-0.32	0.32	0.32
Sep	35.7	0.0	7.14	19.61	2.05	10.53	183.7	1.03	189.21	0	15.37	-3.10	3.1	3.1
Oct	28	33.0	5.6	13.58	1.61	4.77	147.8	0.98	144.84	33	17.84	2.47	-2.47	-2.47
Nov	18.3	53.9	3.66	7.13	1.05	1.17	18.72	0.88	16.47	16.47	23.13	5.29	32.14	32.14
Dec	12.5	26.9	2.5	4	0.72	0.34	5.44	0.87	4.73	4.73	50.07	26.94	-4.77	-4.77
SUM		142.9		173.86										44.02

Year: 1998 , I = 173.84 , a = 3.28

Month	TC⁰	R (mm)	(T/5)	(T/5)^1.514	(T * 10)/I	[(T * 10)/I]^a	PE (mm)	K	PEc (mm)	AE (mm)	SM (mm)	ΔSM (mm)	WS R - (AE + ΔSM) (mm)	RGW WS - RO (mm)
Jan	11.8	32.5	2.36	3.67	0.68	0.28	4.48	0.89	3.99	3.99	53.81	3.74	24.77	24.77
Feb	12.5	18.4	2.5	4	0.72	0.34	5.44	0.86	4.68	4.68	59.12	5.31	8.41	8.41
Mar	20	32.9	4	8.16	1.15	1.58	25.28	1.03	26.04	26.04	61.66	2.54	4.32	4.32
Apr	30	2.1	6	15.07	1.73	6.04	162.1	1.08	175.07	2.1	66.75	5.09	-5.09	-5.09
May	33.5	0.800	6.7	17.81	1.93	8.64	179	1.19	213.01	0.8	49.96	-16.79	16.79	16.79
June	35.8	0.0	7.16	19.69	2.06	10.7	184.3	1.19	219.32	0	40.85	-9.11	9.11	9.11
July	42.4	0.0	8.48	25.44	2.44	18.65	185	1.21	223.85	0	29.19	-11.66	11.66	11.66
Aug	44	0.000	8.8	26.91	2.53	21	185	1.15	212.75	0	25.72	-3.47	3.47	3.47
Sep	38.7	0.0	7.74	22.16	2.23	13.88	185	1.03	190.55	0	20.47	-5.25	5.25	5.25
Oct	32.4	0.0	6.48	16.93	1.86	7.66	175.3	0.98	171.79	0	19.44	-1.03	1.03	1.03
Nov	19.4	9	3.88	7.79	1.12	1.45	23.2	0.88	20.42	9	17.7	-1.74	1.74	1.74
Dec	16.7	0.0	3.34	6.21	0.96	0.87	13.92	0.87	12.11	0	19.52	1.82	-1.82	-1.82
SUM		95.7		173.84										79.64

Year: 1999 , I = 185.54 , a = 3.47

Month	TC⁰	R (mm)	(T/5)	(T/5)^1.514	(T * 10)/I	[(T * 10)/I]^a	PE (mm)	K	PEc (mm)	AE (mm)	SM (mm)	ΔSM (mm)	WS R - (AE + ΔSM) (mm)	RGW WS - RO (mm)
Jan	10.4	35.5	2.08	3.03	0.56	0.13	2.08	0.89	1.85	1.85	18.79	-0.73	34.38	34.38
Feb	13.8	7.8	2.76	4.65	0.74	0.35	5.6	0.86	4.82	4.82	22.92	4.13	-1.15	-1.15
Mar	22	3.7	4.4	9.42	1.19	1.83	29.28	1.03	30.16	3.7	23.56	0.64	-0.64	-0.64
Apr	35	0	7	19.03	1.89	9.11	182.9	1.08	197.53	0	30.85	7.29	-7.29	-7.29
May	33.4	0.0	6.68	17.73	1.8	7.69	179	1.19	213.01	0	20.96	-9.89	9.89	9.89
June	37.6	0.0	7.52	21.21	2.03	11.67	185	1.19	220.15	0	19.35	-1.61	1.61	1.61
July	45.7	0.0	9.14	28.5	2.46	22.73	185	1.21	223.85	0	13.89	-5.46	5.46	5.46
Aug	45.7	0.0	9.14	28.5	2.46	22.73	185	1.15	212.75	0	18.42	4.53	-4.53	-4.53
Sep	38	0.0	7.6	21.56	2.05	12.07	185	1.03	190.55	0	17.47	-0.95	0.95	0.95
Oct	30.5	0.0	6.1	15.45	1.64	5.57	165.2	0.98	161.9	0	18.04	0.57	-0.57	-0.57
Nov	19	6.0	3.8	7.55	1.02	1.07	17.12	0.88	15.07	6	16.9	-1.14	1.14	1.14
Dec	21.2	12.1	4.24	8.91	1.14	1.58	25.28	0.87	21.99	12.1	21.82	4.92	-4.92	-4.92
SUM		54.8		185.54										34.33

Year: 2000 , I = 172.65 , a = 3.26

Month	TC^0	R (mm)	(T/5)	(T/5)^1.514	(T * 10)/I	[(T * 10)/I]^a	PE (mm)	K	PEc (mm)	AE (mm)	SM (mm)	ΔSM (mm)	WS R - (AE + ΔSM) (mm)	RGW WS - RO (mm)
Jan	12.2	10.0	2.44	3.86	0.71	0.33	5.28	0.89	4.7	4.7	20.61	-1.21	6.51	6.51
Feb	13.2	1.6	2.64	4.35	0.76	0.41	6.56	0.86	5.64	1.6	20.42	-0.19	0.19	0.19
Mar	18	0.3	3.6	6.95	1.04	1.14	18.24	1.03	18.79	0.3	19.06	-1.36	1.36	1.36
Apr	33.7	1.5	6.74	17.97	1.95	8.82	179	1.08	193.32	1.5	27.85	8.79	-8.79	-8.79
May	33	0.0	6.6	17.41	1.91	8.24	177.2	1.19	210.87	0	19.56	-8.29	8.29	8.29
June	38	0.0	7.6	21.56	2.2	13.07	185	1.19	220.15	0	18.65	-0.91	0.91	0.91
July	43.2	0.0	8.64	26.17	2.5	19.83	185	1.21	223.85	0	13.29	-5.36	5.36	5.36
Aug	44.2	0.0	8.84	27.1	2.56	21.42	185	1.15	212.75	0	14.42	1.13	-1.13	-1.13
Sep	36.3	0.0	7.26	20.11	2.1	11.23	184.7	1.03	190.24	0	12.37	-2.05	2.05	2.05
Oct	29.2	5.4	5.84	14.47	1.69	5.53	155.4	0.98	152.29	5.4	13.64	1.27	-1.27	-1.27
Nov	17.3	34.09	3.46	6.55	1	1	16	0.88	14.08	14.08	23.25	9.61	10.4	10.4
Dec	16.6	10.0	3.32	6.15	0.96	0.88	14.08	0.87	12.25	10	22.72	-0.53	0.53	0.53
SUM		62.9		172.65										24.41

Year: 2001 , I = 188.76 , a = 3.52

Month	TC^0	R (mm)	(T/5)	(T/5)^1.514	(T * 10)/I	[(T * 10)/I]^a	PE (mm)	K	PEc (mm)	AE (mm)	SM (mm)	ΔSM (mm)	WS R - (AE + ΔSM) (mm)	RGW WS - RO (mm)
Jan	9.1	12.1	1.82	2.48	0.48	0.08	1.28	0.89	1.14	1.14	29.36	6.64	4.32	4.32
Feb	12.6	9.9	2.52	4.05	0.67	0.24	3.84	0.86	3.3	3.3	36.87	7.51	-0.91	-0.91
Mar	17.6	4.0	3.52	6.72	0.93	0.77	12.32	1.03	12.69	4	40.56	3.69	-3.69	-3.69
Apr	32.5	25.7	6.5	17.01	1.72	6.75	175.3	1.08	189.32	25.7	47.7	7.14	-7.14	-7.14
May	32.6	1.4	6.52	17.09	1.73	6.89	175.3	1.19	208.61	1.4	35.06	-12.64	12.64	12.64
June	37.7	0.0	7.54	21.3	2	11.47	185	1.19	220.15	0	30.05	-5.01	5.01	5.01
July	46.4	0.0	9.28	29.17	2.46	23.77	185	1.21	223.85	0	21.49	-8.56	8.56	8.56
Aug	48	0.0	9.6	30.7	2.54	26.61	185	1.15	212.75	0	20.17	-1.32	1.32	1.32
Sep	38.8	0.000	7.76	22.25	2.06	12.73	185	1.03	190.55	0	16.57	-3.60	3.6	3.6
Oct	31.3	0.4	6.26	16.07	1.66	5.95	170.7	0.98	167.29	0.4	16.94	0.37	-0.37	-0.37
Nov	25	2.2	5	11.44	1.32	2.66	42.56	0.88	37.45	2.2	16.7	-0.24	0.24	0.24
Dec	23.6	19.3	4.72	10.48	1.25	2.19	35.04	0.87	30.48	19.3	20.82	4.12	-4.12	-4.12
SUM		75.0		188.76										19.46

| Year: 2002 , I = 185.81 , a = 3.47 | | | | | | | | | | | | | WS | RGW |
Month	TC^0	R (mm)	(T/5)	(T/5)^1.514	(T * 10)/I	[(T * 10)/I]^a	PE (mm)	K	PEc (mm)	AE (mm)	SM (mm)	ΔSM (mm)	R - (AE + ΔSM) (mm)	WS - RO (mm)
Jan	11	5.0	2.2	3.3	0.59	0.16	2.56	0.89	2.28	2.28	23.31	2.49	0.23	0.23
Feb	15	4.5	3	5.28	0.81	0.48	7.68	0.86	6.6	4.5	26.82	3.51	-3.51	-3.51
Mar	23.4	9.3	4.68	10.35	1.26	2.23	35.68	1.03	36.75	9.3	27.76	0.94	-0.94	-0.94
Apr	32.5	23.3	6.5	17.01	1.75	6.97	175.3	1.08	189.32	23.3	38.75	10.99	-10.99	-10.99
May	35.8	4.0	7.16	19.69	1.93	9.79	184.7	1.19	219.79	4	28.26	-10.49	10.49	10.49
June	37.5	0.0	7.5	21.13	2.02	11.47	185	1.19	220.15	0	24.65	-3.61	3.61	3.61
July	44.8	0.0	8.96	27.66	2.41	21.16	185	1.21	223.85	0	17.59	-7.06	7.06	7.06
Aug	46	0.0	9.2	28.79	2.48	23.37	185	1.15	212.75	0	26.52	8.93	-8.93	-8.93
Sep	37.3	0.0	7.46	20.96	2.01	11.27	185	1.03	190.55	0	31.37	4.85	-4.85	-4.85
Oct	32.2	0.4	6.44	16.77	1.73	6.7	173.1	0.98	169.64	0.4	27.84	-3.53	3.53	3.53
Nov	20.8	5.3	4.16	8.66	1.12	1.48	23.68	0.88	20.84	5.3	25.7	-2.14	2.14	2.14
Dec	16.7	12.4	3.34	6.21	0.9	0.69	11.04	0.87	9.6	9.6	28.02	2.32	0.48	0.48
SUM		64.2		185.81										-1.68

| Year: 2003 , I = 177.46 , a = 3.34 | | | | | | | | | | | | | WS | RGW |
Month	TC^0	R (mm)	(T/5)	(T/5)^1.514	(T * 10)/I	[(T * 10)/I]^a	PE (mm)	K	PEc (mm)	AE (mm)	SM (mm)	ΔSM (mm)	R - (AE + ΔSM) (mm)	WS - RO (mm)
Jan	10.5	6.1	2.1	3.07	0.59	0.17	2.72	0.89	2.42	2.42	27.11	-0.91	4.59	4.59
Feb	13.6	0.0	2.72	4.55	0.77	0.42	6.72	0.86	5.78	0	28.62	1.51	-1.51	-1.51
Mar	21.3	0.4	4.26	8.97	1.2	1.84	29.44	1.03	30.32	0.4	27.06	-1.56	1.56	1.56
Apr	32.2	6.8	6.44	16.77	1.81	7.26	173.1	1.08	186.95	6.8	36.25	9.19	-9.19	-9.19
May	31.6	2	6.32	16.3	1.78	6.86	170.7	1.19	203.13	2	26.06	-10.19	10.19	10.19
June	38	0.0	7.6	21.56	2.14	12.69	185	1.19	220.15	0	23.05	-3.01	3.01	3.01
July	48.4	0.0	9.68	31.09	2.73	28.63	185	1.21	223.85	0	16.39	-6.66	6.66	6.66
Aug	46.8	0.0	9.36	29.55	2.64	25.6	185	1.15	212.75	0	16.52	0.13	-0.13	-0.13
Sep	35.5	0.0	7.1	19.44	2	10.13	183.7	1.03	189.21	0	13.87	-2.65	2.65	2.65
Oct	27.6	0.500	5.52	13.28	1.56	4.42	143.7	0.98	140.83	0.5	14.54	0.67	-0.67	-0.67
Nov	18	37.93	3.6	6.95	1.01	1.03	16.48	0.88	14.5	14.5	27.05	12.51	10.92	10.92
Dec	16.2	20.4	3.24	5.93	0.91	0.73	11.68	0.87	10.16	10.16	27.22	0.17	10.07	10.07
SUM		74.1		177.46										38.15

Year: 2004 , I = 193.82 , a = 3.6

Month	TC[0]	R (mm)	(T/5)	(T/5)^1.514	(T * 10)/I	[(T * 10)/I]^a	PE (mm)	K	PEc (mm)	AE (mm)	SM (mm)	ΔSM (mm)	WS R - (AE + ΔSM) (mm)	RGW WS - RO (mm)
Jan	10	38.6	2	2.86	0.52	0.09	1.44	0.89	1.28	1.28	38.76	11.54	25.78	25.78
Feb	16.2	1.2	3.24	5.93	0.84	0.53	8.48	0.86	7.29	1.2	34.42	-4.34	4.34	4.34
Mar	28	1.0	5.6	13.58	1.44	3.72	147.8	1.03	152.23	1	33.16	-1.26	1.26	1.26
Apr	33	4.4	6.6	17.41	1.7	6.75	177.2	1.08	191.38	4.4	41.95	8.79	-8.79	-8.79
May	32.5	7.2	6.5	17.01	1.68	6.47	175.3	1.19	208.61	7.2	30.96	-10.99	10.99	10.99
June	35.7	0.0	7.14	19.61	1.84	8.98	183.7	1.19	218.6	0	26.65	-4.31	4.31	4.31
July	46	0.0	9.2	28.79	2.37	22.34	185	1.21	223.85	0	19.09	-7.56	7.56	7.56
Aug	48.6	0.0	9.72	31.28	2.51	27.47	185	1.15	212.75	0	18.42	-0.67	0.67	0.67
Sep	37	0.0	7.4	20.7	1.91	10.27	184.9	1.03	190.45	0	15.17	-3.25	3.25	3.25
Oct	29.6	0.000	5.92	14.77	1.53	4.62	158.9	0.98	155.72	0	15.24	0.07	-0.07	-0.07
Nov	26	11.1	5.2	12.13	1.34	2.87	45.92	0.88	40.41	11.1	16.9	1.66	-1.66	-1.66
Dec	22.5	1.7	4.5	9.75	1.16	1.71	27.36	0.87	23.8	1.7	22.52	5.62	-5.62	-5.62
SUM		65.2		193.82										42.02

Year: 2005 , I = 182.32 , a = 3.42

Month	TC[0]	R (mm)	(T/5)	(T/5)^1.514	(T * 10)/I	[(T * 10)/I]^a	PE (mm)	K	PEc (mm)	AE (mm)	SM (mm)	ΔSM (mm)	WS R - (AE + ΔSM) (mm)	RGW WS - RO (mm)
Jan	8	38	1.6	2.04	0.44	0.06	0.96	0.89	0.85	0.85	22.61	0.09	37.06	37.06
Feb	14.4	9.7	2.88	4.96	0.79	0.45	7.2	0.86	6.19	6.19	26.32	3.71	-0.2	-0.2
Mar	26	12.8	5.2	12.13	1.43	3.4	54.4	1.03	56.03	12.8	30.06	3.74	-3.74	-3.74
Apr	28.2	12.4	5.64	13.72	1.55	4.48	147.8	1.08	159.62	12.4	39.15	9.09	-9.09	-9.09
May	33.4	0.2	6.68	17.73	1.83	7.9	179	1.19	213.01	0.2	27.36	-11.79	11.79	11.79
June	38.2	0.0	7.64	21.73	2.1	12.65	185	1.19	220.15	0	23.95	-3.41	3.41	3.41
July	46	0.0	9.2	28.79	2.52	23.59	185	1.21	223.85	0	17.09	-6.86	6.86	6.86
Aug	45.7	0.0	9.14	28.5	2.51	23.27	185	1.15	212.75	0	17.12	0.03	-0.03	-0.03
Sep	37.7	0.0	7.54	21.3	2.07	12.04	185	1.03	190.55	0	14.17	-2.95	2.95	2.95
Oct	32	0.300	6.4	16.62	1.76	6.91	173.1	0.98	169.64	0.3	14.64	0.47	-0.47	-0.47
Nov	19.3	6.6	3.86	7.73	1.06	1.22	19.52	0.88	17.18	6.6	15.4	0.76	-0.76	-0.76
Dec	18.2	2.0	3.64	7.07	1	1	16	0.87	13.92	2	20.42	5.02	-5.02	-5.02
SUM		71.7		182.32										42.76

| Year: 2006 , I = 182.88 , a = 3.43 | | | | | | | | | | | | | WS | RGW |
Month	TC⁰	R (mm)	(T/5)	(T/5)^1.514	(T * 10)/I	[(T * 10)/I]^a	PE (mm)	K	PEc (mm)	AE (mm)	SM (mm)	ΔSM (mm)	R - (AE + ΔSM) (mm)	WS - RO (mm)
Jan	12.5	25.5	2.5	4	0.68	0.27	4.32	0.89	3.84	3.84	19.81	-0.61	22.27	22.27
Feb	15.8	43.3	3.16	5.71	0.86	0.6	9.6	0.86	8.26	8.26	24.24	4.43	30.61	30.61
Mar	20	4.2	4	8.16	1.09	1.34	21.44	1.03	22.08	4.2	25.96	1.72	-1.72	-1.72
Apr	33	36.6	6.6	17.41	1.8	7.51	177.2	1.08	191.38	36.6	39.45	13.49	-13.49	-13.49
May	30.8	11.3	6.16	15.68	1.68	5.93	168	1.19	199.92	11.3	31.81	-7.64	7.64	7.64
June	36.6	0.0	7.32	20.36	2	10.78	184.7	1.19	219.79	0	27.35	-4.46	4.46	4.46
July	44.6	0.0	8.92	27.47	2.44	21.32	185	1.21	223.85	0	19.49	-7.86	7.86	7.86
Aug	48.4	0.0	9.68	31.09	2.65	28.3	185	1.15	212.75	0	18.72	-0.77	0.77	0.77
Sep	38	0.0	7.6	21.56	2.08	12.33	185	1.03	190.55	0	15.37	-3.35	3.35	3.35
Oct	30	2.8	6	15.07	1.64	5.46	162.1	0.98	158.86	2.8	18.54	3.17	-3.17	-3.17
Nov	24.5	27.1	4.9	11.09	1.34	2.73	43.68	0.88	38.44	27.1	20.2	1.66	-1.66	-1.66
Dec	15	44.1	3	5.28	0.82	0.51	8.16	0.87	7.1	7.1	23.92	3.72	33.28	33.28
SUM		194.9		182.88										90.20

| Year: 2007 , I = 187.56 , a = 3.5 | | | | | | | | | | | | | WS | RGW |
Month	TC⁰	R (mm)	(T/5)	(T/5)^1.514	(T * 10)/I	[(T * 10)/I]^a	PE (mm)	K	PEc (mm)	AE (mm)	SM (mm)	ΔSM (mm)	R - (AE + ΔSM) (mm)	WS - RO (mm)
Jan	9.3	36.0	1.86	2.56	0.5	0.09	1.44	0.89	1.28	1.28	24.41	0.49	34.23	34.23
Feb	15.2	2.4	3.04	5.38	0.81	0.48	7.68	0.86	6.6	2.4	29.42	5.01	-5.01	-5.01
Mar	29	5.6	5.8	14.32	1.55	4.64	155.4	1.03	160.06	5.6	30.96	1.54	-1.54	-1.54
Apr	30.3	8.3	6.06	15.3	1.62	5.41	165.2	1.08	178.42	8.3	41.35	10.39	-10.39	-10.39
May	33.2	2.300	6.64	17.57	1.77	7.38	177.2	1.19	210.87	2.3	30.56	-10.79	10.79	10.79
June	36	0.0	7.2	19.86	1.92	9.81	184.3	1.19	219.32	0	26.25	-4.31	4.31	4.31
July	47.2	0.0	9.44	29.93	2.52	25.4	185	1.21	223.85	0	18.89	-7.36	7.36	7.36
Aug	43.7	0.0	8.74	26.63	2.33	19.31	185	1.15	212.75	0	18.22	-0.67	0.67	0.67
Sep	41.8	0.0	8.36	24.9	2.23	16.56	185	1.03	190.55	0	14.97	-3.25	3.25	3.25
Oct	32.5	0	6.5	17.01	1.73	6.81	175.3	0.98	171.79	0	15.14	0.17	-0.17	-0.17
Nov	20.2	4.5	4.04	8.28	1.08	1.31	20.96	0.88	18.44	4.5	14.2	-0.94	0.94	0.94
Dec	16	12.8	3.2	5.82	0.85	0.57	9.12	0.87	7.93	7.93	18.22	4.02	0.85	0.85
SUM		71.9		187.56										45.29

Year: 2008 , I = 190.86 , a = 3.55

Month	TC^0	R (mm)	(T/5)	(T/5)^1.514	(T * 10)/I	[(T * 10)/I]^a	PE (mm)	K	PEc (mm)	AE (mm)	SM (mm)	ΔSM (mm)	WS R - (AE + ΔSM) (mm)	RGW WS - RO (mm)
Jan	10.8	28.4	2.16	3.21	0.57	0.14	2.24	0.89	1.99	1.99	28.48	10.26	16.15	16.15
Feb	15	1.0	3	5.28	0.79	0.43	6.88	0.86	5.92	1	25.02	-3.46	3.46	3.46
Mar	23.5	0.5	4.7	10.41	1.23	2.09	33.44	1.03	34.44	0.5	24.86	-0.16	0.16	0.16
Apr	33.6	0.2	6.72	17.89	1.76	7.44	179	1.08	193.32	0.2	32.15	7.29	-7.29	-7.29
May	31.8	2.0	6.36	16.46	1.67	6.18	173.1	1.19	205.99	2	22.16	-9.99	9.99	9.99
June	39	0.0	7.8	22.42	2.04	12.57	185	1.19	220.15	0	19.95	-2.21	2.21	2.21
July	47	0.0	9.4	29.74	2.46	24.42	185	1.21	223.85	0	14.49	-5.46	5.46	5.46
Aug	46.8	0.000	9.36	29.55	2.45	24.07	185	1.15	212.75	0	15.22	0.73	-0.73	-0.73
Sep	37.5	0.0	7.5	21.13	1.96	10.9	185	1.03	190.55	0	13.47	-1.75	1.75	1.75
Oct	32.4	28.8	6.48	16.93	1.7	6.58	175.3	0.98	171.79	28.8	15.94	2.47	-2.47	-2.47
Nov	19.8	0.5	3.96	8.03	1.04	1.15	18.4	0.88	16.19	0.5	19	3.06	-3.06	-3.06
Dec	22.6	19.8	4.52	9.81	1.18	1.8	28.8	0.87	25.06	19.8	23.92	4.92	-4.92	-4.92
SUM		81.2		190.86										20.71

Year: 2009 , I = 187.82 , a = 3.51

Month	TC^0	R (mm)	(T/5)	(T/5)^1.514	(T * 10)/I	[(T * 10)/I]^a	PE (mm)	K	PEc (mm)	AE (mm)	SM (mm)	ΔSM (mm)	WS R - (AE + ΔSM) (mm)	RGW WS - RO (mm)
Jan	11.5	3.4	2.3	3.53	0.61	0.18	2.88	0.89	2.56	2.56	24.48	0.56	0.28	0.28
Feb	18	5.8	3.6	6.95	0.96	0.87	13.92	0.86	11.97	5.8	28.7	4.22	-4.22	-4.22
Mar	22.2	19.5	4.44	9.55	1.18	1.79	28.64	1.03	29.5	19.5	26.06	-2.64	2.64	2.64
Apr	30.8	16.8	6.16	15.68	1.64	5.68	168	1.08	181.44	16.8	25.96	-0.10	0.1	0.1
May	34.4	0.2	6.88	18.54	1.83	8.34	181.8	1.19	216.34	0.2	22.09	-3.87	3.87	3.87
June	38.5	0.0	7.7	21.99	2.05	12.42	185	1.19	220.15	0	19.05	-3.04	3.04	3.04
July	44.8	0.0	8.96	27.66	2.39	21.29	185	1.21	223.85	0	17.84	-1.21	1.21	1.21
Aug	47.6	0.0	9.52	30.31	2.53	26	185	1.15	212.75	0	17.3	-0.54	0.54	0.54
Sep	37.4	0.0	7.48	21.04	1.99	11.19	185	1.03	190.55	0	14.45	-2.85	2.85	2.85
Oct	32.2	7.4	6.44	16.77	1.71	6.57	173.1	0.98	169.64	7.4	10.74	-3.71	3.71	3.71
Nov	22	31.5	4.4	9.42	1.17	1.74	27.84	0.88	24.5	24.5	15.75	5.01	1.99	1.99
Dec	17	9.5	3.4	6.38	0.91	0.72	11.52	0.87	10.02	9.5	22.04	6.29	-6.29	-6.29
SUM		94.1		187.82										9.72

Year: 2010 , I = 193.14 , a = 3.59

Month	TC^0	R (mm)	(T/5)	(T/5)^1.514	(T * 10)/I	[(T * 10)/I]^a	PE (mm)	K	PEc (mm)	AE (mm)	SM (mm)	ΔSM (mm)	WS R - (AE + ΔSM) (mm)	RGW WS - RO (mm)
Jan	10	2.7	2	2.86	0.52	0.1	1.6	0.89	1.42	1.42	27.38	5.34	-4.06	-4.06
Feb	14.6	14.8	2.92	5.07	0.76	0.37	5.92	0.86	5.09	5.09	34.5	7.12	2.59	2.59
Mar	19.6	5.9	3.92	7.91	1.01	1.04	16.64	1.03	17.14	5.9	32.16	-2.34	2.34	2.34
Apr	29.5	13.4	5.9	14.69	1.53	4.6	158.9	1.08	171.61	13.4	31.66	-0.50	0.5	0.5
May	35	8.6	7	19.03	1.81	8.42	182.9	1.19	217.65	8.6	26.99	-4.67	4.67	4.67
June	37.5	0.0	7.5	21.13	1.94	10.79	185	1.19	220.15	0	22.65	-4.34	4.34	4.34
July	48	0.0	9.6	30.7	2.49	26.45	185	1.21	223.85	0	20.54	-2.11	2.11	2.11
Aug	48	0.0	9.6	30.7	2.49	26.45	185	1.15	212.75	0	19.2	-1.34	1.34	1.34
Sep	41.3	0.0	8.26	24.45	2.14	15.35	185	1.03	190.55	0	15.75	-3.45	3.45	3.45
Oct	31.9	0.0	6.38	16.54	1.65	6.04	173.1	0.98	169.64	0	11.44	-4.31	4.31	4.31
Nov	25.5	0.0	5.1	11.78	1.32	2.71	43.36	0.88	38.16	0	14.35	2.91	-2.91	-2.91
Dec	20.2	4.9	4.04	8.28	1.05	1.19	19.04	0.87	16.56	4.9	17.34	2.99	-2.99	-2.99
SUM		50.3		193.14										15.69

Year: 2011 , I = 200.33 , a = 3.71

Month	TC^0	R (mm)	(T/5)	(T/5)^1.514	(T * 10)/I	[(T * 10)/I]^a	PE (mm)	K	PEc (mm)	AE (mm)	SM (mm)	ΔSM (mm)	WS R - (AE + ΔSM) (mm)	RGW WS - RO (mm)
Jan	9.5	35.6	1.9	2.64	0.47	0.06	0.96	0.89	0.85	0.85	20.02	2.68	32.07	32.07
Feb	14	19.8	2.8	4.75	0.7	0.27	4.32	0.86	3.72	3.72	26.4	6.38	9.7	9.7
Mar	30.5	4.8	6.1	15.45	1.52	4.73	165.2	1.03	170.16	4.8	29.06	2.66	-2.66	-2.66
Apr	34.7	21.9	6.94	18.79	1.73	7.64	181.8	1.08	196.34	21.9	28.86	-0.20	0.2	0.2
May	33.5	1.6	6.7	17.81	1.67	6.7	179	1.19	213.01	1.6	23.39	-5.47	5.47	5.47
June	39.5	0.000	7.9	22.86	1.97	12.37	185	1.19	220.15	0	19.95	-3.44	3.44	3.44
July	48	0.0	9.6	30.7	2.4	25.74	185	1.21	223.85	0	18.54	-1.41	1.41	1.41
Aug	48	0.0	9.6	30.7	2.4	25.74	185	1.15	212.75	0	17.9	-0.64	0.64	0.64
Sep	42	0.0	8.4	25.08	2.1	15.68	185	1.03	190.55	0	14.75	-3.15	3.15	3.15
Oct	31	0.3	6.2	15.84	1.55	5.08	168	0.98	164.64	0.3	10.84	-3.91	3.91	3.91
Nov	19	3.400	3.8	7.55	0.95	0.83	13.28	0.88	11.69	3.4	12.85	2.01	-2.01	-2.01
Dec	20	1.1	4	8.16	1	1	16	0.87	13.92	1.1	15.24	2.39	-2.39	-2.39
SUM		78.2		200.33										52.93

Year: 2012 , I = 187.69 , a = 3.5

Month	TC⁰	R (mm)	(T/5)	(T/5)^1.514	(T * 10)/I	[(T * 10)/I]^a	PE (mm)	K	PEc (mm)	AE (mm)	SM (mm)	ΔSM (mm)	WS R - (AE + ΔSM) (mm)	RGW WS - RO (mm)
Jan	12.2	0.2	2.44	3.86	0.65	0.22	3.52	0.89	3.13	0.2	17.18	1.94	-1.94	-1.94
Feb	15	3.9	3	5.28	0.8	0.46	7.36	0.86	6.33	3.9	24.32	7.14	-7.14	-7.14
Mar	22.4	2.8	4.48	9.68	1.19	1.84	29.44	1.03	30.32	2.8	24.96	0.64	-0.64	-0.64
Apr	32	0.2	6.4	16.62	1.7	6.41	173.1	1.08	186.95	0.2	29.16	4.20	-4.2	-4.2
May	33.8	1.7	6.76	18.05	1.8	7.82	180.5	1.19	214.8	1.7	27.84	-1.32	1.32	1.32
June	39	0.0	7.8	22.42	2.08	12.98	185	1.19	220.15	0	23.35	-4.49	4.49	4.49
July	44.8	0.0	8.96	27.66	2.39	21.11	185	1.21	223.85	0	20.94	-2.41	2.41	2.41
Aug	47.8	0.0	9.56	30.51	2.55	26.48	185	1.15	212.75	0	19.5	-1.44	1.44	1.44
Sep	36.6	0.0	7.32	20.36	1.95	10.35	184.7	1.03	190.24	0	15.95	-3.55	3.55	3.55
Oct	30.4	2.4	6.08	15.38	1.62	5.41	165.2	0.98	161.9	2.4	14.74	-1.21	1.21	1.21
Nov	23	15.7	4.6	10.08	1.23	2.06	32.96	0.88	29	15.7	17.65	2.91	-2.91	-2.91
Dec	19.4	21.9	3.88	7.79	1.03	1.11	17.76	0.87	15.45	15.45	18.74	1.09	5.36	5.36
SUM		48.8		187.69										2.95

Year: 2013 , I = 202.76 , a = 3.74

Month	TC⁰	R (mm)	(T/5)	(T/5)^1.514	(T * 10)/I	[(T * 10)/I]^a	PE (mm)	K	PEc (mm)	AE (mm)	SM (mm)	ΔSM (mm)	WS R - (AE + ΔSM) (mm)	RGW WS - RO (mm)
Jan	14.2	27.6	2.84	4.86	0.7	0.26	4.16	0.89	3.7	3.7	21.78	3.04	20.86	20.86
Feb	21.5	3.2	4.3	9.1	1.06	1.24	19.84	0.86	17.06	3.2	29.5	7.72	-7.72	-7.72
Mar	30.2	4.000	6.04	15.22	1.49	4.44	162.1	1.03	166.96	4	29.96	0.46	-0.46	-0.46
Apr	30.2	2.100	6.04	15.22	1.49	4.44	162.1	1.08	175.07	2.1	31.06	1.10	-1.1	-1.1
May	32.9	20.0	6.58	17.33	1.62	6.08	177.2	1.19	210.87	20	26.59	-4.47	4.47	4.47
June	40	0.0	8	23.3	1.97	12.63	185	1.19	220.15	0	22.25	-4.34	4.34	4.34
July	46.7	0.0	9.34	29.45	2.3	22.54	185	1.21	223.85	0	20.34	-1.91	1.91	1.91
Aug	48.6	0.0	9.72	31.28	2.4	26.42	185	1.15	212.75	0	19	-1.34	1.34	1.34
Sep	38.6	0.0	7.72	22.07	1.9	11.03	185	1.03	190.55	0	15.55	-3.45	3.45	3.45
Oct	31.4	1.9	6.28	16.15	1.55	5.15	170.7	0.98	167.29	1.9	11.34	-4.21	4.21	4.21
Nov	22.3	60.6	4.46	9.62	1.1	1.43	22.88	0.88	20.13	20.13	11.65	0.31	40.16	40.16
Dec	21.6	0.1	4.32	9.16	1.07	1.29	20.64	0.87	17.96	0.1	13.04	1.39	-1.39	-1.39
SUM		119.5		202.76										70.07

Month	TC⁰	R (mm)	(T/5)	(T/5)^1.514	(T * 10)/I	[(T * 10)/I]^a	PE (mm)	K	PEc (mm)	AE (mm)	SM (mm)	ΔSM (mm)	WS R - (AE + ΔSM) (mm)	RGW WS - RO (mm)
Jan	13.4	37.7	2.68	4.45	0.77	0.42	6.72	0.89	5.98	5.98	17.08	4.04	27.68	27.68
Feb	18.1	2.6	3.62	7.01	1.03	1.1	17.6	0.86	15.14	2.6	25.1	8.02	-8.02	-8.02
Mar	20.2	26.3	4.04	8.28	1.16	1.63	26.08	1.03	26.86	26.3	23.86	-1.24	1.24	1.24
Apr	28.4	12.6	5.68	13.87	1.62	4.91	151.7	1.08	163.84	12.6	21.86	-2.00	2	2
May	28.3	0.001	5.66	13.8	1.62	4.91	151.7	1.19	180.52	0.001	18.19	-3.67	3.67	3.67
June	37	0.001	7.4	20.7	2.12	11.94	184.9	1.19	220.03	0.001	15.95	-2.24	2.24	2.24
July	44.4	0	8.88	27.28	2.54	21.67	185	1.21	223.85	0	15.94	-0.01	0.01	0.01
Aug	45.3	0	9.06	28.12	2.59	23.11	185	1.15	212.75	0	16	0.06	-0.06	-0.06
Sep	37.6	0	7.52	21.21	2.15	12.5	185	1.03	190.55	0	14.05	-1.95	1.95	1.95
Oct	29.4	2.9	5.88	14.62	1.68	5.54	158.9	0.98	155.72	2.9	12.14	-1.91	1.91	1.91
Nov	20.5	16.0	4.1	8.47	1.17	1.68	26.88	0.88	23.65	16	16.45	4.31	-4.31	-4.31
Dec	18.2	1.8	3.64	7.07	1.04	1.14	18.24	0.87	15.87	1.8	18.74	2.29	-2.29	-2.29
SUM		99.9		174.88										26.02

Year: 2014 , I = 174.88 , a = 3.3

Appendix E

Top Layer   Bottom Layer
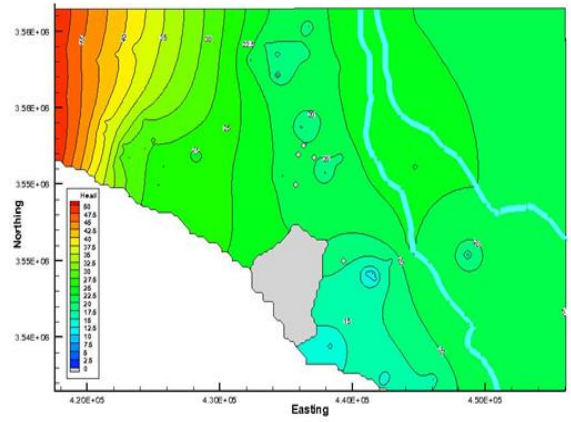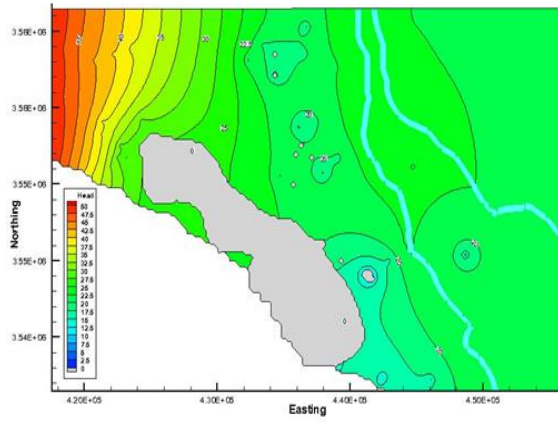
Current Pumping Rate
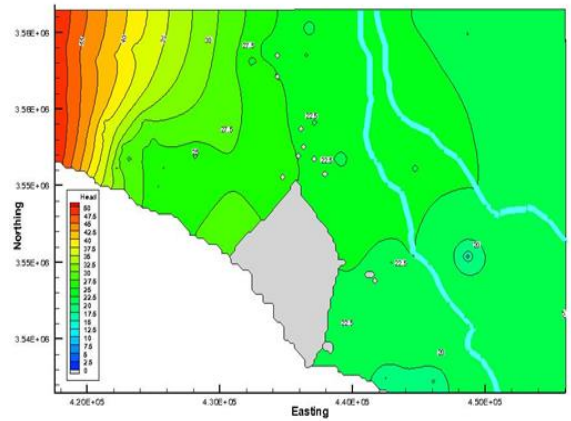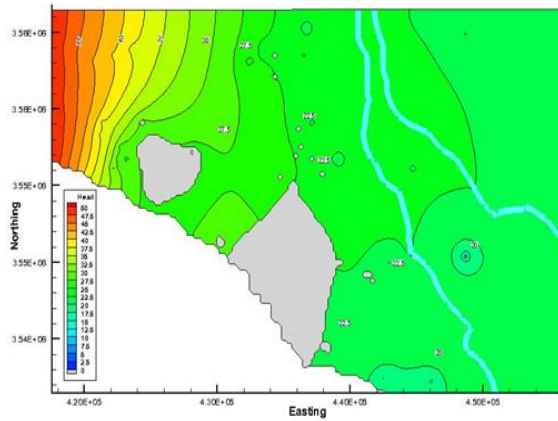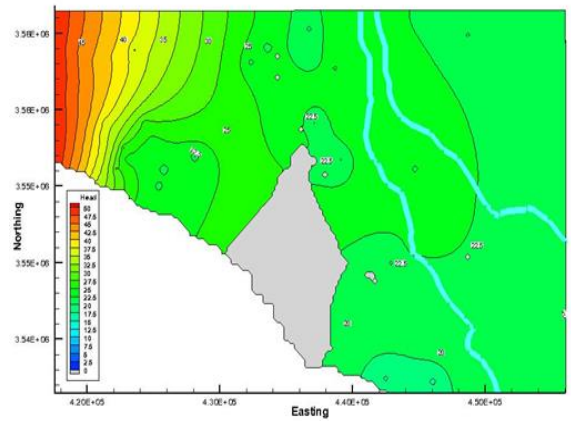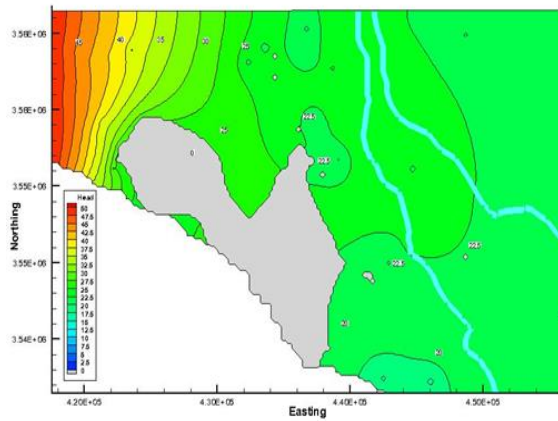
10% Increment
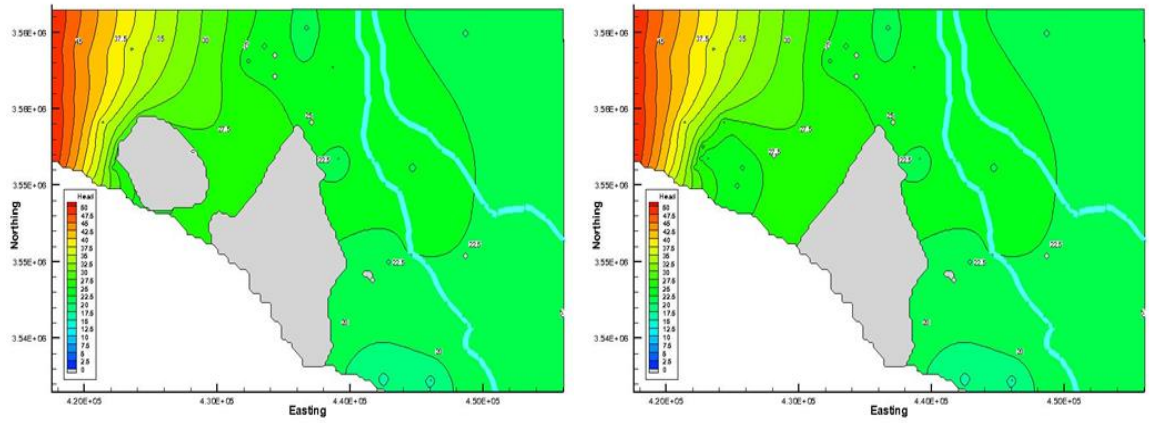
20% Increment
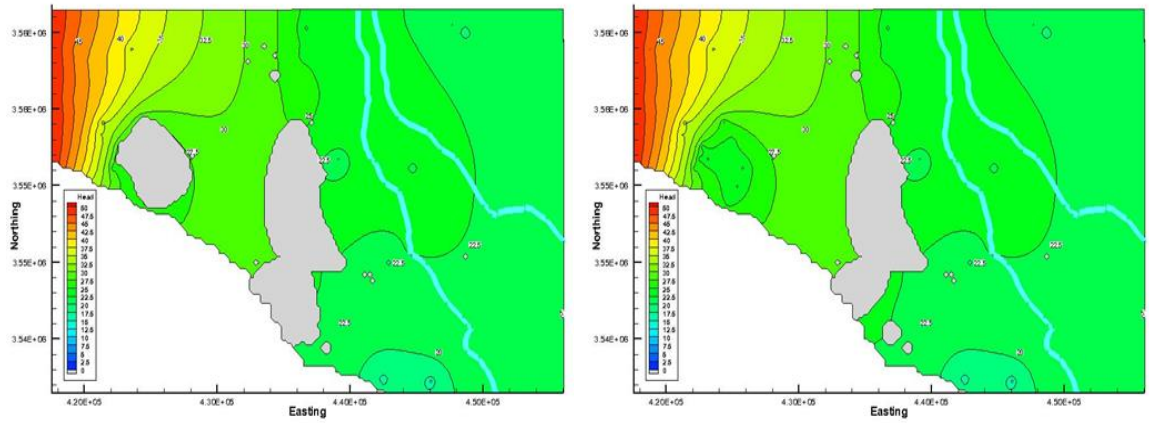
30% Increment
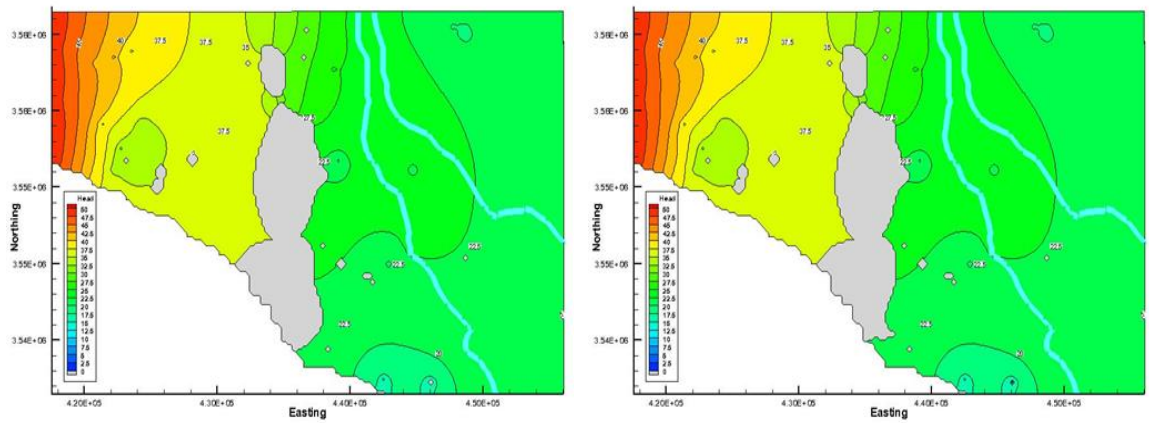
40% Increment

50% Increment

Figure E.1: Computed groundwater tables in the top and bottom layers of the model through the various increments of the pumping rate when the recharge rate reduced by half

Top Layer
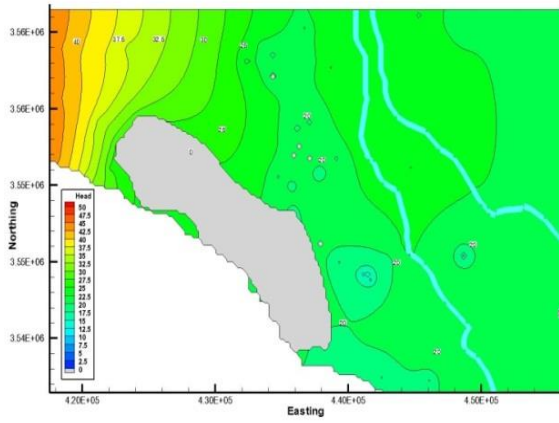
Bottom Layer
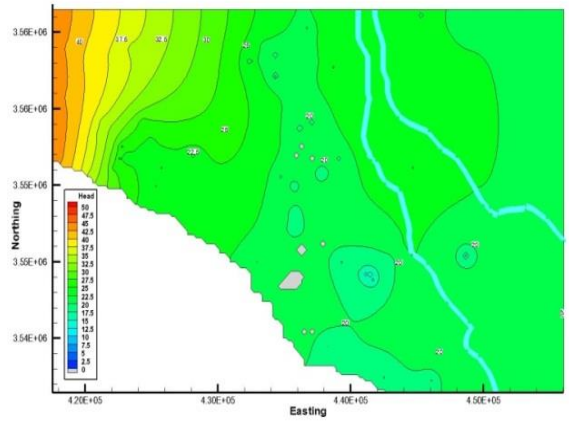
Current Pumping Rate
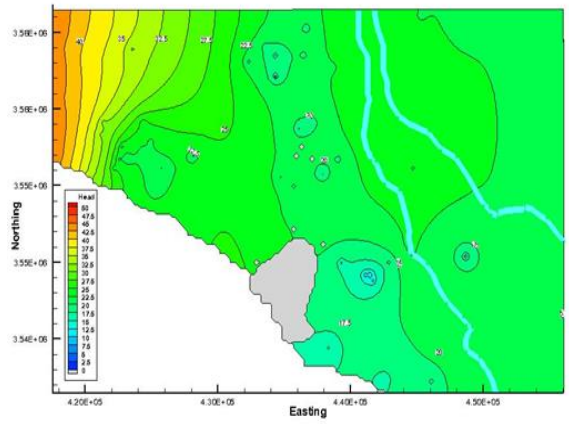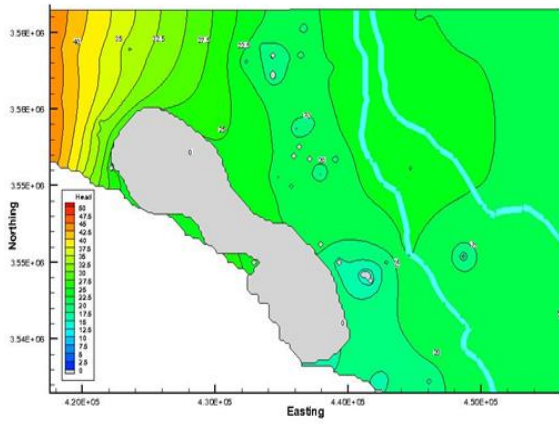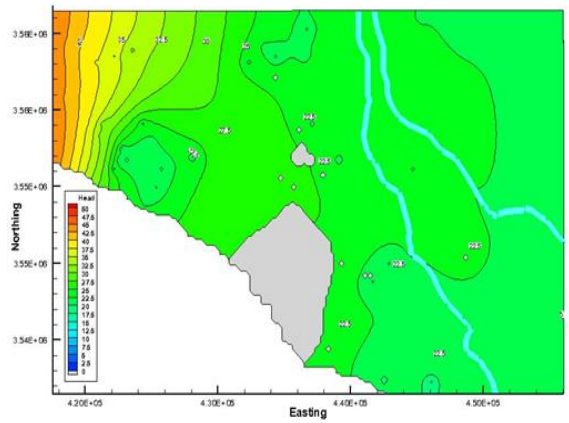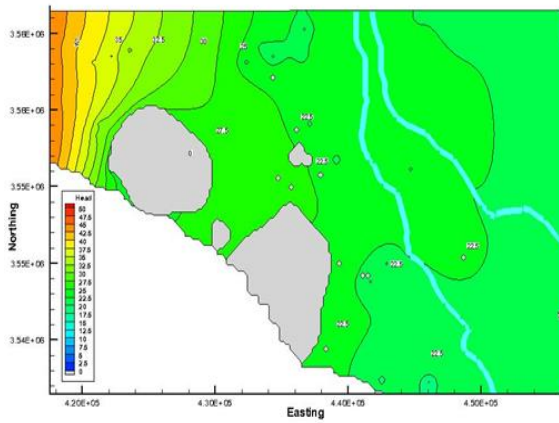
10% Increment
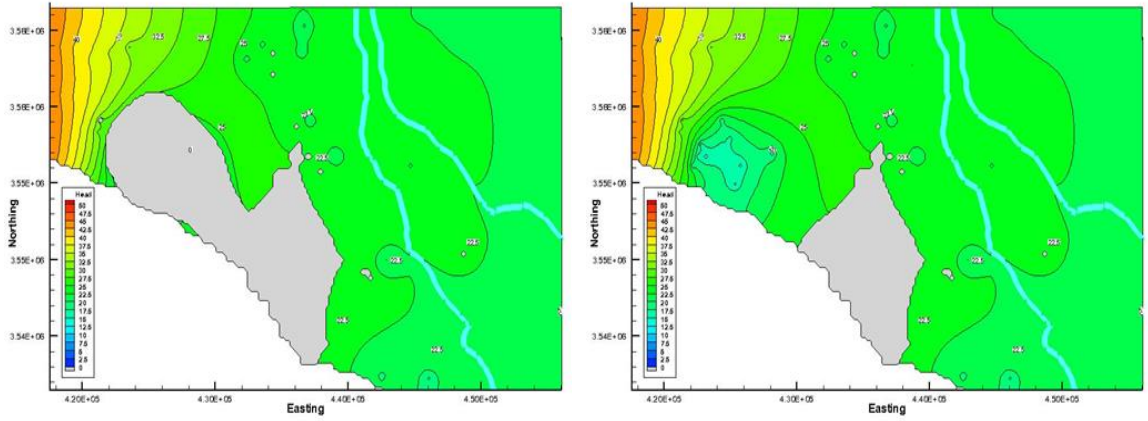
20% Increment
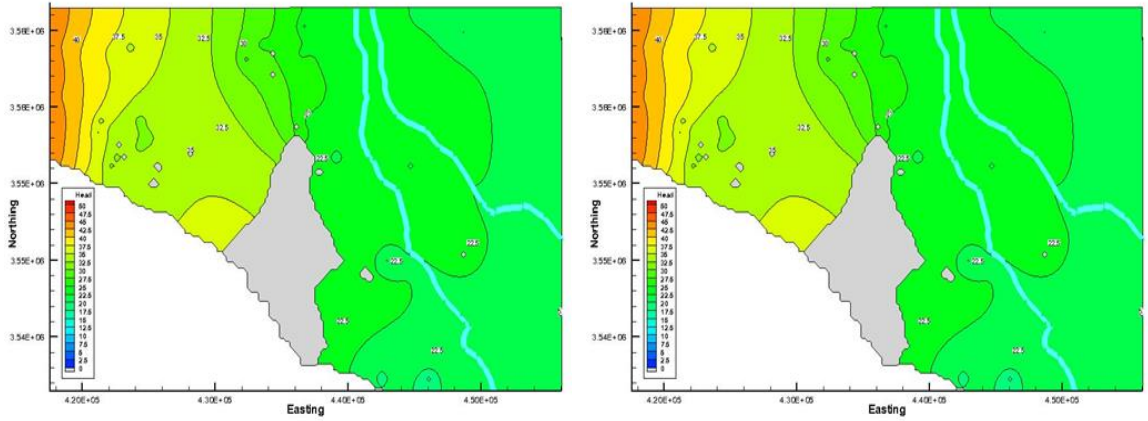
30% Increment
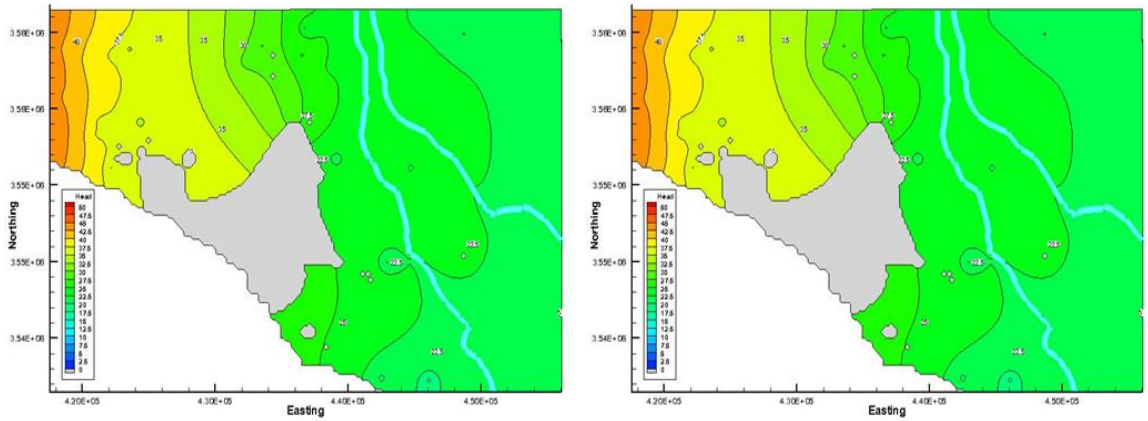
40% Increment

50% Increment

Figure E.2: Computed groundwater tables in the top and bottom layers of the model through the various increments of the pumping rate when reducing the western constant head to be 45m

Top Layer
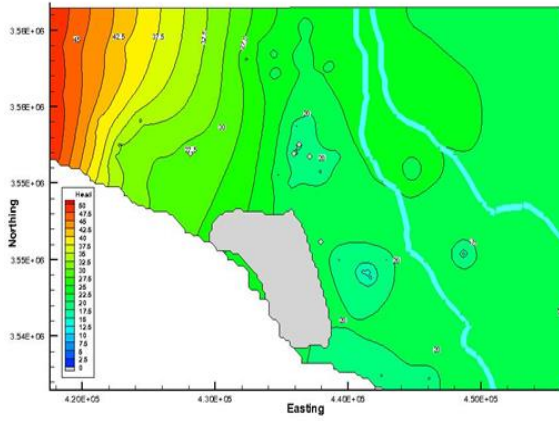
Bottom Layer
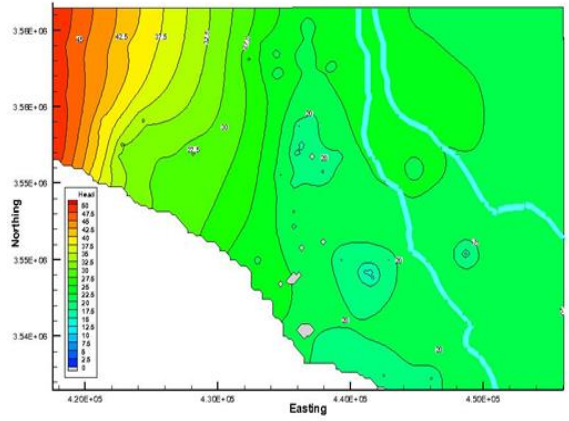
Current Pumping Rate
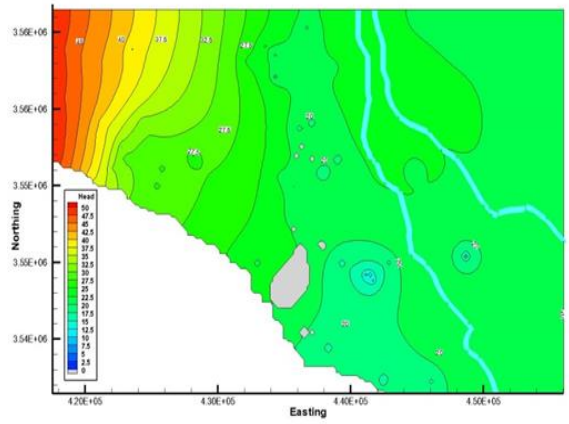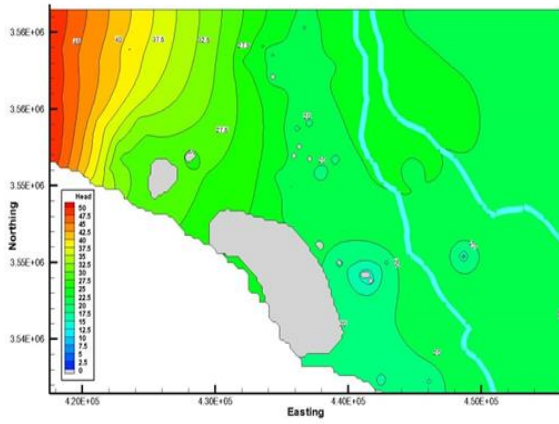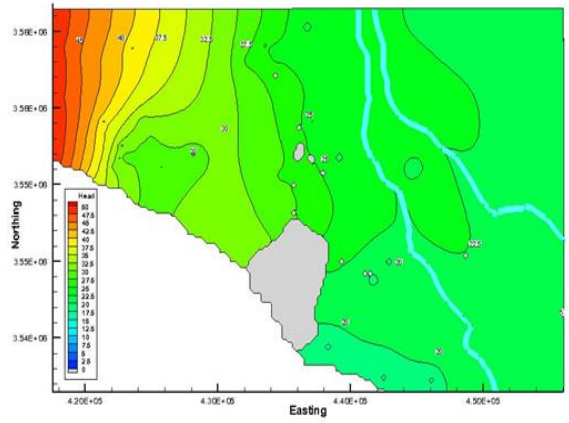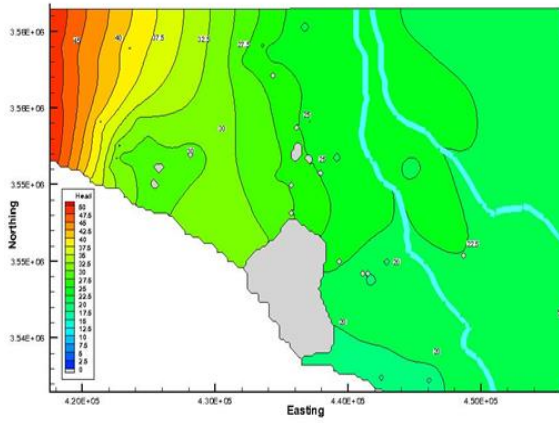
10% Increment
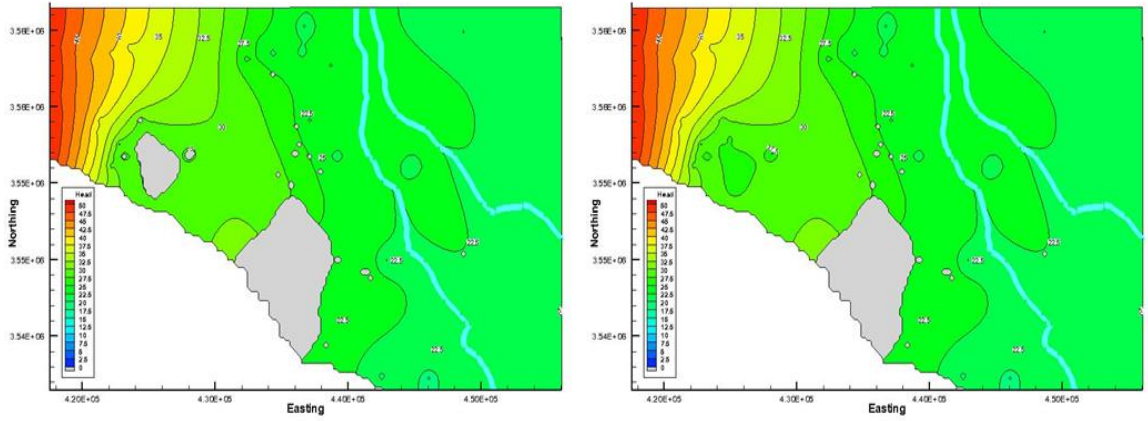
20% Increment
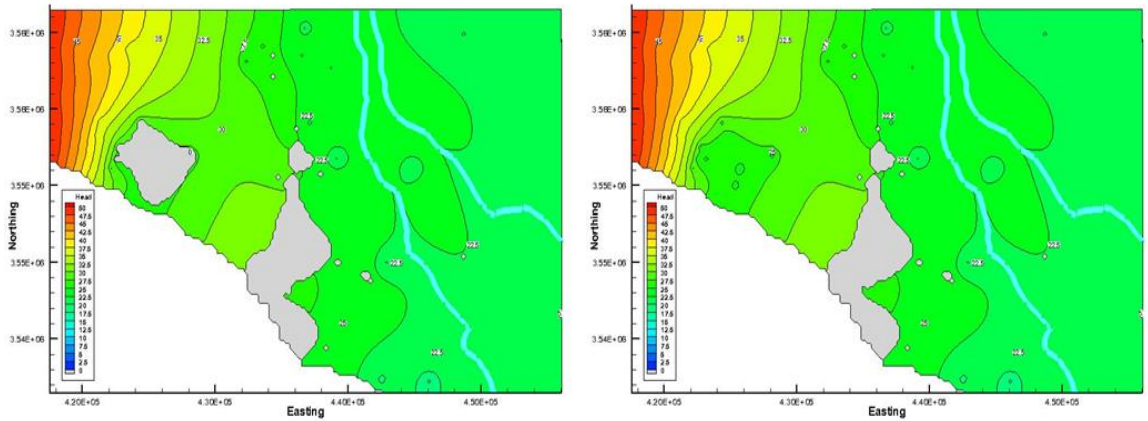
30% Increment
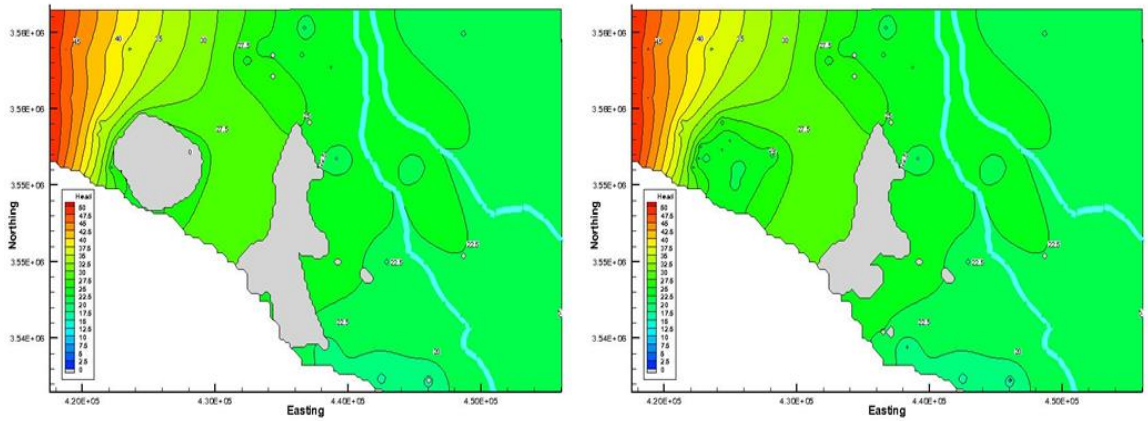
40% Increment

50% Increment

Figure E.3: Computed groundwater table levels in the top and bottom layers of the model through various increments of the pumping rate when reducing the Euphrates River level by 1m

Top Layer
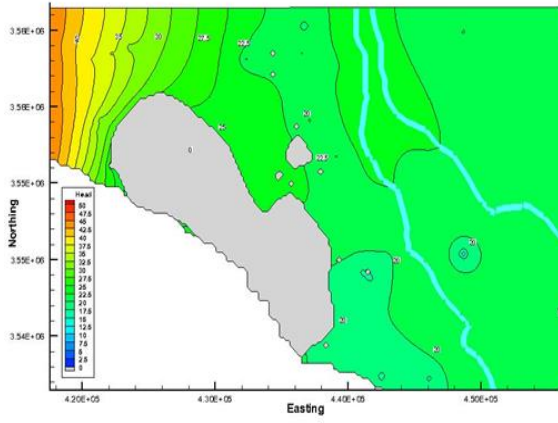
Bottom Layer
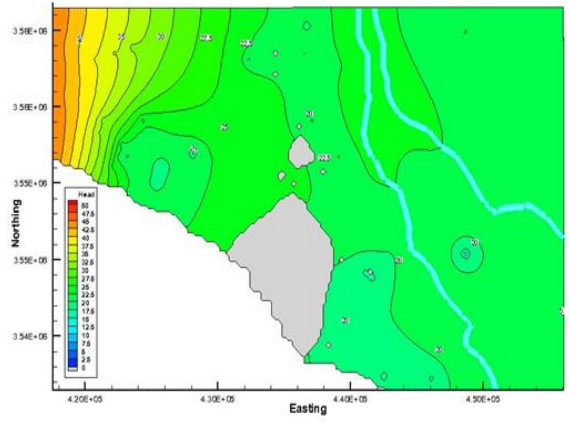
Current Pumping Rate
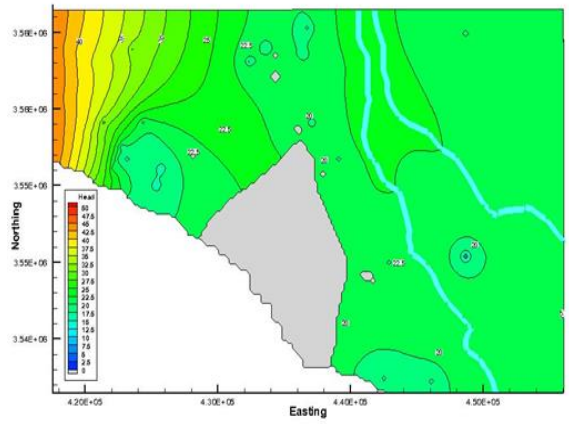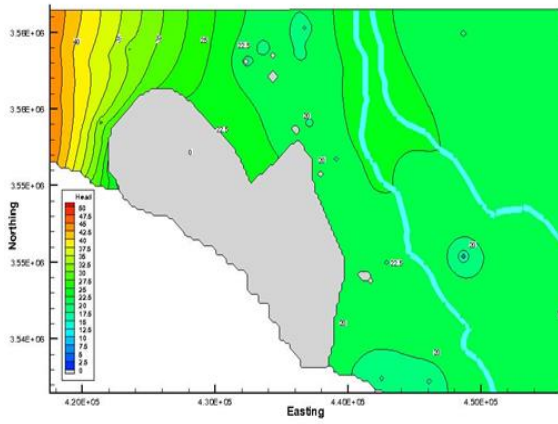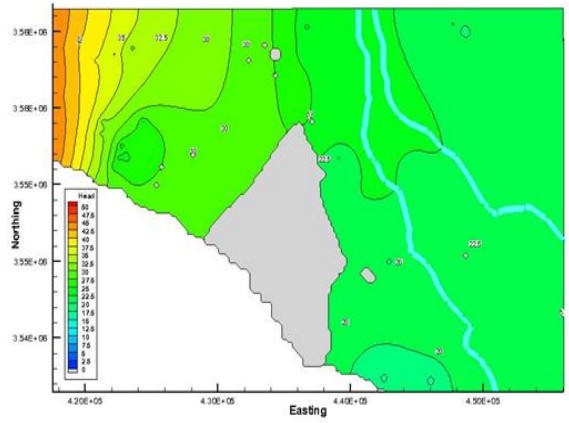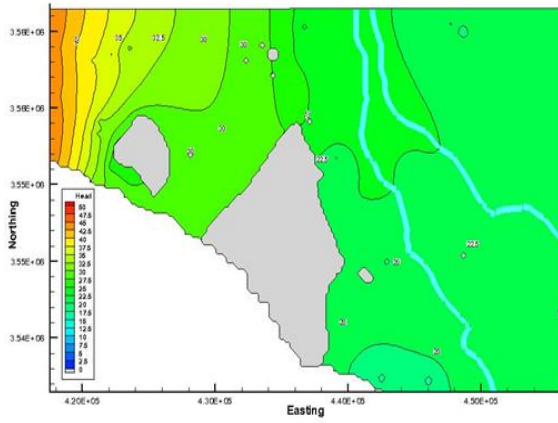
10% Increment
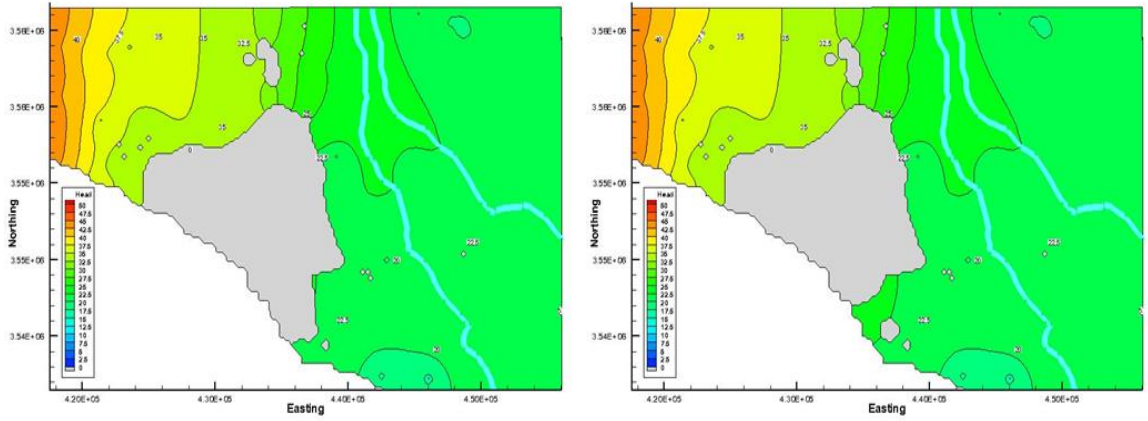
20% Increment
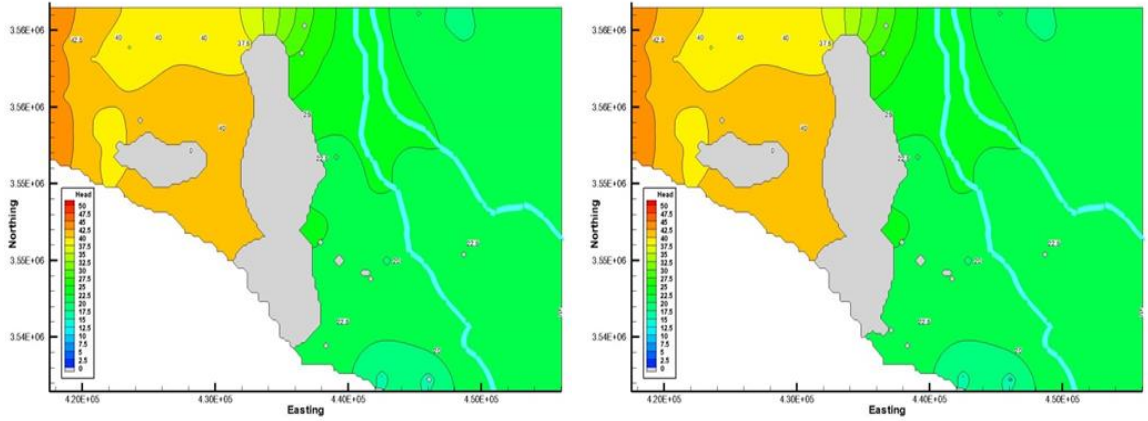
30% Increment
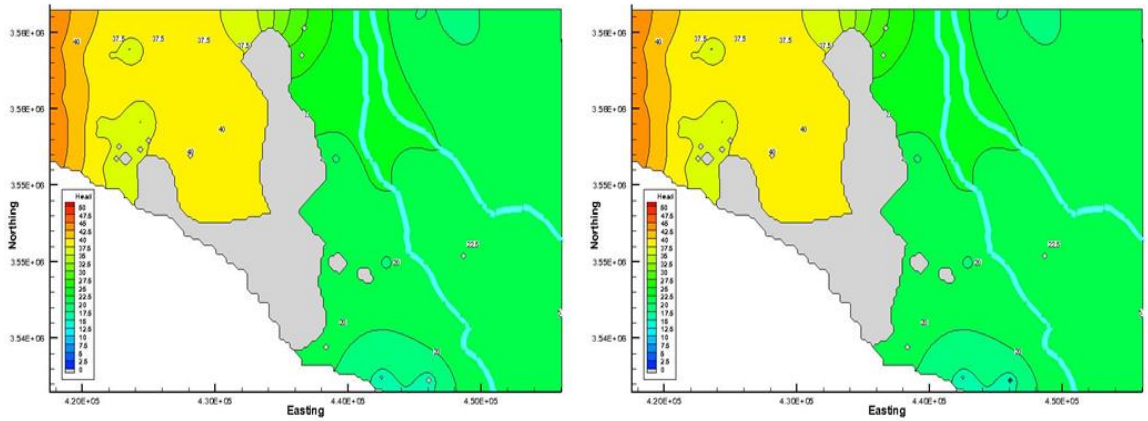
40% Increment

50% Increment

Figure E.4: Computed groundwater table levels in the top and bottom layers of the model through various increments of the pumping rate when reducing the recharge rate by half, reducing the western constant head to 45m, and reducing the Euphrates River level by 1m